UNIVERSITY OF NOTTINGHAM

DEPARTMENT OF CIVIL ENGINEERING

DEVELOPMENTS IN THE ANALYTICAL DESIGN OF ASPHALT PAVEMENTS USING COMPUTERS

BY

JANET M. BRUNTON

May 1983

UNIVERSITY OF NOTTINGHAM

DEPARTMENT OF CIVIL ENGINEERING

DEVELOPMENTS IN THE ANALYTICAL DESIGN OF ASPHALT PAVEMENTS USING COMPUTERS

BY

JANET M. BRUNTON, B.Sc., C.ENG., M.I.C.E.

Thesis submitted to the University of Nottingham
for the degree of Doctor of Philosophy

May 1983

CONTENTS

ABSTRACT

The aim of this research was to develop practical and implementable analytical procedures for the design of asphalt pavements. Use was made of the considerable knowledge which exists on the mechanical properties of the bituminous mixes and previous research done at the University of Nottingham on the analytical approach to pavement design. As the main structural layers in the pavement are bituminous, linear elastic layered systems were used to produce design procedures which are as simple as possible yet realistic. However, values for the sub-base stiffness modulus have been taken from earlier calculations using a non-linear finite element computer program.

Detailed studies of asphalt pavement design against fatigue cracking and permanent deformation have been carried out. These led to the development of revised design criteria for both failure modes.

A suite of programs based on simplified pavement design computations have been written for use on a microcomputer. The programs calculate the asphalt base thickness or the mix proportions for a pavement with equal resistance to permanent deformation and fatigue cracking, or the design life. A further program which considers the effect of cumulative damage in fatigue has also been written.

The development work on the microcomputer has been extended to produce two main frame computer programs, ANPAD and CUDAM. These programs have been used to investigate the effects of varying the asphalt mix proportions and to produce a series of pavement design charts. The advantages of using modified base materials have been demonstrated. Comparisons have been made between the design method developed, other analytical design procedures and current empirical practice.

In order to assess the validity of the analytical approach to design and the practicalities of using novel mixes, several full scale trials have been conducted.

Following a review of procedures for pavement evaluation and overlay design methods using analytical techniques, a computer program has been written for overlay design.

ACKNOWLEDGEMENTS

The author wishes to thank all those who have given help and advice in this research project. In particular:-

Professor R.C. Coates, B.Sc.(Eng.), Ph.D., C.Eng., F.I.C.E., F.I.Struct.E., and Professor P.S. Pell, B.Sc.(Eng.), Ph.D., C.Eng., F.I.C.E., F.I.Struct.E., for providing all the facilities in the Department of Civil Engineering;

Dr. S.F. Brown, B.Sc., Ph.D., D.Sc., C.Eng., F.I.C.E., F.I.H.E., and Professor P.S. Pell, for their helpful supervision and guidance throughout this research;

Mr. B.V. Brodrick, M.Phil, and Mr. K.E. Cooper, M.Phil., for their practical advice and whose experimental work provided such useful information;

Miss J. Shadforth, for typing the thesis;

and all other members of staff in the Department.

Excellent cooperation was also received from a number of outside organisations in connection with the full scale trials. These include Derbysire, Northamptonshire and Leicestershire County Councils and Tarmac Roadstone, Hoveringham Stone, ECC Quarries, Bardon Hill Quarries and BOMAG (GB) Ltd.

Furthermore, the author recognises the excellent service provided by the Cripps Computing Centre of the University of Nottingham and appreciates the use of the computer programs BISTRO, PONOS and CHEVRON developed by the Shell and Chevron Oil Companies.

Final acknowledgement must go to the Science and Engineering Research Council and the Mobil Oil Company for their generous financial sponsorship, without which this project would not have been possible.

NOTATION

CBR	California bearing ratio.
E	Modulus of elasticity. (Numerical suffices indicate the layer, counting from the surface downward.)
EF_w	Equivalence factor for wheel load W.
G_a	Specific gravity of mixed aggregate.
G_b	Specific gravity of bitumen.
I_p	Plasticity Index.
M_A	Percentage of aggregate in mix by mass.
M_B	Percentage of bitumen in mix by mass, (percentage binder content).
N	Design life.
P_i, P_r	Initial and recovered bitumen penetration.
PI_r	Recovered penetration index of bitumen.
S_b	Bitumen stiffness.
S_m	Asphalt mix stiffness.
SP_i, SP_r	Initial and recovered softening point of bitumen.
T	Temperature.
V	Average speed of commercial vehicles (km/hr).
V_B	Percentage volume of binder.
VMA	Voids in mixed aggregate.
V_v	Percentage volume of voids.
h	Thickness of layer. (Numerical suffices indicate the layer.)
p	Normal stress.
q	Deviator stress.
t	Loading time.

x	Design life in years.
δ	Deflection.
ϵ_t	Maximum tensile strain in asphalt.
ϵ_z	Maximum vertical compressive strain in subgrade.
ν	Poisson's ratio.
$\sigma_1, \sigma_2, \sigma_3$	Principal stresses.
τ	Shear stress.

Other symbols are defined and used in restricted conditions as the need arises.

CHAPTER ONE

INTRODUCTION

The economy of a country is, to a great extent, dependent on a reliable means of transport for both people and, more importantly, goods. For this reason it would be logical to expect high financial investment in pavement design and construction but, unfortunately, the level of expenditure is limited by the general economic climate in the United Kingdom. It is, therefore, vital to provide a method of designing pavements which is both accurate and economic, particularly as the numbers and weights of commercial vehicles using the highway network continue to escalate.

1.1 THE PAVEMENT STRUCTURE

A typical flexible pavement consists of several layers of bound and/or unbound materials, (see Fig.1.1). The purpose of the uppermost layer is to provide a good quality riding surface and adequate resistance to skidding. Most surface layers or wearing courses are impervious to prevent water from entering and damaging the lower structural layers. However, in some cases an open textured upper layer, which allows rapid drainage of surface water in order to minimise spray, is used together with an impervious lower layer. As this thesis is only concerned with structural aspects of pavement design, surface texture and skid resistance are not discussed. The basecourse provides an even, working platform for the surface layer and also contributes to the strength of the pavement. The wearing course and basecourse are collectively known as the surfacing layers and are bitumen bound. Below these layers is the road base which is the main structural component of the pavement and is used to distribute the

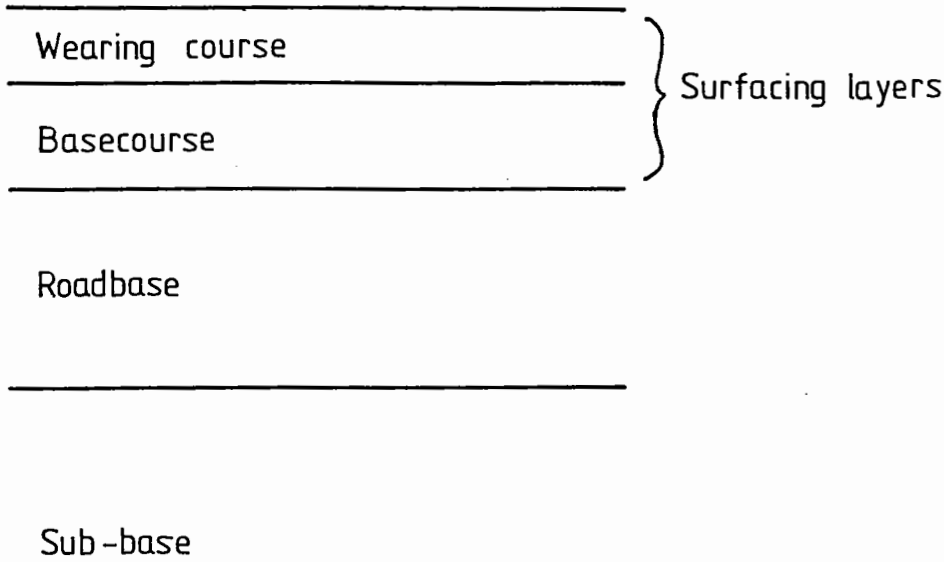

FIG 1·1 TYPICAL FLEXIBLE PAVEMENT

traffic induced stresses and strains to acceptable levels in the lower sub-base layer and subgrade. Although the unbound sub-base layer helps to distribute the load, the main intentions are to provide a working platform for construction of the upper layers and protection to the subgrade from frost.

1.2 CURRENT DESIGN PRACTICE

The fundamental engineering properties of the different pavement materials vary considerably, not only from one material to another but also with temperature and loading conditions, (see section 1.3). Due to these complexities, pavement designs traditionally rely on empirical methods.

Current British practice for pavement design follows the empirical recommendations of the Department of Transpsort (DTp) in Road Note 29 Third Edition (1). These recommendations are based on experience gained from earlier construction and information from full scale trials (2,3). A series of design charts is provided in which the required thickness of each layer may be selected for a known pavement life. For lives in excess of 11 million standard 80 kN axles, the recommendations are extrapolations of measured performance. Standard specifications are also given for the bituminous materials (4,5), effectively restricting the use of some local materials which may fall just outside the permitted range and new or modified mixes.

By following these design procedures, gross failures are very rare provided that the loading conditions remain unchanged. However, empirical design cannot be confidently extrapolated to cover new loadings, materials or construction techniques and the advantages of analytical methods are becoming more widely recognised.

Many other countries such as France (6), Germany (7) and the United States (8), have developed their own empirical or semi-empirical design procedures each applicable to conditions and materials typical for that country.

1.3 ANALYTICAL DESIGN OF PAVEMENTS

Instead of using empirical pavement design methods, an alternative approach is to use theoretically based design procedures which consider the pavement in exactly the same way as a typical civil engineering structure. The selected pavement is subjected to a specified loading and a structural analysis is performed to determine the stresses, strains and deflections at critical points in the structure. These are then compared with the maximum allowable values to assess whether or not the design is acceptable. If the design is unsatisfactory, the layer thicknesses are adjusted and the procedure is repeated.

1.3.1 Traffic Loading and Environmental Conditions

The structural design of pavements is complicated by variations in both environmental and loading conditions. Since pavements are subjected to many types of vehicles travelling at different speeds, the magnitude of the load, the axle configuration and the loading time all vary for each loading application. The engineering properties of the bituminous materials are dependent on temperature and loading time, (see Section 1.3.2) and, therefore, vary throughout the pavement life. Frost and thaw can also significantly affect the strength of the sub-base and subgrade layers. Although it is particularly important to consider freezing effects in countries where the range of temperatures experienced is large, such as the United States, they can generally be ignored in the United Kingdom where the climate is much milder.

In order to perform a detailed analysis each temperature and loading condition should be considered separately and the resulting damage caused to the pavement added together using some form of cumulative damage approach. However, this is impractical due to the number of computations involved and simplifications, such as the use of a standard axle and average monthly temperatures, have been introduced into most design procedures.

1.3.2 Material Properties

To assess the pavement's response to a given load application under known environmental conditions, some knowledge of the mechanical behaviour of each material in the structure is required. For a bituminous material the ratio of applied stress to resulting strain depends on the temperature and loading time for which the stress is applied. Therefore, as the ratio is not constant, a single Young's modulus cannot be assigned to these materials. In 1954 Van der Poel (9) developed from experimental data a nomograph for predicting the 'stiffness' (ratio of stress to strain at a particular temperature and loading time), of bitumen (S_b). As a result of further extensive tests (10) he also showed that the stiffness of an asphalt mix is primarily dependent on the bitumen stiffness and volume concentration of the aggregate. Ten years later Heukelom and Klomp (11) and Van Draat and Sommer (12) extended Van der Poel's work to derive equations for calculating the stiffness of the asphalt mixes. Subsequently, in 1977, a new nomograph was produced by the Shell organisation (13) to predict the stiffness of bituminous materials. Although at high temperatures and long loading times bitumen exhibits viscous behaviour, under the dynamic conditions relevant to pavement design, (low temperatures and short loading times), bituminous materials can be considered as linear elastic.

Unlike bituminous materials, soils and granular materials are markedly non-linear, and their stiffness modulus is clearly stress dependent. Investigations into the resilient behaviour of these materials have been carried out by a number of researchers, including Hicks (14), Seed et al (15), Boyce et al (16), Pappin and Brown (17) and Shaw (18).

For a linear elastic analysis the Poisson's ratio of each material is also required. Poisson's ratio for bituminous materials varies with temperature from about 0.35 at low temperatures to 0.5 at high

temperatures (19,20). Typical values in the United Kingdom are 0.4 for bituminous materials and subgrade, and 0.3 for granular sub-bases (21).

1.3.3 Pavement Failure Modes

The objective of any pavement design procedure is to provide a structure which can maintain an acceptable riding quality throughout its design life. However, pavements do deteriorate with time as a result of traffic load repetitions. The two modes of failure caused by traffic are cracking and permanent deformation. Analytical design methods attempt to control these failure mechanisms by using design criteria which limit the predicted stress and strain levels in the materials.

Cracking in the asphalt layers was shown by Hveem (22) to be a fatigue phenomenon. Cracks generally initiate at the bottom of the asphalt layers, where the repeated tensile strains are maximum and propagate upwards towards the surface. This mode of failure is particularly common in both the United States of America (23) and South Africa (24) though there is much less evidence of it in the United Kingdom. Early notable research into the fatigue behaviour of asphalts was carried out by Pell (25) and Monismith et al (26). By 1973 many more investigations into the fatigue cracking of bituminous materials had been undertaken and a number of these are discussed in Special Report 140 of the Highway Research Board (27).

In the United Kingdom permanent deformation is a far more common cause of pavement failure than fatigue cracking. The rut developed at the pavement surface is the sum of the permanent deformation of each of the layers and the subgrade. Two general approaches are used to design against rutting from repeated traffic loading. The first limits the vertical stress or strain in the subgrade, by controlling the characteristics of the materials through suitable mix design, good

compaction and adequate layer thicknesses and is intended to ensure that the permanent deformation in the subgrade does not result in excessive rutting at the surface. A number of limiting criteria have been developed using data obtained from actual pavements. Peattie (28) and Barksdale and Miller (29) suggested limiting the vertical stress in the subgrade, whilst Dorman and Metcalf (30), Monismith and McLean (31), Hicks and Finn (32), Witczak (33) and Brown et al (34) all developed limiting criteria for the vertical compressive subgrade strain. The second method used to design against permanent deformation involves estimating the actual amount of rutting which may occur using layered elastic or visco-elastic analysis. This type of procedure requires the relation between permanent or plastic strain and applied stress for each material. A number of papers concerning permanent deformation were included in Transportation Research Record 616 (35) and Session 5 at the Fourth International Conference on the Structural Design of Asphalt Pavements (36).

1.3.4 Analysis

Since Burmister (37) first used elastic theory to formulate equations for the deflections and stresses in aircraft runways in 1943, there have been enormous developments in analytical design procedures for pavements. At first, the use of realistic models to represent the pavement structures was seriously hampered by the difficulties in solving the complex mathematical equations. However, the advance of computer technology in the 1960's led to a number of computer programs being developed. Two of these, which considered the pavement as multi-layered elastic systems, were developed by the Shell (38) and Chevron (39) oil companies. Other solutions for the pavement's response to traffic loading have been derived using the more complex visco-elastic analysis, fracture mechanics and non-linear finite element procedures.

As the main structural layers in the pavement are bituminous materials, which can be considered to be linear-elastic under the dynamic conditions relevant to pavement design, a linear-elastic layered system is used in this research in order to keep the design procedures as simple as possible. Many investigations have shown close agreement between measured stresses, strains and deflections in pavements, and predicted values using linear elastic theory (40,41,42,43). Results from earlier computations using a non-linear finite element program developed at the University of Nottingham (44) are used to obtain realistic values for the sub-base stiffness moduli.

1.4 OUTLINE OF THE RESEARCH

The main objective of this research was to produce practical and implementable pavement design procedures based on analytical methods. This was achieved by developing and extending existing design procedures in use at the University of Nottingham, to produce new and versatile computer design programs. Obviously, due to the complex nature of the problem, many simplifications were necessary but it is believed that these are realistic and do not cause significant inaccuracies to the resulting pavement designs. The work reported in this thesis makes use of existing research knowledge of the mechanical properties of typical bituminous materials and did not involve further laboratory testing.

Detailed studies were made of the design of asphalt pavements against fatigue cracking and permanent deformation. Cumulative fatigue damage effects due to variations in temperature and loading were analysed and a revised fatigue criterion was derived. A new computation procedure for the design against excessive rutting has been developed using data produced in a laboratory testing programme carried out at the University of Nottingham at the same time as this research

(45,46,47,48). The procedure involves adjustment to the relationship between the allowable subgrade strain and the design life, depending on the type of road base material used.

A further important aspect of this research was to demonstrate the advantages which could be achieved by using new and improved materials. Novel mixes developed at the University of Nottingham were incorporated into full scale trial pavements designed using the new computer programs.

CHAPTER TWO

REVIEW OF PREVIOUS WORK AT NOTTINGHAM

This research is a continuation of previous work carried out at the University of Nottingham on the development of analytical methods for the design of asphalt pavements. This Chapter, therefore, briefly reviews the design procedures and computer programs which have resulted from this earlier effort.

2.1 THE SIMPLIFIED DESIGN METHOD

The 'simplified design method' for flexible pavements is based on a rational simplification of the complex pavement design problem. It presents a design procedure in the form of charts and equations which is intended for use in the United Kingdom. The original version (49), developed for teaching and preliminary design studies, has been further improved and the results published in a book by Brown (50). A brief description is given below.

2.1.1 Pavement Structure

The major simplifications in the design method concern the form of structure and the number of variables which are allowed. The pavement structure is assumed to consist of three linear-elastic layers, as shown in Fig.2.1. The top layer represents all the bituminous bound materials and varies in thickness between 100 and 500 mm. The second layer is a 200mm thick granular layer and the bottom layer is the subgrade. The elastic properties of each layer, (the stiffness modulus and Poisson's ratio), are required. A Poisson's ratio of 0.4 is used for the asphalt layer and the subgrade and a value of 0.3 is taken for the granular layer. To eliminate the stiffness modulus of the granular

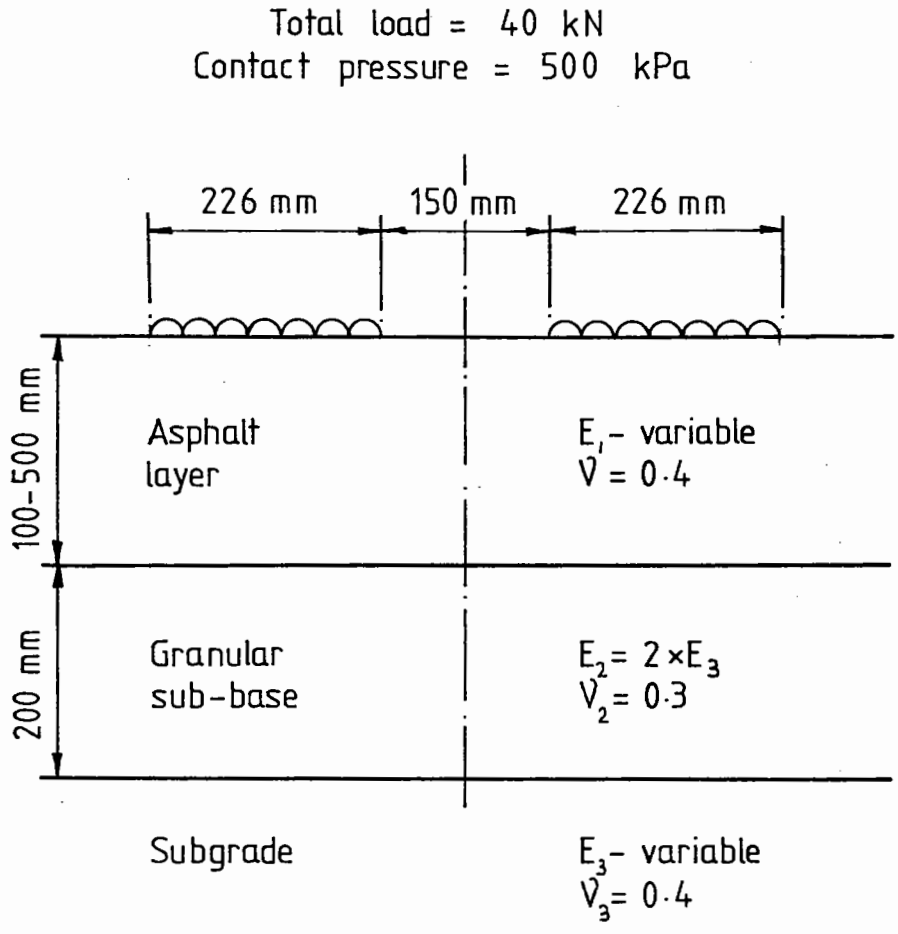

FIG 2.1 PAVEMENT STRUCTURE FOR SIMPLIFIED DESIGN METHOD

layer as a variable, a fixed modular ratio of 2 is used between the sub-base and subgrade. This was considered to be a typical value based on data from site and laboratory testing (51,52). The stiffness moduli of the asphalt layer and subgrade are determined as described in Section 2.1.3.

2.1.2 Traffic Loading and Environmental Conditions

The simplified design method is based on computations using a standard 40 kN dual wheel axle loading arrangement (see Fig.2.1).

A further simplification in the design approach is that variations in temperature are not taken into account directly. An average annual design temperature for the asphalt base is used. This is taken as equal to the average annual air temperature plus 3°C. The 3°C increase is due to the thermal characteristics of the material and the fact that most traffic loading occurs during the day when the temperatures are higher.

2.1.3 Stiffness Moduli

Bituminous Materials Brown (50) provides two methods for deriving the bituminous mix stiffness (S_m), one using equations, the other using nomographs (see Fig.2.2). Both methods require the determination of the recovered binder properties, loading time (t) and binder stiffness (S_b).

The equations given to estimate the recovered penetration (P_r), the recovered softening point (SP_r), and the recovered penetration index (PI_r) are as follows:

$$P_r = 0.65\ P_i \qquad (2.1)$$

$$SP_r = 98.4 - 26.4 \log P_r \qquad (2.2)$$

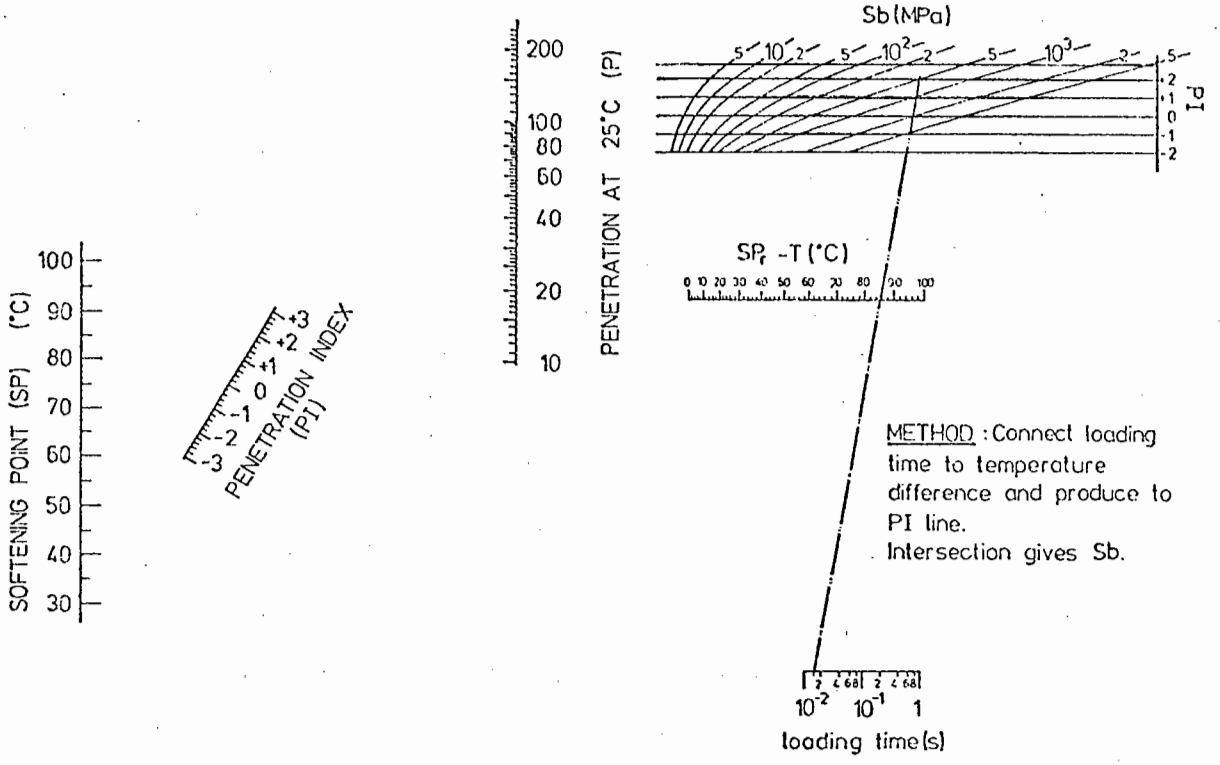

a. Nomograph for penetration index of bitumen (after Van der Poel (9))

c. Nomograph for bitumen stiffness (derived from Van der Poel (9))

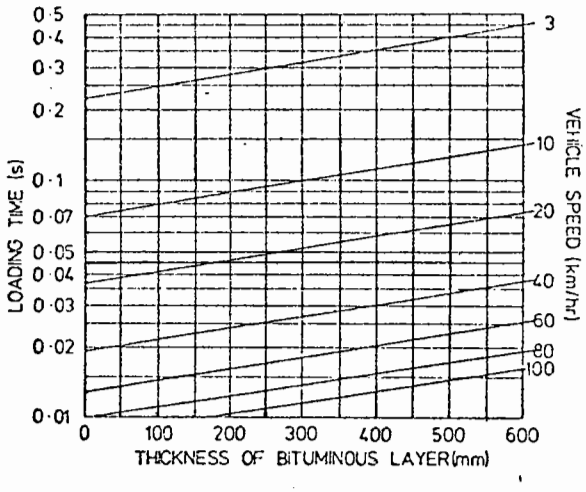

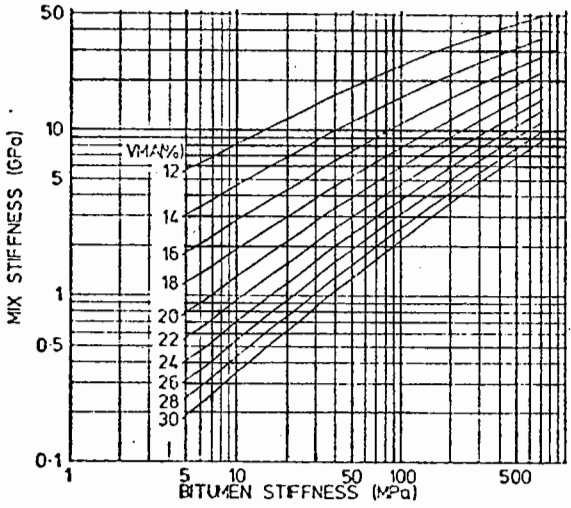

b. Loading time as a function of vehicle speed and layer thickness

d. Relationship between mix stiffness binder stiffness and VMA

FIG 2·2 NOMOGRAPHS FOR MIX STIFFNESS DETERMINATION (AFTER BROWN (50))

$$PI_r = \frac{1951 - 500 \log P_r - 20\ SP_r}{50 \log P_r - SP_r - 120.1} \qquad (2.3)$$

where P_i is the initial penetration of the binder.

Equation (2.4) is used to calculate the loading time (t in seconds), from the average speed of commercial vehicle (V in km/hr) and the layer thickness (h in mm).

$$\log t = 5 \times 10^{-4} h - 0.2 - 0.94 \log V \qquad (2.4)$$

Alternatively, equation (2.5) may be used to obtain a reasonable estimate of loading time for 100-350mm thick asphalt layers.

$$t = \frac{1}{V} \qquad (2.5)$$

The following equation, derived by Ullidtz (53) from Van der Poel's nomograph (9), is used to calculate the binder stiffness over a given range of conditions.

$$S_b = 1.157 \times 10^{-7}\ t^{-0.368}\ 2.718^{-PI_r(SP_r - T)^5} \qquad (2.6)$$

where S_b = binder stiffness (MPa)

t = loading time ($0.01 \leqslant t \leqslant 0.1$ secs)

PI_r = Penetration Index ($-1 \leqslant PI_r \leqslant 1$)

SP_r = Recovered Softening Point (°C)

T = average annual pavement temperature

($20 \leqslant (SP_r - T) \leqslant 60$°C)

Finally, the mix stiffness is determined from the binder stiffness and voids in mixed aggregate (VMA) using the following relationship established by Brown (54) on the basis of earlier work by the Shell Laboratories (11,12) for void contents greater than 3%.

$$S_m = S_b \left[1 + \frac{257.5 - 2.5\ VMA}{n\ (VMA - 3)} \right]^n \qquad (2.7)$$

where, $n = 0.83 \log \left[\frac{4 \times 10^4}{S_b} \right]$

S_b is in MPa and VMA is a percentage.

Brown (50) also provides charts for determining the mix stiffness of three typical mixes depending on the design temperature and vehicle speed.

Subgrade The elastic modulus of the subgrade is estimated from its California Bearing Ratio (CBR) using the approximation:

$$E_{subgrade} = 10 \times CBR \qquad (2.8)$$

where, E is in MPa.

An alternative method for determining the elastic modulus of clays directly from the plasticity index (I_p) based on research at TRRL (55), is also given by Brown (50), viz.,

$$E_{subgrade} = 70 - I_p \qquad (2.9)$$

where, E is in MPa and I_p is a percentage.

2.1.4 Maximum Allowable Strain

The design parameters used in the simplified design method are the maximum tensile strain at the bottom of the asphalt layer and the maximum compressive strain at the top of the subgrade. The maximum allowable asphalt strain is calculated from the relationship between tensile strain (ϵ_t) and the number of cycles to failure (N), binder content by volume (V_B) and the initial softening point of the binder (SP_i) based on the work of Cooper and Pell (56) and Brown et al (34) viz.,

$$\log \epsilon_t = \frac{14.39 \log V_B + 24.2 \log SP_i - 40.7 - \log N}{5.13 \log V_B + 8.63 \log SP_i - 15.8} \quad \text{microstrain} \qquad (2.10)$$

In this equation, laboratory lives have been increased by a factor of 5 to allow for rest periods and an additional factor of 20 to allow for crack propagation and transverse wheel distribution (34). As an alternative to equation (2.10) the nomograph shown in Fig.2.3a may be used. Brown (50) also provides a graph giving the fatigue lines for three typical mixes.

The simplified design method uses the following equation or Fig.2.3b to determine the maximum allowable subgrade strain (ϵ_z) from the number of load applications (N).

$$\epsilon_z = \frac{21600}{N^{0.28}} \quad \text{microstrain} \qquad (2.11)$$

This relationship was established (49) by analysing British pavements of known performance taken from Road Note 29 (1) and using an average annual pavement temperature of 15°C and typical mix proportions for a rolled asphalt (50).

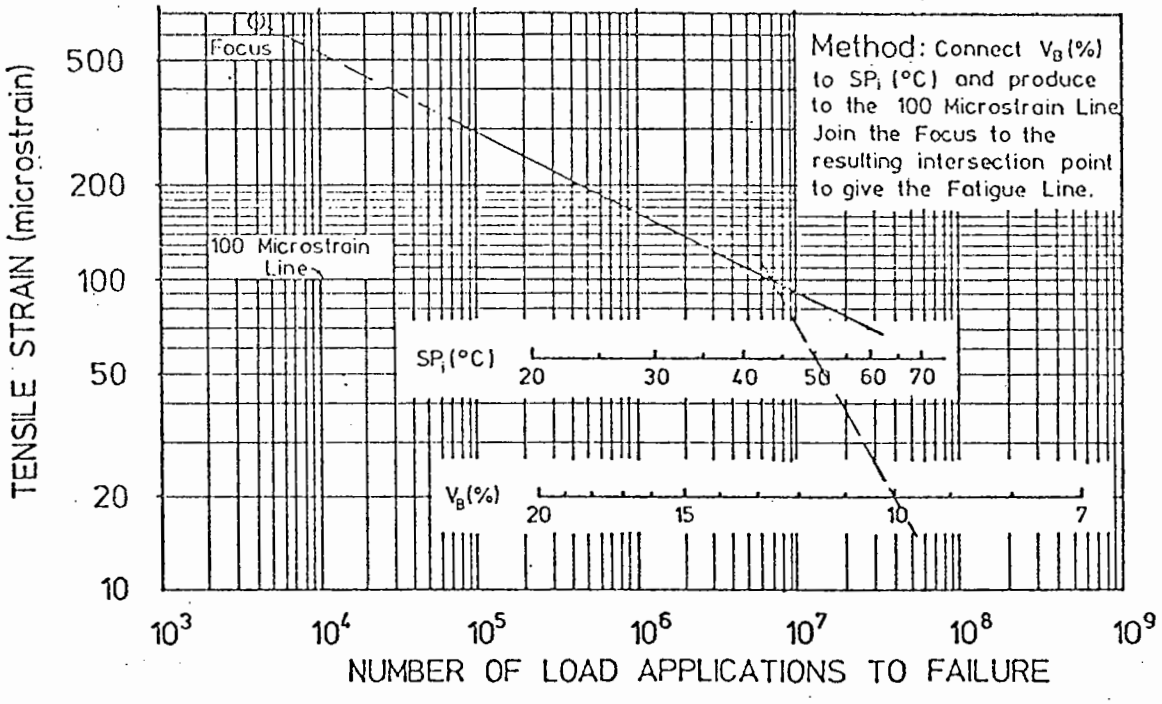

a. Maximum allowable asphalt strain

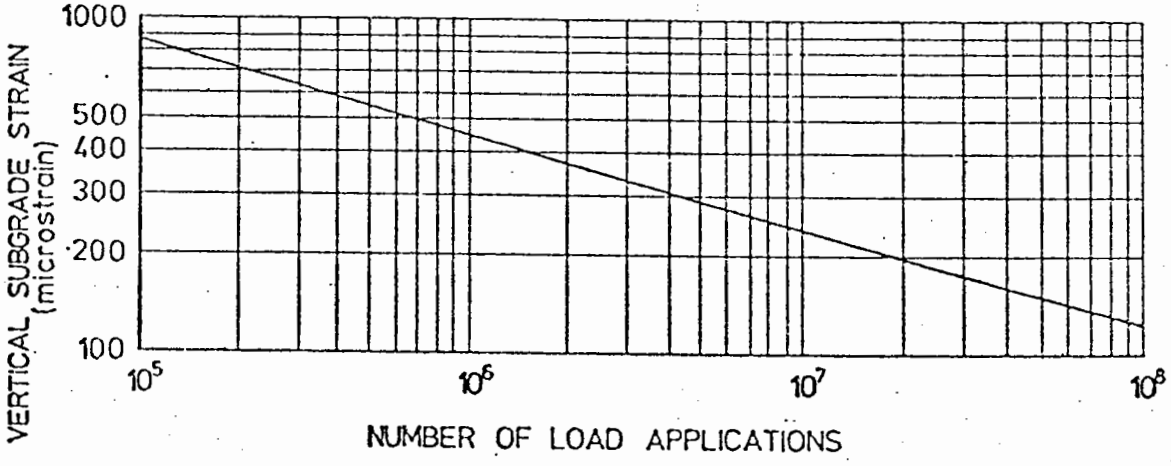

b. Maximum allowable subgrade strain

FIG 2·3 DESIGN CRITERIA FOR SIMPLIFIED DESIGN METHOD (AFTER BROWN (50))

2.1.5 Structural Analysis

Using the simplified structure and loading arrangement given in Fig.2.1, calculations were performed with the BISTRO computer program (38) for a range of asphalt thicknesses (100-500mm), subgrade moduli (20-70 Mpa) and mix stiffness (3-19 GPa). The results of these are contained in four charts for subgrade moduli of 20, 30, 50 and 70 MPa. A typical chart is shown in Fig.2.4. The simplified design method uses these charts to determine the required thickness of bituminous material having a given stiffness so as to satisfy each of the two strain criteria.

2.1.6 Design Methods

In his book, Brown (50) describes in detail three design procedures to calculate either the required asphalt thickness, the bituminous mix properties for a pavement with equal lives against fatigue cracking and permanent deformation, or the design life of the pavement. A flow diagram for the design thickness procedure is given in Fig.2.5a. The average temperature of the asphalt, average speed of commercial vehicles and asphalt mix details are all used to calculate the asphalt mix stiffness (see Section 2.1.3). Then, using the cumulative number of standard axles in the design life, the two maximum allowable strains are determined (see Section 2.1.4). From these, a minimum asphalt layer thickness for each criterion is derived using the relevant design chart (see Fig.2.4). The final design thickness is taken as the larger of the two thicknesses with the pavement overdesigned for the other criterion.

The second procedure described by Brown (50) introduces the concept of a 'balanced design' to produce a pavement which has equal lives based on both design criteria. A flow diagram is given in Fig.2.5b. For this procedure the thickness of the asphalt layer must

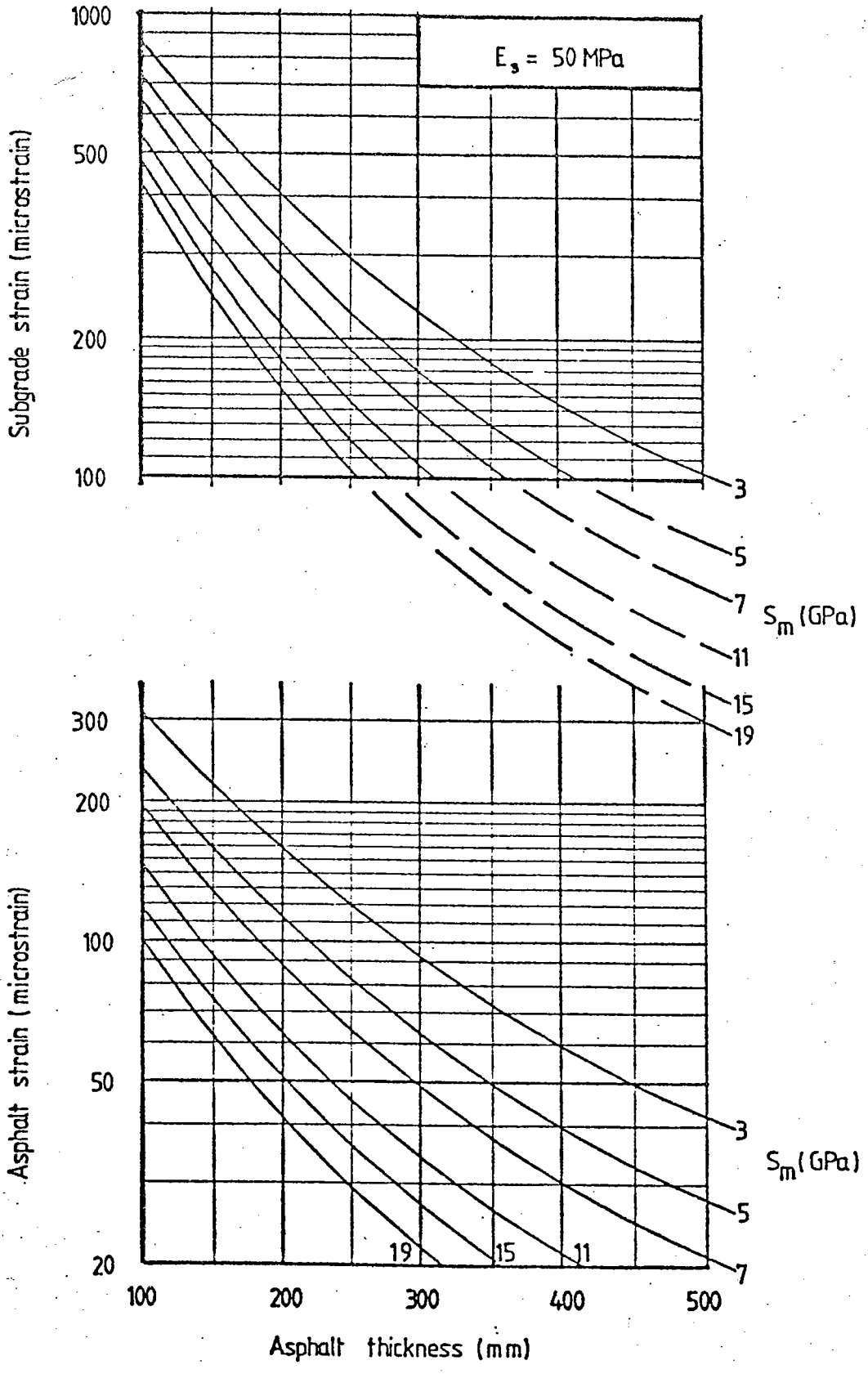

FIG 2.4 CRITICAL STRAINS AS FUNCTIONS OF STIFFNESS AND THICKNESS OF ASPHALT (SUBGRADE MODULUS OF ELASTICITY = 50 MPa) (AFTER BROWN (50))

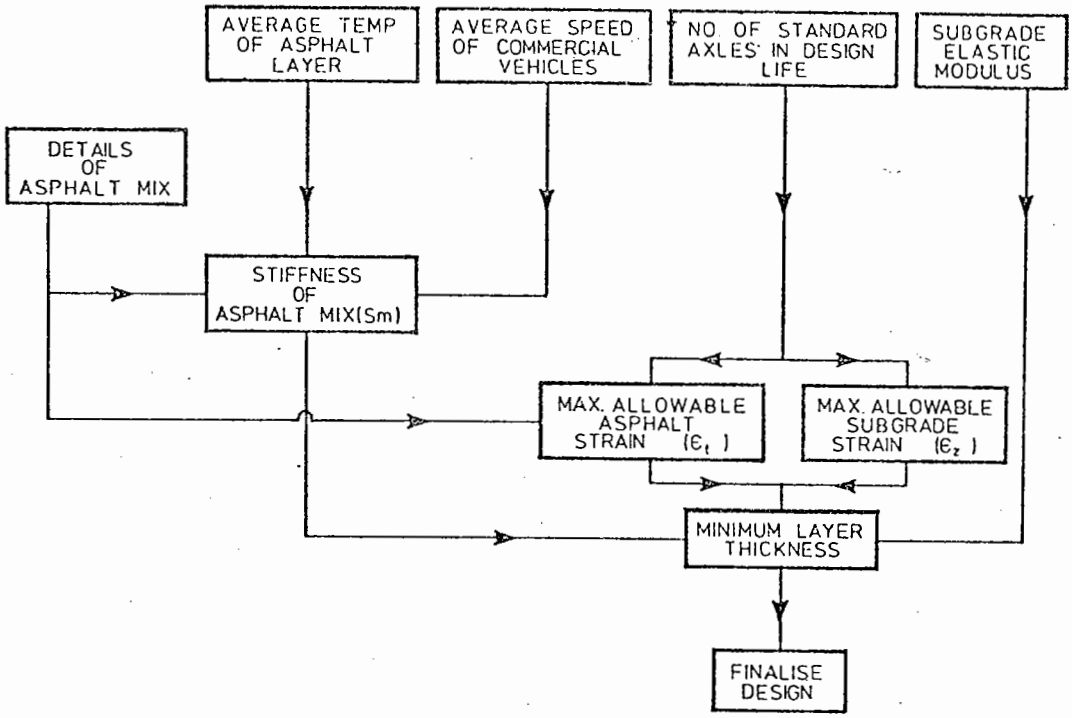

a. Design procedure

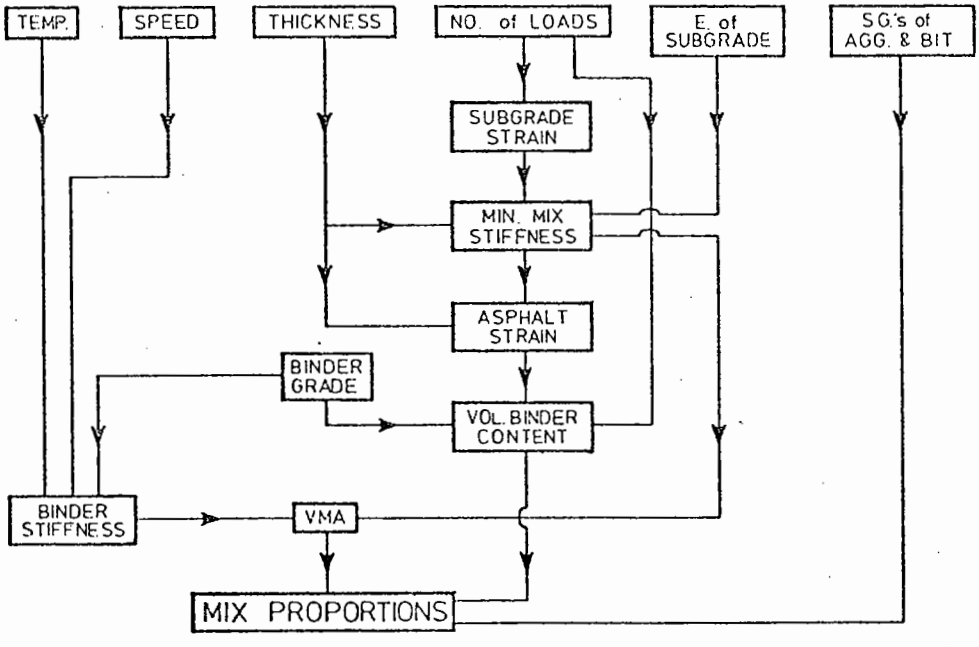

b. Balanced design method

FIG 2·5 FLOW DIAGRAMS FOR SIMPLIFIED DESIGN METHOD (AFTER BROWN (50))

be specified. The first step is to calculate the maximum allowable subgrade strain from the design life. This enables the minimum mix stiffness of the asphalt layer to be determined from the design charts (see Fig.2.4a). Then the asphalt strain can be derived using the same mix stiffness (see Fig.2.4b). Assuming a given initial penetration of binder and corresponding recovered binder properties, the volume of binder in the asphalt mix is obtained from Fig.2.3a or by rearranging equation (2.10). The binder stiffness is then determined from Fig.2.2c or equation (2.6). From the binder stiffness and mix stiffness the required value of the voids in mixed aggregate can be derived (see equation (2.7) or Fig.2.2d). The volumetric proportions of the mix are now fixed by the voids in mixed aggregate (VMA) and volume of binder (V_B), so that the void content (V_v), which is the numerical difference between the two (VMA - V_v), and the binder content (M_B) can be calculated.

The calculated mix proportions may be impractical and a trial mix should be prepared for laboratory testing.

The third design procedure described by Brown (50) assesses the life of a given pavement. The mix stiffness is determined first then the load induced asphalt and subgrade strains followed by the life for each design criterion. The actual life is the smaller of the two lives.

2.2 THE COMPUTER PROGRAM ADEM

The main frame computer program ADEM (Analytical DEsign Method) was developed by Stock (57). The program calculates the required thickness of a bituminous road base in a 3,4 or 5 layer pavement using a similar procedure to that described in Section 2.1 for the simplified design method. However, it offers greater flexibility than a method based on charts. A typical 4-layer system is shown in Fig.2.6. ADEM

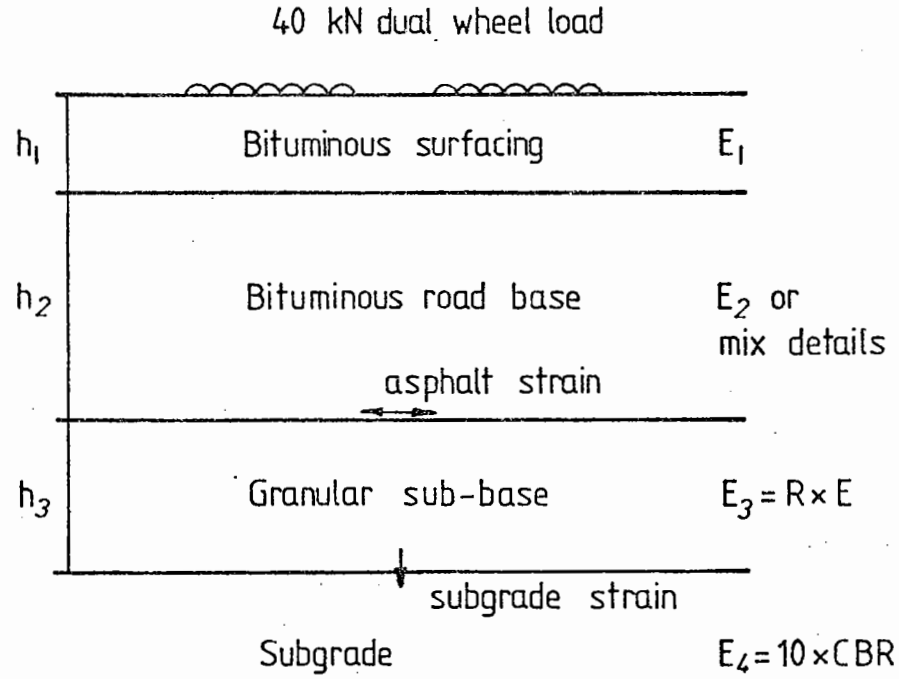

Input data : h_1, h_3, E_1, E_2 (or mix details), CBR
Design criteria : Asphalt strain, subgrade strain
Output : h_2

FIG 2·6 THE ADEM FOUR-LAYER SYSTEM

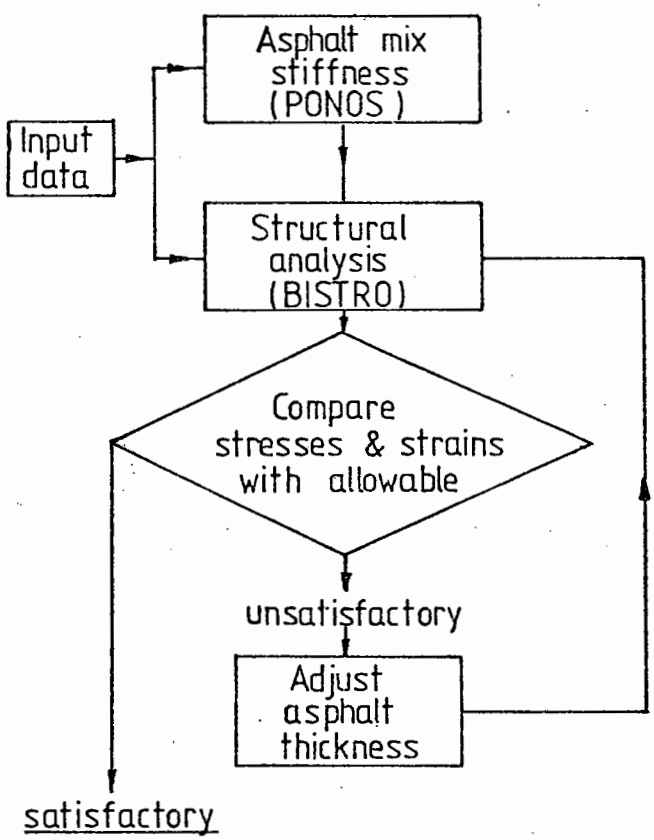

FIG 2·7 SIMPLIFIED FLOW DIAGRAM FOR ADEM

uses the same standard dual wheel loading arrangement, design temperature and criteria as the simplified design method.

Fig.2.7 shows a simplified flow diagram for ADEM. It incorporates the computer program BISTRO (38) to perform the structural analysis and parts of the program PONOS (58) to estimate the bituminous mix stiffness if it is not known. The initial analysis is carried out with a base thickness of 160mm. If this is unsatisfactory due to the traffic induced strains being too large or too small compared with the allowable values, then the base thickness is appropriately increased or decreased by 10mm and the analysis repeated. This iteration procedure continues until the design is satisfactory. Fig.2.8 shows the typical computer output information.

There are two versions of the program, one using linear elastic analysis the other treating the granular layer as non-linear. The linear version is usually quite adequate, unless the thickness of the non-linear granular material is large in relation to the bituminous materials, and uses approximately one-fifth the computer units required for the non-linear version. For the non-linear method the granular layer is divided into 4 sub-layers and an initial estimated value of modulus is assigned to each. The moduli of the sub-layers are then determined from the calculated stresses at the centre of the sub-layer directly under the load using a relationship of the general form shown in equation (2.12) with a failure criterion developed by Boyce (59) superimposed (see Fig.2.9).

$$E = K_1 \theta^{K_2} \qquad (2.12)$$

where θ = sum of the principal stresses, arising from both overburden and traffic loading,

K_1, K_2 = constants which depend on the material type and condition.

TYPICAL INPUT DATA

Initial binder penetration = 50.0
Binder content = 4%
Void content = 6.5%
Binder S.G. = 1.02
Aggregate S.G. = 2.70
Mean pavement temperature = 15°C
Mean traffic speed = 80 km/hr
Design life = 20 msa
Subgrade CBR = 3%
Sub-base thickness = 200 mm

OUTPUT

DESIGN CRITERIA

Asphalt fatigue strain = 75.1 microstrain
Subgrade strain = 193 microstrain

State of Parameters

Iteration Number	Layer Thickness (mm)	Mix Stiffness (MN/m^2)	Asphalt Strain (microstrain)	Subgrade Strain (microstrain)	
1	250	11739	51.1	178	Design conservative
2	240	11767	54.4	190	Design conservative
3	230	11796	58.1	205	Subgrade strain critical
NSTP = 1					
4	240	11767	54.4	190	

DESIGN COMPLETE

Asphalt layer thickness = 0.2400 metres
+++++ +++++

ASPHALT
Thickness = 0.24 m
Stiffness = 11767 MN/m^2
Poisson's ratio = 0.4

SUB-BASE
Thickness = 0.20 m
Stiffness = 75 MN/m^2
Poisson's ratio = 0.3

SUBGRADE
CBR = 3%
Poisson's ratio = 0.4

FIG 2.8 OUTPUT INFORMATION FROM ADEM FOR THREE-LAYER STRUCTURE

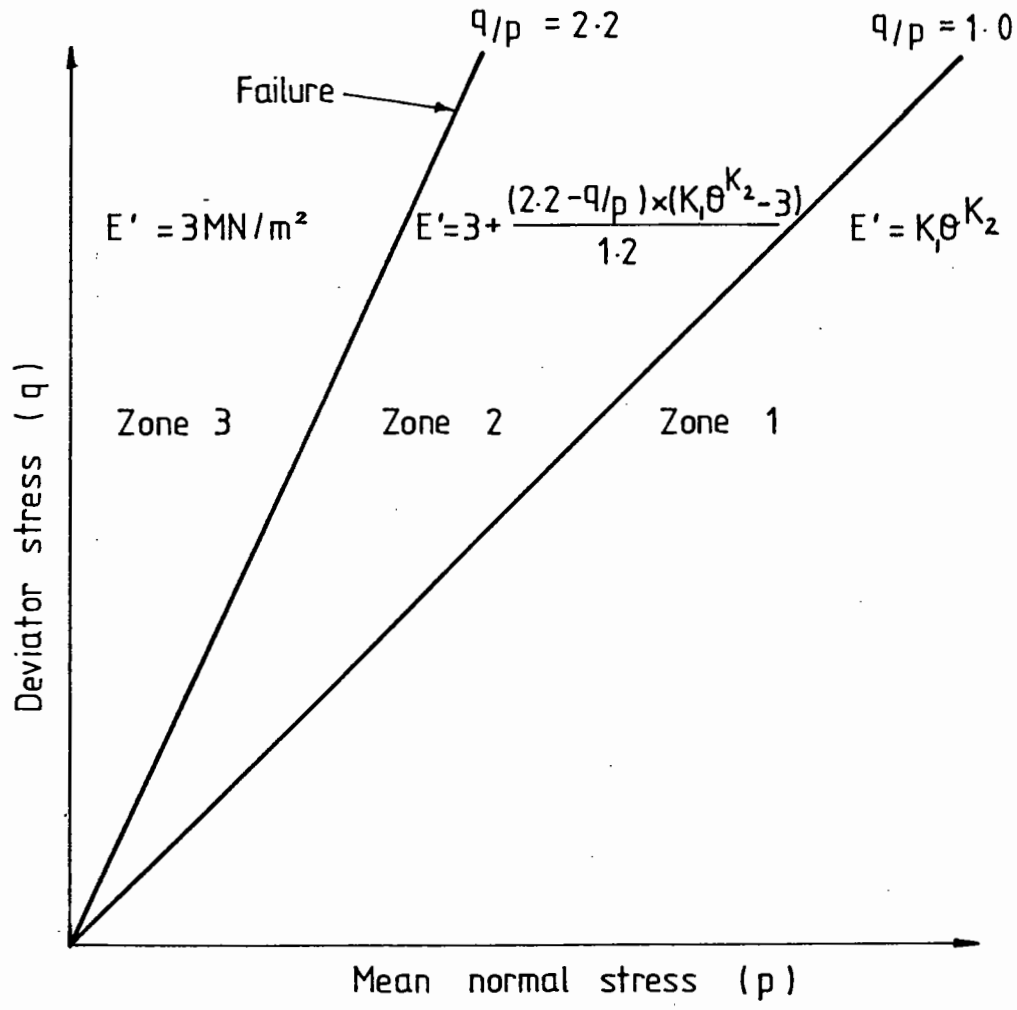

FIG 2·9 MODULUS DETERMINATION FOR UNBOUND GRANULAR MATERIAL (AFTER STOCK (57))

If the calculated modulus differs significantly from the initial estimate then the procedure is repeated with an adjusted modulus value (mid-way between the two) until compatibility is obtained. There were, however, problems in achieving this compatibility for pavements with thin bituminous layers. Further details of the computer program ADEM are given elsewhere (57,60).

2.3 THE COMPUTER PROGRAM SENOL

2.3.1 General Description

The non-linear finite element computer program SENOL, (SEcant NOn-Linear) was developed by Pappin (44) specifically to deal with pavements containing significant thicknesses of materials having non-linear stress-strain relationships. The non-linear models implemented within the program were derived from extensive testing of granular materials (17,61). Because of the complexities and running costs involved, this type of program is, unfortunately, impractical for routine design procedures. However, SENOL does provide a valuable research tool for the investigation of special cases.

The structure is considered as an axisymmetric system and divided both vertically and horizontally into a large number of rectangular elements (see Fig.2.10). Each element can be ascribed different values of modulus. A flow diagram of SENOL is shown in Fig.2.11. A detailed description of the program is given elsewhere (62). The basic computational procedure begins by applying overburden (body) forces and then adds the wheel load in ten gradually increasing steps (see Fig.2.12). At each step the element stresses are calculated and new values of modulus derived from the behaviour model for the material. Once all the load is added the computation is iterated until satisfactory convergence is obtained.

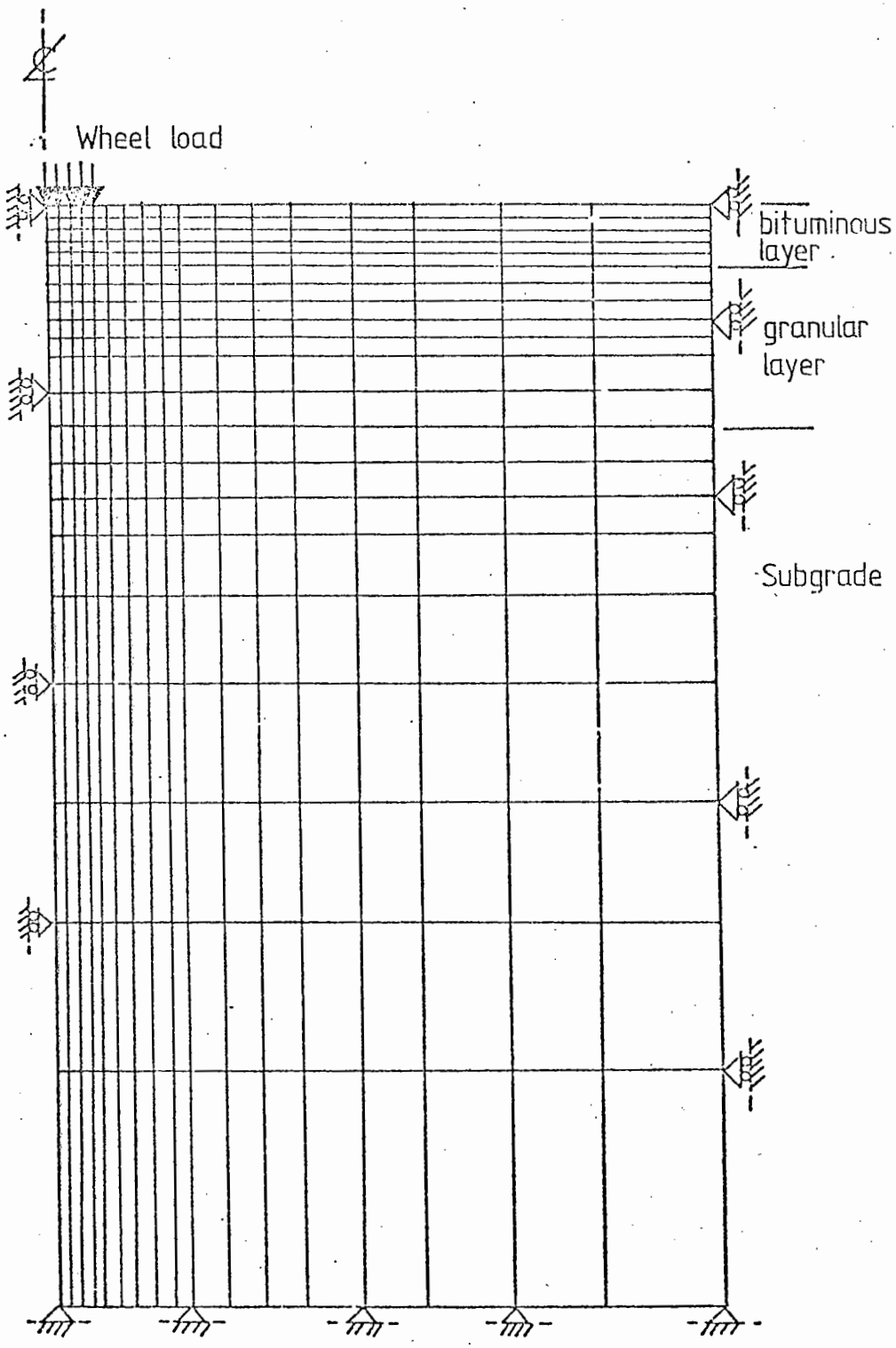

FIG 2·10 TYPICAL ARRANGEMENT OF ELEMENTS FOR ANALYSIS

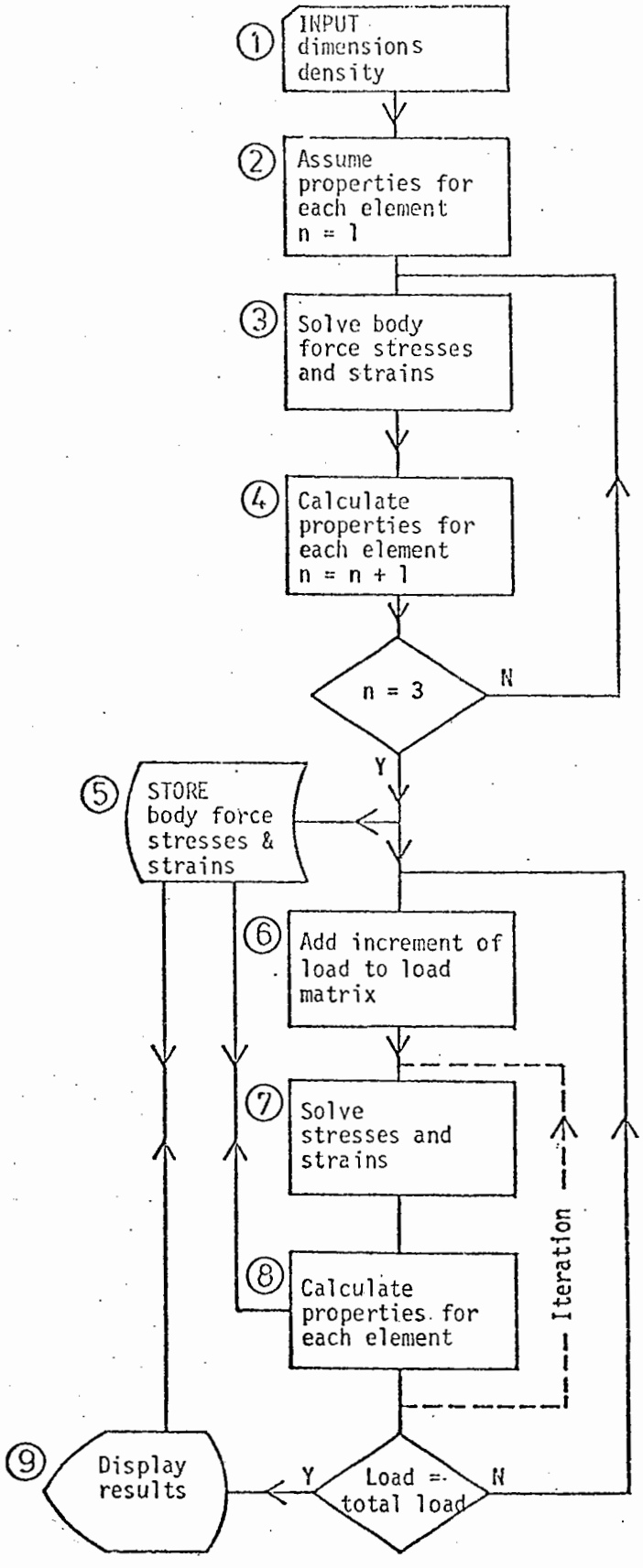

FIG 2·11 FLOW DIAGRAM FOR SENOL

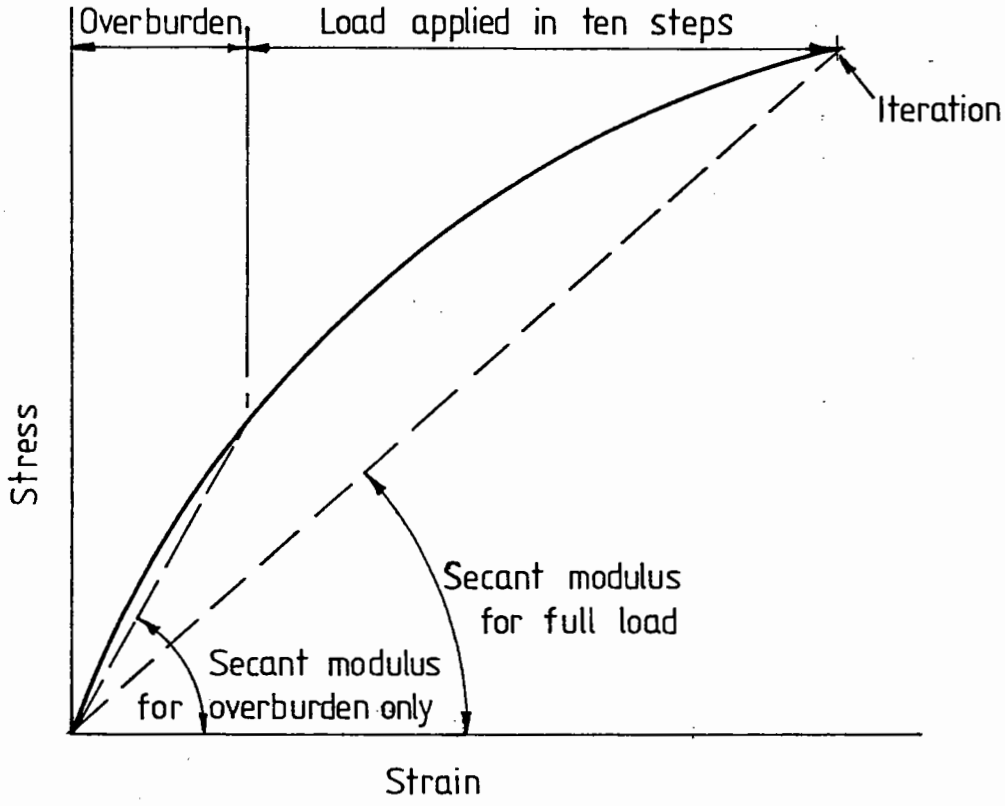

FIG 2·12 BASIS OF SENOL COMPUTATION USING SECANT MODULUS

2.3.2 Determination of Typical Granular Sub-base Moduli

In order to determine realistic moduli for granular sub-bases which could be used in both the simplified design method and the computer program ADEM, a number of designs were carried out by Pappin and Brown using the computer program SENOL. These designs covered a wide range of 3-layered structures as shown in Table 2.1. The top bituminous layer and the subgrade were both considered to be linear elastic, having a Poisson's ratio of 0.4. However, the granular layer was treated as non-linear using a detailed model developed in earlier work by Pappin and Brown (17). The model was in the form of stress dependent, secant bulk and shear moduli (K,G) and was based on repeated load triaxial compression and extension tests using continuously graded limestone covering a wide range of stress paths. From the SENOL computations, average values were derived for the sub-base to subgrade modular ratio and the sub-base modulus. These are given in Table 2.1 and 2.2. A second study was carried out for six of the structures using a weak granular sub-base material in which the secant bulk modulus (K_2) and the secant shear modulus (G_2) were assumed to be those derived by Pappin and Brown (17) divided by 1.2 and 3 respectively, (i.e., $K_2 = K/1.2$, $G_2 = G/3$). The results of this study are given in Tables 2.3 and 2.4.

A further study was also carried out by Shaw (18) to compare the critical strains and modular ratios resulting from using two different non-linear models in SENOL with those calculated using BISTRO (38).

2.4 DISCUSSION

In order to improve the existing analytical pavement design procedures in use at the University of Nottingham, the design criteria against fatigue cracking and permanent deformation have been reviewed and further developed (see Chapters 4 and 5). For the design against

Table 2.1 AVERAGE MODULAR RATIO BETWEEN GRANULAR LAYER AND SUBGRADE

E_1 = 4 GPa										
h_1 (mm)		50			100			200		
h_2 (mm)		200	450	700	200	450	700	200	450	700
E_3 (MPa)	20								4.0	6.0
	30						5.0	2.5	3.5	4.0
	50					2.5	3.0	1.5	2.0	2.5
	70					2.0		1.5	1.5	

E_1 = 7 GPa										
h_1 (mm)		50			100			200		
h_2 (mm)		200	450	700	200	450	700	200	450	700
E_3 (MPa)	20					5.5	5.5	3.5	5.0	5.0
	30			6.0		3.5	3.5	2.5	3.0	4.0
	50		2.0	3.5	2.0	2.0	2.5	1.5	2.0	
	70	2.5	2.5		1.5	1.5		1.5		

E_1 = 12 GPa										
h_1 (mm)		50			100			200		
h_2 (mm)		200	450	700	200	450	700	200	450	700
E_3 (MPa)	20				3.5	4.5	7.5	3.0		
	30		5.5	6.0	2.5	3.5				
	50		3.5	4.0	2.0	2.0				
	70		2.5		1.5					

Table 2.2 AVERAGE MODULI FOR GRANULAR SUB-BASE LAYER

E_1 = 4 GPa										
h_1 (mm)		50			100			200		
h_2 (mm)		200	450	700	200	450	700	200	450	700
E_3 (MPa)	20								80	120
	30						150	75	105	120
	50					125	150	75	100	125
	70					140		105	105	

E_1 = 7 GPa										
h_1 (mm)		50			100			200		
h_2 (mm)		200	450	700	200	450	700	200	450	700
E_3 (MPa)	20					110	110	70	100	100
	30			180		105	105	75	90	120
	50		100	175	100	100	125	75	100	
	70	175	175		105	105		105		

E_1 = 12 GPa										
h_1 (mm)		50			100			200		
h_2 (mm)		200	450	700	200	450	700	200	450	700
E_3 (MPa)	20				70	90	150	60		
	30		165	180	75	105				
	50		175	200	100	100				
	70		175		105					

Table 2.3 AVERAGE MODULAR RATIO BETWEEN WEAK GRANULAR LAYER AND SUBGRADE

E_1 = 4 GPa										
h_1 (mm)		50			100			200		
h_2 (mm)		200	450	700	200	450	700	200	450	700
E_3 (MPa)	20									
	30									1.3
	50							0.8		
	70									

E_1 = 7 GPa										
h_1 (mm)		50			100			200		
h_2 (mm)		200	450	700	200	450	700	200	450	700
E_3 (MPa)	20						2.0			
	30									
	50									
	70				0.7					

E_1 = 12 GPa										
h_1 (mm)		50			100			200		
h_2 (mm)		200	450	700	200	450	700	200	450	700
E_3 (MPa)	20					1.8				
	30									
	50									
	70				0.5					

Table 2.4 AVERAGE MODULI FOR WEAK GRANULAR SUB-BASE LAYER.

E_1 = 4 GPa										
h_1 (mm)		50			100			200		
h_2 (mm)		200	450	700	200	450	700	200	450	700
E_3 (MPa)	20									
	30									40
	50							40		
	70									

E_1 = 7 GPa										
h_1 (mm)		50			100			200		
h_2 (mm)		200	450	700	200	450	700	200	450	700
E_3 (MPa)	20						40			
	30									
	50									
	70				50					

E_1 = 12 GPa										
h_1 (mm)		50			100			200		
h_2 (mm)		200	450	700	200	450	700	200	450	700
E_3 (MPa)	20					35				
	30									
	50									
	70				35					

fatigue cracking, the preliminary work carried out by Stock (57) on the consideration of cumulative damage effects due to both temperature and loading considerations has been extended.

Unfortunately, analytically based procedures have not yet reached the stage where the rut depth can be accurately predicted and a cumulative damage approach applied to permanent deformation. Stock (57) presents a comprehensive literature review on the different approaches used to limit permanent deformation in a pavement. He also attempted to develop an improved deformation criterion using regression equations obtained from a detailed study of the Alconbury Hill trial (62), which predicted the rate of rutting as a function of certain parameters in the pavement. However, these equations did not give reasonable predictions for other structures and Stock used the simple permanent deformation design criterion (see equation (2.11)) in ADEM.

CHAPTER THREE

DEVELOPMENT OF SIMPLIFIED DESIGN PROGRAMS

During the first six months of this research project, a suite of simplified design programs for pavements were written in BASIC for use on a Commodore PET 8k microcomputer. These programs closely follow the simplified design procedures described by Brown (50), (see Chapter 2).

In the Simplified Design Method, developed by Brown (50), three calculation procedures are described in detail:

(a) The Simplified Design Method, which determines layer thickness for given input parameters.
(b) The Balanced Design Method, which allows mix proportions to be calculated for a given asphalt layer thickness.
(c) Pavement Assessment, which is referred to herein as the 'Design Life Method'. This provides for the computation of pavement life.

Each of these procedures has been programmed for the PET computer and details are provided below. All the work with this computer makes use of the analysis charts in Brown (50) prepared by using the BISTRO (38) program. A typical chart is shown in Fig.2.4 of Chapter 2. There are, therefore, certain limitations, the most notable of which are that all asphaltic materials are considered as one layer and that the granular layer is of a fixed thickness. The range of asphalt thickness is from 100 to 500mm and that of asphalt stiffness from 3 to 19 GPa. In addition, subgrade moduli must be between 20 and 70 MPa, corresponding roughly to a CBR range of 2 to 7%.

Despite these limitations, the resulting PET programs proved to be very useful for preliminary designs, studying mix variables and

educational purposes. They also acted as a 'testbed' for new developments.

3.1 SIMPLIFIED DESIGN METHOD

Fig.3.1 is a flow chart for this program (SDM) which follows the procedures of Chapter 5 in Brown (50). Table 3.1 gives a list of the input data required. There are two options in the program, one for an approximate design and the other for a detailed design. For the approximate design there is a choice between a typical hot rolled asphalt or dense bitumen macadam base whose mechanical properties are derived from the mix proportions near the centre of the current British Standard specifications (4,5). For the detailed design, more information is required, though some of the binder properties may be estimated within the program, assuming they are typical binders.

The following equations are used to estimate the initial and recovered softening points (SP_i and SP_r) in the program from the corresponding penetration (P_i or P_r):

$$SP_i = 97.63 - 26.35 \log P_i \qquad (3.1)$$

$$SP_r = 99.13 - 26.35 \log P_r \qquad (3.2)$$

These equations take into account that the softening point used for the recovered properties refers to the value from the ASTM test which gives results about 1.5°C higher than those from the BS test. In Brown (50) a single equation is used for both the softening points. This equation is shown below and is approximately equal to the average of the above two. It is used for simplification.

$$SP = 98.4 - 26.4 \log P \qquad (3.3)$$

Table 3.1 INPUT DATA REQUIRED FOR PROGRAMS ON THE PET MICROCOMPUTER

INPUT	S D M		BDM	DLM	UNITS
Average annual pavement temperature	✓		✓	✓	^{0}C
Thickness of asphalt layer	X		✓	✓	mm
Average speed of commercial vehicles	✓		✓	✓	km/hr
Cumulative number of standard axles or,				X	msa
Initial no. of comm. vehs. per day and				0	
Percentage of grwoth rate and	✓		✓	0	
Design life				X	years
Subgrade modulus or CBR or Plasticity Index	✓		✓	✓	MPa,%,%
	Approx. design	Detailed design			
Material type, HRA or DBM	✓	X	X	X	
Initial penetration	X	✓	✓	✓	
Recovered penetration	X	0	0	0	
Initial softening point	X	0	0	0	
Recovered softening point	X	0	0	0	
Recovered penetration index	X	0	0	0	
Binder content	X	✓	X	✓	%
Void content	X	✓	X	✓	%
Specific gravity of aggregate	X	✓	✓	✓	
Specific gravity of binder	X	✓	✓	✓	

Where data required ✓
optional 0
not required X

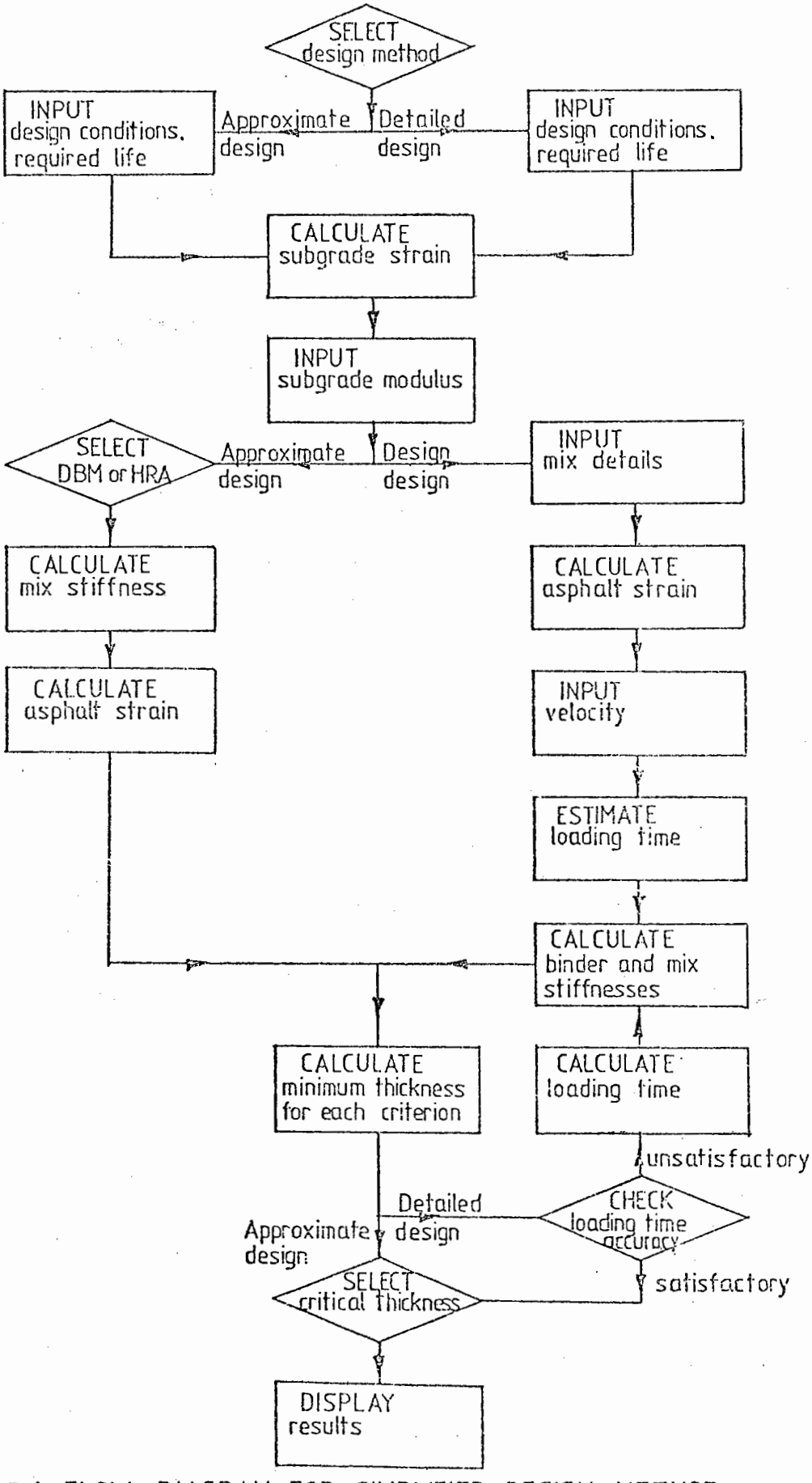

FIG3.1 FLOW DIAGRAM FOR SIMPLIFIED DESIGN METHOD

ACMA (64) have recently proposed the use of the following amended relationship:

$$SP_r \text{ (ASTM)} = 94.75 - 24.28 \log P_r \qquad (3.4)$$

The final design thicknesses determined by the program would only differ slightly whichever of the above equations had been adopted.

The subgrade modulus can either be input directly into the program or it can be calculated within the program from one of the alternative inputs, the California Bearing Ratio (CBR) or the plasticity index (I_p), using the following equations given by Brown (50):

$$E = 10 \times CBR \qquad (3.5)$$

$$E = 70 - I_p \qquad (3.6)$$

where E is in MPa and both CBR and I_p are percentages.

The program next calculates the allowable subgrade strain ϵ_z, which is the same for both options. The maximum allowable value for this parameter depends on the number of standard axles (N) given by the relationship (50):

$$\epsilon_z = \frac{21600}{N^{0.28}} \quad \text{microstrain} \qquad (3.7)$$

The allowable asphalt strain, ϵ_t, for the approximate design, is calculated using the equations based on the selected mix alternative.

i.e. for a rolled asphalt: $\epsilon_t = 3567/N^{0.21}$ (3.8)

for a dense bitumen macadam: $\epsilon_t = 9193/N^{0.32}$ (3.9)

where N is the number of standard axles.

For the detailed design it is calculated from the general relationship based on mix proportions and binder softening point for the particular mix based on the work of Cooper and Pell (56), and Brown et al (34), viz;

$$\log \epsilon_t = \frac{14.39 \log V_B + 24.2 \log SP_i - 40.7 - \log N}{5.13 \log V_B + 8.63 \log SP_i - 15.8} \quad (3.10)$$

where V_B is the volume of binder (%).

The mix stiffness is calculated in two different ways. For the approximate method, quadratic equations have been fitted to the two relationships, shown in Brown (50), between stiffness for the typical mixes and temperature and vehicle speed. These equations take the form:

$$\log S_m = m_1 + m_2 T + m_3 T^2 \quad (3.11)$$

Where T is the pavement temperature (°C)

S_m is the mix stiffness (GPa)

and $m_n = a_n + b_n \log V + c_n (\log V)^2$ (3.12)

where V is the vehicle speed (km/hr)

and a_n, b_n, c_n are constants with suffix n = 1 to 3.

For the detailed design method, the binder stiffness is calculated using an initial estimate for loading time, viz:

$$t = \frac{1}{V} \text{ seconds} \quad (3.13)$$

The mix stiffness is based on this value of binder stiffness. The program then continues to run until a design thickness is obtained. If

the resulting thickness is greater than 350mm, then the actual value is used in the following equation to more accurately determine loading time (65):

$$\log t = 5 \times 10^{-4} h - 0.2 - 0.94 \log V \qquad (3.14)$$

where h is the asphalt layer thickness (mm).

The program then proceeds to recalculate binder stiffness, mix stiffness and design thickness until the resulting design thickness is within ±50mm of the estimate used in the loading time calculation.

When using the design charts (50), the allowable strains and mix stiffnesses are used to determine the asphalt thicknesses required to satisfy each of the strain criteria. This is done with the aid of one of the analysis charts, such as Fig.2.4. Each chart was transferred into a set of equations, for use on the computer, by a curve fitting procedure. These equations are in the form shown below but with different constant values for each of the four subgrade moduli of elasticity, 20, 30, 50 and 70 MPa:

$$h_z = g_1 + g_2 \log \epsilon_z + g_3(\log \epsilon_z)^2 \qquad (3.15)$$

$$h_t = h_1 + h_2 \log \epsilon_t + h_3(\log \epsilon_t)^2 \qquad (3.16)$$

where h_z and h_t are the layer thicknesses based on subgrade and asphalt strains respectively, and g_1 to g_3 and h_1 to h_3 are all constants in the form shown below but each have different values for constants p, q, r and s.

$$g_n = p + q \log S_m + r(\log S_m)^2 + s(\log S_m)^3 \qquad (3.17)$$

A linear interpolation is then made so that any value of subgrade

modulus between 20 and 70 MPa can be used.

The final output of design thickness is given for the critical case, either fatigue cracking or permanent deformation (asphalt or subgrade strain). Fig.3.2 shows the input and output data for a typical computation using the SDM Pet program.

3.2 BALANCED DESIGN METHOD

A flow chart for this program (BDM) is given in Fig.3.3 whilst Table 3.1 lists the input data required. The program closely follows the procedure in Chapter 6 of Brown (50).

In this program, the subgrade strain is calculated first and this allows the minimum mix stiffness to be determined using equations fitted to the analysis charts relating subgrade strain to stiffness and thickness. The mix stiffness is determined from the cubic equation:

$$A + B \log S_m + C(\log S_m)^2 + D(\log S_m)^3 - h = 0 \qquad (3.18)$$

where h is the asphalt thickness in mm, and A, B, C, D are all constants in the form:

$$A = K_1 + K_2 \log \epsilon_z + K_3 (\log \epsilon_z)^2 - R(K_4 + K_5 \log \epsilon_z + K_6 (\log \epsilon_z)^2) \qquad (3.19)$$

but each having different values for constants K_1 to K_6, which can be calculated from equations (3.15) to (3.17) used in the simple design method. R is a constant proportion based on the value for the subgrade modulus which allows interpolation between the values of 20, 30, 50 and 70 MPa.

```
UNIVERSITY OF NOTTINGHAM
DEPARTMENT OF CIVIL ENGINEERING

SIMPLIFIED DESIGN METHOD OF ANALYSIS FOR PAVEMENTS


INPUT
 NO OF DESIGNS= 1


INPUT
 TEMP= 14 'C
 N= 50
 E3= 40 MPA
 INIT PEN= 50
 MB= 5 %
 VV= 6 %
 GA= 2.65
 GB= 1.02
 VEL= 80 KPH



OUTPUT
 MIX STIFFNESS.....SM= 9771 MPA
 SUBGRADE STRAIN....EZ= 151  HE
 ASPHALT STRAIN.....ET= 78  HE
THICKNESS DUE TO SUBGRADE STRAIN= 273 MM
THICKNESS DUE TO ASPHALT STRAIN = 190 MM
 DESIGN THICKNESS.....= 280 MM

 RESULTING DESIGN:-
   ASPHALT LAYER      H1= 280 MM
                      E1= 9771 MPA
                     \)1=0.4
              <------> ET NOT CRITICAL
   GRANULAR SUB-BASE  H2=200
                      E2=2*E3
                   |  \)2=0.3
   ////////////////|////////////////
   SUBGRADE        |   E3= 40 MPA
                   |  \)3=0.4
                   V   EZ= 151  HE
```

FIG 3.2 TYPICAL OUTPUT FROM SDM PROGRAM ON THE PET MICROCOMPUTER

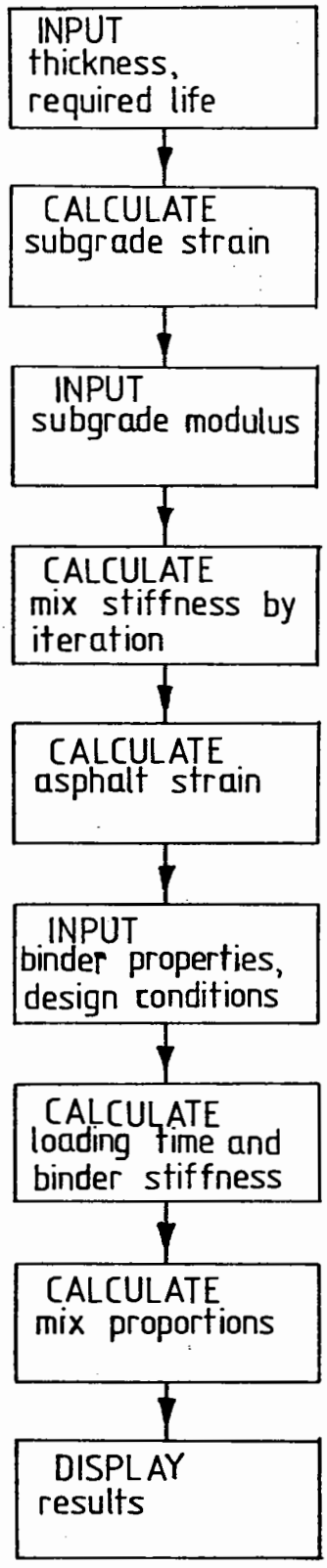

FIG 3·3 FLOW DIAGRAM FOR BALANCED DESIGN METHOD

There are three sets of values for the constants A, B, C, D; one for each of the ranges of subgrade modulus 20-30 MPa, 30-50 MPa and 50-70 MPa.

There would be one unique value, or root, for stiffness of the mix typically within the range 3 to 19 GPa covered by the analysis charts. A value of just less than 3 GPa is initially assigned to the mix stiffness. This is then increased in increments such that there would be 82 values for mix stiffness to reach a value just greater than 19 GPa, i.e. to cover the available range. For each increment, the value of the left hand-side of equation (3.18) is calculated and the one nearest to zero is taken as involving the best estimate for mix stiffness. If this value is within the range $3 \leqslant S_m \leqslant 19$ GPa, then the program continues, otherwise it is terminated since the mix stiffness will be outside the allowable range of the analysis charts.

The equations fitted to the analysis charts (Fig.2.4) giving critical asphalt strain as a function of stiffness and thickness for the simple design method, are arranged in this program to calculate asphalt strain. The equations are now similar to equation (3.14) but this time the thickness is known for a certain value of subgrade modulus. Therefore, an equation, as below, is derived for each of the subgrade modulus ranges, 20-30 MPa, 30-50 MPa and 50-70 MPa with different values for the constants:

$$h_t = L + M \log \epsilon_t + N (\log \epsilon_t)^2 \qquad (3.20)$$

where L, M and N are all constants in the form shown below, but each having different values for the constants p, q, r, s, p', q', r' and s'.

$$L = p + q \log S_m + r(\log S_m)^2 + s(\log S_m)^3 - R(p' + q' \log S_m + r'(\log S_m)^2 + s'(\log S_m)^3) \quad (3.21)$$

where R is a constant proportion based on the subgrade modulus.

The asphalt strain can, therefore, be calculated by solving the quadratic equation in the normal manner. The range for the asphalt strain is between 20 and 300 microstrain. The solution to the equation which lies within this range is the value required.

Once the binder properties and design conditions such as vehicle speed and temperature have been read in, the program calculates the mix properties required to provide a balanced design.

The results of a typical balanced design exercise are given in Fig.3.4

3.3 DESIGN LIFE METHOD

The aim of this program (DLM) is to calculate the life of a pavement either in terms of standard axles or years. In order to do this both the thickness and mix details of the asphalt layer are required, together with the design conditions. Table 3.1 lists all the input data required. Fig.3.5 gives a flow diagram for this program which closely follows the procedure of Chapter 7 in Brown (50).

The loading time, binder stiffness and mix stiffness can all be calculated in the usual way. In order to calculate the subgrade strain, equations (3.15) and (3.16) for thickness in the simple design method program are rearranged as a quadratic equation in a similar form to equation (3.20) used in the balanced design method program for calculating the asphalt strain. The equation is then solved in the same manner using the known range of subgrade strain, i.e. 100 to 1000 microstrain. This procedure is also followed for the asphalt strain, again using similar equations to those used in the balanced design program.

```
UNIVERSITY OF NOTTINGHAM
DEPARTMENT OF CIVIL ENGINEERING

DESIGN OF A BALANCED MIX FOR A GIVEN THICKNESS


INPUT
  NO OF DESIGNS= 1


INPUT
  THICKNESS= 250 MM
  N= 25 MSA
  E3= 30 MPA
  INIT PEN= 100
  TEMP= 14 'C
  VEL= 75 KPH
  GA= 2.7
  GB= 1.02



OUTPUT :-
  SUBGRADE STRAIN.......EZ= 183  HE
  ASPHALT STRAIN........ET= 52  HE
BALANCED MIX:-
  MIX STIFFNESS.........SM= 10644 MPA
  BINDER STIFFNESS......SB= 50 MPA
  VOLUME OF BINDER......VB= 9.48 %
  MASS OF BINDER........MB= 4.01 %
  SG OF BINDER..........GB= 1.02
  SG OF AGGREGATE.......GA= 2.7
  VOLUME OF VOIDS.......VV= 4.68 %
```

FIG 3.4 TYPICAL OUTPUT FROM BDM PROGRAM ON THE PET MICROCOMPUTER

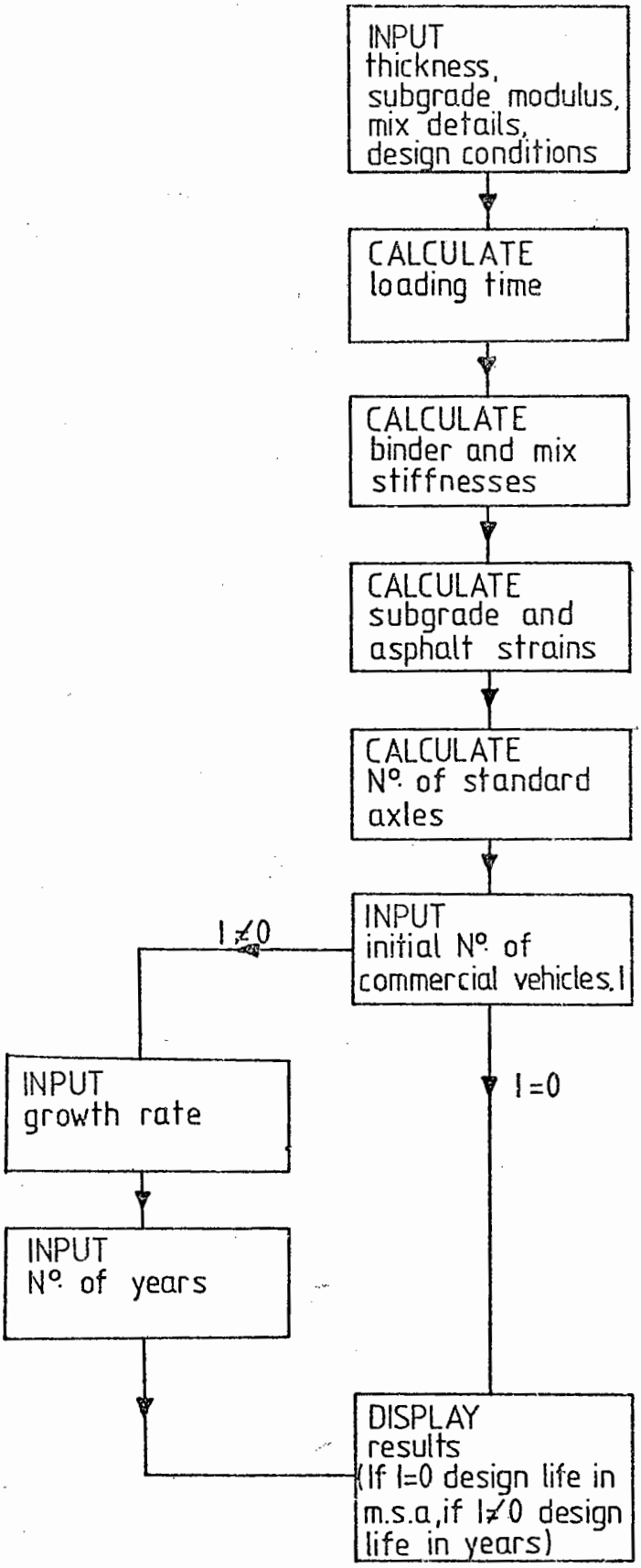

FIG 3·5 FLOW DIAGRAM FOR DESIGN LIFE METHOD

From the two values of strain, the cumulative number of standard axles in the design life can be calculated in each case. For the subgrade strain:

$$N = 3.02 \times 10^{15} / \epsilon_z^{3.57} \qquad (3.22)$$

where N is the number of standard axles.

For the asphalt strain, equation (3.10) is used.

If the initial traffic volume and average annual growth rate are known, then the program proceeds to calculate the design life in years. Alternatively, the result remains in terms of standard axles. Once again, the design life is based on the most critical criterion; either fatigue cracking or permanent deformation.

Typical output from an DLM computation is shown in Fig.3.6.

```
UNIVERSITY OF NOTTINGHAM
DEPARTMENT OF CIVIL ENGINEERING

TO CALCULATE THE DESIGN LIFE OF A GIVEN PAVEMENT


INPUT
  NO OF DESIGNS= 1


INPUT
  THICKNESS= 220 MM
  ES= 35 MPA
  INIT PEN= 50
  TEMP= 12.5 'C
  VB= 5.5 %
  VV= 5 %
  GA= 2.7
  GB= 1.02
  VEL= 60 KPH
  INITIAL NO OF COMM VEHS/DAY= 1000
  GROWTH RATE= 1 %


OUTPUT :-

  MIX STIFFNESS.............SM= 9472 MPA
  SUBGRADE STRAIN...........EZ= 231  HE
  N(MSA) FOR SUBGRADE STRAIN..= 10.8
  ASPHALT STRAIN............ET= 67  HE
  N(MSA) FOR ASPHALT STRAIN...= 175.8
  DESIGN N(MSA)..............= 10.8

  DESIGN LIFE= 13 YEARS
```

FIG 3.6 TYPICAL OUTPUT FROM DLM PROGRAM ON THE PET MICROCOMPUTER

CHAPTER FOUR

DETAILED STUDY OF DESIGN AGAINST FATIGUE CRACKING

4.1 ASSESSMENT OF PRESENT DESIGN PROCEDURE

4.1.1 Existing Design Criterion

The critical parameter used in pavement design against fatigue cracking is the maximum tensile strain in the asphalt, which occurs at the bottom of the base. The maximum allowable strain is calculated from:

$$\log \epsilon_t = \frac{14.39 \log V_B + 24.2 \log SP_i - 40.7 - \log N}{5.13 \log V_B + 8.63 \log SP_i - 15.8} \qquad (4.1)$$

where V_B = binder content by volume (%)

SP_i = initial binder softening point (°C)

N = number of load applications to failure

ϵ_t = tensile strain ($\mu\epsilon$).

This expression was derived from the work of Cooper and Pell (56) and Brown et al (34). The equation includes a factor of 100 on the material life (N) to allow for differences between the laboratory test conditions and those in the pavement. This factor is made up of 5 for rest periods between load applications and 20 for other factors, including time for cracks to propagate through the layer and lateral distribution of wheel loads. Hence, the life of an asphalt layer in situ is taken to be 100 times that in the laboratory. Various evidence was used to establish this factor of 100 and it is this which has been examined afresh and extended for this chapter.

4.1.2 Laboratory Testing at Nottingham

A comprehensive study was undertaken at Nottingham to establish the effect of various mix variables on the fatigue life and performance of bituminous materials. The details were reported by Cooper and Pell (56). The testing was carried out at various temperatures, though most work was at 10°C, in controlled stress rotating bending machines. Hence the fatigue lives which were established were for life to crack initiation, since, in this type of test, the crack propagates very rapidly. Using the general fatigue relationship developed in this work and extended by Brown et al (34), Fig.4.1 was produced showing fatigue lives for typical hot rolled asphalt and dense bitumen macadam road base mixes. The details of these typical mixes are given in Table 4.1. Fig.4.1 includes both laboratory and design lines, these differing by the factor of 100.

4.1.3 The Effect of Rest Periods

The effects of rest periods on fatigue life have been studied by several investigators, notably Raithby and Sterling (66,67), McElvaney and Pell (68), and Van Dijk (69). In each case, different loading conditions were used and these should be considered together with the resulting factors.

In the earlier work of Raithby and Sterling (66) at TRRL it was concluded that a factor of 5 could be used to account for rest period effects. However, their subsequent report (67) suggested a range of values from 5 to 25. These fatigue tests were carried out at three different frequencies (16.7, 25 and 2.5 Hz) and varying temperatures (10, 25 and 40°C). The rest periods were up to 1 sec. Once the rest period exceeded 0.5 s, then the life ratio (life with rest period : life without) was constant. Table 4.2 gives a summary of the conditions and life factors established from the experiments. For the

Table 4.1 PROPERTIES OF TYPICAL MIXES

Mix Type	Binder content (%)	Void content (%)	VMA	Binder properties				
				Initial		Recovered		
				P_i	SP_i	P_r	SP_r	PI_r
HRA	5.7	6.0	19.0	50	52.9	32.5	59.3	-0.1
DBM	3.5	10.0	17.9	100	44.9	65.0	51.4	-0.2

Specific gravity of aggregate = 2.7; specific gravity of bitumen = 1.02.

Table 4.2 REST PERIOD FACTORS FROM RAITHBY AND STERLING (67)

Temperature (^oC)	Stress (MN/m^2)	Factor $\frac{N_{\text{rest periods}}}{N_{\text{continuous}}}$
40	0.2	5
25	0.43	25
25	0.76	25
10	1.0	25
10	1.5	15

Table 4.3 DESIGN FACTORS RELATING DESIGN LIFE TO CALCULATED LIFE INCORPORATED IN THE SHELL METHOD

Variable corrected	Factor	Values governing range of factors
Laterial wheel distribution	2.5	
Healing and intermittent loading	1.25→1.0	lean/open mixture → rich/dense
Temperature gradient	0.5→1.0	thick/high temp. → thin/low temp.
Crack propagation	≈ 20	from Van Dijk (70)

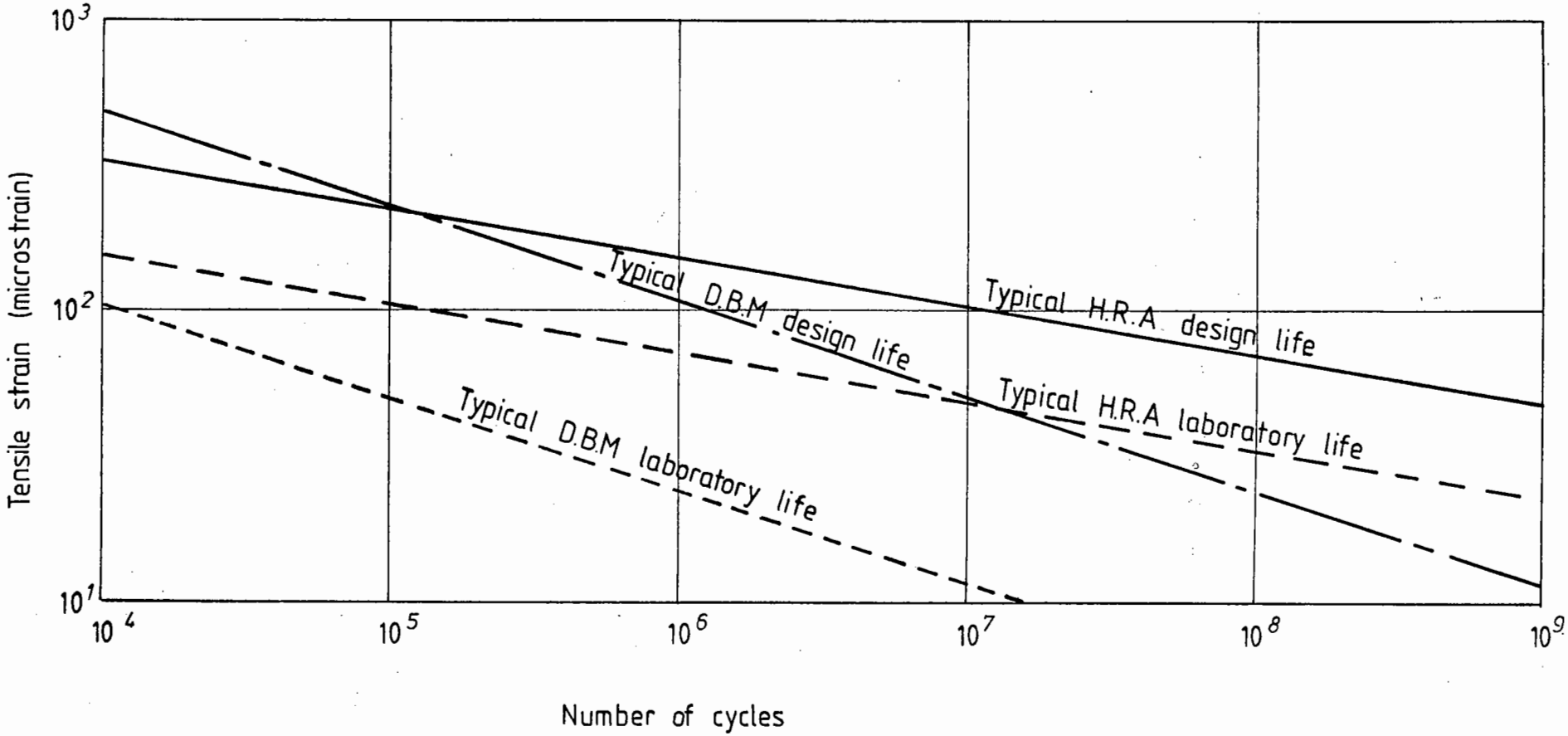

FIG 4·1 TYPICAL FATIGUE LIVES - NOTTINGHAM METHOD

stress range generally required and for average annual temperatures between 10 and 25°C, these results suggest a factor from 15 to 25, provided that the rest periods exceeded 0.5 s, which could generally be taken as the case. The shape of the wave form was also seen to affect the life by a factor ranging from 0.42 to 1.45, with sinusoidal loading being 1.0. The dynamic stiffness was noted to change during the test. It decreased quite sharply during continuous loading and more gradually with rest periods. It was also concluded that the strain recovery time was dependent on temperature and rate of loading. At high temperatures the material is softer and more viscous, so that deflections are larger and a longer time is required for delayed elastic recovery.

The fatigue tests carried out by McElvaney and Pell (68) were also of the constant stress type. They used a typical hot rolled asphalt basecourse. The majority of their tests were carried out at 10°C and a frequency of 16.7 Hz. However, the applied loading in these tests consisted of several successive blocks of loading cycles followed by a rest period. There was not a rest period after each load application. This is, therefore, not so compatible with the pavement situation involving a short rest between each axle load, as the TRRL work. The material is unable to recover some of its strain after each loading. Hence, as would be expected, the resulting factors between life with rest periods to life without rest periods are considerably lower (approximately 2) than those of Raithby and Sterling (67).

The loading conditions used by Van Dijk et al (69) were similar to those used at TRRL in that there were rest periods between each loading application. A controlled cyclic stress was applied at 50 Hz. The rest periods, however, were of 0.12 s maximum duration. The factors obtained from this work indicated an increase in life of 3.5 to 5 times that for continuous loading for a typical hot rolled asphalt at 10°C. If this is compared with the work of Raithby and Sterling (67), then it

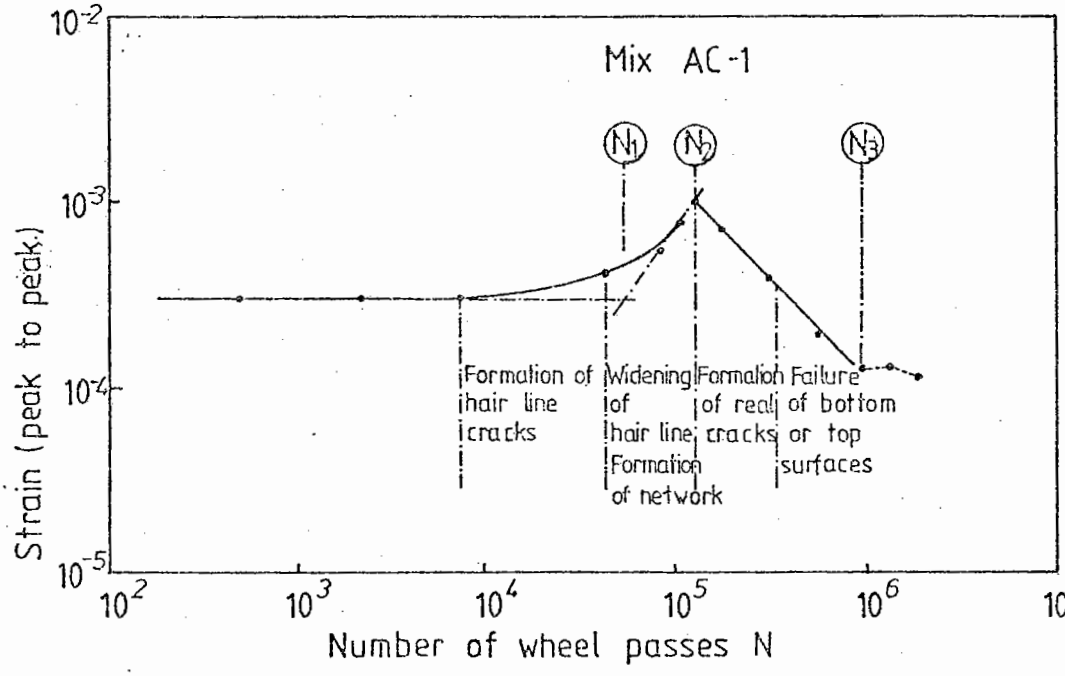

FIG 4·2 CRACK DEVELOPMENT AS A FUNCTION OF STRAIN READINGS AT EQUIVALENT NUMBER OF WHEEL PASSES (AFTER VAN DIJK (70))

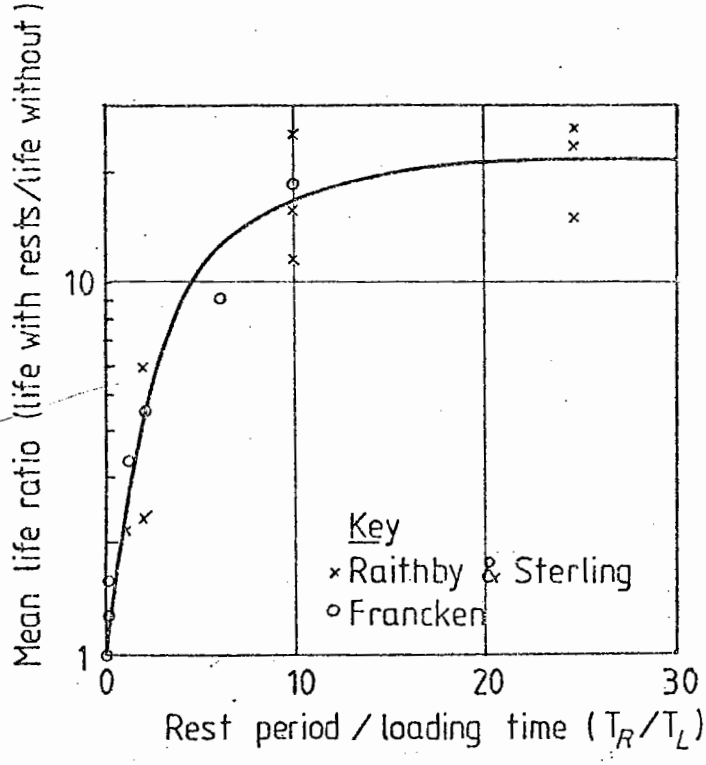

FIG 4·3 VARIATION OF MEAN LIFE RATIO IIN TERMS OF REST PERIOD DIVIDED BY LOADING TIME (AFTER VERSTRAETEN(78))

is seen to be in close agreement as it is in the range of their values for short duration rest periods, whilst the factor is still increasing with rest duration.

From the three references discussed above, it can be seen that the effects of rest periods vary considerably with duration, temperature and loading sequence. In a typical UK situation, the average asphalt temperature will be about 15°C and the duration should be greater than 0.5 s between each load. Although values from the three sources cannot be compared for this particular case, they are in agreement where comparisons can be made. The only experiments which cover this realistic situation appear to be those of Raithby and Sterling (67) where a value of 15 to 25 was obtained. This value is considerably higher than the factor 5 used at the present time. This factor was partially based on the earlier work of Raithby and Sterling (66) where a factor of 5 was suggested.

4.1.4 The Effect of Crack Propagation

Crack propagation is much more difficult to study as it generally requires the construction of a slab and wheel tracking apparatus. Van Dijk (70) carried out a detailed investigation on crack propagation using such equipment at the Shell laboratories in Amsterdam. Fig.4.2 is taken from his paper and shows crack development as a function of measured strain at the bottom of the slab. At equivalent numbers of wheel passes, three distinctive points were identified. The first (N_1) represents the initial formation of cracks where strains start to increase. It is at this point that constant stress flexural fatigue tests generally fail. The second point (N_2) shows when the strains start to decrease, and the third point (N_3) represents the total failure of the structure when no further change of strain occurs since movement is concentrated at the cracks. This corresponds to in situ

pavement failure. Three materials were investigated by Van Dijk in this work. They included a typical Dutch graded mix, a Californian medium grade and a British hot rolled asphalt. In each case the ratio of lives $N_2:N_1$ was approximately 3.5. The ratio $N_3:N_2$ varied between 4 and 6. Hence, the overall ratio of lives $N_3:N_1$ representing the life exepectation between crack initiation and complete failure is of the order 14 to 21. Life N_2 relates to the results of constant strain flexure tests, since it incorporates some crack propagation time. All these experiments were carried out at 20°C for a loading time of 0.1 s.

Further work carried out by Ramsamooj, Majidzadeh and Kauffman (71) indicated a similar factor (about 20) between fatigue lives of slabs and those of beams. Again, controlled stresses were applied as half sinusoidal waveforms with a period of 1 s and impulse duration of 0.2 s at 25°C. The resulting factor relating the final failure of slabs to those of the beams (i.e. crack initiation condition) was 20. This research was reviewed when the original factor of 100 was developed at Nottingham.

4.1.5 Other Design Methods

In order to establish revised design factors, or check those already used, the various factors incorporated in design methods developed elsewhere were studied. In many instances it is difficult to isolate the factors.

The Shell method reported by Claessen et al (72) used the computer program BISAR (73) to calculate stresses, strains and displacements. The permissible value for the horizontal tensile asphalt strain was developed from laboratory testing and allowed for the influence of transverse distribution of wheel loads, "healing" of cracks and intermittent loading. The mean annual or monthly air temperatures were related to an effective asphalt temperature which depended on the layer

thickness. A series of design charts was produced, which incorporated the several factors to relate design lives to calculated lives. These are summarised in Table 4.3.

The overall range of factors, relating pavement design life to the original calculated life based on laboratory data and excluding any effects of crack propagation which are incorporated in the design charts range from 3 to 25. Although there is no specific factor stated for crack propagation, there are references to the work of Van Dijk's wheel tracking tests. As noted above, this work showed a factor of about 20. It can be assumed that the Shell design charts include this factor for crack propagation. Combining their various factors gives overall values between 30 and 500 depending on the mix type.

Another design program, DAMA, developed by Witczak (74) as part of the Asphalt Institute's revision of the design manual MS-1 (75), uses CHEVRON (39) to calculate the stresses and strains in the pavement. It also uses a regression model for calculating the mix stiffness, rather than the Shell method used at Nottingham. The resulting stiffnesses, therefore, differ somewhat from those calculated at Nottingham. For the asphalt strain criterion the following equation is used:

$$N_f = f_o(10^M)\ (f_1 \epsilon_t^{-f_2} E^{-f_3}) \qquad (4.2)$$

where $$M = \left[f_4 \frac{V_B}{V_V + V_B} - f_5 \right] \qquad (4.3)$$

Equation (4.2) has three distinct components; laboratory to field performance factor, mix adjustment factor and laboratory fatigue equation. The f_o factor is the first of these and represents the shift required to relate crack initiation to a failure condition of cracking

in the road. The typical value used by the Asphalt Institute for its MS-1 study was $f_o = 18.4$. f_1, f_2 and f_3 should be found from a regression analysis of laboratory fatigue data. The mix adjustment factor M corrects for changes in void content and volumetric binder content. The Asphalt Institute took $f_o = 18.4$, $f_1 = 0.004325$, $f_2 = 3.291$, $f_3 = 0.834$, $f_4 = 4.84$, $f_5 = 0.69$. These figures were based on an asphalt concrete mix with $V_V = 5\%$ and $V_B = 11\%$. Those for the mix adjustment factor, M, were proposed by Santucci (76) and also used in the San Diego County base experiment (77).

The Belgium design method developed by Verstraeten et al (78) has a slightly different approach to design against fatigue cracking and factors are more difficult to isolate as various values are substituted at an early stage and then a cumulative damage method adopted. However, they have performed a large number of fatigue tests to establish the effect of rest periods (78). Fig.4.3, taken from their work, shows the comparison of results for the mean life ratio (life with rests/life without rests) versus rest duration/loading time, for experiments carried out by Francken (79) and those performed by Raithby and Sterling (67). The graph shows good correlation over certain ranges. These values for life ratios are used in the Belgian design for each type and frequency of loading and summations made for cumulative damage using Miner's rule (see Section 4.2). Therefore, provided conditions are similar in Belgium to the UK, the factors used for rest periods should be in close agreement with those adopted by using information from Raithby and Sterling (67). For a typical commercial vehicle speed of 60 km/hr and rest period of 0.1 s (between tandem axles), a factor of 7 is given. The rest period assumed appears to be low since it relates to the gap between tandem axles of 1 vehicle rather than between vehicles, or between front and rear axles of a vehicle (0.3 s). Although the Belgian method acknowledges the fact

that once the crack has been initiated on the pavement, the riding surface is still satisfactory for a period, they do not consider it practical to extend the life of their pavements into the crack propagation phase. Hence, their design criterion is crack initiation for their design charts.

They did, however, measure the amount of cracking on an experimental section of road against time and the result is given in Fig.4.4. The increase obtained from this graph is only of the order 3-4 rather than 20 as suggested by Van Dijk (70) and Majidzadeh (71). A further factor of 1 to 2.5 is also incorporated to take into account lateral distribution of traffic.

Another design method considered was that produced by Kasianchuk (80). For fatigue testing he carried out different tests depending on the pavement. For an asphalt thickness less than 50mm, controlled strain tests were used and failure was defined as the number of load repetitions to reduce the mix stiffness to 50% of its original value at 20°C. For thicknesses greater than 150mm, controlled stress tests were considered appropriate. Some comparisons were made between predicted life and actual life for an experiment at Morro Bay. The predicted values tended to underestimate the life by a factor of approximately 2.2. These predictions were based on the controlled strain tests as the pavement was thin. For a thicker pavement in the Ygnacio Valley Road test the design thickness for a life of 10 years was determined using controlled stress test data. In each case, cumulative damage was used to calculate the life for various types of loading and temperature.

The National Institute for Road Research, South Africa, have developed a fatigue prediction program, described by Freeme and Marais (24) which was originally based on the computer program reported by Kasianchuk (80), but with additional features. This program not only calculates the onset of crack initiation, but also the rate of decrease

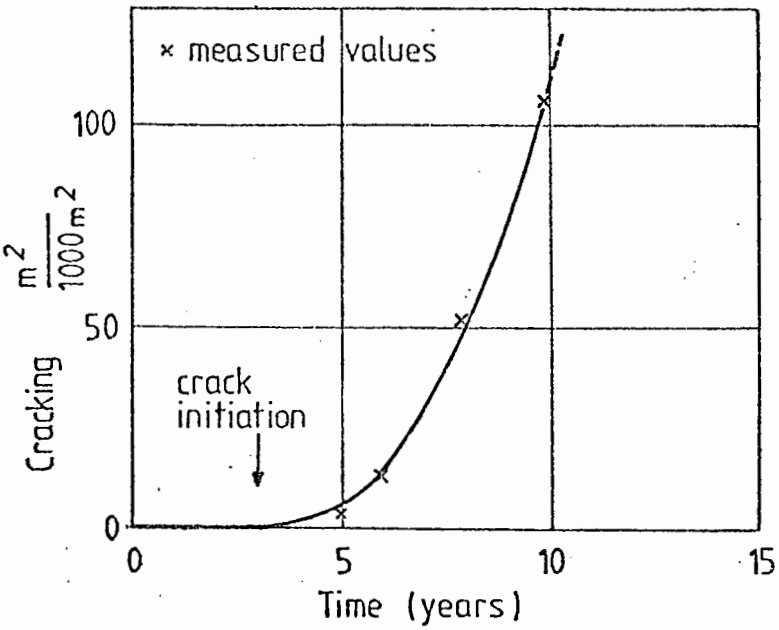

FIG 4.4 EVOLUTION OF CRACKING (AFTER VERSTRAETEN et al (78))

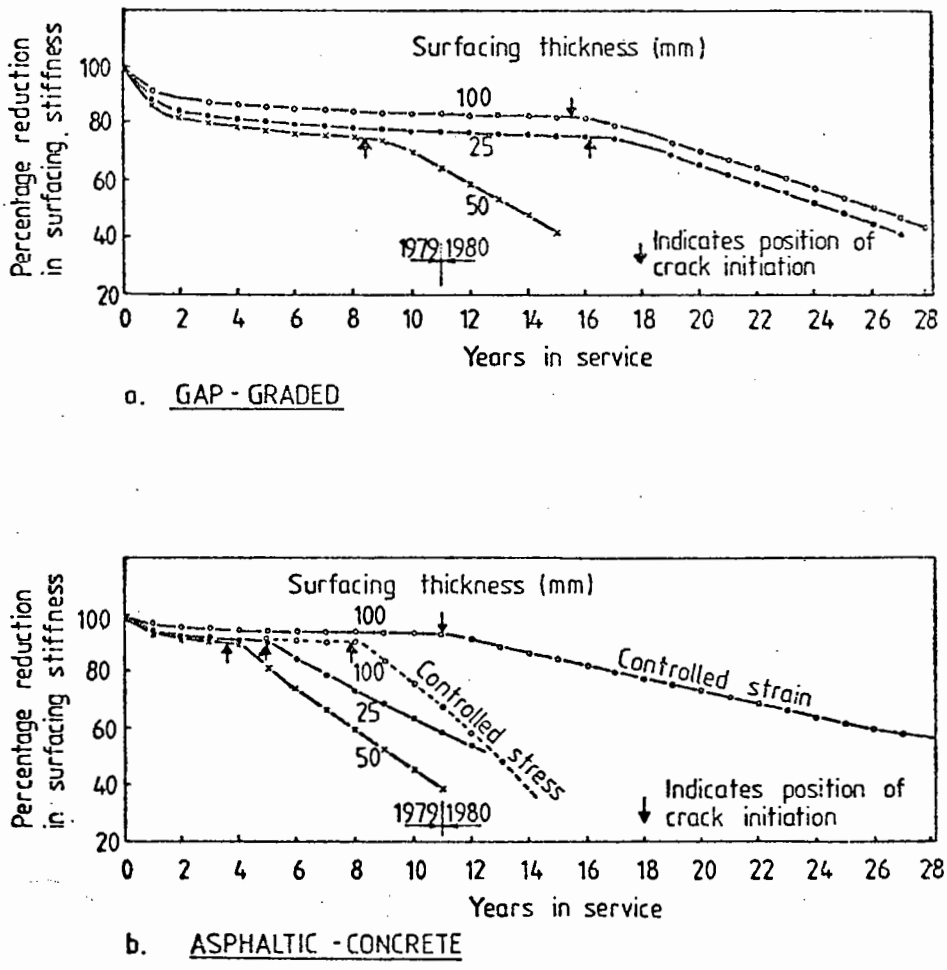

FIG 4.5 REDUCTION IN SURFACE STIFFNESS WITH NUMBER OF YEARS (24)

in stiffness. The results of either controlled stress or strain testing can be used. Fig.4.5 shows how the stiffness of a pavement decreases rapidly in the first year, then very slowly until crack initiation occurs. It is, therefore, suggested that the pavement stiffness could be monitored. Failure can be taken to occur when the stiffness is reduced by 50%. However, there do appear to be differences in lives depending on whether controlled stress or strain conditions are used (see Fig.4.5). Freeme and Marais (24) reported fairly large discrepancies between predictions using their method and that developed at Nottingham.

4.1.6 Comparison with Road Note 29

In order to assess the validity of design factors used at Nottingham, comparisons should be made with designs given by Road Note 29 (1). These design charts are based on the findings of full scale trials by TRRL. Similar comparisons have been made in earlier work (60), but the properties of the typical mixes have been adjusted slightly as a result of more recent experience. These properties are given in Table 4.1. In each case the design conditions which were used involved a mean speed of 80 km/hr for commercial vehicles and an average annual pavement temperature of 14°C. Six designs were selected from Road Note 29, see Table 4.4. The lives for each of these were then calculated using the simple design method on the PET computer, (see Chapter 3). This uses a design life to laboratory life ratio of 100.

Comparisons with Road Note 29 must be made against the background of the full scale trial conditions on which they were based. Recommendations for designs in excess of 11 msa are extrapolations of measured performance. Pavement failure was determined as a limiting rut depth and, hence, detailed checks of an analytical procedure for

Table 4.4 COMPARISON OF FATIGUE LIVES FOR TYPICAL MIXES

Mix	Subgrade CBR (%)	Road Note 29 design life (msa)	Road Note 29 thickness (mm)	Fatigue life (msa) (F=100)	Subgrade strain design life (msa)	Fatigue life (msa) (F=400)	Required factor (F)	Design Thickness (mm) (F=100)	Design Thickness (mm) (F=400)
Typical Dense Bitumen Macadam	5	0.5	145	0.3	0.8	1.2	170	165	113
	6	10.0	240	2.4	12.8	9.2	430	330	241
	7	70.0	350	13.1	136.4	52.4	530	490	372
Typical Hot Rolled Asphalt	5	0.5	135	7.2	1.0	-	-	-	-
	6	10.0	220	159.5	15.3	-	-	-	-
	7	70.0	300	1480	118.6	-	-	-	-

where $F = \frac{\text{design life}}{\text{laboratory life}}$

fatigue cracking can only be made with caution. However, it is important that for similar conditions, the design thicknesses resulting from each method should be of a similar magnitude.

The results in Table 4.4 show that when a factor of 100 is used, the DBM designs are fatigue critical, i.e. shorter lives are predicted by the fatigue criterion than by the subgrade strain (permanent deformation) criterion. The reverse is true for rolled asphalt because it has a similar stiffness, but better fatigue cracking resistance.

Predicted fatigue lives for the DBM are all low compared with Road Note 29. Therefore, further computations were performed to investigate a laboratory to field factor of 400 and also to determine the required factor to produce exact agreement with Road Note 29. The calculations were also performed the other way round, with layer thicknesses being determined for the three Road Note 29 lives using fatigue factors of 100 and 400. All the results are summarised in Table 4.4. Since fatigue is not critical for rolled asphalt, the calculations were only performed for the DBM.

Fig. 4.6 has been developed from Croney (63) in order to put these comparisons in perspective. It shows the performance of experimental sections with asphalt surfacings and dense bitumen macadam road bases in comparison with Road Note 29 recommendations. It clearly demonstrates how the recommendations were derived. For a subgrade CBR of 5%, the total bituminous thickness recommended in Road Note 29 is always greater than in the experimental sections. For the 4% CBR subgrade, the Road Note 29 thicknesses are less for the bituminous materials, but much greater for the sub-base. Hence, detailed comparisons between the analytical design and Road Note 29 are not always reliable, it being better to consider the actual pavement performance. However, details concerning fatigue cracking of actual pavements are in short supply in the UK.

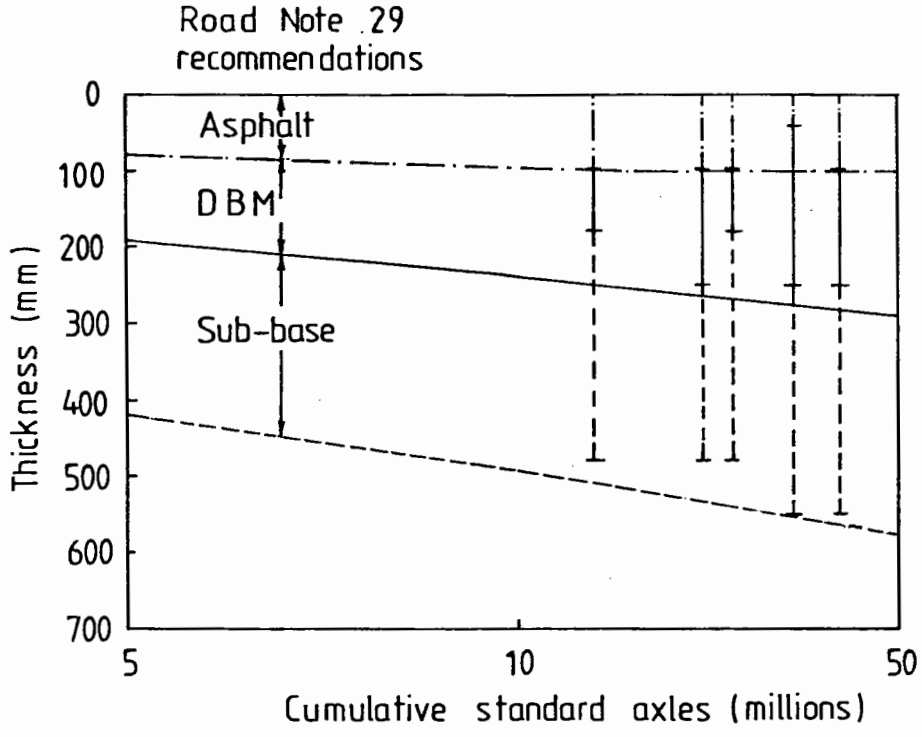

a. CBR = 5 %

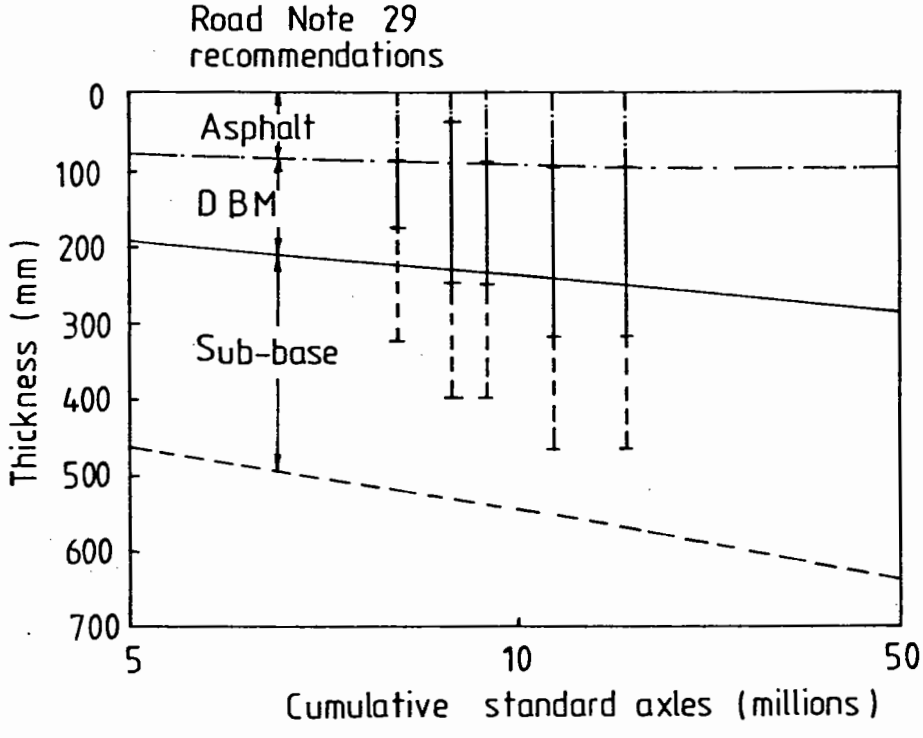

b. CBR = 4%

FIG 4·6 PERFORMANCE OF EXPERIMENTAL SECTIONS WITH ASPHALT SURFACING AND DBM ROADBASES (AFTER CRONEY (63))

Thrower (81) also compared results of analytical design computations with Road Note 29 recommendations and obtained very large discrepancies between the two. The ratio for life in terms of standard axles between the Road Note 29 design and those calculated being 760-4300. The factors said to account for these differences being rest periods, wheel tracking and crack propagation. These ratios, however, are particularly large. Thrower also questioned the use of the fourth power law for converting different wheel loads to standard axles. He suggested that the fourth power law applies consistently to thicker pavements, but for thinner pavements the power factor varies from about 1.8 to 4. For thin pavements and heavy loads the pavement thickness will be underestimated by up to 15mm but for a thin pavement and a light load spectrum the error will be +10mm. That is, for heavy loads on thin pavements, life is underestimated, while for light loads on thin pavements it is overestimated. The power law is discussed in more detail in Section 4.3. Thrower also considers the effect of temperature variations using a cumulative damage approach. This is discussed in Section 4.2.

4.1.7 Full Scale Road Tests

In making comparisons with Road Note 29, only British full scale trials have been considered. However, there are trial sections elsewhere which should also be considered.

Kingham (82) examined the results from the AASHO road test pavements and produced a series of relationships between different tensile strain and number of load repetitions for various asphalt stiffnesses. The stiffnesses were determined from two equations derived from deflection measurements and material properties. A typical fatigue life for a stiffness of about 1.7 GPa is given in Fig.4.7.

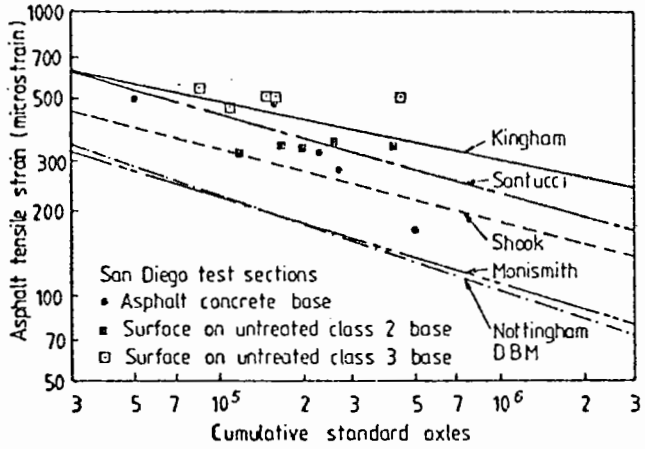

Fatigue lines

Monismith - pure laboratory data } Failure at crack initiation
Shook - " " "
Kingham - developed from AASHO road test data } Failure during crack propogation
Santucci - developed from laboratory data with a laboratory to field conversion factor ≃11
Nottingham- developed from laboratory data with a laboratory to field conversion factor of 100

FIG 4·7 COMPARISON OF FATIGUE LINES AND EXPERIMENTAL DATA (AFTER SHOOK (77))

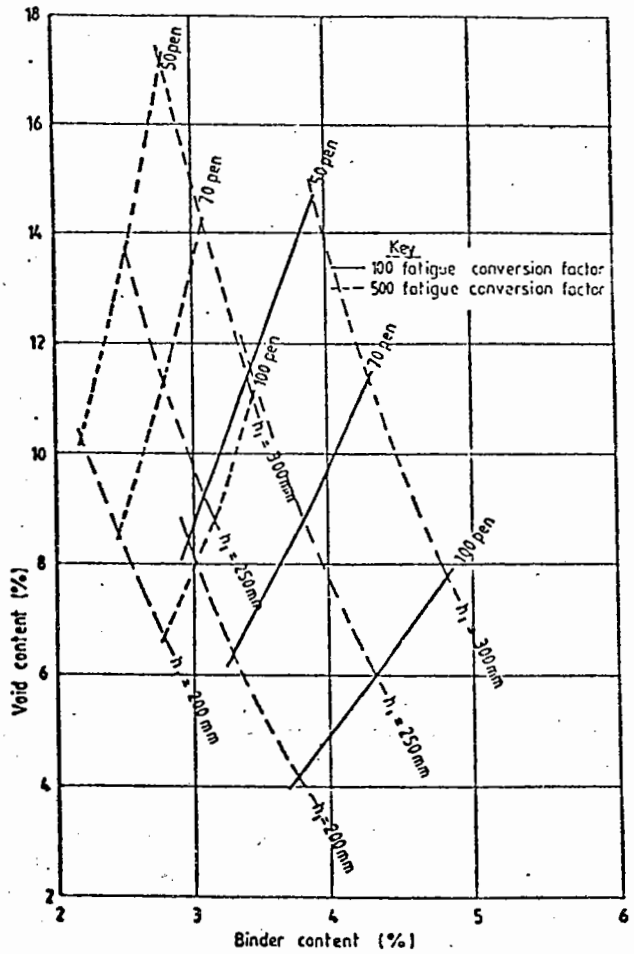

FIG 4·8 TO SHOW THE EFFECT OF VARYING THE FATIGUE LABORATORY TO FIELD CONVERSION FACTOR ON BALANCED DESIGNS

Another full scale experiment was investigated by Kallas and Shook (77) at San Diego. In this experiment, there were 35 different test sections. The sections were constructed of different bases and thicknesses with the intention of providing the same life. Comparisons were made between the stiffnesses of a laboratory prepared specimen before ageing, after one year and a cored specimen after one year. Assuming the site specimen stiffness to be 100%, then the stiffnesses were 72%, 90% and 100% respectively. This indicates the error that can arise in stiffness estimates alone, depending on preparation and time factors. In this study laboratory fatigue curves which have been shifted to the right to account for the differences between laboratory and field observations such as crack propagation and rest periods, pure laboratory curves and curves derived from field studies were compared (see Fig.4.7). The line in this figure proposed by Santucci (76) was taken from a set of fatigue curves based on laboratory stress controlled tests recommended by Monismith (83) but which have been shifted by a factor of about 11 to account for field conditions. These curves accounted for mix variables in the manner discussed in connection with the Asphalt Institute design method (75). The curves proposed by Shook, Santucci and Monismith were for the same stiffness (1.7 GPa) as that of Kingham and corresponded to a temperature of about 28°C. Although a typical British DBM would have a similar stiffness at 28°C, the fatigue line, shown in Fig.4.7, appears conservative when compared with the others except Monismith's pure laboratory data.

4.1.8 Balanced Design

A balanced design is one in which equal lives based on fatigue and permanent deformation are achieved by selection of mix proportions. A series of designs were carried out using the BDM PET program, see Chapter 3, to note the effect on the mix proportions of varying the

laboratory to field life conversion factor for fatigue. The input data which was used is given in Table 4.5 and the results are summarised in Fig.4.8. For the 100 conversion factor, the most practical mixes derived were for 100 pen bitumen. However, for a conversion factor of 500 no practical mix proportions were obtained with the 50, 70 or 100 pen binders. In practice, failure by deformation is preferable to cracking, since a deformed pavement can be overlaid whilst a cracked pavement must be reconstructed. This can be incorporated into the design by multiplying the required pavement life by a factor of, say, 1.2, for fatigue only. For the lines given in Fig.4.8 using the 500 fatigue conversion factor, this results in a small shift back towards those given for the 100 conversion factor, but practical mixes are still not obtained. For a particular binder, all the mix proportions to the lower right-hand side of the line *re*presenting balanced designs in Fig.4.8 will be deformation critical and all those to the left-hand side will be fatigue critical. The majority of the materials in this country lie in the deformation critical zone and this is confirmed in practice by the number of roads which deform compared with those which crack. However, some of the typical DBM bases with 3.5% of 100 pen binder, and void contents of 10 to 12% are close to the line and may fail by fatigue.

The lines given in Fig.4.8 are for a life of 10 msa and subgrade modulus of elasticity of 30 MPa. Further calculations were carried out for lives up to 100 msa and increased subgrade stiffnesses up to 70 MPa. These all resulted in diagrams similar to Fig.4.8.

This study shows that balanced designs will be impractical for increased fatigue conversion factors of the order of 400 to 500. In general, as permanent deformation is the critical criterion, more effort needs to be put into designing mixes with higher dynamic stiffness and resistance to rutting whilst still checking for fatigue cracking.

Table 4.5 INPUT DATA FOR BALANCED DESIGN EXERCISE

Parameter	Value
Asphalt thickness (mm)	200, 250 and 300
Life N (msa)	10
Subgrade modulus of elasticity (MPa)	30
Initial penetration of bitumen	50, 70 and 100
Pavement temperature (^{o}C)	15
Speed (km/hr)	80
Specific gravity of aggregate	2.7
Specific gravity of binder	1.02

4.1.9 Summary

Table 4.6 summarises the different factors applied to convert design lives (based on laboratory fatigue tests) to field lives.

It can be concluded that, for crack propagation, the factor of 20 used to date is approximately correct (70,71). The factor for rest periods, however, appears to be low, particularly when the more recent work of Raithby and Sterling (67) and Francken (79) are considered. For a rest period of 0.5 s, the value could be more realistically increased to 20. A further factor may then be thought necessary for lateral wheel distribution, but the evidence available suggests this is dependent on the road situation and the range of values is only of the order 1 to 2.5, from Belgian investigations and 2 to 5 from work by Shell. An overall factor of 440 would, therefore, seem more appropriate than the present 100 factor.

This consists of 20 for crack propagation, 20 for rest periods and 1.1 for lateral wheel distribution. An increase of this order is compatible with the Road Note 29 comparisons, and the American data in Fig.4.7.

4.2 CUMULATIVE FATIGUE DAMAGE EFFECTS DUE TO TEMPERATURE VARIATIONS

One of the simplifications in ADEM (57) and the simplified approach to design (50), was to assume that the seasonal temperature changes could be ignored and that an average annual air temperature, plus 3°C, could be used for the pavement temperature. The increase of 3°C is a combination of 2°C, which is added to the air temperature to take into consideration the fact that most traffic is on the road between 6 am and 10 pm when the temperature is higher, and a further 1°C which is added to allow for the difference between air temperature and pavement temperature. However, seasonal temperature variations do result in different degrees of damage throughout the year. The aim of

Table 4.6 SUMMARY OF LOAD FACTORS

Design method	Rest period	Lateral wheel distribution	Crack propagation	Overall factor	Reference for determination of factor
Nottingham present method	5		20	100	(66) (69) Rest period (70,71) Crack propagation
Shell method Claessen et al	1.25 → 10	2.5	20	65→1000	(67) Rest (70) Crack propagation
DAMA Witczak			18.4		
Belgium Verstraeten et al	7+	1 to 2.5	0	7→17.5	(67) (79) Francken
Laboratory testing	(1.5 → 2) (3.5 to 5) 0 15→25		16→21 20 ≃11		(68) McElvaney and Pell (69,70) Van Dijk (71) Majidzadeh et al (67) Raithby and Sterling (76) Santucci

this section is to take into account both daily and seasonal temperature changes together with traffic variation.

While detailed techniques have yet to be developed for dealing with cumulative damage due to permanent deformation, though the principles are established (84), there are procedures for considering fatigue cracking. Cumulative damage in fatigue has been studied in the laboratory by Deacon and Monismith (85) and by McElvaney and Pell (86). Futhermore, Miner's rule has been applied to design computations by a number of workers including Monismith (23) and Santucci (87). These ideas have been applied to the UK situation using the PET computer programs and drawing on earlier studies by Stock (57).

Miner's rule for evaluating cumulative damage (D) states that:

$$D = \sum_{i=i}^{j} \frac{n_i}{N_i} \qquad (4.4)$$

and failure occurs when $D \geq 1$

where n_i = number of applications at strain level i

N_i = number of applications to cause failure in simple loading at strain level i

D = total cumulative damage

j = number of strain levels.

Fig.4.9 illustrates the linear summation of cycle ratios used in Miner's rule.

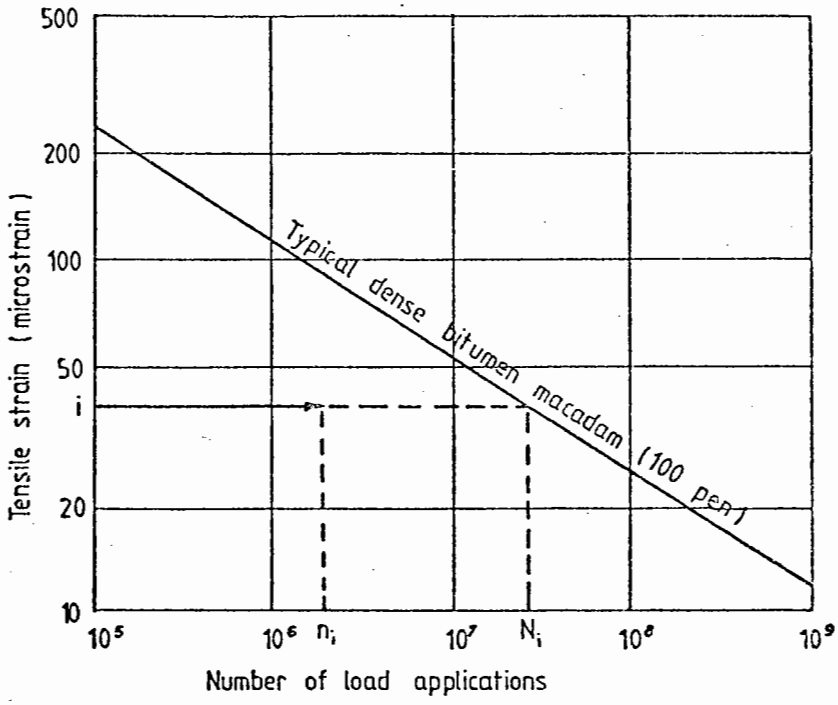

FIG 4.9 TENSILE STRAIN AS A FUNCTION OF NUMBER OF LOAD APPLICATIONS

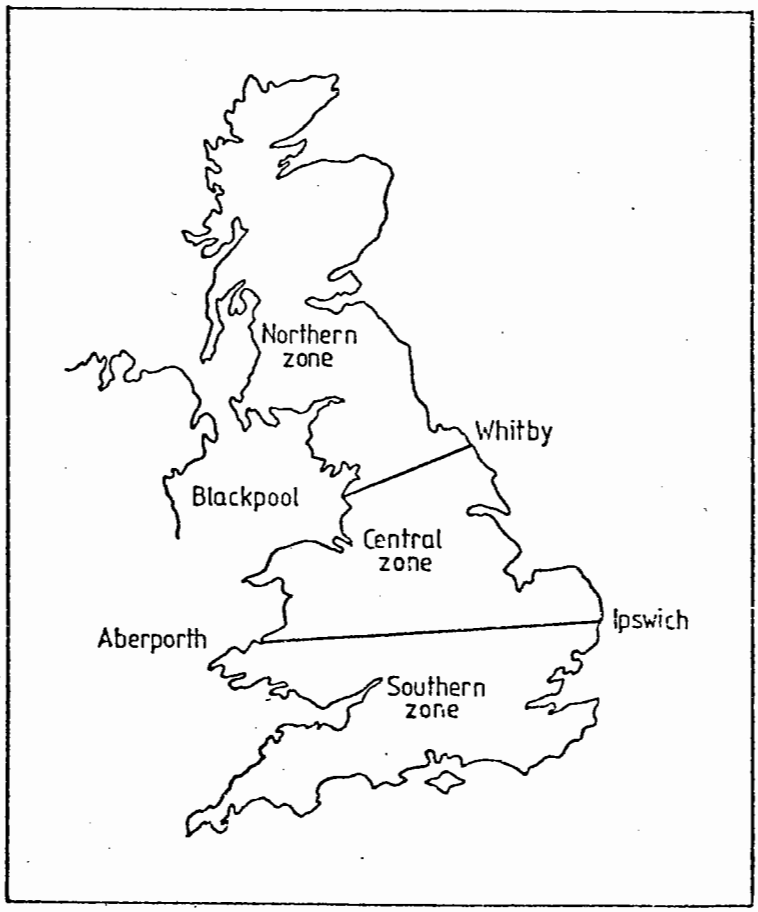

FIG 4.10 SUB DIVISION OF UNITED KINGDOM INTO TEMPERATURE ZONES (AFTER CRONEY (63))

4.2.1 Temperature Conversion Factor

A simple relationship is required to convert air temperatures into design temperatures. Stock (57) considered the effects of diurnal variations in both temperature and traffic loading for a typical pavement consisting of 101mm rolled asphalt, 254mm bitumen macadam, 152mm sub-base and subgrade for which data was available (63). Hourly and daily damage indices were calculated according to Miner's rule for April, July, October and January. Using the central temperature zone for the UK (see Fig.4.10) and associated monthly air temperatures from Croney (63), Stock then derived factors for these months to convert the average monthly air temperature to a pavement design temperature which when used would result in the same damage. Factors for the other months were determined by interpolation. Table 4.7(a) gives the conversion factors which varied between 1.17 and 1.71 with an average of 1.47.

Santucci (87) used a linear relationship based on an average of Witczak's (74) original correlations between air temperatures and pavement temperatures at various thicknesses. This did not include for hourly traffic variations. The equation for this line is approximately:

$$T_d = (1.1 \times T_a) + 3.45 \qquad (4.5)$$

where T_d is the pavement design temperature in °C

T_a is the average monthly air temperature in °C.

Figure 4.11(a) shows the line representing the above relationship together with a plot of pavement design temperature as a function of average monthly air temperature using the conversion factors from Table 4.7(a). The line representing the following equation is also included:

Table 4.7 TEMPERATURE CONVERSION FACTORS FOR EACH REGION

Month	Av. monthly air temp. Ta (°C)	Conversion Factor F	Ta×F	Design Temp. Td=Ta×1.47
Jan	3.3	1.52	5.0	4.9
Feb	3.7	1.58	5.8	5.4
Mar	5.7	1.60	9.1	8.4
Apr	8.5	1.71	14.5	12.5
May	11.3	1.62	18.3	16.6
Jun	14.4	1.53	22.0	21.2
Jul	16.0	1.47	23.5	23.5
Aug	15.6	1.45	22.6	22.9
Sep	14.0	1.37	19.2	20.6
Oct	10.2	1.17	11.95	15.0
Nov	6.6	1.35	8.9	9.7
Dec	4.5	1.46	6.6	6.6
Average	9.5	1.47	14	14

(a) Central Region

Month	Av. monthly air temp. Ta (°C)	Conversion Factor F	Ta×F	Design Temp. Td=Ta×1.47
Jan	4.2	1.52	6.4	6.2
Feb	4.7	1.54	7.2	6.9
Mar	6.2	1.60	9.9	9.1
Apr	8.7	1.71	14.9	12.8
May	11.4	1.62	18.5	16.8
Jun	14.5	1.52	22.0	21.3
Jul	16.0	1.47	23.5	23.5
Aug	15.9	1.46	23.2	23.4
Sep	14.3	1.32	18.9	21.0
Oct	12.5	1.17	14.6	18.4
Nov	7.5	1.38	10.4	11.0
Dec	5.2	1.48	7.7	7.6
Average	10.1	1.48	14.8	14.8

(b) Southern Region

/contd

Table 4.7 contd.

Month	Av. monthly air temp. Ta (^{o}C)	Conversion Factor F	Ta×F	Design Temp. Td=Ta×1.47
Jan	3.0	1.52	4.6	4.4
Feb	2.9	1.52	4.4	4.3
Mar	5.1	1.61	8.2	7.5
Apr	7.3	1.71	12.5	10.7
May	9.7	1.63	15.8	14.3
Jun	12.7	1.52	19.3	18.7
Jul	14.1	1.47	20.7	20.7
Aug	14.0	1.46	20.4	20.6
Sep	12.4	1.36	16.9	18.2
Oct	9.4	1.17	11.0	13.8
Nov	5.9	1.36	8.0	8.7
Dec	3.9	1.47	5.7	5.7
Average	8.4	1.48	12.3	12.3

(c) Northern Region

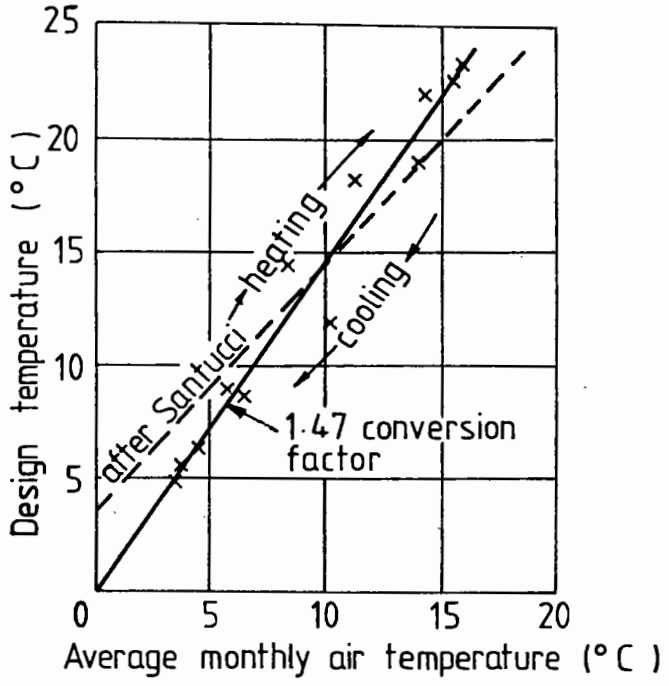

a. Central region

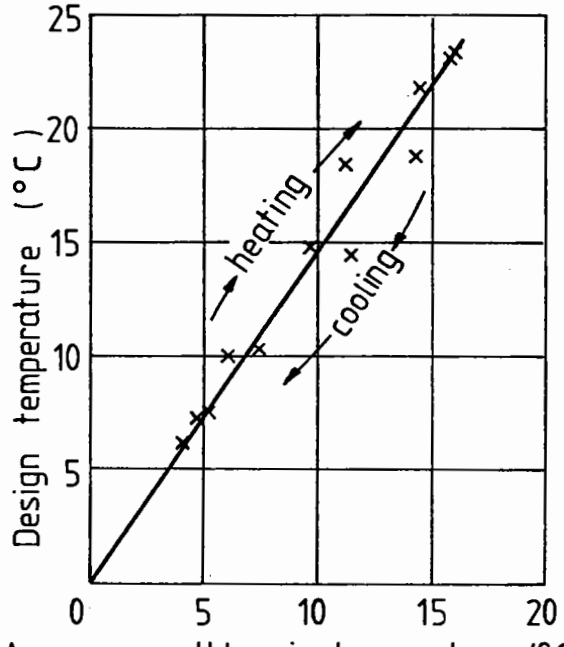

b. Southern region

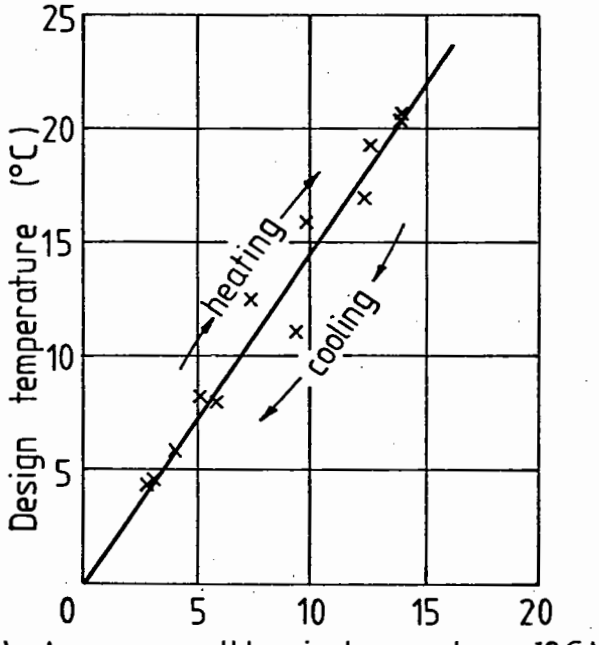

c. Northern region

FIG 4.11 DESIGN TEMPERATURE AS A FUNCTION OF AVERAGE MONTHLY AIR TEMPERATURE

$$T_d = 1.47 \times T_a \qquad (4.6)$$

From Fig.4.11(a), it can be seen that by applying a single conversion factor of 1.47 an acceptable relationship is obtained. The deviation about this line is quite small and evenly distributed. The line used by Santucci gives lower design temperatures at higher air temperatures and vice versa. It could, therefore, lead to unsatisfactory designs, as most damage is done at high temperatures. The conversion factor of 1.47 was therefore adopted.

4.2.2 Method of Analysis

The simple criterion used in assessing subgrade strain is semi-empirical, being based on back analysis of pavements with known performance at an average annual pavement temperature of 15°C. It is, therefore, inappropriate to calculate cumulative damage at various temperatures based on subgrade strain. This parameter was, therefore, calculated using the same method as described in Chapter 3. The average annual pavement design temperature for this calculation was, however, based on equation (4.6) applied on an annual basis, viz.

$$T_D = 1.47 \times T_A \qquad (4.7)$$

where T_A is the average annual air temperature.

For asphalt strain, the analysis uses Miner's rule to calculate cumulative damage. Using 12 average monthly design temperatures (T_{d1} to T_{d12}) each month has a particular strain level and hence life associated with it (N_{Td}), therefore,

$$D = \sum_{T_{d1}}^{T_{d12}} \frac{n_{Td}}{N_{Td}} \qquad (4.8)$$

The number of standard axles at each strain level (n_{Td}) is taken as one twelfth of the total number of standard axles to failure (N). Hence,

$$D = \frac{N}{12} \sum_{T_{d1}}^{T_{d12}} \frac{1}{N_{Td}} \qquad (4.9)$$

where D is damage factor

N is required total number of standard axles for design

T_{d1} to T_{d12} are twelve monthly design temperatures

N_{Td} is the number of standard axles to cause failure at temperature T_d

From two damage factors for two thicknesses of asphalt material, Santucci (87) used a linear interpolation to calculate the minimum design thickness of the asphalt material (due to the asphalt strain), relating to a damage factor of 1, by assuming a linear relationship for damage factor as a logarithmic function of thickness. In order to verify this relationship, an example was tested, with specific gravity of aggregate equal to 2.7, specific gravity of bitumen equal to 1.02 (see Fig.4.12). Damage factors were calculated at various thicknesses and a curve drawn through these values. From the results shown in Fig.4.12, it is evident that the relationship is not linear. A substantial error can arise in the final design thicknesses if a linear relationship is assumed to determine the thickness corresponding to a damage factor of 1 unless the inital thicknesses are selected carefully.

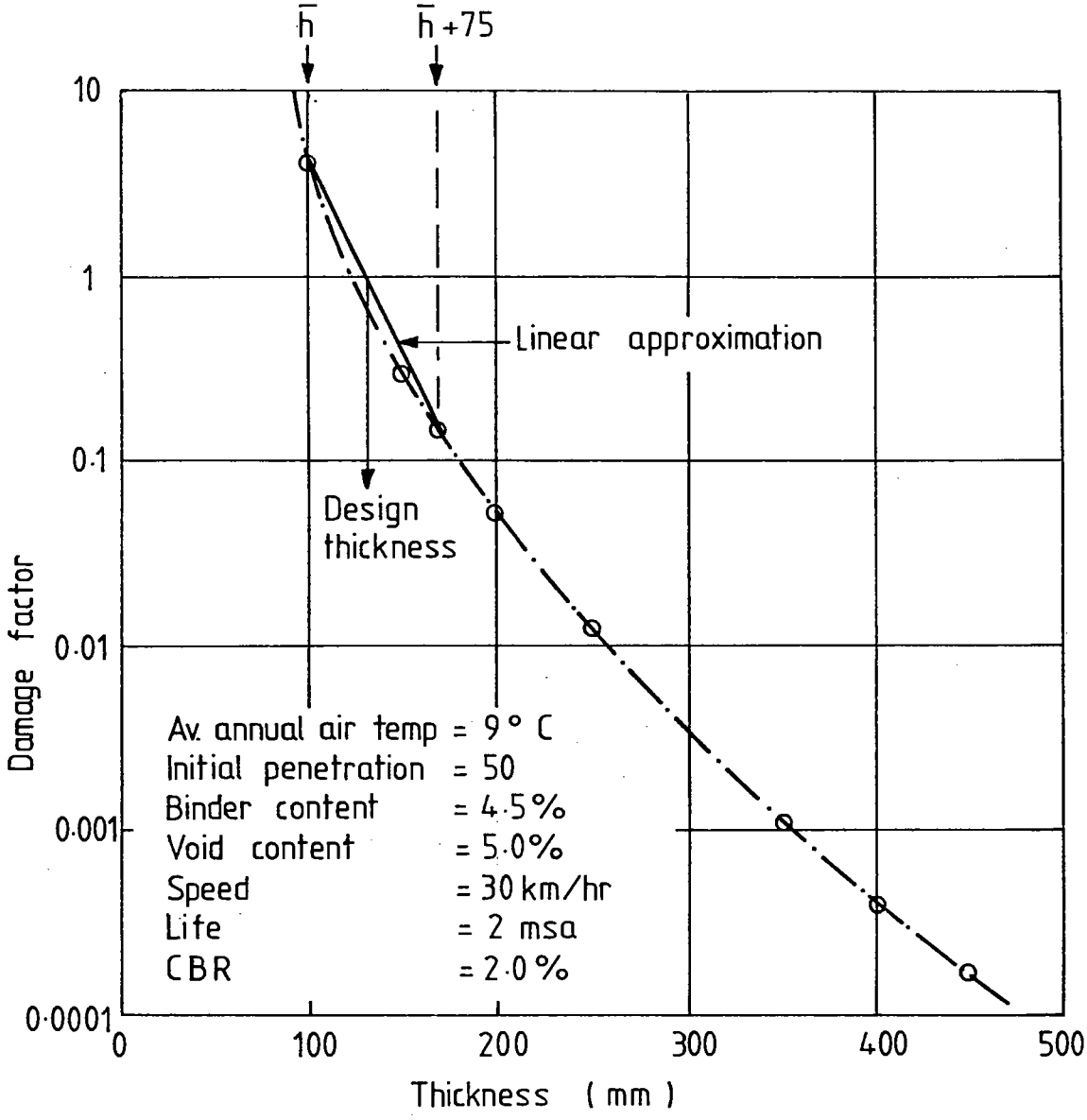

FIG 4·12 RELATIONSHIP BETWEEN DAMAGE FACTOR AND LAYER THICKNESS

Preliminary computations showed that the cumulative damage method produced designs up to 75mm thicker than the simple design method using an average annual pavement temperature equal to 1.47 times the average annual air temperature when asphalt fatigue was critical. Therefore, the two initial thicknesses used in the cumulative design method were taken as that calculated by the simple design method and the same plus 75mm (see Fig.4.12).

Once a method had been established for calculating thicknesses of asphaltic material due to cumulative damage, three examples were checked in order to verify the conversion factor of 1.47 (see Tables 4.8 and 4.9). In each case, the discrepancies between the thicknesses calculated using the 1.47 factor to those using the individual monthly factors in Table 4.7(a) for the central region were insignificant.

4.2.3 Alternative Temperature Regions

Having established a satisfactory single conversion factor of 1.47 for the central region, the other two temperature regions were considered. For the southern and northern regions, as defined in Fig.4.10, a similar set of data to that used for the central region was required. As this data was unavailable, further assumptions had to be made. Fig.4.13 expressing temperature conversion factor as a function of mean monthly air temperature from Stock (57) for the central region, was applied to the southern and northern regional air temperatures, given by Croney (63) (Table 4.7(b) and (c)), using Stock's proposal. This involves extrapolation parallel to the temperature axis for each of the months January, April, July and October, so that although the temperatures for these months change, the conversion factors remain the same (see Fig.4.13). The conversion factors are unlikely to change significantly, from one region to another, as they largely vary due to

Table 4.8 INPUT DATA FOR DESIGN CASES

Design Case	No. of std axles (msa)	Subgrade modulus (MPa)	Initial Pen	Binder content (%)	Void content (%)	Specific gravity of aggregate	Specific gravity of bitumen	Vehicle speed km/hr
1	2	20	50	4.5	5.0	2.7	1.02	30
2	3	60	100	4.5	5.0	2.7	1.02	55
3	15	25	50	5.0	7.0	2.7	1.02	30

Table 4.9 COMPARISON OF DESIGN THICKNESSES BASED ON FATIGUE CRACKING USING VARIOUS METHODS TO DEFINE TEMPERATURE CONDITIONS

Design Case (see Table 4.8)	Temperature region	Calculated asphalt thickness (mm)		
		Monthly temp. conversion factors for cumulative damage		Annual temp. conversion factor for simple design of 1.92
		As per Table 4.7	1.47	
1	Central	149	148	147
2		193	192	189
3		249	249	242
1	Southern	150	151	153
2		196	198	201
3		254	254	254
1	Northern	136	136	137
2		171	171	171
3		224	224	223

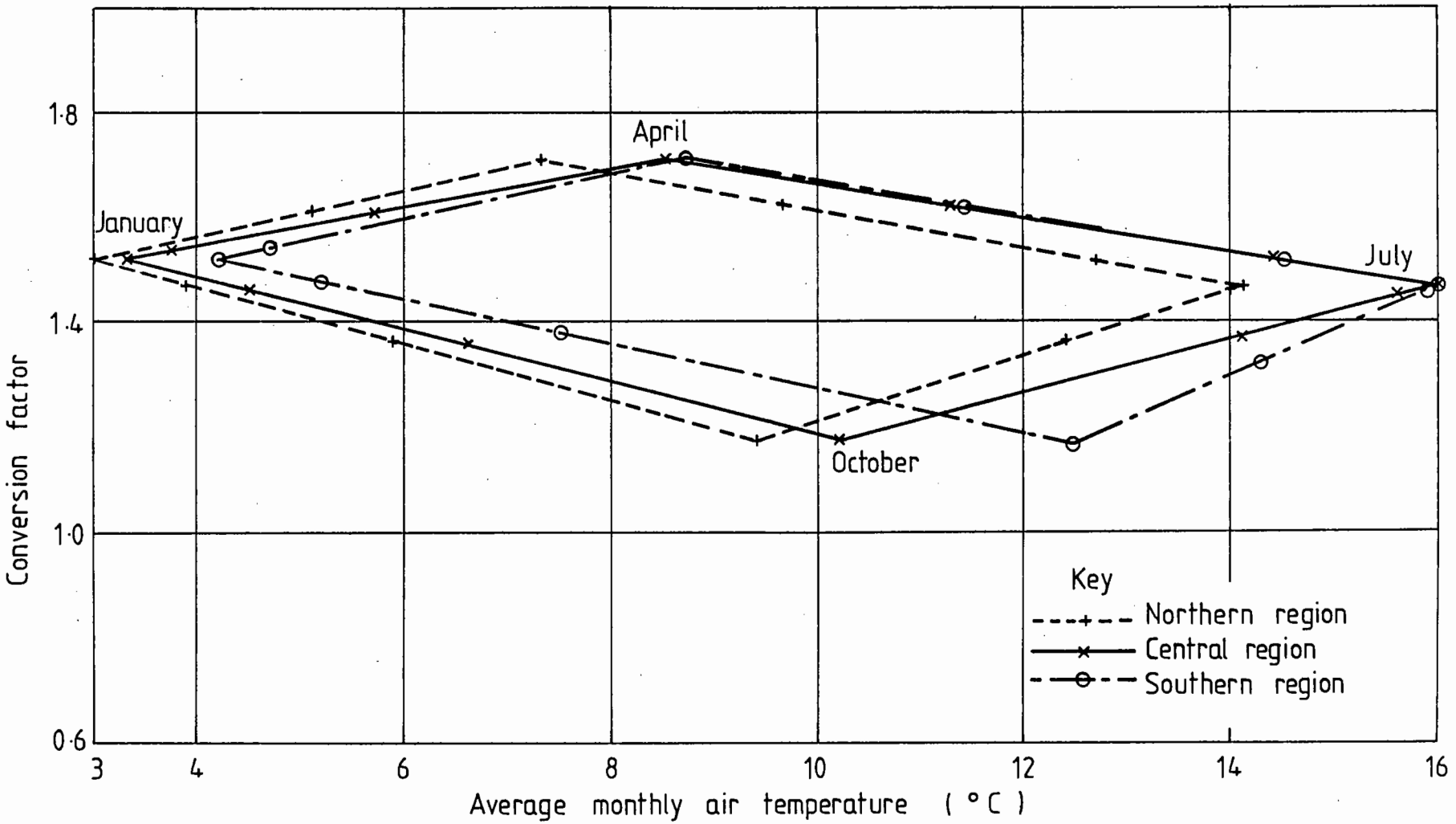

FIG 4·13 TEMPERATURE CONVERSION FACTOR AS A FUNCTION OF AVERAGE MONTHLY AIR TEMPERATURE

the rate of heating and cooling at a particular time of the year. The points for these four months were then joined together, in sequence, by straight lines so that the corresponding conversion factors for the intermediate months could be read off. These factors are given in Table 4.7(b) and (c). Stock used only four reference months, since these were the ones for which detailed data was available (63).

The monthly pavement design temperatures were calculated using the average monthly air temperatures and the corresponding conversion factors. Figs.4.11(b) and (c) were then plotted for these design temperatures as a function of the average monthly air temperatures. The line representing design temperature equal to 1.47 x average monthly air temperature was also drawn. Once again, the distribution about the line is small and shows a hysteresis effect as the pavement heats up from January to July and then cools down again to December.

Examples using both the individual monthly factors and the constant factor of 1.47 were checked for each region. The results in Table 4.9 show that the discrepancies in thickness are insignificant.

4.2.4 Equivalent Annual Design Temperatures

Considering the three typical regions, and using a typical set of input data (see Fig.4.12), equivalent temperatures for the year were calculated. These equivalent annual design temperatures are such that when used in the simple design method program, they give the same design asphalt thickness based on asphalt strain, as that calculated using the monthly temperatures and a cumulative damage method. Table 4.10 shows the results obtained for this example.

From Table 4.10, a mean factor of 1.92 emerges as the average value for all regions. This factor gives a good estimate when calculating the asphalt strain and thickness using the simple design method for any of the temperature regions (see Table 4.9).

Table 4.10 AVERAGE ANNUAL AIR TEMPERATURES AND EQUIVALENT ANNUAL PAVEMENT DESIGN TEMPERATURES

Region	T_A (°C)	T_E (°C)	$\frac{T_E}{T_A}$
Southern	10.1	19.1	1.89
Central	9.5	18.6	1.96
Northern	8.4	16.0	1.90

Table 4.11 TYPICAL MIX PROPERTIES FOR STRUCTURES USED IN CUMULATIVE ANALYSIS OF VARIOUS AXLE LOADINGS

Mix property	HRA wearing course	HRA basecourse	DBM base
Initial Penetration	50	50	100
Binder Content (%)	7.9	5.7	3.5
Void Content (%)	5.0	5.0	10.0
Volume of Binder (%)	17.6	13.0	7.9

Table 4.12 CALCULATED ASPHALT MIX STIFFNESSES USED IN CUMULATIVE ANALYSIS OF AXLE LOADINGS

Material	Asphalt stiffness (MPa)		
	Summer (22.5°C)	Winter (5.6°C)	Spring/Autumn (13.8°C)
HRA wearing course	2450	8560	5050
HRA basecourse	4060	12560	7830
DBM, thin structure, 5 msa	2310	9550	5350
DBM, thick structure, 50 msa	2390	9830	5490

The use of this factor means that the method is still an approximation compared with consideration of the twelve monthly temperatures. However, one advantage is that it only requires an average annual air temperature . Another advantage is that, for some of the higher or lower monthly temperatures, the appropriate mix stiffness (S_m) could be outside the allowable range of the PET programs, $3 \leqslant S_m \leqslant 19$ GPa. In such cases, the approximate method, based on the average annual air temperature, is more likely to calculate a mix stiffness within the allowable range.

The data in Table 4.9 for three typical cases in each of the three temperature regions shows that the resulting thicknesses are in close agreement.

The implications of these results for use of the three simple design programs are that the pavement temperature used in each of them depends on which design criterion is critical. For asphalt strains, air temperature should be multiplied by 1.92, while for subgrade strains the factor is only 1.47. These differences detract from the simplicity of the method, since, in effect, the computations need to be done twice. This could be programmed so that the user simply inputs the air temperature.

4.2.5 Microcomputer Program for Cumulative Damage Analysis

A program was developed for use on the Commodore PET microcomputer based on the method of analysis described in Section 4.2. The program is called CDM from Cumulative Damage Method. It has been written to include all the following options:

1. Typical regional data, southern, central and northern.
2. Specific input data.
3. Approximate design method using an equivalent annual pavement design temperature to calculate the asphalt strain.

4. Cumulative design method using average monthly air temperatures.

The flow chart in Fig.4.14 illustrates how each of the above alternatives is incorporated in the program. The same assumptions and ranges of parameters apply to this program as for the other three simple design programs (see Chapter 3).

Since the cumulative design method is more complex, a 16 or 32K storage microcomputer is required (the other three programs only require 8K storage).

4.3 CUMULATIVE FATIGUE DAMAGE EFFECTS DUE TO LOADING VARIATIONS

In Section 4.2 cumulative damage concepts have only been applied to temperature variations. However, other factors also influence the magnitude of tensile strain, and amongst these, wheel load and arrangement are of most importance. Both ADEM and the simplified PET programs consider a standard 40 kN dual wheel loading as shown in Fig.4.15a with the contact pressure, p, being taken as 500 kPa. However, the actual loading of a pavement is by means of a number of commercial vehicles with various axle arrangements and axle loads. The following exercise has been carried out to investigate the cumulative effects of these.

A number of practical simplifications were required. Two typical pavements were selected from Road Note 29 (1) for lives of 5 and 50 msa. These are detailed in Fig.4.16. Three pavement temperatures were selected to represent an average for the summer, winter and spring/autumn seasons, these were 22.5, 5.6 and 13.8°C respectively, based on a central region temperature distribution (63). The summer and winter temperatures are each an average for three months' duration and the autumn/spring temperature is an average for six months' duration.

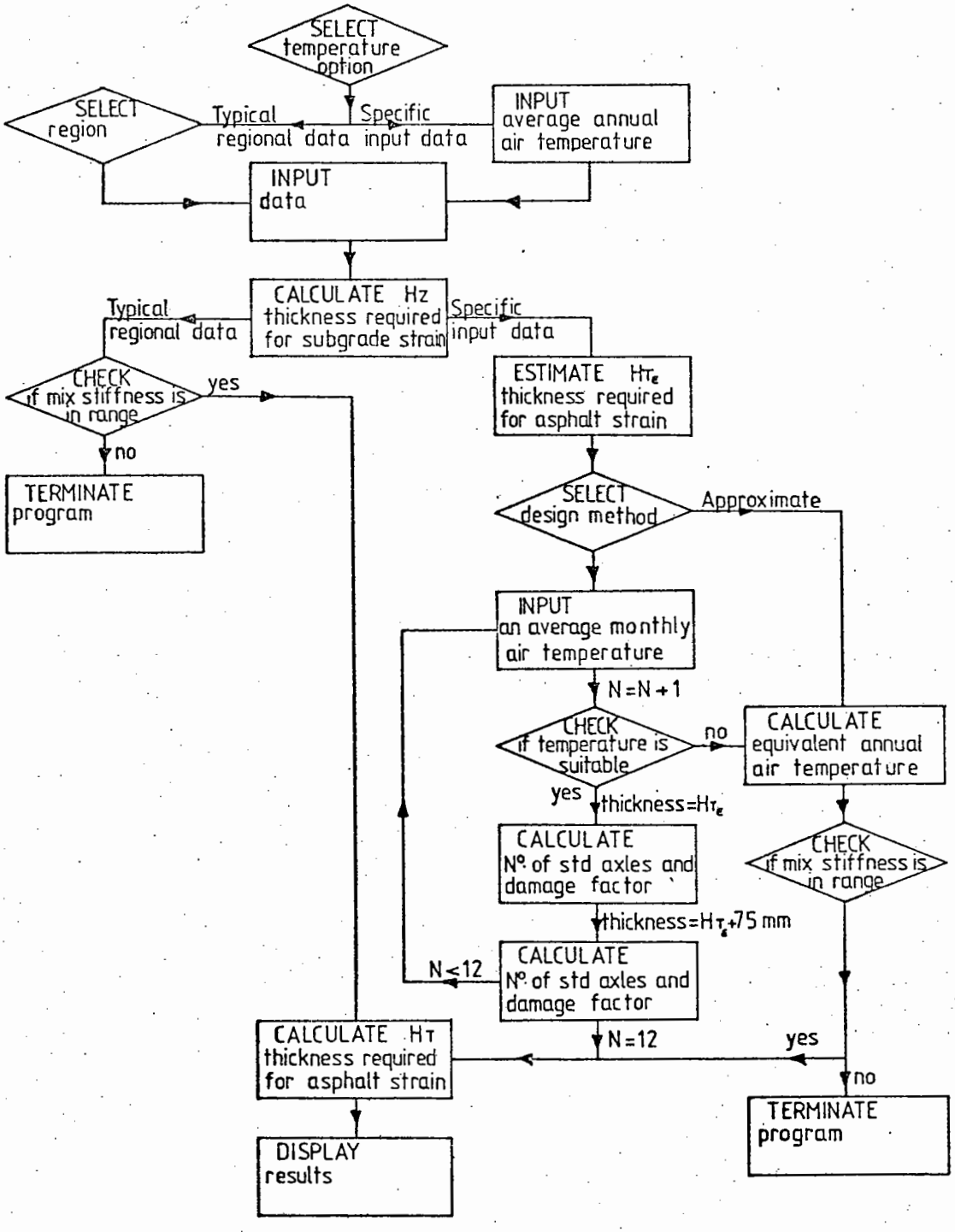

FIG 4.14 FLOW DIAGRAM FOR CDM

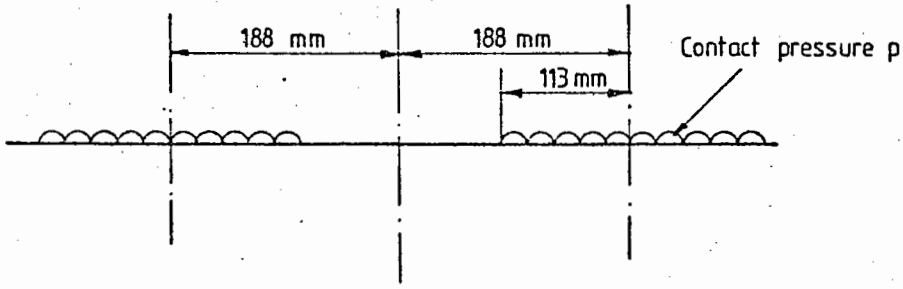

a. Standard dual wheel arrangement

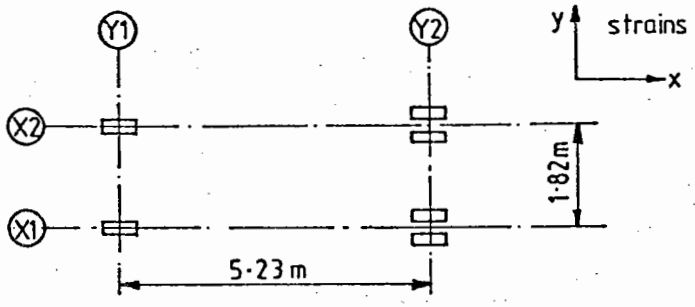

Payload	axle Y1	axle Y2	total
0 T	3·94 T ≙ 2·0 T/wheel	1·86 T ≙ 0·5 T/wheel	5·80 T
max 10·4 T	6·18 T ≙ 3·0 T/wheel	10·02 T ≙ 2·5 T/wheel	16·20 T

b. 2-axle rigid vehicle

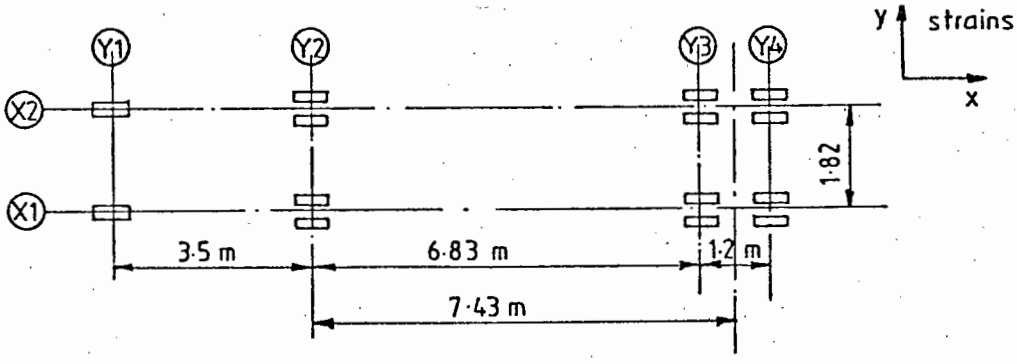

Payload	axle Y1	axle Y2	bogie axles Y3 & Y4	total
0 T	3·85 T ≙ 2·0 T/wheel	2·76 T ≙ 0·7 T/wheel	3·89 T ≙ 0·5 T/wheel	10·5 T
max 22·0 T	5·06 T ≙ 2·5 T/wheel	9·78 T ≙ 2·5 T/wheel	17·68 T ≙ 2·2 T/wheel	32·51 T

c. 4-axle articulated vehicle

FIG 4·15 ARRANGEMENT AND LOADING OF TYPICAL COMMERCIAL VEHICLES

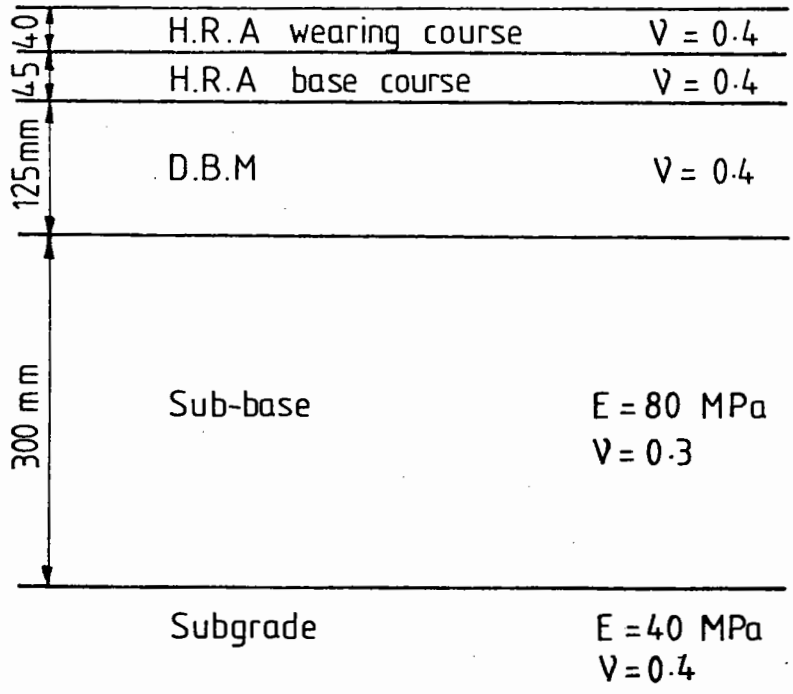

a. Thin structure (5 m.s.a)

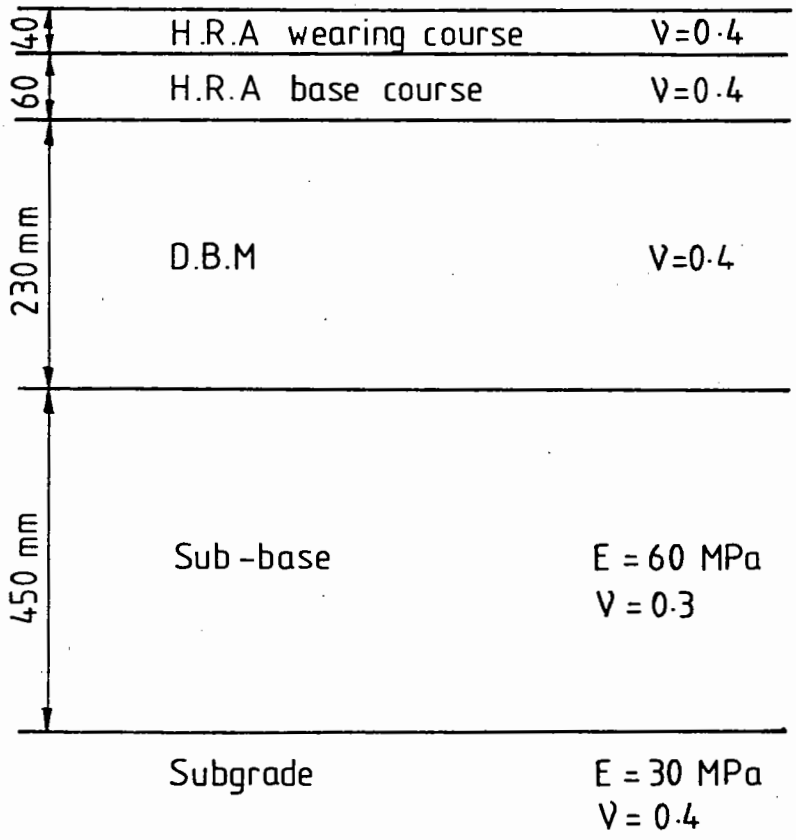

b. Thick structure (50 m.s.a)

FIG 4·16 STRUCTURES FOR CUMULATIVE ANALYSIS OF AXLE LOADINGS

The properties assumed for the hot rolled asphalt wearing course and basecourse and the dense bitumen macadam base are given in Table 4.11. These were used with an average speed for commercial vehicles of 80 km/hr and the seasonal temperatures stated above to calculate the mix stiffnesses given in Table 4.12. Hence, there were six structures to be analysed (two pavements x three temperatures).

The most commonly used commercial vehicles are the two-axle rigid lorry (approximately 65% of the total) and the four-axle articulated lorry (approx. 20%) (88). Fig.4.15 (b) and (c) shows the axle arrangements and wheel loadings, which were taken as typical, for these calculations.

The computer program BISTRO (38) was used to calculate the horizontal strains at the bottom of the asphalt layer. Each vehicle was considered both with no pay load and with maximum pay load. This resulted in the following loading cases; 2, 2.5 and 3 tonne single wheel loads and 0.5, 0.7, 2.0, 2.2 and 2.5 tonne per wheel for dual wheel loads. For the single wheel loads the required contact pressure was calculated for a circular contact area of 113mm radius. For the dual wheel loads the required contact pressure was calculated for the standard dual wheel loading arrangement given in Fig.4.15(a), each of which has the same 113mm radius. The longitudinal and transverse strains at the bottom of the road base were calculated at the centre of loading and along each axis. Fig.4.17 to 4.23 show the results plotted along the axes defined in Fig.4.15(b) and (c). If the corresponding strains are summed at each point along an axis, then the maximum tensile strains are generally in the longitudinal direction at the centre of each load.

Table 4.13 and 4.14 summarise the maximum horizontal strains in the wheel track (axis X1) beneath the centre of the wheel and corresponding lives in millions of standard axles (msa) based on the

Table 4.13 MAXIMUM TENSILE STRAINS AND CORRESPONDING LIVES IN A WHEEL TRACK (AXIS XI) FOR FULL PAY LOAD

Loading conditions	Maximum horizontal strains (με)				Life (msa)			
	Axle				Axle			
	Y1	Y2	Y3	Y4	Y1	Y2	Y3	Y4
4-axle articulated								
Thin Pavement								
Summer	156	231	182	182	0.30	0.09	0.19	0.19
Spring/Autumn	85	133	104	104	1.95	0.49	1.05	1.05
Winter	58	87	69	69	6.28	1.81	3.69	3.69
Thick Pavement								
Summer	82	139	113	113	2.18	0.43	0.82	0.82
Spring/Autumn	44	76	65	65	14.66	2.75	4.44	4.44
Winter	27	49	41	41	65.45	10.54	18.20	18.20
2-axle rigid								
Thin Pavement								
Summer	192	231	-	-	0.16	0.09	-	-
Spring/Autumn	106	132	-	-	0.99	0.51	-	-
Winter	68	87	-	-	3.86	1.82	-	-
Thick Pavement								
Summer	103	142	-	-	1.08	0.40	-	-
Spring/Autumn	55	78	-	-	7.40	7.54	-	-
Winter	35	51	-	-	29.60	9.33	-	-

Table 4.14 MAXIMUM TENSILE STRAINS AND CORRESPONDING LIVES IN A WHEEL TRACK (AXIS XI) FOR NO PAY LOAD

Loading conditions	Max. horizontal strains (με)				Life (msa)			
	Axle				Axle			
	Y1	Y2	Y3	Y4	Y1	Y2	Y3	Y4
4-axle articulated								
Thin Pavement								
Summer	128	57	41	41	0.55	6.63	18.20	18.20
Spring/Autumn	70	32	22	22	3.53	38.89	122.57	122.57
Winter	46	20	15	15	12.79	164.14	396.28	396.28
Thick Pavement								
Summer	73	36	26	26	3.10	27.11	73.47	73.47
Spring/Autumn	37	19	14	14	24.92	192.07	489.56	489.56
Winter	23	12	8	8	106.97	785.07	2718.98	2718.98
2-axle rigid								
Thin Pavement								
Summer	128	41	-	-	0.55	18.20	-	-
Spring/Autumn	70	22	-	-	3.53	122.57	-	-
Winter	46	15	-	-	12.79	396.28	-	-
Thick Pavement								
Summer	73	26	-	-	3.1	73.47	-	-
Spring/Autumn	37	14	-	-	24.92	489.56	-	-
Winter	23	8	-	-	106.47	2718.98	-	-

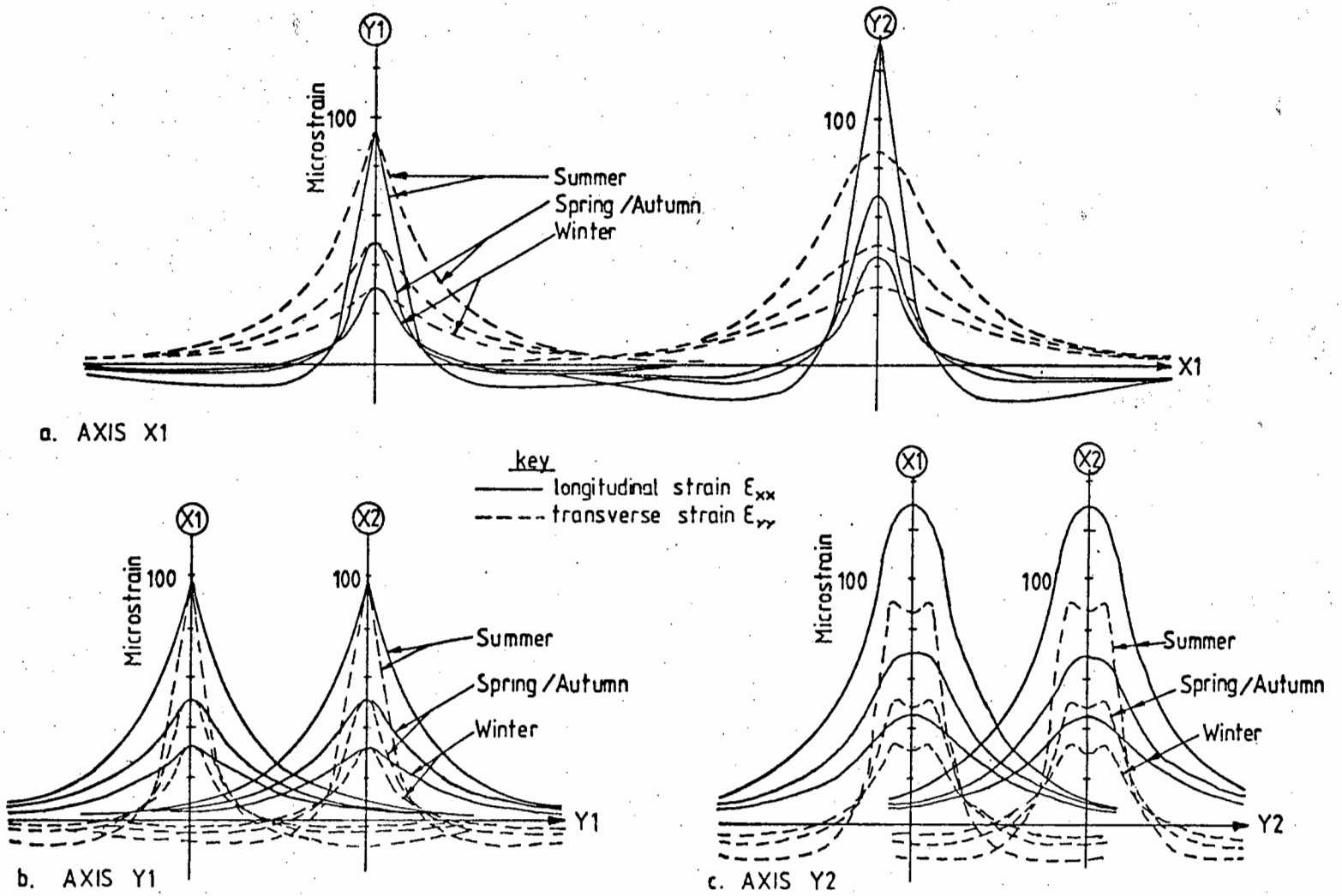

FIG 4.17 HORIZONTAL STRAINS ALONG AXES X1, Y1 AND Y2 FOR A 2-AXLE RIGID VEHICLE WITH MAXIMUM PAYLOAD AND A THICK PAVEMENT STRUCTURE

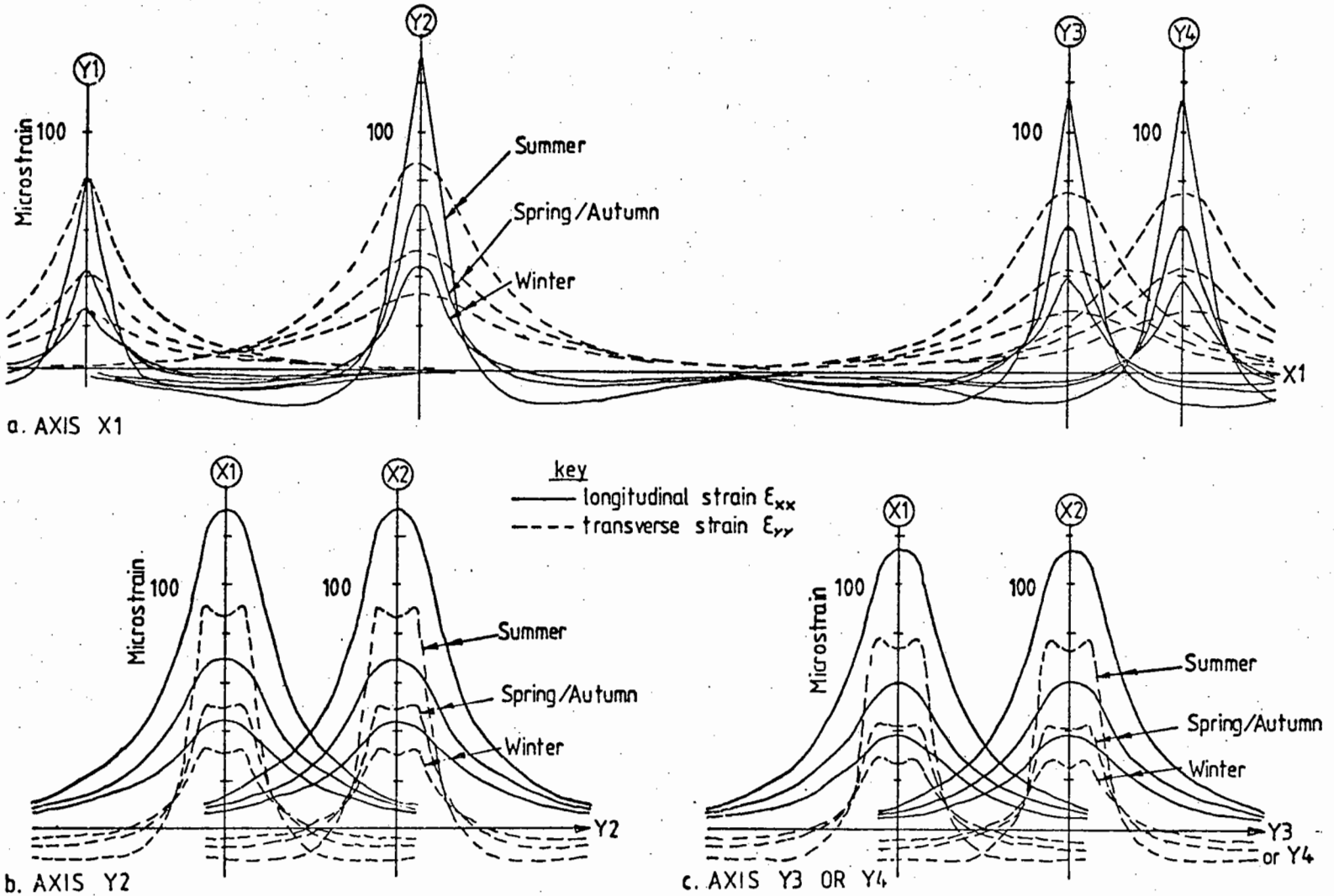

FIG 4·18 HORIZONTAL STRAINS ALONG AXES X1 Y2 Y3 AND Y4 FOR A 4-AXLE ARTICULATED VEHICLE WITH MAXIMUM PAYLOAD AND A THICK PAVEMENT STRUCTURE

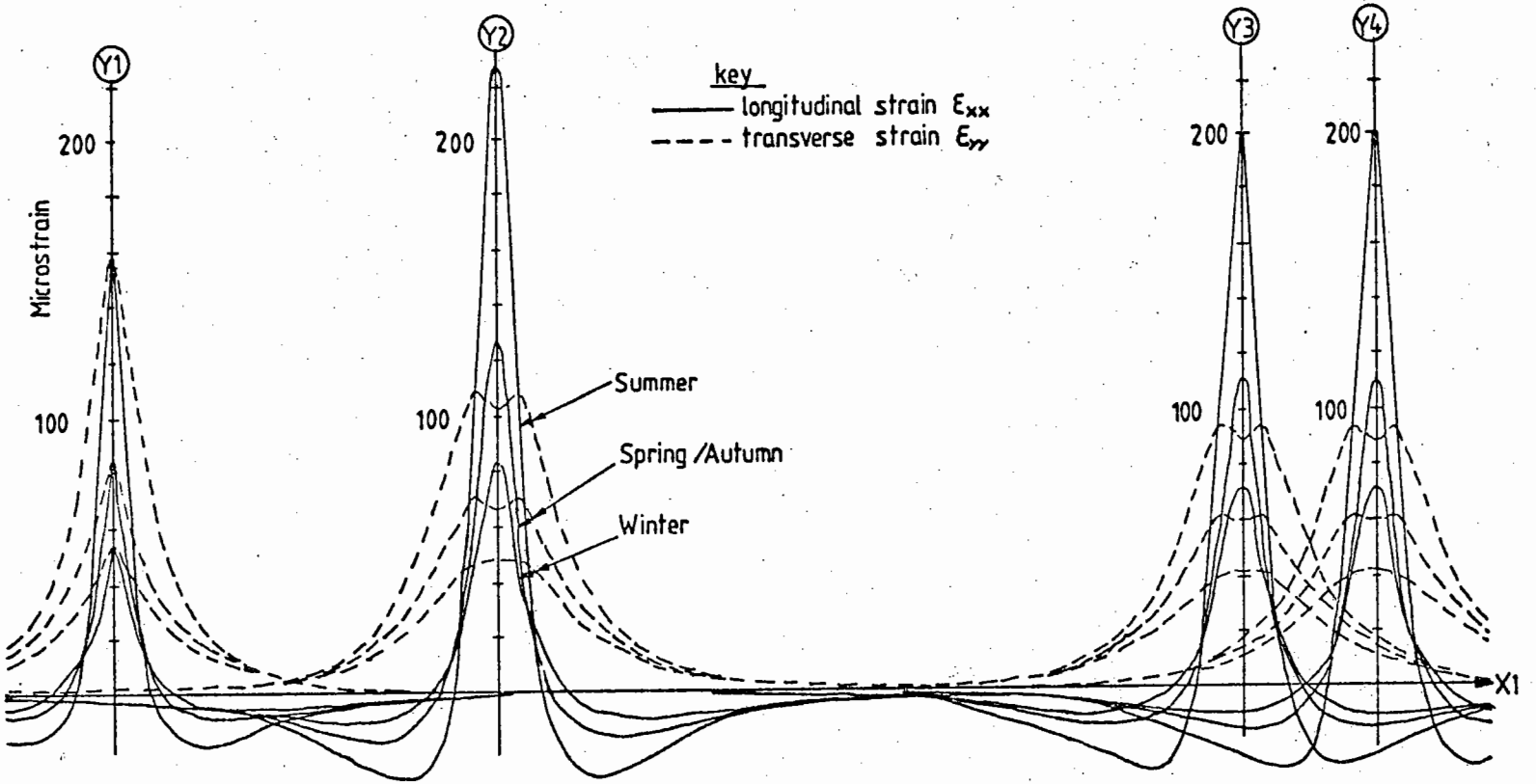

FIG 4.19 HORIZONTAL STRAINS ALONG AXIS X1 FOR A 4-AXLE ARTICULATED VEHICLE WITH MAXIMUM PAYLOAD AND A THIN PAVEMENT STRUCTURE

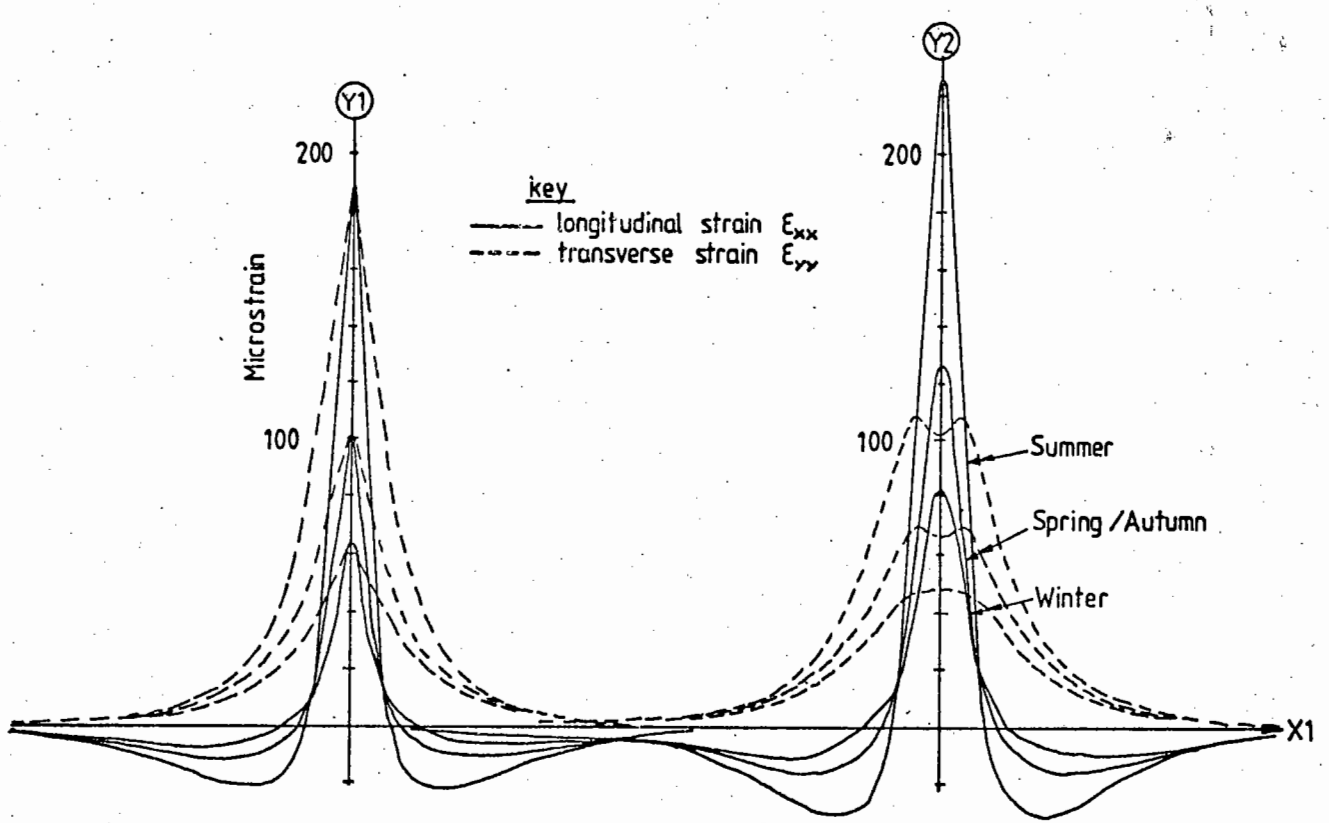

FIG 4.20 HORIZONTAL STRAINS ALONG AXIS X1 FOR A 2-AXLE RIGID VEHICLE WITH MAXIMUM PAYLOAD AND A THIN PAVEMENT STRUCTURE

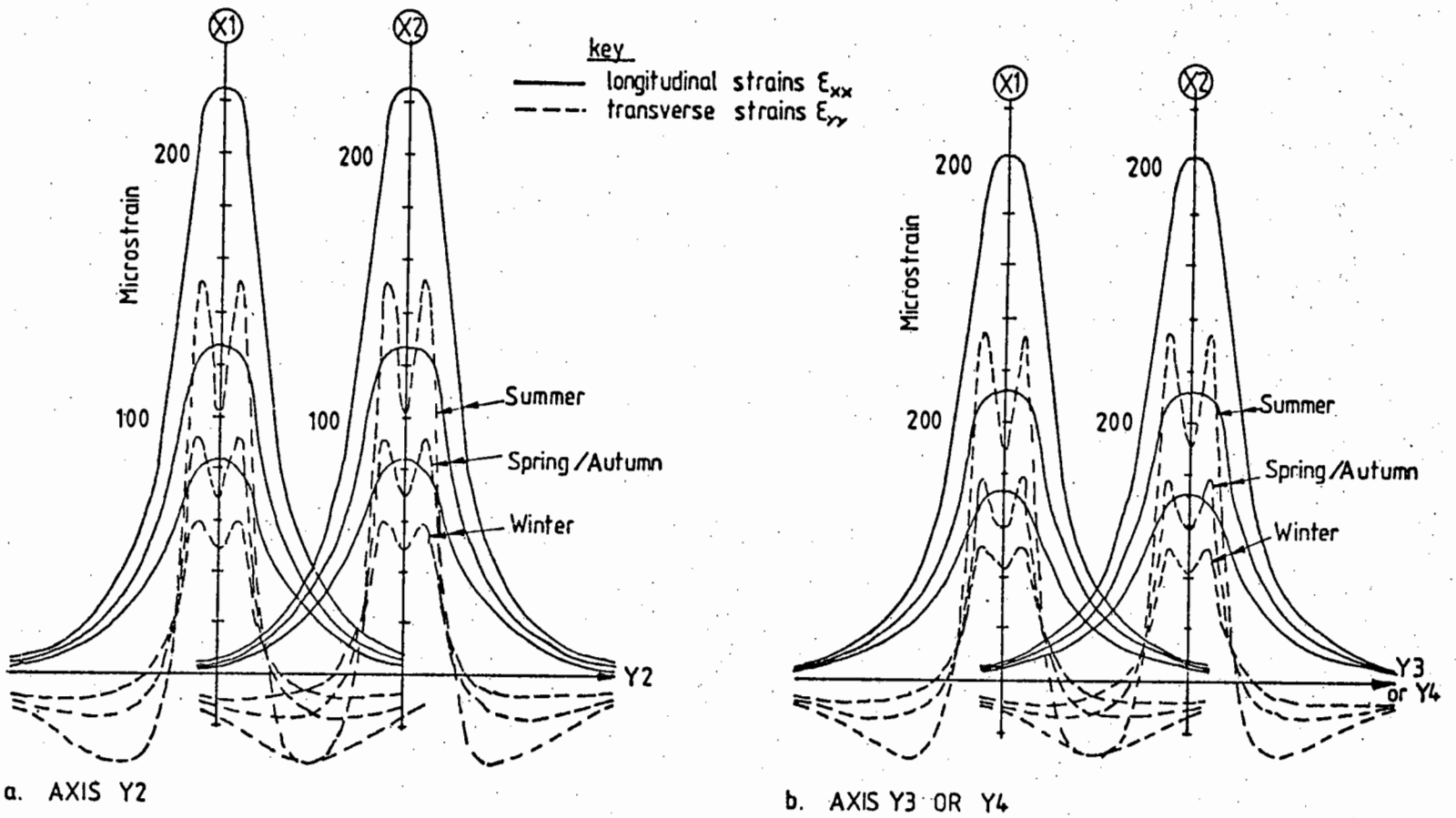

FIG 4·21 HORIZONTAL STRAINS ALONG AXIS Y2 FOR A 2-AXLE RIGID VEHICLE AND AXES Y2 Y3 AND Y4 FOR A 4-AXLE ARTICULATED VEHICLE AND A THIN PAVEMENT STRUCTURE (BOTH WITH MAXIMUM PAYLOADS)

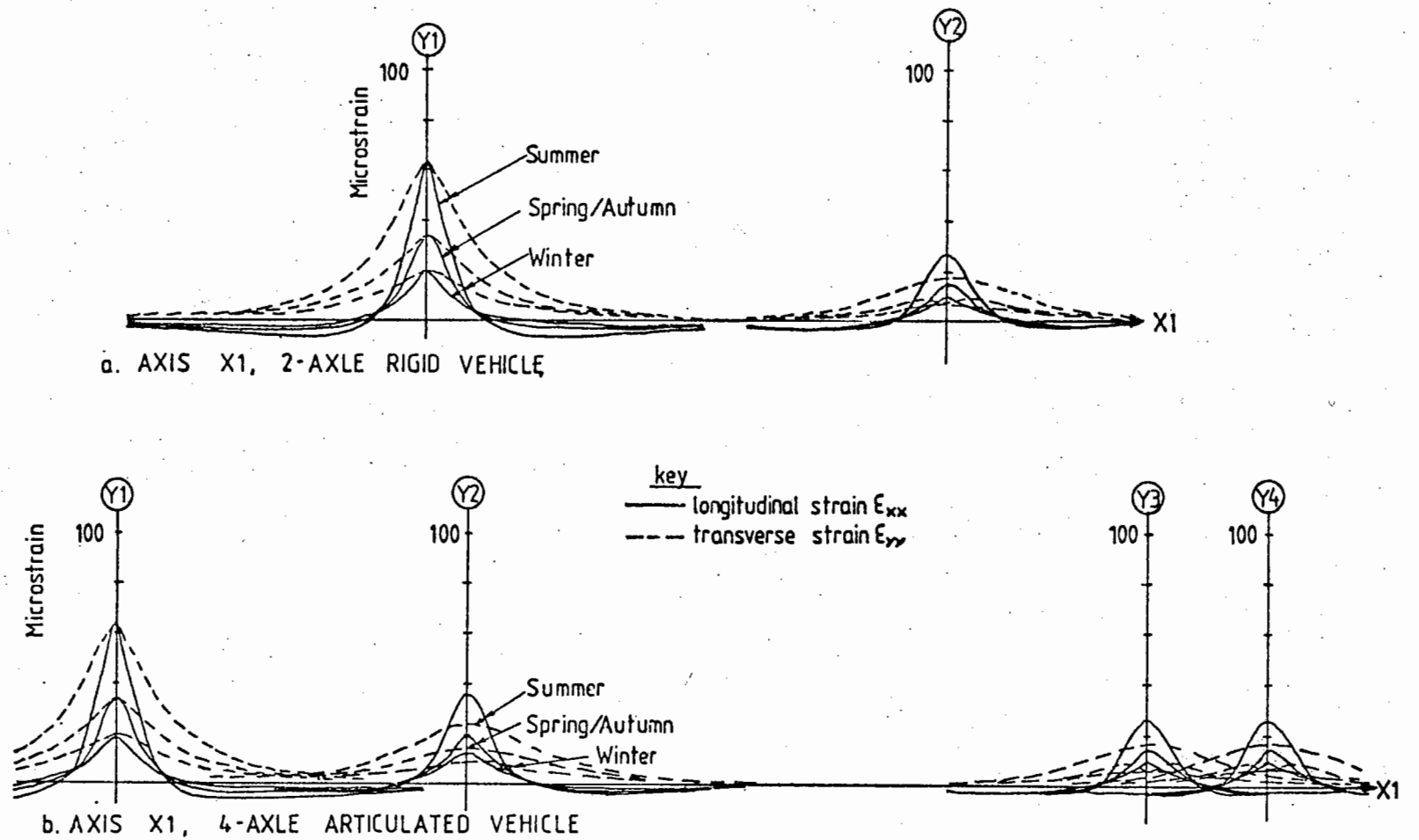

FIG 4.22 HORIZONTAL STRAINS ALONG AXIS X1 FOR A 2-AXLE RIGID VEHICLE AND A 4-AXLE ARTICULATED VEHICLE WITH NO PAYLOAD AND A THICK PAVEMENT STRUCTURE

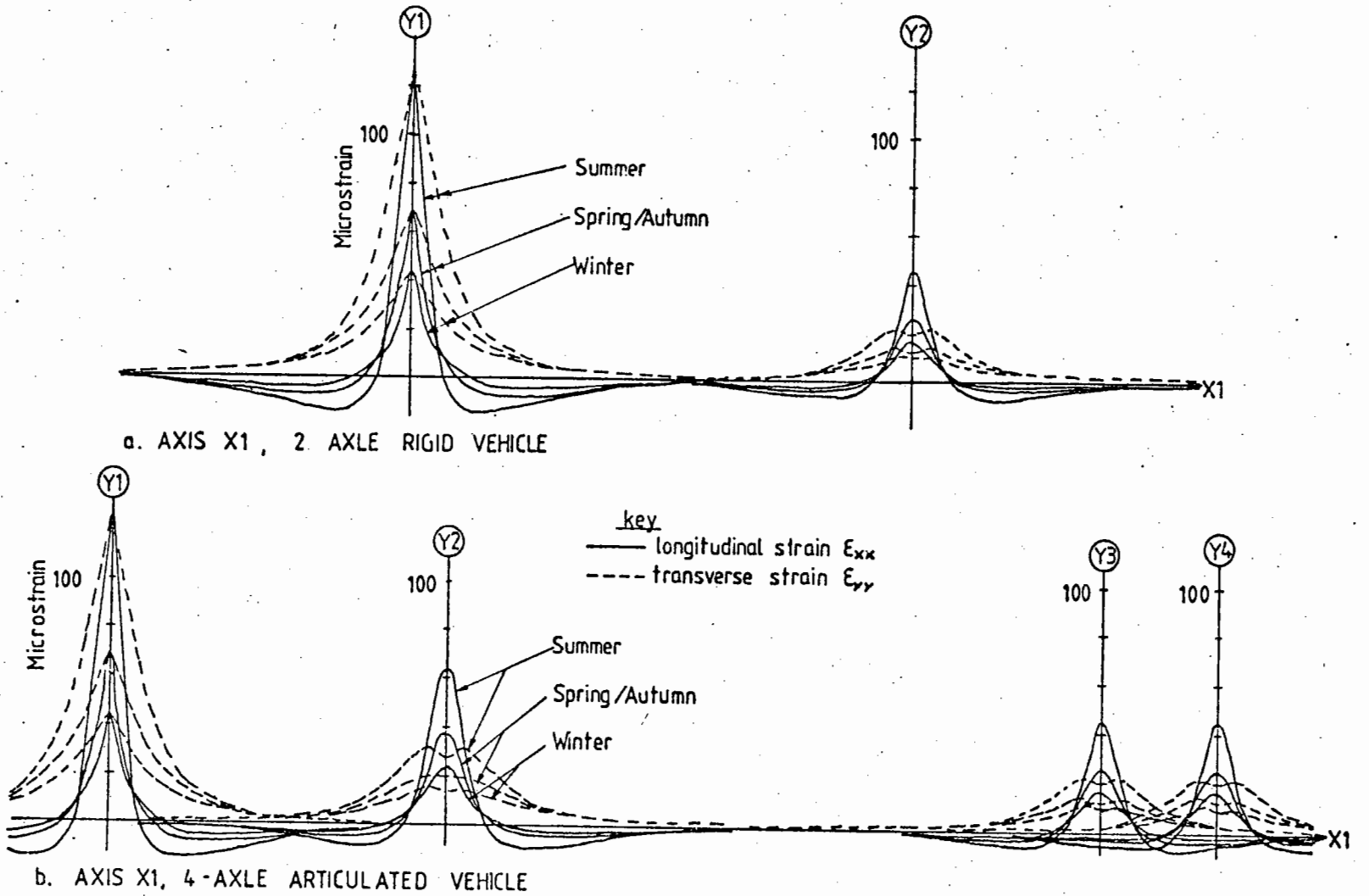

FIG 4.23 HORIZONTAL STRAINS ALONG AXIS X1 FOR A 2-AXLE RIGID VEHICLE AND A 4-AXLE ARTICULATED VEHICLE WITH NO PAYLOAD AND A THIN PAVEMENT STRUCTURE

fatigue characteristics of the DBM base. Table 4.15 gives the lives related to each axle load (N_A) using the cumulative damage approach as follows:

$$N_A = \frac{4}{\left[\frac{1}{N_S} + \frac{1}{N_W} + \frac{2}{N_{SA}}\right]} \qquad (4.10)$$

where N_S, N_W, N_{SA} = lives for Summer, Winter and Spring/Autumn temperature conditions.

The strains and lives were also calculated for the standard dual wheel load (Fig.4.15(a)) and these are given in Table 4.16. The total lives in the extreme right hand column were determined from the seasonal values using Equation (4.10). The laboratory to site conversion factor used in the fatigue criterion for calculating lives was 100. Although later work, discussed in Section 4.1, increased this factor to 440 the relative lives for each axle loading remain the same.

For these typical loading conditions, the life of the pavement due to each axle configuration was given in terms of millions of standard axles. The life of the same pavement was also calculated assuming a standard dual wheel arrangement. Therefore, the equivalent number of standard axles (E_e) for each of the typical axles could be calculated from the following relationship:

$$E_e = \frac{\text{life of pavement (msa) due to standard axle load}}{\text{life of pavement (msa) due to known axle load}} \qquad (4.11)$$

and the results are shown in Table 4.17. In order to avoid this detailed analysis, axle loads are generally converted to standard axles by calculating an equivalence factor using a power law, viz:

Table 4.15 PAVEMENT LIVES FOR EACH AXLE LOADING

Vehicle and pavement	Life (msa)							
	Maximum pay load				No pay load			
	Axle				Axle			
	Y1	Y2	Y3	Y4	Y1	Y2	Y3	Y4
4-axle articulated								
Thin Pavement	0.89	0.25	0.54	0.54	1.62	19.20	54.21	54.21
Thick Pavement	6.55	1.27	2.32	2.32	9.70	82.35	221.43	221.43
2-axle rigid								
Thin Pavement	0.47	0.26	--	--	1.62	54.51	--	--
Thick Pavement	3.25	1.18	--	--	9.70	221.32	--	--

Table 4.16 STRAINS AND PAVEMENT LIVES DUE TO STANDARD DUAL WHEEL LOADING

	Maximum horizontal strain (με)	Life (msa)	
		Seasonal	Total
Thin Pavement			
Summer	180	0.20	)
Spring/Autumn	102	1.12	)0.57
Winter	66	4.23	)
Thick Pavement			
Summer	104	1.05	)
Spring/Autumn	56	7.00	)3.14
Winter	35	29.56	)

Table 4.17 EQUIVALENT NUMBER OF STANDARD AXLES FOR EACH TYPICAL VEHICLE

	With maximum payload			With no pay load		
	Equivalent no. of standard axles		Calculated n	Equivalent no. of standard axles		Calculated n
	Analysis	4th power law		Analysis	4th power law	
4-axle articulated						
Thin Pavement Axle						
Y1	0.64	0.15	0.95	0.35	0.063	1.51
Y2	2.28	2.44	3.69	0.03	0.015	3.34
Y3	1.06	1.46	0.61	0.01	0.004	3.32
Y4	1.06	1.46	0.61	0.01	0.004	3.32
per vehicle	5.04	5.51		0.04	0.09	
Thick Pavement Axle						
Y1	0.48	0.15	1.56	0.32	0.063	1.64
Y2	2.47	2.44	4.05	0.04	0.015	3.07
Y3	1.35	1.46	3.15	0.01	0.004	3.32
Y4	1.35	1.46	3.15	0.01	0.004	3.32
per vehicle	5.65	5.51		0.38	0.09	
2-axle rigid						
Thin Pavement Axle						
Y1	1.21	0.32	-0.66	0.35	0.063	1.51
Y2	2.19	2.44	3.51	0.01	0.004	3.32
per vehicle	3.40	2.76		0.36	0.07	
Thick Pavement Axle						
Y1	0.96	0.32	0.14	0.32	0.063	1.64
Y2	2.66	2.44	4.38	0.01	0.004	3.32
per vehicle	3.62	2.76		0.33	0.07	

$$EF_W = \left[\frac{W}{80}\right]^n \qquad (4.12)$$

where EF_W is the equivalent factor

W is the axle load in KN

and 80 KN is the standard axle load

n is usually taken as 4.

This law was based on overall performance of the AASHO road test pavement and therefore results from pavement deterioration due to other factors as well as fatigue cracking. However, it was used to calculate the equivalent number of standard axles for each of the actual axle loads and the results are also shown in Table 4.17. There is a large discrepancy between the equivalent numbers of standard axles determined by the two methods in some cases. The power n, used in Equation (4.12), was calculated so as to give agreement between the two approaches and these values are also included in Table 4.17.

The fourth power law appears to be inaccurate when each axle is considered separately. However, for the 4-axle articulated vehicle, the total number of equivalent standard axles for a maximum payload is reasonably accurate. The largest discrepancies arise for cases with no pay load. The errors in this case, for the second, third and fourth axles of the articulated truck, were of the order of 50%. For the first axle, however, which was the only one with a significant load, the errors are about 80%. The largest discrepancies with the fourth power law occur for the single wheels.

Although this analysis suggests that the cumulative damage approach should be adopted for variations of load as well as temperature for every pavement, particularly when the loading is light, this would be unrealistic. In this study only two vehicles were

considered, either with zero or full loading. The equivalent number of standard axles per vehicle for the maximum loading case was as much as 12 times that of the unloaded case. The number of each type or classification of vehicle could be assessed quite simply in traffic surveys, but the actual axle loads are not so readily available. The factors used to convert the number of commercial vehicles to standard axles, depending on the initial number of commercial vehicles per day given in Road Note 29 are based on data from comprehensive traffic studies and, therefore, they should be more reliable than using cumulative damage methods where the percentage of pay load must be estimated.

4.4 APPLICATION OF REVISED FATIGUE DESIGN CRITERION

The revised laboratory to field fatigue conversion factor of 440 was incorporated into the PET computer programs. The progams were also amended to account for cumulative damage effects in fatigue by using an asphalt design temperature equal to 1.92 times the average annual air temperature when considering fatigue cracking only. This factor is discussed in Section 4.2.4. It comprises a 1.47 factor to obtain the average annual pavement temperature (used for the subgrade criterion), and a 1.31 factor for cumulative damage effects (1.31 x 1.47 = 1.92). The 1.31 factor is only approximate. The balanced design method for the PET computer program was further amended to include a 1.2 safety factor on the fatigue design life to ensure a failure by permanent deformation.

Fig.4.24 shows the effect of the revised design criterion on balanced designs. These were calculated using the PET computer program with the same input data as for Fig.4.8, given in Table 4.5. Although Fig.4.8 was prepared to show the effect of varying the laboratory to field conversion factor, it did not include the 1.2 safety factor on

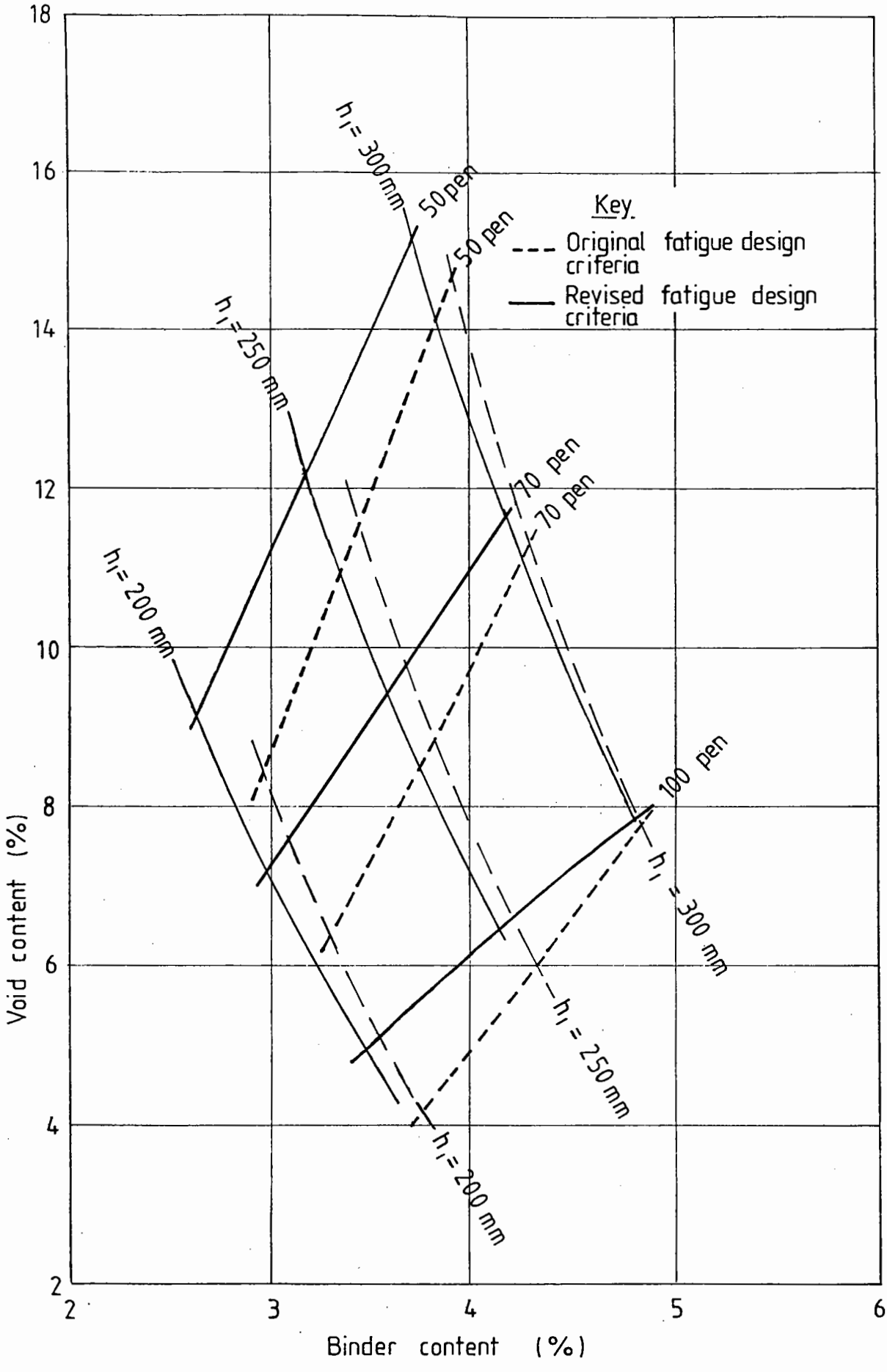

FIG 4·24 TO SHOW THE EFFECT OF THE REVISED FATIGUE DESIGN CRITERION ON BALANCED DESIGNS

fatigue life, nor did it use the higher pavement temperature to account for cumulative damage effects in fatigue. Fig.4.24 shows that for both the original and revised fatigue design criteria, practical mixes are more likely to occur when 100 pen bitumen is used. For 50 pen binders, the mixes required for a balanced design are generally too lean and have high void contents.

As a further check on the validity of the revised fatigue criterion, the typical DBM Road Note 29 designs analysed in Section 4.1.6, were re-examined using the amended PET programs, SDM and DLM. The assumed mix details are given in Table 4.1. As before, the design conditions adopted were a mean speed of 80 km/hr and an average annual pavement temperature of 14°C, which was adjusted by a factor of 1.31 to 18.3°C for the fatigue calculations. Table 4.18 summarises the results.

Using the original fatigue criterion, the calculated lives were all less than given by Road Note 29. All these lives were increased when the revised fatigue criterion was applied. For the thinnest pavement, a longer life was predicted using the revised criterion than from Road Note 29. However, for the two thicker pavements, the lives were still conservative by a factor of approximately 2. A similar trend was observed when the Road Note 29 design lives were used to calculate the pavement thicknesses.

The design thicknesses for the 10 and 70 msa lives, using the revised fatigue criterion, were greater than those required by Road Note 29, and vice versa for the 0.5 msa life. The comparisons are shown graphically in Fig.4.25.

As discused in detail in Section 4.1.6, precise agreement with Road Note 29 should not be expected. However, it can be concluded that whilst the revised fatigue criterion no longer gives conservative designs for very short lives (or thin pavements), it does result in

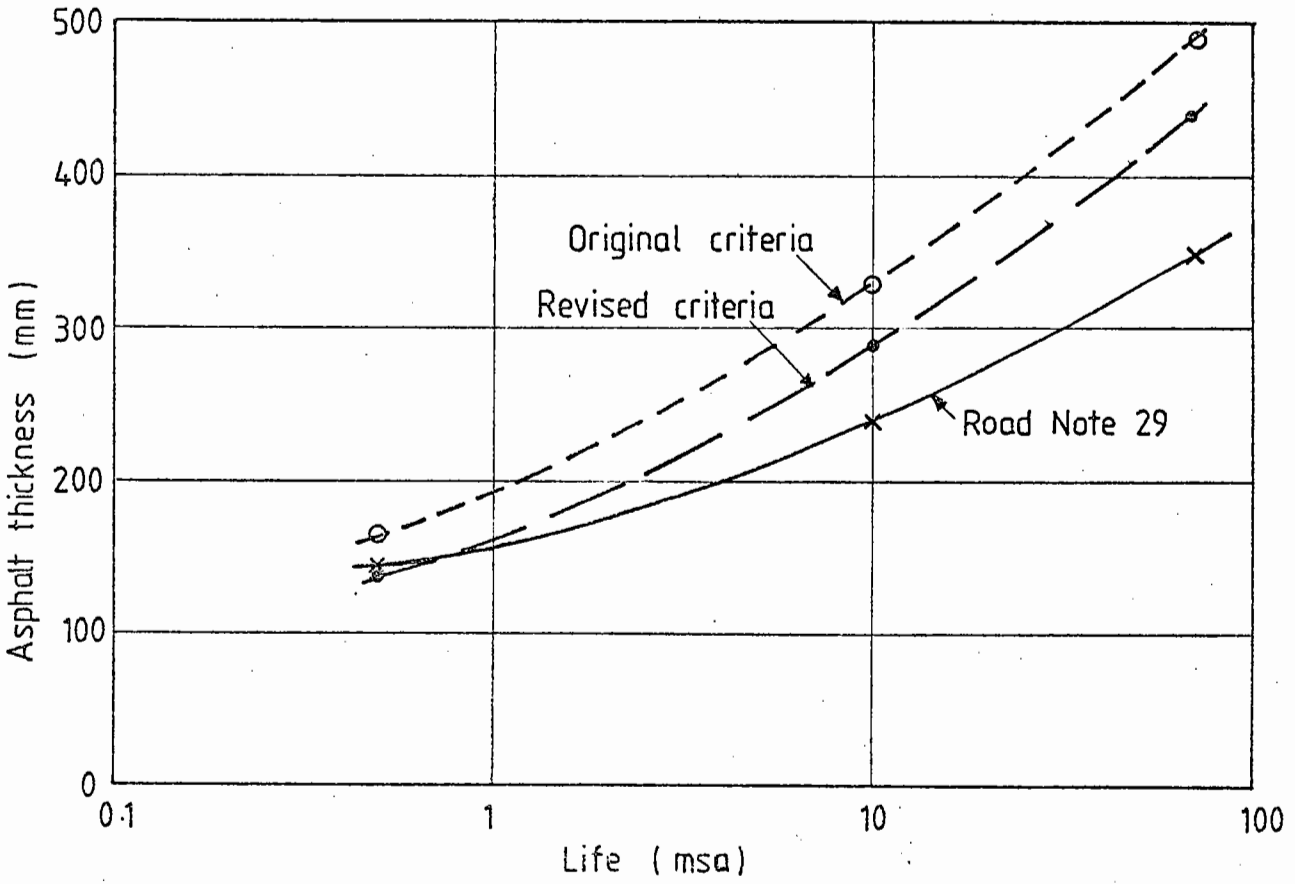

FIG 4·25 COMPARISON OF FATIGUE LIVES FOR A TYPICAL DBM

Table 4.18 COMPARISON OF FATIGUE LIVES FOR TYPICAL DBM

Subgrade CBR (%)	Road Note 29		Original fatigue criterion		Revised fatigue criterion	
	Design life (msa)	Thickness (mm)	Life* (msa)	Thickness+ (mm)	Life* (msa)	Thickness+ (mm)
5	0.5	145	0.3	165	0.7	140
6	10.0	240	2.4	330	4.7	290
7	70.0	350	13.1	490	24.6	440

* Calculations based on Road Note 29 thickness.
+ Calculations based on Road Note 29 design life.

closer agreement with Road Note 29 for the other situations considered.

4.5 SUMMARY

1. The PET microcomputer program CDM was developed.
2. Application of the cumulative damage approach to variations of load as well as temperature was generally found to be impracticable and it was decided that the use of the fourth power law was a reasonable general approach.
3. An increase from 100 to 440 was proposed for the fatigue "shift factor", which takes into account the differences between conditions in situ (where longer lives are obtained) and those in laboratory testing.
4. Cumulative fatigue damage effects due to temperature variations were incorporated in the simple design method of the PET programs by using a factor of 1.92 to convert the average annual air temperature to a pavement design temperature (for fatigue only).
5. The balanced design method of analysis was amended to include a 1.2 safety factor on the fatigue design life to ensure failure by permanent deformation.
6. The revised fatigue criterion no longer gives conservative designs for very short lives (or thin pavements), but it does result in closer agreement with Road Note 29 for the other situations considered.

CHAPTER FIVE

DETAILED STUDY OF DESIGN AGAINST PERMANENT DEFORMATION

5.1 EXISTING DESIGN CRITERION

The simple criterion used to design against rutting is the vertical compressive strain at the top of the subgrade. The maximum allowable value of this parameter depends on the number of standard axles (N) given by the relationship:

$$\epsilon_z = \frac{21600}{N^{0.28}} \quad \text{microstrain} \qquad (5.1)$$

Equation (5.1) was derived by back analysis of British pavements of known performance at an average annual pavement temperature of 15°C,(50). These pavements had hot rolled asphalt bases and the analysis assumed a mix stiffness of 6200 MPa. This is appropriate for a typical HRA with 5.7% of 50 pen bitumen, compacted to a void content of 6%, using a design speed of 40km/hr.

The existing design criterion assumes that the same subgrade strain criterion can be applied to all types of base materials. If a HRA base in a structure is replaced by a DBM base of the same stiffness and thickness then the calculated vertical compressive strain and corresponding design life would be identical. However, in practice the DBM has better resistance to deformation than the HRA. The aim of this study is to provide a means by which this discrepancy can be taken into account.

5.2 LABORATORY TEST DATA

Tables 5.1 and 5.2 summarise the properties of seventeen mixes tested at Nottingham (45,46,47). The mixes can be categorized into

Table 5.1 SUMMARY OF MIXES TESTED AT NOTTINGHAM

Mix No.	Mix Type	Aggregate			Binder		Void Content (%)	VMA (%)
		Type	Max. particle size (mm)	Grading	Grade (pen)	Content (%)		
1	DBM base	Dene limestone	40	Cont.	200	3.9	10.4	19.1
2	DBM base	Dene limestone	40	Cont.	100	3.5	10.4	18.3
3	HRA b/c	Dene limestone	28	Gap	50	5.4	5.0	17.5
4	HRA b/c	Boreham gravel	28	Gap	50	5.3	3.1	15.4
5	Mod. HRA	Boreham gravel	28	Gap	50	5.3	4.2	16.4
6	DBM b/c	Dene limestone	40	Cont.	100	4.4	9.8	19.6
7	DBM base	B. Hill granite	40	Cont.	200	5.0	7.6	19.3
8	DBM b/c	B. Hill granite	40	Cont.	100	4.3	10.0	20.0
9	HRA b/c	B. Hill granite	28	Gap	50	5.5	5.3	18.1
10	Mod. HRA	Croft granite	28	Gap	50	4.4	4.9	15.2
11	Mod. DBM	Croft granite	20	Cont.	50	4.4	8.9	18.8
12	Mod. HRA	M. Peak limestone	37.5	Gap	50	5.2	3.4	15.8
13	Mod. HRA	M. Peak limestone	28	Gap	50	5.8	3.0	16.5
14	DBM b/c	Sanford slag	40	Cont.	100	6.9	8.0*	22.2*
15	Grave bitume	Tilbury granite	20	Cont.	50	4.6	4.4	16.1
16	HRA w/c	Dene granite	14	Gap	50	8.3	4.0	22.6
17	Grave bitume	Limestone	28	Gap	50	3.6	-	-

* Tentative results.

Table 5.2 COMPARISON OF DYNAMIC STIFFNESSES AT 80 km/hr and 15°C FOR MIXES TESTED AT NOTTINGHAM

Mix No.	Mix type	VMA (%)	Binder stiffness (MPa)	Mix stiffness (GPa)		Predicted / Measured
				Measured	Predicted	
1	DBM base	19.1	12	6.0	1.5	0.25
2	DBM base	18.3	48	6.0	5.0	0.83
3	HRA b/c	17.5	105	12.5	9.5	0.76
4	HRA b/c	15.4	105	-	12.0	-
5	Mod. HRA	16.4	105	10.5	10.5	1.0
6	DBM b/c	19.6	48	-	4.0	-
7	DBM base	19.3	12	2.0	1.5	0.75
8	DBM b/c	20.0	48	5.0	4.0	0.80
9	HRA b/c	18.1	105	10.5	8.0	0.76
10	Mod. HRA	15.2	105	15.0	12.0	0.80
11	Mod. DBM	18.8	105	11.0	7.5	0.68
12	Mod. HRA	15.8	105	12.0	11.5	0.96
13	Mod. HRA	16.2	105	11.0	10.5	0.95
14	Slag DBM	20.5	48	3.0	3.5	1.17
15	Grave bit.	16.1	105	12.0	10.5	0.88
16	HRA w/c	22.5	105	10.0	4.5	0.45

four different types of material, typical HRA, typical DBM, Modified HRA and Modified DBM. Triaxial creep and repeated load triaxial tests were carried out on each mix. The results from the repeated load tests are considered more representative of site conditions and are, therefore, those used in the following study. Fig.5.1 summarises the repeated loading test conditions.

For each mix, graphs of permanent shear strain against number of cycles were plotted for confining stresses between 100 and 300 kPa. Fig.5.1 shows a typical graph. From the broad spectrum of results a single line has been selected to represent the mid-range value for the mix. Figs.5.2 and 5.3 give these lines for each mix. It can be seen that there is a general trend for the four groups. In order to obtain a practical solution a single line has been chosen to represent each material, a typical HRA, DBM and Modified HRA and DBM, as shown in Fig.5.4.

5.3 DEVELOPMENT OF DESIGN CRITERION FOR PERMANENT DEFORMATION

5.3.1 Application of Laboratory Data

The horizontal scale in Fig.5.4 was converted to a number of standard axles N, to make it appropriate for design use. The procedure involved use of the Van der Poel nomograph (9) in which loading time (t) is related to test frequency (f) using $t = \frac{1}{2\pi f}$.

Hence, total loading time in a repeated load test

$$= \frac{\text{No. of cycles}}{2\pi f} \qquad (5.2)$$

For example, 10^3 cycles represents a total loading time of 159 seconds, since f = 1Hz.

For the 50 pen mixes, a recovered softening point of 59°C and a recovered penetration index of -0.1 were assumed. Hence, the

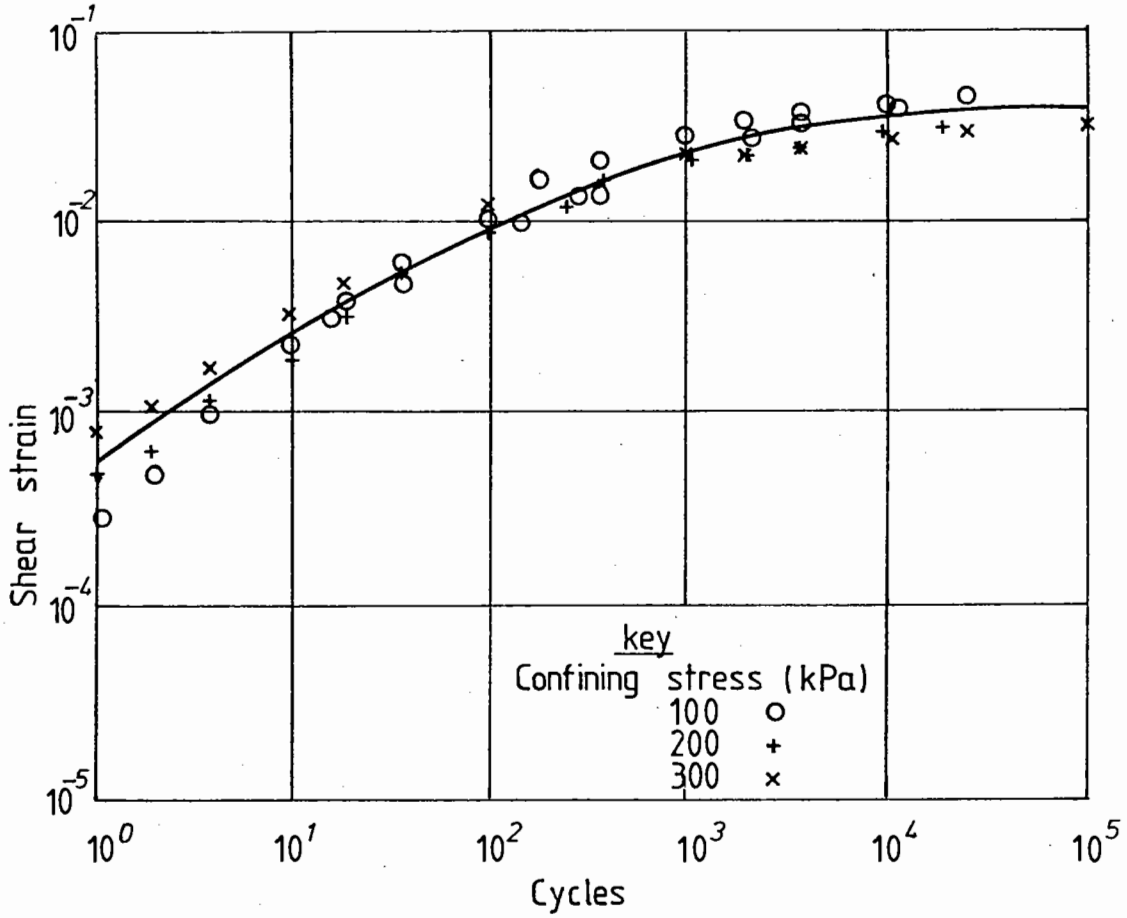

Repeated load test conditions

Deviator stress (q) = 200 kPa
Frequency = 1 Hz
Temperature = 30 °C
Waveform - sinusoidal

FIG 5.1 TRIAXIAL TEST RESULTS FOR HOT ROLLED ASPHALT BASECOURSE (crushed granite, 50 pen bitumen) Mix no. 9 - Bardon Hill

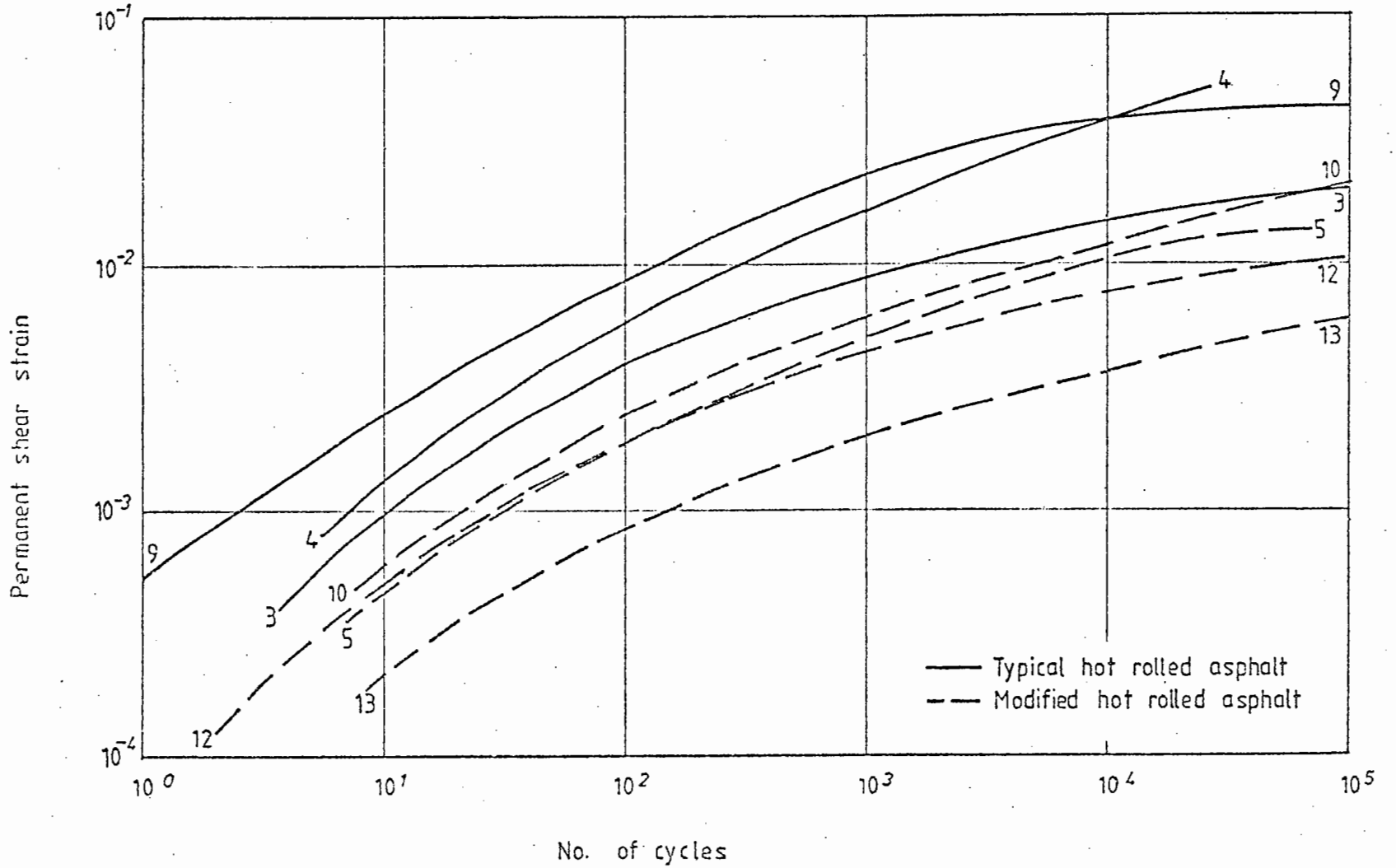

FIG 5·2 REPEATED LOAD TRIAXIAL TEST RESULTS FOR HOT ROLLED ASPHALTS

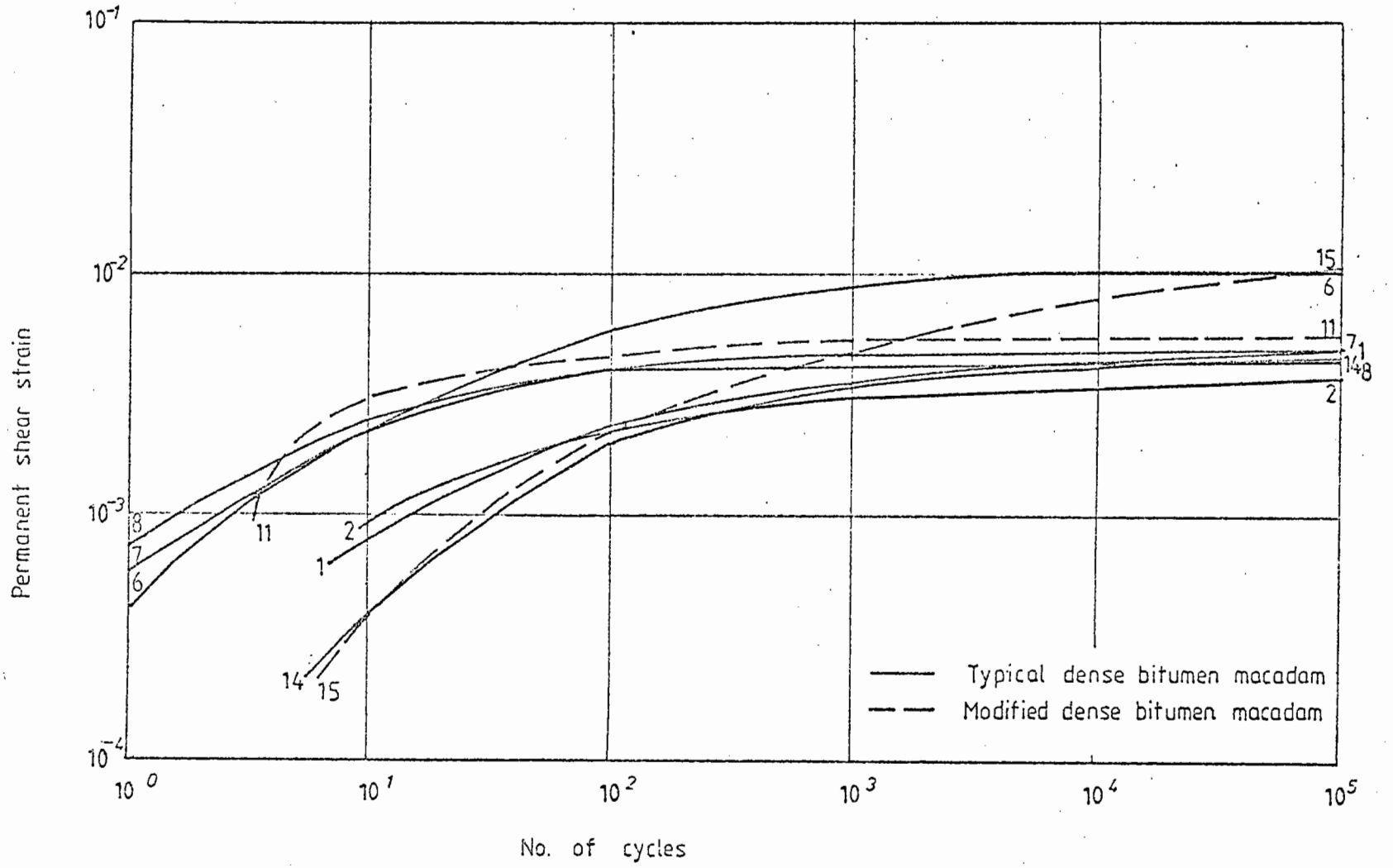

FIG 5.3 REPEATED LOAD TRIAXIAL TEST RESULTS FOR DENSE BITUMEN MACADAMS

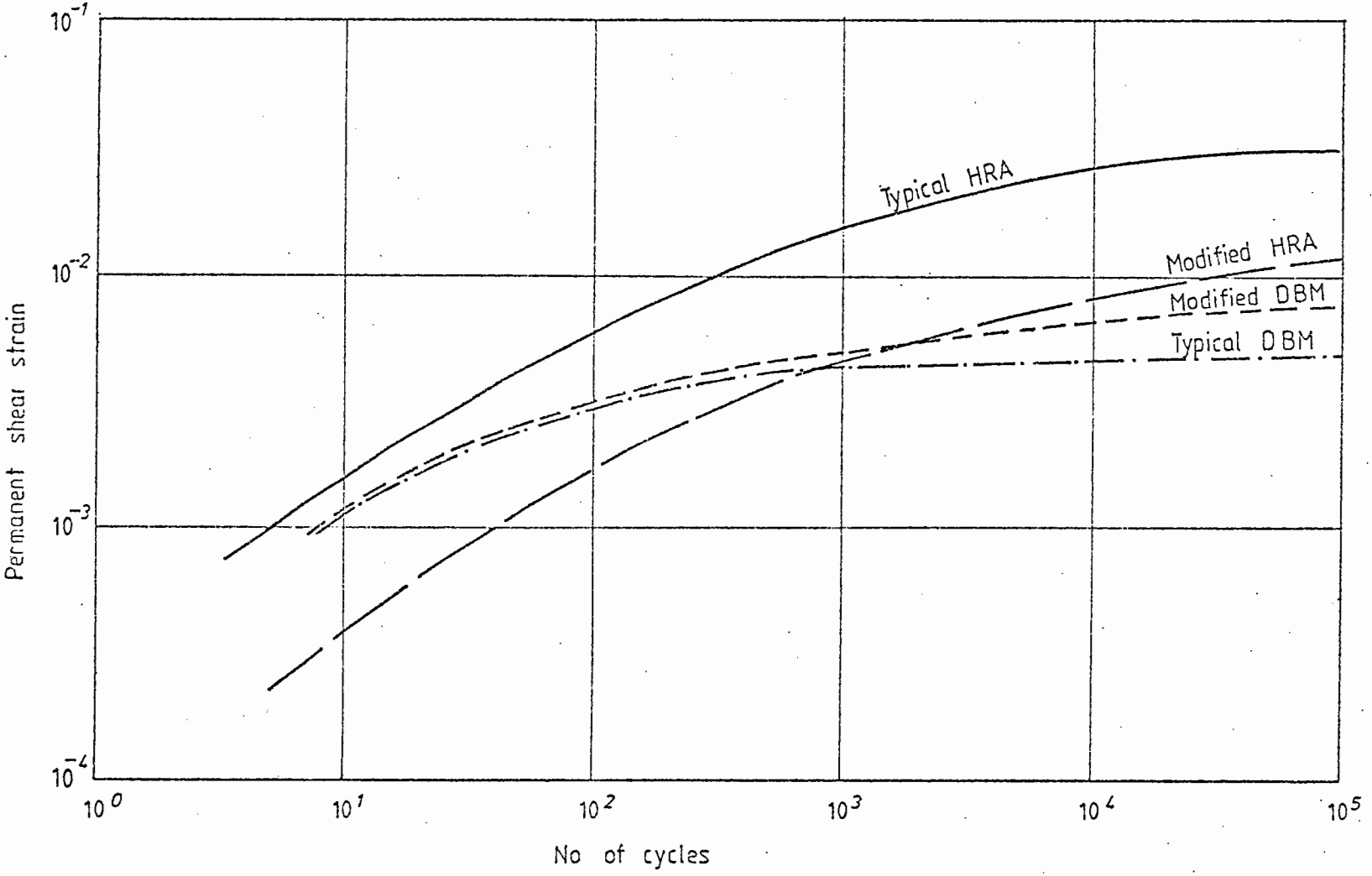

FIG 5.4 REPEATED LOAD TRIAXIAL TEST RESULTS FOR TYPICAL MIXES

temperature difference between recovered softening point and test temperature (30°C) was 29°C. For a known loading time, say 159 seconds, the binder stiffness can be determined using Van der Poel's nomograph as shown in Fig.5.5. In order to have the same binder stiffness under site conditions (15°C), the total loading time required is 10^4 seconds. (see Fig.5.5.) For a speed of 40km/hr the loading time for 1 standard axle can be estimated using the simple empirical relationship:-

$$t = \frac{1}{V} \quad \text{seconds} \qquad (5.3)$$

where V is the speed in km/hr. Therefore, the number of standard axles required for a total loading time of 10^4 seconds is,

$$N = \frac{10^4}{t} = 4 \times 10^5 \quad \text{standard axles}$$

In a similar way the loading time for a 100 pen mix was also converted to number of standard axles. The recovered softening point used was 51°C and the recovered penetration index -0.2. For a loading time of 159 seconds under test conditions (10^3 cycles), the site loading time is 6×10^3 seconds and the equivalent number of standard axles is 2.4×10^5. Fig.5.6 shows the four mix types and the various horizontal scales derived. Fig.5.7 is the resultant graph of permanent shear strain against number of standard axles.

In practice pavement design lives vary between 0.5 msa and 300 msa. Over this range the values of permanent shear strain tend to level out, and an average value is assumed for each material, (see Fig.5.7). These values are given in Table 5.3.

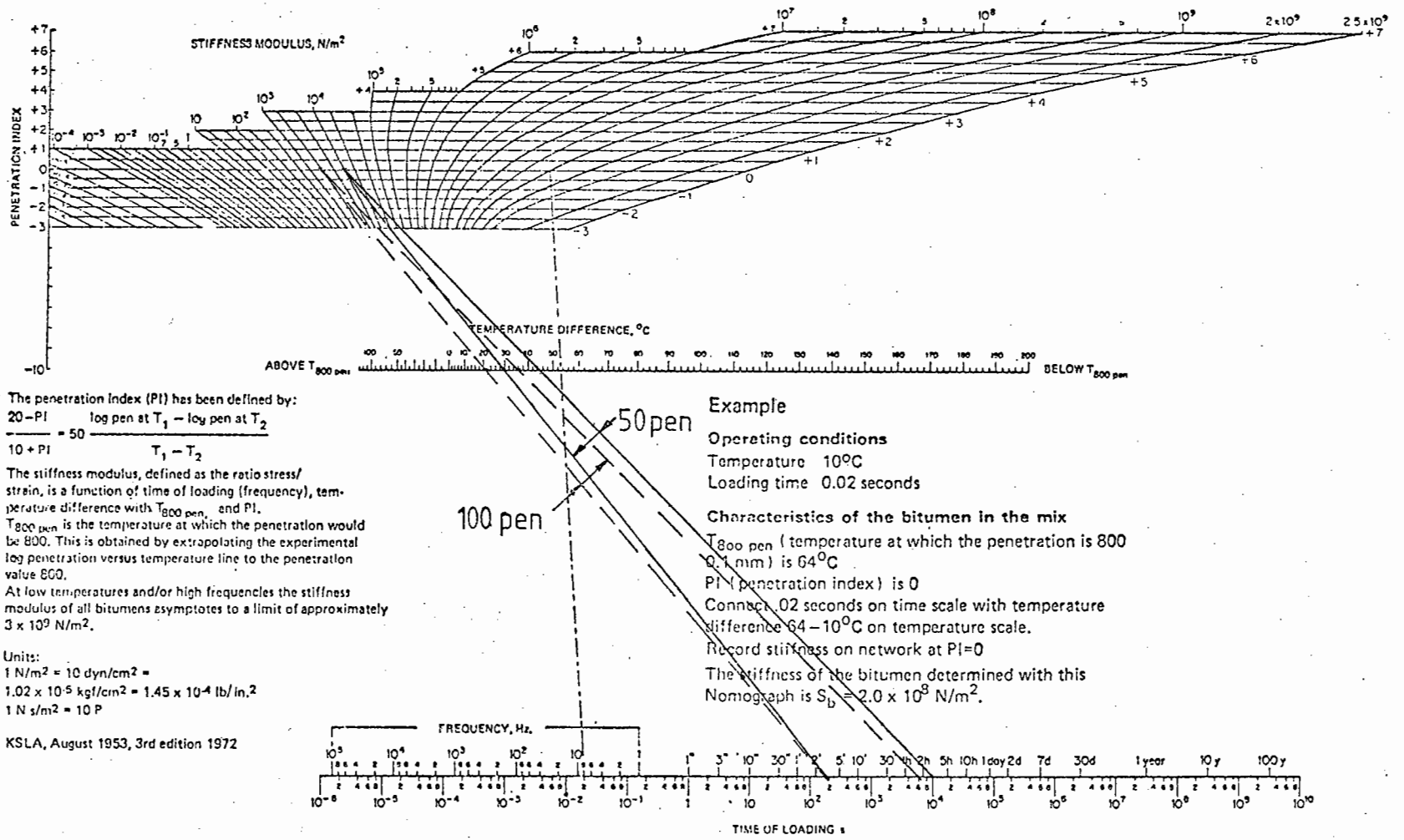

The penetration index (PI) has been defined by:

$$\frac{20-PI}{10+PI} = 50\,\frac{\text{log pen at } T_1 - \text{log pen at } T_2}{T_1 - T_2}$$

The stiffness modulus, defined as the ratio stress/strain, is a function of time of loading (frequency), temperature difference with $T_{800\,pen}$, and PI.
$T_{800\,pen}$ is the temperature at which the penetration would be 800. This is obtained by extrapolating the experimental log penetration versus temperature line to the penetration value 800.
At low temperatures and/or high frequencies the stiffness modulus of all bitumens asymptotes to a limit of approximately 3×10^9 N/m².

Units:
1 N/m² = 10 dyn/cm² =
1.02×10^{-5} kgf/cm² = 1.45×10^{-4} lb/in.²
1 N s/m² = 10 P

KSLA, August 1953, 3rd edition 1972

Example

Operating conditions
Temperature 10°C
Loading time 0.02 seconds

Characteristics of the bitumen in the mix
$T_{800\,pen}$ (temperature at which the penetration is 800 0.1 mm) is 64°C
PI (penetration index) is 0
Connect .02 seconds on time scale with temperature difference 64 – 10°C on temperature scale.
Record stiffness on network at PI=0
The stiffness of the bitumen determined with this Nomograph is $S_b = 2.0 \times 10^8$ N/m².

FIG 5.5 NOMOGRAPH FOR DETERMINING THE STIFFNESS OF BITUMENS (AFTER VAN DER POEL (9))

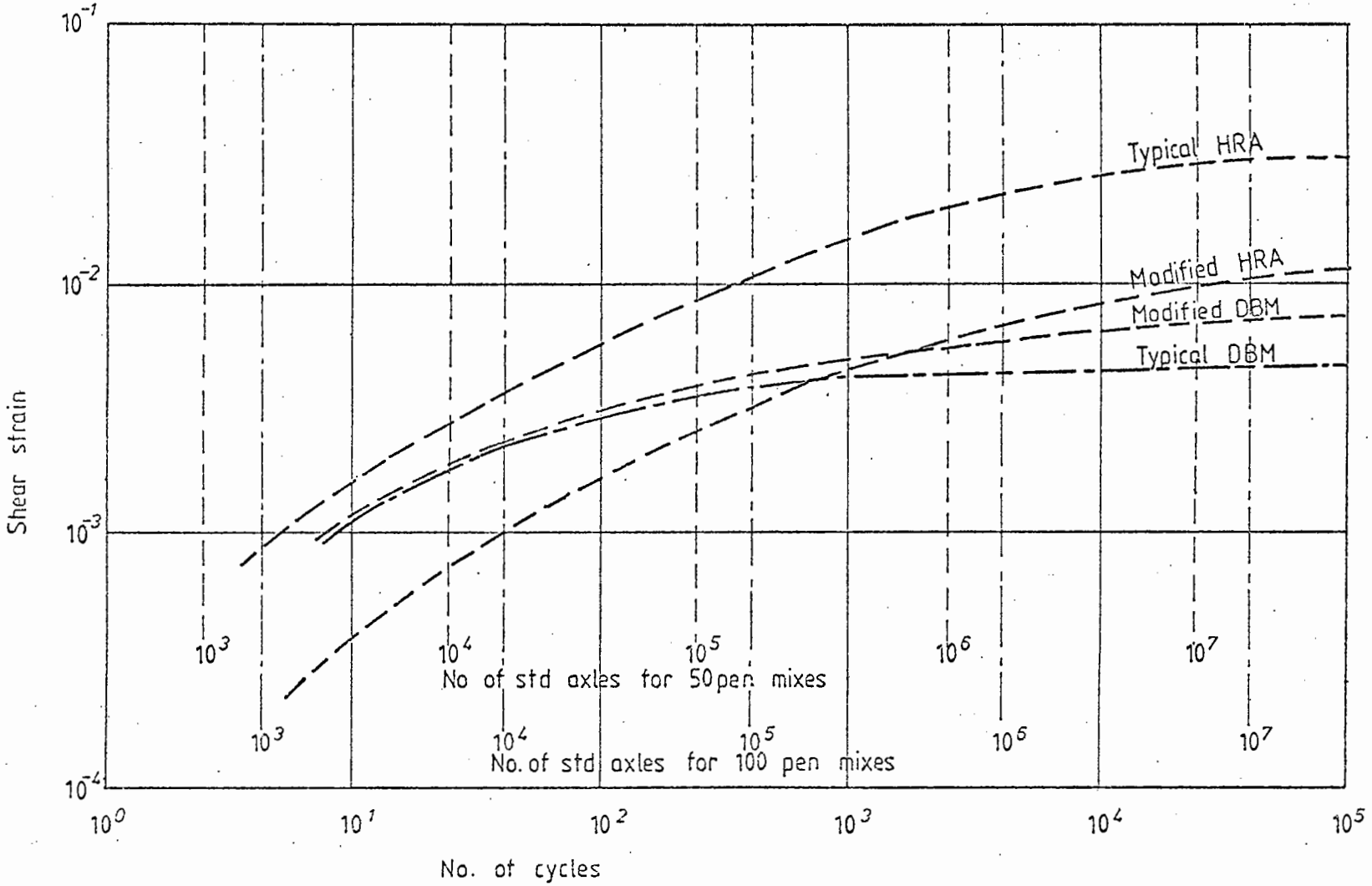

FIG 5·6 NUMBER OF STANDARD AXLES EQUIVALENT TO NUMBER OF CYCLES FOR REPEATED LOAD TEST

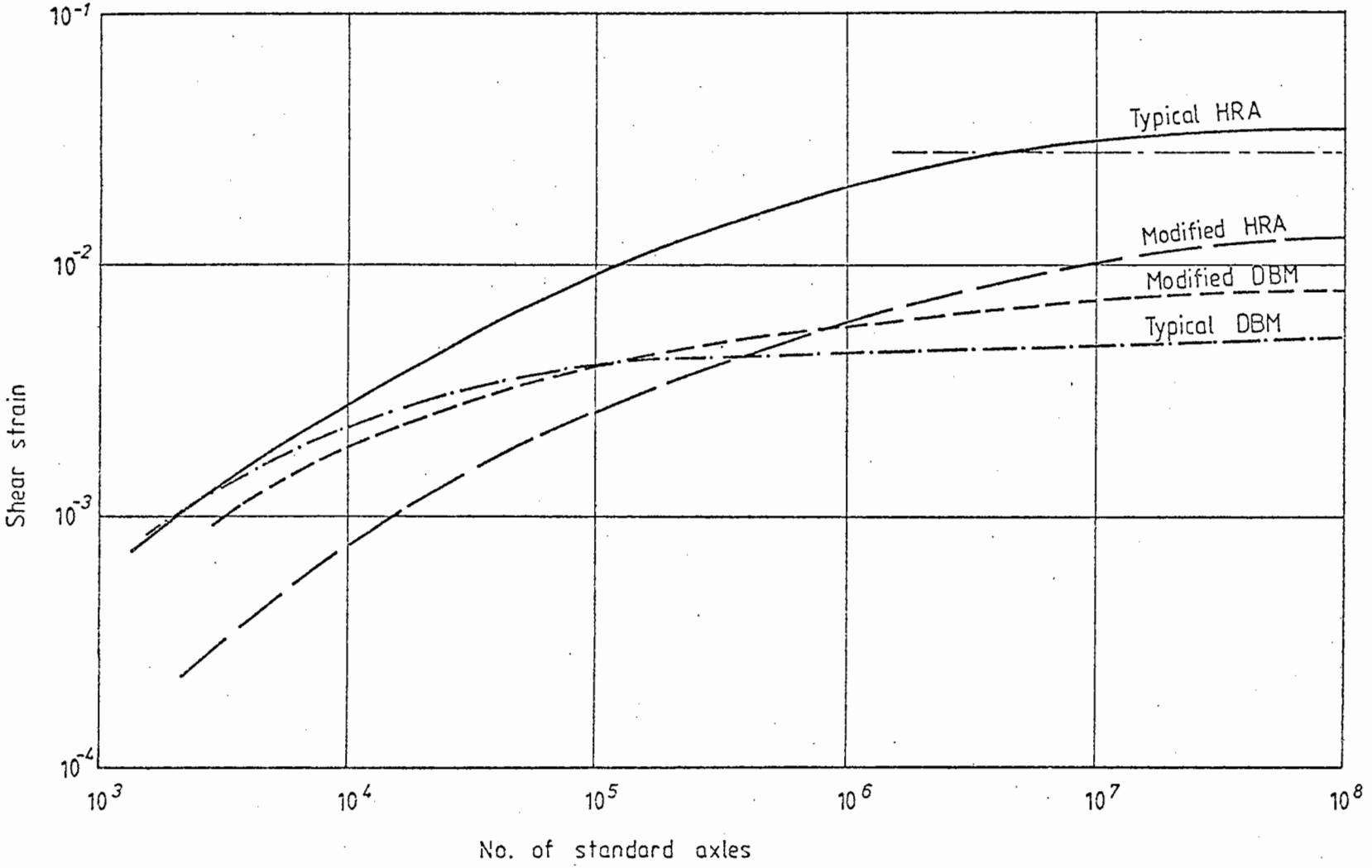

FIG 5·7 SHEAR STRAIN AS A FUNCTION OF NUMBER OF STANDARD AXLES FOR TYPICAL MIXES

In the triaxial test the measured volumetric and shear strains are:

$$\text{Volumetric strain, } \epsilon_v = \epsilon_a + 2\epsilon_c \qquad (5.4)$$

$$\text{Shear strain, } \epsilon_s = \frac{2}{3}(\epsilon_a - \epsilon_c) \qquad (5.5)$$

where ϵ_a = axial strain

ϵ_c = radial strain

Brown and Cooper (89) have shown that the volumetric strain in repeated load triaxial tests is dependent on the type of applied loading wave. (see Fig.5.8) These tests were carried out on a typical DBM using a mean normal stress p and deviator stress q as given in the figure. Typically, for the sinusoidal waveform used in the repeated load tests considered in this report, the volumetric strain fluctuated about zero and was small. This wave form is close to that which occurs in a pavement under passing wheel loads.

Assuming the volumetric strain can be taken as zero.

$$\epsilon_a = -2\epsilon_c \qquad (5.6)$$

$$\text{and} \quad \epsilon_s = \epsilon_a \qquad (5.7)$$

The values for shear strain can therefore be considered as equal to the axial strain. The axial strain is the deformation divided by the length of the specimen. For the triaxial tests these lengths were between 250 and 300mm. Using an average of 275mm and the strain values previously stated, the deformation of each material was calculated and the values are shown in Table 5.3.

Table 5.3 PERMANENT SHEAR STRAINS AND CORRESPONDING DEFORMATIONS OBTAINED FROM THE TRIAXIAL TEST RESULTS

Material	Permanent Shear Strain (%)	Deformation (mm)
Typical HRA	2.82	7.8
Typical DBM	0.53	1.5
Modified HRA	1.0	2.7
Modified DBM	0.72	2.0

Table 5.4 PROPERTIES FOR BISTRO CALCULATIONS

	HRA Surfacing	HRA base	Sub-base	Subgrade
Initial Penetration	50	50		
Binder Content (%)	7.9	5.7		
Void Content (%)	5.0	6.0		
Specific gravity of aggregate	2.7	2.7		
Specific gravity of binder	1.02	1.02		
Stiffness (MPa)	3400*	6190*	75	50
Poissons Ratio	0.4	0.4	0.3	0.4

* at 15°C and 40 km/hr.

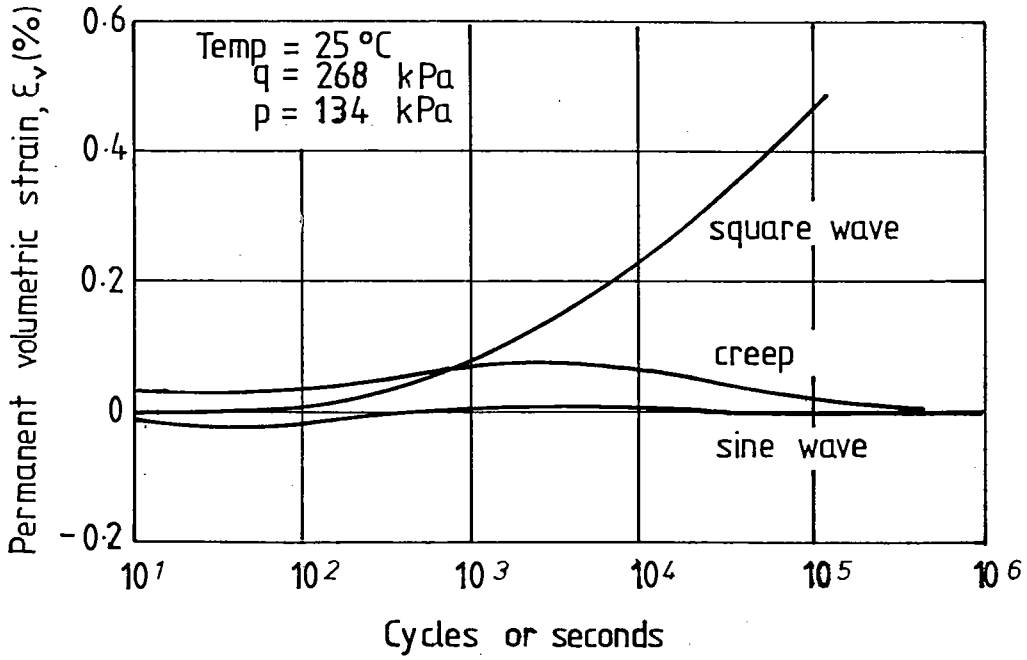

FIG 5·8 EFFECT OF MODE OF LOADING ON PERMANENT VOLUMETRIC STRAIN (AFTER BROWN AND COOPER (89))

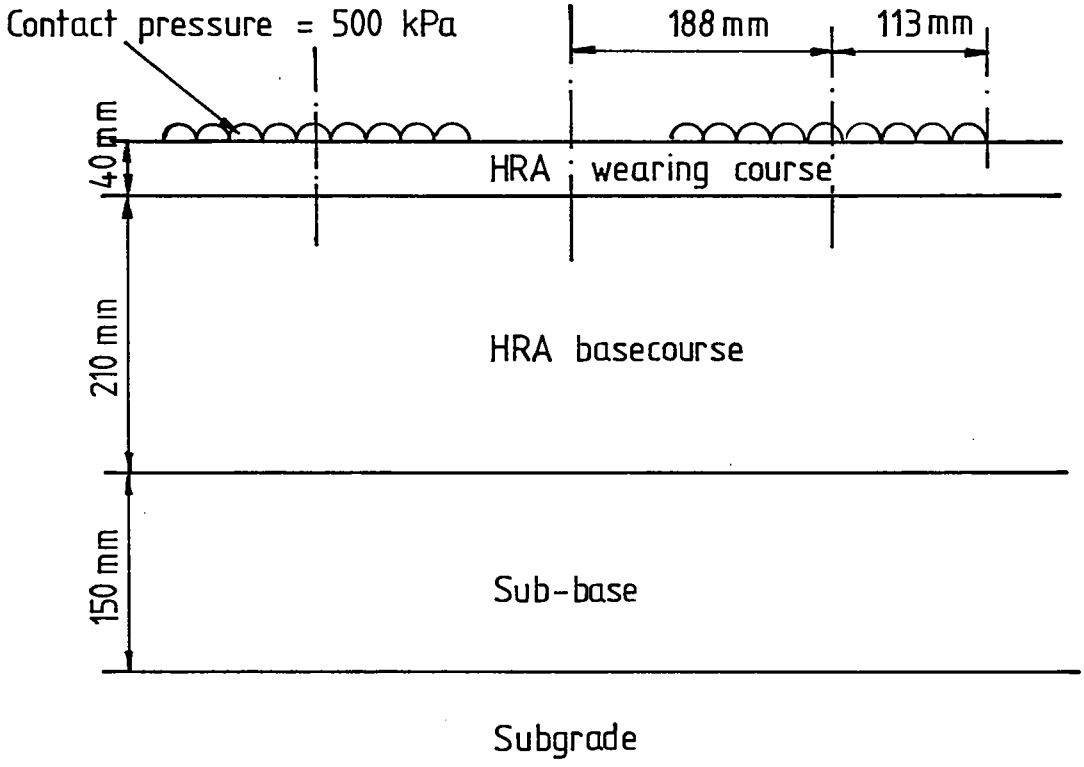

FIG 5·9 PAVEMENT STRUCTURE A1 CONINGTON LODGE

5.3.2 Relative contribution of layers to rutting

Lister (90) studied the development of permanent deformation in each layer of a typical structure at Conington Lodge on the A1. The structure consisted of 100mm of HRA, (say 40mm wearing course and 60mm base course), 150 HRA base and 150mm sub-base on a heavy clay. For the purposes of this study the HRA base course and base were combined to be a single layer, and the resulting structure is given in Fig.5.9. Using the results of Lister's work (see Fig.5.10) the permanent deformations of each layer in Spring 1971 were:-

HRA base + surfacing	4.0	mm
Sub-base	1.0	mm
Subgrade	4.0	mm
TOTAL	9.0	mm

The failure criterion for deformation is the development of a 20mm rut. For the structure at Conington Lodge, the deformation of the sub-base was constant and about 1mm. It was assumed that the sub-base contribution to a 20mm rut was the same so that the other layers contributed the remaining 19mm. The relative contribution to rutting of each layer is approximately proportional to the deformation of the layer. Since the base and surfacing together, and the subgrade, each had equal deformations then their contribution to a 20mm rut, will be the same. Hence, for a 20mm rut the contribution to rutting of each layer will be:-

HRA base + surfacing	9.5	mm
Sub-base	1.0	mm
Subgrade	9.5	mm
TOTAL	20	mm

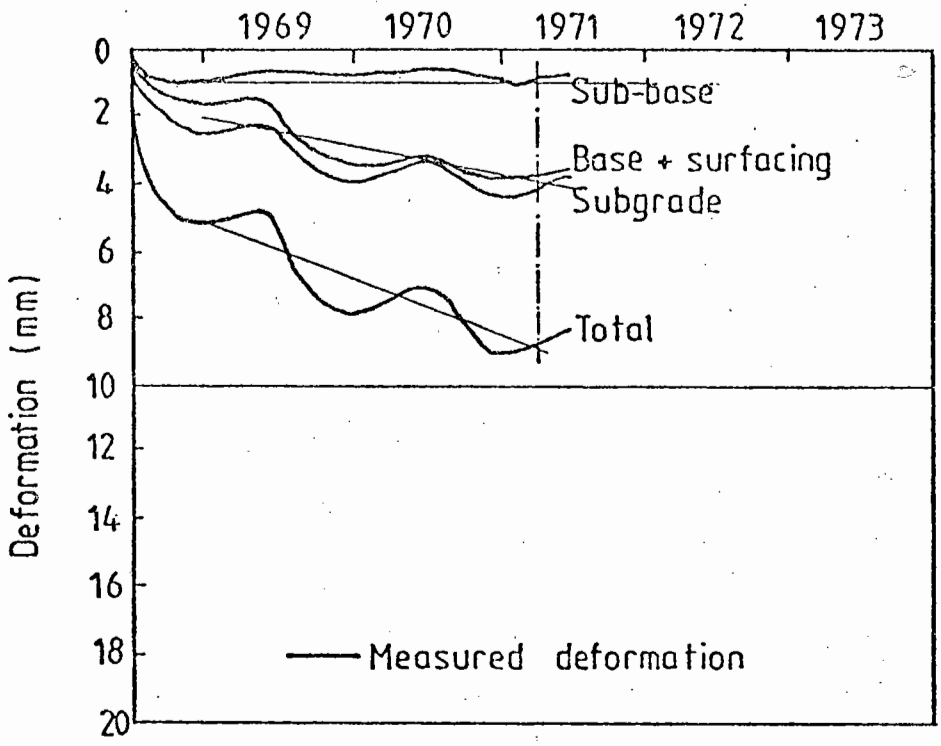

FIG 5·10 DEVELOPMENT OF PERMANENT DEFORMATION IN A PAVEMENT WITH A ROLLED ASPHALT BASE (AFTER LISTER (90))

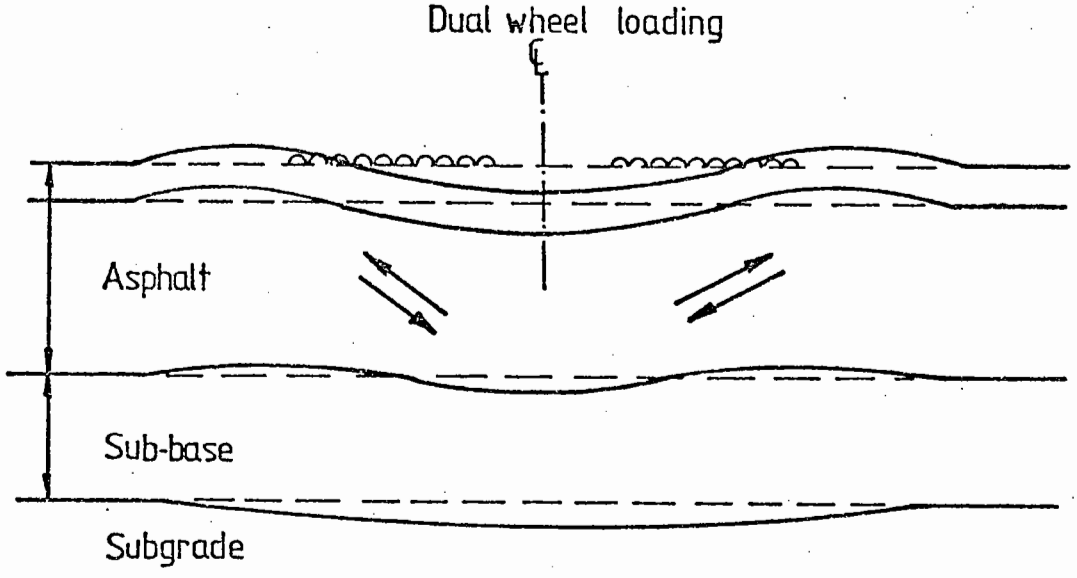

FIG 5·11 DEVELOPMENT OF PERMANENT DEFORMATION IN A PAVEMENT

In order to assess the effects of using various types of bituminous base materials, it is necessary to determine the separate contribution to rutting of the HRA surfacing and HRA base layers.

Fig.5.11 demonstrates that the developments of permanent deformation in an asphalt pavement layer is a shearing action in the absence of volumetric strain or compaction under traffic. The rut depth of a pavement can be calculated from the following relationship:-

$$\text{Rut depth, } R = \sum \epsilon_{pz} h \qquad (5.8)$$

where ϵ_{p_z} is the permanent vertical strain and

h is the layer thickness.

By considering a section of pavement which includes both the haunches and the rut then the total volumetric change in the asphalt layers will be approximately zero, (see Fig.5.11). From the previous discussion of the triaxial test it was shown that if the volumetric strain was zero then the axial strain was equal to the shear strain for conditions of axial symmetry. The permanent shear strain can be related to the shear stress and it is this latter parameter which has been used in the following analysis, assuming that the contribution to rutting is proportional to the shear stress times the layer thickness or:-

$$\frac{r_1}{r_2} = \frac{\tau_1 h_1}{\tau_2 h_2} \qquad (5.9)$$

where $r_1, r_2, \tau_1 \tau_2, h_1$ and h_2 are the contributions to rutting, average maximum shear stresses and thicknesses of the surfacing and base layers respectively.

The computer program BISTRO (38) was used to calculate the stress conditions at the mid-depths of the two asphalt layers at various distances from the centre line of a standard dual wheel load (see Fig.5.12). The properties used for each layer are given in Table 5.4. Table 5.5 tabulates the vertical stress, σ_z, the horizontal stress, σ_y and the shear stress, τ_{yz}, on the vertical and horizontal planes. The maximum shear stresses at each point were then calculated using Mohr's Circle and the values are shown in Fig.5.12.

The average maximum shear stresses for the surfacing layer and for the base layer were calculated as follows:-

$$\tau_{1\ Av\ Max} = \frac{161 + 2(169+41.4+165+99+69.3)}{11} \text{ kPa}$$

$$= \underline{113.5 \text{ kPa}}$$

$$\tau_{2\ Av\ Max} = \frac{18.6 + 2(68.1+122.7+151.5+122.4+89)}{11} \text{ kPa}$$

$$= \underline{102.4 \text{ kPa}}$$

The corresponding rut contributions for the two asphalt layers using equation(5.9) were, therefore;

$$\frac{r_1}{r_2} = \frac{113.5 \times 40}{102.4 \times 210}$$

Therefore, $$\frac{r_1}{r_2} = 0.211 \qquad (5.10)$$

but $$r_1 + r_2 = 9.5 \text{ mm} \qquad (5.11)$$

Therefore $r_1 = 1.9\text{mm}$ and $r_2 = 7.8\text{mm}$

Table 5.5 STRESSES AT MID-DEPTH IN THE BITUMINOUS LAYERS AS CALCULATED BY BISTRO

z coordinate (mm)	y coordinate (mm)	σ_y (KPa)	σ_z (KPa,	τ_{yz} (KPa)
20	0	321	0.1	0
20	75	449	236	131
20	188	576	495	-8.35
20	301	380	236	-149
20	376	193	0	-22.5
20	451	135	0	-15.7
145	0	6.61	43.8	0
145	75	-11.4	95.6	42.1
145	188	-421	187	-44.0
145	301	-11.7	94.3	-142
145	376	4.58	24.3	-122
145	451	2.6	6.2	-89.0

Table 5.6 COMPARATIVE RUT DEPTHS FOR STRUCTURES USING DIFFERENT BASE MATERIALS

Base	Total Rut Depth (mm)
HRA	20
DBM	13.7
Modified HRA	14.9
Modified DBM	14.2

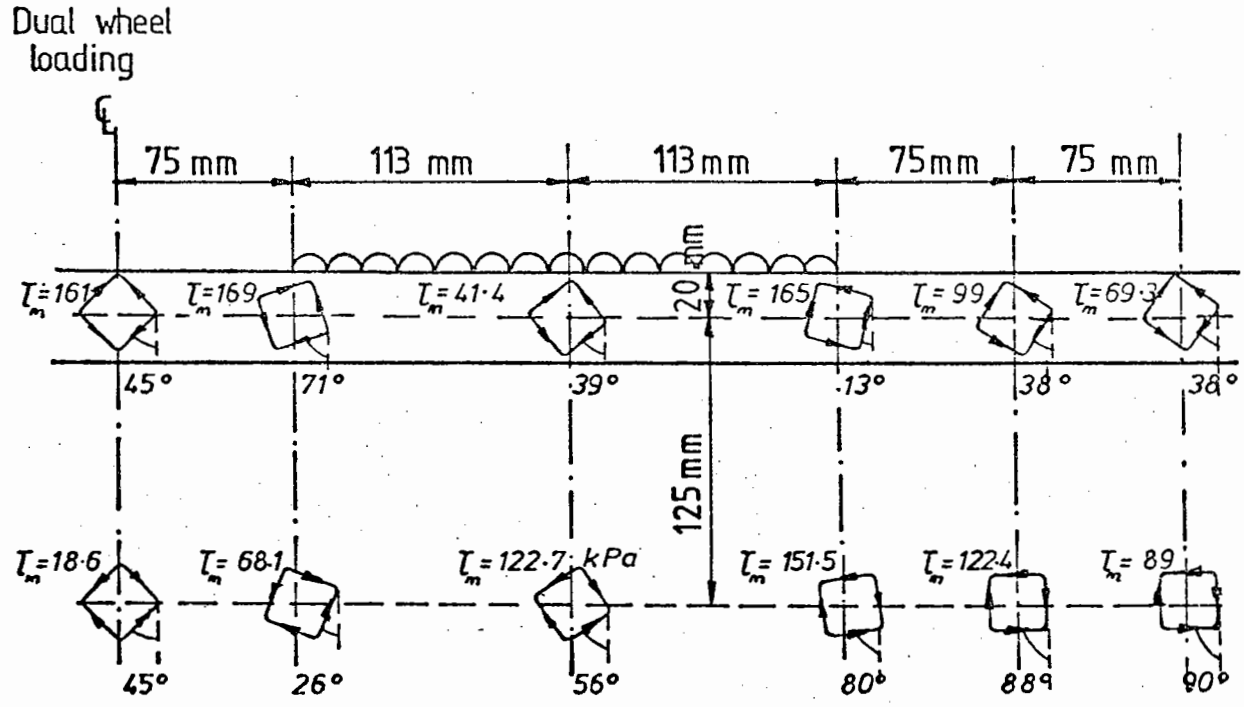

FIG 5·12 MAXIMUM SHEAR STRESSES AT MID DEPTH OF THE ASPHALT LAYERS

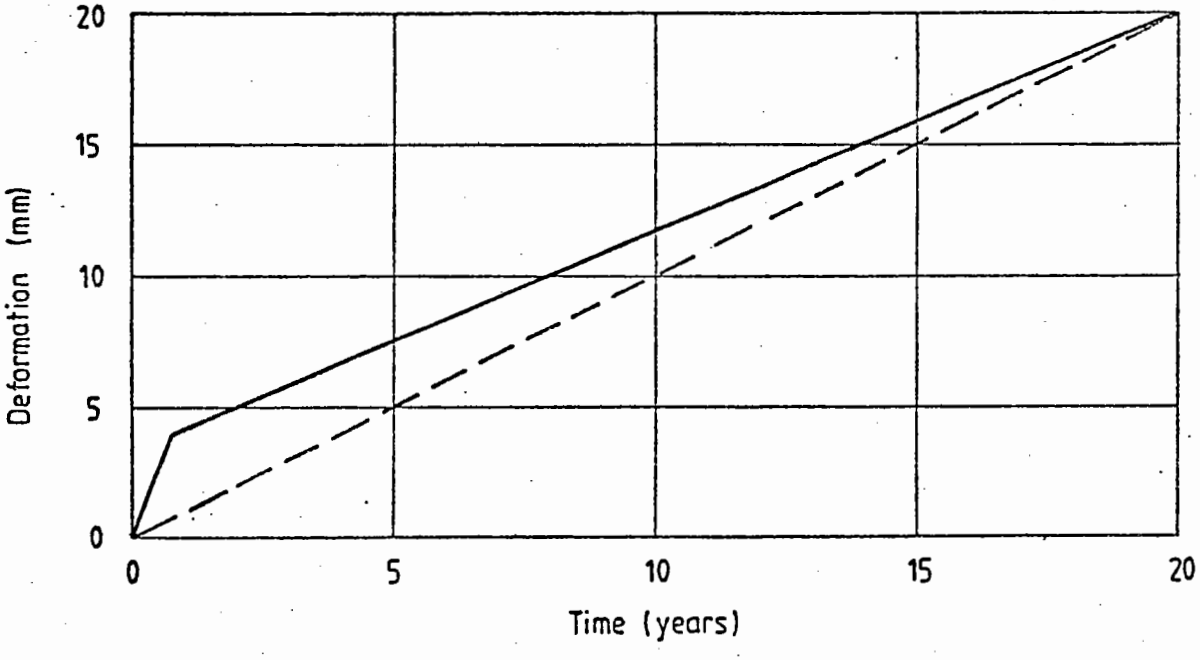

FIG 5·13 TYPICAL DEVELOPMENT OF DEFORMATION IN A PAVEMENT

Hence, the resultant contribution of each layer to the 20mm rut was:

HRA surfacing	1.7mm
HRA base	7.8mm
Sub-base	1.0mm
Subgrade	9.5mm

5.3.3 Development of rutting factors on life

Coincidentally, the deformation for the HRA base in Table 5.3 is the same (7.8mm) as the contribution to rutting calculated above for the Conington Lodge pavement. Therefore, if the HRA base in a structure was replaced by the same thickness of one of the other three types of materials with the same mix stiffness, after the same number of load applications, the total rut depths for the other structures would be as given in Table 5.6, i.e. the values in Table 5.3 + 12.2mm (for the remaining layers).

The dynamic stiffnesses of the four materials may not, in practice, be identical. For the typical mix proportions and binders given in Table 5.7 the stiffnesses range from 4310 to 6920 MPa compared with a value of 6190 MPa used in the computations for HRA described above. The Conington Lodge structure was, therefore, re-analysed with base stiffnesses of 4310 and 6290 MPa in order to check the influence of the mix stiffness on the original determinations of maximum shear stress and relative rut contribution. Table 5.8 gives the results of this analysis showing that, for the higher mix stiffness, the effects were negligible. For the stiffness of 4310 MPa there was a small increase in the contribution (+0.5mm) to rutting from the wearing course and a reduction for the base course (-0.5mm). The overall effect of varying the mix stiffness on the calculations for relative

Table 5.7 MIX DETAILS OF REPRESENTATIVE MATERIALS

	Typical Hot Rolled Asphalt	Typical Dense Bitumen Macadam	Modified Hot Rolled Asphalt	Modified Dense Bitumen Macadam
Initial Penetration	50	100	50	50
Binder Content (%)	5.7	3.5	4.5	4.5
Void Content (%)	6.0	10.0	8.0	8.0
Specific Gravity of Aggregate	2.7	2.7	2.7	2.7
Specific Gravity of Bitumen	1.02	1.02	1.02	1.02
Mix Stiffness* (MPa)	6200	4310	6920	6920

* Mix stiffnesses calculated at 15^0C and 40 km/hr.

Table 5.8 RELATIVE RUT CONTRIBUTIONS AND SHEAR STRESSES FOR DIFFERENT HRA BASE MIX STIFFNESSES

	HRA Base Mix Stiffness (MPa)		
	4310	6190	6920
Average maximum shear stress (kPa)			
layer (1) $\tau_{max(1)}$	146.4	113.5	112.3
layer (2) $\tau_{max(2)}$	93.7	102.4	95.7
Ratio of rut contribution			
r_1/r_2	0.298	0.211	0.224
Rut contribution (mm)			
r_1	2.2	1.7	1.7
r_2	7.3	7.8	7.8

Where $r_1 + r_2 = 9.5$mm

rut contributions from the bituminous layers in the Conington Lodge structure is therefore small. Hence, the remaining calculations were based on the contributions determined from the analysis using an HRA base stiffness of 6190 MPa.

From Table 5.6 it can be seen that the pavements with a typical DBM, modified HRA or modified DBM base layer can carry more traffic than the same pavement with the HRA base before a 20mm rut develops.

There are, typically, two stages of rut development; an initial fairly rapid one, followed by a second more gradual one as shown by the solid line in Fig.5.13. In practice the slope of the second stage does tend to decrease with time (see Fig.5.10). As an approximation, the dotted line in Fig.5.13 has been assumed to apply. The discrepancy is not very significant towards the end of the pavement life. Fig.5.7, produced from the triaxial test results, shows that beyond 0.5msa the shear strains in the HRA and modified HRA and, therefore, their contributions to rutting are continuing to increase. However, for the DBM and modified DBM, the shear strains and corresponding rut contributions are approximately constant. From Fig.5.10 it can also be seen that, whilst the subgrade deformation increases with time, the sub-base deformation is constant at 1mm. Hence, in order to obtain the additional life of the pavements with DBM, modified HRA and modified DBM base materials, the rut contribution of the subgrade, HRA wearing course and HRA base materials are taken to continue at the same rate, whilst the DBM, modified DBM and sub-base are taken to remain constant once the life of a similar pavement with an HRA base (generally greater than 0.5msa) has been reached. Fig.5.14 illustrates, diagramatically the relative pavement lives determined by this method.

N_{HRA} is the life of a pavement structure with a HRA base when a rut of 20mm has formed. The other three structures have the same thickness and stiffness but different types of base material and their

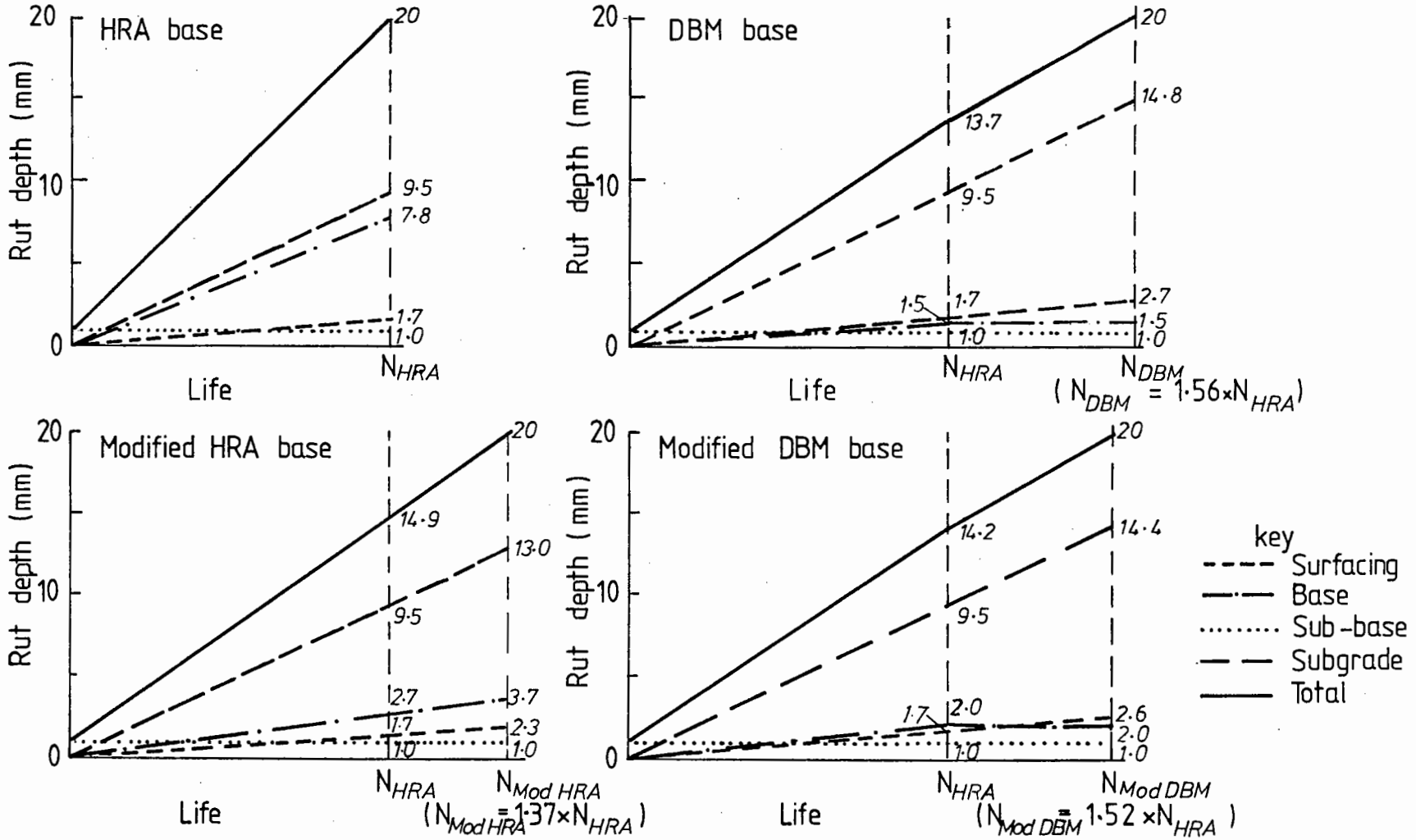

FIG 5.14 RUT DEPTHS AND RELATIVE LIVES DEVELOPED FOR DIFFERENT BASE MATERIALS

rut depths, after the same number of standard axles, are given in Table 5.6. The contributions to rutting of the individual layers were then adjusted as described above until a 20mm rut had been developed. At this point the life of the pavement is equal to N_{HRA} multiplied by a rut factor (f_r) as given in the diagram. These are 1.56, 1.37 and 1.52 for the DBM, modified HRA and modified DBM respectively.

Fig.5.15 shows the original allowable subgrade strain line, which applied for HRA bases, together with the proposed 'shifted' line for DBM obtained using the factor of 1.56. The other two materials fall in between.

5.4 APPLICATION OF CRITERION TO FULL DEPTH ASPHALT PAVEMENTS

The subgrade strain criterion was originally derived for pavements with a granular sub-base. Therefore, some justification is required before it can be applied to full depth asphalt pavements. The same criterion could be used if the rut depths developed for the two types of pavements are equal when their subgrade strains are equal. In this case, as the development of rutting is a shearing action, the maximum shear stresses in the asphalt layers should be similar.

This was checked using the Conington Lodge structure, (Fig.5.9 and Table 5.4). The computer program BISTRO calculated a vertical subgrade strain of 181 microstrain under a standard dual wheel loading arrangement. An equivalent full depth asphalt pavement with approximately the same subgrade strain (182$\mu\epsilon$) was determined by replacing the 150mm of granular sub-base in the Conington Lodge structure with an additional 10mm of the HRA base. The stress conditions in the full depth asphalt pavement were then calculated at the same positions as previously and the values are given in Table 5.9. Fig.5.16 shows the resulting maximum shear stresses obtained by Mohr's circle. Table 5.10 compares the maximum shear stresses for the two

Table 5.9 STRESSES IN THE BITUMINOUS LAYERS OF THE FULL DEPTH ASPHALT STRUCTURE

z coordinate (mm)	y coordinate (mm)	σ_y (kPa)	σ_z (kPa)	τ_{yz} (kPa)
20	0	311	0	0
20	75	438	236	131
20	188	566	495	-7.9
20	301	373	236	-148
20	376	189	0.5	-21.3
20	451	134	0	-14.7
145	0	31	46.3	0
145	75	12.9	99.7	41.0
145	188	-19.5	19.4	-43.6
145	301	6.3	98.4	-139
145	376	18.1	25.3	-120
145	451	11.9	5.7	-87.8
150	0	5.3	45.1	0
150	75	-12.0	94.0	38.1
150	188	-41.0	181	-43.4
150	301	-12.9	92.6	-136
150	376	2.8	24.9	-118
150	451	1.1	6.0	-87.8

Table 5.10 COMPARISON OF MAXIMUM SHEAR STRESSES

	y coordinate (mm)	Maximum Shear Stress (kPa)	
		Structure 1 Conington Lodge	Structure 2 Full Depth Asphalt
At depth 20mm	0	161	155.5
	75	169	165.5
	188	41.4	36.4
	301	165	163
	376	99	96.6
	451	69.3	68.6
Average for layer		113.5	110.5
At depth 145mm	0	18.6	7.7
	75	68.1	59.7
	188	122.7	115.3
	301	151.5	146.4
	376	122.4	120
	451	89	87.9
Average for layer		102.4	96.9
At depth 150mm	0		19.9
	75		56.3
	188		119.7
	301		145.9
	376		118.5
	451		87.5
Average for layer			97.8

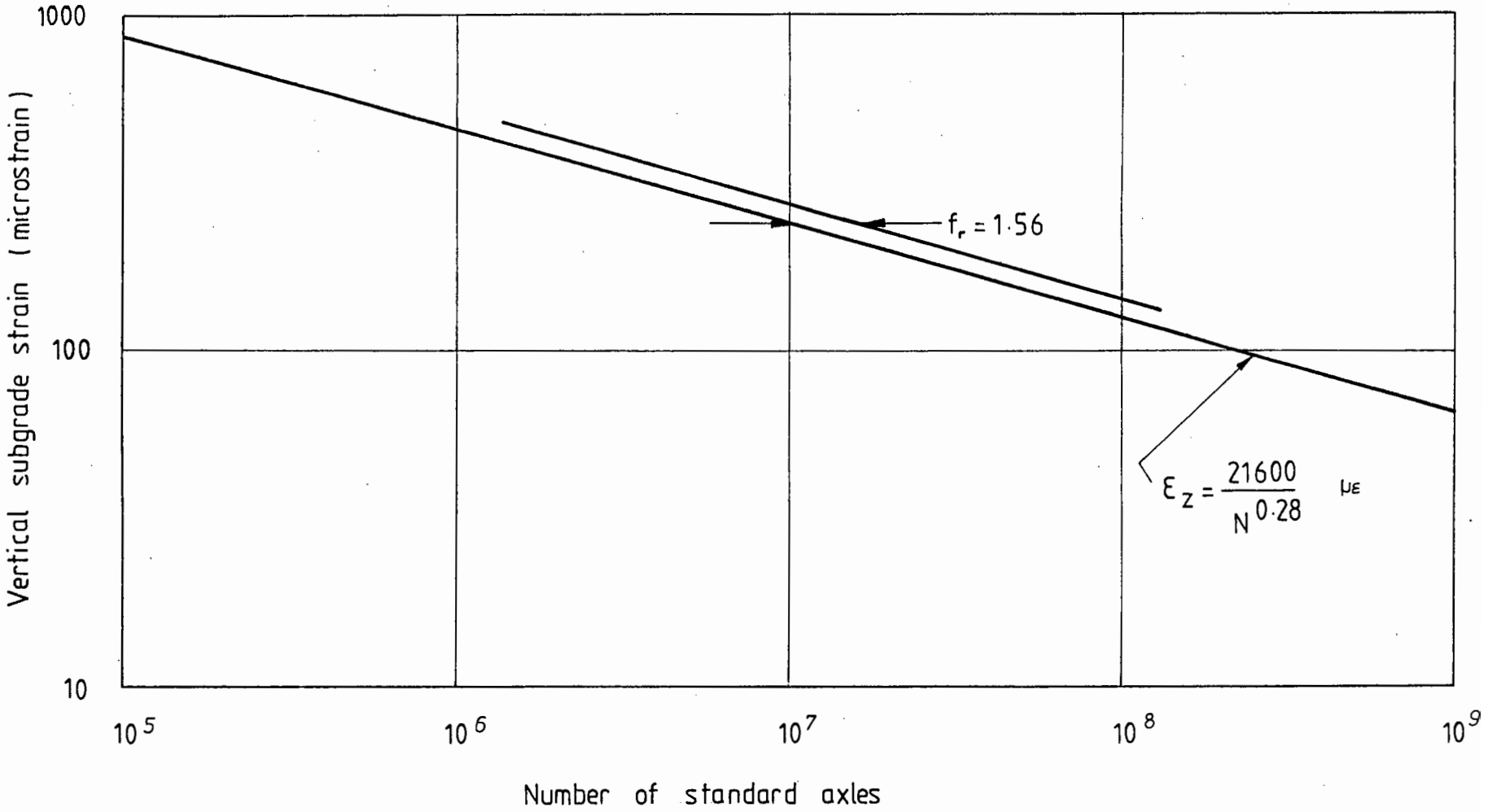

FIG 5·15 MAXIMUM ALLOWABLE SUBGRADE STRAIN CRITERION

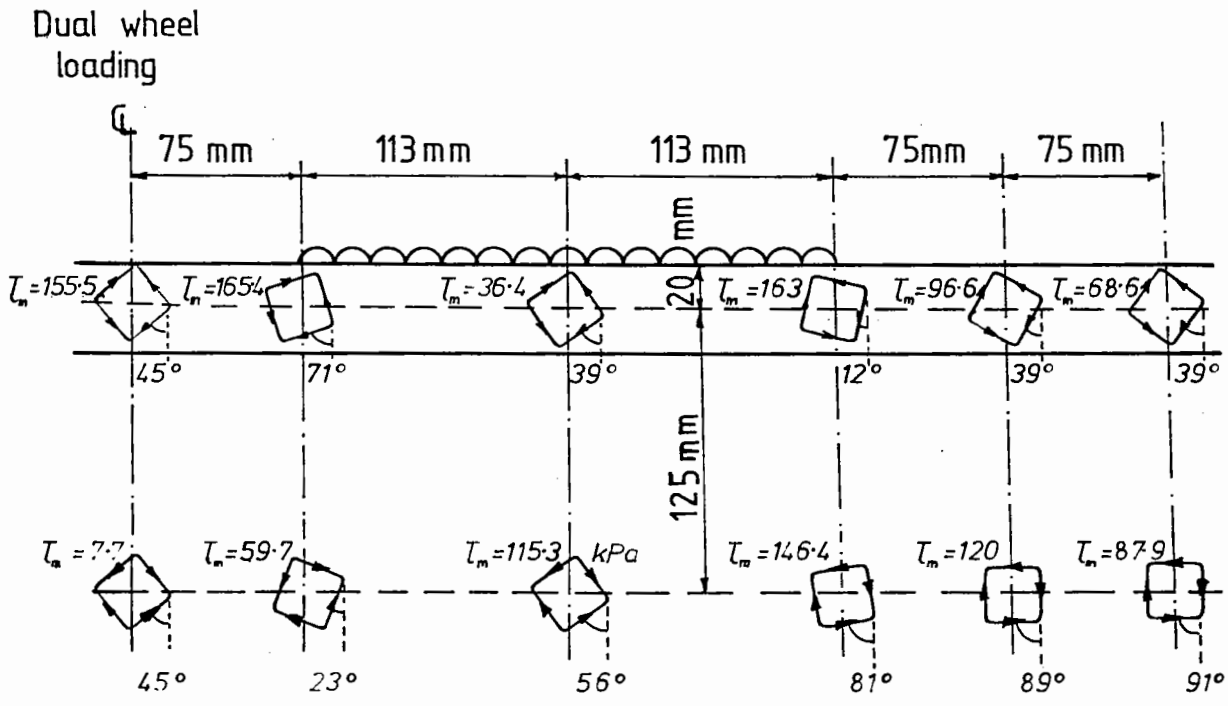

FIG 5·16 MAXIMUM SHEAR STRESSES IN A FULL DEPTH ASPHALT STRUCTURE

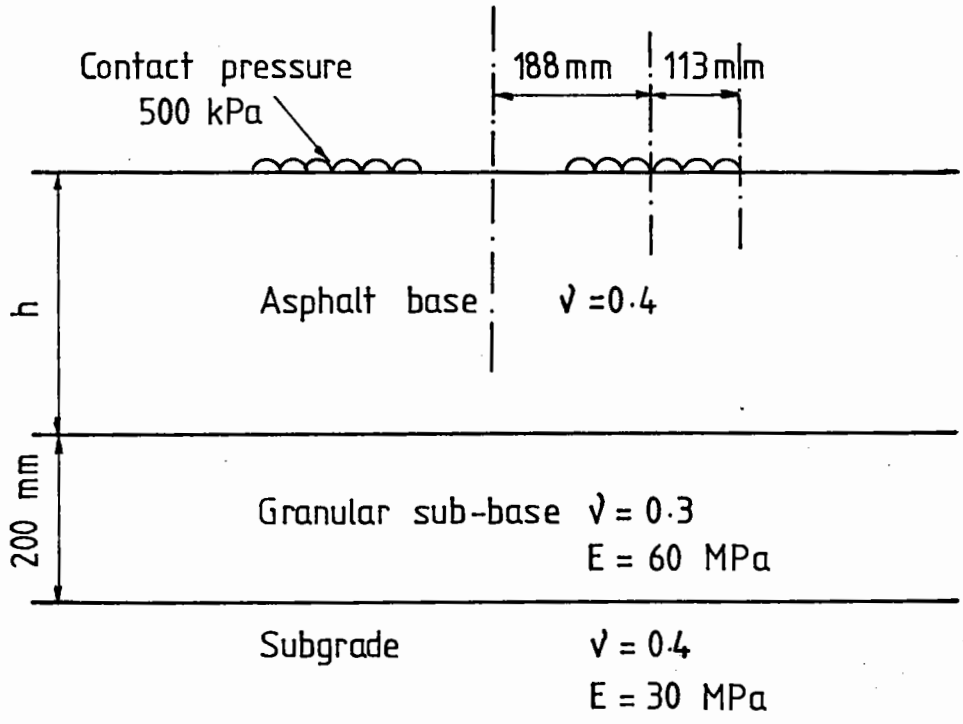

FIG 5·17 TYPICAL THREE LAYERED STRUCTURE

structures at the same points and also at the mid depth of the asphalt base layer in the full depth pavement.

Although the maximum shear stresses at the same depth in the two structures are in fairly close agreement, those in the full depth structure are always slightly smaller. If the maximum shear stresses in the HRA base layers are compared at their mid-depths then there is better agreement. As the maximum stresses developed in the two are of similar magnitude, then the ruts developed should be approximately equal. Therefore, it is appropriate to adopt the same subgrade strain criterion for full depth asphalt structures.

5.5 ASSESSMENT OF REVISED PERMANENT DEFORMATION CRITERION

The effect of introducing the revised subgrade strain criterion is to increase the pavement life against deformation for structures with DBM or modified mix bases. However, the deformation criterion is not always the critical design case. A simple three layered structure, (see Fig.5.17) with varying base materials and thicknesses has been analysed by using the PET programs to determine the effect on the design life. The mix details and loading conditions are given in Table 5.11.

Fig.5.18 shows the results of these computations. For the pavement with the HRA base the design life remains the same. The figure for the DBM base illustrates the fact that although the life for the pavement based on deformation has increased, for this particular mix, the design life is determined by the fatigue criterion. However, for the two modified mixes the design life of the pavement has shifted to the right, representing an increase in life of approximately 50%, because the deformation criterion was the critical case. Alternatively, it represents a saving of 15 mm in the thickness of the asphalt base required for a specific design life.

Table 5.11 INPUT PARAMETERS FOR PET PROGRAM DESIGN CALCULATIONS

	HRA base	DBM base	Modified HRA base	Modified DBM base
Mix Details				
Initial Penetration	50	100	50	50
Binder Content (%)	5.7	3.5	4.5	4.5
Void Content (%)	6.0	10.0	8.0	8.0
Specific Gravity of Aggregate	2.7	2.7	2.7	2.7
Specific Gravity of Bitumen	1.02	1.02	1.02	1.02
Design Conditions				
Speed (km/hr)	40	40	40	40
Average Annual Air Temperature (^{0}C)	9.5	9.5	9.5	9.5

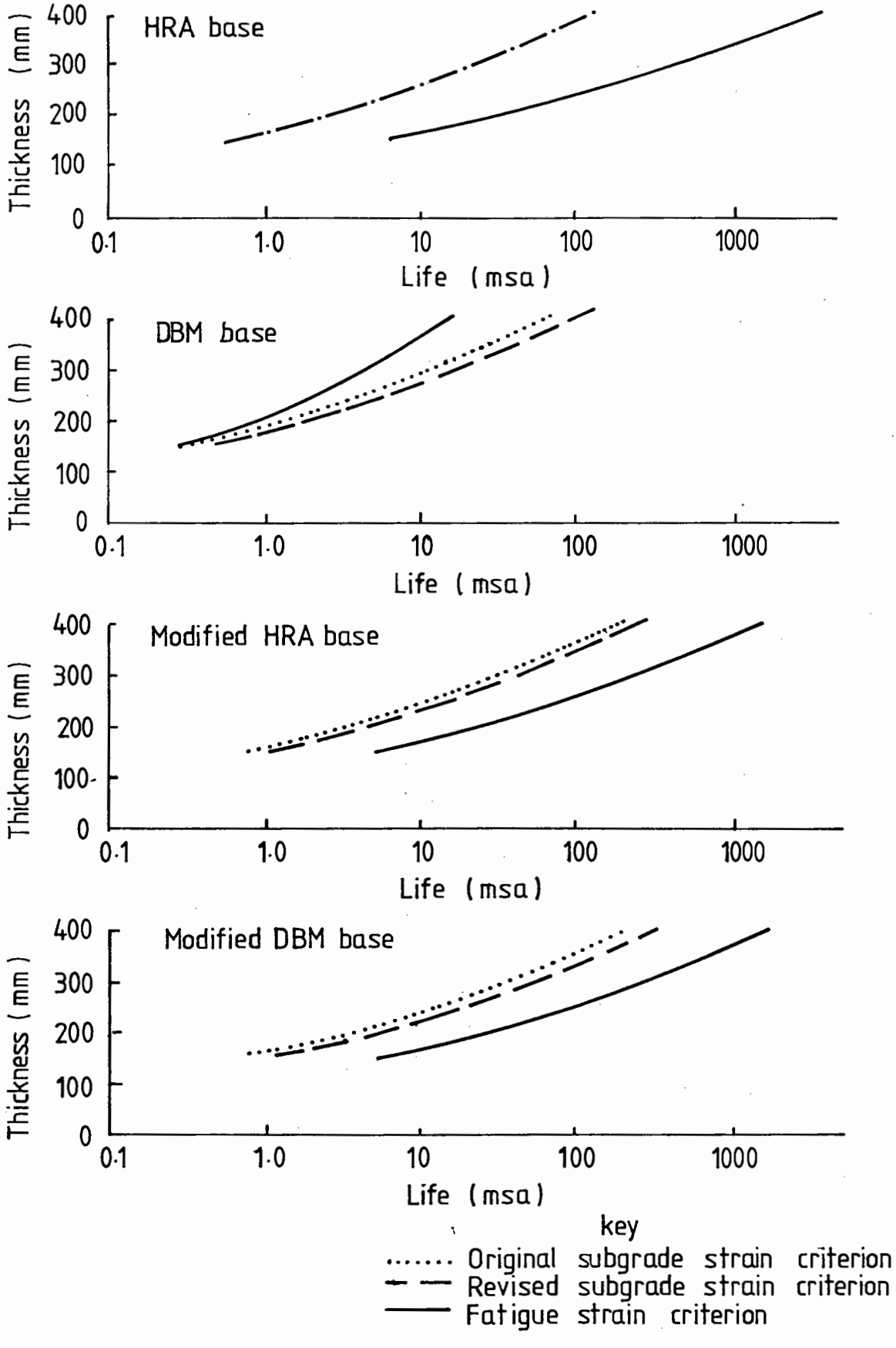

FIG 5.18 EFFECT OF REVISED SUBGRADE STRAIN CRITERION ON THICKNESS

CHAPTER SIX

DEVELOPMENT OF COMPUTER PROGRAMS FOR DESIGN

The development of four simple pavement design programs for use on the Commodore Pet microcomputer was discussed in Chapters 3 and 4. These programs were:

Simple design method (SDM)

Balanced design method (BDM)

Design life method (DLM)

Cumulative damage method (CDM)

Since they were first written, several changes have been made to the programs. These changes were mainly due to the development of the temperature conversion factors and revised design criteria against fatigue cracking and permanent deformation, (see Chapters 4 and 5). A user manual for the present version of the PET microcomputer programs has been written (48).

The principles established in these simple microcomputer programs have been used to develop more flexible packages for the main frame computer. This has resulted in the development of two new programs; ANPAD and CUDAM.

6.1 ANPAD COMPUTER PROGRAM

6.1.1 General Description

ANPAD (ANalytical PAvement Design) is a computer program based on the use of linear elastic analysis. It incorporates three design alternatives, calculating the design thickness, mix proportions for a balanced design or the design life. A user manual for ANPAD has been written (48). It includes flow diagram (Fig.6.1) and listing of the required input data (Table 6.1). Some of the data which is required

Table 6.1 INPUT DATA REQUIRED FOR ANPAD

Input Data	Design Option			Format (FC.0 unless otherwise specified)	Examples	Units
	Design Thickness	Balanced Design	Design Life			
1. TEXT, DATA	X	X	X	15A4	Test 23/5/82	
2. NO. OF DESIGNS	X	X	X	I1	1	
3. OPTION 1 for design thickness 2 for balanced design 3 for design life	X	X	X	I1	1	
4. TEMPERATURE: Average annual air temperature	X	X	X		9.0	°C
5. SPEED: Average speed of commercial vehicles	X	X	X		35.0	km/hr
6. LIFE: Design life in millions of standard axles	+	+	-	F10.0	30.0	msa
7. LIFE: Design life in years. This is only required for options 1 and 2 if input 6 is left blank	+	+	-	F10.0	20.0	years
8. INITIAL NO. OF COMMERCIAL VEHICLES: Only required for options 1 and 2 if the design life is given in years (Input 7) Optional for design life method	+	+	+	F10.0	1000.0	
9. PERCENTAGE GROWTH RATE Only required for options 1 and 2 if the design life is given in years. Optional for design life method.	+	+	+	F10.0	1.1	%
10. NO. OF LAYERS (N)	X	X	X	I2	04	
When applicable Inputs 11 to 16 are required for the upper bituminous layers, starting with the surfacing layer 1 to layer (N-3)						
11. THICKNESS	X	X	X		0.060	metres
12. BINDER CONTENT	X	X	X		7.2	%
13. VOID CONTENT	X	X	X		4.0	%
14. SPECIFIC GRAVITY OF AGGREGATE	X	X	X		2.7	
15. SPECIFIC GRAVITY OF BITUMEN	X	X	X		1.02	

Contd...

Table 6.1 Cont'd.

Input Data	Design Option			Format. (F0.0 unless otherwise specified)	Examples	Units
	Design Thickness	Balanced Design	Design Life			
16. INITIAL PENETRATION, INITIAL SOFTENING POINT, RECOVERED PENETRATION and RECOVERED SOFTENING POINT. That is 4 inputs but only the Initial Penetration is essential, the others may be estimated within the program.	X+++	X+++	X+++		50.0	4F10.0
For the Base Layer						
17. THICKNESS	-	X	X		0.300	metres
18. BINDER CONTENT	X	-	X		4.2	%
19. VOID CONTENT	X	-	X		6.0	%
20. SPECIFIC GRAVITY OF AGGREGATE	X	X	X		2.65	
21. SPECIFIC GRAVITY OF AGGREGATE	X	X	X		1.01	
22. INITIAL PENETRATION etc.	X+++	X+++	X+++	4F10.0	50.0	
23. TYPE OF BASE MATERIAL. 1,2,3 or 4 depending on whether the base material is a HRA, DBM, Modified HRA or Modified DBM respectively	X	X	X		3	
24. SUBBASE THICKNESS	X	X	X		0.250	metres
25. SUBGRADE CBR	X	X	X		2.3	%
26. SUB-BASE TO SUBGRADE MODULAR RATIO. This is generally between 1.5 and 5.0, typcially 2.0 say.	X	X	X		2.0	
If no. of structures is greater than 1 then repeat 3 to 26.						

KEY

X required

+ optional

- not required

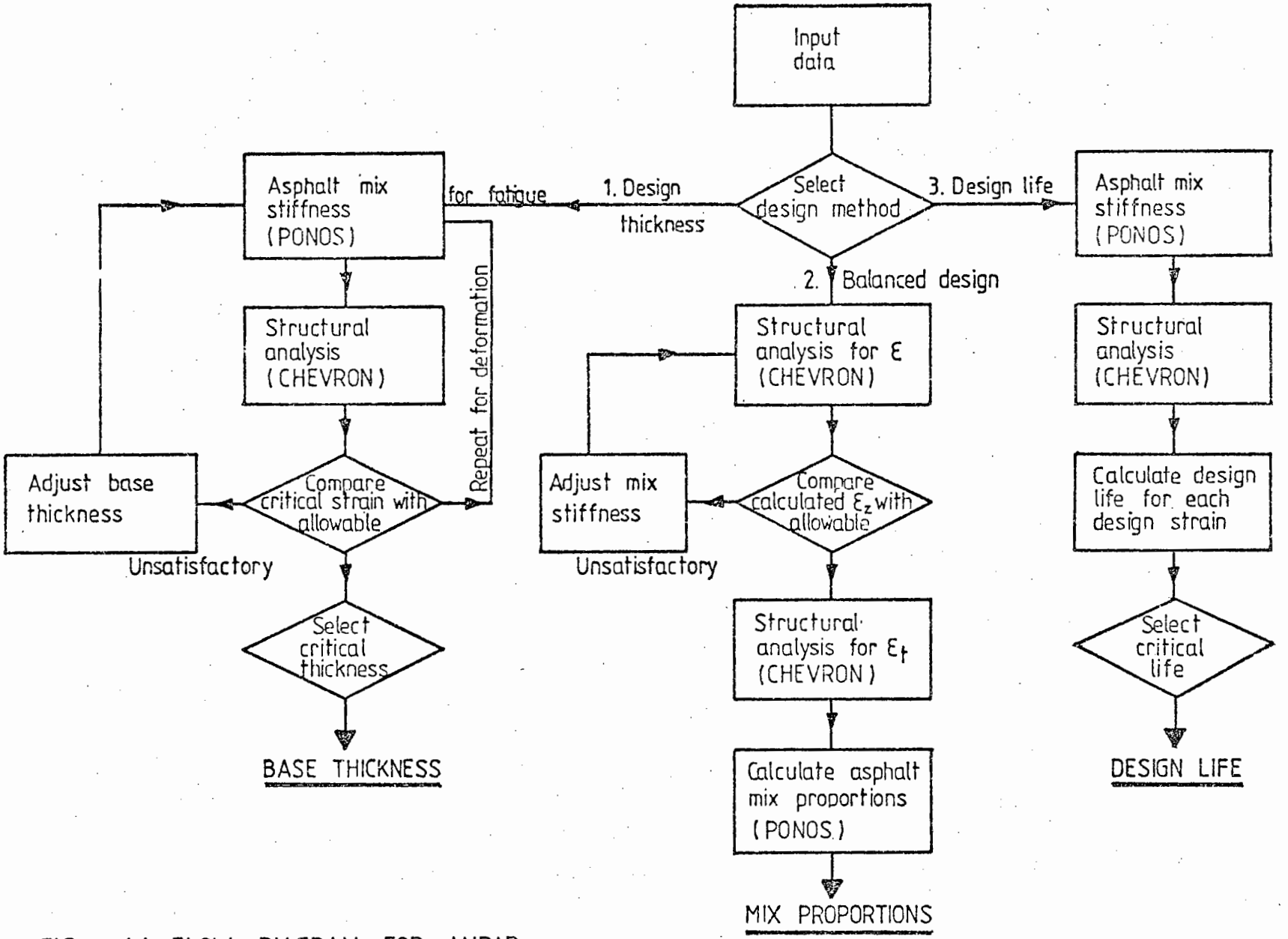

FIG 6.1 FLOW DIAGRAM FOR ANPAD

depends on the selected design calculation. Certain data can be estimated from within the program if necessary. Parts of the program PONOS (58) are used to calculate the dynamic stiffness of the asphalt layers. ADEM, a less versatile computer program to calculate pavement design thickness only (57), was developed in earlier research at Nottingham sponsored by ACMA using the Shell program, BISTRO, for the structural analysis. For this research project, for the programs ANPAD and CUDAM, however, it was decided to use the Chevron N-layer program (39) as the central analytical tool. The critical strains calculated with it are very similar to those obtained using BISTRO. Fig.6.2 illustrates a typical pavement configuration with the applied dual wheel loading which is used. The designer can incorporate three or more layers. In all cases the subgrade is overlain by a granular sub-base followed by one or more upper bitumen bound layer(s). The lowest bitumen bound layer in the pavement is the design layer, and is the main structural component; in conventional practice, the road base.

6.1.2 Maximum Allowable Strains

The critical parameters used in ANPAD are the same as those used in the simple PET programs, i.e. the maximum asphalt tensile strain at the bottom of the base and the vertical compressive strain at the top of the subgrade.

The maximum allowable asphalt strain is calculated within the program from the revised fatigue strain criterion developed in Chapter 4. The criterion, given in equation (6.1), incorporates a factor of 440 to convert design lives (based on laborataory fatigue tests) to field lives.

$$\log \epsilon_t = \frac{14.39 \log V_B + 24.2 \log SP_i - 40.06 - \log N}{5.13 \log V_B + 8.63 \log SP_i - 15.8} \qquad (6.1)$$

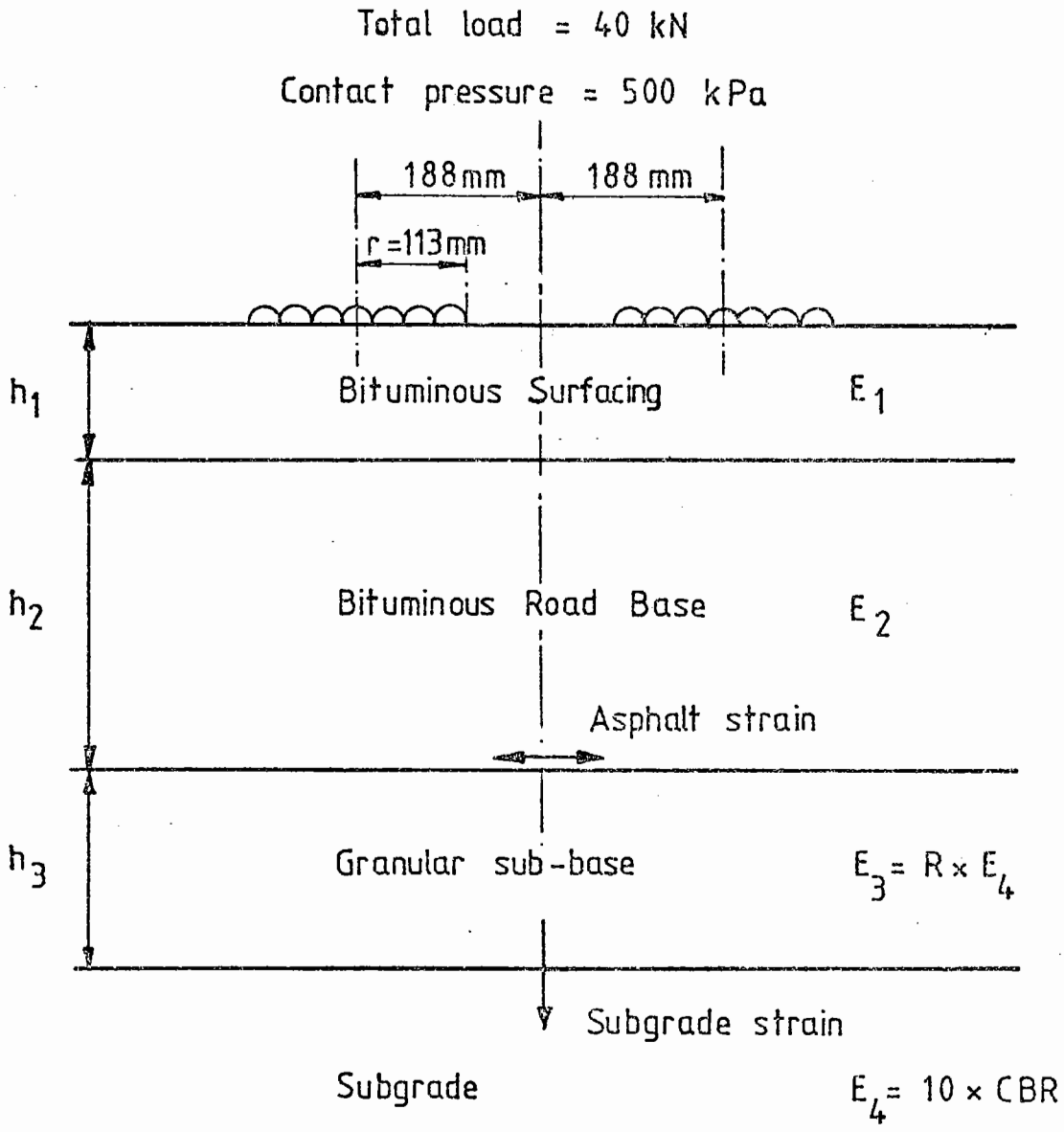

FIG. 6.2 TYPICAL FOUR LAYERED STRUCTURE FOR ANPAD

where V_B = binder content by volume (%)

SP_i = initial binder softening point (°C)

N = number of load applications to failure

ϵ_t = tensile strain ($\mu\epsilon$)

The maximum allowable subgrade strain ϵ_z, is calculated using the following equation developed in Chapter 5:

$$\epsilon_z = \frac{21600}{(N/fr)^{0.28}} \qquad (6.2)$$

where ϵ_z = subgrade strain ($\mu\epsilon$)

N = number of load applications to failure

fr = rut factor varying between 1.0 and 1.56, depending on the base material, see Chapter 5.

6.1.3 Temperature

The temperature input should be the average annual air temperature (which can be estimated from local meteorological data). This temperature is converted, within the program, into two design temperatures using the following relationships derived in Chapter 4;

For the subgrade strain calculations,

Design Temperature = 1.47 x Average annual air temperature (6.3)

For the fatigue strain calculations,

Design Temperature = 1.92 x Average annual air temperature (6.4)

The 1.92 factor used in equation (6.4) takes account of cumulative damage for fatigue cracking.

6.1.4 Stiffness Moduli

The binder stiffnesses of each bituminous layer, (apart from the base layer for a balanced design), are calculated within the program using the PONOS sub-routine (58) together with the known binder properties, for the relevant design temperature. The equation used to calculate the loading time, t seconds, for a particular layer, at speed V km/hr is:

$$\log_{10} t = 0.5\ Z - 0.2 - 0.945 \log V \qquad (6.5)$$

where Z is the depth in metres to the centre of the layer.

The mix stiffness is determined from the binder stiffness and percentage voids in mixed aggregate (VMA) using the same equation as adopted in the PET programs and Brown's simplified design method (50), i.e.,

$$S_m = S_b \left[1 + \frac{257.5 - 2.5\ VMA}{n(VMA - 3)} \right]^n \qquad (6.6)$$

$$\text{where } n = 0.83 \log \left[\frac{4 \times 10^4}{S_b} \right]$$

S = mix stiffness (MPa)

VMA = voids in mixed aggregate

Void contents > 3%.

For the design thickness alternative the mix stiffness of the base layer is recalculated when its thickness is adjusted, (see Section 6.1.6), as this affects the loading time.

The subgrade modulus of elasticity is estimated within the program from the CBR using the following equation:

$$E_{subgrade} = 10 \times CBR \quad MPa \qquad (6.7)$$

The sub-base modulus is calculated from the subgrade modulus using the selected modular ratio. Previous studies using the SENOL non-linear finite element computer program (44) have shown that the modular ratio lies between 1.5 and 7.5 depending on the relative thicknesses and stiffnesses of the other layers, (see Table 2.2). A typical value is about 2 as used in the simple PET programs.

6.1.5 Vehicle Damage Factors

TRRL Laboratory Report 910 (91) gives background information on the determination of vehicle damage factors recommended in Road Note 29 (1) and subsequently by the Department of Transport (92) and LR 910 (91). Tables 6.2 and 6.3, taken from LR 910, give the damage factors and the year for which they were selected. Table 6.3 shows that there is a large step in the vehicle damage factors at 250, 1000, and 2000 initial number of commercial vehicles. Hence, the resulting number of standard axles determined for vehicle figures close to these limits can vary substantially. A more practical method was therefore considered necessary.

Figs.6.3 and 6.4, taken from LR 910, show the estimated changes in the number of axles per commercial vehicle and standard axles per commercial axle for the four traffic categories. Table 6.4 gives the number of axles per commercial vehicle and the maximum and minimum number of standard axles per commercial axle for the year when the recommended vehicle damage factor was determined. These values were read from Figs.6.3 and 6.4. The maximum number of standard axles per

Table 6.2 VEHICLE DESIGN FACTORS RECOMMENDED FOR THE DESIGN OF NEW ROADS (after Currer et al (91))

CATEGORY OF ROAD (Commercial vehicles per day in one direction)	STANDARD AXLES PER COMMERCIAL VEHICLE	
	Road Note 29 (1970)	Present
>2000	1.08	2.9
1000–2000	1.08	2.25
250–1000	0.72	1.25
<250	0.45	0.75

Table 6.3 VEHICLE DAMAGE FACTORS RECOMMENDED FOR THE ESTIMATION OF THE REMAINING LIVES OF EXISTING ROADS AND FOR THE DESIGN OF PAVEMENT STRENGTHENING MEASURES (after Currer et al (91))

Year	CATEGORY OF ROAD (Commercial vehicles per day in one direction)			
	<250	250-1000	1000-2000	>2000
1945	0.15	.25	.40	
6				
7	0.20	.30	.45	
8				
9				
1950				
1				
2		.35	.50	
3				
4				
5			.55	
6	.25	.40	.60	
7				
8				
9		.45	.65	
1960			.70	
1				
2			.75	
3		.50	.80	
4				
5	.30		.85	
6		.55	.90	
7				
8			.95	
9		.60		
1970			1.00	1.00
1	.35	.65	1.05	1.05
2				1.20
3		.70	1.15	1.35
4		.75	1.20	1.50
5	.40		1.25	1.60
6		.80	1.30	1.80
7			1.35	1.95
8		.85	1.40	2.05

Year	CATEGORY OF ROAD (Commercial vehicles per day in one direction)			
	<250	250-1000	1000-2000	>2000
9	.45	.90	1.50	2.20
1980		.95	1.60	2.30
1			1.65	2.40
2	.50	1.00	1.75	2.45
3	.55	1.05	1.85	2.55
4	.60		1.95	2.65
5		1.10	2.00	2.70
6		1.15	2.05	2.80
7		1.20	2.15	2.85
8	.65		2.20	2.90
9	.70	1.25	2.25	2.95
1990		1.30	2.30	3.00
1	.75	1.35		
2			2.35	3.05
3	.80	1.45	2.40	3.10
4			2.45	3.15
5	.85	1.50		
6		1.55	2.50	
7	.90		2.55	3.20
8	.95	1.60	2.60	3.25
9		1.65	2.65	
2000	1.00			3.30
1		1.70	2.70	
2	1.05	1.75		3.35
3			2.75	
4	1.10	1.80		
5	1.15	1.85	2.80	3.40

Table 6.4 VEHICLE DAMAGE FACTORS

Commercial Vehicles per day	Year (see table 6.3)	Axles per commercial Vehicle A	Standard axles per commercial axle, S		Vehicle damage factor, A x S	
			Max	Min	Max	Min
> 2000	1988	3.12	1.07	0.87	3.34	2.71
1000-2000	1989	2.93	0.88	0.64	2.58	1.88
250-1000	1989	2.62	0.64	0.4	1.68	1.05
< 250	1991-2	2.45	0.39	0.21	0.96	0.51

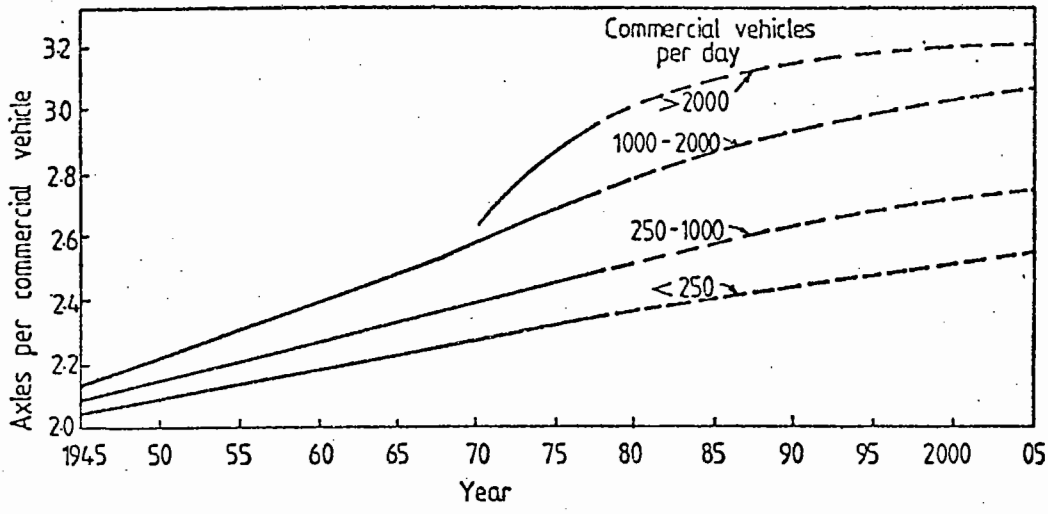

FIG 6·3 ESTIMATED CHANGES IN THE NUMBER OF AXLES PER COMMERCIAL VEHICLE FOR FOUR LEVELS OF TRAFFIC (After Currer et al (91))

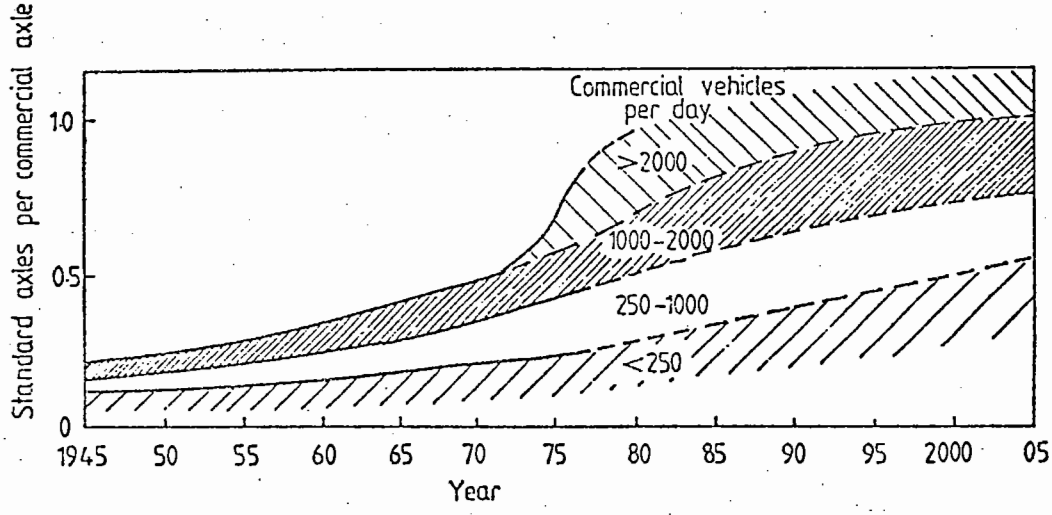

FIG 6·4 ESTIMATED CHANGES IN STANDARD AXLES PER COMMERCIAL AXLE FOR FOUR LEVELS OF TRAFFIC (After Currer et al (91))

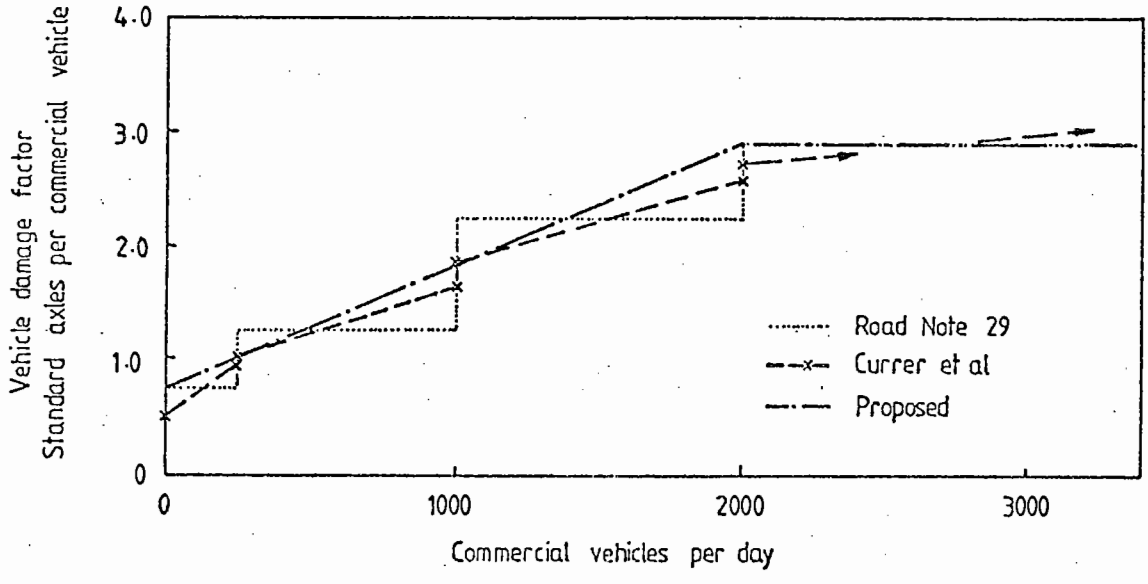

FIG 6·5 VEHICLE DAMAGE FACTORS FOR DIFFERENT TRAFFIC LEVELS

commercial axle is the value for the upper limit of the vehicle range and vice versa. Table 6.4 also gives the maximum and minimum vehicle damage factors for the traffic ranges. These are equal to the product of axles per commercial vehicle and standard axles per commercial axle. Fig.6.5 compares the DTp recommendations for vehicle damage factors with the values derived from the TRRL report (see Table 6.3). At the mid point of each vehicle range the values approximately agree. A further line is also shown which is the proposal for realistic design. It represents a steady increase in vehicle damage factor from 0.75 to 2.9 as the number of commercial vehicles rises from 0 to 2000 per day. Beyond 2000 the vehicle damage factor is constant at 2.9.

Between 250 and 450, and between 1000 and 1400 vehicles per day, the proposed line is less than current practice. However, it gives the same or slightly higher vehicle damage factors than those derived from the TRRL report on which the recommendations are based.

6.1.6 Design Thickness Procedure

An outline of this procedure is given in the flow diagram in Fig.6.1. The following design method is carried out twice, first for resistance to fatigue cracking then for resistance to permanent deformation. Each time the mix stiffnesses of the bituminous layers must be calculated for the appropriate design temperature, (see Sections 6.1.3 and 6.1.4).

At the start of the design, the asphalt base layer is assigned a thickness of 160mm. The traffic induced asphalt or subgrade strain, depending on the mode of failure under consideration, is calculated (using CHEVRON) and compared with the allowable value. If this strain is too great, then the thickness is increased (or vice versa) and the structural analysis repeated. The thickness is adjusted in 10mm increments unless the calculated strain differs substantially from the

allowable strain, in which case the increment is increased. The design is completed when the calculated strain equals the allowable strain ±5 microstrain.

Once the required thickness of the asphalt base layer has been determined for each criterion the program proceeds to select the larger of the two thicknesses as the final design thickness. The pavement will then be overdesigned for the other criterion.

The output data for typical examples using each design procedure of ANPAD is given in the user manual (48).

6.1.7 Balanced Design Procedure

This design procedure follows a similar method of calculation to that used for the PET program. A summary of the steps involved is given in the flow diagram (Fig.6.1). From the direct relationship between design life and allowable subgrade strain, the strain is calculated. The program then checks that the mix stiffness for the asphalt base lies within the range 2 to 20 GPa set by the program. The mix is then assigned an initial value of 11 GPa (i.e. mid range value) and the traffic induced subgrade strain calculated using the mix stiffnesses for the upper asphalt layers based on the subgrade strain design temperature. If the compressive strain is greater than the allowable value, then the new value is calculated from the previous value, until the strain is within the allowable tolerance, using the following equation:

$$E_N = E_{N-1} \pm \frac{18000}{2^N} \qquad (6.8)$$

where E_N is the Nth estimate of the mix stiffness, and

E_1 is the initial estimate = 11,000 MPa.

PONOS is then used to determine the binder stiffness of the base layer at both design temperatures. As the percentage voids in mixed aggregate of the base layer is constant, the mix stiffness of the base layer at the fatigue design temperature can also be calculated using two simultaneous equations of the form shown in equation (6.6).

The traffic induced asphalt strain is calculated next, using the appropriate asphalt mix stiffness for fatigue, and substituted into the relationship between the allowable asphalt strain and the design life, given in equation (6.1). A factor of 1.2 is applied to the design life for fatigue to ensure that the pavement fails in permanent deformation (see Chapter 4). Hence, for a particular grade of binder the required volume of binder (V_B) can be determined.

If the void content is less than 3%, then the following relationship established by Heukelom and Klomp can be applied:

$$S_m = S_b \left[1 + \frac{2.5C_v}{n(1-C_v)} \right]^n \qquad (6.9)$$

where $n = 0.83 \left[\log \frac{4 \times 10^4}{S_b} \right]$ (S_b in MPa)

and C_V = the volume concentration of aggregate.

Rearranging, C_V can be calculated and fed into the following equation to derive volume of voids, V_V:

$$C_v = \frac{1 - V_V - V_B}{1 - V_V} \qquad (6.10)$$

If the calculation is performed and V_V is greater than 3%, then it must be adjusted. Van Draat and Sommer (12) proposed replacing C_V by C_V' for mixes of >3% volume of voids, where:

$$C_V' = \frac{C_V}{0.97 - V_V} \qquad (6.11)$$

From equation (6.10) and (6.11) the following relationship can be used to determine void content:

$$V_V = \frac{(1 + 0.03\ C_V') - \sqrt{1 + C_V'(3.8809C_V' - 3.94 + 4\ V_B)}}{2C_V'} \qquad (6.12)$$

The final output gives the mix proportions as the binder content by mass volume, void content and voids in mixed aggregate.

6.1.8 Design Life Procedure

The third option available in ANPAD is to calculate the life of a given pavement. This is the simplest procedure and is shown in the flow diagram, Fig.6.1. The input required is listed in Table 6.1. CHEVRON is used to calculate the two critical strains. Rearranging the equations for allowable strains, the life of the pavement for each criterion is calculated in terms of millions of standard axles. Then the program selects the lower life as the design life. When the input data includes values for the initial number of commercial vehicles and percentage growth rate, then the program also determines the pavement life in years. This calculation is based on the method used in Road Note 29 (1) together with the appropriate vehicle damage factor (see Section 6.1.5), and is also incorporated in the PET programs.

6.1.9 Check on Accuracy

As stated previously, for the design thickness procedure the calculated critical strain must be within ±5 microstrain of the allowable value. This represented improved accuracy over the ADEM program in which the criterion was ±10 microstrain. For pavements that require large base thicknesses, ±5 microstrain can make a substantial difference to the result as the slope of the graph of calculated strain as a function of thickness reduces as the required thickness increases, Fig.6.6 has been prepared to show the errors which can arise within these limits, for a three-layered structure with a typical dense bitumen macadam base. A subgrade CBR of 3% was used together with a sub-base to subgrade modular ratio of 3.0. The thickness of the sub-base was 300mm. The average speed of commercial vehicle assumed was 80 km/hr and the average annual air temperature, 9.5°C. The mix details used for the base layer were, 3.5% of 100 pen binder, a void content of 10% and specific gravities of the aggregate and binder of 2.7 and 1.02 respectively.

For a design life of 1 million standard axles (msa) the ranges of calculated design thicknesses, which satisfied either the allowable asphalt or subgrade strain ±5 microstrain, were only small, (see Fig.6.6). However, for a design life of 100 msa the calculated design thickness varied by as much as ±20mm for the critical asphalt strain criterion, see Fig.6.6. It is, therefore, recommended that the output should be checked to see how close the calculated strain for the design thickness is to the allowable strain. If the thickness is large and the strain near the limit of the allowable range, then the error can be reduced by plotting the results and reading the design thickness corresponding to the allowable strain.

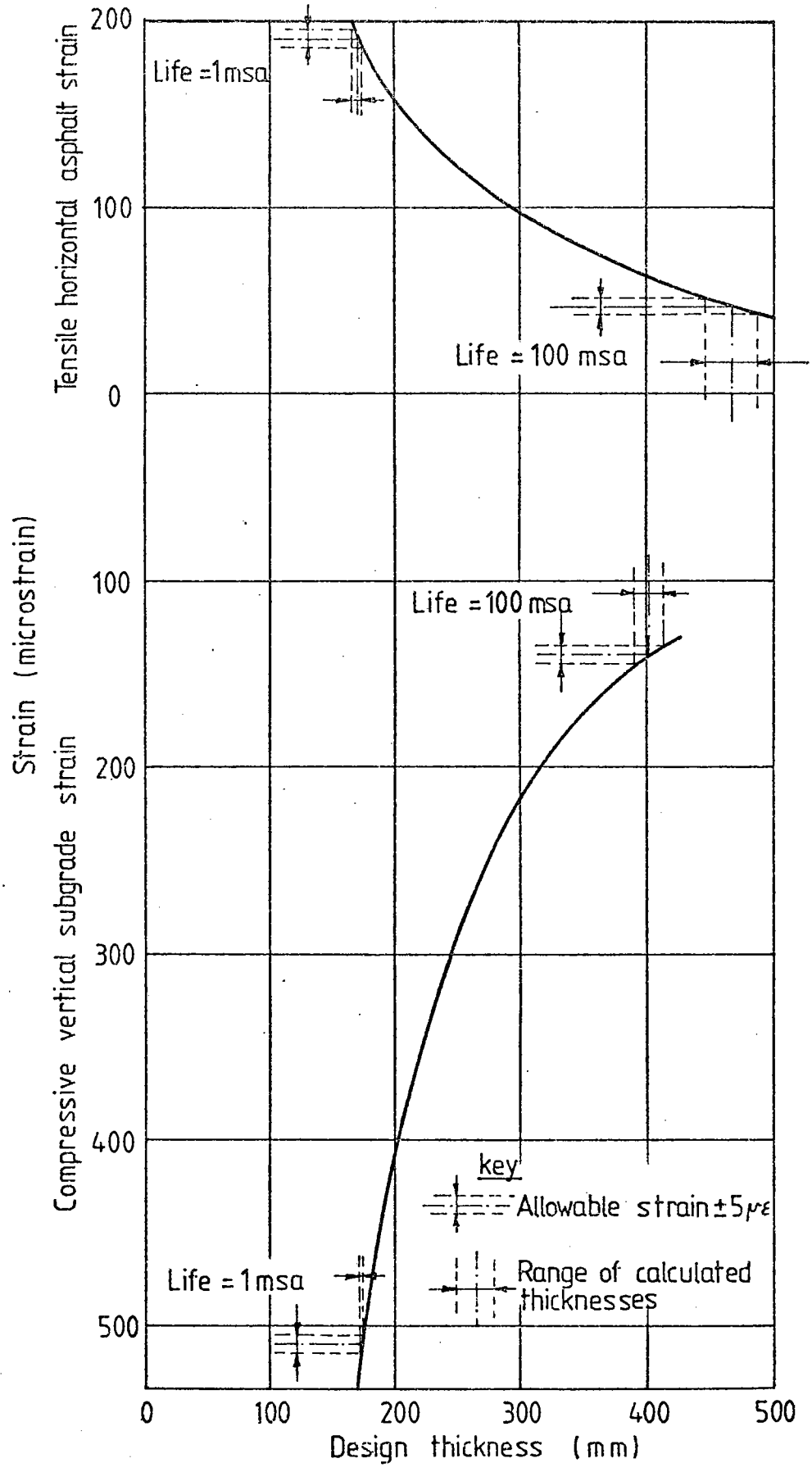

FIG 6·6 ACCURACY OF DESIGN THICKNESS PROCEDURE OF ANPAD

6.2 CUDAM COMPUTER PROGRAM

6.2.1 General Description

CUDAM (CUmulative DAMage) is a further development of ANPAD based on the principles established for the simple PET program CDM which was described in Chapter 4. The central analytical tool is, again, the CHEVRON n-layer program (39). CUDAM calculates the design thickness for a pavement with a specified life or the design life for a known base thickness. A flow diagram is given in Fig.6.7. The required input is listed in Table 6.5. It is similar to that required for ANPAD but twelve average monthly air temperatures must be given instead of the average annual air temperature.

The maximum allowable strains are identical to those used in ANPAD and the same equations are used to determine the loading time and the stiffness moduli.

6.2.2 Design Thickness Procedure

The thickness necessary for the subgrade strain criterion is calculated in exactly the same way as in ANPAD. It uses the average annual air temperature, calculated in CUDAM from the twelve monthly air temperatures, multiplied by 1.47. A cumulative damage approach is not adopted because the allowable vertical subgrade strain has been determined semi-empirically.

For the asphalt strain criterion, the twelve monthly air temperatures are converted into twelve monthly pavement temperatures using the 1.47 factor. The asphalt strain and corresponding life are then determined, using CHEVRON, for each pavement temperature. This is done for two thicknesses, $\bar{h}$ − 30mm, and $\bar{h}$ + 30mm, where $\bar{h}$ is the thickness calculated for the fatigue criterion using the average annual air temperature multiplied by 1.92.

Table 6.5 INPUT DATA REQUIRED FOR CUDAM

Input Data	Design Option		Format (F0.0 unless otherwise stated)	Units
	Design thickness	Design life		
1. TEXT, DATE	X	X	15A4	
2. NO. OF DESIGNS	X	X	I1	
3. OPTION: 1 for design thickness or 2 for design life	X	X	I1	
4. TEMPERATURE: Average monthly air temperature	X	X	12F6.0	°C
5. SPEED: Average speed of commercial vehicle	X	X		km/hr
6. LIFE: Design life in millions of standard axles	X	-		msa
7. NO. OF LAYERS (N)	X	X	I2	
When applicable Inputs 8-15 are required for the upper bituminous layers, starting with surfacing layer 1 to layer (N-3)				
8. THICKNESS	X	X		metres
9. BINDER CONTENT	X	X		%
10. VOID CONTENT	X	X		%
11. SPECIFIC GRAVITY OF AGGREGATE	X	X		
12. SPECIFIC GRAVITY OF BITUMEN	X	X		
13. INITIAL PENETRATION, INITIAL SOFTENING POING RECOVERED PENETRATION AND RECOVERED SOFTENING POINT that is 4 Inputs but only the Initial penetration is essential the others may be estimated within the program	X+++	X+++	4F10.0	

Contd...

Table 6.5 Contd.

Input Data	Design Option		Format (F0.0 unless otherwise stated)	Units
	Design thickness	Design life		
For the base layer:				
14. THICKNESS	-	X		metres
15. BINDER CONTENT	X	X		%
16. VOID CONTENT	X	X		%
17. SPECIFIC GRAVITY OF AGGREGATE	X	X		
18. SPECIFIC GRAVITY OF BINDER	X	X		
19. INITIAL PENETRATION, etc.	X+++	X+++	4F10.0	
20. TYPE OF BASE MATERIAL 1,2,3 or 4 is input depending on whether the base is a typical HRA, typical DBM, modified HRA or modified DBM respectively	X	X		
21. SUBBASE THICKNESS Thickness of granular layer	X	X		metres
22. SUBGRADE CBR	X	X		%
23. SUB-BASE TO SUBGRADE MODULAR RATIO. This is generally between 1.5 and 5.0, typcially 2.0 say.	X	X		
If No. of structures is greater than 1 then repeat 3 to 23.				

KEY

X required

\+ optional

\- not required

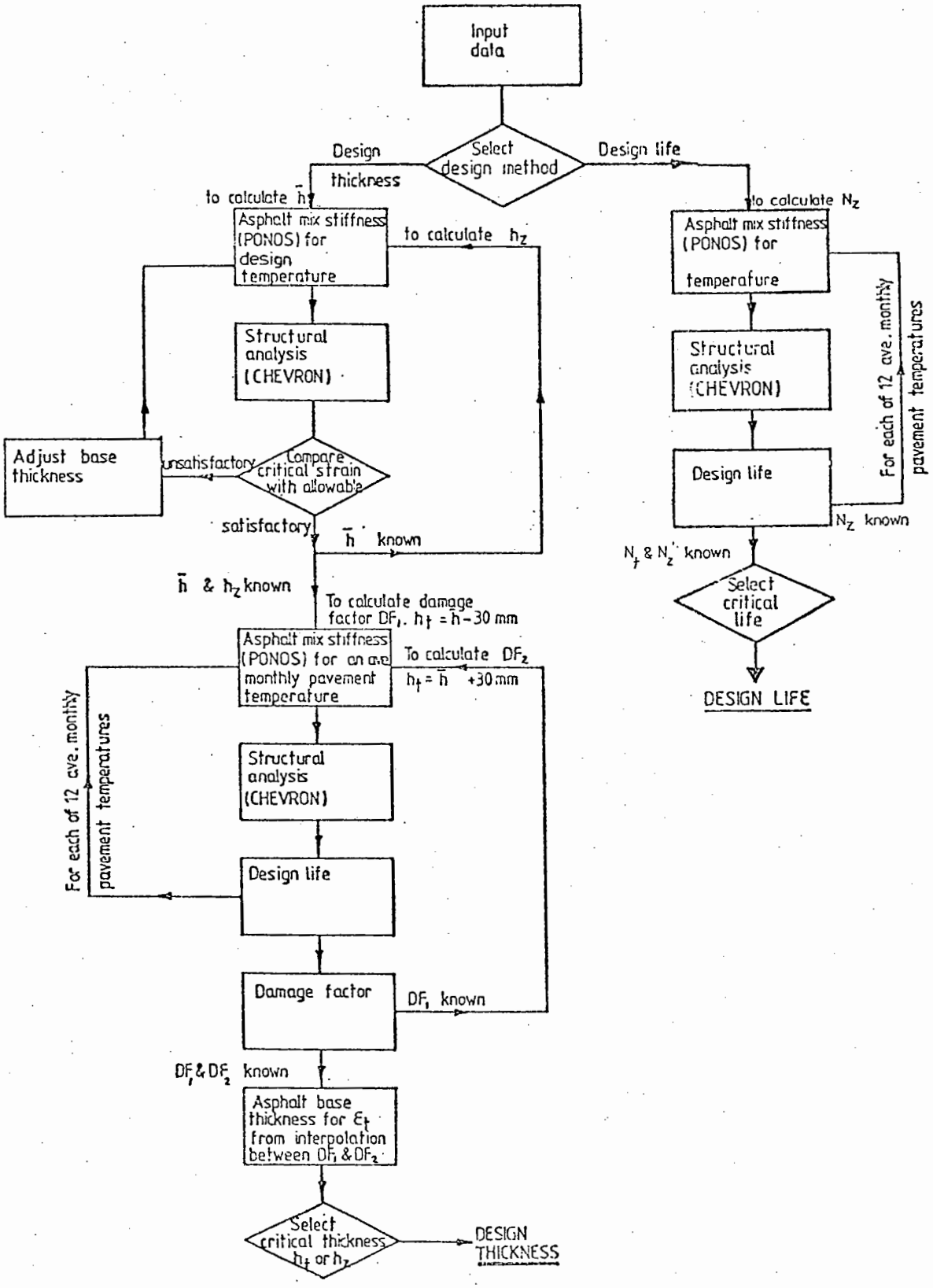

FIG 6.7 FLOW DIAGRAM FOR CUDAM

The actual pavement thickness required for the asphalt strain can then be found using a cumulative damage approach. Details of this method of calculation were included in Section 4.2.2 the only difference being that the increment used for the second initial estimate of thickness has been changed to 60mm.

The final design thickness is given for the critical case, either permanent deformation or fatigue cracking.

6.2.3 Design Life Procedure

The life of the pavement against permanent deformation is calculated in exactly the same way as in ANPAD. It uses the average annual air temperature, calculated in CUDAM, multiplied by 1.47.

For the asphalt strain criterion, the twelve monthly air temperatures are converted into twelve monthly pavement temperatures using the 1.47 factor. The asphalt strain and corresponding life are then determined, using CHEVRON, for each pavement temperature. Assuming that one twelfth of the total number of load applications occur at each temperature, the design life is calculated from the following equation:

$$N = \frac{12}{\sum_{T_{d1}}^{T_{d12}} \frac{1}{N_{Td}}} \qquad (6.13)$$

where N is the design life against fatigue cracking in standard axles

T_{d1} to T_{12} are the twelve monthly pavement temperatures

N_{Td} is the number of standard axles to cause failure at temperature Td.

Equation (6.13) is derived from equation (4.9) using a damage factor of 1.0.

Finally, the program selects the smaller of the two lives, (life against permanent deformation or life against fatigue cracking), as the design life.

CHAPTER SEVEN

APPLICATIONS OF COMPUTER PROGRAM

The computer program ANPAD can be used for a number of purposes. In the first section of this Chapter it was utilised to study the effect of mix variables on pavement performance. Similar calculations were also carried out using CUDAM and good agreement between the two programs is demonstrated.

Secondly ANPAD was used to develop a pavement design manual in the form of a series of charts. Two of the three structures considered were of full depth asphalt whilst the third had a conventional granular sub-base. Additional charts are also provided to show the effects of using different types of structures, base materials, subgrade moduli, temperatures and speeds.

7.1 MATERIAL VARIABLES

Once ANPAD had been developed it was used to study the effects of varying the asphalt base mix proportions on either pavement life or layer thickness. In each example, a three-layered structure with a 3% CBR subgrade and sub-base to subgrade modular ratio of 3.0 was analysed. The average speed of commercial vehicle assumed was 80 km/hr and the average annual air temperature 9.5°C. Specific gravities of 2.7 for the aggregate and 1.02 for the binder were taken. A range of typical mix proportions for a hot rolled asphalt base and a dense bitumen macadam base were considered, as shown in Table 7.1.

In Figs.7.1 (a) and (c) the asphalt base design thicknesses, calculated by the design thickness procedure of ANPAD, have been plotted against binder content for lives of 1, 10 and 100 million standard axles (msa). For the hot rolled asphalt base permanent

Table 7.1 VOIDS IN MIXED AGGREGATE FOR TYPICAL MIX PROPORTIONS

(a) Hot Rolled Asphalt

Void Content (%) \ Binder Content (%)	4	5	6
4	13.5	15.7	17.9
6	15.3	17.5	19.6
8	17.1	19.3	21.3

(b) Dense Bitumen Macadam

Void Content (%) \ Binder Content (%)	3	4	5
8	15.0	17.1	19.3
10	16.8	18.9	21.0
12	18.7	20.7	22.8

Table 7.2 COMPARISON OF ANPAD AND CUDAM DESIGNS

Base Material	Binder Content (%)	Design Thickness (mm)	
		ANPAD	CUDAM
HRA	4	200	200
	5	225	225
	6	250	250
DBM	3	320	320
	4	300	305
	5	300	310

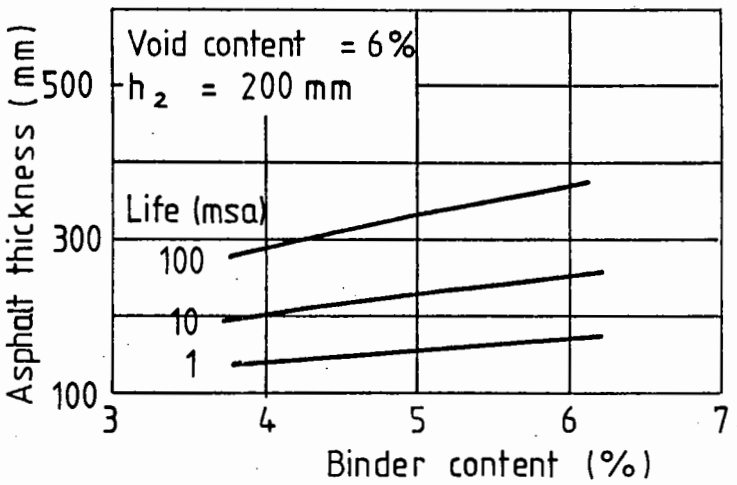

a. HRA base 50 pen

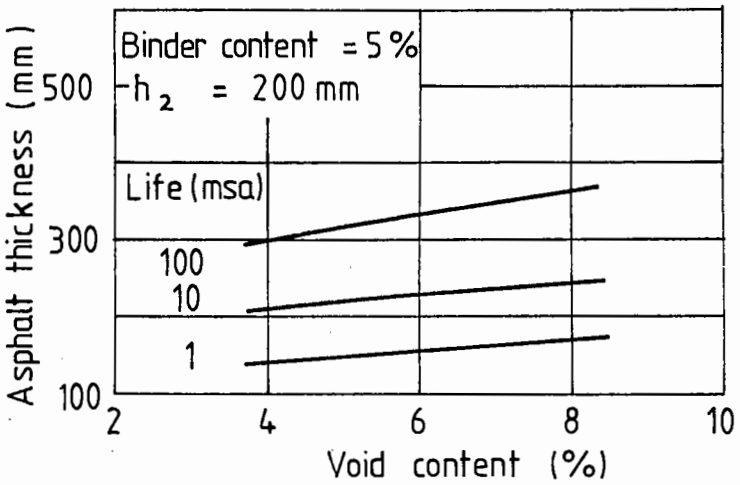

b. HRA base 50 pen

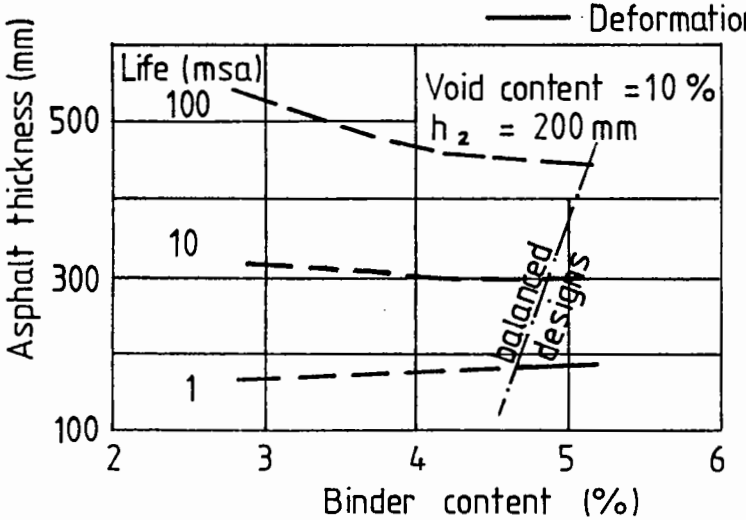

c. DBM base 100 pen

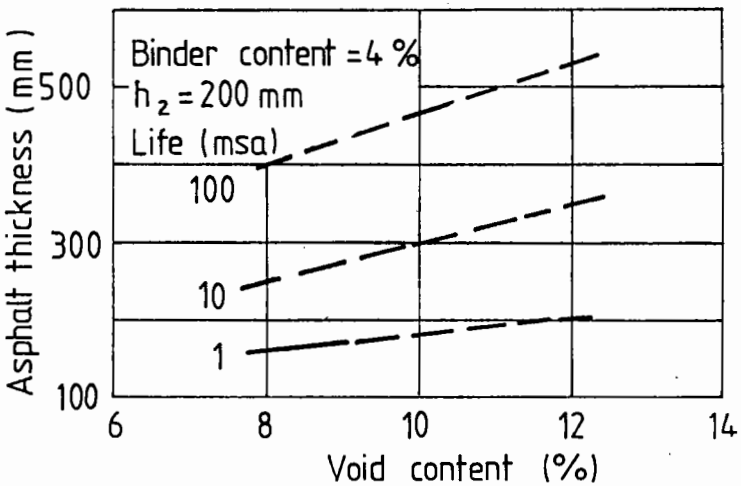

d. DBM base 100 pen

FIG 7.1 DESIGN THICKNESS AS A FUNCTION OF BINDER CONTENT AND VOID CONTENT

deformation was always critical. Therefore, as the binder content is lowered, the design thickness reduced. For the dense bitumen macadam base, fatigue was generally critical. However, as the binder content is increased the design thickness for permanent deformation is also increased until, at a binder content of approximately 5%, both criteria are critical and the design is balanced. Figs.7.1 (b) and (d) demonstrate that by improving compaction (reducing void content) the required thickness of base material is reduced.

The effect of varying the binder and void content on the design life of a pavement has also been studied using the design life option of the computer program (see Fig.7.2). Two thicknesses of asphalt base material were used, 200 and 400mm. For a 200mm hot rolled asphalt base, a reduction in binder content from 6 to 4% increases the life by 3.5 times. But for the dense bitumen macadam base, there is an optimum binder content of about 4.2 and 5.1% for base thicknesses (h_1) of 200 and 400mm respectively. For both these base materials improved compaction results in longer lives, (see Figs.7.2 (b) and (d)).

An increase in sub-base thickness (h_2) generally results in small savings in asphalt base thickness because of the much lower modulus of granular material. For example, Fig.7.3 shows that for an increase in sub-base thickness of 300mm, the average saving in asphalt thickness is about 40mm. However, the life of the pavement can be nearly doubled by providing the extra 300mm of sub-base.

Similar investigations were also carried out using the computer program CUDAM. The average monthly air temperatures were taken as those for the central region of Britain (see Chapter 4), and correspond to an average annual air temperature of 9.5°C as used in the ANPAD designs. Fig.7.4 shows the effect of varying binder content on the design thicknesses. The results are very similar to those produced using ANPAD (see Table 7.2).

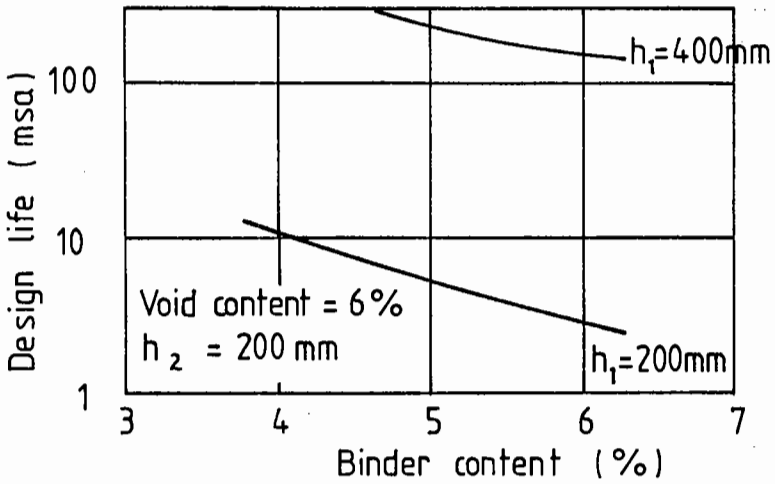

a. HRA base 50 pen

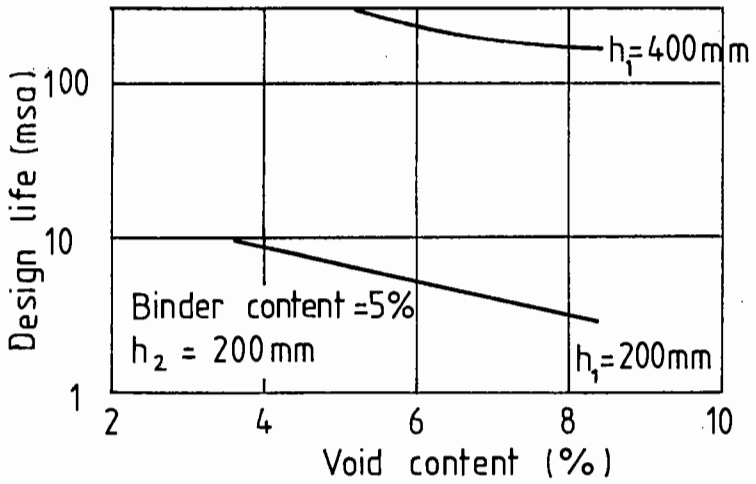

b. HRA base 50pen

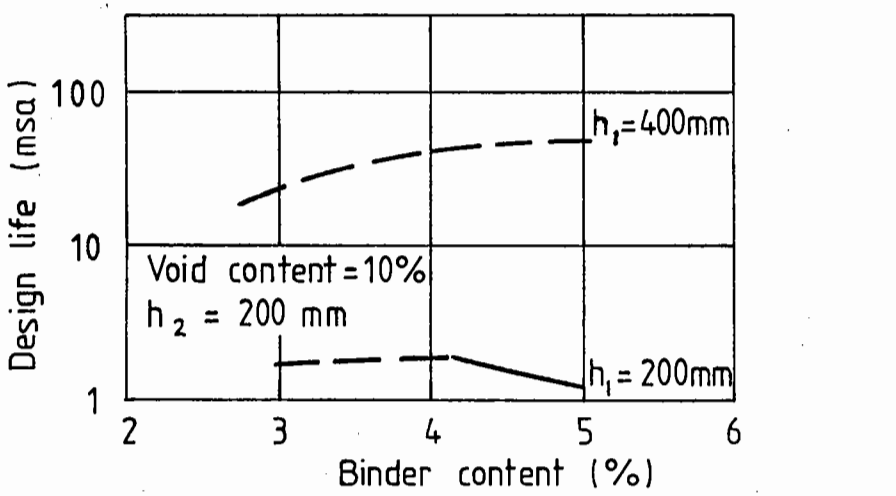

c. DBM base 100 pen

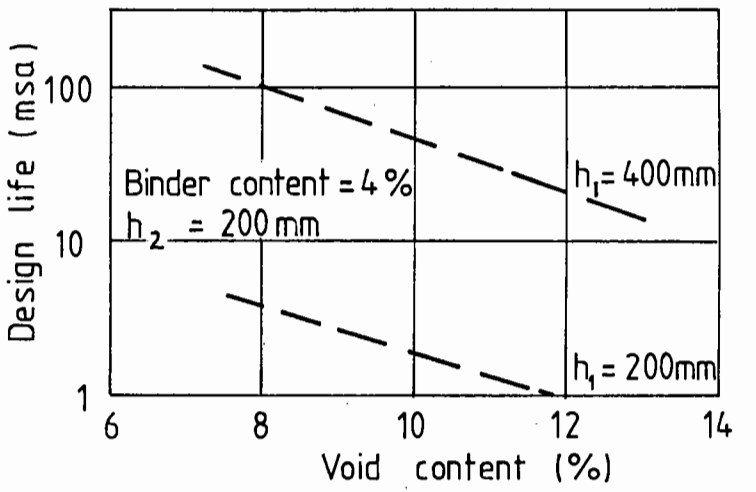

d. DBM base 100 pen

FIG 7.2 DESIGN LIFE AS A FUNCTION OF BINDER CONTENT AND VOID CONTENT

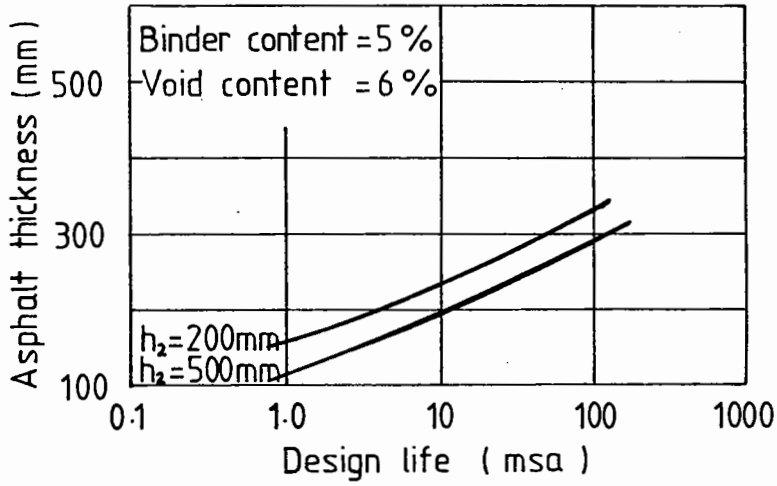

a. HRA base 50pen

— — Fatigue critical

——— Deformation critical

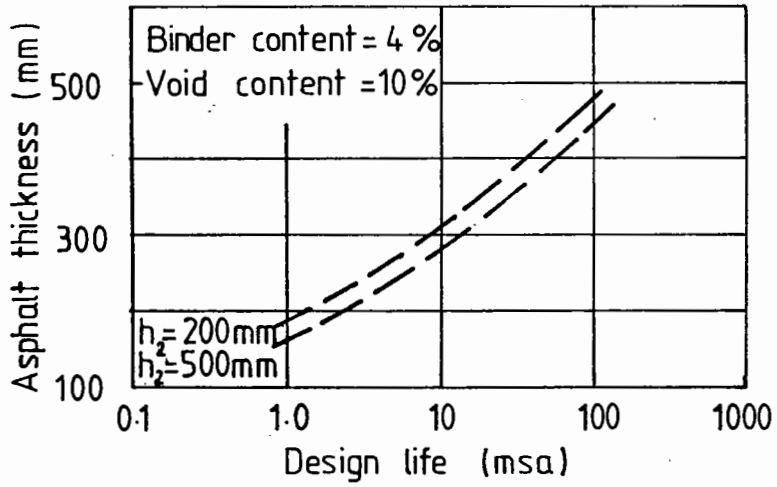

b. DBM base 100 pen

FIG 7·3 DESIGN THICKNESS AS A FUNCTION OF LIFE

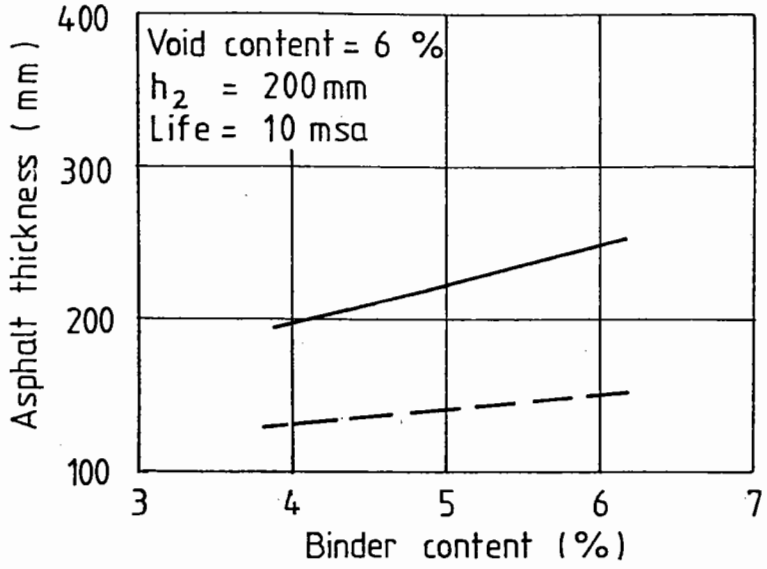

a. HRA base 50 pen

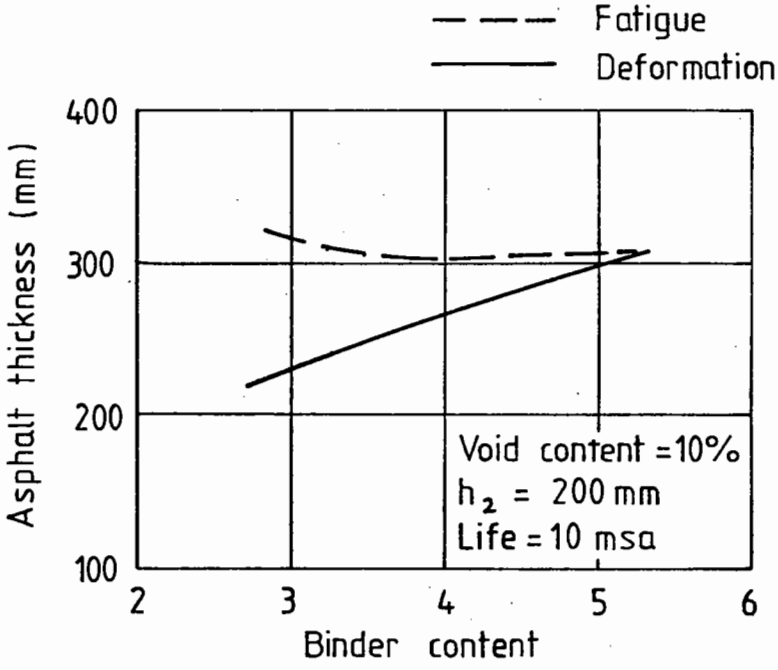

b. DBM base 100 pen

FIG 7.4 DESIGN THICKNESS AS A FUNCTION OF BINDER CONTENT USING CUDAM

7.2 DEVELOPMENT OF DESIGN CHARTS

A number of calculations were carried out using ANPAD in order to produce a design guide in the form of a series of charts. The resulting design manual is included in Appendix A. Three structures, each having 40mm HRA wearing course and a DBM, HRA or design mix base layer were considered, as shown in Fig.7.5. The mix details of the bituminous materials are given in Table 7.3. The first two structures were of full depth asphalt, type A and type B. Type A assumed a single uniformly compacted base layer, whilst type B assumes poorer compaction in the first lift of the asphalt base due to potential difficulties in laying the material directly onto the subgrade. Thus, in the analysis of the type B structure, the base is considered as two separate layers. The lower base thickness equals one third the total base thickness but with a minimum of 50mm and a maximum of 100mm. The calculations for both full depth asphalt structures assume a dummy 5mm thick sub-base to satisfy the requirements of ANPAD. The dummy sub-base has the same stiffness modulus as the subgrade.

Structure 3 includes a conventional granular sub-base 200mm thick. The sub-base to subgrade modular ratios used in the program were estimated from earlier studies using the SENOL non-linear finite element computer program.

7.2.1 Analysis

The design life option of the computer program ANPAD was used for various base layer thicknesses. Two average annual air temperatures, 8.4 and 10.1°C, were assumed, representing the typical Northern and Southern temperature zones for Great Britain, (see Fig.7.6). A typical value for the central temperature zone would be 9.5°C. Average speeds of commercial vehicles of 30 and 80 km/hr were selected. In order to cover a practical range of subgrade conditions, CBR values of 2, 5 and

Table 7.3 MIX DETAILS OF BITUMINOUS MATERIALS

	HRA wearing course	DBM base	HRA base	Design Mix base
Initial penetration	50	100	50	50
Binder Content (%)	7.9	4.7	5.7	4.5
Void content (%)	4.0	9.0 or 11.0*	6.0 or 8.0*	8.0 or 10.0*
Specific gravity of aggregate	2.7	2.7	2.7	2.7
Specific gravity of bitumen	1.02	1.02	1.02	1.02

* The higher void contents are used for the poorly compacted lower base layers, full depth asphalt type B structure.

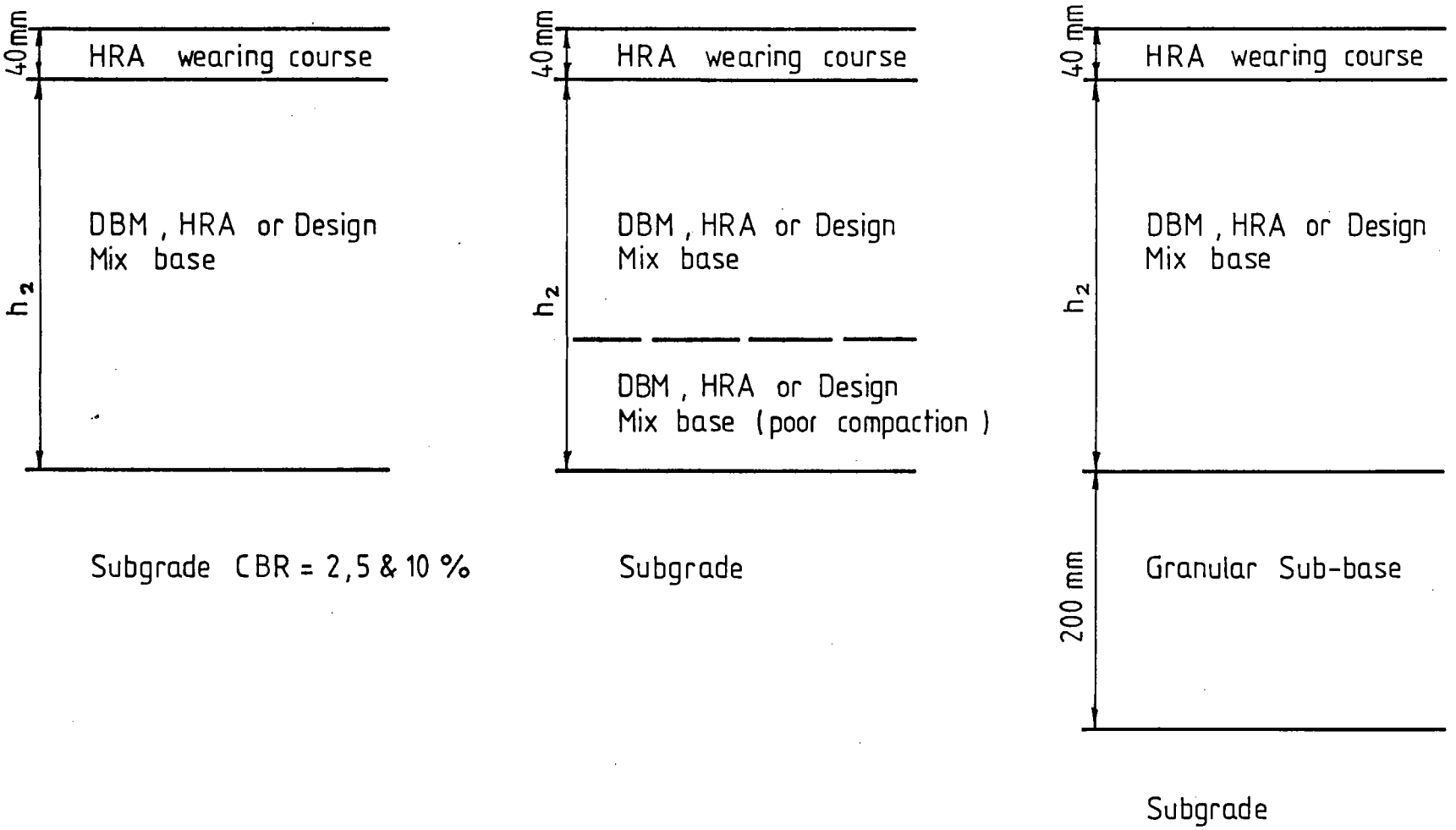

Full depth asphalt Type A

Full depth asphalt Type B

Granular Sub-base

FIG 7·5 TYPICAL DESIGN STRUCTURES

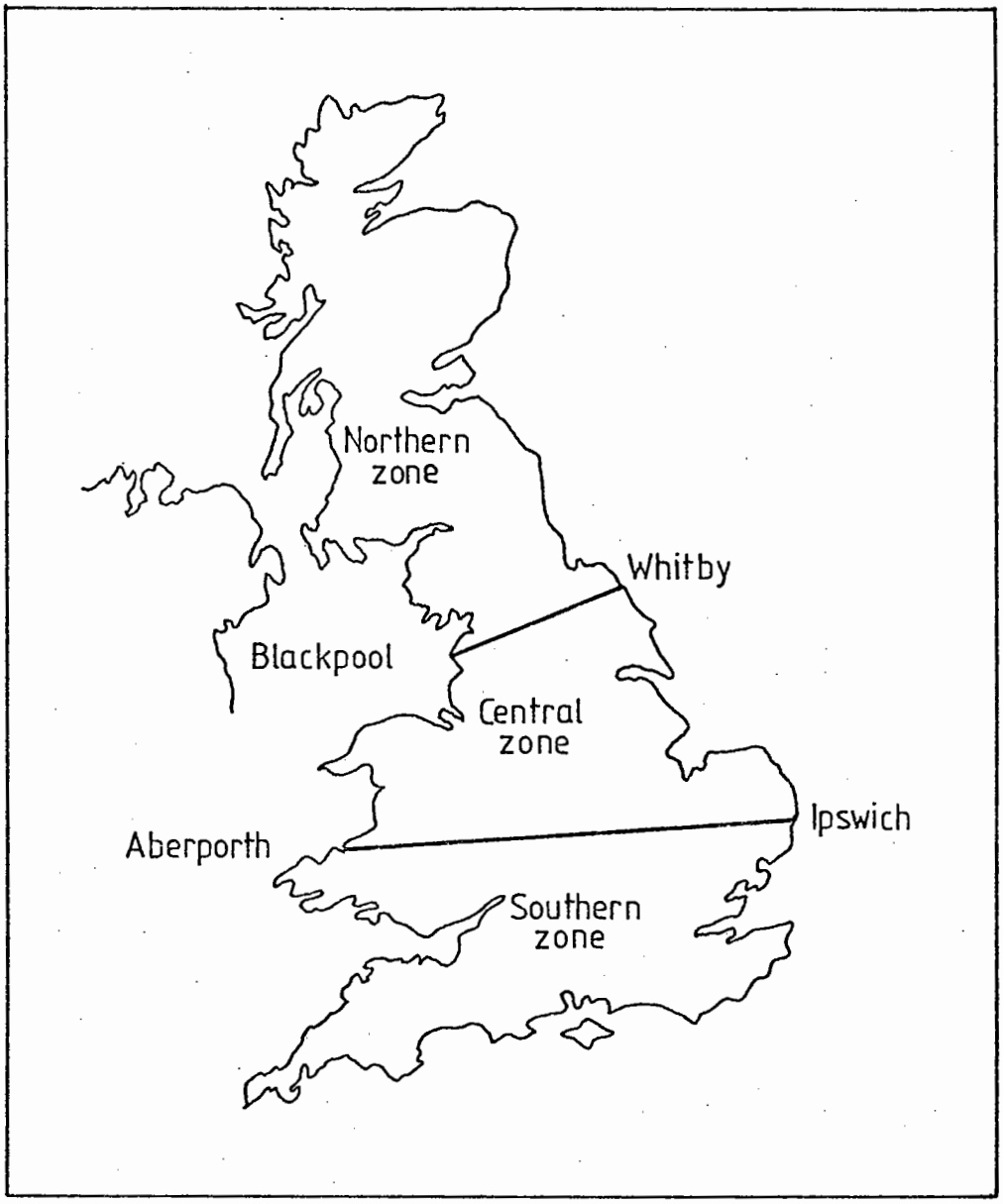

FIG 7·6 SUBDIVISION OF UNITED KINGDOM INTO TEMPERATURE ZONES (AFTER CRONEY (63))

10% were used. For each combination of temperature, speed, CBR, base material and type of structure, three base thicknesses were selected to give design lives between 0.1 and 500 million standard axles. Tables D1 to D9 in Appendix B give the input data and results from which the charts 1S to 9N in Appendix A were plotted. Fig.7.7 shows a typical chart 1S. The suffices S and N refer to the Southern and Northern temperature zones. Each chart consists of three graphs representing the different CBRs.

7.2.2 Interpolation of Results

When the design speed, temperature or CBR differ from those used in the charts the results may be interpolated. This interpolation procedure has been checked using the PET Programs, for convenience, and the results are given in Tables 7.4 and 7.5. Speeds of 30, 50 and 80 km/hr and air temperatures of 8, 9 and 10°C were used. Base thicknesses of 200 and 300mm were adopted for the design life calculations while lives of 5 and 50 msa were used for the design thickness calculations. These Tables also give the estimated design life and design thicknesses for the intermediate speeds and temperatures (50 km/hr and 9°C). These were obtained using linear interpolation between the two outer values assuming natural scales, log scales or a combination of the two. The scales used made very little difference to the estimated values, each demonstrating close agreement with the calculated value. Hence, for simplicity, natural scales are recommended.

Each design case is repeated for three CBR values. Several designs have been performed using the design charts and the results plotted in Figs. 7.8 and 7.9. Curves have been drawn through the design points to allow interpolation between the CBR values. However, the use of linear interpolation between either 2 and 5% CBR or 5 and

Table 7.4 CALCULATED AND ESTIMATED DESIGN LIVES

	Calculated Lives (msa) using PET Programs			Estimated Lives for a temperature of 9 °C using linear interpolation			
	Temperature °C			log life, log temp.	log life, temp.	life, log temp.	life, temp.
	8	10	9				
CBR 5% Speed 50 km/hr Base thickness 200mm							
DBM Base	4.1	1.7	2.7	2.6	2.6	2.8	2.9
HRA Base	7.5	5.3	6.3	6.2	6.3	6.3	6.4
Design Mix base	12.5	8.8	10.5	10.4	10.5	10.6	10.7
Base thickness 300mm							
DBM Base	27.5	9.7	16.6	15.9	16.3	18.1	18.6
HRA Base	79.3	51.6	64.0	63.2	64.0	64.7	65.5
Design Mix base	138	90.3	112	110.3	111.6	112.8	114.2
				Estimated lives for a speed of 50 km/hr using linear interpolation			
	Speed Km/hr			Log life, Log speed	Log Life, Log speed	Log Life, speed	life speed
	30	80	50				
Air temperature 9.°C Base thickness 200mm							
DBM Base	2.0	3.5	2.7	2.7	2.5	2.8	2.6
HRA Base	5.2	7.5	6.3	6.3	6.0	6.4	6.1
Design Mix base	8.7	12.5	10.5	10.5	10.1	10.7	10.2
Base thickness 300mm							
DBM Base	12.0	22.3	16.6	16.6	15.4	17.4	16.1
HRA Base	50.6	79.9	64.2	6.2	60.7	65.9	62.3
Design Mix base	88.5	139	112	112.0	106.0	114.8	108.7

Table 7.5 CALCULATED AND ESTIMATED DESIGN THICKNESSES

	Calculated thickness (mm) using PET program			Estimated thicknesses for a temperature of 9°C using linear inerpolation			
	Temperature °C			log thickness, log temp.	log thickness, temp.	thickness, log temp.	thickness, temp.
	8	10	9				
CBR 5% Speed 50 km/hr 5 msa							
DBM Base	208	256	230	232	231	233	232
HRA Base	185	198	191	192	191	192	192
Design Mix base	168	179	174	174	173	174	174
50 msa							
DBM Base	330	412	371	371	369	373	371
HRA Base	277	296	286	287	286	287	287
Design Mix base	254	270	262	262	262	262	262
				Estimated thicknesses for a speed of 50 km/hr using linear interpolation			
	Speed (km/hr)			log thickness, log speed	log thickness, speed	thickness, log speed	thickness, speed
	30	80	50				
Air temperature 9°C 5msa							
DBM Base	246	215	230	229	233	230	234
HRA BAse	199	185	191	192	193	192	193
Design Mix base	180	168	174	174	175	174	175
50msa							
DBM BAse	396	342	371	367	373	367	374
HRA Base	297	276	286	286	288	286	289
Design Mix base	272	253	262	262	264	262	264

SOUTHERN TEMPERATURE ZONE

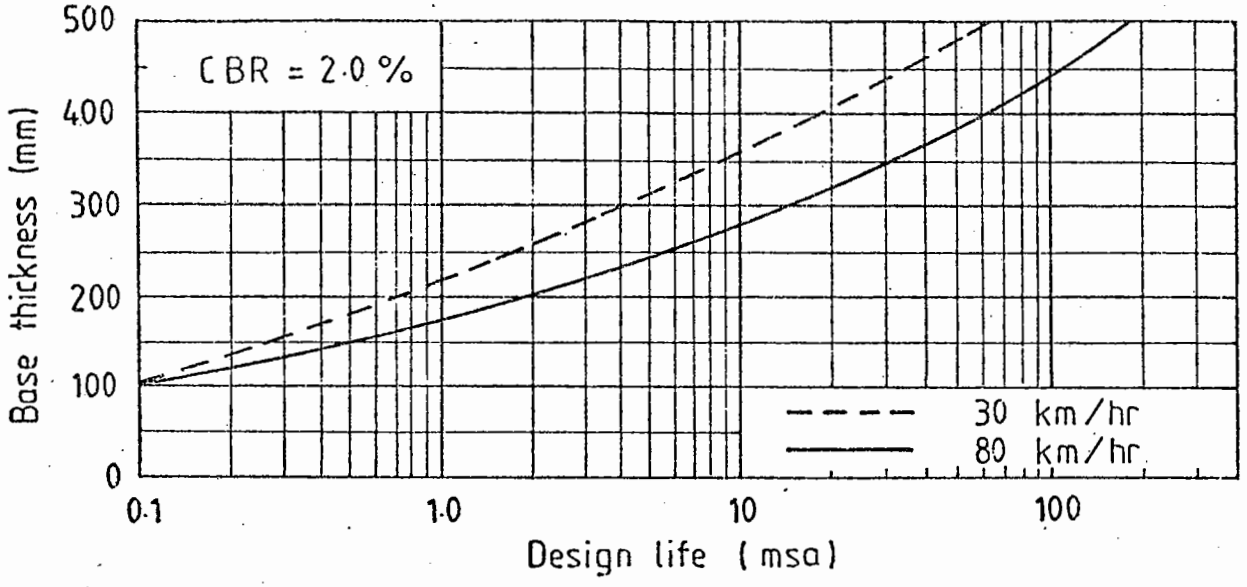

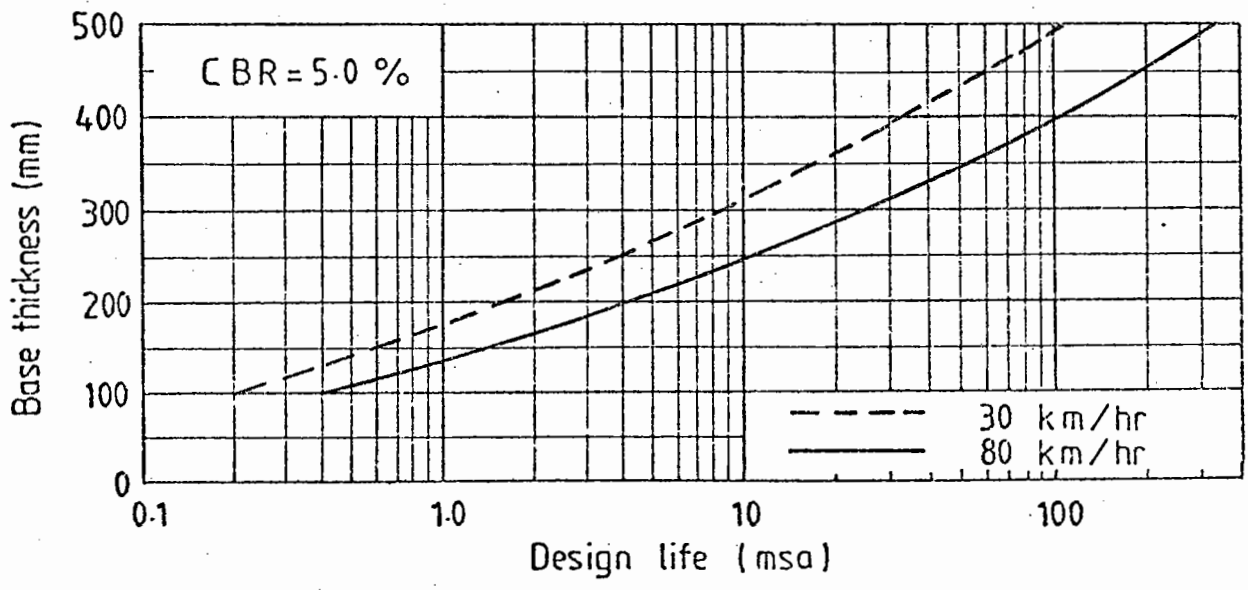

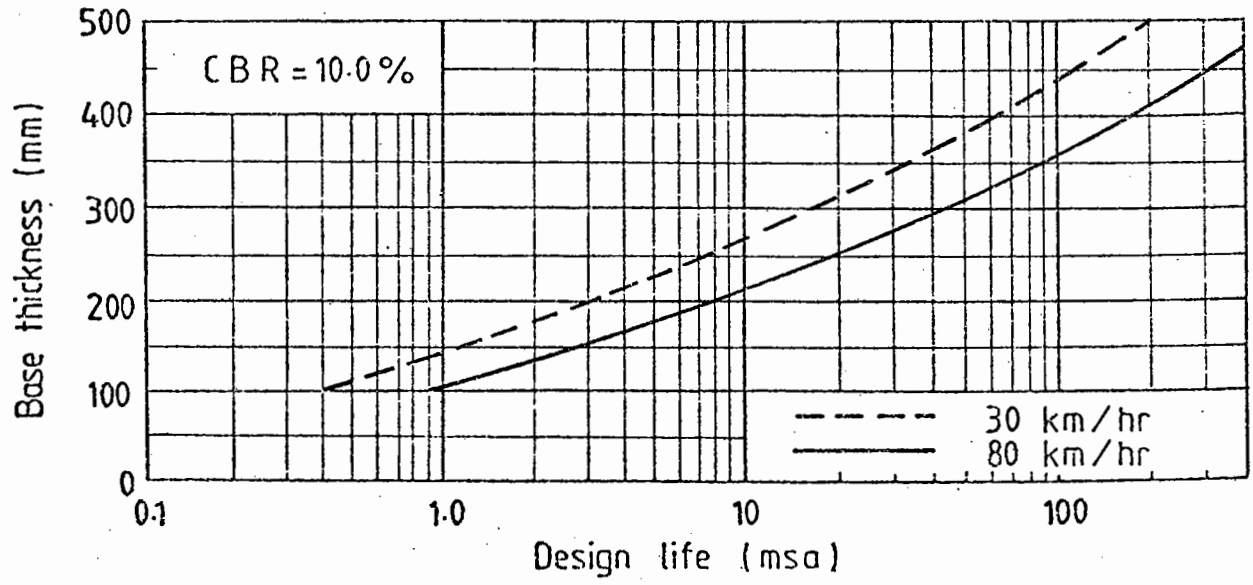

FIG 7·7 CHART 1S DBM BASE, FULL DEPTH ASPHALT TYPE A

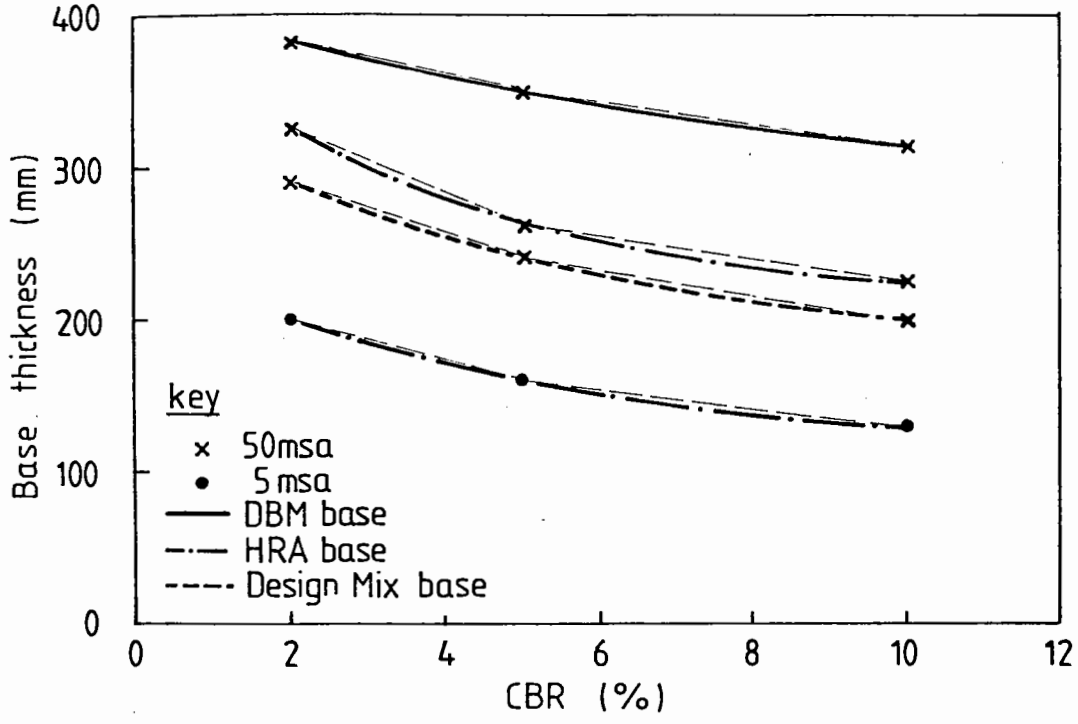

FIG 7·8 BASE THICKNESS AS A FUNCTION OF CBR, FULL DEPTH ASPHALT TYPE A

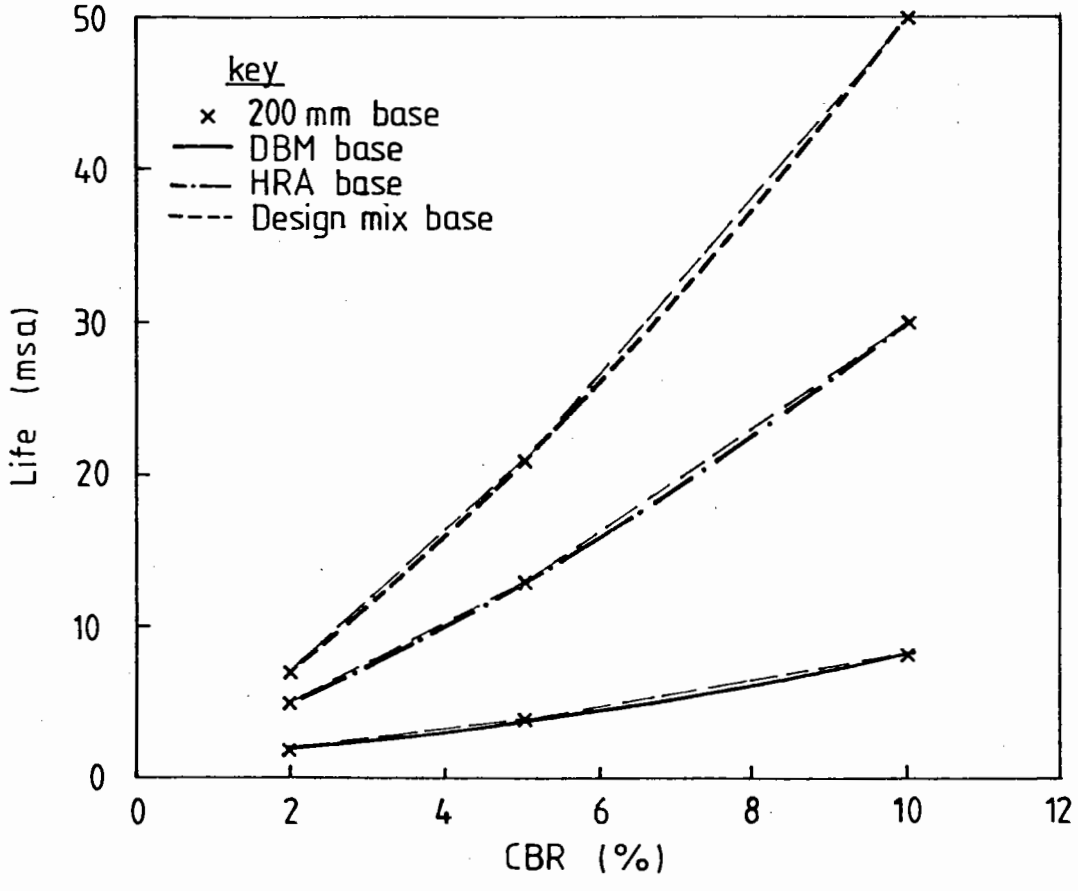

FIG 7.9 DESIGN LIFE AS A FUNCTION OF CBR FULL DEPTH ASPHALT TYPE A

10% CBR shown by the fine dashed lines also leads to a reasonable estimate, and is therefore recommended.

The order in which the interpolations are made should not effect the result. However, a logical order would be speed, CBR and then temperature so that the calculated values can be checked more easily from the charts.

Equations are provided in the Design Manual (Appendix A) to facilitate interpolations.

Table 7.6 gives the results of two examples using interpolation. In both cases design mix base, full depth asphalt type A structures have been used. The design speed was 50 km/hr, CBR, 3% and air temperature, 9.5°C. The design life calculation was for a base thickness of 200mm and the design thickness calculation for a life of 50msa. The interpolated results from the charts agree reasonably well with those calculated directly by ANPAD, but are slightly on the conservative side.

7.2.3 Effect of Design Parameters

Figs.7.10 to 7.11 have been prepared to show the effects of varying the design parameters. Fig.7.10 demonstrates how the type of structure influences the design thickness or life of the pavement, for each of the three base materials. The full depth asphalt type B structure is the weakest followed by the type A structure. For the DBM bases in particular, there is very little difference between the full depth asphalt type A structure and the structure with the 200mm granular sub-base.

Fig.7.11 compares designs using the three base materials for each structure. The design mix base provides the longest lives or the most savings in base thickness followed by the HRA. The influences of CBR on design thickness or life for a full depth asphalt type A structure

Table 7.6 TWO DESIGN EXAMPLES

Example 1 Design thickness 50 msa, speed 50 km/hr, CBR 3% and air temperature 9.5°C

			Thickness (mm)				
Temperature (°C)	CBR (%)	Speed (km/hr)	Using design charts 3S and 3N	Corrected to 50 km/hr	Corrected to CBR 3%	Corrected to 9.5°C	Calculated Using ANPAD
10.1	2	30	330	} 310	} 290	} 280	270
		80	290				
	5	30	270	} 260			
		80	240				
8.4	2	30	290	} 280	} 260		
		80	270				
	5	30	240	} 230			
		80	220				

Example 2 Data Base thickness 200mm, speed 50 km/hr, CBR 3% and air temperature 9.5°C

			Life (msa)				
Temperature (°C)	CBR (%)	Speed (km/hr)	Using design charts 3S and 3N	Corrected to 50 km/hr	Corrected to CBR 3%	Corrected to 9.5°C	Calculated using ANPAD
10.1	2	30	5.6	} 6.2	} 9.5	} 11.3	11.7
		80	7.0				
	5	30	12.0	}16.0			
		80	22.0				
8.4	2	30	7.5	} 9.5	}14.6		
		80	12.5				
	5	30	20.0	}24.8			
		80	32.0				

SOUTHERN TEMPERATURE ZONE

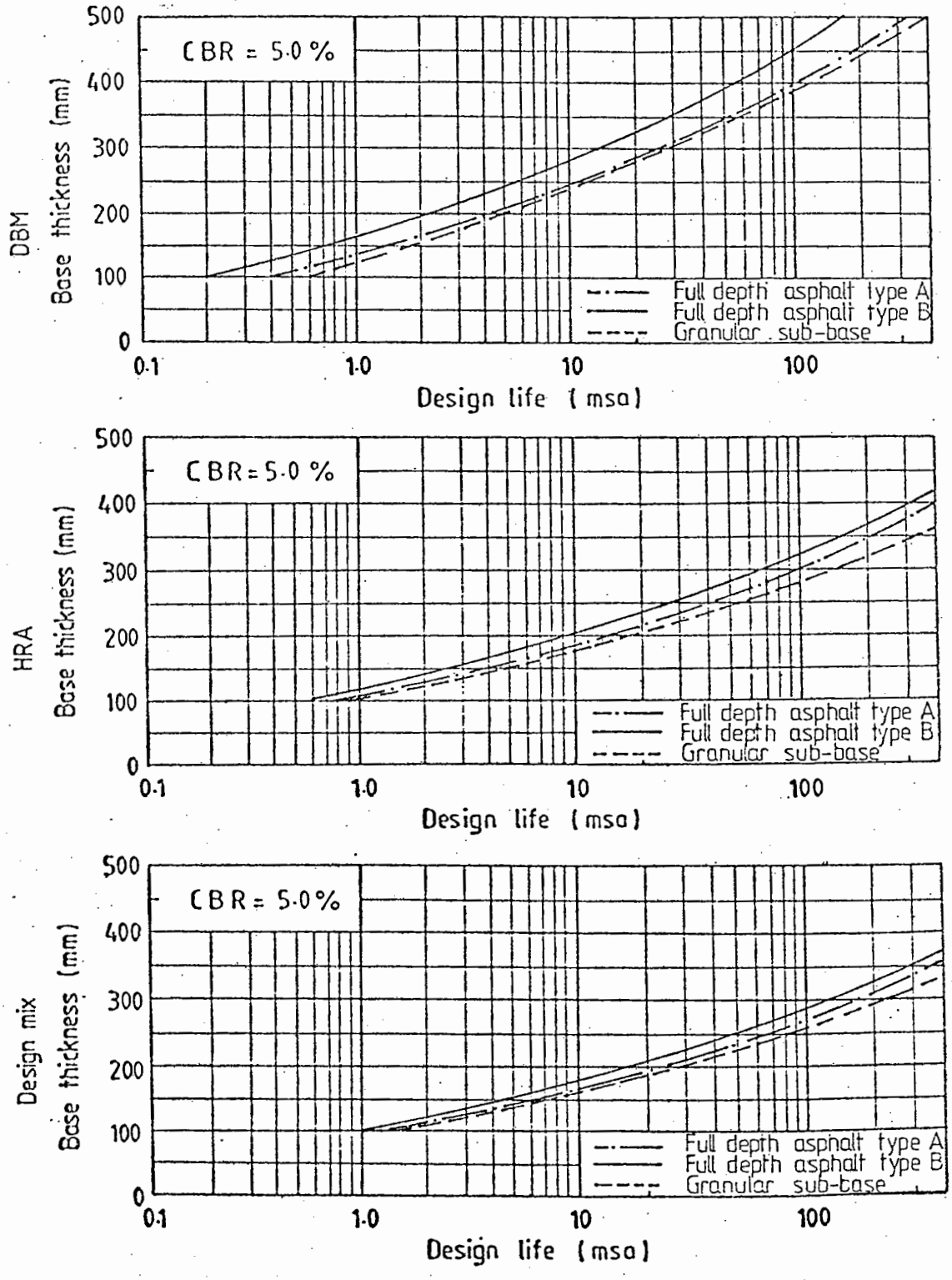

FIG 7·10 COMPARISON OF CHARTS FOR DIFFERENT TYPES OF STRUCTURES, SPEED 80 km/hr

SOUTHERN TEMPERATURE ZONE

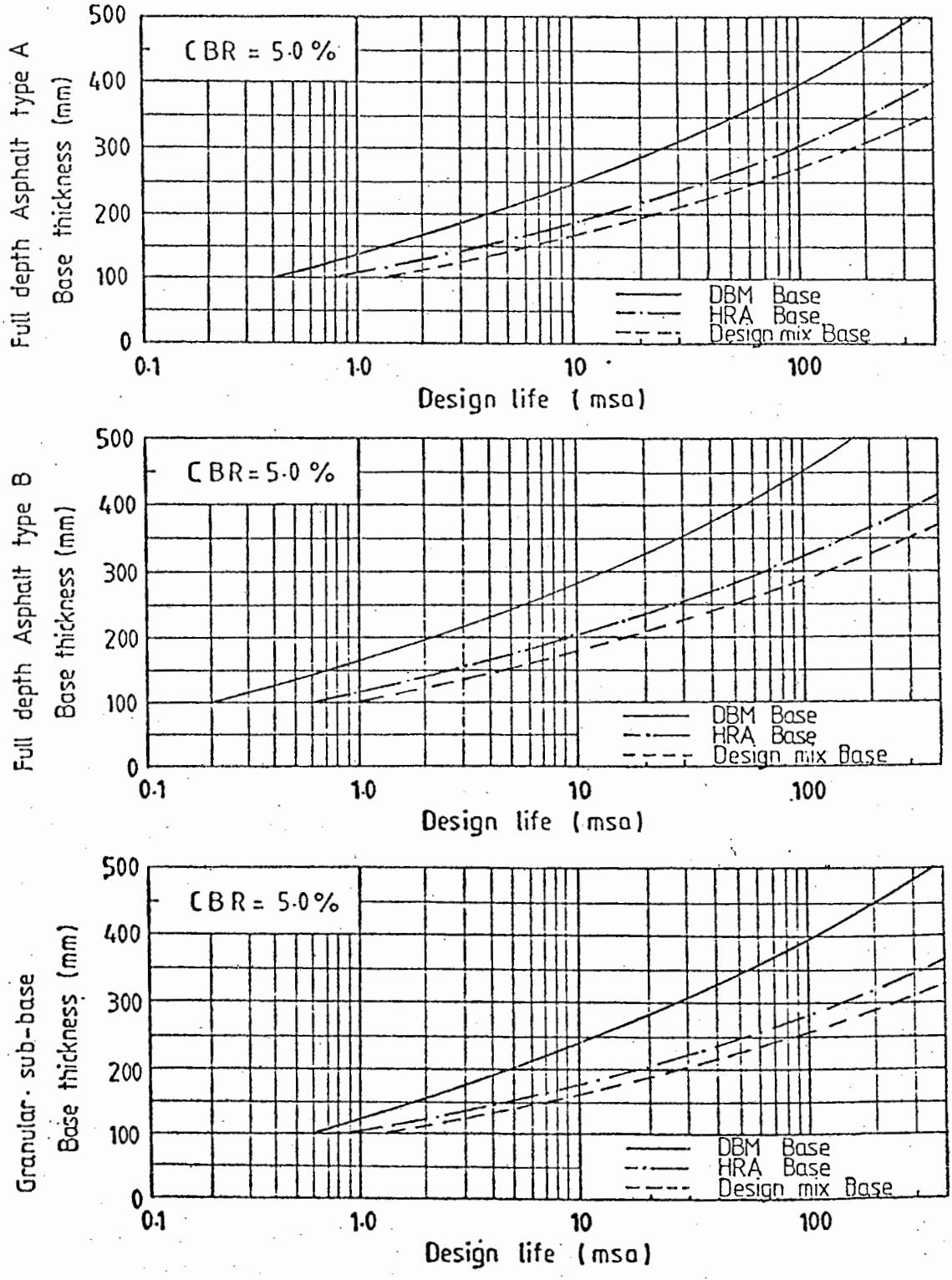

FIG 7·11 COMPARISON OF CHARTS FOR DIFFERENT BASE MATERIALS, SPEED 80 km/hr

SOUTHERN TEMPERATURE ZONE

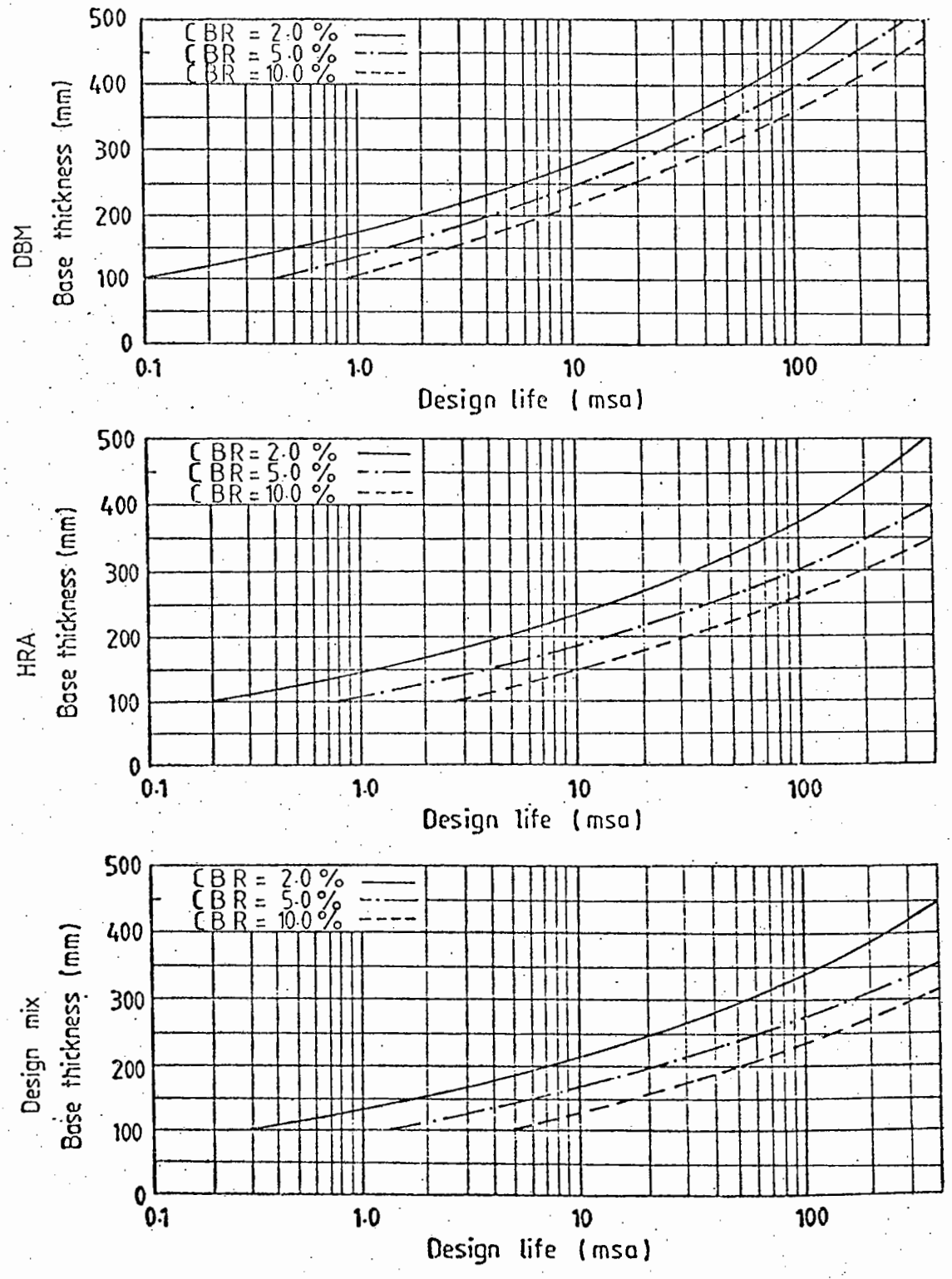

FIG 7·12 COMPARISON OF CHARTS FOR CBR S OF 2, 5 AND 10%, FULL DEPTH ASPHALT TYPE A AND SPEED 80 km/hr

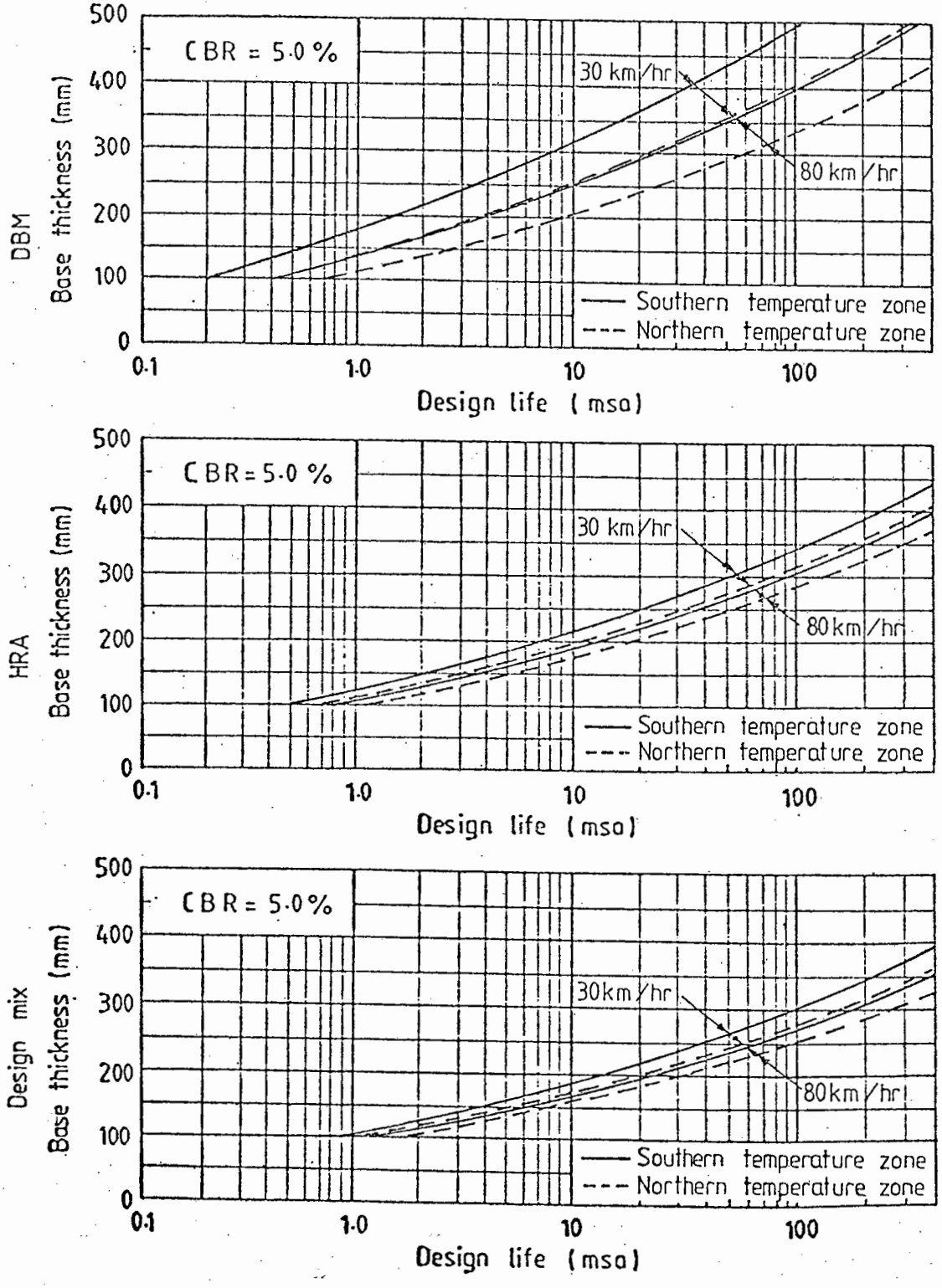

FIG 7·13 COMPARISON OF CHARTS FOR SOUTHERN AND NORTHERN TEMPERATURE ZONES, FULL DEPTH ASPHALT TYPE A

is shown in Fig.7.12. The CBR value affects the HRA and design mix bases slightly more than the DBM bases.

Fig.7.13 shows the combined effects of temperature and speed. Temperature effects are greater for the DBM bases than for the HRA or design mix bases. It is also interesting to note that designs for 30 km/hr in the Northern temperature zone are very similar to designs for 80 km/hr in the Southern temperature zone.

CHAPTER EIGHT

COMPARISON OF DESIGN METHODS

There are a number of different design systems in existence but only a few are applicable to conditions in the United Kingdom. This Chapter compares designs carried out using Road Note 29 (1), the TRRL design method (81,93) and the Shell design manual (94) with those using the computer program ANPAD. A review of the Asphalt Institute design procedure (75) is also given, although this has been developed for use in the United States.

8.1 REVIEW OF TRRL DESIGN PROCEDURE FOR FATIGUE

The effect of temperature on the fatigue life of a typical DBM roadbase is discussed in detail by Thrower (81) and Goddard et al (95). The laboratory testing reported by Thrower lacks full details. However, the frequency of loading was 25 Hz and the mix was a dense bitumen macadam. The binder content was estimated as 3.5-4.0% of 100 pen bitumen, depending on the type of aggregate, by the superimposition of the laboratory fatigue lines for known mixes provided by Goddard et al (given in Fig.8.1) on to those established at various temperatures for the particular mix used by Thrower (see Fig.8.2). The fact that TRRL consider the fatigue line for a particular mix to shift with temperature is contrary to the approach adopted at Nottingham where a unique fatigue line is used for each mix which is independent of temperature. The different results may be explained by the testing techniques involved. Although controlled stress testing was used in both cases, TRRL used axial loading and superimposed an additional deformation control so that the mean position of the specimen remained at its starting point (zero strain position). This results in longer

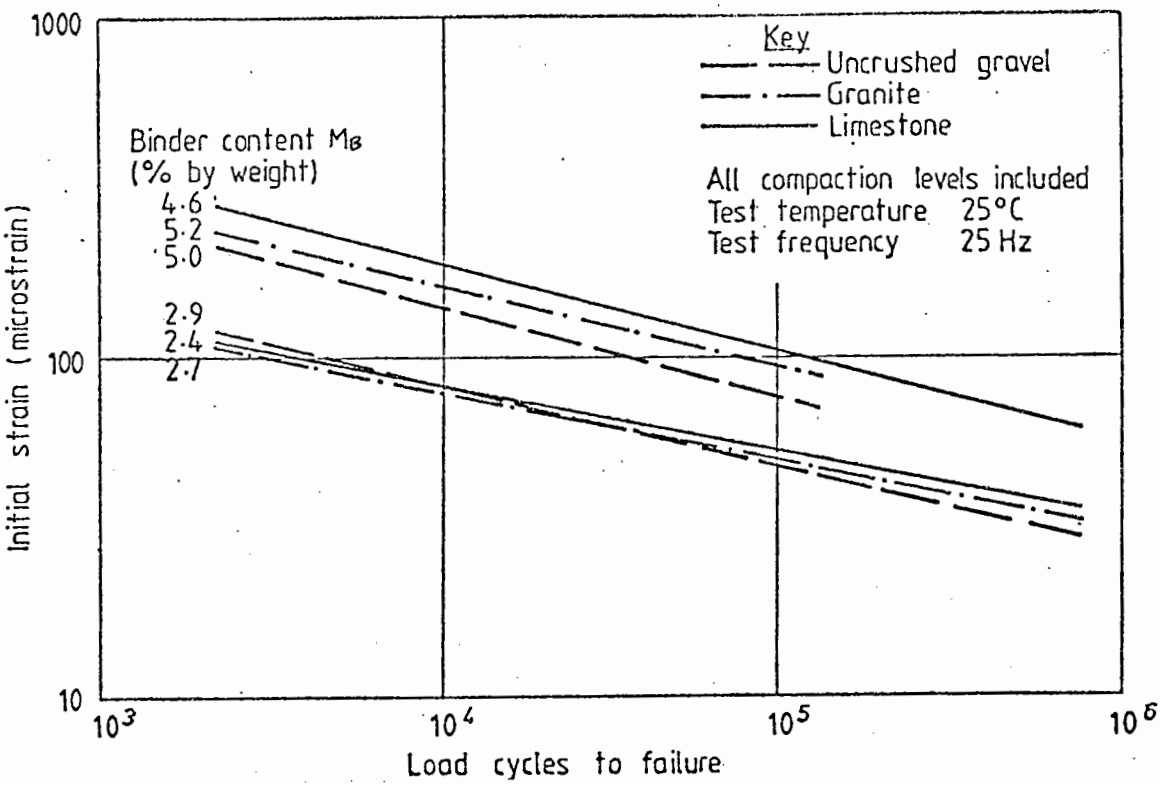

FIG 8.1 EFFECT OF BINDER CONTENT ON THE RELATIONSHIP BETWEEN INITIAL STRAIN AND FATIGUE LIFE (AFTER GODDARD ET AL(95))

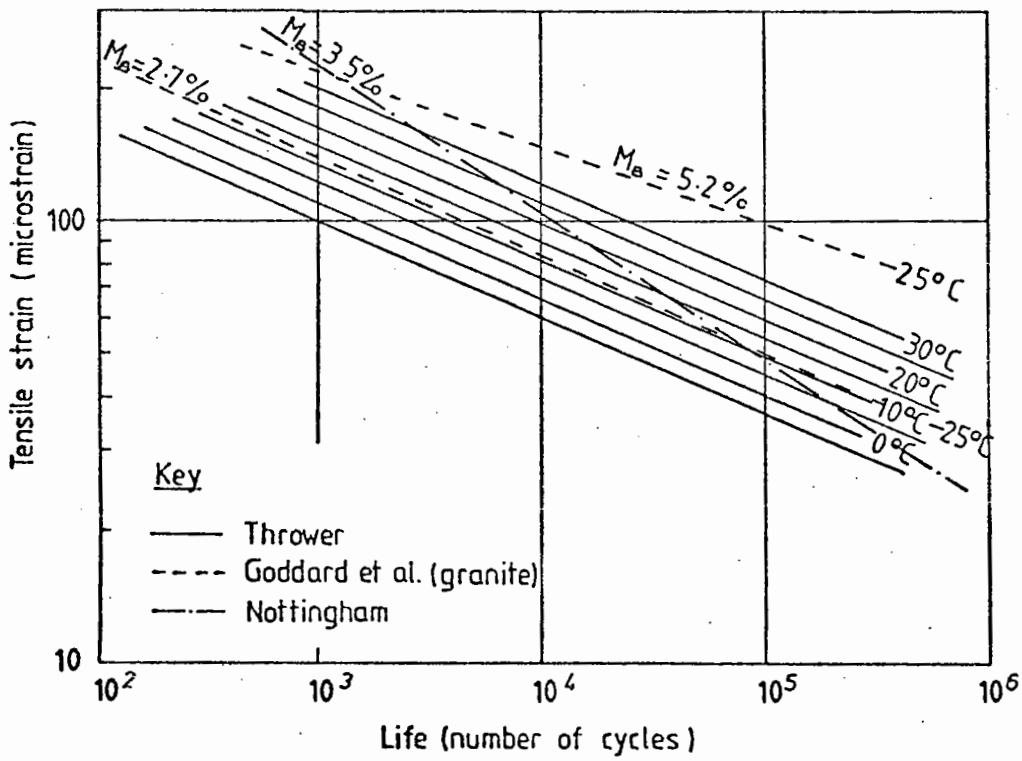

FIG 8.2 LABORATORY FATIGUE RESULTS

measured laboratory lives than those determined at Nottingham where pure stress control was used both in rotating bending cantilever and axial loading tests.

All the lives quoted by Thrower (81) are laboratory lives and are expressed as the number of load applications to failure. The lines given in Fig.8.2 can generally be related by the following equation:

$$N = d\epsilon^{\alpha} \qquad (8.1)$$

where N is the laboratory life, in no. of applications

$d = 10^{-n}$

$$n = \left[15.65 - 0.2\left[\frac{T+5}{5}\right]\right]$$

T = Pavement temperature in °C

$\alpha = -4.66$

8.1.1 Pavement Structure

Thrower (81) analysed 8 different pavement structures. In each case the subgrade and sub-base had moduli of elasticity of 40 and 270 MPa and Poisson's ratios of 0.45 and 0.35 respectively. The total bound layer thickness varied from 120mm to 370mm and consisted of a surfacing layer and a roadbase.

Thrower determined the stiffness and Poisson's ratio of the asphalt layer from Fig.8.3. The same values were assigned to both the surfacing and roadbase layers with no adjustment for their different mix details. The variation of stiffness due to the influence of layer thickness on the loading time was also ignored, but this is less important. To keep computations to a minimum, only the 120 and 370mm total asphalt layers are analysed here.

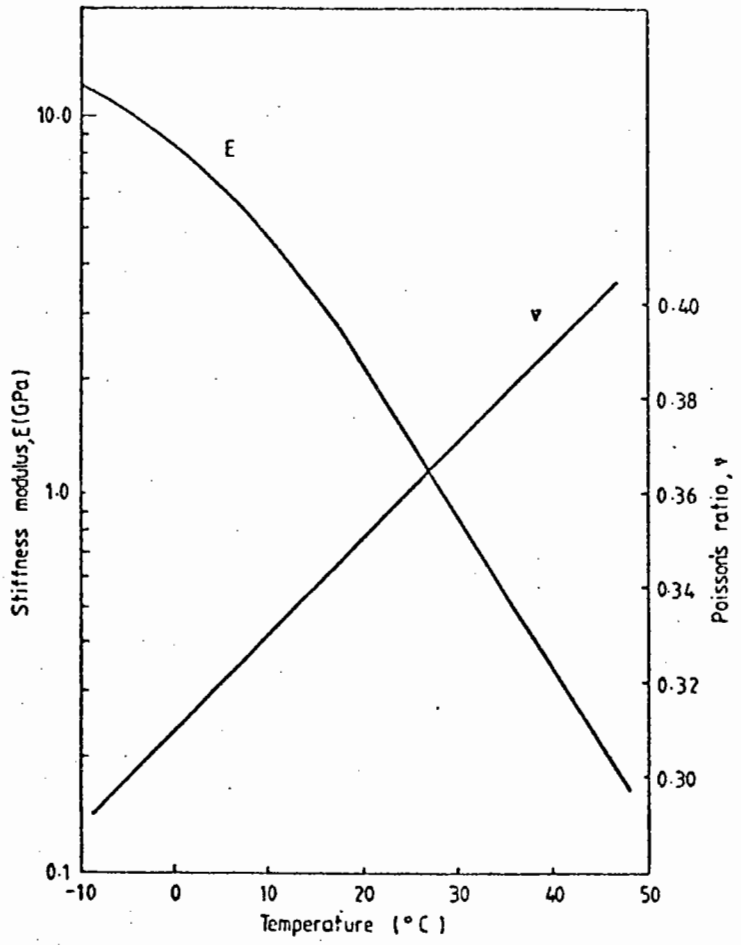

FIG 8.3 ELASTIC PARAMETERS OF BITUMINOUS MATERIALS (AFTER THROWER(81))

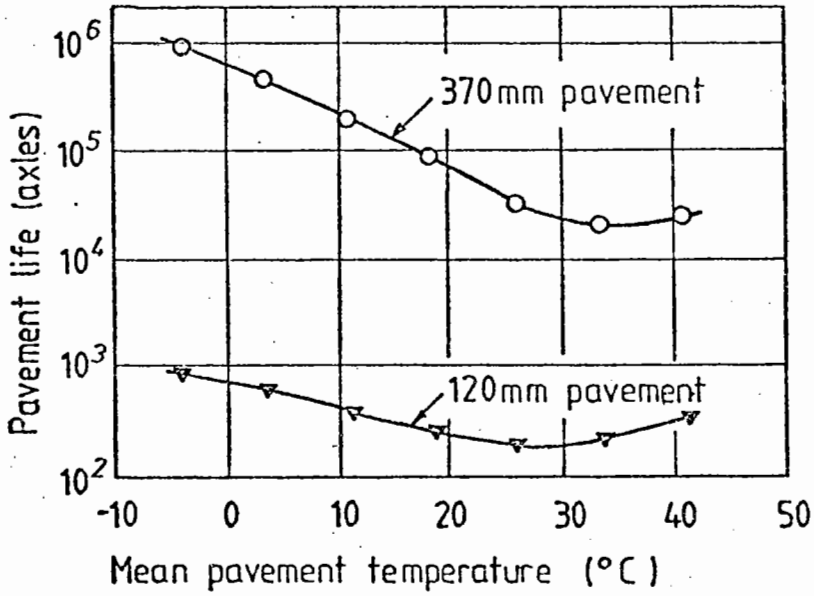

FIG 8.4 RELATIONS BETWEEN PAVEMENT LIFE AND MEAN PAVEMENT TEMPERATURE (AFTER THROWER(81))

8.1.2 Temperature

In his analysis, Thrower used three temperature distributions through the pavement; the one with zero temperature gradient was used for these calculations. He used seven temperature classes covering a wide range. These were derived from the extensive observations at Alconbury by-pass and are shown in Table 8.1.

A mean value, weighted to allow for traffic variations, was determined as 14.5°C which falls between two of the temperature classes considered in Table 8.1 (11.3 and 18.8°C).

In order to compare the design method adopted by Thrower at TRRL with that used at Nottingham, the long term average monthly air temperatures for Alconbury by-pass (96) are also required. These are given in Table 8.3. The simple Nottingham design method uses an average annual design temperature for fatigue equal to 1.31 times the average annual pavement temperature. A factor of 1.47 is used to convert the monthly air temperatures to pavement temperatures. This factor incorporates the effects of diurnal variations in both temperature and traffic loading.

8.1.3 Analysis

Fig.8.4 is reproduced from Thrower (81). It shows the pavement life in axles for the two pavement structures at various temperatures. This data has been reproduced in Table 8.1. The corresponding tensile strains have been added by use of Thrower's fatigue lines in Fig.8.2. The lives for each pavement have been added to Table 8.1, both the simple and cumulative damage approaches having been used. The simple approach took an annual pavement temperature of 14.5°C (Thrower's weighted mean for Alconbury by-pass) and Thrower's results from Fig.8.4. The cumulative approach used his data, from the same source, which gave the number of axle loads in each of his seven temperature

Table 8.1 TRRL LABORATORY LIVES FOR TEMPERATURE CLASS DISTRIBUTION

	Temperature Class (^{o}C)							Pavement life	
	-3.75	3.75	11.25	18.75	26.25	33.75	41.25	Using Miner's rule	Using axle weighted mean temp. (14.45^{o})
Fraction of axles	0.102	0.056	0.388	0.252	0.170	0.029	0.002		
120 mm pavement									
Strain × 10^{6}	115	132	170	211	264	293	312		
life	850	610	370	270	190	230	340	310	316
370 mm pavement									
Strain × 10^{6}	23.8	32	44.5	61.3	87.7	113.8	126.7		
life	890000	440000	190000	85000	32000	19000	23000	82140	143000

classes. Miner's rule was applied as follows:

$$N = \frac{1}{\sum \frac{f}{N_t}} \qquad (8.2)$$

where N is the pavement life in axles,

f is the fraction of axles in temperature class t,

N_t is the life for pavement temperature t.

Table 8.2 gives the laboratory lives for the same temperature classes, but the asphalt mix stiffnesses were calculated using the equations adopted at Nottingham and Nottingham based fatigue lines as discussed in more detail later. Thrower considered both asphalt layers as one, so the same assumption was made for the Notingham design calculations. This layer was assumed to be a typical DBM having a 100 pen binder content of 3.5% and a 10% void content. A plot of mix stiffness against temperatures for each pavement thickness is given in Fig.8.5. A constant Poisson's ratio of 0.35 was assigned to the asphalt layer in order to reduce the number of computations. This value was taken as fairly typical from Thrower, Fig.8.3. The computer program BISTRO (38) was used to determine the strains.

The laboratory lives in Table 8.2 were also calculated by two different methods. The first used the Nottingham fatigue line given in Fig.8.2, for every temperature. In the second method, this fatigue line shifted to give a range of parallel lines for different temperatures, as shown in Fig.8.6, in an attempt to more closely simulate the TRRL data. The particular fatigue line used in the first method was taken to represent a temperature of 10°C, since this was the temperature at which the majority of the fatigue tests had been carried out at Nottingham. The adjustment in life, for each 5°C temperature

Table 8.2 NOTTINGHAM LABORATORY LIVES FOR TEMPERATURE CLASS DISTRIBUTION

	Temperature Class (°C)							Pavement life	
	-3.75	3.75	11.25	18.75	26.25	33.75	41.25	Using Miner's rule	Using axle weighted mean temp. (14.45°C)
Fraction of axles	0.102	0.056	0.388	0.252	0.170	0.029	0.002		
120 mm pavement									
Asphalt stiffness (MPa)	16580	11230	6870	3640	1548	680	290		
Strain × 10^6	76	95	122	159	196	196	143		
Life using Nottingham fatigue line	27400	13800	6420	2850	1500	1500	3940	3450	4500
Life using Nottingham fatigue line with temp. variation	7690	7750	7206	6400	6735	13470	70760	7086	6790
370 mm pavement									
Asphalt stiffness (MPa)	15700	10600	6450	3400	1440	640	280		
Strain × 10^6	18	25	36	54	87	115	123		
Life using Nottingham fatigue line	2250000	823000	269500	77900	18080	7690	6260	54700	168110
Life using Nottingham fatigue line with temp. variation	631380	461890	302500	174880	81180	69054	112430	180562	253620

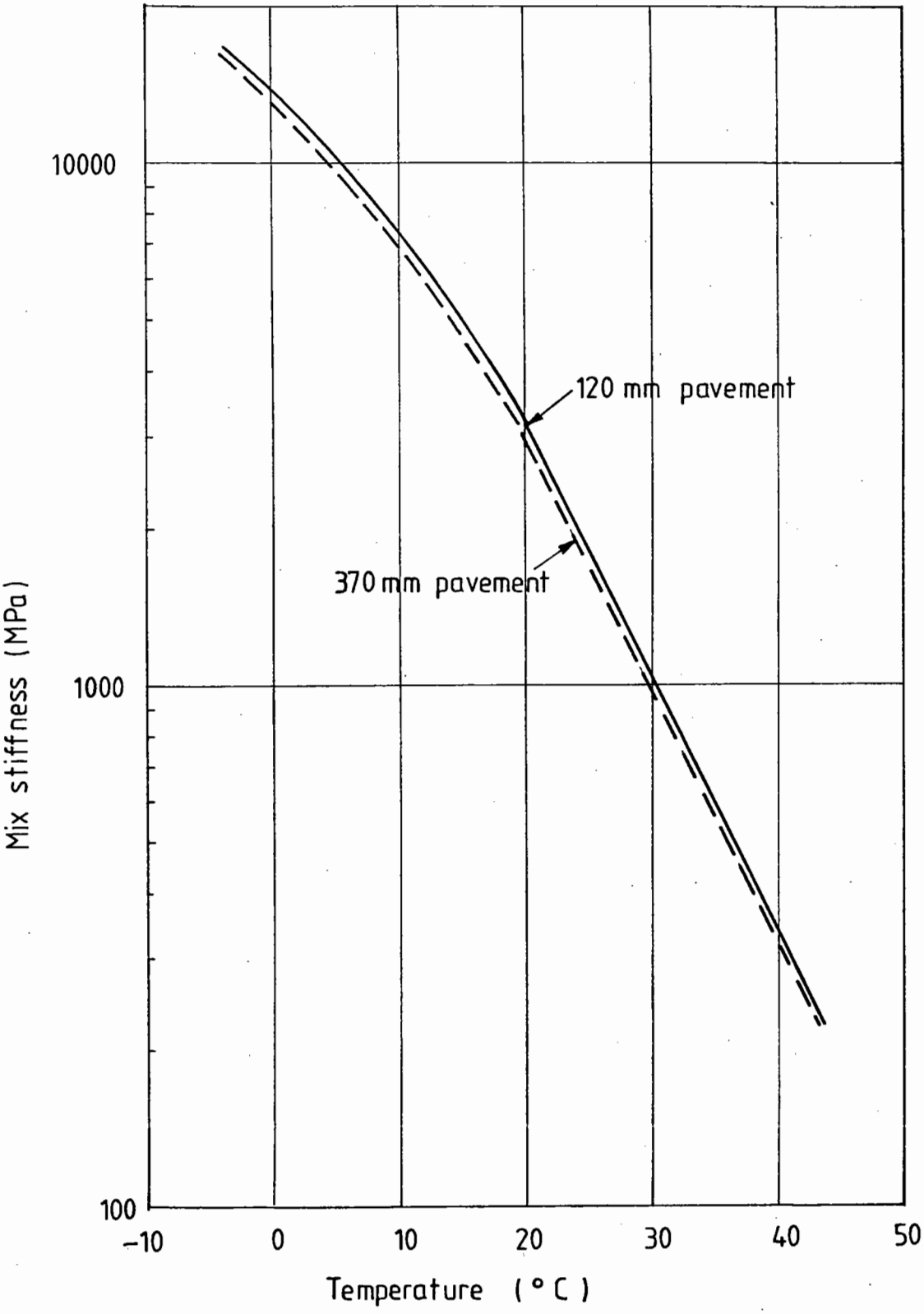

FIG 8·5 MIX STIFFNESS AS A FUNCTION OF TEMPERATURE

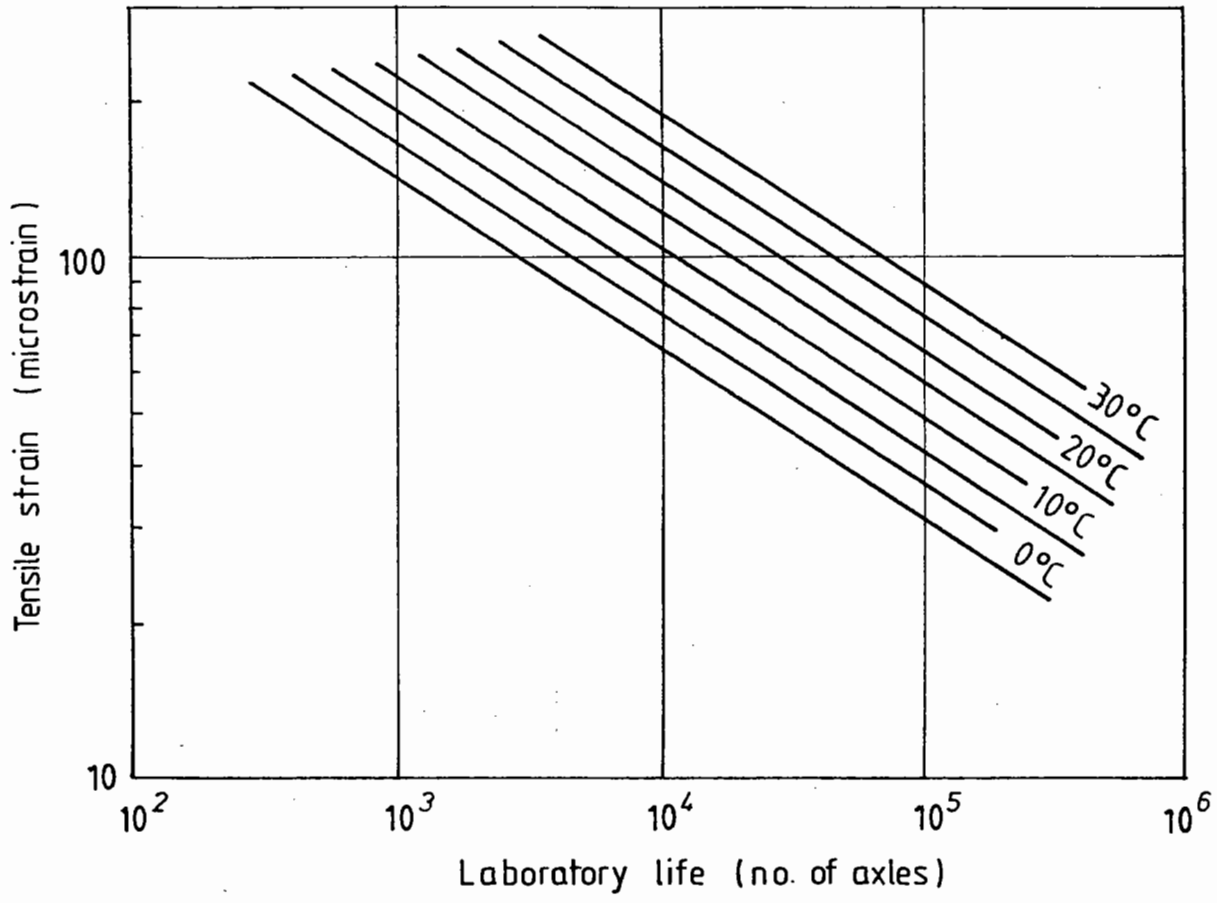

FIG 8.6 NOTTINGHAM FATIGUE LINE WITH ADJUSTMENTS FOR TEMPERATURE

increment was the same as that given by Thrower in Fig.8.2. This relationship between the life at temperature t (°C), (N_t) and the standard life at a temperature of 10°C, (N_{10}), can be expressed as follows:

$$N_t = \frac{N_{10}}{4} \times 16^{\left[\frac{t+5}{30}\right]} \qquad (8.3)$$

Table 8.3 was prepared to indicate the lives calculated using the methods adopted at Nottingham, which are incorporated in the programs ANPAD and CUDAM. This involves use of an average annual design temperature for the simple analysis and average monthly pavement temperatures for considering cumulative damage. Cumulative damage analysis used Miner's rule for the twelve lives (N_{t_1} to $N_{t_{12}}$) obtained for each average monthly temperature (t_1 to t_{12}), as follows:

$$N = \frac{1}{12} \sum_{t_1}^{t_{12}} \frac{1}{N_{t_i}} \qquad (8.4)$$

8.1.4 Summary

Table 8.4 gives a summary of each of the design approaches that was tried - cases 1 to 4. The longest pavement lives were calculated when the temperature adjusted Nottingham fatigue lines were used as the fatigue criteria (case 2). These were considered unrealistic, as the temperature adjustments were based purely on the laboratory fatigue lines established by TRRL.

For the thinner pavement, there was a large discrepancy between the lives calculated using the TRRL fatigue criterion (case 1) and those calculated using the single Nottingham fatigue line (cases 3 and 4). The latter were approximately ten times greater. However, there was no significant difference between the life calculated using Miner's rule and that calculated for a mean annual temperature for the TRRL

Table 8.3 NOTTINGHAM LABORATORY LIVES USING MONTHLY PAVEMENT TEMPERATURES

	Monthly temperature (°C)												Pavement life		
	J	F	M	A	M	J	J	A	S	O	N	D	Using Miner's rule	Using average annual pavement temperature (14·2 °C)	Using design temperature (18·6 °C)
Average monthly air temperature, T_A	3.3	3.7	5.9	8.5	11.5	14.7	16.6	16.2	14.1	10.2	6.6	4.5			
Average monthly pavement temp., $T_A \times 1.47$	4.9	5.4	8.7	12.5	16.9	21.6	24.4	23.8	20.7	15.0	9.7	6.6			
120 mm pavement															
Mix stiffness (MPa)	10500	10180	8230	6250	4330	2720	1960	2110	2990	5110	7680	9450			
Strain × 10^6	99	100	112	128	149	174	189	186	169	140	116	104			
Life (axles)	12180	11180	8340	5540	3480	2170	1680	1770	2370	4210	7490	10470	3670	4600	2940
370 mm pavement															
Mix stiffness (MPa)	9890	9590	7740	5870	4050	2540	1830	1970	2790	4790	7220	8900			
Strain × 10^6	26	27	31	38	49	65	78	75	62	44	33	28			
Life (axles)	729880	650230	425970	228380	104860	44150	25260	28490	51020	145790	351760	581710	81340	168110	78500

Table 8.4 SUMMARY OF PAVEMENT LIVES USING DIFFERENT METHODS OF CALCULATION

Case No.		120mm pavement				370 mm pavement			
		Laboratory life			Ratio $\frac{\text{Life}_{\text{mean temp.}}}{\text{Life}_{\text{Miner's rule}}}$	Laboratory life			Ratio $\frac{\text{Life}_{\text{mean temp.}}}{\text{Life}_{\text{Miner's rule}}}$
		Using Miner's rule	Using mean pavement temperature	Using design temperature		Using Miner's rule	Using mean pavement temperature	Using design temperature	
1	TRRL Method TRRL temperature classes and TRRL fatigue lines	310	316 *		1.02	82140	143000 *		1.74
2	TRRL temperature classes and temperature adjusted Nottingham fatigue lines	7090	6790 *		0.96	180560	253620 *		1.40
3	TRRL temperature classes and Nottingham fatigue line	3450	4500 *		1.30	54700	168110 *		3.07
4	Nottingham Method Monthly temperatures and Nottingham fatigue line	3670	4600 +	2940 ×	1.25	81340	168110 +	78500 ×	2.07

* TRRL weighted mean pavement temperature (14·45°C)

\+ Nottingham mean pavement temperature equal to 1·47 times average annual air temperature. (14·2°C)

× Nottingham design temperature (18·6°C)

design method (case 1). Using the Nottingham fatigue criterion, however, (cases 3 and 4), the life calculated for a mean annual pavement temperature was 30% greater than that calculated using Miner's rule. However, when the annual design temperature was used the life was 20% less than that calculated using Miner's rule.

For the thin pavement, the effect of using TRRL's temperature classes as opposed to traffic weighted average monthly pavement temperatures was minimal. For the thick pavement, there was some discrepancy when using Miner's rule.

For the 370mm pavement, there was close agreement between the lives calculated by the TRRL design method (case 1) and those determined from the Nottingham design method (case 4). For this thicker pavement, the lives calculated using the mean annual pavement temperature rather than the cumulative approach were 1.7 and 2.0 times greater, but close agreement was achieved using the annual design temperature.

This exercise has shown that the approach to temperature and traffic variations both during a 24-hour period and from month to month, which had been used in the Nottingham computations, is realistic. The TRRL data, based on numbers of axles actually observed during various temperature ranges, when used for design, gives similar results.

The main discrepancies between the TRRL work and that at Nottingham, is caused by the different nature of the basic fatigue relationship derived from laboratory testing. For the particular mix examined here (a typical DBM), the Nottingham fatigue line is much steeper. In addition, no temperature dependence was observed in the Nottingham work.

Comparisons with fatigue data used elsewhere, discussed in Chapter 4, indicates that the Nottingham fatigue law has more similarities to the results obtained in other countries.

8.2 COMPARISON OF TRRL DESIGNS FOR HEAVY TRAFFIC WITH DESIGNS USING ANPAD

The design of a bituminous road pavement against fatigue cracking under heavy traffic is discussed in detail by Goddard (93), who also provides a new design curve for heavy traffic. The design curve enables a direct comparison to be made between TRRL pavement designs for heavily trafficked roads and designs carried out by the computer program ANPAD when detailed information about the materials is considered.

8.2.1 Pavement Structure

The TRRL design structure for heavy traffic is shown in Fig.8.7. It differs from conventional structures in that it has two base layers. The upper base layer is a DBM which has good resistance to permanent deformation, whilst the lower is a HRA which provides better resistance to fatigue cracking. The HRA is placed below the DBM as the maximum tensile strains generally occur at the bottom of the asphalt layers.

An alternative approach is to use a single base material which provides good resistance to both permanent deformation and fatigue cracking, such as the modified bases developed at Nottingham, or the improved DBM described by Leech (97). This approach is discussed in more detail in section 8.2.5.

8.2.2 Analysis

A review of the TRRL design procedure reported by Thrower (81) has been included in Section 8.2.1. There are several differences between the TRRL design method and that adopted at Nottingham and some of these are summarised below:

Fatigue criterion: TRRL consider the fatigue line, (a logarithmic plot of the maximum allowable tensile strain in the asphalt against

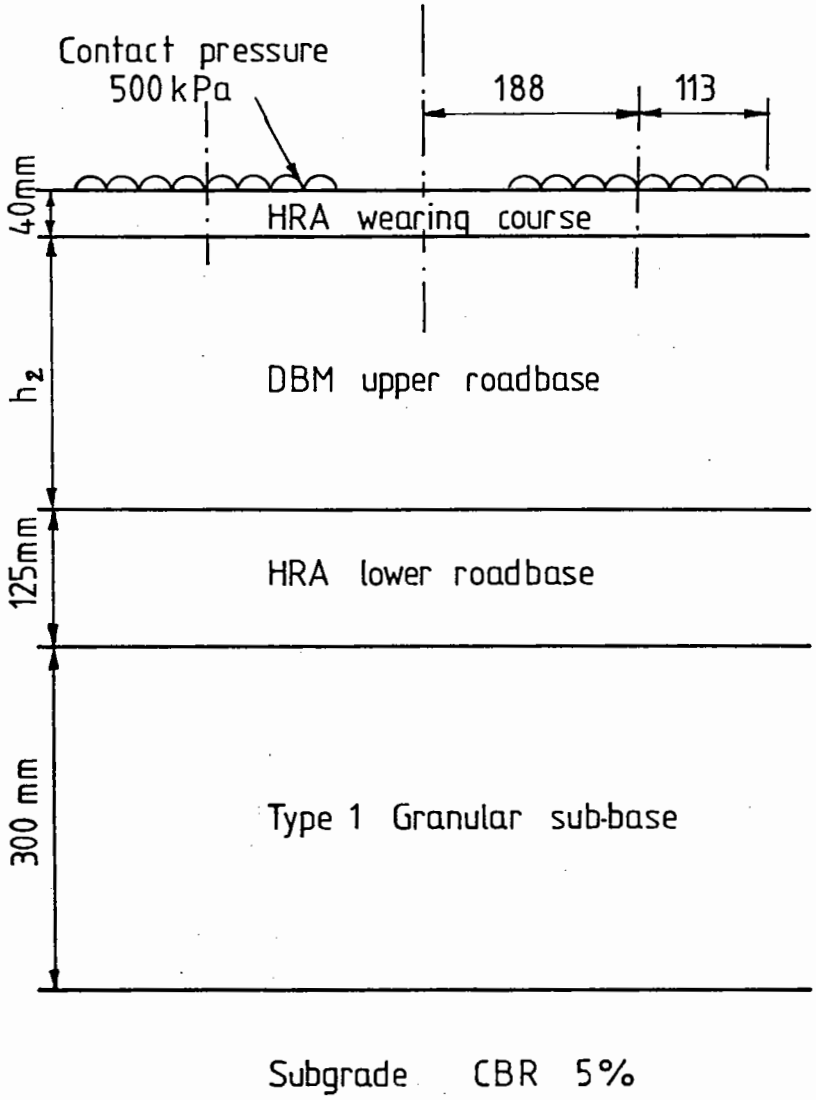

FIG 8.7 TRRL DESIGN STRUCTURE FOR HEAVY TRAFFIC

life in millions of standard axles), for a particular mix to shift with temperature. At Nottingham a unique fatigue line is used for each mix.

Goddard (93) adopts a factor of 700 to convert the laboratory fatigue lives to those for pavement design. This factor does not include any allowance for crack propagation. ANPAD uses a laboratory to field fatigue life conversion factor of 440 of which a factor of 20 is included for crack propogation.

Temperature: TRRL use a cumulative damage approach when designing against fatigue cracking as demonstrated by Thrower (81). Typically, the pavement is designed for seven pavement temperature classes (−3.75°C to 41.25°C). Then, using the fraction of axles likely to occur in each temperature class, the relative damage of each temperature class may be assessed and summed using Miner's rule to obtain the pavement life. A simplified distribution of commercial vehicle wheel loading under different temperature regimes is given by Goddard (95).

ANPAD uses just two pavement design temperatures to calculate the bituminous mix stiffness in the sub-routine PONOS (58). To calculate the subgrade strain, when designing against permanent deformation, the design temperature equals 1.47 times the average annual air temperature (°C). The 1.47 factor is used to convert the air temperature to a design temperature and incorporates the effects of diurnal variations in both temperature and traffic loading. The cumulative damage effects in fatigue are taken into consideration by using a further factor of 1.31 on the design temperature when calculating the tensile strains.

Traffic loading: The TRRL design method uses a spectrum of loads. For the particular structure under consideration a heavy traffic load spectrum was used as described by Thrower (81). ANPAD uses a standard (80 kN) dual wheel loading arrangement.

8.2.3 Materials

Dense bitumen macadam: Goddard (93) used a DBM with a measured binder content of 3.5% and void content 7.5%. The stiffness moduli were also measured and the results for frequencies of 5 and 8 Hz are duplicated in Fig.8.8a. Using the same mix proportions and a frequency of loading of 5 Hz, the stiffness moduli were calculated for a range of temperatures following the relationship established by Brown (54) based on that of Van der Poel (9). Assumed specific gravities of the aggregate and binder were 2.7 and 1.02 respectively. The calculated stiffness moduli were higher than those measured by TRRL and are shown in Fig.8.8a. Further calculations were made using an increased void content of 10%. These resulted in mix stiffnesses closer to those measured and are also shown in the same figure.

Hot rolled asphalt: No details were given by Goddard (93) of the mix proportions of the HRA, but the mix stiffnesses of the HRA wearing course and road base were determined by laboratory measurements on materials from a full scale pavement. The figures for road base are given in Fig.8.8b. The typical binder content and void content of a HRA base are 5.7% and 6% respectively. Using these values,the calculated mix stiffnesses for 5 Hz closely agreed with those measured by TRRL (see Fig.8.2b).

Sub-base and subgrade: The TRRL designs used a subgrade stiffness modulus of 45 MPa and sub-base modulus of 150 MPa, the subgrade value representing a CBR of 5%. Following the design procedure used at Nottingham for a CBR of 5% the subgrade stiffness modulus was taken as 50 MPa. The stiffness modulus of the sub-base was taken as 100 MPa based on a study of sub-base to subgrade modular ratio using the SENOL non-linear finite element computer program (44).

TRRL assumed Poisson's rations of 0.35, 0.4 and 0.4 for the bituminous materials, sub-base and subgrade respectively. The designs

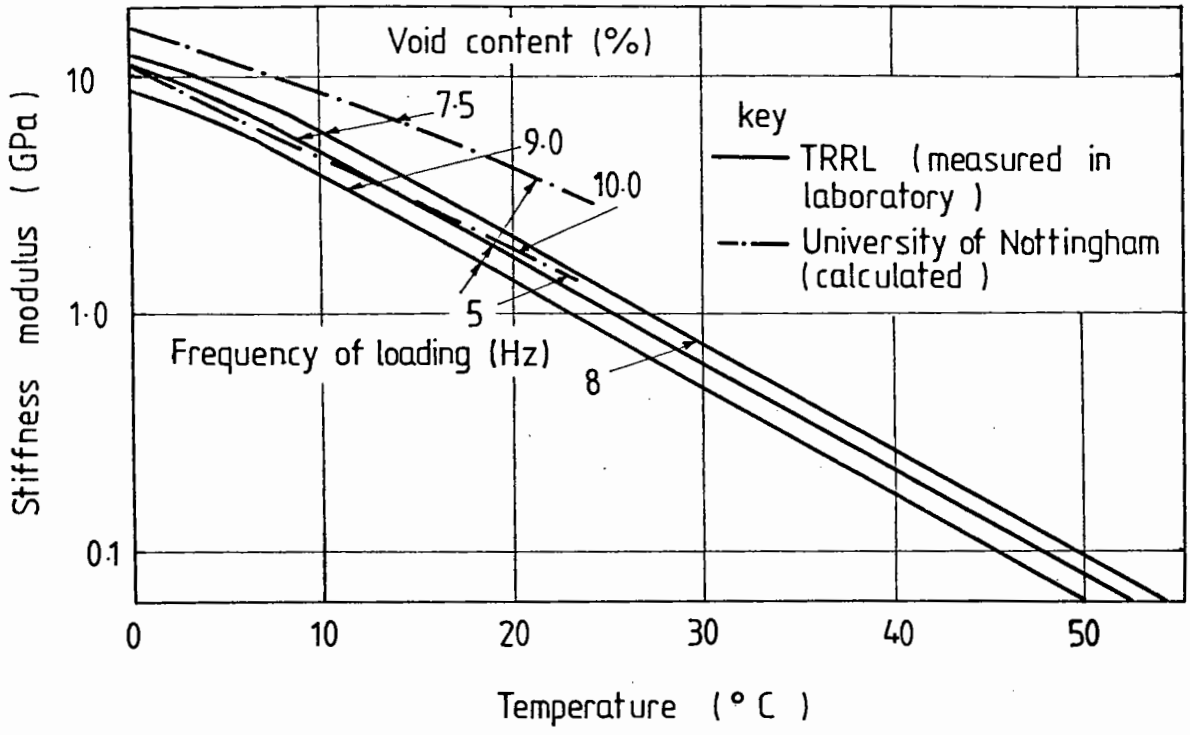

a. Dense Bitumen Macadam

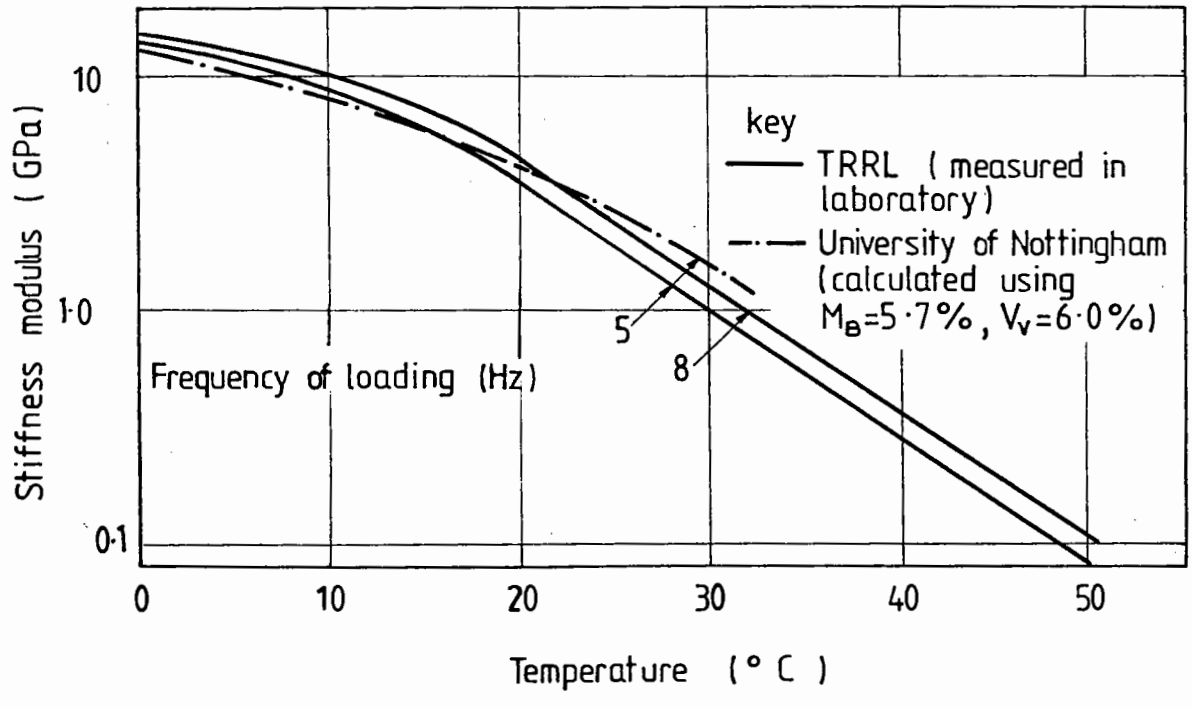

b. Hot Rolled Asphalt

FIG 8·8 STIFFNESS MODULI OF BITUMINOUS MATERIALS

made using the computer program ANPAD used Poisson's ratios of 0.4, 0.3, 0.4 for the bituminous materials, sub-base and subgrade.

8.2.4 Comparison of designs

Fig.8.9 compares the TRRL design curve produced by Goddard (93) with the design curves produced by ANPAD for the same structure (see Fig.8.7). When the DBM void content of 7.5% was used, the ANPAD computer program designs were about 20mm thinner than the TRRL ones. However, when the DBM void content was increased to 10% the design curves for ANPAD agreed closely with TRRL. In this case, the mix stiffnesses of the bituminous layers also showed good agreement.

The TRRL design curve gives the thickness of the DBM upper road base to prevent fatigue cracking which is, hence, the critical design case. For the same structure, the critical case using ANPAD is permanent deformation. A comparison of design lives is given in Table 8.5

8.2.5 Use of Alternative Materials

An alternative approach is to provide a single base layer which has good resistance to both fatigue cracking and permanent deformation. Two types of novel mix have been developed at Nottingham which have these properties. The first is a modified HRA with less 50 pen binder and more filler than a typical HRA. The second is a modified DBM made with a 50 pen binder rather than 100 pen binder. The aggregate grading is also adjusted to give a material which is easier to compact. The material is similar to that described by Leech (97).

The pavement designs performed earlier by ANPAD were repeated but with a single modified base layer replacing the two base layers in the TRRL structure. The base thicknesses were calculated for lives of 100, 140 and 200 msa and the results are plotted in Fig.8.10, which also

Table 8.5. COMPARISON OF LIVES FOR TRRL STRUCTURE FOR HEAVY TRAFFIC

Upper road base conditions	Calculated Lives using Nottingham Design Method (msa)				TRRL design lives (msa)
	Life against fatigue cracking		Life against permanent deformation	Design life	
	DBM upper* Road base	HRA lower Road base			
DBM upper road base, V_v = 7.5%					
Thickness (mm) 190	370	> 800	142	142	97
210	380	> 800	195	195	140
230	400	> 800	263	263	205
DBM upper road base, V_v = 10%					
Thickness (mm) 190	470	750	105	105	
210	445	> 800	142	142	
230	430	> 800	187	182	

* Calculated using BISTRO

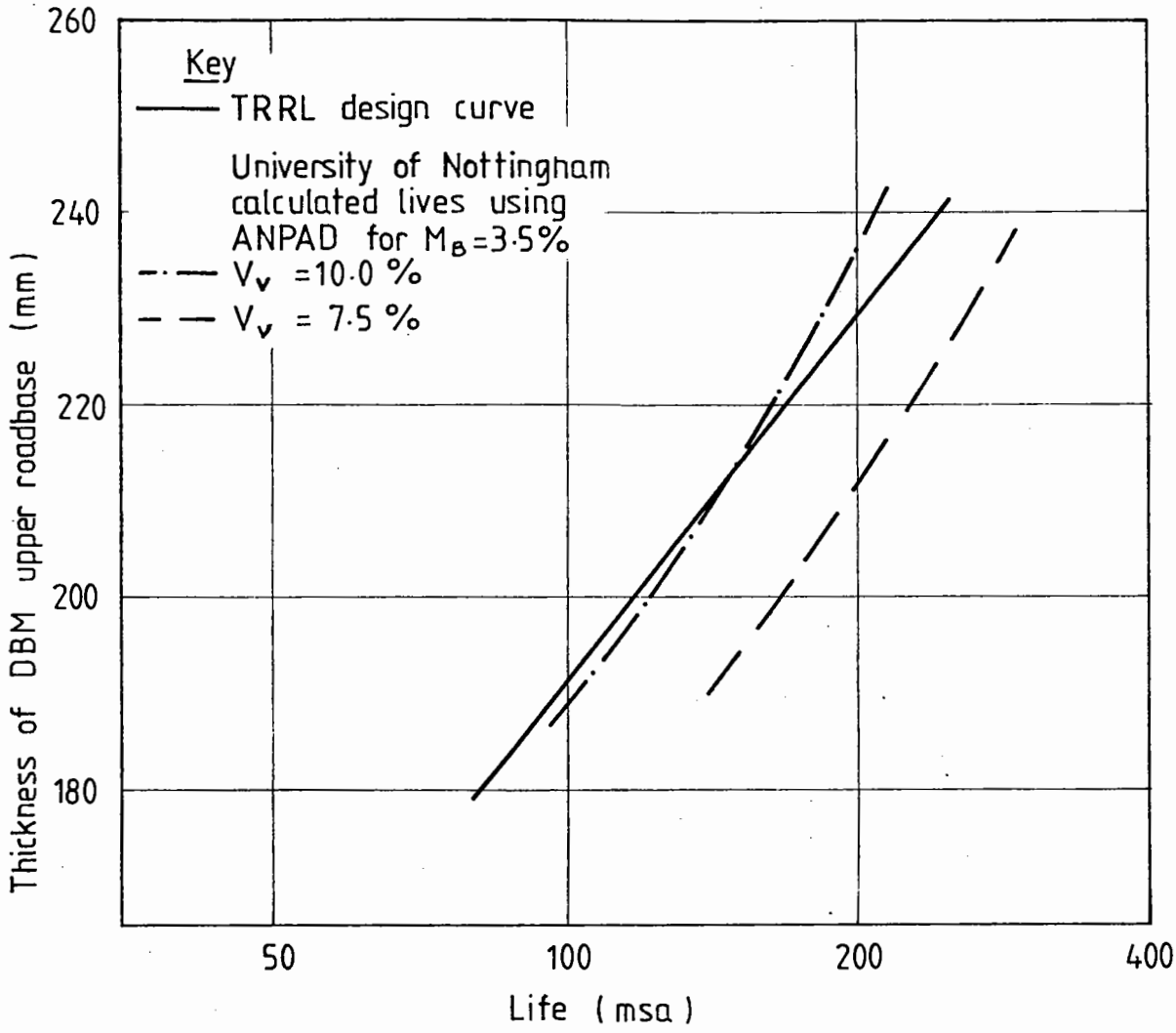

FIG 8·9 COMPARISON OF TRRL DESIGN CURVE FOR HEAVY TRAFFIC WITH ANPAD DESIGNS FOR THE SAME STRUCTURE

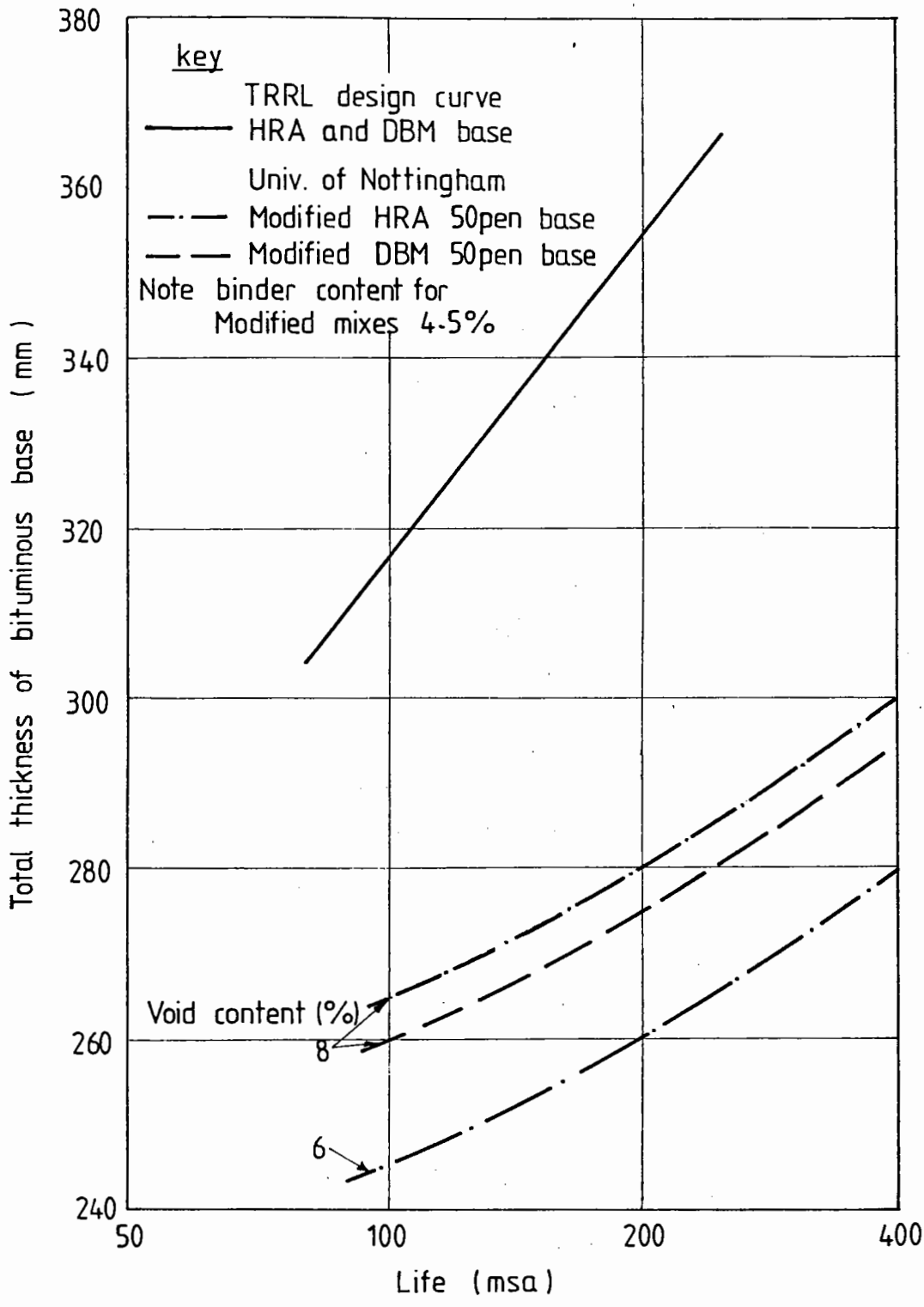

FIG 8·10 EFFECT OF BASE MATERIAL ON DESIGN LIFE

shows the total base thickness for the TRRL designs (i.e. road base plus lower road base). The effect of using the single modified base layer is to produce a saving on total base thickness of 60 to 100 mm when compared to the TRRL designs. The saving is still 40 to 80 mm when compared to the designs made by the computer program ANPAD for the TRRL structure.

8.2.6 Conclusions

1. The calculated mix stiffnesses for the DBM base were higher than those measured by TRRL assuming a void content of 7.5%.
2. The calculated mix stiffnesses for the HRA base agreed reasonably well with those measured by TRRL.
3. The TRRL designs required about 20mm more of the DBM base than determined by the computer program ANPAD for the same structure with a DBM having a void content of 7.5%.
4. The critical design criterion in the TRRL designs was fatigue cracking whilst for the designs by ANPAD it was permanent deformation.
5. Considerable savings in total base thickness may be achieved by replacing the two base layers in the TRRL pavement structure with a single modified base layer.

8.3 COMPARISON OF ROAD NOTE 29 DESIGNS AND THOSE USING THE SHELL PAVEMENT DESIGN MANUAL WITH THOSE USING ANPAD

In section 11.2 of the Shell Pavement Design Manual (94) a comparison is made between the Shell designs and those recommended in Road Note 29 (1) for use in Britain. The structures cover a range of design lives from 1 to 100 msa and use subgrades with CBR values of 5 and 2.5%. As a further comparison, these Road Note 29 structures have now been analysed using the computer program ANPAD to calculate the

required base thickness for the same design lives. The lower layers of each structure are detailed in Table 8.6. Designs were produced for bases with hot rolled asphalt (HRA) and dense bitumen macadam (DBM). Details of surfacing layers are noted beneath Table 8.6.

8.3.1 Design Conditions

Speed: A loading time of 0.02 seconds was adopted by Shell as being fairly typical. This corresponds to an average speed of commercial vehicles of approximately 50 km/hr which was used in the designs carried out with ANPAD.

Loading: Both the Shell calculations and ANPAD computer program use similar loading arrangements based on a standard dual wheel load of 40 kN.

Temperature: The Shell design charts use a weighted mean annual air temperature (w-MAAT) for design which takes into account daily and monthly variations in the pavement temperatures. For London, a recommended w-MAAT of 12°C is given. A check on this weighted temperature was made using the average monthly air temperatures for the Central Region of England as given by Croney (63) and the corresponding weighting factors taken from chart W of the Shell Manual. The results are tabulated in Table 8.7. The average weighting factor calculated in Table 8.7 corresponds to a w-MAAT of 12°C in the Shell chart W.

An average annual air temperature of 9.5°C was assumed for the ANPAD designs. This is adjusted within the program to give two pavement design temperatures. The first is 14.5°C, (9.5 x 1.47), which is used to calculate the subgrade strain where the 1.47 factor converts the air temperature into a design temperature taking account of both diurnal variations in temperature and traffic. The second design temperature, 18.3°C, (9.5 x 1.47 x 1.31) is used for dealing with fatigue cracking. The additional 1.31 factor takes into consideration cumulative damage effects.

Table 8·6 DETAILS OF SUBGRADES AND SUB-BASES FOR STRUCTRES RECOMMENDED BY ROAD NOTE 29 AND ANALYSED BY ANPAD

CBR (%)	Life (msa)	Subbase thickness (mm)
5	1	210
	10	260
	100	310
2.5	1	380
	10	460
	100	540

Note: 1. Each structure has 40mm HRA wearing course.

2. Structures with a design life of 1 msa also have 30mm HRA base course.

3. Structures with a design life of 10 and 100 msa also have 60mm HRA base course.

Table 8.7 DETERMINATION OF WEIGHTED MEAN ANNUAL AIR TEMPERATURE FOLLOWING THE SHELL DESIGN PROCEDURE

Month	Average monthly Air Temperature (^{0}C)	Shell Weighting Factor
Jan	3.3	0.105
Feb	3.7	0.115
Mar	5.7	0.15
Apr	8.5	0.225
May	11.3	0.32
Jun	14.4	0.44
Jul	16.0	0.62
Aug	15.6	0.6
Sep	14.0	0.47
Oct	10.2	0.29
Nov	6.6	0.17
Dec	4.5	0.125
Average	9.5	0.3

Corresponding Shell weighted mean annual air temperature = 12^{0}C

8.3.2 Materials

Bituminous Materials: Typical details of the bituminous materials used in Britain are given in Table 8.8. These are also those used in the ANPAD design calculations. The Shell design manual defines the bituminous material by its mix stiffness, fatigue resistance and initial penetration of the binder. Figs. 8.11 and 8.12 show the stiffness relationships S1 and S2 adopted by Shell for bituminous materials using 50 and 100 pen bitumens. In order to determine into which category the British mixes fall, calculated values have been superimposed on to Figs. 8.11 and 8.12 for the typical mixes given in Table 8.8. The HRA base and basecourse and the DBM base show good agreement with the S1 curves for the relevant binder penetration. However, the HRA wearing course lies somewhere mid-way between the S1 and S2 curves on the plot of mix stiffness against bitumen stiffness (see Fig.8.11), and between the S1-50 and S2-50 plots in Fig.8.12.

The two design methods assume different fatigue relationships. Fig.8.13 shows fatigue lines for the typical mixes. These were derived from equations based on laboratory testing at Nottingham by Cooper and Pell (56) together with a shift factor of 440 for converting laboratory lives to design lives. This factor takes into consideration crack propagation, rest periods and lateral wheel distribution. Fig.8.13 also gives the Shell fatigue lines for the two characteristic categories F1 and F2 for mix stiffnesses of 5800 and 7900 MPa. These mix stiffnesses were selected as being representative of the DBM and HRA bases respectively, using the mix details given in Table 8.8 and a weighted mean annual air temperature of 12°C. Hence, these lines would represent the choice of fatigue lines available following the Shell design procedure. Both the F1 and F2 curves give shorter fatigue lives for the HRA base material, but these designs are usually deformation critical. The slope of the F1 and F2 curves is less than that for the

Table 8.8 TYPICAL MIX DETAILS OF THE BITUMINOUS MATERIALS

	Initial Penetration	Binder Content (%)	Void Content (%)	Specific gravity of aggregate	Specific gravity of aggregate
HRA wearing course	50	7.9	4.0		
HRA base course	50	5.7	6.0	} 2.7	} 1.02
HRA base	50	5.7	6.0		
DBM base	100	3.5	10.0		

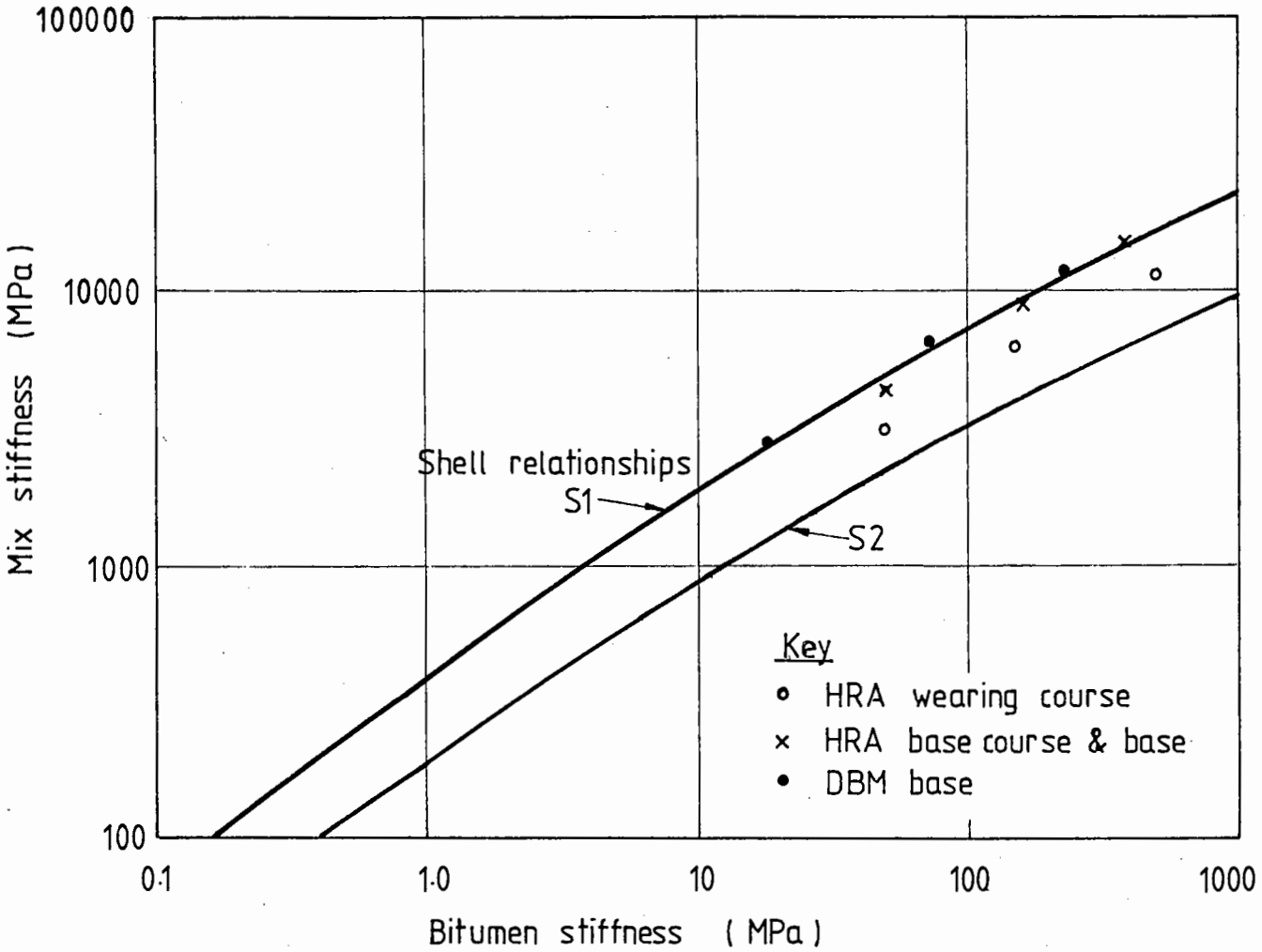

FIG 8.11 RELATIONSHIPS BETWEEN MIX STIFFNESS AND BITUMEN STIFFNESS

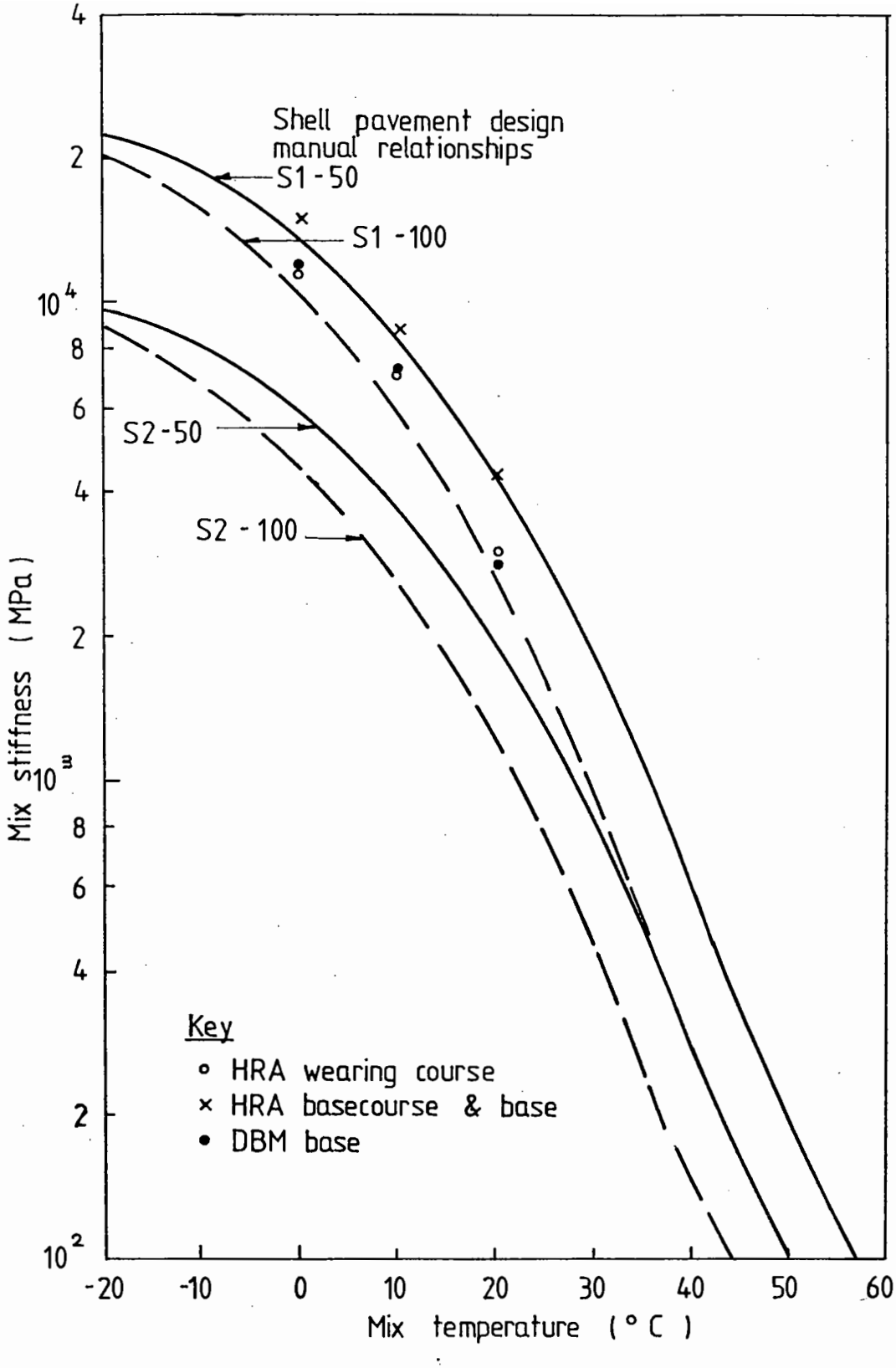

FIG 8·12 RELATIONSHIPS BETWEEN MIX STIFFNESS AND MIX TEMPERATURE AT A LOADING TIME OF 0·02 SECONDS

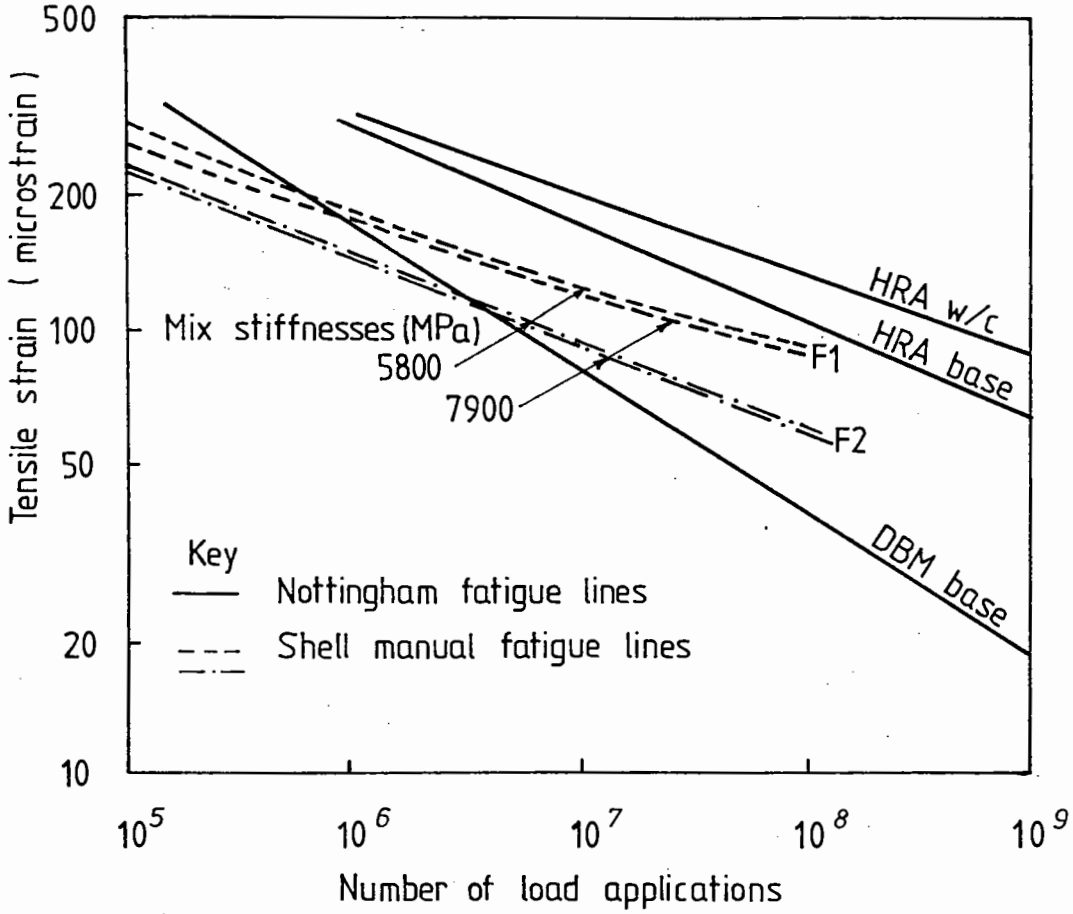

FIG 8·13 FATIGUE LINES FOR THE TYPICAL MIXES

Nottingham DBM fatigue line. Although a shorter fatigue life is given by the Shell lines at high tensile strains, at lower strains the lives are much longer than those predicted by the Nottingham fatigue line. In the Shell comparison with Road Note 29 it is interesting to note that the F2 fatigue curve is used.

Sub-base and Subgrade: Both the Shell Design Manual (94) and the computer program ANPAD use a factor of 10 to convert the subgrade CBR value to Young's modulus in MPa. In order to obtain the stiffness modulus of the sub-base, the computer program ANPAD uses a sub-base to subgrade modular ratio. This ratio has been studied using the SENOL non-linear finite element program (44). For each of the structures analysed by ANPAD, a sub-base stiffness modulus of 100 MPa was used. The Shell design manual specifies minimum stiffness moduli for the sub-base depending on its position in the structure and the subgrade modulus. These range from 100 to 800 MPa. Thus the Shell design procedure divides the total Road Note 29 sub-base into several sub-layers of different thickness and modulus. Table 8.9 gives an example of the relative thicknesses and stiffness moduli for the Shell designs using the S1-F2-100 design charts for 12°C. The sub-base moduli assumed by the Shell designs are, therefore, considerably higher than those used in the ANPAD computer program.

8.3.3 Comparison of Designs

Table 8.10 compares the design base thicknesses from the ANPAD calculations with those recommended by Road Note 29 (1) and the Shell Pavement Design Manual (94). The Shell base thicknesses are given for both the S1 and S2 stiffness models although, as shown in Figs. 8.11 and 8.12, the S1 curves appear to be more appropriate. The F2 fatigue lines were used even though they do not agree with the Nottingham fatigue lines (see Fig.8.13). The F2 fatigue lines are more

Table 8.9 MINIMUM SUB-BASE THICKNESS AND STIFFNESS MODULI FOR THE SHELL DESIGN PROCEDURE USING THE S1-F2-100 DESIGN CHARTS FOR 12°C

CBR (%)	Life (msa)	Total sub-base thickness (mm)	Sub-base sublayer thickness (mm)			
			h_{2-1} (E_{2-1}= 800 MPa)	h_{2-2} (E_{2-2}= 400 MPa)	h_{2-3} (E_{2-3}= 200 MPa)	h_{2-4} (E_{2-4}= 100 MPa)
5.0	1	210	-	50	160	-
	10	260	-	90	170	-
	100	310	30	100	180	-
2.5	1	380	20	100	90	170
	10	460	80	110	100	170
	100	540	120	120	120	180

Table 8.10 COMPARISON OF REQUIRED BASE THICKNESSES FOR EACH DESIGN METHOD

Subgrade CBR (%)	Life (msa)	Sub-base thickness (mm)	Total Asphalt Thicknesses (mm)							
			Road Note 29		A N P A D		Shell Pavement Design Manual			
			HRA base	DBM base	HRA base	DBM base	S1-F2-50	S1-F2-100	S1-F2-50	S2-F2-100
5	1	210	150 (70+80)	160 (70+90)	150 (70+80)	170 (70+100)	100	130	150	170
	10	260	220 (100+120)	240 (100+140)	220 (100+120)	310 (100+210)	160	200	240	250
	100	310	320 (100+220)	370 (100+270)	310 (100+210)	490 (100+390)	230	280	320	350
2.5	1	380	150 (70+80)	160 (70+90)	160 (70+90)	180 (70+100)	110	150	190	210
	10	460	220 (100+120)	240 (100+140)	240 (100+140)	320 (100+220)	170	230	270	300
	100	540	320 (100+220)	370 (100+270)	350 (100+250)	510 (100+410)	250	310	370	400

Note: The figures in brackets, for example, (70+80) refer to the thicknesses of the asphalt layers. The first figure, 70, is the thickness (mm) of the HRA wearing course plus HRA base course. The second figure, 80, is the thickness (mm) of the base layer.

conservative than the F1 fatigue lines and are also those previously chosen by Shell in their comparison with Road Note 29 designs.

The HRA base thicknesses for the range of design lives and the DBM base thicknesses for 1 msa as calculated by the computer program ANPAD, agree to within 20mm with those recommended by Road Note 29. However, greater thicknesses were calculated for the DBM bases for 10 and 100 msa. The majority of both the ANPAD and Road Note 29 total asphalt thicknesses lie within the range obtained using the Shell Pavement Design Manual for mix stiffness curves S1 and S2. However, they should really be compared with Shell asphalt thicknesses obtained for mix stiffness curve S1 (see Figs. 8.11 and 8.12). This comparison indicates that the Shell designs require substantially less asphalt base material than the Road Note 29 or ANPAD structures. There could be several reasons for this, such as the differences in design temperatures used, fatigue models or elastic moduli of the sub-base.

A further comparison was made between the same ANPAD design structures and designs for a full depth structure using the Shell Pavement Design Manual. The results are given in Table 8.11. In the majority of cases the base thickness required by the Shell designs was still less than for the designs made using the computer program ANPAD even though these also had a substantial thickness of sub-base.

8.4 REVIEW OF THE ASPHALT INSTITUTE DESIGN PROCEDURE

The ninth edition of the Asphalt Institute Manual MS-1 (75) presents a structural design procedure for pavements. Details on the development of the manual are described by Shook et al (98,99). A series of charts are provided to determine the required thickness of each layer for a given life, expressed in terms of equivalent 80 KN standard axle loads (EAL), depending on the type of material and subgrade stiffness modulus. As these charts were developed for use in

Table 8.11 COMPARISON OF THE DESIGNS MADE USING THE COMPUTER PROGRAM ANPAD WITH FULL DEPTH DESIGNS USING THE SHELL PAVEMENT DESIGN MANUAL

CBR (%)	Life (msa)	ANPAD design thickness (mm)			Shell Full depth asphalt thickness (mm)	
		Sub-base	HRA	DBM	S1-F1-50	S1-F1-100
5	1	210	150	170	150	180
	10	260	220	310	210	260
	100	310	310	490	280	340
2.5	1	380	160	180	130	150
	10	460	240	320	180	230
	100	540	350	510	250	310

the United States, a wide temperature range was used and the subgrade modulus adjusted for periods of frost and thaw. It is, therefore, unrealistic to compare designs taken directly from the MS-1 charts with those calculated using ANPAD, which was developed for use in the United Kingdom where a much narrower range of temperatures is experienced.

8.4.1 Methods of Analyis

The design charts were prepared using a computer program DAMA (74) which, like ANPAD and CUDAM, incorporates the CHEVRON N-layer elastic program (39) to perform the structural analysis. The program examines both fatigue and permanent deformation on the basis of monthly cumulative damage concepts. Each month is analysed separately, and the damage summed until it equals 1 using Miner's rule (see Chapter 4).

8.4.2 Temperature

Table 8.12 summarises the three temperature regimes which were analysed by DAMA in the preparation of the design charts. For the first two regimes, frost effects were included by adjusting the stiffness moduli of the sub-base and subgrade layers each month (98,99). For example, the subgrade modulus was increased for the freezing period and reduced for the thaw period, as shown in Fig.8.14. Three normal subgrade moduli were used 31, 83 and 155 MPa.

In order to determine the stiffness moduli of the bituminous layers, the mean monthly air temperatures (MMAT) were converted to mean monthly pavement temperatures (MMPT) using the following equation developed by Witczak (33) from correlations between air temperatures and pavement temperatures at various thicknesses:

Table 8.12 MEAN MONTHLY AIR TEMPERATURE FOR THREE REPRESENTATIVE TEMPERATURE REGIMES

MAAT	Mean Monthly Air Temperature (°C)											
	Jan	Feb	Mar	Apr	May	Jun	Jul	Aug	Sep	Oct	Nov	Dec
7°C New York	-4	-4	-10	-3	6	9	19	21	18	13	9	5
15.5°C South Carolina	7	3	6	7	13	21	26	27	26	23	14	12
24°C Arizona	13	16	16	23	32	33	33	34	34	30	22	13

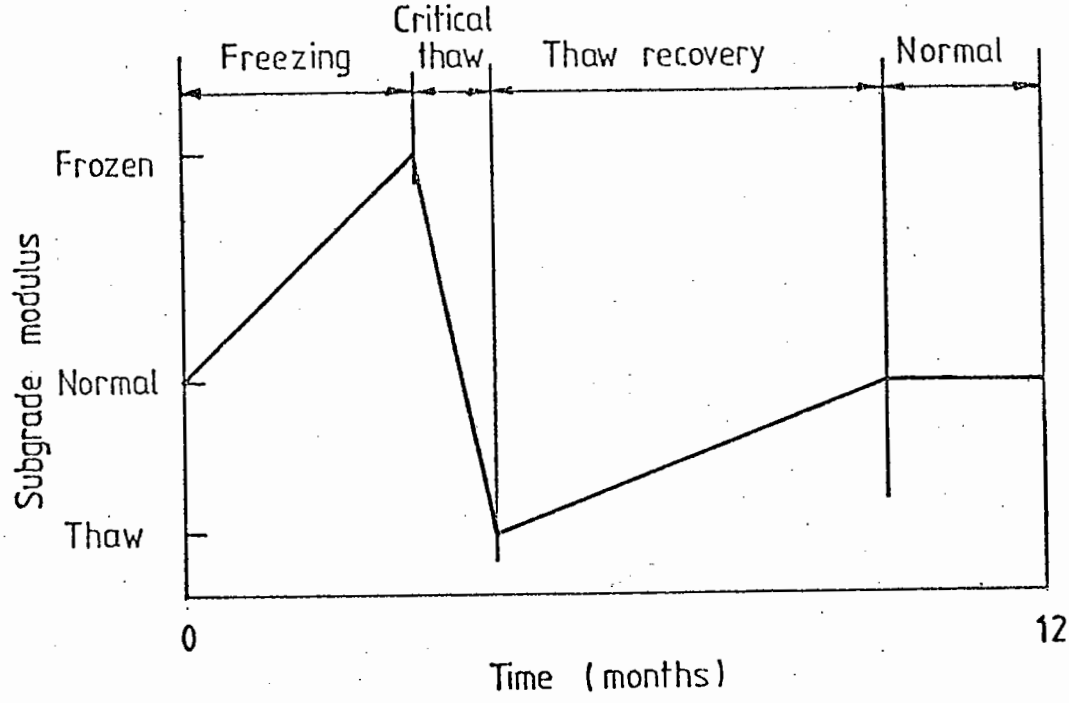

FIG 8.14 VARIATIONS IN SUBGRADE MODULUS THROUGHOUT THE YEAR

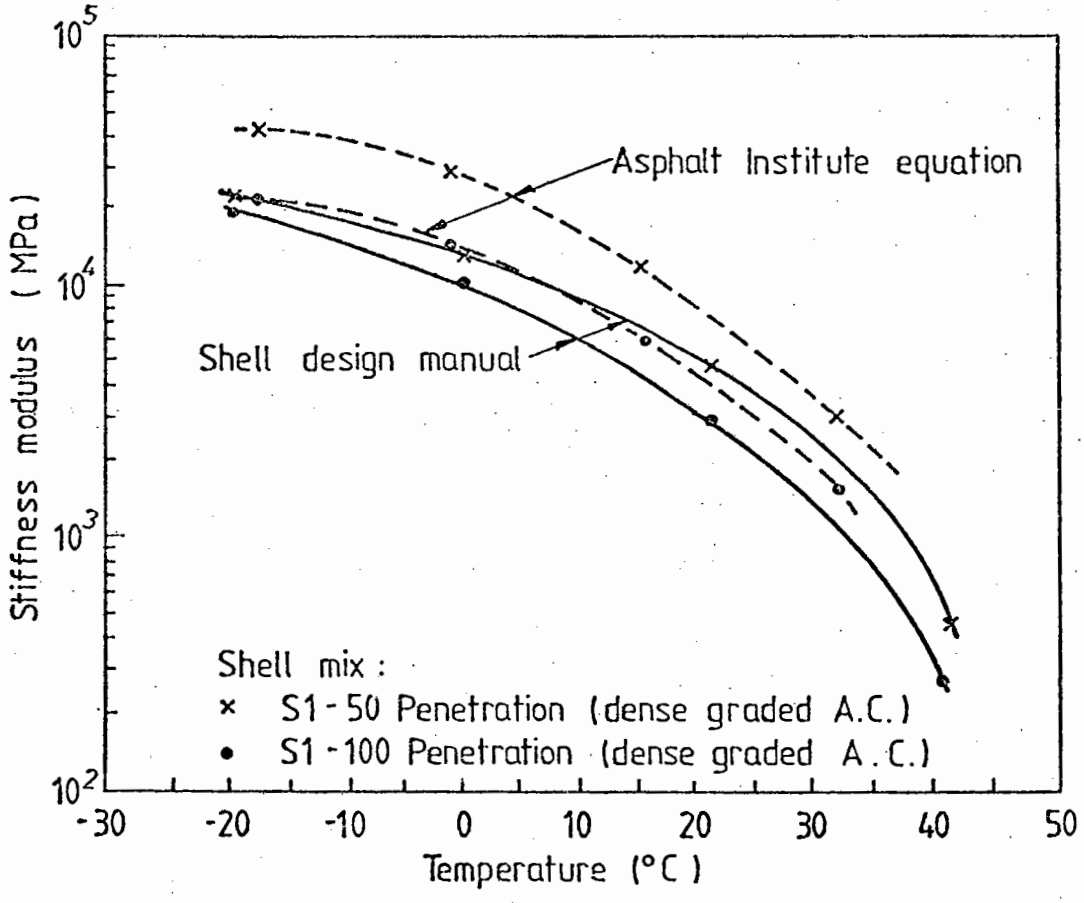

FIG 8.15 COMPARISON OF SHELL STIFFNESS MODULI TO THE ASPHALT INSTITUTE PREDICTION FOR THE SHELL MIXES

$$MMPT = MMAT \left[1 + \frac{1}{(z+4)}\right] - \frac{34}{z+4} + 6 \qquad (8.5)$$

where the temperatures are in degrees Farenheit and z is the depth equal to one-third the layer thickness in inches.

For typical conditions in the United Kingdom, Table 8.13 shows that there is reasonable agreement between pavement temperatures calculated using equation (8.5) and those obtained by the 1.47 conversion factor developed at Nottingham (see Chapter 4). However, for high air temperatures the Nottingham pavement design temperatures are higher than those calculated by equation (8.5) and lower for low air temperatures. This is due to the fact that the 1.47 conversion factor also takes into consideration hourly traffic variations, (see Chapter 4).

8.4.3 Bituminous Mix Stiffnesses

The computer program DAMA predicts the bituminous mix stiffnesses from a regression equation, developed by the Asphalt Institute (99), based on laboratory stiffness data. The general form of this equation is:

$$|E^*| = \text{Function}\ (f,\ p_{200},\ V_b,\ V_v,\ \eta_{70°F},\ T) \qquad (8.6)$$

where $|E^*|$ = dynamic modulus

f = load frequency

p_{200} = per cent aggregate passing No.200 sieve

V_b = volume of binder (%)

V_v = volume of voids (%)

$\eta_{70°F}$ = original absolute viscosity of asphalt used in mix at 70°F

T = mix temperature.

Table 8.13 COMPARISON OF PAVEMENT TEMPERATURES FOR DESIGN

Air Temperature (^{0}C)	Pavement Temperature (^{0}C)			
	Asphalt Institute (Equation 8.5)			Nottingham 1.47 factor
	Thickness of Asphalt Layer (mm)			
	100	200	300	
5	9.1	8.9	8.8	7.4
10	15.0	14.7	14.9	14.7
15	20.9	20.4	20.1	22.1

The Asphalt Institute (99) has shown that the above equation predicts higher stiffness moduli than the Shell Design Manual (94) for similar materials (see Fig.8.15). Since the procedure for calculating bituminous mix stiffnesses in ANPAD, (see Chapter 6) is based on that derived by Shell (11,12) then equation (8.6) also calculates higher stiffness moduli than ANPAD. The design charts in MS-1 were developed using the following mix parameters:

P_{200} = 5%

f = 10 Hz

V_v = 4% for the surface course

V_v = 7% for the base course

V_b = 11% for both mixes

$\eta_{70°F}$ = 0.3 to 5.0 depending on the asphalt grade for the different climate regimes (99)

T = mean monthly pavement temperature.

For emulsified mixes, a six month cure period was used to prepare the charts and the stiffness moduli of the mix adjusted accordingly (99).

8.4.4 Design Criteria

The critical design parameters used in DAMA are the same as those used in ANPAD; the horizontal strain at the bottom of the asphalt layers and the vertical compressive strain at the top of the subgrade. The equation for the maximum allowable asphalt strain has already been discussed in Chapter 4.1. Fig.8.16 compares the asphalt strain criterion used in DAMA for a bituminous material with a 5% void content and an 11% volume of binder (99) with that used in ANPAD, (see Chapter 5), for a similar mix. The specific gravities of the aggregate and

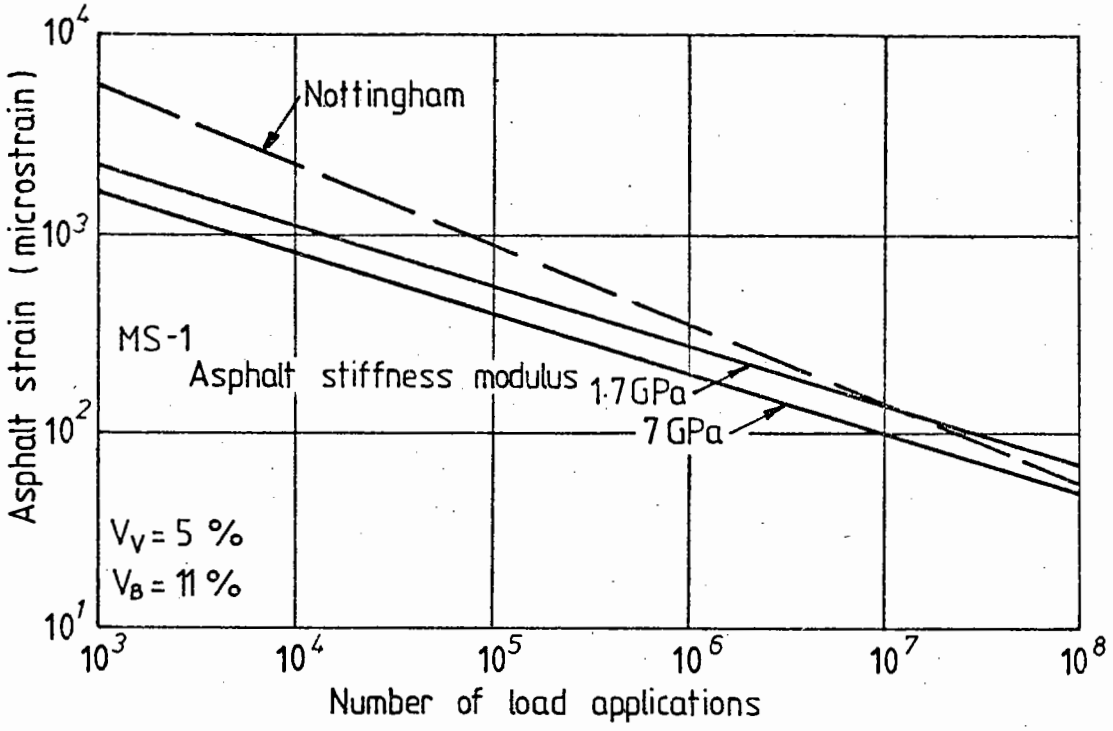

FIG 8·16 COMPARISON OF FATIGUE LINES

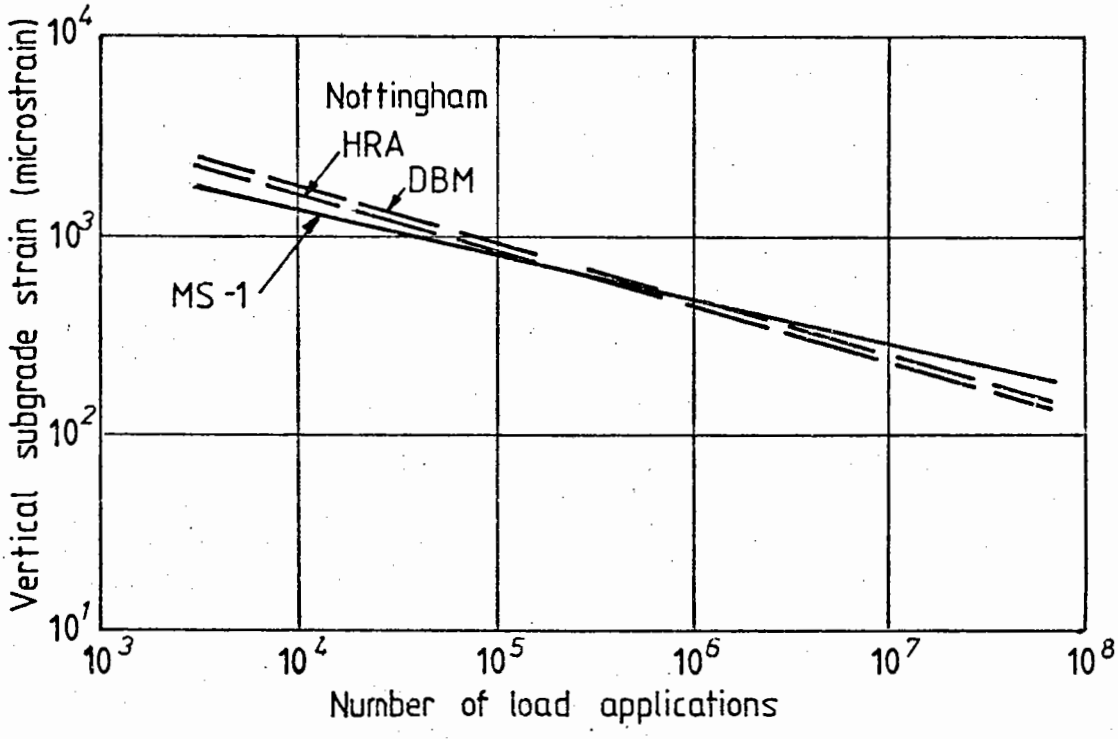

FIG 8·17 COMPARISON OF SUBGRADE STRAIN CRITERIA

bitumen were taken as 2.7 and 1.02 respectively, and the initial penetration of the binder was assumed to be 100. At high strain levels the Asphalt Institute fatigue criterion gives longer lives than the revised Nottingham fatigue criterion but, at lower strain levels, the Nottingham fatigue line is more conservative. The design criterion for permanent deformation used in DAMA agrees closely with that used at Nottingham as shown in Fig.8.17.

8.4.5 Summary

1. The Asphalt Institute design method is based on cumulative damage effects for both fatigue cracking and permanent deformation.
2. The sub-base and subgrade stiffness moduli are adjusted for frost and thaw effects.
3. The Asphalt Institute predicts higher bituminous mix stiffnesses than the Nottingham design method and Shell.
4. The slope of the Nottingham fatigue line is slightly steeper than the Asphalt Institute fatigue line.
5. The Asphalt Institute subgrade strain criterion agrees closely with that used at Nottingham.

CHAPTER NINE

FULL SCALE TRIALS

Full scale trials are essential for establishing confidence in analytical design methods. They can also be used to compare conventional and experimental pavement structures and to demonstrate the advantages of analytical designs and new materials. For example, a conventional pavement structure can be compared with a designed structure having either the same life but a reduced overall thickness or, the same overall thickness but an increased life. Typically, in these designed structures, the base course and base layer of a conventional pavement is replaced by a single structural layer of an asphalt mix with improved mechanical properties. Such novel mixes have been developed at the University of Nottingham (45,46,47,48) and have been used in the full scale trials described in this Chapter. Because the void contents of the bituminous materials are so important to the design calculations, particular effort was made during construction to ensure proper compaction (46,47,48).

The designs of three full scale trials at Theddingworth (Leicestershire), Carsington (Derbyshire) and Nottingham, are discussed in detail. Further information on the instrumentation, construction and mix analysis is given elsewhere (46,47,48). The designs were carried out during the research project before the design criteria had been finalised. Both the Theddingworth and Carsington designs are based on the existing Nottingham design criteria described at the beginning of Chapters 4 and 5. The design of the A52 Nottingham trial is also based on the existing permanent deformation criterion but, for fatigue, the revised criterion is used. The effect of changing from the existing to the revised fatigue criterion is to slightly increase

the fatigue life (see Section 4.4). The revised permanent deformation criterion allows the life calculated in accordance with the existing criterion to be increased when a dense bitumen macadam or modified mix base is used (see Section 5.3).

Data from two other full scale trials constructed at Hasland (Derbyshire) and Braintree (Essex) and additional data from Theddingworth has also enabled comparison to be made between observed measurements and theoretical computations.

9.1 A427, THEDDINGWORTH

This overlay experiment was on a 575 metre length of the A427 just east of Theddingworth in South Leicestershire. A plan of the road is given in Fig.9.1. Section 1 and 2 were the experimental ones, with novel basecourse mixes, as proposed by the University. Each of these sections was 140m long, at the eastern end of the scheme, with bends as shown in the plan. Section 3 used conventional materials, in accordance with Leicester County Council's standard specifications. It consisted of a steep downward stretch from the village with one bend.

Before any analysis could commence, Northamptonshire County Council carried out a deflection beam survey in June 1980 on both the nearside and offside of each carriageway. The results are shown in Figs.9.2 and 9.3. Twelve cores were also taken at intervals along both carriageways and the data from these is given elsewhere (46).

Although a computer program for designing overlays is described in Chapter 10 this design was carried out before the program was developed.

9.1.1 Analysis of Existing Structure

In order to be in a position to design the overlays, it was necessary to perform a back analysis on the existing pavement to

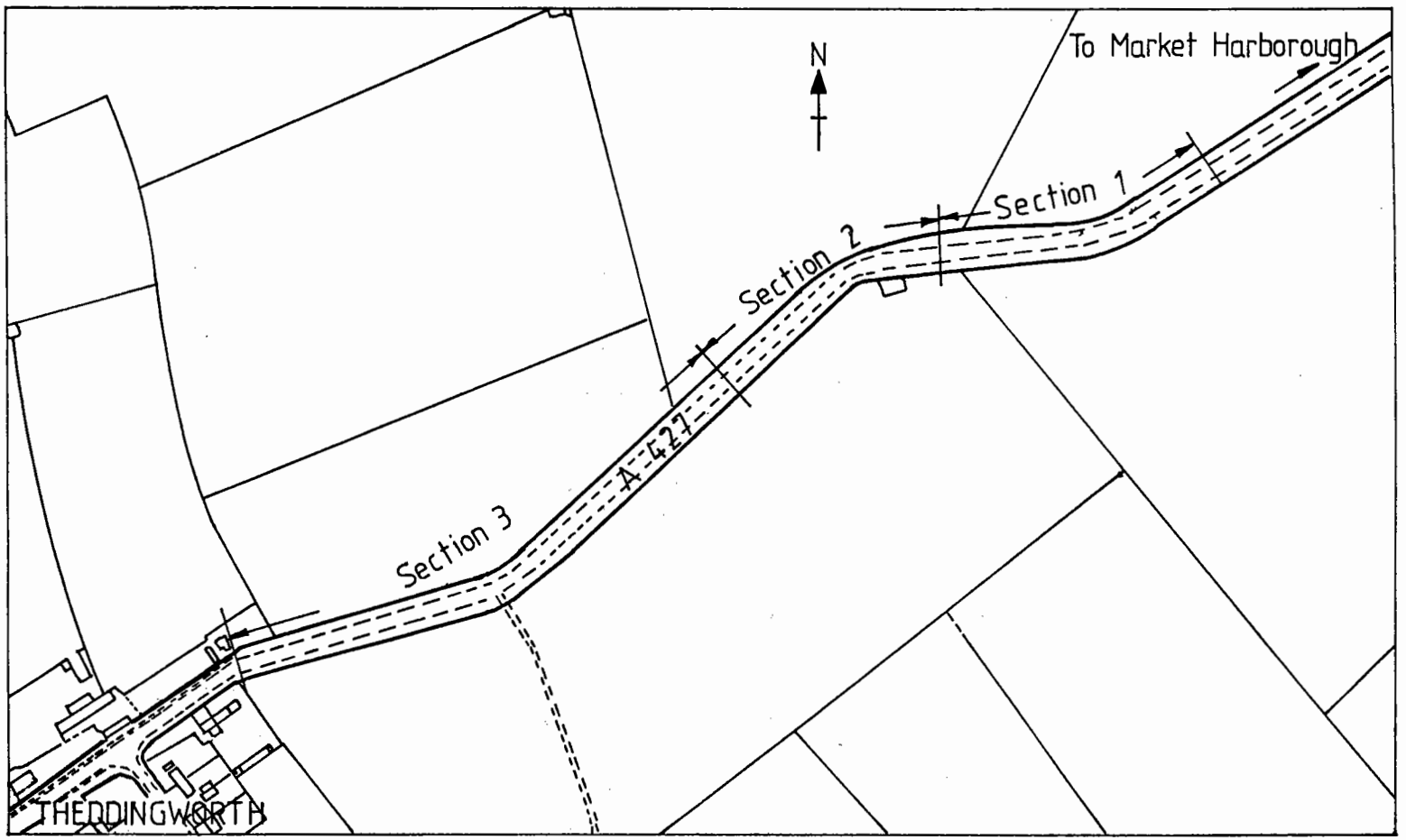

FIG 9.1 SITE PLAN OF OVERLAY EXPERIMENT A 427 THEDDINGWORTH

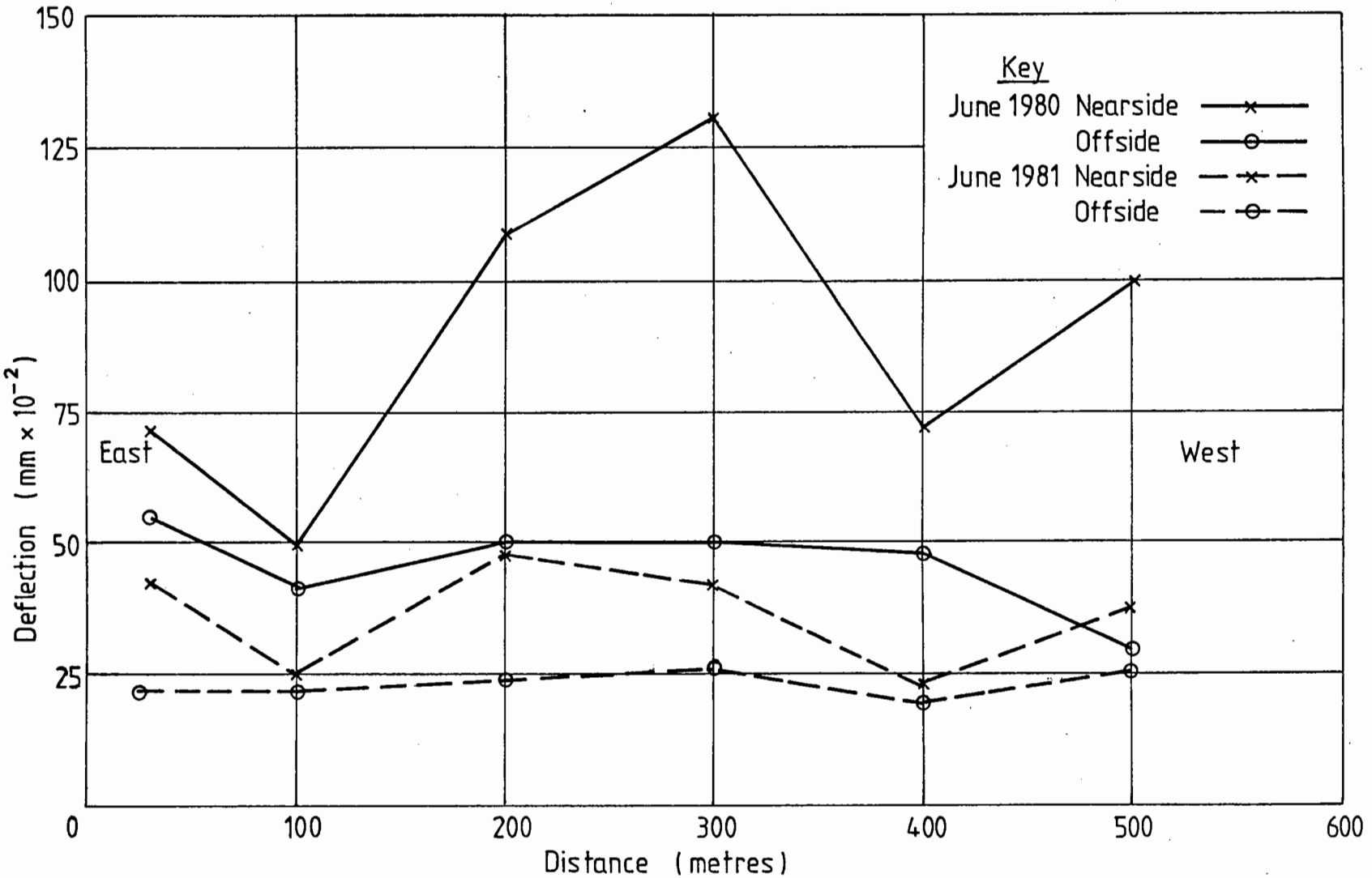

FIG 9.2 DEFLECTION BEAM RESULTS FOR WESTBOUND CARRIAGEWAY, A 427 THEDDINGWORTH

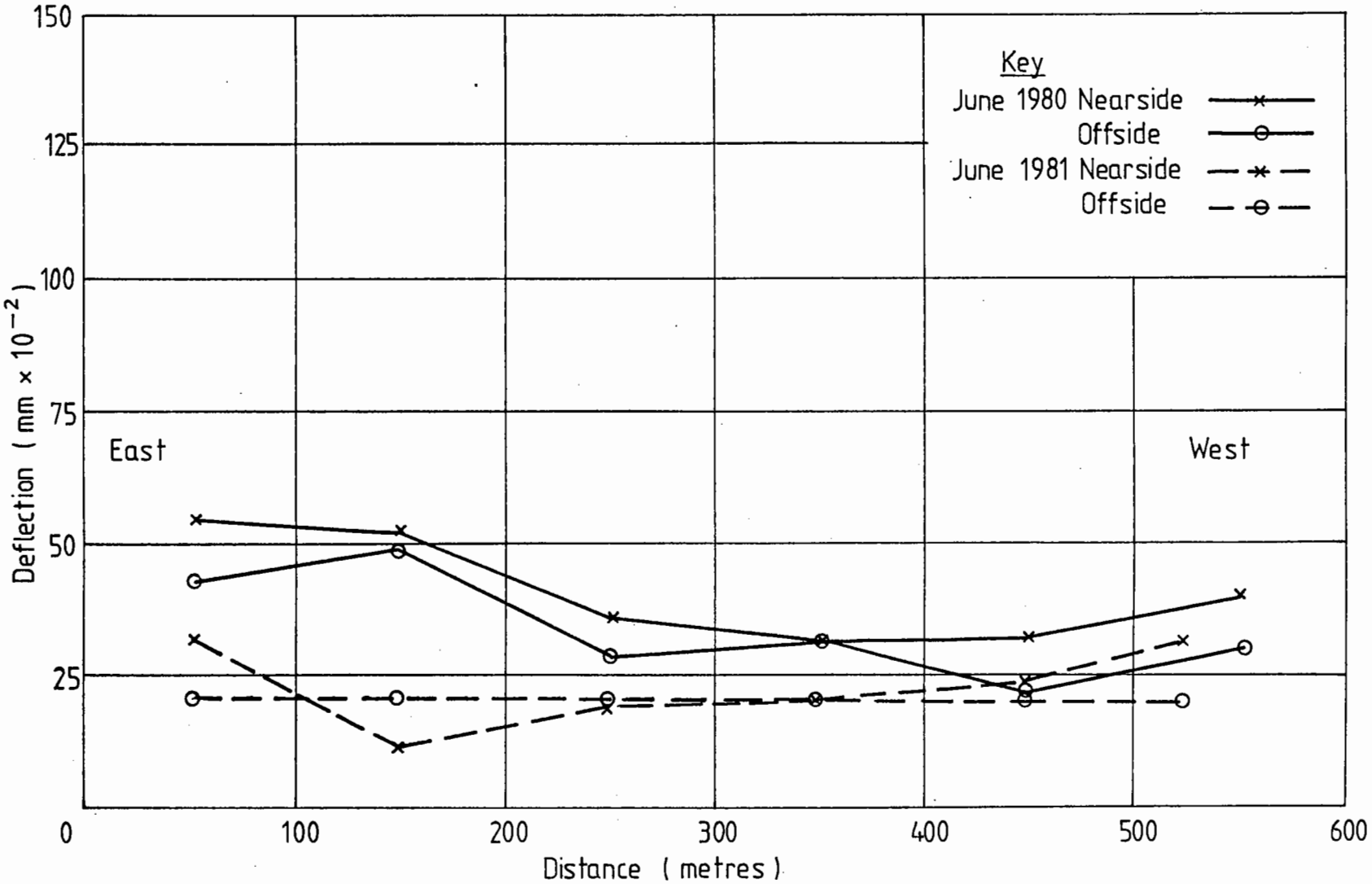

FIG 9.3 DEFLECTION BEAM RESULTS FOR EASTBOUND CARRIAGEWAY, A 427 THEDDINGWORTH

determine a thickness and stiffness for each of its layers.

Two simple models of the existing pavements resulted from a comparison of the general thicknesses of both asphalt and sub-base materials for the twelve cores (46). The first of these (the stronger structure) was representative of most of the road and consisted of 380mm of asphaltic material over a 120mm unbound sub-base. The second model represented a short length of weaker pavement consisting of 250mm of asphaltic material over a 120mm of sub-base. A section through each of these structures is given in Fig.9.4.

From the deflection beam results (Figs.9.2 and 9.3), a typical figure of 50 x 10^{-2}mm was selected as appropriate for the majority of the road, i.e. for the stronger model. The higher deflections corresponded to the region where the weaker model was appropriate, and an average value of 100 x 10^{-2}mm was taken for this model. The standard conditions for deflection measurements were taken as (100):

Vehicle speed	1.8 km/hr
Pavement temperature	20°C

with a dual wheel load arrangement as shown in Fig.9.4.

A stiffness, or modulus of elasticity, and a Poisson's ratio were assigned to each layer of each model. The two models were then analysed, using the BISTRO computer program, to obtain the surface deflections under the same loading conditions as applied in the deflection beam test. These deflections were compared with the actual measured deflections and the stiffnesses and Poisson's ratio were adjusted until the results from the analysis closely represented those which had been measured. Fig.9.4 shows the two models which gave satisfactory comparisons.

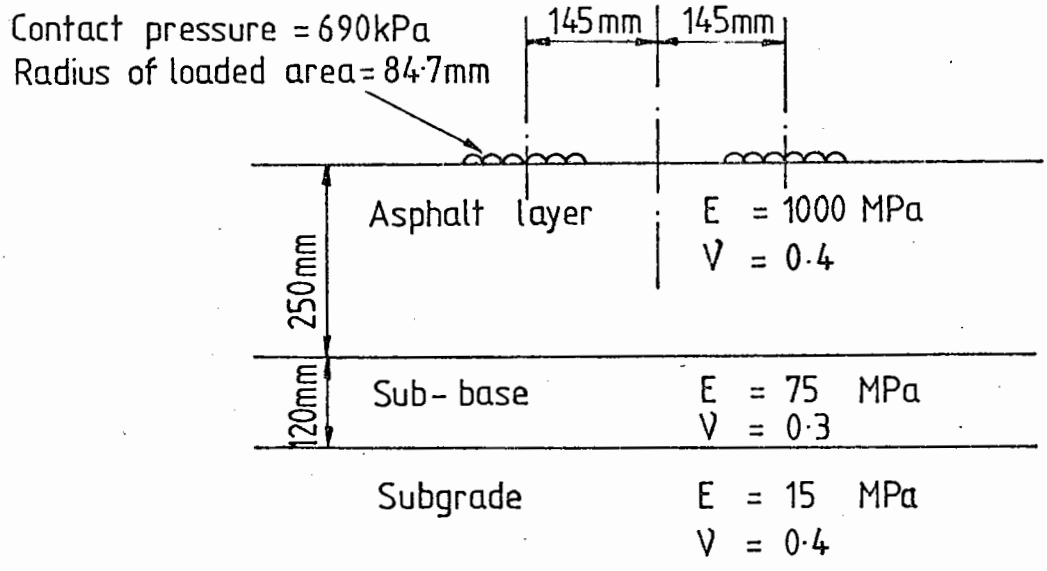

a. WEAKER STRUCTURE

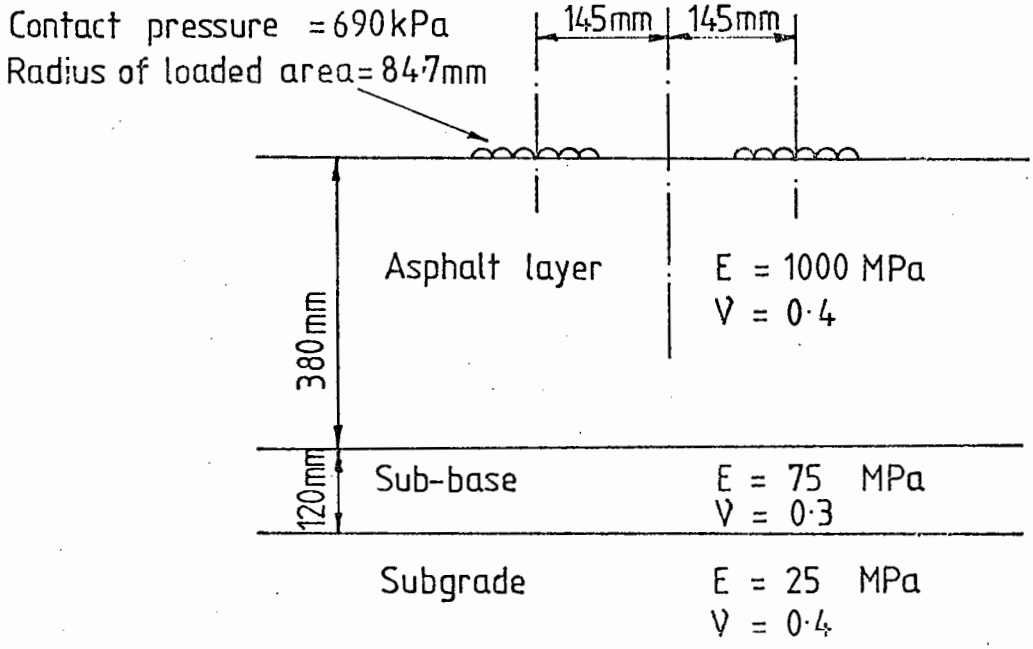

b. STRONGER STRUCTURE

FIG 9·4 MODELS OF EXISTING PAVEMENT DERIVED FOR DEFLECTION BEAM LOADING, A 427 THEDDINGWORTH

The existing asphaltic material was assumed to have a typical 100 pen binder. For this grade of binder to have a mix stiffness of 1000 MPa (see Fig.9.4), when subjected to the deflection beam loading conditions, the binder stiffness was calculated to be 2 MPa and the voids in mixed aggregate (VMA) 16%. Using this information, the following range of properties for the existing material were calculated and considered reasonable.

Initial penetration	=	100
Binder content	=	4.0 to 4.5%
Void content	=	6.0 to 7.0%
Specific gravity of aggregate	=	2.6
Specific gravity of bitumen	=	1.02

9.1.2 Design of Overlay

For the overlay design the loading conditions are those related to normal traffic and were taken as follows:

Vehicle speed	=	40 km/hr
Pavement temperature	=	15°C
Standard 40 kN dual wheel loading (see Fig.9.5(a))		

The mix stiffness for the existing asphaltic material under the design conditions and using the properties stated above, was calculated as 6300 MPa.

Following discussions with Leicestershire County Council, it was decided that the overall thickness of the overlays would be 100mm, there being no specified design information on projected traffic volume.

Sections 1 and 2 were used to experiment with novel basecourse mixes. A decision was made to use a dense bitumen macadam basecourse incorporating 50 pen bitumen for one section, while the other would be a modified hot rolled asphalt.

The DBM was similar to that used as a main structural layer in the Hasland By-Pass experiment in Derbyshire (101). The HRA was modified in an attempt to produce optimum mechanical properties, viz., dynamic stiffness, fatigue resistance and resistance to permanent deformation based on earlier research (56,102).

The mix proportions selected were as follows:-

Section 1: A dense bitumen macadam of crushed rock aggregate with 20mm maximum particle size to the grading of BS 4987, Table 25. Binder content to be 4.5% of 50 pen bitumen; void content 5%.

Section 2: A modified hot rolled asphalt to the following composition:

60% 20mm crushed rock coarse aggregate

25.5% sand fines

10% filler

4.5% 50 pen bitumen

Void content to be 5%.

Each of these materials was to be placed to a thickness of 70mm with a 30mm friction course above having the following specifications:

Crushed rock aggregate to the following grading:

Sieve Size	% Passing
14mm	100
10mm	90-100
6.35mm	35-45
3.35mm	20-26
75μm	3-6

Binder content to be 5.0% of 100 pen bitumen.

Both basecourse materials were supplied by ECC Quarries at Croft and the friction course was supplied by Bardon Hill Quarries. For the purposes of design, the volumetric proportions of the two basecourse mixes and their binder grade were identical, viz., 4.5% of 50 pen bitumen compacted to a void content of 5%. The specific gravities of aggregate and binder were taken as 2.7 and 1.02 respectively.

It was anticipated that the volume of voids in the friction course would be 15%. The mix stiffnesses were then calculated under the design conditions for both the two basecourses (11,000 MPa) and the friction course (1,375 MPa).

Section 3 of the scheme, proposed by Leicestershire County Council, consisted of 60mm of a typical hot rolled asphalt basecourse and 40mm of hot rolled asphalt wearing course. For the purpose of design the following properties were assumed:

	HRA Base Course	HRA Wearing Course
Initial penetration	50	50
Binder content (%)	5.7	7.9
Void content (%)	8.0	5.0
Specific gravity of aggregate	2.7	2.7
Specific gravity of bitumen	1.02	1.02

The mix stiffnesses for the design conditions were calculated to be 4900 MPa and 3900 MPa for the hot rolled asphalt basecourse and wearing course, respectively.

Having calculated the mix stiffnesses for both the overlays and the existing materials, each structure was then analysed using BISTRO for the standard 40 kN dual wheel loading conditions. Full details of the structures and layer stiffnesses are shown in Fig.9.5. Using the tensile strain at the base of the asphalt layer (ϵ_t) and the vertical

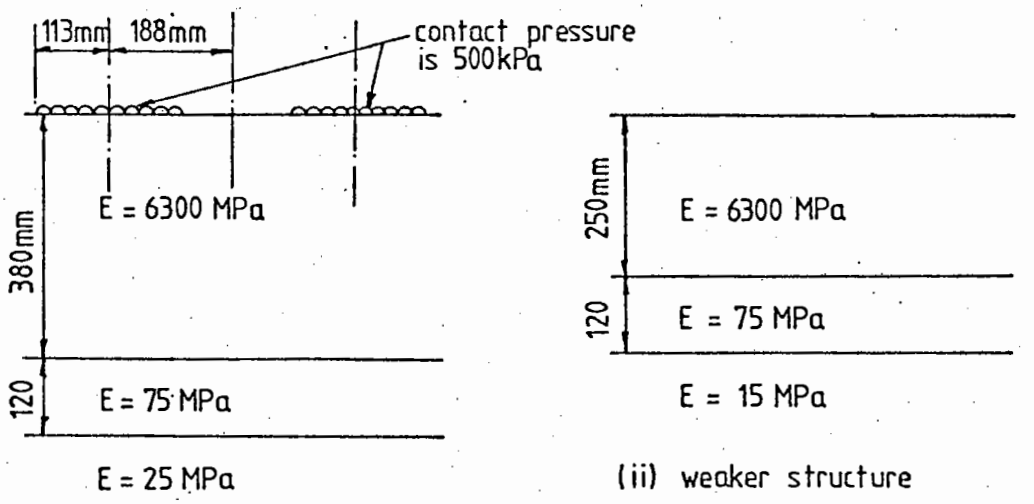

(i) stronger structure (ii) weaker structure

a. Existing pavement

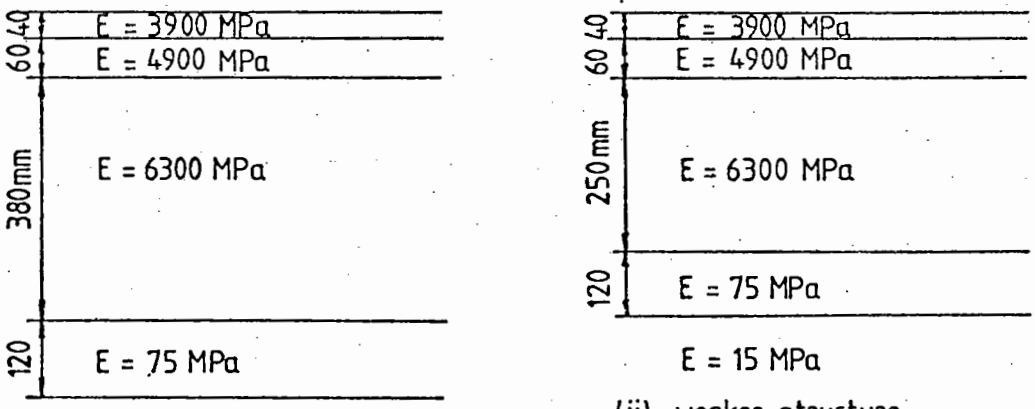

(i) stronger structure (ii) weaker structure

b. Conventional overlay

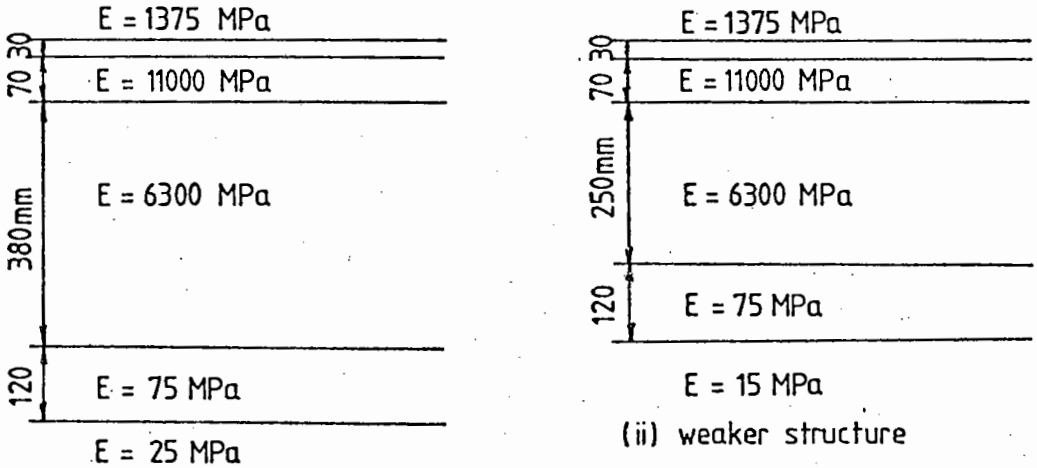

(i) stronger structure (ii) weaker structure

c. Experimental overlay

FIG 9.5 PAVEMENT MODELS FOR DESIGN CONDITIONS
A 427 THEDDINGWORTH

strain at the top of the subgrade (ϵ_z), the pavements were checked for fatigue cracking and permanent deformation respectively. In each case the life of the pavement was determined in terms of millions of standard axles. The strains and pavement lives are given in Table 9.1.

The projected lives are similar for both the experimental and conventional constructions. For the stronger structural section, lives are increased by factors of 3.5 and 3.9 for the conventional and experimental structures respectively. The corresponding figures for the weak structure are 4.8 and 5.8.

The present traffic using the road is equivalent to 1233 standard axles per day in each direction. Assuming a growth rate of 2% per annum over 20 years, gives a cumulative loading of 10 million standard axles. All the designs provide lives in excess of this figure.

9.1.3 Overlay Deflection Survey

The overlay was constructed in September 1980, and in June 1981 a deflection survey was made on the overlaid structure. The results of this survey have been superimposed on those obtained prior to the overlay in Figs.9.2 and 9.3 in order to illustrate the reduction in deflection.

An attempt was made to predict these new deflections using the mix proportions for the in situ materials as determined at the time of construction. The details are given in Table 9.2

For the second deflection survey, the total axle loading was 58.9 kN. The calculations assumed dual wheel loading consisting of two circular contact areas of 110mm radius and a contact pressure of 387 kPa. Table 9.3 compares the measured and calculated deflections for the original survey, before construction, and the survey after the overlay construction. It can be seen that the actual effect of the overlay was to reduce the measured deflections by more than was indicated by the computed values.

Table 9.1 RESULTS OF PAVEMENT ANALYSES, A427 THEDDINGWORTH

	Stronger structure				Weaker structure			
	ε_t (με)	ε_z (με)	Life (msa)		ε_t (με)	ε_z (με)	Life (msa)	
			Due to ε_t	Due to ε_z			Due to ε_t	Due to ε_z
Existing Pavement	42	148	37	50	88	348	3.1	2.5
Conventional Overlay	29	98	129	159	55	210	15	15
Experimental Overlay	28	90	145	179	52	193	18	21

Table 9.2 MIX PROPERTIES OF AS LAID ASPHALT OVERLAY FOR DEFLECTION CALCULATIONS, A427 THEDDINGWORTH

	Section 1	Section 2	Sections 1 & 2	Section 3	
	DBM	HRA	Friction course	HRA b/c	HRA w/c
Initial Penetration	50	50	100	50	50
Specific gravity of aggregate	2.7	2.7	2.7	2.7	2.7
Specific gravity of binder	1.02	1.02	1.02	1.02	1.02
Binder content (%)	4.2	4.36	5.0	5.7	7.9
Void content (%)	9.4	7.3	15.0	4.9	5.0
Mix stiffness (MPa)	1250	1690	225	1460	655

Table 9.3 COMPARISON OF MEASURED AND CALCULATED DEFLECTIONS, A427 THEDDINWORTH

	Measured deflection ($mm \times 10^{-2}$)	Calculated deflection ($mm \times 10^{-2}$)	Measured / Calculated
Initial Survey			
Weaker structure	100	104	0.96
Stronger structure	50	53	0.94
Second Survey after overlay construction			
Weaker structure	45	76	0.60
Stronger structure	20 to 25	42	0.5 to 0.6
Initial Survey / Second Survey			
Weaker structure	2.2	1.4	1.6
Stronger structure	2.0 to 2.5	1.3	1.6 to 1.9

Table 9.4 RELATIVE LIVES OF CONVENTIONAL AND EXPERIMENTAL CONSTRUCTION FOR CARSINGTON

Structure	ε_t ($\mu\varepsilon$)	ε_z ($\mu\varepsilon$)	N (msa) due to ε_t	N (msa) due to ε_z
Conventional	132	456	0.63	0.67
Experimental	91	390	17.9	1.68

Table 9.3 COMPARISON OF MEASURED AND CALCULATED DEFLECTIONS, A427 THEDDINWORTH

	Measured deflection ($mm \times 10^{-2}$)	Calculated deflection ($mm \times 10^{-2}$)	Measured / Calculated
Initial Survey			
Weaker structure	100	104	0.96
Stronger structure	50	53	0.94
Second Survey after overlay construction			
Weaker structure	45	76	0.60
Stronger structure	20 to 25	42	0.5 to 0.6
Initial Survey / Second Survey			
Weaker structure	2.2	1.4	1.6
Stronger structure	2.0 to 2.5	1.3	1.6 to 1.9

Table 9.4 RELATIVE LIVES OF CONVENTIONAL AND EXPERIMENTAL CONSTRUCTION FOR CARSINGTON

Structure	ε_t ($\mu\varepsilon$)	ε_z ($\mu\varepsilon$)	N (msa) due to ε_t	N (msa) due to ε_z
Conventional	132	456	0.63	0.67
Experimental	91	390	17.9	1.68

9.2 CARSINGTON BY-PASS

The Carsington By-Pass is part of the ancilliary works associated with the construction of a reservoir at Carsington in Derbyshire. The section offered by Derbyshire County Council for experimental construction involves 200 metres of new construction 6.75 metres wide, the purpose of which is to straighten out a bend in the B5035 Wirksworth to Ashbourne Road south west of Carsington. The CBR of the formation as measured by Derbyshire County Council was initially reported to vary between 1.5 and 2%, and the conventional construction which they would have normally used, was as follows:

410mm type 1 sub-base
100mm DBM base
50mm DBM basecourse
25mm HRA wearing course

The road was lightly trafficked and the following figures were available:

16-hour flow	1856	axle pairs
24-hour flow	1970	" "
Peak hour flow	230	" "

11% heavy vehicles.

Using Road Note 29, it is apparent that the conventional design was intended for a cumulative traffic volume of about 2 msa. Using the traffic data above, this implies a growth rate of 6% per year which is a high figure perhaps compatible with the increase in traffic expected in the area due to the reservoir construction.

Attempts were made initially to produce a balanced design for an asphaltic mix placed to a thickness of 150mm which would be a saving of

25mm on the conventional design. However, the design parameters were such that satisfactory mix proportions could not be achieved.

It was, therefore, decided that the asphalt layer should be similar in thickness to the conventional design at 170mm and that a modified hot rolled asphalt, like the one used at Theddingworth, should be adopted (4.5% of 50 pen bitumen with a high filler content). In view of the difficulties in obtaining good riding quality with the Hasland experiment (101), it was decided that the top 50mm of asphalt should be separately placed and have a higher binder content. The overall objective of this experiment, therefore, became mainly one of mix design. Skid resistance was to be achieved by surface dressing.

For the purposes of design computations the two mixes were characterised on the basis of the following mix proportions:

50mm basecourse:	5% of 50 pen binder
	5% void content
120mm base:	4.5% of 50 pen binder
	5% void content.

The specific gravities of aggregate and binder for both mixes were assumed to be 2.7 and 1.02 respectively. Other parameters for design were as follows:

Pavement temperature	= 13°C
Vehicle speed	= 30 km/hr
Cumulative no. of standard axles	= 2 msa
Modulus of elasticity of subgrade	= 20 MPa

The sub-base thickness was increased from the initial proposal of 200mm to 300mm with a layer of Terram 1000 fabric at formation level.

This change was agreed in conjunction with Derbyshire C.C. engineers in view of the site conditions and their concern to establish a sound platform for compaction of the asphalt layers.

The resulting structure was then compared to the conventional design (see Fig.9.6). Each structure was analysed using the BISTRO computer program with standard dual wheel loading and the same pavement temperature and vehicle speeed as before. The life of each pavement was then calculated using both asphalt and subgrade strains (fatigue cracking and permanent deformation) and the results are given in Table 9.4.

The life of the experimental section, at 1.68 msa, is less than the value of 2 msa. However, as the traffic computations were very approximate and the life of the conventional design was even lower, the solution was considered satisfactory.

9.3 A52 DERBY ROAD, NOTTINGHAM

The experimental section was 190 metres long on the westbound carriageway of the A52 Derby Road between Sandy Lane and an electricity substation (metreage 915), as shown in the site plan, Fig.9.7. The total length of reconstruction was from Sandy Lane to the Sherwin Arms roundabout. Fig.9.8 gives a section through the existing pavement. The structural problem was identified from core samples as sulphate attack of the lean mix concrete. Therefore, the road was excavated to a depth of 300mm removing the existing 100mm of asphalt surfacing and 200mm of lean concrete.

Below the lean concrete was a red shale sub-base which crumbled easily to a fine material with lumps of hard red shale. The thickness of the sub-base varied between 100 and 500mm and it was wet in places. Under the sub-base was a sandstone subgrade which varied between 'loosely compacted' and 'well consolidated'.

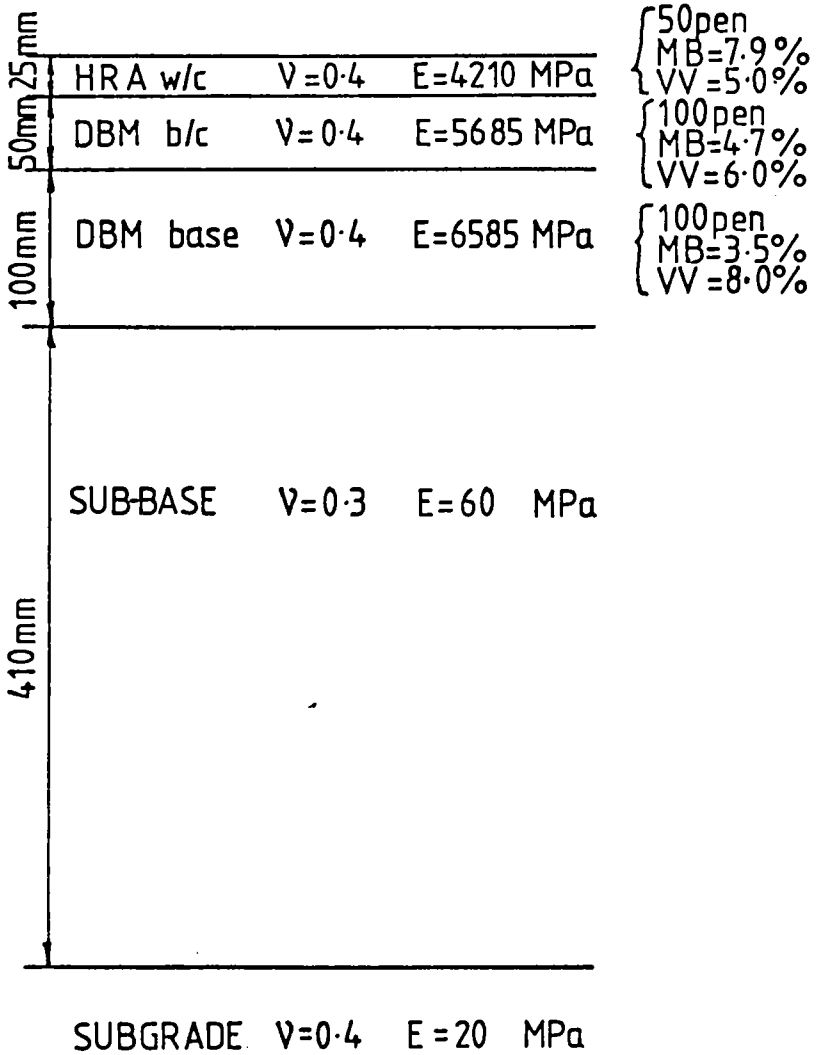

a TYPICAL CONSTRUCTION

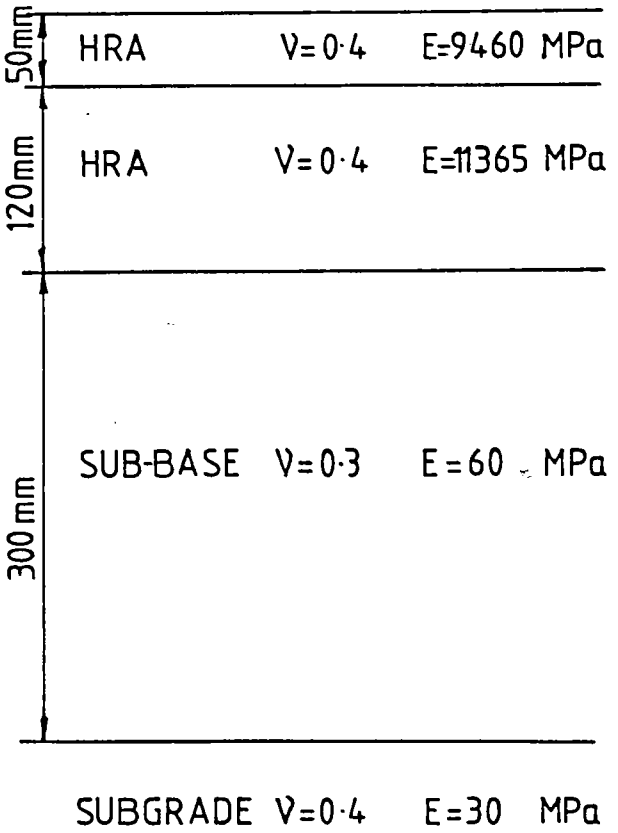

b DESIGN STRUCTURE

FIG 9·6 PAVEMENT STRUCTURES CONSIDERED FOR ANALYSIS CARSINGTON BY-PASS

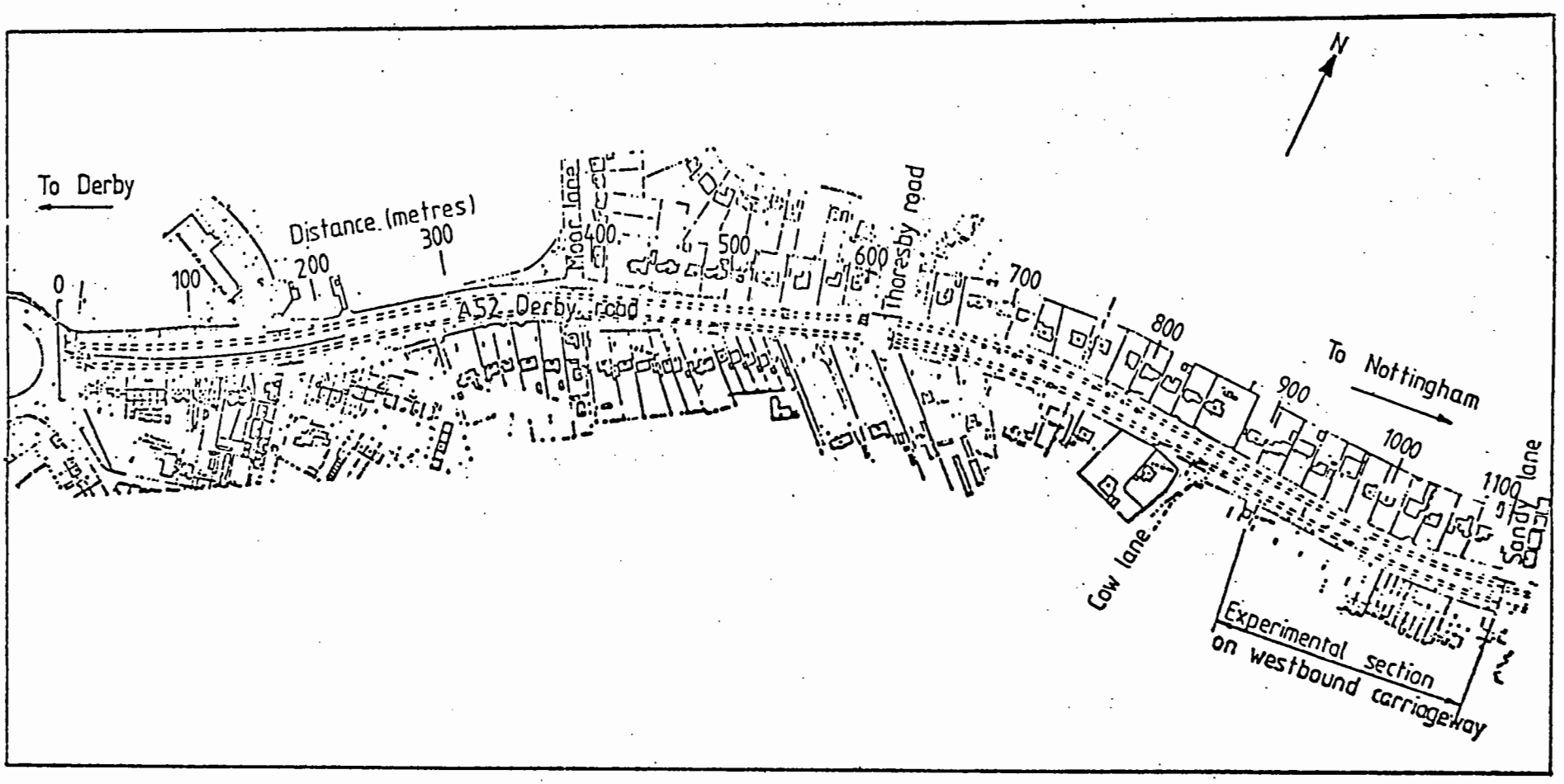

FIG 9.7 SITE PLAN OF RECONSTRUCTION A52 DERBY ROAD, NOTTINGHAM

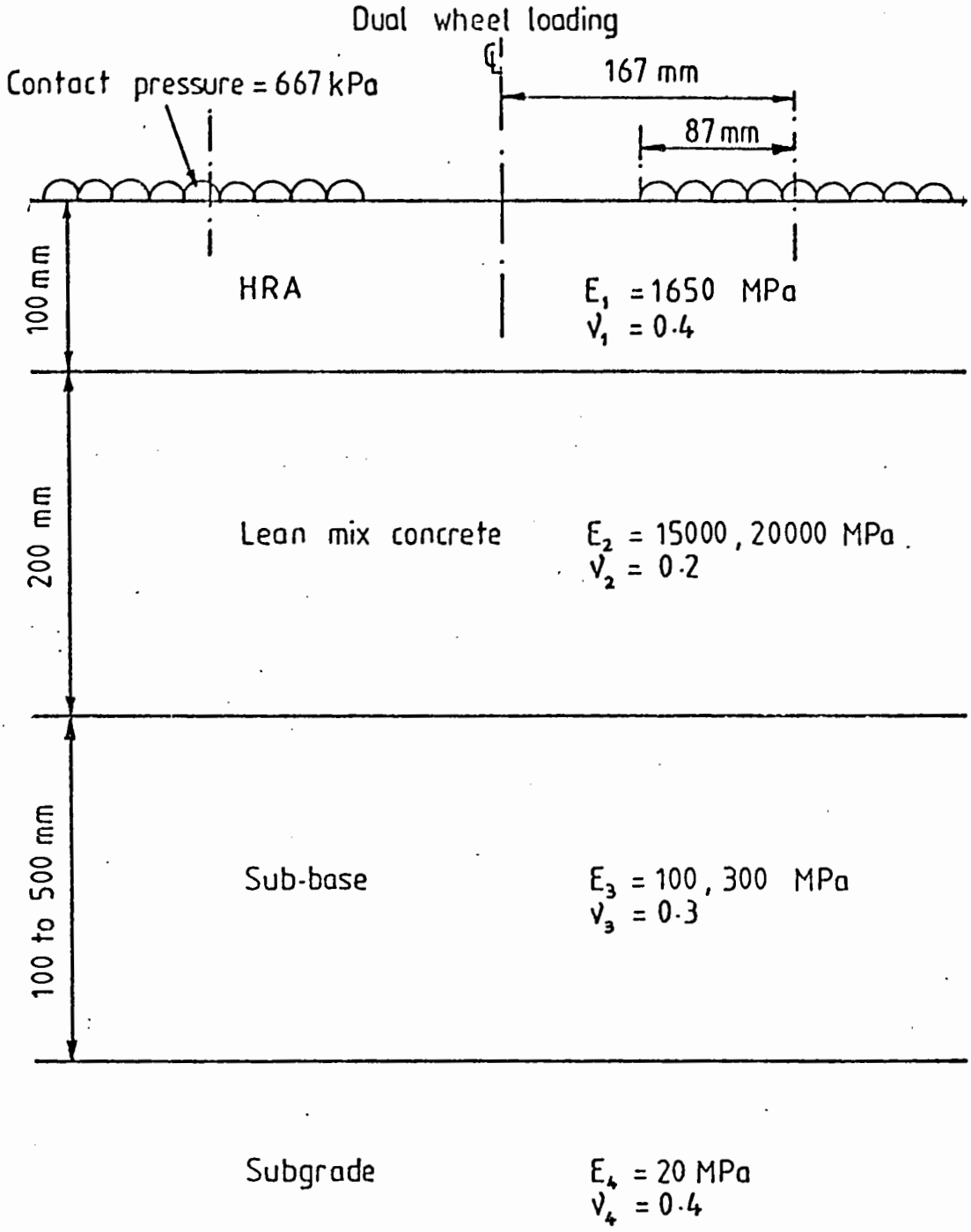

FIG 9·8 EXISTING STRUCTURE AND LOADING ARRANGEMENT USED IN DEFLECTION CALCULATIONS A 52 DERBY ROAD NOTTINGHAM

Nottinghamshire County Council proposed to partially reconstruct the road with 200mm HRA road base and 100mm HRA surfacing. The proposal for the experimental section was 40mm HRA wearing course, 60mm modified HRA base course and 200mm modified DBM road base. A friction course was considered but would have caused problems with the existing drainage channels.

The modified materials proposed for the base and basecourse were derived from earlier trials and laboratory work. The basecourse HRA was to have a lower binder content and higher filler content than the BS 594 specified material. The DBM base was to have a dense grading, specified to suit the quarry involved, and a higher binder content than BS 4987 involving a harder grade of bitumen.

A deflection study was made by Nottinghamshire County Council on the existing structure using a Deflectograph. The loading arrangement for the vehicle is given in Fig.9.8. The results of the survey are shown in Fig.9.9 for the nearside lane of both carriageways. Each point represents an average of 14 or 15 measurements taken over 50 metres. The range of deflections measured for the existing pavement was between 15 and 100mm x 10^{-2} with an average measured deflection of 40mm x 10^{-2}.

The County Council had also taken plate bearing tests on the subbase in March 1982. These indicated a CBR of 30%.

9.3.1 Design Requirements

The specified traffic volume for design was 35 msa. This was determined by the County from traffic flow counts taken in 1980. The traffic flow was 1700 commercial vehicles per day, 90% of which were considered to be in the slow lane. The required design life was 20 years and so for a growth rate of 2.5% and 2.75 standard axles per vehicle, the life required was 35 msa. However, the deflection survey

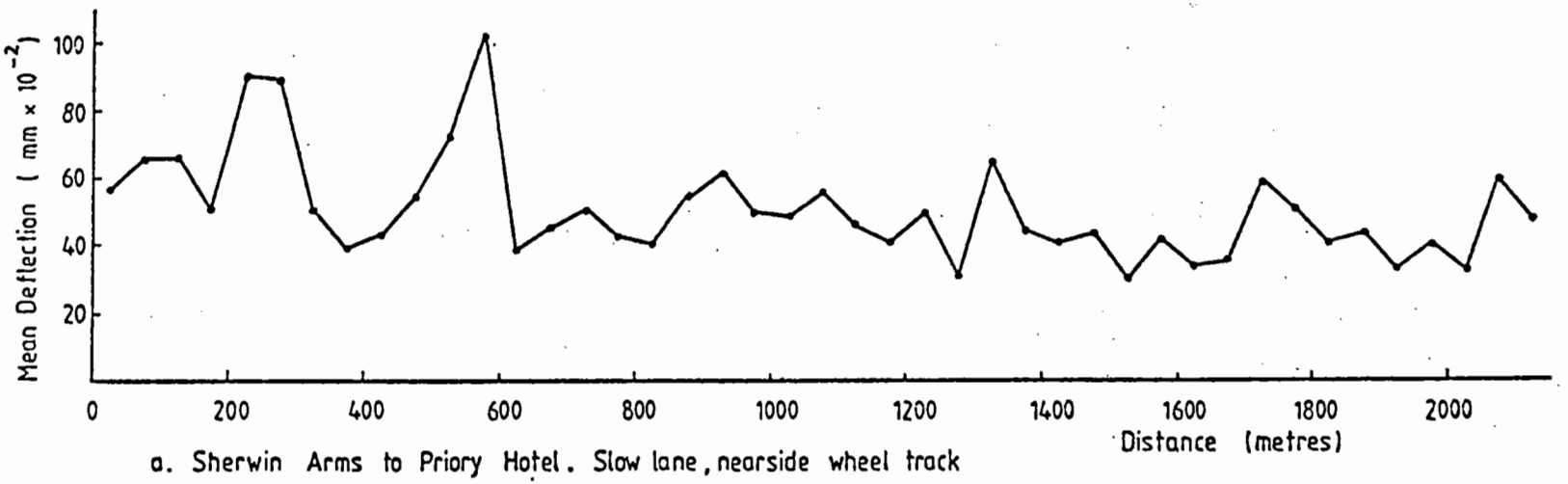

a. Sherwin Arms to Priory Hotel. Slow lane, nearside wheel track

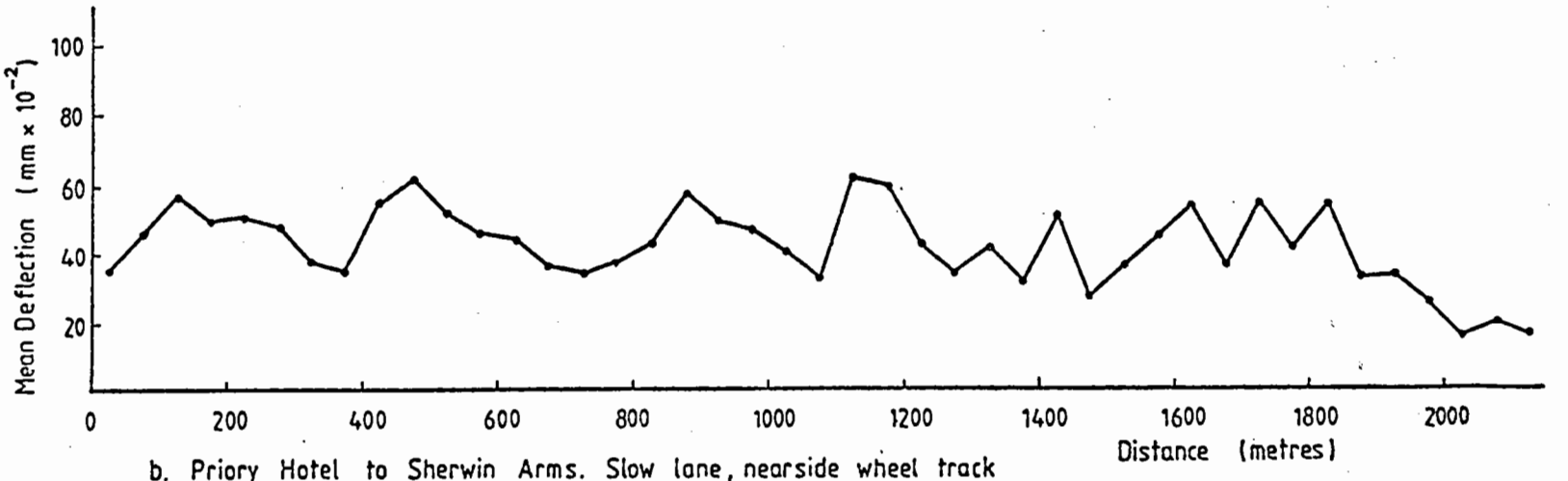

b. Priory Hotel to Sherwin Arms. Slow lane, nearside wheel track

FIG 9.9 DEFLECTOGRAPH DEFLECTION SURVEY A 52 DERBY ROAD

print out used 1665 commercial vehicles per day in the slow lane and calculated the required design life to be 44 msa.

9.3.2 Analysis

A back analysis was performed on the existing pavement to determine the effect of varying some of the parameters on the calculated deflections. The structure and loading arrangement are given in Fig.9.8. The asphalt mix stiffness was determined from the data listed below:

Mix Details

Initial penetration		50
Binder content	(%)	5.7
Void content	(%)	6.0
Specific gravity of aggregate		2.7
Specific gravity of bitumen		1.02

Loading Conditions

Speed of Deflectograph (km/hr)		2
Temperature	(°C)	20

The stiffness modulus of the lean concrete was estimated as between 15 and 20 GPa. The modulus of the sub-base, based on the CBR was 300 MPa. This value was initially considered rather high and a second value of 100 MPa was also chosen. Two sub-base thicknesses were used, 100 and 500mm. The results of the deflection calculations using the computer program BISTRO are given in Table 9.5.

The calculated deflections agreed fairly well with the average measured deflection. However, when the sub-base modulus of 300 MPa was used together with a sub-base thickness of 500mm, then the calculated

Table 9.5 CALCULATED DEFLECTIONS FOR THE EXISTING A52 PAVEMENT STRUCTURE

lean Concrete Modulus (GPa)	Sub-base Modulus (MPa)	Sub-base Thickness (mm)	Calculated deflection ($mmx10^{-2}$)	Average Measured deflection ($mmx10^{-2}$)
15	100	100	44	40
		500	40	
	300	100	44	
		500	34	
20	100	100	41	
		500	37	
	300	100	41	
		500	33	

Table 9.6 MIX DETAILS AND STIFFNESS MODULI FOR BITUMINOUS MATERIALS USED IN DESIGN ANALYSIS

	HRA wearing course	HRA base course and base	Modified HRA base course	Modified DBM base
Mix Details				
Initial penetration	50	50	50	50
Binder content (%)	7.9	5.7	5.0	4.5
Void content (%)	5.0	6.0	5.0	8.0
Specific gravity of aggregate	2.7	2.7	2.7	2.7
Specific gravity of bitumen	1.02	1.02	1.02	1.02
Poissons Ratio	0.4	0.4	0.4	0.4
Mix Stiffnesses (MPa)				
At 40 km/hr for deformation	3900	6190	8880	6920
for fatigue	2670	4390	6460	4940
At 80 km/hr for deformation	4620	6190	10220	8040
for fatigue	3180	4390	7490	5780

deflections were rather lower than the average measured value.

For the reconstructed pavement design, the top of the sub-base was considered to be the new subgrade level. This avoided problems with variations in sub-base thickness. A subgrade stiffness modulus of 300 MPa was thought to be rather high and so a value of 100 MPa was used.

Table 9.6 gives the mix details of the bituminous materials together with their stiffness moduli determined using an average annual air temperature of 10.1°C and average speeds of commercial vehicles of both 40 and 80 km/hr. Two speeds were used as the road is a busy dual carriageway with several junctions having traffic lights. Fig.9.10 shows the two structures and the standard dual wheel loading arrangement used in the analysis.

The results of the structural analysis performed by the computer program BISTRO are given in Table 9.7. The maximum tensile strains (ϵ_t) were calculated at the bottom of the asphalt layers, and the subgrade strains (ϵ_z), were calculated at the top of the subgrade.

In each case the subgrade strain was the critical criterion. Increasing the speed of the commercial vehicles from 40 to 80 km/hr increased the lives by about 40%. However, the design case must be for the speed of 40 km/hr which is a more representative value for the commercial vehicles, particularly at peak loading times. The predicted life of the pavement proposed by Nottinghamshire County Council was therefore 39 msa whilst for the experimental section it was 52 msa, an increase in life of 33%.

9.3.3 Analysis in Region of Trial Section

After the existing road had been excavated small trial pits were made in the experimental section. These revealed that, locally, the sub-base was approximately 200mm thick. Nottinghamshire County Council also performed a series of plate bearing tests on the sub-base between

Table 9.7 CALCULATED STRAINS AND PREDICTED DESIGN LIVES OF THE RECONSTRUCTED PAVEMENTS

	Asphalt strain ε_t (microstrain)	Subgrade strain ε_z (microstrain)	Fatigue life N_t (msa)	Deformation life N_z (msa)
Nottingham County Council				
Proposed reconstruction				
40 km/hr	66	162	912	39*
80 km/hr	58	147	1690	55
University of Nottingham				
Proposed experimental section				
40 km/hr	59	149	437	52*
80 km/hr	53	135	689	74

* Design lives

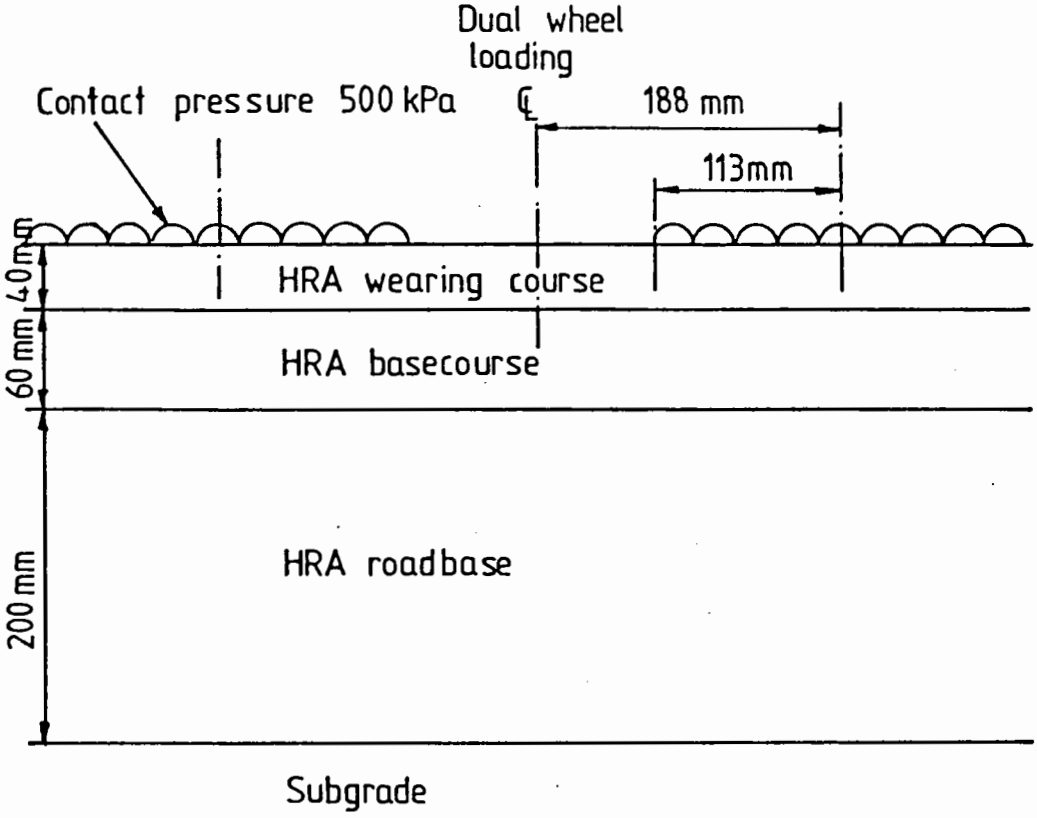

a. Nottingham County Council proposed reconstruction.

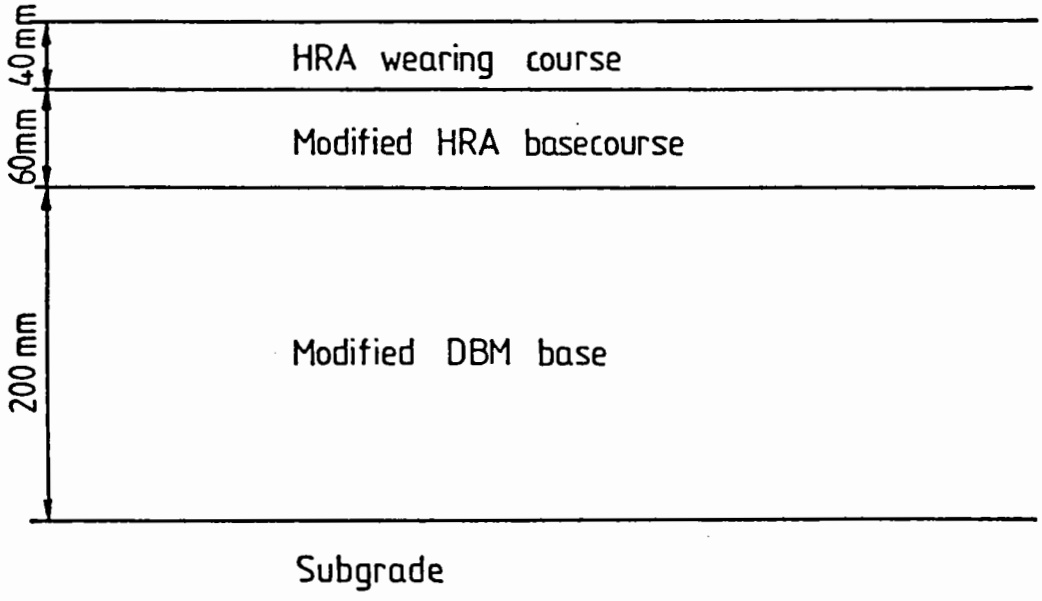

b. University of Nottingham proposed experimental section

FIG 9.10 DESIGN STRUCTURES FOR A 52 DERBY ROAD, NOTTINGHAM

metreage 700 and 1200. The results of these tests are given in Fig.9.11. The CBRs varied between 5 and 50%. At the intersection between the experimental section and the control section (metreage 915) the CBR was about 25%. Fig.9.11 also compares the CBR values with the measured deflections on the old pavement along the westbound carriageway and shows a reasonable correlation.

Deflection measurements also were taken on the sub-base using a Benkelman Beam. The results are given in Table 9.8 together with those calculated using the data given in Table 9.9. From these results it can be seen that better agreement is recorded when a subgrade modulus of 30 MPa is used.

The proposed reconstructed pavements were re-analysed using the same bituminous mix stiffnesses but with a 200mm sub-base. The stiffness moduli of the sub-base and subgrade were 250 and 30 MPa respectively. An average speed of 40 km/hr and an average annual air temperature of 10.1°C were also used. The results of the analysis are given in Table 9.10. The design lives calculated for the control and experimental sections were 17 and 23 msa, respectively. In each case the subgrade strain was the critical design criterion. Although these lives are less than the required design life they are probably conservative. The proportion of deformation occurring in the subgrade will be less than normal. The rate of deformation decreases with time and the majority of the subgrade deformation will have taken place in the original pavement. The effect of this deformation on the rut is therefore removed when overlaid.

The trial section was re-analysed using the measured binder and void contents (see Tables 9.11 and 9.12). The effect of these changes was to increase the calculated lives of the control and experimental sections to 31 and 50 msa respectively.

Table 9.8 CALCULATED AND MEASURED DEFLECTIONS ON SUB-BASE

	Deflection mm. x 10^{-2}
Measured	
At Metreage 915	67
925	163
933	119
945	128
Average	120
Calculated	
Using Subgrade Modulus 20MPa	172
Using Subgrade Modulus 30MPa	127

Table 9.9 INPUT DATA FOR DEFLECTION CALCULATIONS

Parameter		Input
Sub-base modulus	(MPa)	250
Sub-base thickness	(mm)	200
Subgrade modulus	(MPa)	20 and 30
Dual wheel loading		
Contact pressure	(kPa)	476
Radius of loading	(mm)	102
Distance between wheel loads	(mm)	290

Table 9.10 CALCULATED STRAINS AND DESIGN LIVES OF THE RECONSTRUCTED PAVEMENTS LOCALLY TO THE CONTROL SECTION AND EXPERIMENTAL SECTION

Location	Asphalt Strain, ϵ_t (microstrain)	Subgrade Strain, ϵ_z (microstrain)	Fatigue life, N_t (msa)	Deformation life, N_z (msa)
Nottingham C.C. Control Section	71	204	643	17
University of Nottingham Proposed experimental section	65	188	290	23

Table 9.11 MEAN VOID CONTENTS

Material	Void Content (%)			VMA(%)
	Upper layer	Lower layer	Overall	Overall
Modified DBM base	3.8	4.4	4.7	4.6
Modified HRA basecourse	-	-	6.2	17.6
Conventional HRA base	3.4	2.2	2.8	16.1

Table 9.12 SUMMARY OF NINETEEN MIX ANALYSES CARRIED OUT ON ROAD BASE MIX BY TARMAC ROADSTONE AND SEVENTEEN MIX ANALYSES CARRIED OUT ON BEHALF OF NOTTS. C.C.

		Tarmac (%)	Notts.C.C (%)
Passing 20mm	minimum	68	64.1
Spec: 70-80%	maximum	80	80
	mean	74.5	72.3
Passing 10mm	minimum	50	49
Spec: 55-65%	maximum	65	63
	mean	57.4	55.6
Passing 5mm	minimum	33	33
Spec: 35.45%	maximum	47	43
	mean	39.2	38.4
Passing 2.36mm	minimum	25	23
Spec: 32-38%	maximum	33	31
	mean	28.4	27.6
Passing 1.18mm	minimum	17	16.4
Spec: 22-28%	maximum	22	23
	mean	19.8	19.6
Passing .600mm	minimum	12	12
Spec: 17-23%	maximum	16	17
	mean	14.2	14.1
Passing .300mm	minimum	9	8.3
Spec: 9-15%	maximum	11	13.1
	mean	10.2	10.2
Passing .150mm	minimum	7	6
Spec: 7-12%	maximum	8	10
	mean	7.5	7.7
Passing .075mm	minimum	5.6	5.0
Spec: 4-8%	maximum	6.9	8.1
	mean	6.4	5.9
Binder Content	minimum	3.8	3.9
Spec: 3.9-4.7%	maximum	4.6	4.5
	mean	4.24	4.15

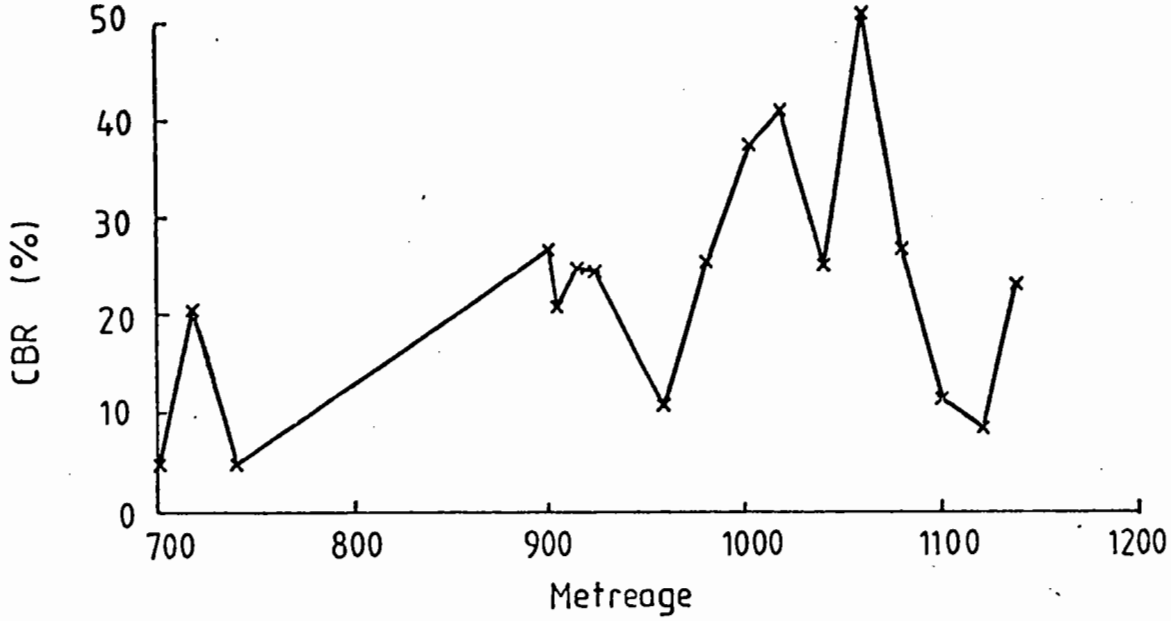

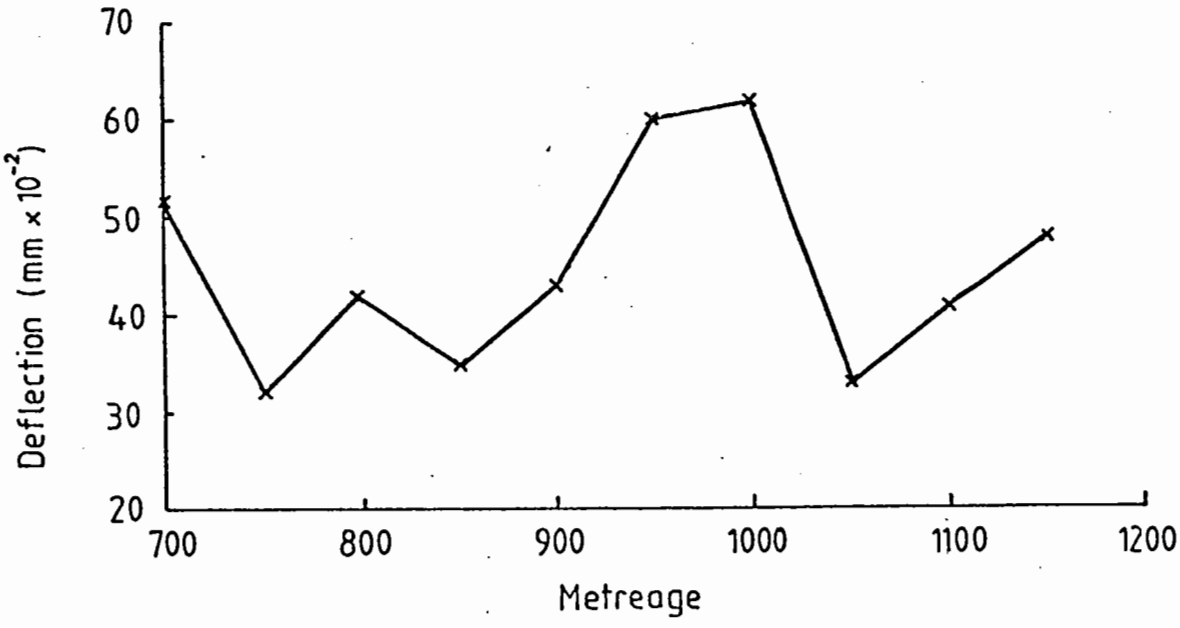

FIG 9·11 COMPARISON OF SUB-BASE CBR AND MEASURED DEFLECTIONS ON WESTBOUND CARRIAGEWAY OF EXISTING PAVEMENT

Instruments to measure transient stresses and strains were installed in both the experimental and control sections, but as yet no readings have been taken.

9.4 HASLAND BY-PASS

The experimental dual carriageway on the A617 Hasland by-pass near Chesterfield was constructed in 1978 for Derbyshire County Council. Fig.9.12 shows a typical section through the experimental pavement. Pressure cells and strain coils were installed in the wheel tracks of the west bound carriageway to measure the vertical stresses and strains in the subgrade, 100mm below the granular layer, and strain coils were installed in the east bound carriageway to measure the horizontal strains at the interface between the bituminous and granular layers.

Regular deflection surveys and stress/strain measurements have been made since construction. Three typical surveys in July 1978, October 1979 and April 1981 are discussed here. Both carriageways have differences in binder and void contents and in the support conditions. However, for simplification, this analysis assumes that the east bound carriageway is typical. The asphalt mix details and subgrade modulus of elasticity which were used in the analysis are, therefore, averages for the east bound carriageway.

9.4.1 Support Conditions

The subgrade was variable over the length of the project. In situ CBR measurements varied between about 5% and 28%, the average value on the experimental section of the eastbound carriageway being 10.6%. A design CBR of 3% was taken by Derbyshire C.C. The in situ measurements were probably high because they were obtained on exposed formation in early summer, when the moisture content was lower than that expected for equilibrium under the completed road. A CBR of 5.3% was chosen as

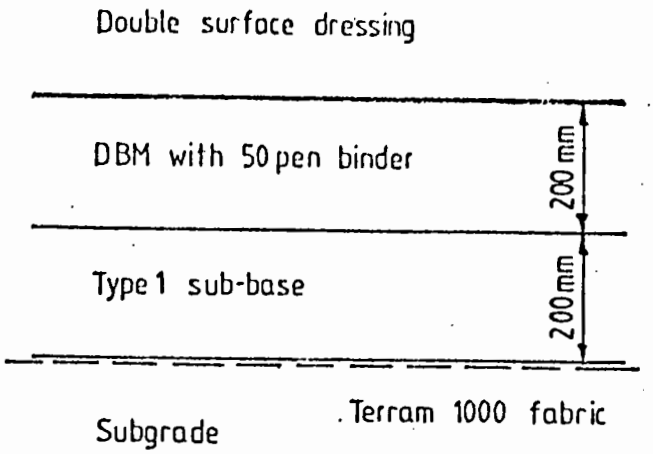

FIG 9.12 EXPERIMENTAL SECTION STRUCTURE FOR HASLAND BY-PASS

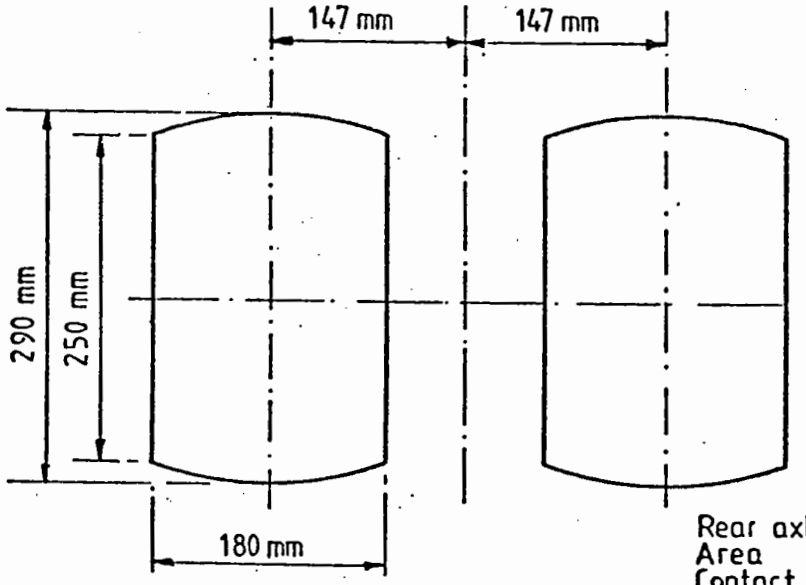

a. Measured tyre inprint (April 1981)

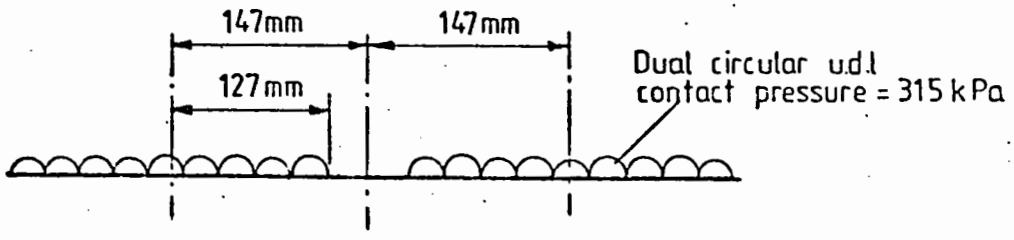

b. Equivalent loading arrangement for analysis

FIG 9.13 LOADING ARRANGEMENT FOR HASLAND BY-PASS

a basis for analysis, being half the average measured value and rather closer to the design figure of 3%.

A sub-base to subgrade modular ratio of 1.5 was assumed. This was selected on the basis of a previous study using the SENOL non-linear finite element computer program (44).

9.4.2 Asphalt Mix Details

The designed asphalt mix had a binder content of 4%. The void content measured from cores varied between 4% and 7% with an average value of 6.2% taken for analysis. The specific gravity of the aggregate was 2.71 and the binder, 1.02.

9.4.3 Surface Deflection

For deflection surveys, the measurements were corrected to a standard temperature of 20°C following the TRRL procedure (103). Therefore, the analyses were carried out at this temperature. In order to cover the range of measured values, average, maximum and minimum design cases were considered. The conditions for each design case are given in Table 9.13. A standard speed of 1.8 km/hr was used as representative of conditions for deflection surveys (100). The dimensions of the dual wheels on the deflection beam lorry were obtained in April 1981 and are recorded in Fig.9.13, together with the equivalent loading arrangement used for analysis. Although the rear axle loading varied for the other two surveys and the pressure was adjusted for the stress and strain calculations, just the one case was taken as typical for deflection computations.

The results of the analysis are given in Table 9.14 with the average, maximum and minimum values recorded during the three surveys shown for comparison. The computed deflections agreed closely with those measured. The important influence of the subgrade stiffness is

Table 9.13 VARIOUS PARAMETERS USED FOR DEFLECTION CALCULATIONS ON HASLAND BY-PASS

Parameter	For Average Deflection	For Maximum Deflection	For Minimum Deflection
Binder Content (%)	4.0	4.0	4.0
Void Content (%)	6.2	7.2	4.0
Mix Stiffness (MPa)	2530	2030	4210
Sub-base Modulus of Elasticity (MPa)	80	37	210
Sub-base to Subgrade Modular Ratio	1.5	1.5	2.0
Subgrade Modulus of Elasticity (MPa)	53	25	140

Table 9.14 COMPARISON BETWEEN MEASURED AND CALCULATED DEFLECTIONS FOR HASLAND BY-PASS

	Average Deflection ($mm \times 10^{-2}$)	Maximum Deflection ($mm \times 10^{-2}$)	Minimum Deflection ($mm \times 10^{-2}$)
Measured:			
July 1978	38	61	25
Oct. 1979	38	75	21
April 1981	42	80	19
Average	39	79	22
Calculated	44	78	18
$\frac{\text{Average Measured}}{\text{Average Calculated}}$	0.9	1.0	1.2

demonstrated by the computations. This is confirmed by the measured data in Figs.9.14 and 9.15 which shows the correlation between CBR and deflection along the eastbound carriageway.

9.4.4 Stress and Strain Measurements

The stresses and strains were also measured in July 1978, October 1979 and April 1981. The pavement temperatures and rear axle loading varied and these are given in Table 9.15. The mix stiffness of the asphalt layer had to be adjusted to accommodate the temperature variations. The values which were adopted in the analysis are given in Table 9.15.

For each survey, the average stress and strain were determined for each instrument. These figures were then averaged to give the measured values shown in Table 9.16 where they are compared with the computations. There is better agreement between the calculated and measured values of vertical stress than for either of the strains. The measured vertical strains in the subgrade were, on average, 2.7 times those calculated and the transverse asphalt strains 4.0 times those calculated.

The effects of variations to the subgrade stiffness (30-110 MPa), the sub-base to subgrade modular ratio (1.5-2.5), and stiffness of the asphalt layer (1.5-6.0 GPa), were investigated in an attempt to improve the accuracy of the computed parameters. Although slight improvements in stress or strain predictions were noted in certain instances, these were inconsistent with each other and of little overall significance.

9.5 AETHERIC ROAD, BRAINTREE

The installation of the instrumentation in the full depth asphalt construction at Aetheric Road, Braintree, is described elsewhere (46). The actual thickness of the asphalt layer as detemined from coring

Table 9.15 LOADING CONDITIONS FOR STRESSES AND STRAINS, HASLAND BY-PASS

Loading condition	July 1978	October 1979	April 1981
Temperature (°C)	23	17	14
Mix Stiffness (MPa)	2540	4925	5950
Rear axle load (kN)	56.9	68.7	63.5
Pressure (kPa)	280	340	315

Table 9.16 COMPARISON OF MEASURED AND CALCULATED STRESSES AND STRAINS, HASLAND BY-PASS

	July 1978			October 1979			April 1981		
	Meas.	Calc.	Meas./Calc.	Meas.	Calc.	Meas./Calc.	Meas.	Calc.	Meas./Calc.
Vertical stress (kPa)									
In subgrade	23.6	14.8	1.6	14	13.6	1.0	18.6	11.6	1.6
Vertical strain (με)									
In subgrade	745	260	2.9	425	232	1.8	662	196	3.4
Lateral strain (με)									
In asphalt	463	87	5.3	277	71	3.9	168	58	2.9

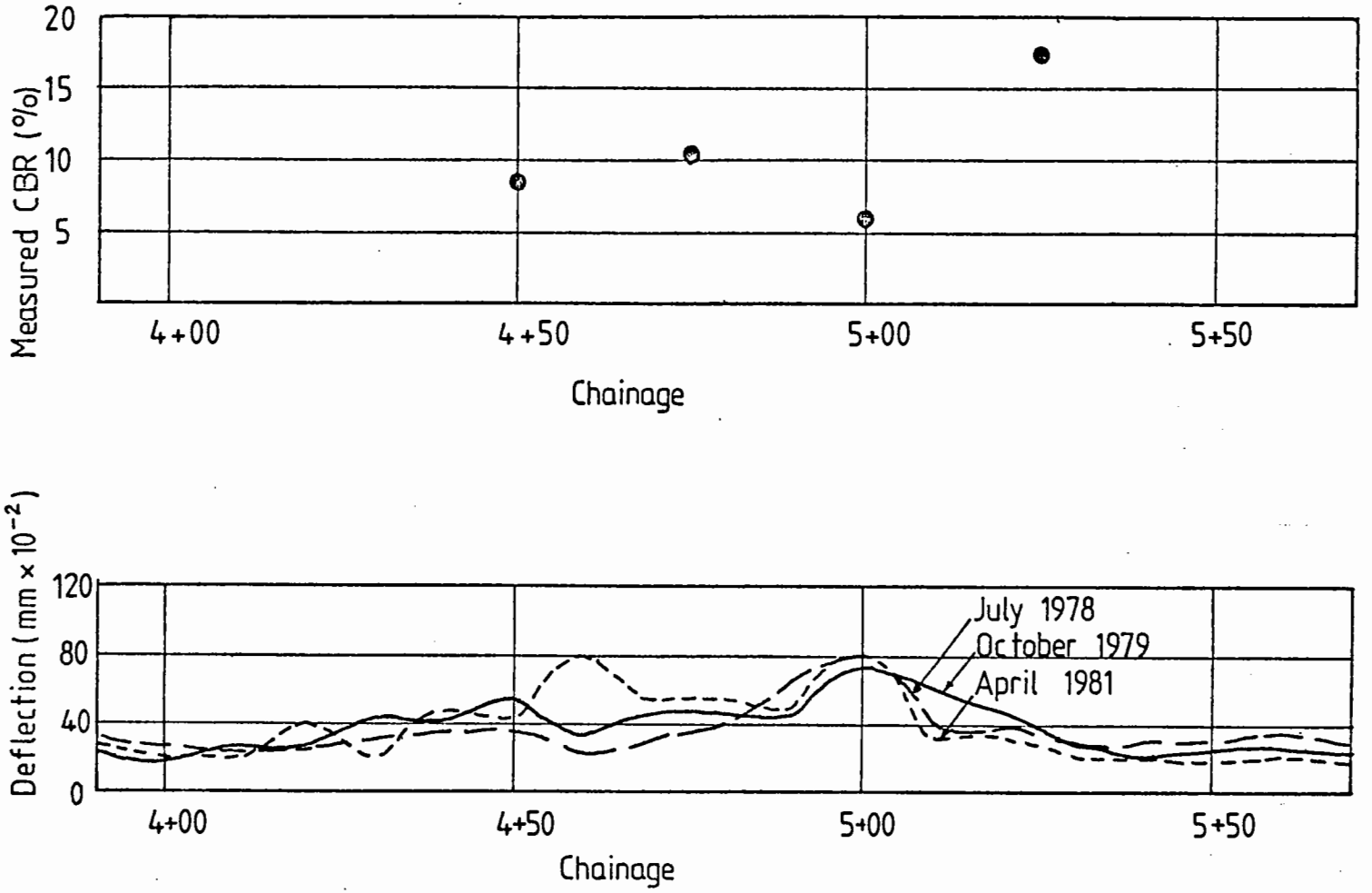

FIG 9·14 MEASURED CBR AND DEFLECTION EASTBOUND CARRIAGEWAY HASLAND BY PASS

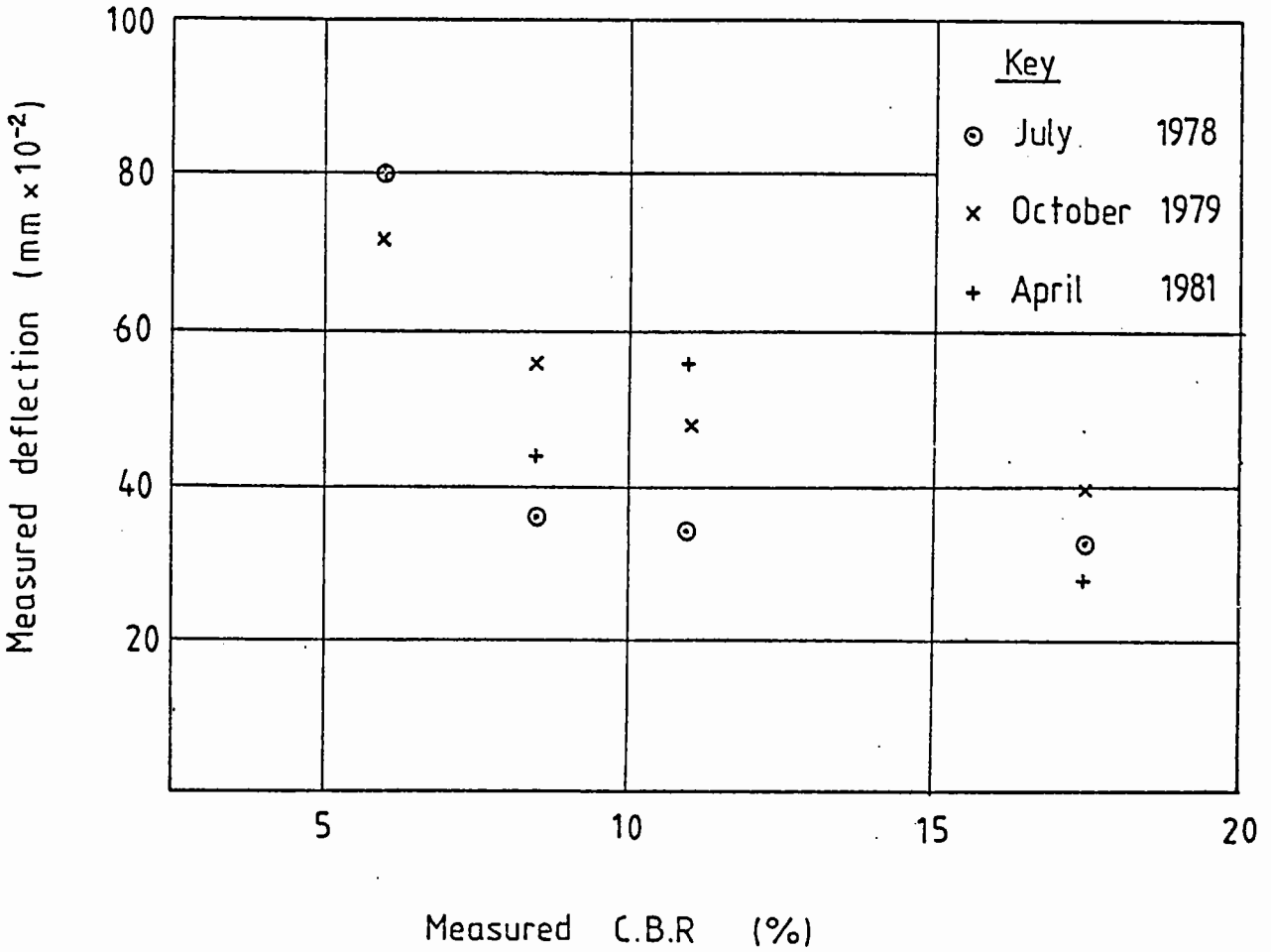

FIG 9·15 MEASURED DEFLECTION AS A FUNCTION OF MEASURED C.B.R ALONG EASTBOUND CARRIAGEWAY

varied but, for these calculations, an overall asphalt depth of 300mm was taken. This incorporates 50mm of wearing course and 250mm of asphalt base. Fig.9.16 shows a cross section of the pavement and the loading arrangement. This was derived from site measurements and, in each case, the contact pressure was calculated from the rear axle loading using the contact area shown in Fig.9.16.

Measurements of stresses, strains and deflections were taken in April and September 1980. Table 9.17 gives a summary of each loading condition, while Table 9.18 lists the mix properties assumed in calculating the asphalt stiffnesses. Table 9.19 summarises the layer stiffnesses which were used for each computation.

The measurements recorded on the site included vertical stress and strain at formation level, and both longitudinal and lateral horizontal strain at the bottom of the asphalt layer. In Table 9.20, the average values for these parameters are compared with those calculated using the BISTRO computer program.

The deflection measurements shown in Fig.9.17 were corrected, for temperature, to the standard of 20°C. The average deflections from this figure have been converted back to those measured at the actual pavement temperatures and are compared with the calculated deflections in Table 9.20. The calculated deflections were 1.6 times larger than those measured, whereas the calculated vertical stress was approximately 0.6 that measured. In order to improve the accuracy of these two factors, an increased subgrade modulus of elasticity of 50 MPa, corresponding to a CBR of 5%, was used and the calculations repeated. However, this was of limited significance, reducing the calculated deflection to 1.43 times that measured and increasing the calculated vertical stress to 0.67 times the measured value. The calculated vertical and lateral strains, however, were also reduced, decreasing their accuracy still further as they were already lower than those measured.

Table 9.17 SUMMARY OF LOADING CONDITIONS FOR AETHERIC ROAD, BRAINTREE

Loading condition	14.4.80	18.9.80
Pavement temperature (°C)	15	19
Rear axle load (kN)	79.0	60.8
Contact pressure (p) (kPa)	510	400
Speed (for stress, strain measurements) (km/hr)	4.0	4.0
Speed (for deflection measurements) (km/hr)	1.8	1.8

Table 9.18 DETAILS OF ASPHALTIC MATERIALS, AETHERIC ROAD, BRAINTREE

Mix property	Wearing course	Base
Initial penetration	50	50
Binder content	7.9	5.3
Void content	5.0	6.0
Specific gravity of aggregate	2.7	2.7
Specific gravity of binder	1.02	1.02

Table 9.19 STIFFNESS MODULI FOR AETHERIC ROAD, BRAINTREE

	Stiffness Modulus (MPa)			
	14.4.80		18.9.80	
	Stress, Strain Calculation	Deflection Calculation	Stress, Strain Calculation	Deflection Calculation
Wearing Course	1815	1470	1425	1045
Base	3385	2860	2470	1810
Subgrade	40	40	40	40

Table 9.20 COMPARISON OF MEASURED AND CALCULATED STRESSES, STRAINS AND DEFLECTIONS, AETHERIC ROAD, BRAINTREE

	14.4.80			18.9.80		
	Meas.	Calc.	Meas./Calc.	Meas.	Calc.	Meas./Calc.
Vertical stress (kPa)	18.4	12.9	1.4	23.7	12	2.0
Vertical strain (με)	649	292	2.2	438	280	1.6
Longitudinal strain (με)	232	107	2.1	189	107	1.8
Lateral strain (με)	167	80	2.1	172	79	2.2
Deflection ($mm \times 10^{-2}$)	25	47	0.53	30	42	0.71

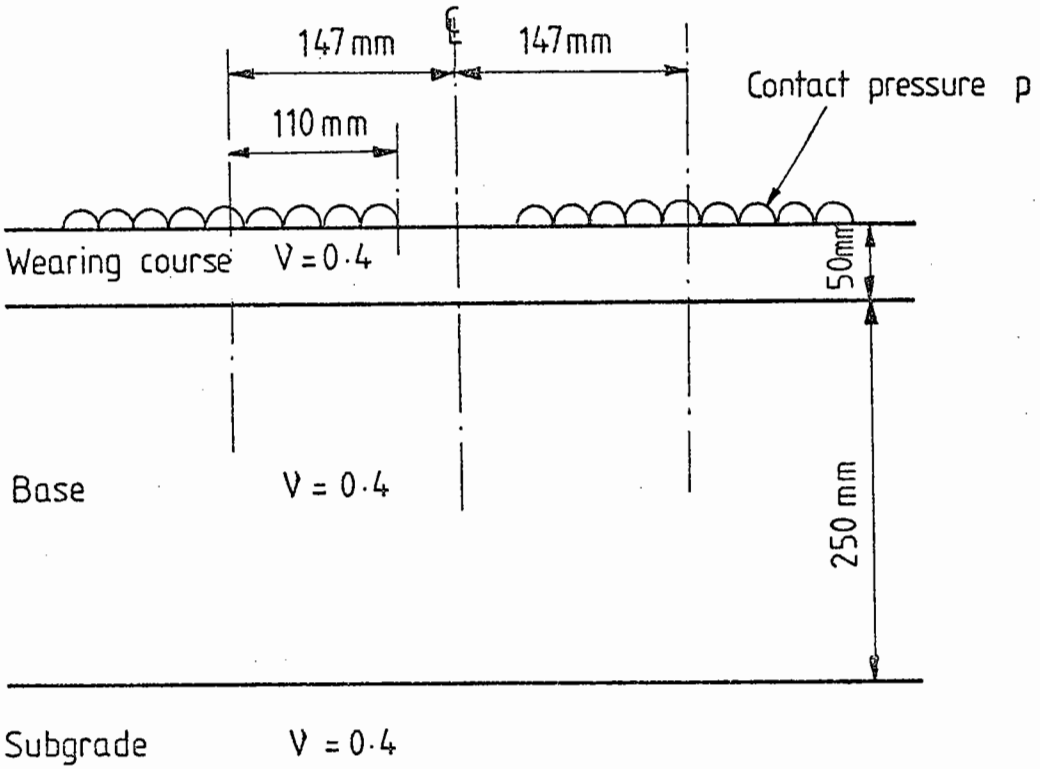

FIG 9·16 PAVEMENT STRUCTURE AND LOADING ARRANGEMENT FOR AETHERIC ROAD

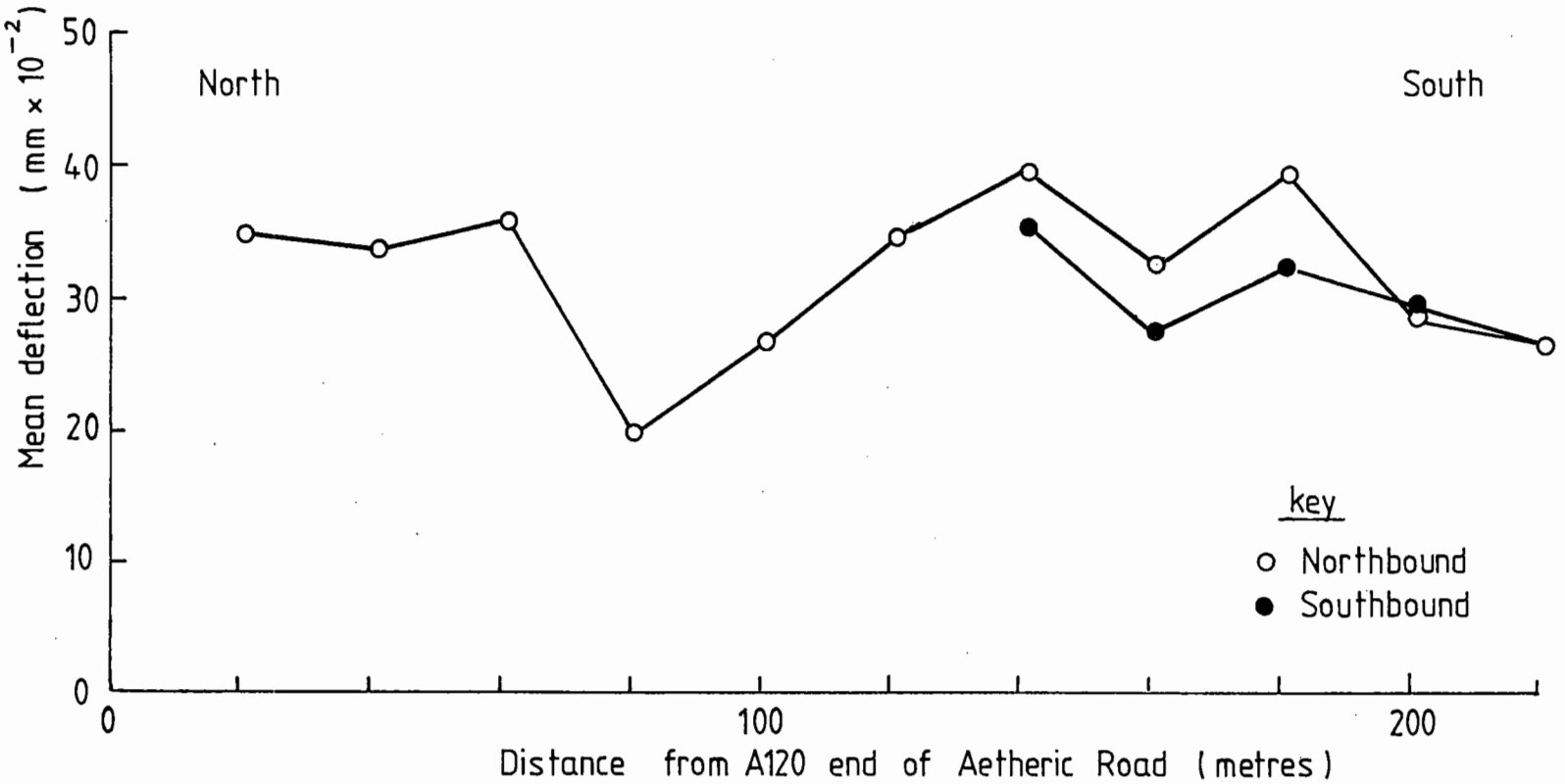

FIG 9·17 BENKELMAN BEAM DEFLECTION SURVEY, AETHERIC ROAD

9.6 SUMMARY

Analytical design methods have been used on an overlay at Theddingworth, a by-pass at Carsington and the reconstruction of the upper layers of the A52 Derby Road, Nottingham. The use of modified materials in the experimental sections has led to designs which compare favourably with the conventional alternatives.

From this study of full scale trials it can also be concluded that theoretical computations of deflection agree reasonably well with those measured. An average ratio of measured to calculated deflection of 1.0 was obtained for Hasland and the initial survey (before overlay construction) at Theddingworth, by varying the input parameters, particularly layer stiffnesses, for the analysis. This ratio was 0.6 at Aetheric Road and for the deflection survey after construction at Theddingworth.

The average ratio between measured and calculated vertical stresses at Hasland and Aetheric Road were 1.4 and 1.7 respectively. Although this discrepency appears to be fairly substantial, it is considered reasonable, as the actual values recorded for the stress were 15 to 25 kPa and the accuracy of the pressure cells about ±7 kPa.

The measured vertical and horizontal strains were substantially higher than those computed. For Hasland the average measured vertical strain was 2.7 times that calculated, and the average measured horizontal strain 4.0 times that calculated. At Aetheric Road the average measured to calculated ratios were somewhat better, being about 2.0 for both the vertical and horizontal strains.

This exercise has indicated the need for further work in this area. The accuracy of in situ measurements is probably not high since relatively few instruments were used and they were installed under somewhat difficult circumstances. Calibration work under ideal conditions has shown that about six duplicate readings of in situ

stress or strains are required to develop a reliable mean. Deflection measurements are more reliable and it has been possible to model these by adjustments to layer stiffnesses. This is encouraging for future work on overlay design.

CHAPTER TEN

OVERLAY DESIGN

In recent years the rate of deterioration of pavements has increased as traffic loads and the number of commercial vehicles have risen and many pavements constructed in Britain during the last 25 years are reaching the end of their design lives. Rising costs in materials and labour have emphasised the importance of strengthening existing roads by overlaying. The main difference between designing overlays and new pavements is that the strength of the existing pavement has to be determined and its residual life assessed. Generally, it is more economical to construct a thin overlay before major deterioration of a pavement than a thicker overlay or a new pavement at a later date.

Unfortunately, within the time available, it is impossible to consider the design of overlays in great detail. However, because overlays are so important to the highway network, this Chapter incorporates a literature review and provides details of a computer program developed to model surface deflections and determine the residual life of a pavement together with its required overlay thickness.

10.1 USE OF DEFLECTION MEASUREMENTS FOR DETERMINING PAVEMENT MATERIAL PROPERTIES

In order to evaluate the structural properties of a pavement, the pavement response (stresses, strains or displacements) for a given loading condition must be measured. The transient displacement or deflection of the road surface under an applied load is the easiest response to measure by rapid, non-destructive tests. As the surface

deflection represents the sum of all the vertical strains in the pavement and subgrade, it has been used for many years as an indicator of pavement performance. In 1955, limiting values of allowable maximum deflection were established from the results of the WASHO Road test (104,105) for flexible pavements in spring and autumn. Since then, deflection limits have been related to traffic, layer thicknesses and type of asphalt material. Hoffman and Thompson (106) summarize some typical limiting deflection criteria reported in the literature. Kennedy and Lister (107) provide a series of charts for use in the United Kingdom showing the relation between deflection and life for pavements with different road bases (see Section 10.2.4).

10.1.1 Deflection Measuring Devices

Current non-destructive deflection measuring devices can be classified under four loading modes; static, vehicular, vibrating and impulse. The typical device in the static loading category, is the plate bearing test. The load is applied for several minutes over a fixed point in the pavement surface. The large loads and static nature of the test make it unsuitable as a means of defining the pavement's response under the action of a moving wheel load.

Typical vehicular loading devices in common use because of their easy operation, are the Deflection Beam and Lacroix Deflectograph. The Deflection Beam was originally designed by Benkelman (104,105) for use in the WASHO Road test in the United States and is often referred to as the Benkelman Beam (BB). It has since been modified by different research organisations and road authorities. The Lacroix deflectograph is an automated form of the BB developed in France. Kennedy (100,103) describes in detail standardised versions of these devices and their operating procedures for use in the United Kingdom. Both devices use a dual wheel load of 3175 kg ±10% moving at creep speeds of between 1 and

3 km/hr. The magnitude of the wheel load used is different in other countries. In vehicular loading devices there is a horizontal relative motion between the load and the testing point. A moving wheel passing a point in the pavement produces a loading function which starts at zero, reaches a peak, then falls to zero again. The peak amplitude of the load decreases with depth whilst the loading time increases with depth.

Vibratory loading devices induce a steady-state harmonic vibration in the pavement with a dynamic generator. One example of this type of loading device is the Road Rater which is used in the United States and several other countries. Hoffman and Thompson (106) describe in detail the equipment and its operating procedures. Another example of this type of device used in the United States and Italy is the Dynaflect. Bandyopadhyay (108) discusses the Dynaflect equipment and presents a method for flexible pavement evaluation using the Dynaflect deflections.

The Falling Weight Deflectometer (FWD) is an impulse loading device which was developed in France. It has since been used in Denmark by Ullidtz (109) and Holland by Claessen et al (110). The force impulse is generated by a mass falling down a vertical rod on to a system of springs connected to a circular plate. The magnitude of the force depends on the size of the mass and the height through which it falls. The duration of the pulse load is fixed and controlled by the damping system. Typically it is between 0.02 and 0.03 seconds. The pulse duration is essentially constant with depth as reported by Bohn et al (111). Both the vibratory loading devices and the FWD measure the deflected shape of the surface by the use of several geophones at various radial distances from the loaded plate.

Hoffman and Thompson (106,112,113) performed an extensive programme of selected non-destructive testing of flexible pavements

using the road rater, BB and FWD. Correlations and comparisons between the different devices are presented. The FWD was considered the best device for simulating pavement response under a moving wheel load as the force amplitude and duration are of a similar magnitude to those for a moving heavy wheel load. The road rater induced lower pavement deflections than the FWD because of its harmonic loading without rest periods and static pre-load. The BB loading induced the highest pavement deflections.

The choice of equipment for measuring the deflections in an overlay design procedure depends to some extent on the design method adopted. The BB and deflectograph equipment are inaccurate at significant distances from the load because the deflection gauge is supported within the basin itself. However, Kennedy and Lister (107) use these devices since their design procedure depends only on the maximum central deflections. When the shape of the deflection bowl is required to determine material properties of the pavement, it is better to use a vibratory device or FWD.

10.1.2 Estimation of Material Properties

In order to study the effect that variations in stiffness moduli have on surface deflections, a typical structure has been analysed using the computer program BISTRO (38). The structure consisted of 4 layers; 2 bituminous layers 40 and 150mm thick, representing a wearing course and a base layer, a 300mm thick granular sub-base and a subgrade. A single 40 kN load was applied using a pressure of 565 kPa and radius 150mm. The surface deflections were calculated at radii of 0, 0.3, 0.6 and 0.9 metres. The stiffness modulus of each layer in turn was varied over a practical range of values and the results are shown in Fig.10.1. In each diagram the stiffness moduli of the other layers are kept constant at their middle values, that is, 5000, 7000,

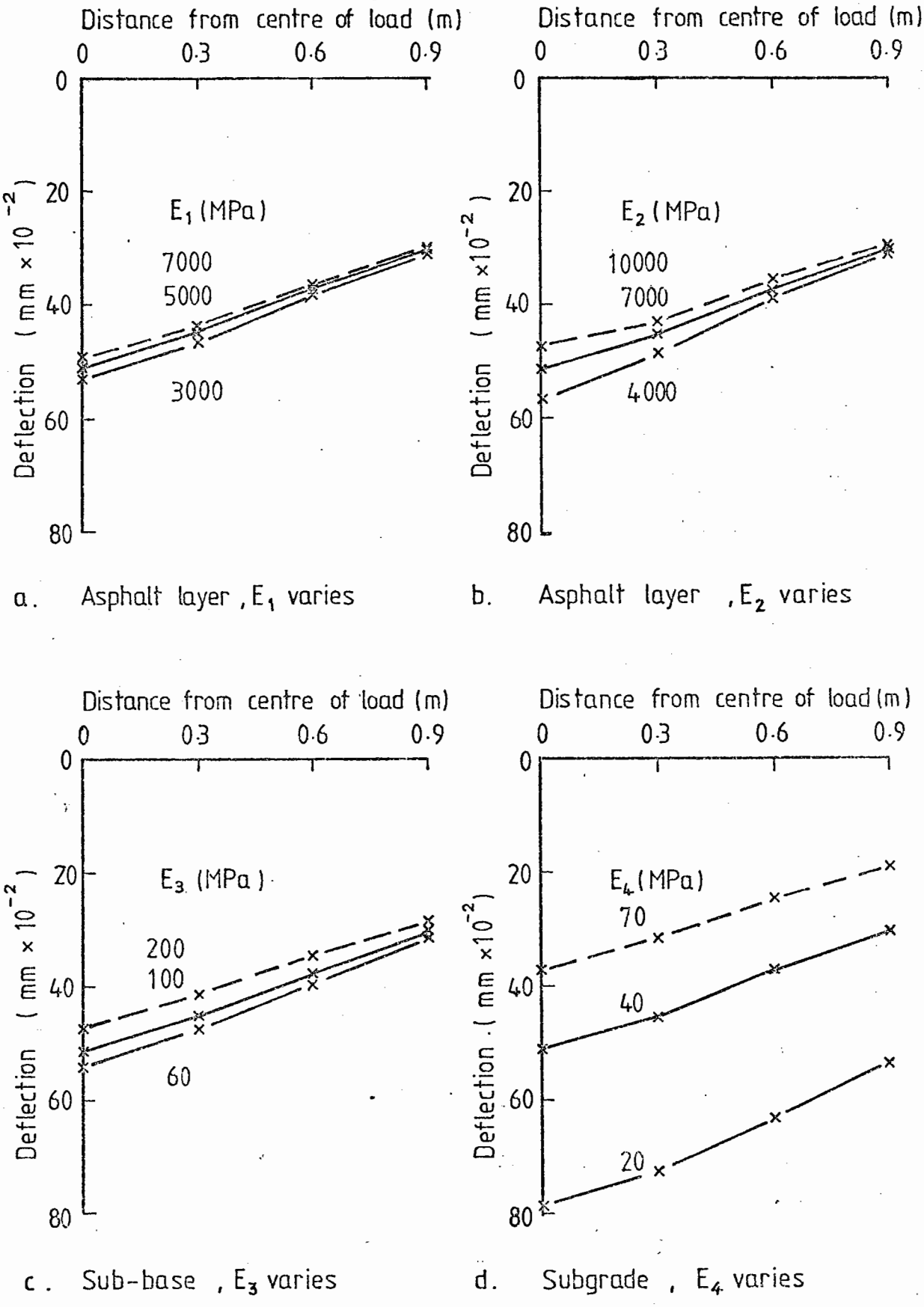

a. Asphalt layer , E_1 varies

b. Asphalt layer , E_2 varies

c. Sub-base , E_3 varies

d. Subgrade , E_4 varies

FIG 10·1 EFFECT OF VARYING STIFFNESS MODULUS FOR EACH LAYER ON SURFACE DEFLECTION

100 and 40 MPa for the wearing course, base, sub-base and subgrade respectively. From Fig.10.1 it can be noted that whilst changes in the moduli of the bituminous layers effect the surface deflections close to the centre of the load, they have very little effect on the surface deflections at distances of 0.6 and 0.9 metres from the load. Variations in the sub-base modulus have slightly more effect on the surface deflection at a distance of 0.6 metres but still hardly effect the deflection at 0.9 metres. The changes in subgrade modulus have by far the greatest effect on all the deflections. Because of this it is usually the first modulus to be derived. Similar studies on the effects of varying the stiffness moduli of pavement layers are reported by Kilareski et al (114) and McCullough et al (115).

A number of analytically based methods for the design of overlays were described at both the 4th and 5th International Conferences on the Structural Design of Asphalt Pavements. In most methods, the existing pavement is evaluated by measuring the surface deflection and radius of curvature or the deflected shape of the surface.

The Shell method for pavement evaluation and overlay design, is described by Claessen and Ditmarsch (110). The pavement structure is represented by three linear elastic layers, the asphalt layer, sub-base and subgrade. The deflection measurements required are the maximum deflection at the centre and the shape of the deflection bowl defined by the ratio of the deflection at a fixed offset distance to the maximum deflection. Assuming that the stiffness modulus of the asphalt layer, thickness of sub-base and sub-base to subgrade modular ratio are known, then the effective thickness of the asphalt layer and subgrade modulus are determined from a series of charts. These charts have been prepared to cover a wide range of structures using the computer program BISAR (73).

The effective asphalt layer thickness (h_1) takes into account differences between actual and assumed stiffness modulus of the asphalt layer due to the presence of cracks. The FWD was used for the deflection measurements.

Ullidtz (109) also used calculations based on elastic layer theory to construct a series of charts from which the stiffnesses of the layers in an existing pavement could be derived. The moduli may be determined both for structures containing linear elastic materials only and for structures having a non-linear elastic subgrade, for which the stress dependent modulus is approximated by

$$E = C \times \left[\frac{\sigma_1}{\sigma'}\right]^n \qquad (10.1)$$

where E is the modulus, σ_1 the major principal stress, σ' a reference stress and C and n are constants.

Kilareski et al (114) describe a method for evaluating the stiffness moduli of a four-layered pavement from four measured surface deflections at different radii from the centre of the load, (see Fig.10.2). The computer program BISAR (73) is used together with a successive approximation procedure. The first step is to assign a set of initial values of stiffness moduli to the pavement. By adjusting the subgrade stiffness modulus the calculated surface deflection is altered until it agrees with the measured deflection δ_4, (see Fig.10.2). Then, using the new subgrade modulus, the measured surface deflection δ_3 is modelled by adjusting the sub-base modulus. Similarly, using the new sub-base modulus also, δ_2 is modelled by adjusting the base modulus. To complete the first iteration, the maximum deflection at the centre of the load, δ_1, is modelled by altering the stiffness modulus of the surfacing layer. This calculation uses the newly derived moduli for

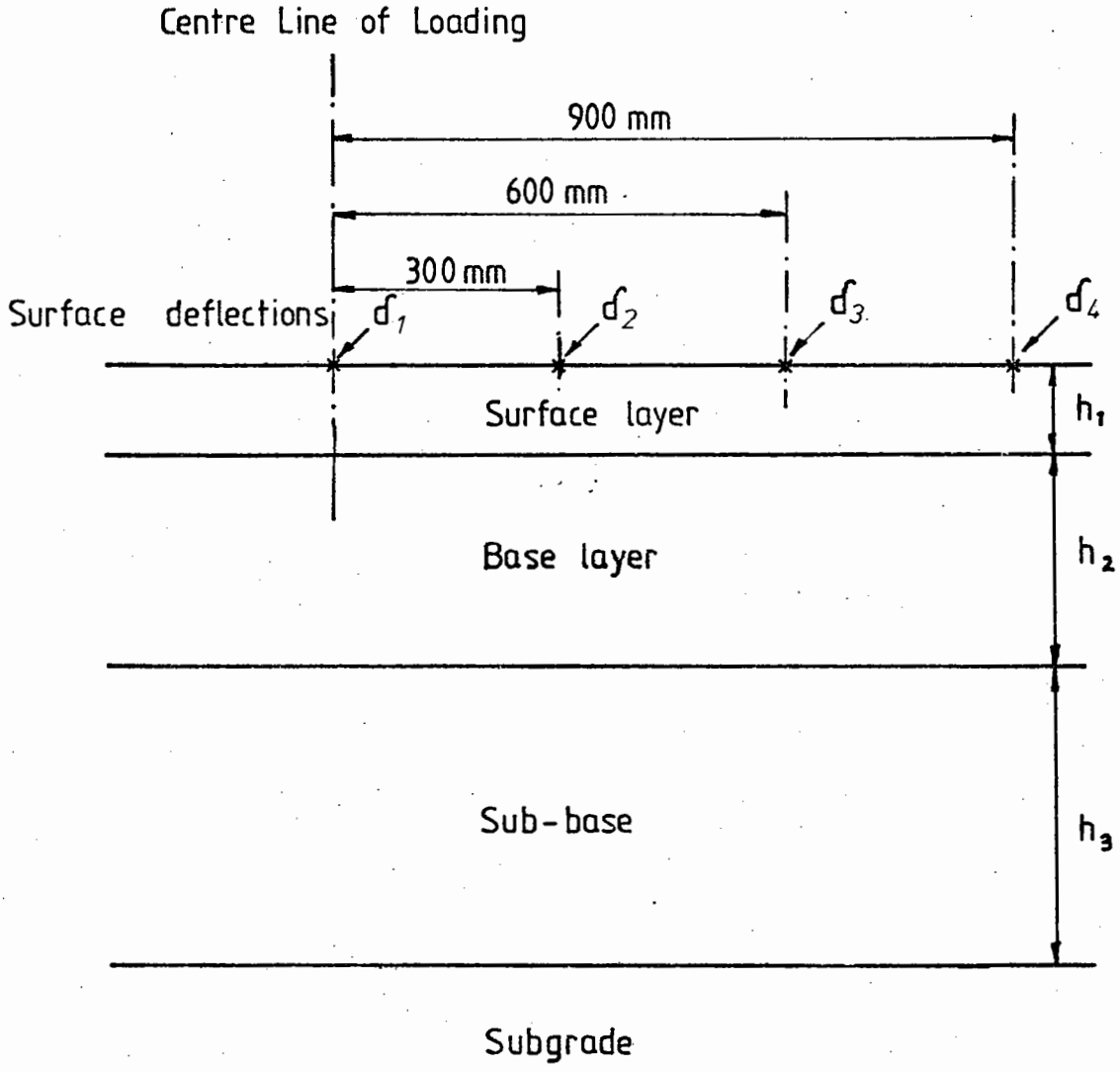

FIG 10.2 PAVEMENT STRUCTURE AND DEFLECTION MEASUREMENTS (AFTER KILARESKI (114))

the three lower layers. Because deflection δ_4, δ_3 and δ_2 were each modelled using at least one of the initial estimates of stiffness moduli, the procedure is repeated with the latest derived stiffness moduli as the initial values. If any of the stiffness moduli require further adjustment in the second iteration then the procedure must be repeated a third time and so on until all the measured deflections are satisfactorily modelled and the stiffness moduli fixed.

Hoffman and Thompson (113) describe a method (ILLI-CALC) for back calculating non-linear resilient moduli based on the interpretation of measured surface deflection basins. A stress dependent finite-element model (ILLI-PAVE) was used to develop nomographs for deflection basin interpretation. Measured surface deflections at radii of 0, 1, 2 and 3 feet are used, together with the deflection basin 'area', a parameter combining the four deflection readings.

Kilareski et al (114), Van der Loo (116) and Bandyopadhyay (108) all use one or more of the following parameters associated with deflection measurements to obtain valuable information about the strength of a pavement system. The surface curvature index (SCI), which is defined as the numerical difference between the first or central deflection and second deflection, is used to indicate the structural condition of the upper layers. The base curvature index (BCI), which is defined as the numerical difference between the two outer surface deflection measurements, measures the strength of the lower portion of a pavement. The slope of the deflection basin also indicates the strength of a pavement. A steep slope is associated with a weak pavement whilst a shallow slope is associated with a strong pavement.

10.2 TRRL OVERLAY DESIGN PROCEDURE

The TRRL design procedure for overlays is described in LR 833 by Kennedy and Lister (107). It has been considerably extended since its introduction in 1973 (117). Further details and examples of the design procedures cost effectiveness have also been reported by Lister et al (118). The design procedure is an empirical method using relationships between maximum surface deflection (measured using a BB) and the structural strength of the road. These relationships were developed from both BB and Deflectograph measurements observed during the last 20 years on TRRL full scale road experiments (119,120).

10.2.1 Traffic Estimation

Estimates are required for both the traffic carried by the pavement since construction (past traffic) and the traffic expected during the design life of the overlay (future traffic). The past traffic figure is used to estimate the remaining life of the pavement. Two nomograms which were developed by Thrower and Castledine (121) are provided (see Fig.10.3) for the direct prediction of both past and future traffic in terms of number of commercial vehicles. The number of commercial vehicles is then converted to an equivalent number of standard axles by using the factors given in Table 2 of Road Note 29 (1) for the past traffic figures and the revised damage factors for future traffic figures recommended by the Department of Transport (92) and TRRL (91).

10.2.2 Adjustment of Measured Deflections

The standard deflection value is the equivalent BB deflection value measured at a pavement temperature of 20°C, 40mm below the surface. Measurements recorded using a Deflectograph are first converted to equivalent BB deflections at the same temperature, and

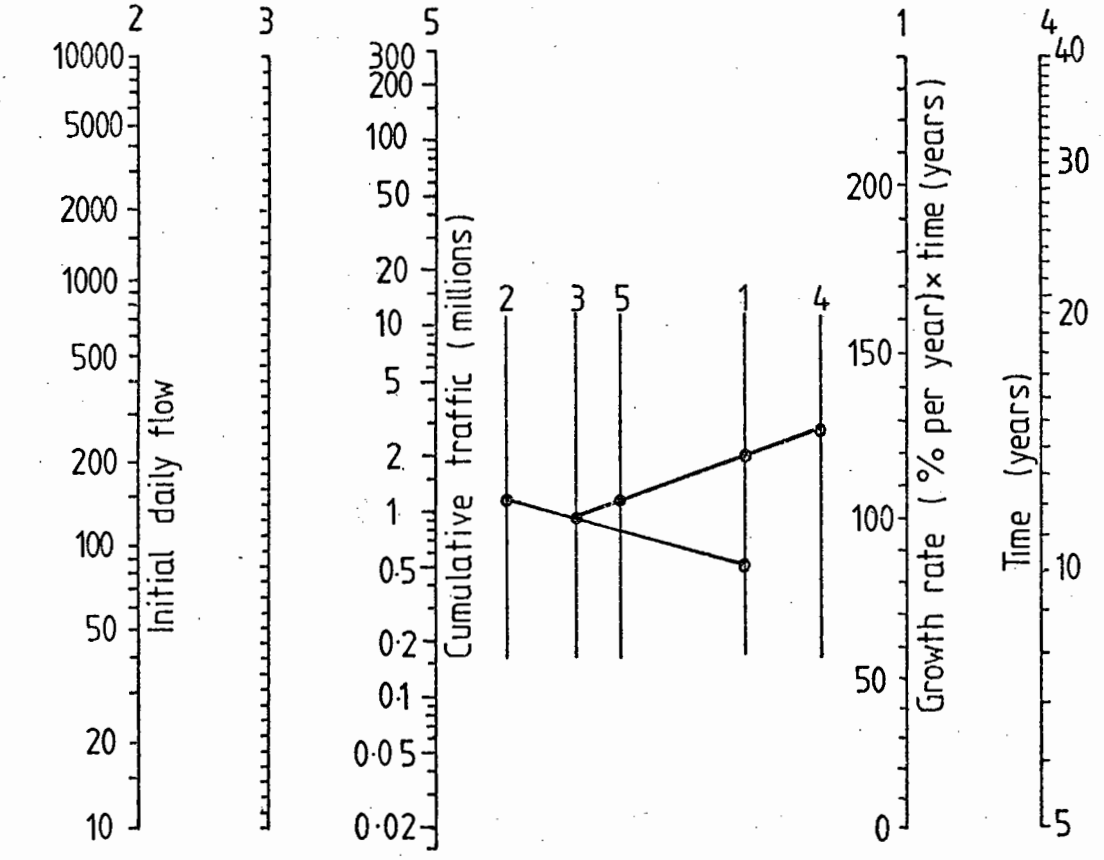

a. Forward

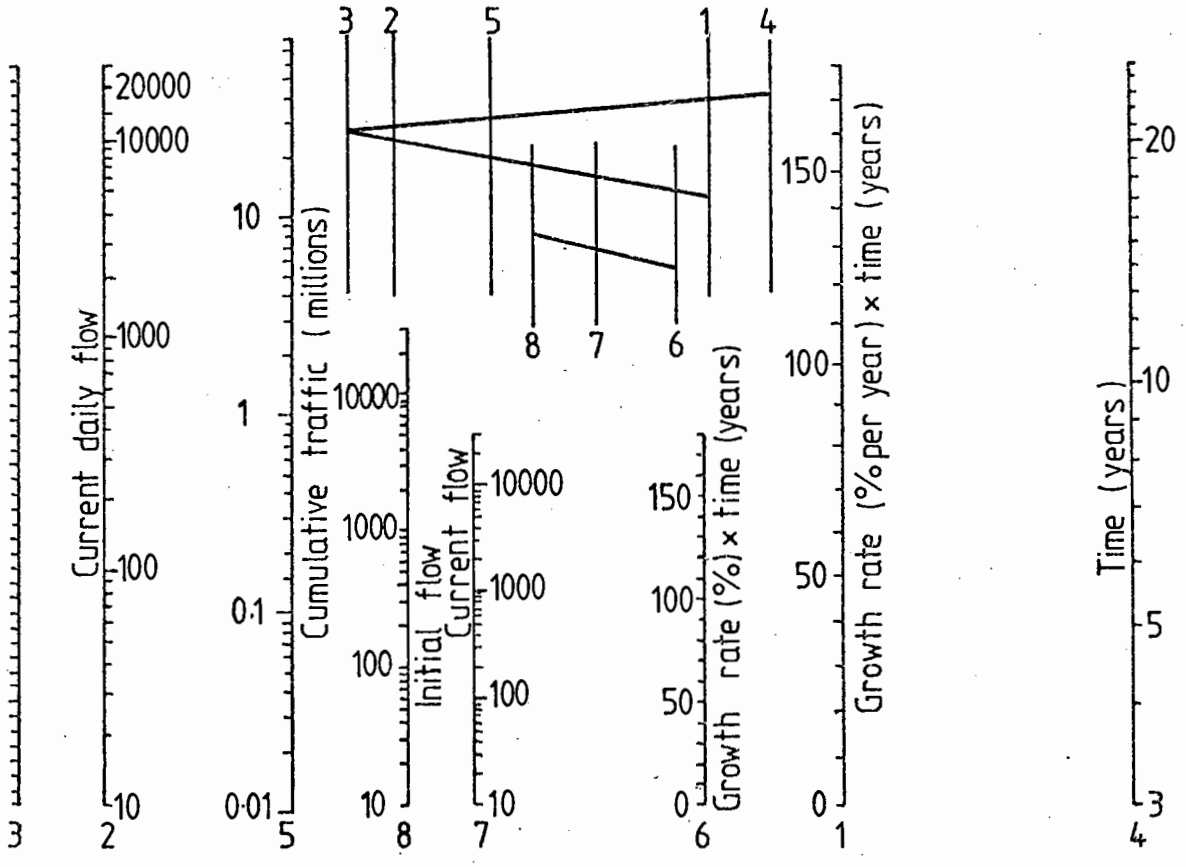

b. Backward

FIG 10·3 NOMOGRAMS FOR ESTIMATION OF CUMULATIVE ONE-WAY TRAFFIC IN THE LEFT HAND LANE (AFTER THROWER & CASTLEDINE (121))

then to equivalent deflections at 20°C. BB values are only corrected for temperature. Fig.10.4 shows the correlation between the deflections measured with the two sets of equipment, and Fig.10.5 shows a typical temperature correction chart.

10.2.3 Assessment of Pavement Performance

The deflection of a pavement is fairly constant during its life until the onset of critical conditions when it begins to increase. A visual assessment of the quality of the pavement and measurements of rut depth in the wheel paths using a 2m straight edge, enable the road to be classified in accordance with Table 2 of LR 833 (107) (see Table 10.1). Deflection histories were used to develop four performance charts showing the relation between standard deflection and life for pavements with different road bases (see Fig.10.6). The critical condition in these charts corresponding approximately to damage visible at the road surface as described in Table 10.1. The residual life of the pavement is determined from the difference between the number of standard axles corresponding to the critical condition and that carried by the pavement up to the time of the deflection survey.

10.2.4 Design of the Overlay

If the residual life of the pavement is considered too short the required overlay is determined from a second set of charts, see Fig.10.7. These charts are for pavements with different road bases and specify the thicknesses of a hot rolled asphalt overlay. Equivalent thicknesses of coated macadam overlays can be determined using multiplication factors given in Table 3 of LR 833. The charts were derived from information reported in references (118, 120).

Table 10.1 PAVEMENT CLASSIFICATION

Classification	Code	Appearance
Sound	1	No cracking. Rutting less than 5 mm.
	2	No cracking. Rutting 5 to 9 mm.
Critical	3	No cracking. Rutting from 10 to 19 mm.
	4	A single crack or extending over less than half the wheel path. Rutting 19 mm or less.
Failed	5	Inter-connected multiple cracking over most of the wheel path. Rutting 19 mm or less.
	6	No cracking. Rutting 20 mm or greater.
	7	A single crack or extending over less than half the wheel path. Rutting 20 mm or greater.
	8	Inter-connected multiple cracking over most of the wheel path. Rutting 20 mm or greater.

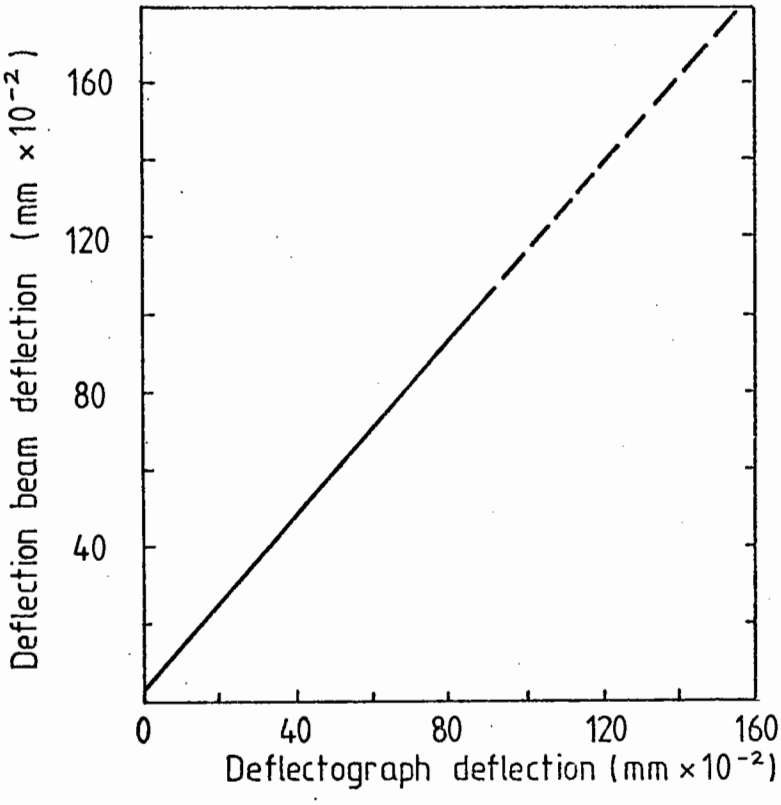

FIG 10·4 CORRELATION BETWEEN DEFLECTION BEAM AND DEFLECTOGRAPH (AFTER KENNEDY AND LISTER (107))

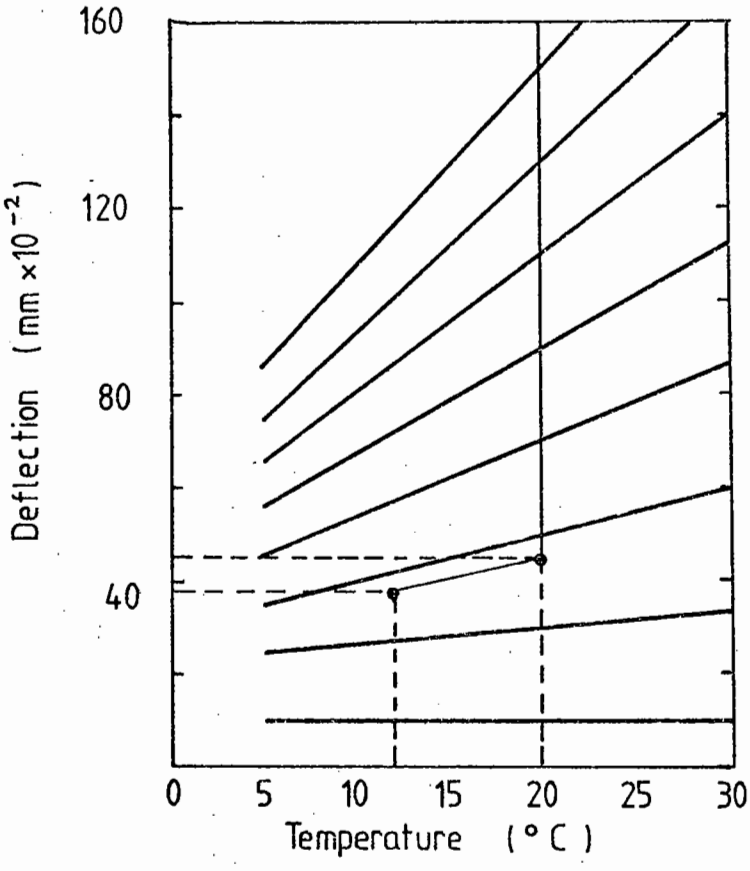

FIG 10·5 TYPICAL RELATION BETWEEN DEFLECTION AND TEMPERATURE (AFTER KENNEDY AND LISTER (107))

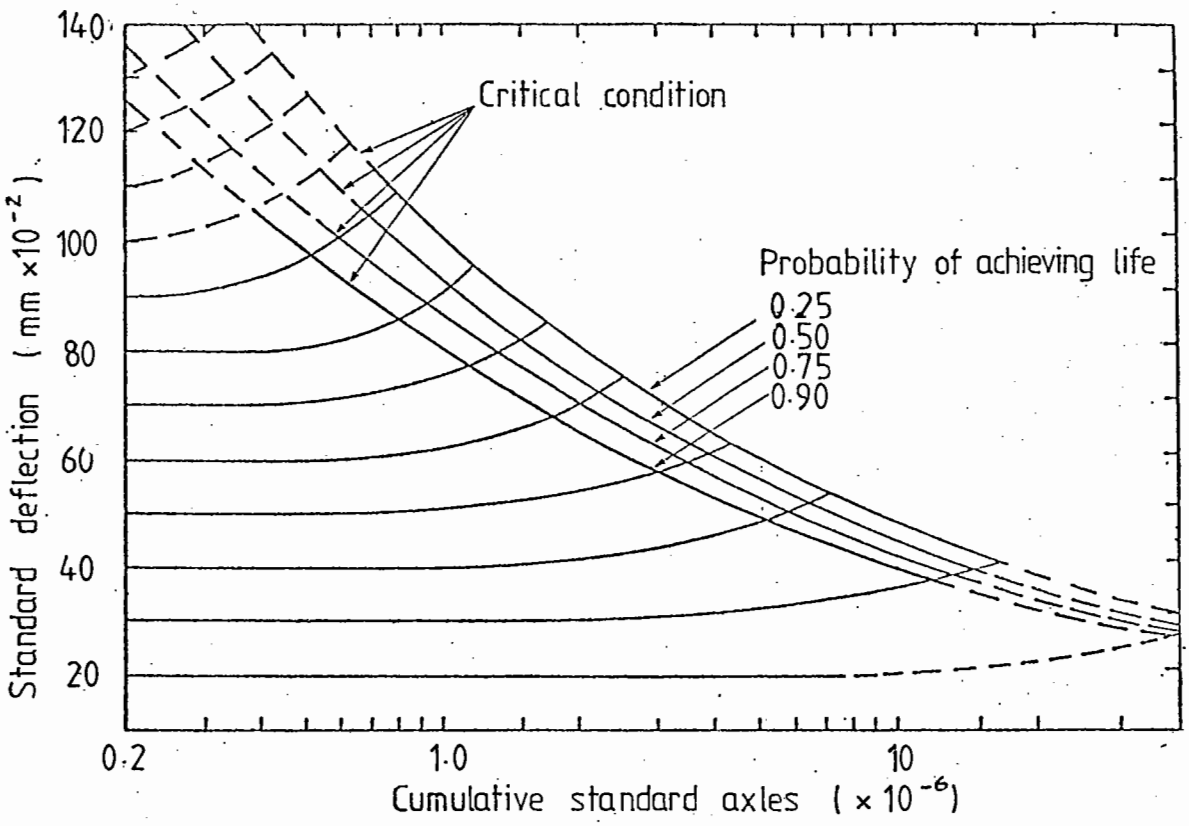

FIG 10·6 RELATION BETWEEN STANDARD DEFLECTION AND LIFE FOR PAVEMENTS WITH BITUMINOUS ROAD BASES (AFTER KENNEDY ET AL(107))

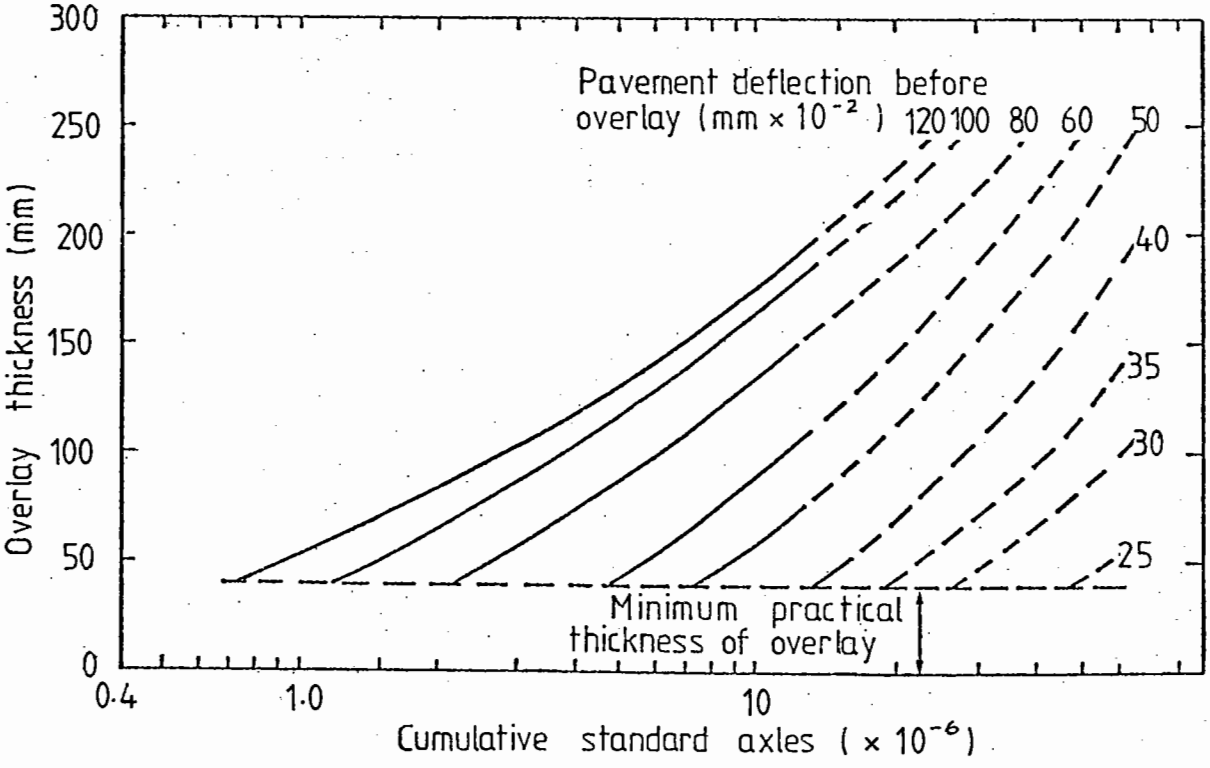

FIG 10·7 OVERLAY DESIGN CHARTS FOR PAVEMENTS WITH BITUMINOUS ROAD BASES (0·50 PROBABILITY) (AFTER KENNEDY ET AL(107))

10.3 DEVELOPMENT OF COMPUTER PROGRAM FOR DEFLECTION MODELLING AND OVERLAY DESIGN

As discussed in Section 10.2, the present method for designing overlays in the United Kingdom relies on an empirical procedure. Although this procedure gives more reliable thicknesses for an overlay than those based solely on engineering judgement, there remain several limitations to its use. The residual lives of an existing pavement and required overlay thicknesses can only be determined for four typical road base materials. It is difficult to adjust the residual lives or overlay thicknesses for variations in the materials even when detailed information is known. It should also be noted that the charts in LR 833 (107) are for existing pavements with design lives less than 40 million standard axles (msa) and for overlaid pavements with design lives less than 80 msa. Nowadays, pavements are frequently designed for lives well in excess of these values and consequently the development of an analytical procedure for overlay design to be used in conjunction with the computer programs developed for designing new pavements is a logical step. Although such a program has been developed, as described in the remainder of this Chapter, it should be remembered that the program may require further modifications once it has been applied to practical situations. It is hoped that this will be one of the first priorities of future work at the University of Nottingham. The name given to the main frame computer program is DEMOD, from DEflection Modelling for Overlay Design.

10.3.1 Choice of Analytical Tool

A major problem in modelling surface deflections due to a known loading is the non-linear characteristics of the materials, particularly those which are unbound and the subgrade. A finite element program, SENOL, has been developed at the University of

Nottingham by Pappin (44) which deals with non-linearity using stress dependent bulk and shear moduli. However, the aim of this work is to develop an analytical procedure which is both realistic and yet as simple as possible. A linear elastic layered system was therefore selected as the analytical tool with the intention of using more accurate finite element computations for calibration.

The CHEVRON N-layer elastic system computer program (39) is incorporated into the overlay progam DEMOD as a subroutine in a similar way to that used in both the ANPAD and CUDAM programs. DEMOD also includes parts of the program PONOS (58) for estimating dynamic stiffness of the bituminous materials. Southgate et al (122) and Van der Loo (116) also use the CHEVRON computer program when evaluating the stiffness moduli of a pavement from deflection measurements.

10.3.2 Method of Analysis

Fig.10.8 shows a flow diagram for the computer program DEMOD. Two sets of measured deflections are required; those in the wheel track and those in the lane centre, (mid-way between the two wheel tracks (see Fig.10.9)). Because the centre of a lane in a pavement carries negligible traffic, only that due to lane changes, when compared to the wheel track section, the lane centre deflections are used to model the stiffness moduli of the existing pavement shortly after it was constructed. These stiffness moduli are required to determine the original fatigue life of the pavement and to assess the amount of damage which has already occurred. Van der Loo (116) also used the lane centre deflections in his pavement evaluation method based on the original design life of the pavement. Although the construction of an overlay reduces the level of tensile strain at the bottom of the bituminous layers, it does not remove any fatigue damage which has already taken place and subsequent damage must be considered as

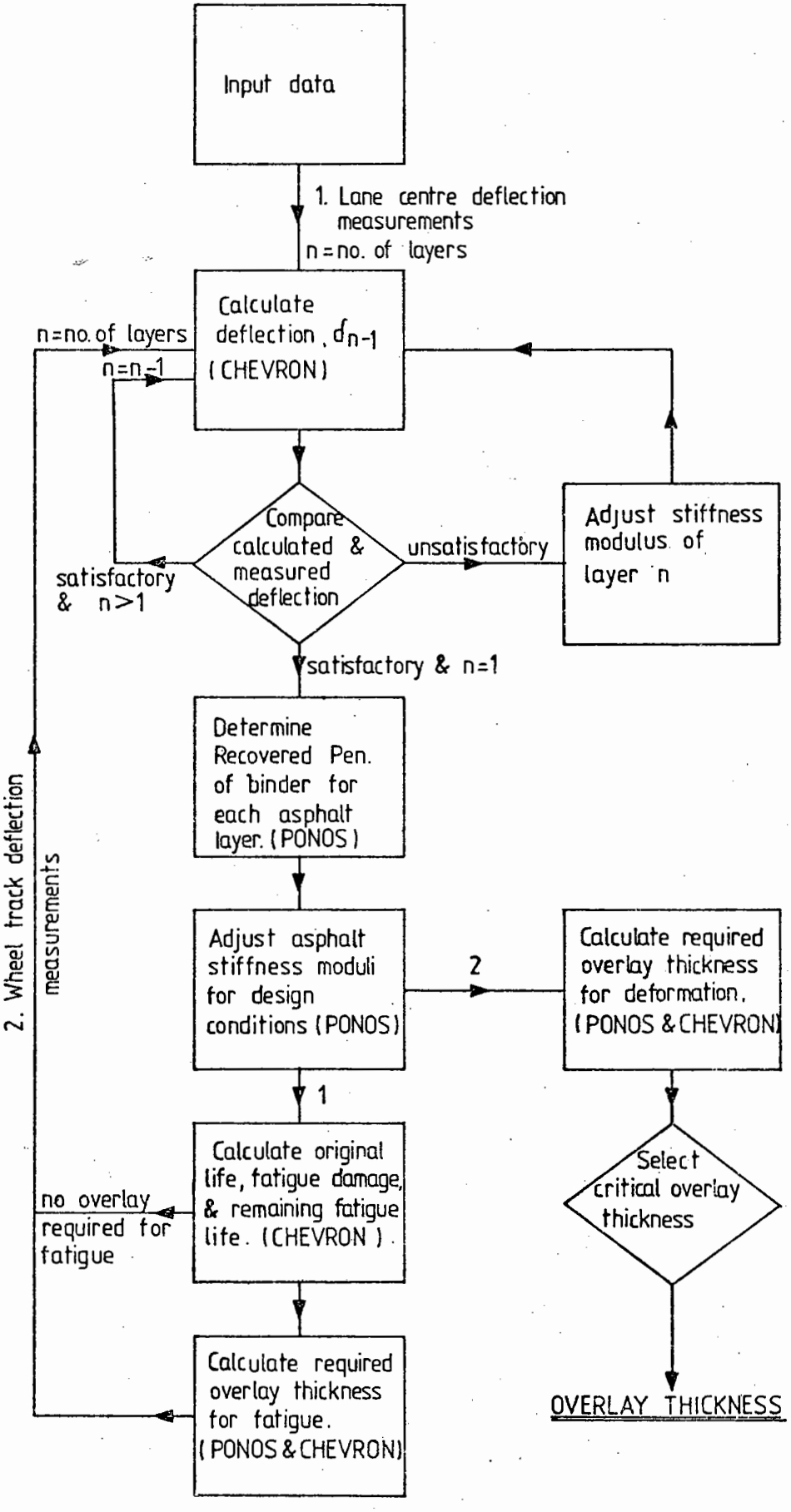

FIG 10·8 FLOW DIAGRAM FOR DEMOD

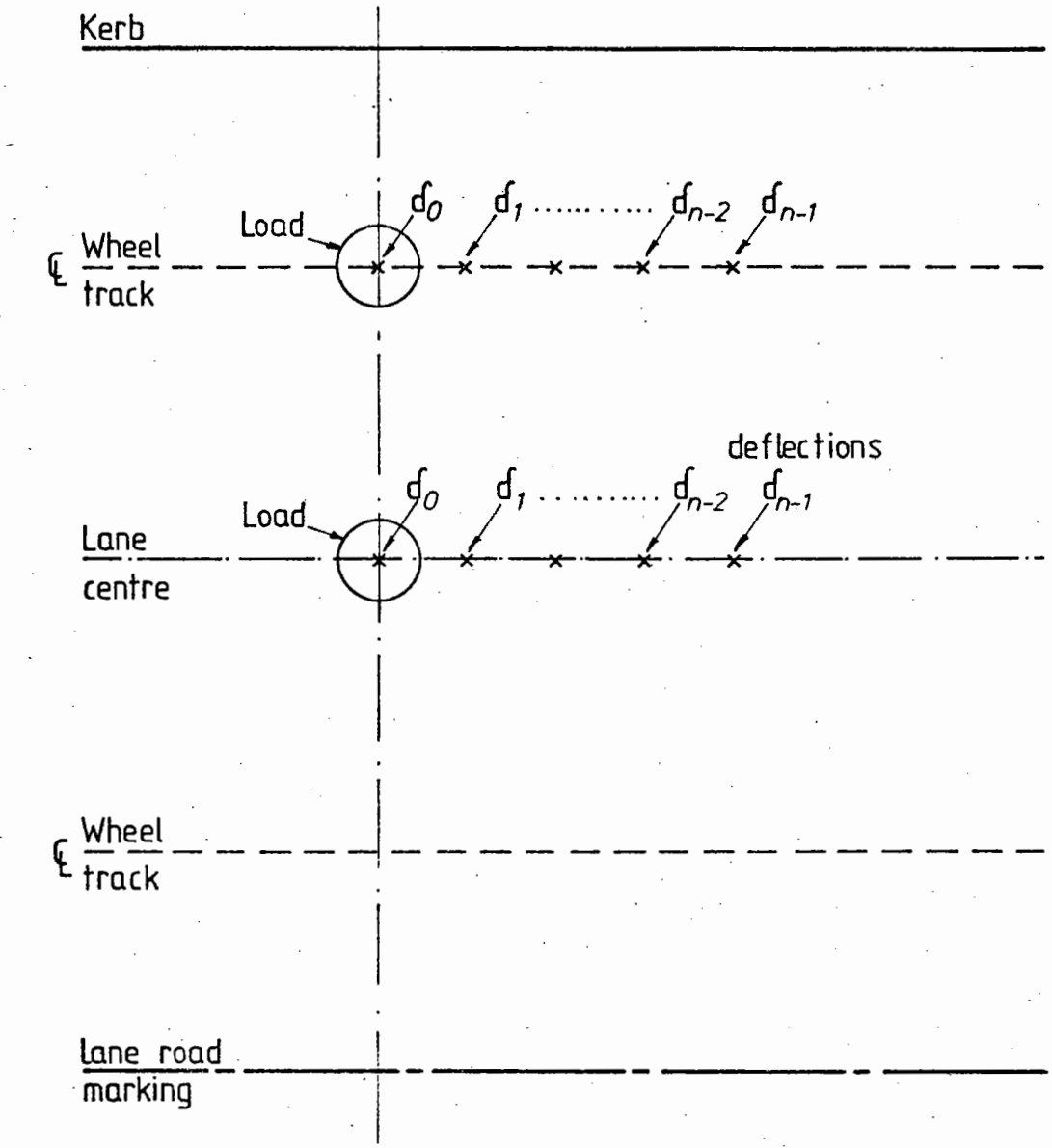

a. Plan

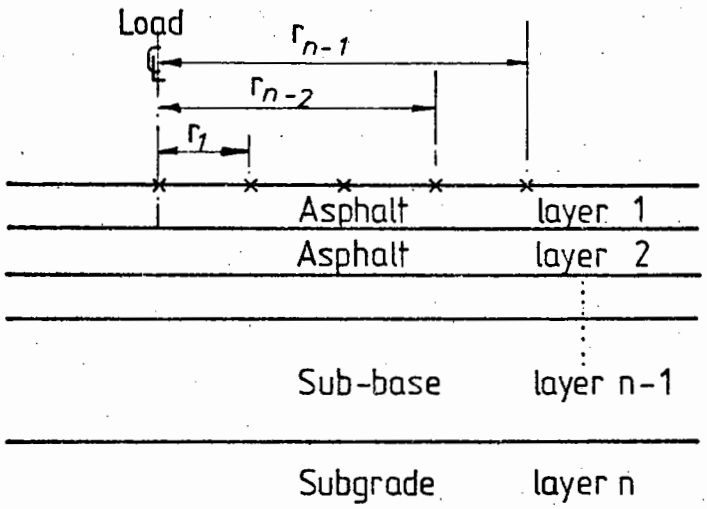

b. Section

FIG 10.9 TYPICAL PAVEMENT STRUCTURE AND DEFLECTION MEASUREMENTS FOR DEMOD

additional. However, when considering the design of an overlay against permanent deformation, the structure can be analysed as a 'new' pavement and the life determined from the maximum allowable subgrade strain (see Chapter 5). The stiffness moduli of the existing structure, just prior to construction of the overlay, are therefore derived from the deflections measured in the wheel track where rutting usually occurs.

A list of input data necessary for running the computer program is given in Table 10.2 whilst Fig.10.9 shows a typical structure and the required deflection measurements. For the deflection analysis DEMOD presently uses a typical FWD loading arrangement with a 35 KN single load, (contact pressure 500 kPa and radius 0.15 metres) but the program can be amended to suit an alternative loading arrangement.

The program first calculates the lane centre deflection at radius r_{n-1}, where n is the number of layers in the structure, (see Fig.10.9), using the estimated stiffness modulus of each layer and the sub-routine CHEVRON. The calculated deflection is compared with the corresponding measured deflection, (δ_{n-1}). If the calculated deflection is not within ±2% of the measured deflection then the stiffness modulus of the subgrade, layer n, is adjusted as follows:

$$E_{i+1} = E_i \times \frac{(\delta_m + \delta_c)}{2 \times \delta_c} \qquad (10.2)$$

where, E_i and E_{i+1} are the i^{th} and $(i+1)^{th}$ estimates of the stiffness modulus (MPa) and δ_m and δ_c are the measured and calculated deflection values.

The same deflection is re-calculated using the new subgrade stiffness modulus and the procedure repeated.

Table 10.2 INPUT DATA REQUIRED FOR DEMOD

Input Data	Format (FQO unless otherwise stated)	Examples	Units
1. Text, Date	15A4	Test 1/3/83	
2. No. of designs			
3. Air temperature for design: average annual air temperature		9.0	^{0}C
4. Design speed: average speed of of commercial vehicles		80	km/hr
5. Past traffic		20.0	msa
6. Future traffic		40.0	msa
7. No. of layers of existing pavement (N). For the overlay inputs 8-12 are required	I1	4	
8. Binder content		4.5	%
9. Void content		6.5	%
10. Specific gravity of aggregate		2.7	
11. Specific gravity of bitumen		1.02	
12. Initial penetration of binder Inputs 13-19 are required for the upper bituminous layers, starting with the surfacing layer 1 to layer (N-2)		50.0	
13. Thickness		0.100	metres
14. Estimated stiffness modulus		3000.0	MPa
15. Binder content		5.0	%
16. Void content		5.0	%
17. Specific gravity of aggregate		2.65	
18. Specific gravity of binder		1.03	
19. Ratio of recovered penetration of binder to initial penetration of binder		0.65	
20. Type of base material, 1,2,3 or 4 depending on whether the base material is a HRA, DBM, Modified HRA or Modified DBM, respectively	I1	1	
21. Sub-base thickness		0.200	metres
22. Estimated stiffness modulus of sub-base		100.0	MPa
23. Estimated CBR of subgrade		4.0	%

Table 10.2 Contd.

Input Data	Format (F 0.0 unless otherwise stated)	Examples	Units
24. Deflection temperature		18.0	^{0}C
25. Deflection loading time Inputs 26-28 are required for each deflection measuring position starting at the centre of loading and working outwards		0.02	seconds
26. Radius		0.000	metres
27. Measured deflection in the lane centre		40.0	mm x 10^{-2}
28. Measured deflection in the wheel track		42.0	mm x 10^{-2}

Once the calculated deflection is satisfactory the program proceeds to model the measured lane centre deflection at radius r_{n-2}, (see Fig.10.9), by adjusting the stiffness modulus of the sub-base (layer n-1). In these calculations the subgrade modulus is taken as that derived from modelling the deflection δ_{n-1}. Then, using the derived sub-base modulus also, the measured deflection at radius r_{n-3} is modelled by altering the stiffness modulus of layer n-2. Following the same procedure the program continues to derive a stiffness modulus for each layer in turn until the stiffness modulus of the surfacing layer is determined from the maximum deflection at the centre of the load using the calculated moduli for all the other layers. As each newly adjusted stiffness modulus may affect an earlier derived modulus for a lower layer, all the deflections are re-checked and further adjustments carried out when necessary.

The next step is to determine a recovered penetration of the binder for each bituminous layer. The input mix details and deflection conditions of temperature and loading time are used in the sub-routine PONOS. The input loading time, (approximately 0.02 seconds), for the FWD is assumed to be constant with depth, as discussed in Section 10.1.1. The mix stiffness is calculated using an initial estimate for the recovered penetration of 50.0 and then compared with that derived from the deflection modelling. An iterative procedure follows in which the recovered penetration is adjusted until the calculated mix stiffness is equal to that derived ±10 MPa. From the input ratio of recovered penetration to initial penetration, the initial penetration is then calculated.

Now that the binder properties have been determined, the design stiffness moduli of the bituminous layers are calculated using the sub-routine PONOS. As in ANPAD, these moduli are based on design temperatures of 1.92 and 1.47 times the average annual air temperature

for fatigue and permanent deformation respectively and loading times derived from the average speed of the commercial vehicles, (see Chapter 6).

Following the arrow 1 on the flow diagram, Fig.10.8, the next step is to calculate the original life of the pavement against fatigue cracking and permanent deformation. An identical method to that adopted in the design life option of ANPAD is used, together with the same critical design criteria (see Chaper 6).

The amount of fatigue which has already taken place is then determined from:

$$\text{Fatigue Damage} = \frac{T_p}{N_{te}} \qquad (10.3)$$

where, T_p is the traffic carried by the existing pavement (past traffic in msa) and N_{te} is the calculated fatigue life of the existing pavement in msa.

If the amount of fatigue damage which has occurred is greater than or equal to 0.5 then the program terminates and suggests that a reconstruction is required. The value of 0.5 was selected in a fairly arbitrary way to limit the amount of cracking and further justification should be sought. However, it is interesting to note that the onset of critical conditions in the TRRL design procedure (107) is denoted by a rut depth of 10mm or more, which is half that which denotes failure (20mm). When the fatigue damage is less than 0.5 then the remaining fatigue life equals the difference between the fatigue life of the existing pavement and the past traffic. If the remaining fatigue life is greater than the input value for future traffic then no overlay is required for fatigue considerations. If, however, the remaining

fatigue life is less than the input value for future traffic then the fatigue design life of the pavement and overlay, N_{to}, is derived from Miners' rule in which the total damage must be less than or equal to 1.

$$\frac{T_p}{N_{te}} + \frac{T_f}{N_{to}} = 1 \qquad (10.4)$$

$$\text{Therefore, } N_{to} = \frac{T_f}{(1-T_p/N_{te})} \qquad (10.5)$$

where, T_p and T_f are the past and future traffic figures respectively and N_{te} is the fatigue design life of the existing pavement. N_{to}, N_{te}, T_p and T_f are all in millions of standard axles.

From the fatigue design life of the pavement and overlay, N_{to}, the required thickness of the overlay is calculated next using a similar procedure to that adopted in the design thickness option of ANPAD. The maximum allowable asphalt strain (ϵ_t) at the bottom of the bituminous layers is calculated within the program from the same relationship used in both ANPAD and CUDAM, (see Chapter 6) viz;

$$\log \epsilon_t = \frac{14.39 \log V_B + 24.2 \log SP_i - 40.06 - \log N}{5.13 \log V_B + 8.63 \log SP_i - 15.8} \qquad (10.6)$$

where, ϵ_t is the tensile strain (microstrain)

V_B is the binder content by volume (%)

SP_i is the initial binder softening point (°C)

and N is the required life of the pavement in standard axles (for the overlay, $N = N_{to} \times 10^6$).

An initial thickness of 100mm is assigned to the overlay and the maximum tensile strain calculated using the CHEVRON subroutine. The

calculated strain is compared with the maximum allowable strain and the thickness of the overlay adjusted by ±10mm until the criterion is just satisfied. The minimum overlay thickness is 40mm for practical considerations and the maximum overlay thickness allowed in the program is 200mm.

Once the thickness of the overlay has been determined for fatigue, permanent deformation must be considered. For this part of the analysis the wheel track deflections are used to determine the present stiffness moduli of the various layers of the pavement, that is just prior to construction of the overlay (see Fig.10.8). The same method is adopted as before when modelling the lane centre deflection measurements, but the initial estimate for each layer stiffness modulus is taken as that derived from the lane centre deflection measurements.

For each bituminous layer the recovered penetration of the binder is determined using the stiffness modulus derived from the wheel track deflections and the same iterative procedure as described earlier when considering the lane centre deflections. Then, the sub-routine PONOS adjusts the stiffness moduli of the bituminous layers to the design conditions, (temperature and loading time).

Using the resulting design stiffness moduli, the next step in DEMOD is to calculate the required thickness of the overlay for permanent deformation. Yet again a similar procedure is adopted to that used in the design thickness option of ANPAD with the same criterion for the maximum allowable compressive strain (ϵ_z) on the subgrade as follows:

$$\epsilon_z = \frac{21600}{(N/f_r)^{0.28}} \qquad (10.7)$$

where, ϵ_z is the subgrade strain (microstrain)

f_r is the rut factor varying between 1.0 and 1.56, depending on the base material, (see Chapter 5)

and N is the number of standard axles.

The thickness of the overlay is adjusted in the same manner and within the same limits (40 to 200mm) for deformation as it was for fatigue until the calculated vertical subgrade strain just satisfies the criterion given in equation (10.7).

The resulting design thickness of the overlay is selected from the two values obtained; one for fatigue and the other for deformation.

An example of the use of DEMOD is given in Fig.10.10.

10.3.3 Practical Adaptations to DEMOD

Before the computer program DEMOD can be used to accurately model the measured deflection of a pavement under a given loading, some adaptations may be necessary. Unfortunately there is insufficient detailed data available at present to allow an investigation into the accuracy of DEMOD. Details of the pavement structure, including the measured stiffness modulus and thickness of each layer and mix deflections and loading conditions, are required to enable comparisons to be made with calculations using DEMOD.

Presently DEMOD adjusts each stiffness modulus until the corresponding calculated deflection is within ±2% of the measured deflection. It may be necessary to alter the allowable percentage error for one or more of the deflections. Kilareski et al (114) permit a 5.0% error in the calculated maximum deflection (δ_o) whilst allowing only 1.0% for the other deflections.

Very little of the pavement deflection is due to compression of the surface layers, mostly it is due to compression of the subgrade.

EXAMPLE

INPUT DATA

Bituminous Mix Details	Overlay	Layer 1	Layer 2 (HRA base)
Binder content	4.5	7.9	5.7
Void content	8.0	4.0	6.0
Specific gravity of aggregate	2.7	2.7	2.7
Specific gravity of bitumen	1.02	1.02	1.02
Initial penetration	50.0	-	-
Recovered penetration/ Initial penetration	-	0.65	0.65

Design Conditions

Average annual air temperature	=	9.5 ^{0}C
Traffic speed	=	80 km/hr
Past traffic	=	5 msa
Future traffic	=	20 msa

Deflection Data

Temperature	=	20 ^{0}C
Loading time	=	0.02 seconds

	Measured Deflections (mm x 10^{-2})	
Radius (m)	Lane Centre	Wheel Track
0.0	60.0	65.0
0.3	50.0	53.0
0.6	40.0	41.0
0.9	32.0	32.0

FIG 10·10 OUTPUT INFORMATION FROM DEMOD

OUTPUT DATA

1. Lane Centre Analysis

	Lane Centre Deflection (mm x 10^{-2})	
Radius (m)	Measured	Calculated
0.0	60.0	58.8
0.3	50.0	50.9
0.6	40.0	40.5
0.9	32.0	31.7

		Stiffness Moduli (MPa)	
Layer	Estimated	For Deflection	For Recovered Penetration
1	3000	2182	2175
2	4500	4500	4494
3	80	80	
4	40	35	

	Binder Properties		
Layer	Init. Pen.	Rec. Pen.	Init. Soft. Point (°C)
1	66.46	43.20	49.61
2	47.72	31.02	53.40

Design Based on Linear Elastic Analysis

Fatigue criterion

Asphalt strain = 123.3 microstrain
Life = 48.9 msa

Deformation criterion

Subgrade strain = 322.9 microstrain
Life = 3.3 msa

Therefore Deformation critical

Structure 1

ASPHALT LAYER 1

Thickness	=	40 mm
Poisson ratio	=	0.4
Effective Stiffness:		
For deformation	=	4445 MPa
For fatigue	=	3182 MPa

ASPHALT LAYER 2

Thickness	=	150 mm
Poisson ratio	=	0.4
Effective Stiffness:		
For deformation	=	7567 MPa
For fatigue	=	5721 MPa

SUB-BASE

Thickness	=	300 mm
Poisson ratio	=	0.4
Stiffness	=	80 MPa

SUBGRADE

CBR	=	3.5 %
Poisson ratio	=	0.40

Existing Pavement Life	=	3.3 msa
Percentage Fatigue Damage	=	10.2

Overlay Design for Fatigue

Remaining life	=	43.9 msa

No overlay required for fatigue

2. Wheel Track Analysis

Wheel Track Deflection (mm x 10^{-2})

Radius (m)	Measured	Calculated
0.0	65.0	63.7
0.3	53.0	53.8
0.6	41.0	41.8
0.9	32.0	32.1

Stiffness Moduli (MPa)

Layer	Estimated	For Deflection	For Rec. Pen.
1	3000	1077	1082
2	4500	3878	3886
3	80	82	
4	40	35	

Binder Properties

Layer	Init. Pen.	Rec. Pen.	Init. Soft Point (°C)
1	127.15	82.65	42.18
2	56.08	36.45	51.55

Structure 2

ASPHALT LAYER 1

Thickness	=	40	mm
Poisson ratio	=	0.4	
Effective Stiffness:			
For deformation	=	2616	MPa
For fatigue	=	1743	MPa

ASPHALT LAYER 2

Thickness	=	150	mm
Poisson ratio	=	0.4	
Effective Stiffness:			
For deformation	=	6882	MPa
For fatigue	=	5085	MPa

SUB-BASE

Thickness	=	300	mm
Poisson ratio	=	0.3	
Stiffness	=	82	MPa

SUBGRADE

CBR	=	3.5	%
Poisson ratio	=	0.4	

Overlay Design for Deformation

Allowable subgrade strain	=	195.1	microstrain
Overlay thickness required	=	70	mm

Overlay Design for both Fatigue and Deformation

Required thickness	=	70	mm
Effective stiffness of overlay			
For deformation	=	8736	MPa
For fatigue	=	6678	MPa

In order to reduce the inaccuracy caused by assuming the subgrade is linear rather than non-linear, McCullough and Taute (115) consider the subgrade to be supported by a more rigid foundation at a depth of about 4 metres. A similar assumption could also be incorporated into DEMOD or the computer program SENOL (44) could be used to develop a relationship by which the stiffness modulus of the subgrade in DEMOD could be increased with depth.

CHAPTER ELEVEN

CONCLUSIONS

The object of this research was to develop analytical design procedures using computers for asphalt pavements. Because the main structural layers of the typical pavements under consideration are bituminous, linear elastic layered systems were selected as the analytical tool in order to keep the design procedures as simple as possible. Realistic values for the sub-base modulus, however, were derived from studies using the non-linear finite element computer program SENOL (44).

The main conclusions of the work described in this thesis are summarised below.

11.1 PAVEMENT DESIGN

Chapters 4 and 5 discuss detailed studies of the design of asphalt pavements against fatigue cracking and permanent deformation. Revised design criteria against these failure modes were derived. Chapters 3 and 6 describe the development of a number of computer programs for pavement design. The overall conclusions of this section of work are as follows:-

a) A revised fatigue design criterion was developed which includes a 'shift factor' of 440 to take into account the differences between conditions in situ (where longer lives are obtained) and those in laboratory testing.

b) Improved procedures have been established for defining temperature conditions in asphalt pavements for design purposes. A factor of 1.47 is used to convert air temperatures into pavement

temperatures. This factor takes into consideration the effects of diurnal variations in both temperature and traffic loading. For fatigue computations only, a further factor of 1.31 has been derived to obtain a single design temperature which takes into consideration cumulative damage effects. Thus, for fatigue, the pavement design temperature is equal to 1.92 times the average annual air temperature (1.47 x 1.31 = 1.92). For the cumulative damage programs (CUDAM and CDM), the twelve average monthly pavement temperatures are used.

c) Application of the cumulative damage approach to variations of load as well as temperature was generally found to be impracticable and it was decided that the use of the fourth power law to calculate the equivalent number of standard axles was a reasonable general approach.

d) The computation procedure for dealing with design against excessive permanent deformation has been brought up to date in the light of data produced in the laboratory testing programme at Nottingham (45,46,47,48) over the past three years. The procedure involves adjustment to the relationship between allowable subgrade strain and design life, depending on the road base mix to be used.

e) A suite of three programs for simplified pavement design computations has been developed for the Commodore PET 8k microcomputer. These are:

SDM A Simplified Design Method used to calculate the required asphalt thickness.

BDM A Balanced Design Method used to determine the asphalt mix proportions.

DLM A Design Life Method used to calculate the life of a given pavement.

f) A program which considers cumulative fatigue damage effects due to temperature variations has been developed for a 16k PET microcomputer. The program is called CDM from Cumulative Damage Method.

g) The development work on pavement design using a microcomputer has been extended to the main frame machine resulting in two versatile computer programs ANPAD and CUDAM.

ANPAD (ANalytical PAvement Design) is a computer program based on linear elastic analysis. It incorporates three design alternatives, calculating the design thickness, mix proportions for a balanced design or the design life of a given pavement.

CUDAM (CUmulative DAMage) carries out a more detailed analysis for the design thickness and design life options of ANPAD by incorporating procedures to deal with cumulative damage in asphalt fatigue. Both ANPAD and CUDAM use the CHEVRON N-layer elastic program (39) to perform the structural analysis and parts of the program PONOS (58) to estimate the dynamic stiffness of the bituminous layers.

11.2 APPLICATIONS OF COMPUTER PROGRAMS

The applications of the computer programs described in Chapter 7 led to the following results and conclusions:-

a) The effect of varying the mix proportions and design conditions on the required thickness of the asphalt layer or life of the pavement, has been studied in detail in Chapter 7. Generally, when the binder content is reduced to 4% for the hot rolled asphalt mixes, the life of the pavement is increased. For a typical dense bitumen macadam, there is an optimum binder content between 4 and 5% depending on the thickness of the asphalt layer

and the void content of the bituminous mix. Improved compaction of the asphalt layers also increases the life of the pavement or reduces the thickness of asphalt required.

b) The ANPAD program has been used to develop a suite of design charts for asphalt pavements. The configurations include full depth asphalt and structures with granular sub-bases. Various material types may be used. The charts are incorporated in a design manual included here as Appendix A. They cover a practical range of temperatures, traffic speeds and CBR values.

c) The merits of using the modified DBM or HRA road base course mixes, suggested by the laboratory testing and field trials, has been well demonstrated in the design studies performed using ANPAD.

11.3 COMPARISON OF DESIGN METHODS

In Chapter 8 careful comparisons have been carried out between the analytical design methods of TRRL, Shell and the Asphalt Institute with that incorporated in ANPAD. Comparisons have also been made with current UK practice as outlined in Road Note 29. The results of these comparisons are listed below:

a) The main discrepancies between the TRRL design procedure for fatigue and that at Nottingham, are caused by the different nature of the basic fatigue relationship derived from laboratory testing. For the typical dense bitumen macadam base examined, the Nottingham fatigue line is much steeper and independent of temperature.

b) The critical design criterion in the TRRL designs for heavy traffic (see Section 8.2), was fatigue cracking whilst for the ANPAD designs it was permanent deformation. Although the detailed

calculations differ, the final results appear somewhat similar.

c) The Shell Design Charts were found to produce significantly thinner asphalt layers than those derived using ANPAD.

d) Comparisons of the Road Note 29 designs with those using ANPAD have shown close agreement for structures with a hot rolled asphalt base and lives between 1 and 100 million standard axles. However, for structures with a dense bitumen macadam base, the required total asphalt thicknesses calculated using ANPAD were greater than those recommended in Road Note 29, particularly for the longer lives.

e) The Asphalt Institute design method is based on cumulative damage effects for both fatigue cracking and permanent deformation. Higher bituminous mix stiffnesses are predicted by this method than by the Nottingham or Shell design methods. The Asphalt Institute design criteria agree closely with those developed in this research.

11.4 FULL SCALE TRIALS

The validity of analytical design methods can only be assessed by their use in practice. A number of full scale trials have been designed using the computer programs developed (see Chapter 9). Additional computations were carried out using measurements of stress, strain and deflection obtained from these and other full scale trials. The conclusions arising from Chapter 9 are:

a) The use of modified materials in the experimental sections have led to designs which compare favourably with the conventional alternatives.

b) By adjustment of layer stiffnesses, theoretical computations of deflection were made to agree reasonably well with those measured.

c) Within the accuracy of the earth pressure cells (±7 kPa), the measured vertical subgrade stresses also demonstrated reasonable agreement with those computed.

d) The measured vertical and horizontal strains were substantially higher than those computed.

11.5 OVERLAY DESIGN

As a result of a detailed literature review, the main frame computer program DEMOD (from DEflection Modelling for Overlay Design) was developed in a preliminary way. DEMOD models the measured surface deflections using an iterative procedure to adjust the stiffness moduli of each layer. The program then calculates the residual life of the existing pavement and the required overlay thickness. Once again the CHEVRON N-layer elastic program (39) was incorporated to perform the structural analysis and parts of the program PONOS (58) used as a sub-routine to determine the bituminous mix stiffnesses.

CHAPTER TWELVE

RECOMMENDATIONS FOR FUTURE WORK

Although this research has led to the develoment of practical design procedures for asphalt pavements based on analytical methods, there is scope for further improvements. With this in mind, a number of recommendations for future work are discussed below.

Additional studies on the propagation of cracks through existing pavements and test slabs could provide useful information relevant to the design of new pavements and, particularly, overlays.

Further research should be directed towards producing a fundamental method for predicting the development of a rut in a pavement. A cumulative damage approach could then be applied to the design of a pavement against permanent deformation as well as fatigue cracking.

The computer programs ANPAD and CUDAM are based on linear elastic layered systems. However, because the sub-base layers have non-linear characteristics, the input values used for the sub-base to subgrade stiffness modular ratios are derived from studies using the SENOL non-linear finite element program (44). A means of directly incorporating the results of these studies into ANPAD and CUDAM is desirable.

There is a need for validation using accelerated testing of pavements or slabs. A notable development in connection with this work will be the new TRRL test facility.

Risk analysis investigations should be carried out to assess the consequences of variations in mix proportions, layer thicknesses, support conditions, temperatures and loading conditions on the overall performance of the pavement.

One of the major problems now is to persuade the engineers responsible for designing the pavements to adopt analytical design methods. Confidence in these methods must be established and this will come only with use. Further full scale trials are therefore essential. Instrumentation of these experimental sections is also recommended to enable more detailed comparisons to be made between site measurements and theoretical computations of stresses, strains and deflections.

A logical extension of this research would be to continue the work described in Chapter 10 on the structural evaluation of pavements using measured surface deflections and the design of overlays. Some modifications to the computer program DEMOD may be required before it can accurately model surface deflections. These modifications should take into consideration the results of actual site measurements of the deflected surface shape of known pavements under a given loading.

REFERENCES

1. Road Research Laboratory, 'A guide to the structural design of pavements for new roads', Road Note 29, 3rd Edition, HMSO, London, 1970.
2. Leigh, J.V. and Croney, D., 'The current design procedure for flexible pavements in Britain', Proc. 3rd Int. Conf. on the Struct. Design of Asphalt Pavements', Vol.1, 1972, pp.1039-1048.
3. Ibid. Thompson, R., Croney, D., and Currer, E.W.H., 'The Alconbury Hill experiment and its relation to flexible pavement design', pp.920-937.
4. British Standards Institution, 'Specification for rolled asphalt (hot process) for roads and other paved areas', BS 594, 1973.
5. British Standards Institution, 'Specification for coated macadam for roads and other paved areas', BS 4987, 1973.
6. Chantereau, M. and Leger, P.H., 'The catalogue of structures on the direction des routes et de la circulation routiere francaise (French Highways Authority)', Proc. 3rd Int. Conf. on the Struct. Design of Asphalt Pavements, Vol.1, 1972, pp.990-1000.
7. Ibid. Vogt, H. and Von Becker, P., 'Design and dimensions of standardised bituminous pavements in the Federal Republic of Germany: data, requirements, performance, developments', pp.1102-1116.
8. The Asphalt Institute, 'Thickness design manual - Asphalt Pavements for Highways and Streets (MS-1)', 7th and 8th Editions, 1963 and 1969 respectively.

9. Van der Poel, C., 'A general system describing the visco-elastic properties of bitumens and its relation to routine test data', Journ. App. Chem., 4, 1954, pp.221-236.

10. Van der Poel, C., "Time and temperature effects on the deformation of bitumen and bitumen-mineral mixtures', Journ. Soc. Plastics Eng., 11, 1955, pp.47-64.

11. Heukelom, W. and Klomp, A.J.G., 'Road design and dynamic loading', Proc. Assn. Asphalt Paving Techn. Vol.33, 1964, pp.92-125.

12. Van Draat, W.E.F. and Sommer, P., 'An apparatus for determining the dynamic elastic modulus of asphalt', (in German), Strasse und Autobahn, 6, 1955, pp.206-211.

13. Bonnaure, F., Gest, G., Gravois, A. and Uge, P., 'A new method of predicting the stiffness of asphalt paving mixtures', Proc. Assn. Asphalt Paving Techn. Vol.46, 1977, pp.64-104.

14. Hicks, R.G. and Monismith, C.L., 'Prediction of the resilient response of pavements containing granular layers using non-linear elastic theory', Proc. 3rd Int. Conf. on the Struct. Design of Asphalt Pavements, Vol.1, 1972, pp.410-429.

15. Seed, H.B., Chan, C.K. and Lee, C.E., 'Resilience characteristics of subgrade soils and their relation to fatigue failures in asphalt pavements', Proc. Int. Conf. on the Struct. Design of Asphalt Pavements, 1962, pp.611-636.

16. Boyce, J.R., Brown, S.F. and Pell, P.S., 'The resilient behaviour of a granular material under repeated loading', Proc. Aust. Road Research Board, Vol.8, 1976, pp.8-19.

17. Pappin, J.W. and Brown, S.F., 'Resilient stress-strain behaviour of a crushed rock', Proc. Int. Symp. on Soils Under Cyclic and Transient Loading, Swansea, Vol.1, 1980, pp.169-177.

18. Shaw, P., 'Stress-strain relationships for granular materials under repeated loading', Ph.D. Thesis, University of Nottingham, 1980.

19. Snaith, M.S., 'Deformation characteristics of dense bitumen', macadam subjected to dynamic loading', Ph.D. Thesis, University of Nottingham, 1973.

20. Monismith, C.L. and Secor, K.E., 'Viscoelastic behaviour of asphalt concrete pavements', Proc. Int. Conf. on the Struct. Design of Asphalt Pavements, 1962, pp.476-521.

21. Pell, P.S. and Brown, S.F., ' The characteristics of materials for the design of flexible pavements', Proc. 3rd Int. Conf. on the Struct. Design of Asphalt Pavements, Vol.1, 1972, pp.326-342.

22. Hveem, F.N., 'Pavement deflections and fatigue failure', Highway Research Board Bulletin, No.114, 1955, pp.44-87.

23. Monismith, C.L., 'Pavement design: The fatigue subsystem', Highway Research Board, Special Report 140, 1973, pp.1-19.

24. Ibid. Freeme, C.R. and Morris, C.P., 'The bituminous surfaces: their fatigue behaviour', pp.158-178.

25. Pell, P.S., 'Fatigue characteristics of bitumen and bituminous mixes', Proc. Int. Conf. on the Struct. Design of Asphalt Pavements, 1962, pp.310-323.

26. Monismith, C.L., Secor, K.E. and Blackmer, E.W., 'Asphalt mixture behaviour in repeated flexure', Proc. Assn. of Asphalt Paving Techs. Vol.39, 1970, pp.207-236.

27. Highway Research Board, 'Structural design of asphalt concrete pavements to prevent fatigue cracking', Special Report, 140, 1973.

28. Peattie, K.R., 'A fundamental approach to the design of flexible pavements', Proc. of the Int. Conf. on the Struct. Design of Asphalt Pavements, 1962, pp.403-411.

29. Barksdale, R.D. and Miller, J.H., 'Development of equipment and techniques for evaluating fatigue and rutting characteristics of asphalt concrete mixes', Georgia Inst. of Tech. SCEGIT-77-149, 1977.

30. Dorman, G.M. and Metcalf, C.T., 'Design curves for flexible pavements based on a layered system theory'. Highway Research Record, No.71, 1965.

31. Monismith, C.L. and McLean, D.B., 'Design considerations for asphalt pavements', Institute of Transportation and Traffic Engineering, Univ. of California, Report TE 71-8, 1971.

32. Hicks, R.G. and Finn, F.N., 'Prediction of pavement performance from calculated stresses and strains at the San Diego Test Road', Proc. Assn. of Asphalt Paving Technologists, Vol.43, 1974, pp.1-40.

33. Witczak, M., 'Design of full-depth asphalt airfield pavements', Proc. 3rd Int. Conf. on the Struct. Design of Asphalt Pavements, Vol.1, 1972, pp.550-567.

34. Brown, S.F., Pell, P.S. and Stock, A.F., 'The application of simplified, fundamental design procedures for flexible pavements', Proc. 4th Int. Conf. on the Struct. Design of Asphalt Pavements, Vol.1, 1977, pp.327-341.

35. Transportation Research Board, 'Soil mechanics:Rutting in Asphalt Pavements, Embankments on Varved Clays and Foundations', Record 616, 1976.

36. Fourth International Conference on the Structural Design of Asphalt Pavements, Ann Arbor, Michigan, 1977.

37. Burmister, D.M., 'The theory of stresses and strains in layered systems and application to the design of airport runways', Proc. Highway Research Board, Vol.23, 1943.

38. Peutz, M.G.F., Van Kempen, H.P.M. and Jones, A., 'Layered systems under normal surface loads', Highway Research Record, 228, 1968.

39. Warren, H. and Dieckmann, W.L., 'Numerical computation of stresses and strains in a multi-layer asphalt pavement system', Unpub. int. rep., Chevron Research Corp., USA, 1963.

40. Brown, S.F. and Pell, P.S., 'An experimental investigation of the stresses, strains and deflections in a layered pavement structure subjected to dynamic loads', Proc. 2nd Int. Conf. on the Struct. Design of Asphalt Pavements, Vol.1, 1967, pp.671-688.

41. Ibid. Klomp, A.J.G. and Niesman, Th.W., 'Observed and calculated strains at various depths in asphalt pavements', pp.671-688.

42. Thrower, E.N., Lister, N.W. and Potter, J.F., 'Experimental and theoretical studies of pavement behaviour under vehicular loading in relation to elastic theory', Proc. 3rd Int. Conf. on the Struct. Design of Asphalt Pavements, Vol.1, 1972, pp.521-535.

43. Bleyenberg, W.G., Claessen, A.I.M., van Gorkum, F., Heukelom, W. and Pronk, A.C., 'Fully monitored motorway trials in the Netherlands corroborate linear elastic design theory', Proc. 4th Int. Conf. on the Struct. Design of Asphalt Pavements, Vol.1, 1977, pp.75-98.

44. Pappin, J.W., 'Characteristics of a granular material for pavement analysis', Ph.D. Thesis, Univ. of Nottingham, 1979.

45. Cooper, K.E., Brown, S.F. and Pell, P.S., 'Developments of improved procedures for asphalt pavement mix design', Report No.KEC/1, Univ. of Nottingham, February, 1980.

46. Brown, S.F., Cooper, K.E., Brunton, J.M., Brodrick, B.V. and Pell, P.S., 'Developments of improved procedures for asphalt pavement mix design', Report No.KEC/JMB/1, Univ. of Nottingham, February, 1981.

47. Brunton, J.M., Cooper, K.E., Brown, S.F., and Pell, P.S., 'Developments of improved procedures for asphalt pavement mix design', Report No.KEC/JMB/2, Univ. of Nottingham, February, 1982.

48. Brunton, J.M., Cooper, K.E., Brown, S.F., Brodrick, B.V. and Pell, P.S., 'Developments of improved procedures for asphalt pavement mix design', Report No.KEC/JMB/3, Univ. of Nottingham, February, 1983.

49. Brown, S.F., 'A simplified, fundamental design procedure for bituminous pavements', The Highway Engineer, Vol.XXI, Nos.8-9, 1974, pp.14-23.

50. Brown, S.F., 'An introduction to analytical design of bituminous pavements', Univ. of Nottingham, 1980.

51. Heukelom, W. and Klomp, A.J.G., 'Dynamic testing as a means of controlling pavements during and after construction', Proc. Int. Conf. on the Struct. Design of Asphalt Pavements, 1962, pp.667-679.

52. Hicks, R.G. and Monismith, C.L., 'Factors influencing the resilient response of granular materials', Highway Research Record 345, 1971, pp.15-31.

53. Ullidtz, P., 'A fundamental method for the prediction of roughness, rutting and cracking in asphalt pavements', Proc. Assn. of Asphalt Paving Techs. Vol.48, 1979, pp.557-586.

54. Brown, S.F., 'Stiffness and fatigue requirements for structural performance of asphaltic mixes', Eurobitume seminar, London, 1978, pp.141-145.

55. Black, W.P.M. and Lister, N.W., 'The strength of clay fill subgtrades: its prediction in relation to road performance', TRRL Report LR 889, 1979.

56. Cooper, K.E. and Pell, P.S., 'The effect of mix variables on the fatigue strength of bituminous materials', TRRL Report LR 633, 1974.

57. Stock, A.F., 'Flexible pavement design, Ph.D. Thesis, Univ. of Nottingham, 1979.

58. de Bats, F.Th., 'The computer programs PONOS and POEL: A computer simulation of Van der Poel's Nomograph', External report, Koninkijke/Shell Laboratorium, Amsterdam, 1972.

59. Boyce, J.R., 'The behaviour of a granular material under repeated loading', Ph.D. Thesis, Univ. of Nottingham, 1976.

60. Brown, S.F., Stock, A.F. and Pell, P.S., 'The structural design of asphalt pavements by computer', The Highway Engineer, Vol.27, No.3, 1980, pp.2-10.

61. Brown, S.F. and Pappin, J.W., 'Analysis of pavements with granular bases', Transportation Research Record 810, 1981, pp.17-22.

62. Brown, S.F., Brodrick, B.V. and Pappin, J.W., 'Permanent deformation of flexible pavements', Final Technical Report to US Army, June, 1980.

63. Croney, D., 'The design and performance of road pavements', HMSO, 1977.

64. Peattie, K.R., Private communication.

65. Brown, S.F., 'Determination of Young's Modulus for bituminous materials in pavement design', Highway Research Record No.431, 1973, pp.38-49.

66. Raithby, K.D. and Sterling, A.B., 'The effect of rest periods on the fatigue performance of a hot-rolled asphalt under reversed axial loading', Proc. Assn. Asphalt Paving Techs., Vol.39, 1970, pp.134-147.

67. Raithby, K.D. and Sterling, A.B., 'Some effects of loading history on the fatigue performance of rolled asphalt', TRRL Report, LR 496, 1972.

68. McElvaney, J. and Pell, P.S., 'Fatigue damage of asphalt: effect of rest periods', Highways and Road Construction, Vol.41, No.1766, October, 1973, pp.16-20.

69. Van Dijk, W., Moreaud, H., Quedeville, A. and Uge, P., 'The fatigue of bitumen and bituminous mixes', Proc. 3rd Int. Conf. on the Struct. Design of Asphalt Pavements, London, 1972, pp.354-366.

70. Van Dijk, W., 'Practical fatigue characteristics of bituminous mixes', Proc. Assn. Asphalt Paving Techn., Vol.44, 1975, pp.38-72.

71. Ramsamooj, D.V., Majidzadeh, K. and Kauffmann, E.M., 'The analysis and design of the flexibility of pavements', Proc. 3rd Int. Conf. on the Struct. Design of Asphalt Pavements, London, 1972, pp.692-704.

72. Claessen, A.I.M., Edwards, J.M., Sommer, P. and Uge, P., 'Asphalt pavement design - the Shell method', Proc. 4th Int. Cont. on the Struct. Design of Asphalt Pavements, Vol.1, Ann Arbor, Michigan, 1977, pp.39-74.

73. De Jong, D.L., Peutz, M.G.F. and Korswagen, A.R., 'Computer program BISAR, Layered systems under normal and tangential surface loads', Koninklijke/Shell Laboratorium, Amsterdam, External Report, AMSR.0006.73, 1973.

74. Witczak, M.W., 'Computer program DAMA, user's manual', Univ. of Maryland, September, 1978.

75. The Asphalt Institute, 'Thickness design - asphalt pavement for highways and streets', Manual Series No.1 (MS-1), 9th Edition, September, 1981.

76. Santucci, L.E., 'Thickness design procedure for asphalt concrete and emulsified asphalt mixes', Presented to Committee A2B02, Transportation Research Board, Washington, January, 1975.

77. Kallas, B.F. and Shook, J., 'San Diego County experimental base project', Final Report, Asphalt Institute Research Report 77-1, November, 1977.

78. Verstraeten, J., Ververka, V. and Francken, L., 'Rational and practical designs of asphalt pavements to avoid cracking and rutting', Proc. 5th Int. Conf. on the Struct. Design of Asphalt Pavements, Vol.1, 1982, pp.45-58.

79. Francken, L., 'Fatigue performance of a bituminous road mix under realistic test conditions', Transportation Researach Record 712, 1979, pp.30-36.

80. Kasianchuk, D.A., 'Fatigue considerations in the design of asphalt concrete pavements', Ph.D. dissertation, Univ. of California, 1968.

81. Thrower, E.N., 'A parametric study of a fatigue prediction model for bituminous road pavements', TRRL Laboratory Report, LR 892, 1979.

82. Kingham, R.I., 'Failure criteria developed from AASHO road test data', Proc. 3rd Int. Conf. on the Struct. Design of Asphalt Pavements, Vol.1, London, 1972, pp.656-669.

83. Monismith, et al., 'Asphalt mixture behaviour in repeated flexure', Report No. TE 70-5, Univ. of California, December, 1970.

84. Brown, S.F. and Bell, C.A., 'The prediction of permanent deformation in asphalt pavements', Proc. Assn. Asphalt Paving Techs. Vol.48, 1979.

85. Monismith, C.L. and Deacon, J.A., 'Fatigue of asphalt paving mixtures', Journ. Transp. Eng. Div., ASCE, TE2, 1969, pp.317-346.

86. McElvaney, J. and Pell, P.S., 'Fatigue damage of asphalt under compound-loading', Journ. Transp. Eng. Div., ASCE, Vol.100, TE3, 1974, pp.101-178.

87. Santucci, L.E., 'Thickness design procedure for asphalt and emulsified asphalt mixes', Proc. 4th Int. Conf. on the Struct. Design of Asphalt Pavements, Vol.1, Ann Arbor, Michigan, 1977.

88. Shane, B.A., 'The relationship between goods movement and road damage', TRRL Supplementary Report, SR 720, 1982.

89. Brown, S.F. and Cooper, K.E., 'A fundamental study of the stress-strain characteristics of a bituminous material', Proc. of the Assn. Asphalt Paving Techs. February, 1980, pp.476-498.

90. Lister, N.W., 'The transient and long term performance of pavements in relation to temperature', Proc. of the 3rd Int. Conf. on the Struct. Design of Asphalt Pavements, 1972, pp.94-100.

91. Currer, E.W.H. and O'Connor, M.G.D., 'Commercial traffic: its estimated damaging effect, 1945-2005', TRRL Report, LR 910, 1979.

92. Department of Transport, 'Road pavement design', Tech. Memo H6/78.

93. Goddard, R.T.N., 'Fatigue resistance of a bituminous load pavement design for very heavy traffic', TRRL Report LR 1050, 1982.

94. Shell International Petroleum Co. Ltd., 'Shell pavement design manual - asphalt pavements and overlays for road traffic', London, 1978.

95. Goddard, R.T.N., Powell, W.D. and Applegate, M.W., 'Fatigue resistance of dense bitumen macadam: the effect of mixture variables and temperature', TRRL Supplementary Report, SR 410, 1978.

96. Forsgate, J., 'Temperature frequency distributions in flexible road pavements', TRRL Report, LR 438, 1972.

97. Leech, D., 'A dense coated roadbase macadam of improved performance', TRRL Report LR 1060, 1982.

98. Shook, J.F., Finn, F.N., Witczak, M.W. and Monismith, C.L., 'Thickness design of asphalt pavements - The Asphalt Institute Method', Proc. 5th Int. Conf., 1982, pp.17-44.

99. The Asphalt Institute, 'Research and Development of the Asphalt Institute's Thickness Design Manual (MS-1), 9th Edition.

100. Kennedy, C.K., Fevre, P. and Clarke, C., 'Pavement deflection: equipment for measurement in the United Kingdom', TRRL Report LR 834, 1978.

101. Brown, S.F., 'Implementation of analytical pavement design: a case study', The Highway Engineer, Vol.27, No.7, 1980.

102. Brien, D., 'Research in the design of asphalt', The Highway Engineer, Vol.24, No.10, 1977, pp.14-21.

103. Kennedy, C.K., 'Pavement deflection: operating procedures for use in the United Kingdom', TRRL Report, LR 835, 1978.

104. Highway Research Board, 'The WASHO Road Test', Special Report 18, 1954.

105. Highway Research Board, 'The WASHO Road Test', Special Report 22, 1955.

106. Hoffman, M.S. and Thompson, M.R., 'Mechanistic interpretation of non destructive pavement testing deflections', Report No.UILU-ENG-81-2010, Univ. of Illinois, June, 1981.

107. Kennedy, C.K. and Lister, N.W., 'Prediction of pavement performance and the design of overlays', TRRL Report LR 833, 1978.

108. Bandyopadhyay, S.S., 'Flexible pavement evaluation and overlay design', Proc. of the ASCE, Vol.108, No.TE6, November, 1982.

109. Ullidtz, P., 'Overlay and stage by stage design', Proc. 4th Int. Conf. Struct. Design of Asphalt Pavements, Vol.1, 1977, pp.722-735.

110. Claessen, A.I.M. and Ditmarsch, R., 'Pavement evaulation and overlay design', Proc. 4th Int. Conf. Struct. Design of Asphalt Pavements, Vol.1, 1977, pp.649-662.

111. Bohn, A., Ullidtz, P., Stubstad, R. and Sorenson, A., 'Danish experiments with the French Falling Weight Deflectometer', Proc. 3rd Int. Conf. on Struct. Design of Asphalt Pavements, 1972, pp.1119-1128.

112. Hoffman, M.S. and Thompson, M.R., 'Field testing program summary', Report No.UILU-ENG-2003, Univ. of Illinois, 1981.

113. Hoffman, M.S. and Thompson, M.R., 'Comparative study of selected non destructive testing devices', Transport Research Record 852, 1982, pp.32-41.

114. Kilareski, W.P. and Anani, B.A., 'Evaluation of in situ moduli and pavement life from deflection basins', Proc, 5th Int. Conf. on Struct. Design of Asphalt Pavements, 1982, pp.349-366.

115. McCullough, B.F. and Taute, A., 'Use of deflection measurements for determining pavement material properties', Transport Research Record, 852, 1982, pp.8-15.

116. Van der Loo, J.M.M., 'Simplified method for evaluation of asphalt pavements', Proc. 5th Int. Conf. on Struct. Design of Asphalt Pavements, Vol.1, 1982, pp.475-481.

117. Norman, P.J., Snowdon, R.A. and Jacobs, J.C., 'Pavement deflection measurements and their application to structural maintenance and overlay design', TRRL Report LR 571, 1973.

118. Lister, N.W., Kennedy, C.K. and Ferne, B.W., 'The TRRL method for planning and design of structural maintenance', Proc. 5th Int. Conf. on Struct. Design of Asphalt Pavements, 1982, pp.709-725.

119. Lister., N.W., 'Deflection criteria for flexible pavements', TRRL Report, LR 375, 1972.

120. Lister., N.W., and Kennedy., C.K., 'A system for the prediction of pavement life and design of pavement strengthening.' Proc 4th Int. Conf. on Structural Design of Asphalt Pavements, 1977, pp 629-650.

121. Thrower, E.N. and Castledine, L.W.E., 'The design of new road pavements and of overlays: estimation of commercial traffic flows', TRRL Report, LR 844, 1978.

122. Southgate, H.F., Sharpe, G.W., Deen, R.C. and Haven, J.H., 'Structural capacity of in-place asphaltic concrete pavements from dynamic deflections', Proc. 5th Int. Conf. on Struct. Design of Asphalt Pavements, pp.422-429, 1982.

APPENDIX A

PAVEMENT DESIGN MANUAL

Written as a separate document for
independent use.

PAVEMENT DESIGN MANUAL

Developed by the Pavement Research Group,
the University of Nottingham,
for Mobil Oil Ltd., 1982,
using the computer program ANPAD.

CONTENTS

CHARTS

1S, 1N	DBM base, full depth asphalt type A
2S, 2N	HRA base, full depth asphalt type A
3S, 3N	Design Mix base, full depth asphalt type A
4S, 4N	DBM base, full depth asphalt type B
5S, 5N	HRA base, full depth asphalt type B
6S, 6N	Design Mix base, full depth asphalt type B
7S, 7N	DBM base, granular sub-base
8S, 8N	HRA base, granular sub-base
9S, 9N	Design Mix base, granular sub-base

Note the suffices S and N represent the Southern and Northern temperature zones respectively.

1. INTRODUCTION

The aim of this manual is to provide a guide for determining pavement thicknesses or lives based on the use of analytical methods. The structures considered are a full depth asphalt or include a 200mm granular sub-base. The design charts 1S to 9N were prepared from numerous designs carried out using the computer program ANPAD, developed at the University of Nottingham. The manual provides a means of interpolating between design speeds, subgrade CBR values and temperatures. Comparisons can also be made between the three pavement structures and/or the type of base material.

2. MATERIAL PROPERTIES AND STRUCTURES

There are three types of structure, as illustrated in Fig.1 and defined as follows:

Full depth asphalt type A: consisting of 40mm HRA wearing course together with a single, uniformly compacted DBM, HRA or design mix base layer and subgrade.

Full depth asphalt type B: consisting of 40mm HRA wearing course together with a DBM, HRA or design mix base layer and subgrade. The first lift of the base layer is assumed to have a higher void content than the rest, due to possible difficulties in laying the material directly onto the subgrade. The base thickness used in the charts is the total base thickness. The thickness of the first lift may be determined as follows:

$$\text{Thickness of Ist lift base, } h_{2,1} = \frac{1}{3} \text{ Total base thickness}$$

$$\text{Minimum value, } h_{2,1} = 50\text{mm}$$

$$\text{Maximum value, } h_{2,1} = 100\text{mm}$$

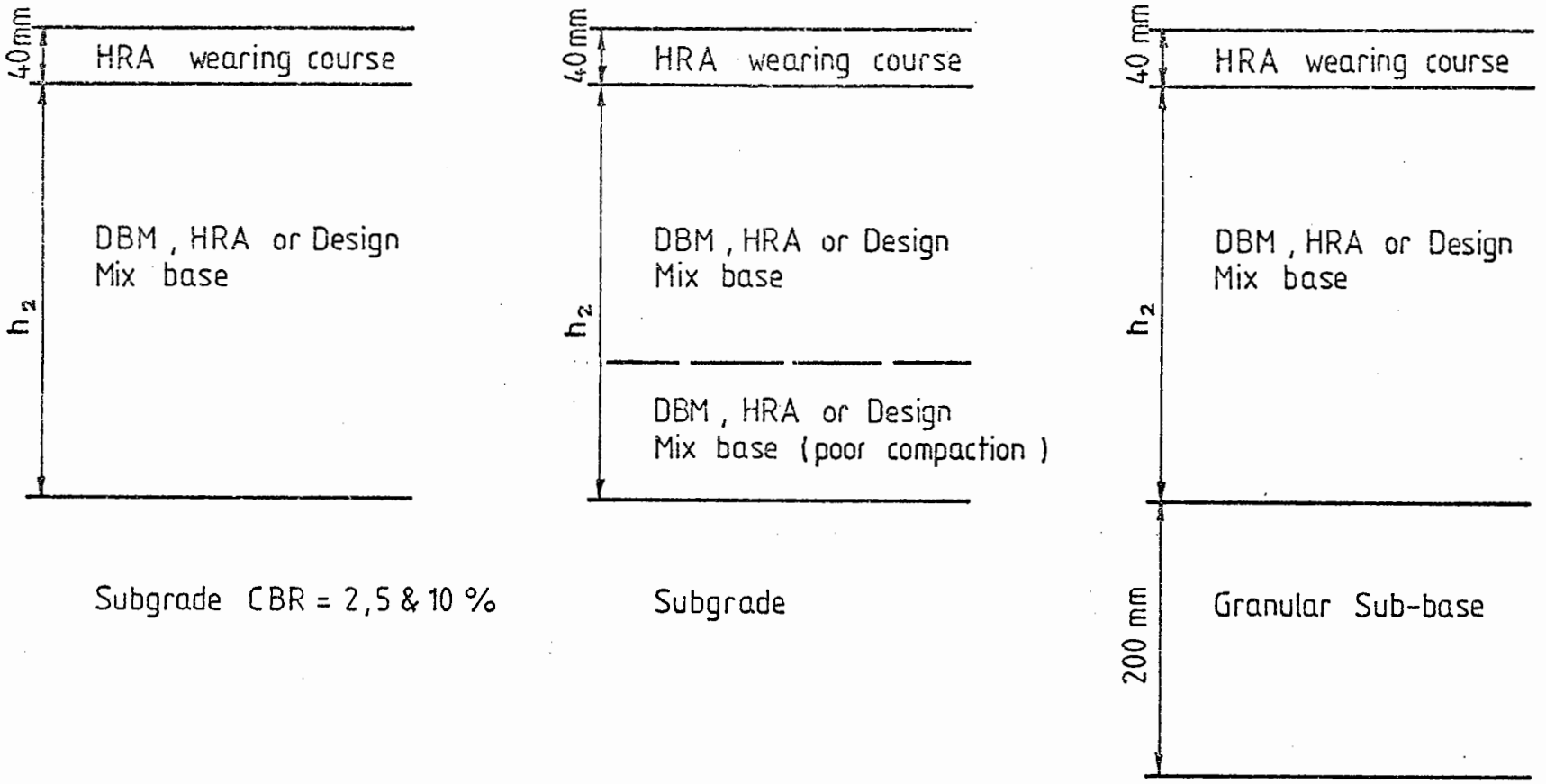

Full depth asphalt Type A

Full depth asphalt Type B

Granular Sub-base

FIGURE 1 TYPICAL DESIGN STRUCTURES

For example, for a total base thickness, h_2 = 240mm,

thickness of 1st lift base $h_{2,1}$ = 80mm

and for a total base thickness, h_2 = 120mm,

thickness of 1st lift base $h_{2,1}$ = 50mm

Granular sub-base: consisting of 40mm HRA wearing course, a single uniformly compacted DBM, HRA or design mix base layer, 200mm granular sub-base and subgrade.

The bituminous mix details are given in Table 1. The DBM and HRA bases are typical mixes as specified by British standards 594 (1) and 4987 (2). The void contents assumed are considered to be realistic practical values. The design mix is either of two novel materials developed at the University of Nottingham. The first is a modified HRA in which the binder content is reduced and the filler content increased. The second is a modified DBM using 50 pen bitumen and having an improved grading to give a denser mix.

3. DESIGN CONDITIONS

Speed: the design speed should be the average speed of commercial vehicles in km/hr. Although two speeds 30 and 80 km/hr are used, interpolation for other speeds within the range 10 to 100 km/hr may be effected.

CBR: the charts have been prepared for three average CBR values of 2, 5 and 10%. Interpolations may be made within this range.

Temperature: the design temperature used should be the average annual air temperature in °C. This can usually be obtained from local meteorological office records. However, if this is impossible Fig.2 (3) can be used to determine the temperature zone for the pavement. The design charts have been prepared for the two extreme temperature zones, North and South. The average annual air temperatures for each

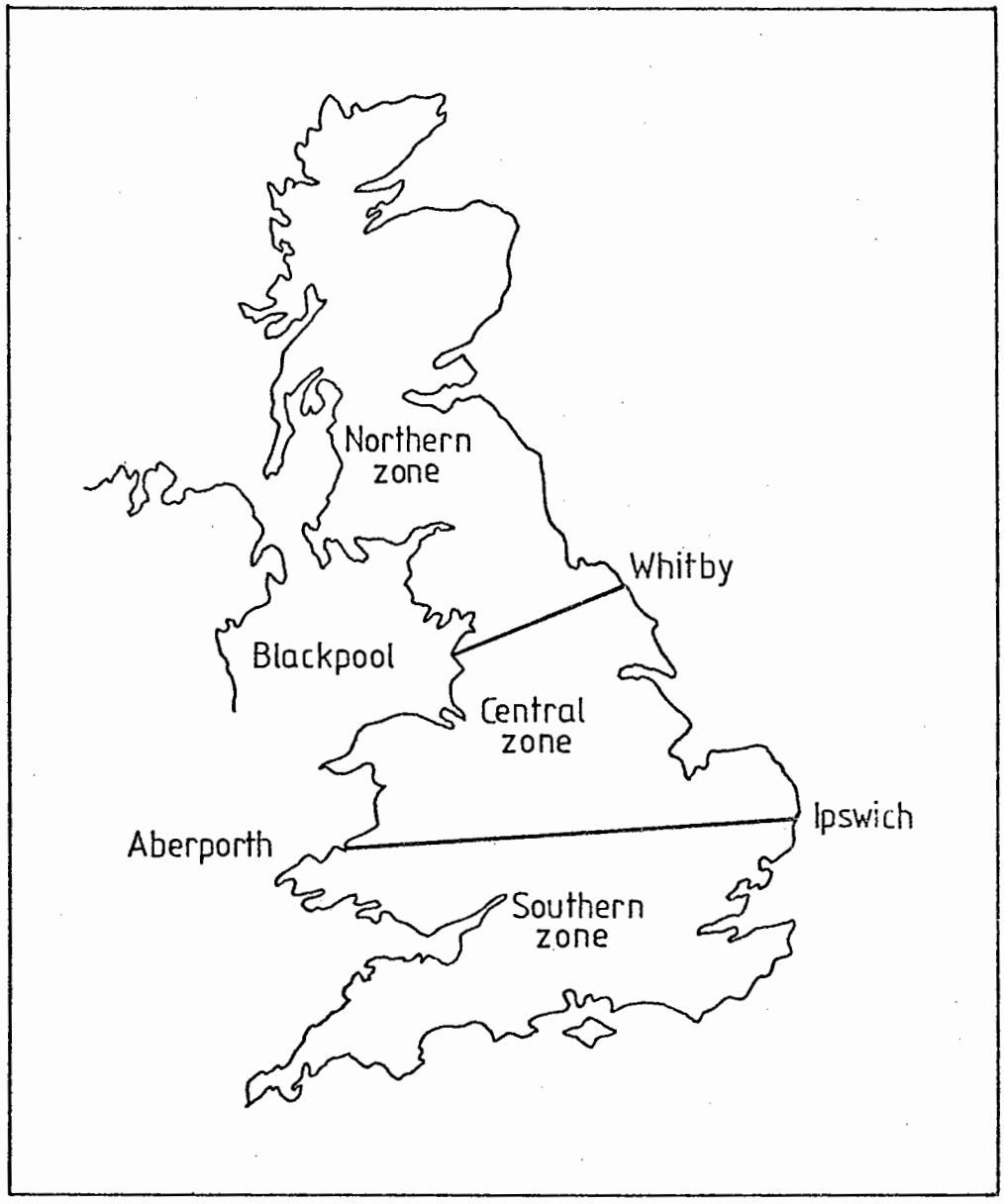

FIGURE 2 SUBDIVISION OF UNITED KINGDOM INTO TEMPERATURE ZONES (AFTER CRONEY (3))

zone are as follows:

Southern temperature zone	10.1°C
Central temperature zone	9.5°C
Northern temperature zone	8.4°C

4. INTERPOLATION OF RESULTS

The following equations are recommended for interpolation between values used in the charts:

Equations for Calculation of Design Life

For Speed:

$$N_v = N_{30} + \frac{(V-30)}{50}(N_{80}-N_{30}) \quad \text{----------(1)}$$

where N_v, N_{30}, N_{80} are the lives in msa at speeds of V, 30 and 80 km/hr.

For CBR:

For CBRs in the range 2<CBR<5%

$$N_{CBR} = N_2 + \left[\frac{CBR-2}{3}\right](N_5-N_2) \quad \text{----------(2)}$$

For CBRs in the range 5<CBR<10%

$$N_{CBR} = N_5 + \left[\frac{CBR-5}{5}\right](N_{10}-N_5) \quad \text{----------(3)}$$

where N_{CBR}, N_2, N_5 and N_{10} are the lives in msa at CBRs of CBR, 2,5 and 10%

For temperature

$$N_T = N_S + \frac{(10.1-T)}{1.7}(N_N-N_S) \quad \text{----------(4)}$$

where N_T, N_N, N_S are the lives at temperatures T, 8.4°C (Northern temperature zone), 10.1°C (Southern temperature zone).

Equations for Calculation of Base Thickness

For Speed

$$h_v = h_{80} + \frac{80-V}{50} (h_{30}-h_{80}) \quad \text{----------(5)}$$

where h_v, h_{30} and h_{80} are the base thicknesses in mm at speeds of V, 30 and 80 km/hr.

For CBR

For CBRs in the range $2<CBR<5\%$

$$h_{CBR} = h_5 + \frac{5-CBR}{3} (h_2-h_5) \quad \text{----------(6)}$$

For CBRs in the range $5<CBR<10\%$

$$h_{CBR} = h_{10} + \frac{10-CBR}{5} (h_5-h_{10}) \quad \text{----------(7)}$$

where h_{CBR}, h_2, h_5 and h_{10} are the base thicknesses in mm at CBRs of CBR 2, 5, 10%.

For temperature

$$h_T = h_N + \frac{(T-8.4)}{1.7} (h_S-h_N) \quad \text{----------(8)}$$

where h_T, h_N, h_S are the base thicknesses in mm at temperatures T°, 8.4°C (Northern temperature zone) and 10.1°C (Southern temperature zone).

5. WORKED EXAMPLES

Using a Design mix base, full depth asphalt structure type A (i.e. charts 3S and 3N) calculate:

a) the design thickness for 50msa
b) the design life for 200mm base thickness.

Use a speed of 50 km/hr, CBR 3% and air temperature 9.5°C.

(a)

Temperature (°C)	CBR (%)	Speed (km/hr)	Thickness (mm) From charts 3S and 3N	Corrected to 50 km/hr (eqn 5)	Corrected to CBR 3% (eqn 6)	Corrected to 9.5°C (eqn 8)
10.1	2	30	330	} 310		
		80	290		} 290	
	5	30	270	} 260		
		80	240			} 280
8.4	2	30	290	} 280		
		80	270		} 260	
	5	30	240	} 230		
		80	220			

Design thickness = 280mm

(b)

Temperature (°C)	CBR (%)	Speed (km/hr	Life (msa) From charts 3S and 3N	Corrected to 50 km/hr (eqn 1)	Corrected to CBR 3% (eqn 2)	Corrected to 9.5°C (eqn 4)
10.1	2	30	5.6			
		80	7.0	} 6.2		
	5	30	12.0		} 9.5	
		80	22.0	}16.0		
8.4	2	30	7.5			} 11.3
		80	12.5	} 9.5		
	5	30	20.0		} 14.6	
		80	32.0	}24.8		

Design life = 11.3mm

Table 1 MIX DETAILS OF BITUMINOUS MATERIALS

	HRA wearing course	DBM base	HRA base	Design Mix base
Initial Penetration	50	100	50	50
Binder Content (%)	7.9	4.7	5.7	4.5
Void Content (%)	4.0	9.0 or 11.0*	6.0 or 8.0*	8.0 or 10.0*
Specific Gravity of Aggregate	2.7	2.7	2.7	2.7
Specific Gravity of Bitumen	1.02	1.02	1.02	1.02

* The higher void contents are used for the poorly compacted lower base layers, full depth asphalt type B structure.

REFERENCES

1. British Standards Institution 'Specification for rolled asphalt (hot process) for roads and other paved areas', BS 594, 1973.

2. British Standards Institution 'Specification for coated macadam for roads and other paved areas', BS 4987, 1973.

3. Croney, D., 'The design and performance of road pavements', HMSO, 1977.

SOUTHERN TEMPERATURE ZONE

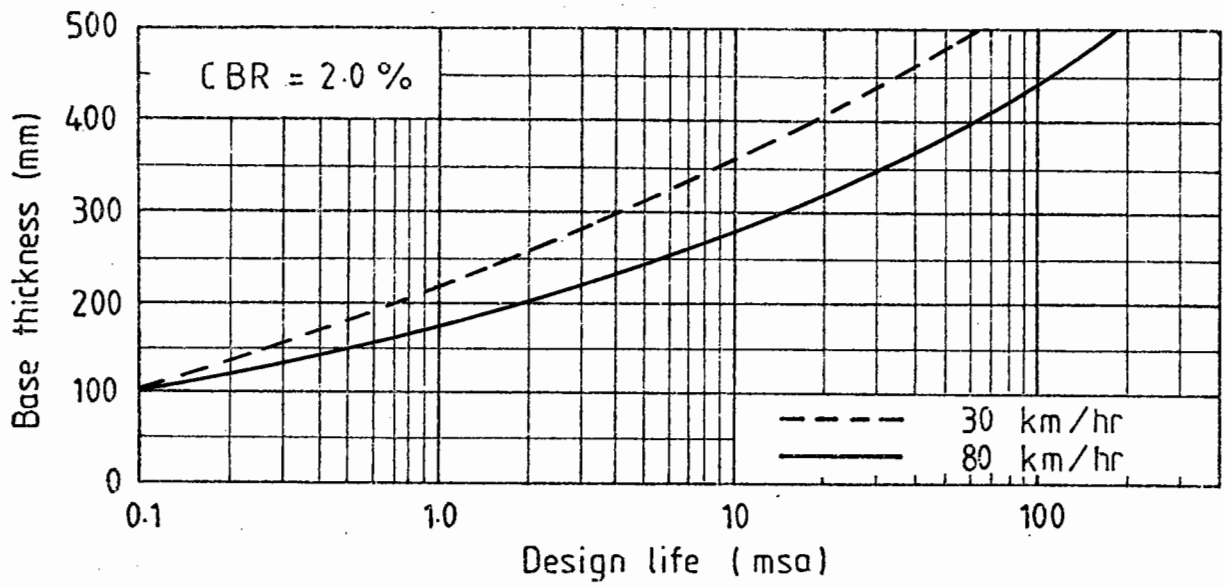

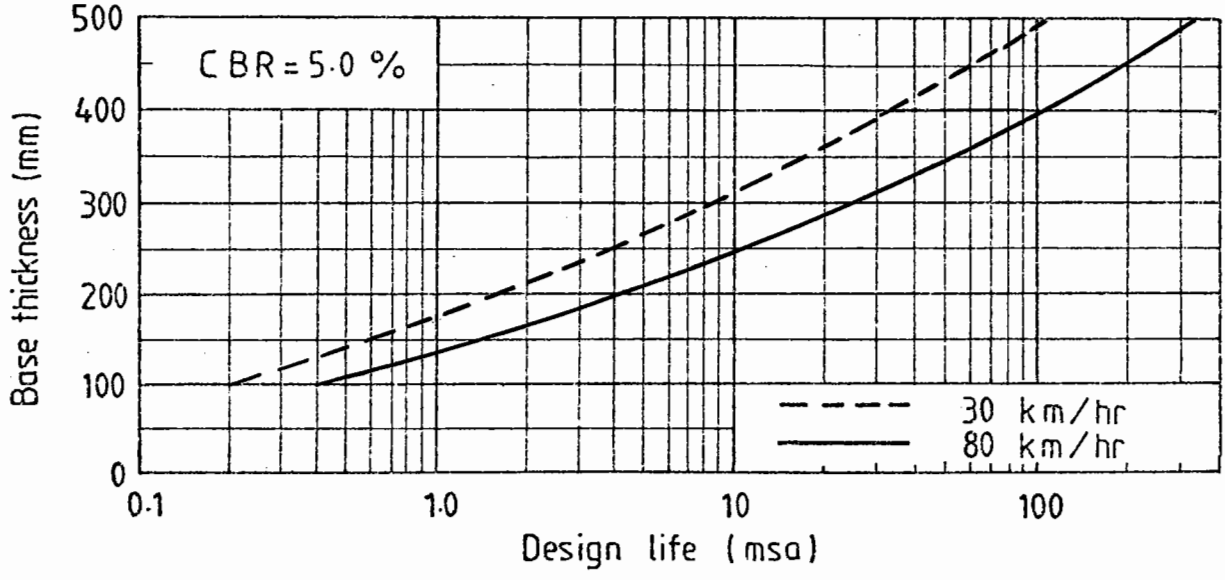

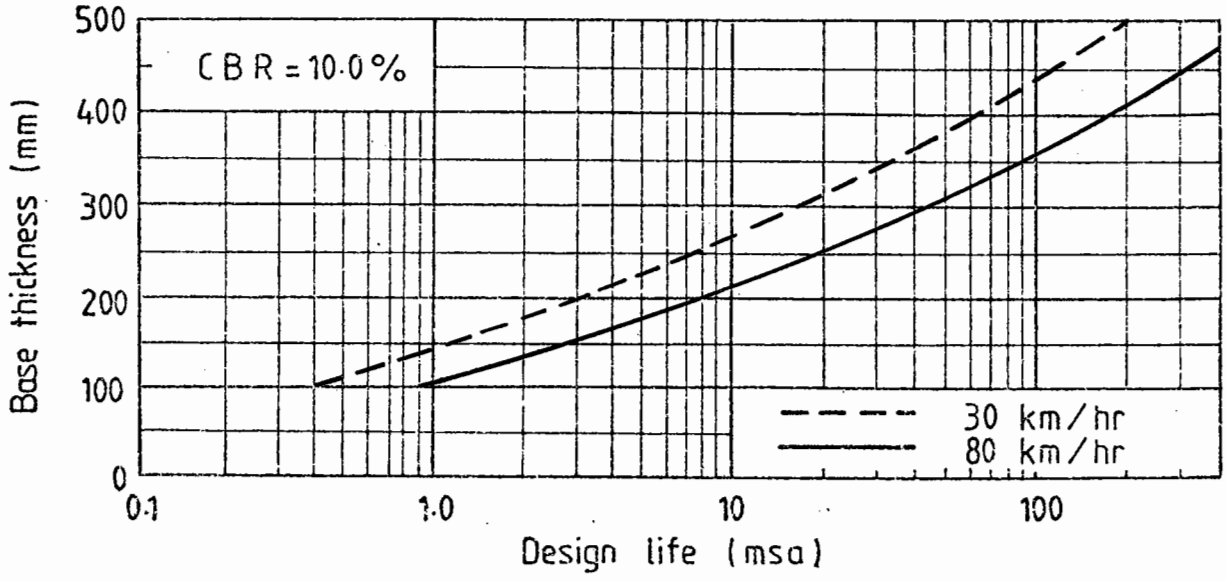

CHART 1S DBM BASE , FULL DEPTH ASPHALT TYPE A

NORTHERN TEMPERATURE ZONE

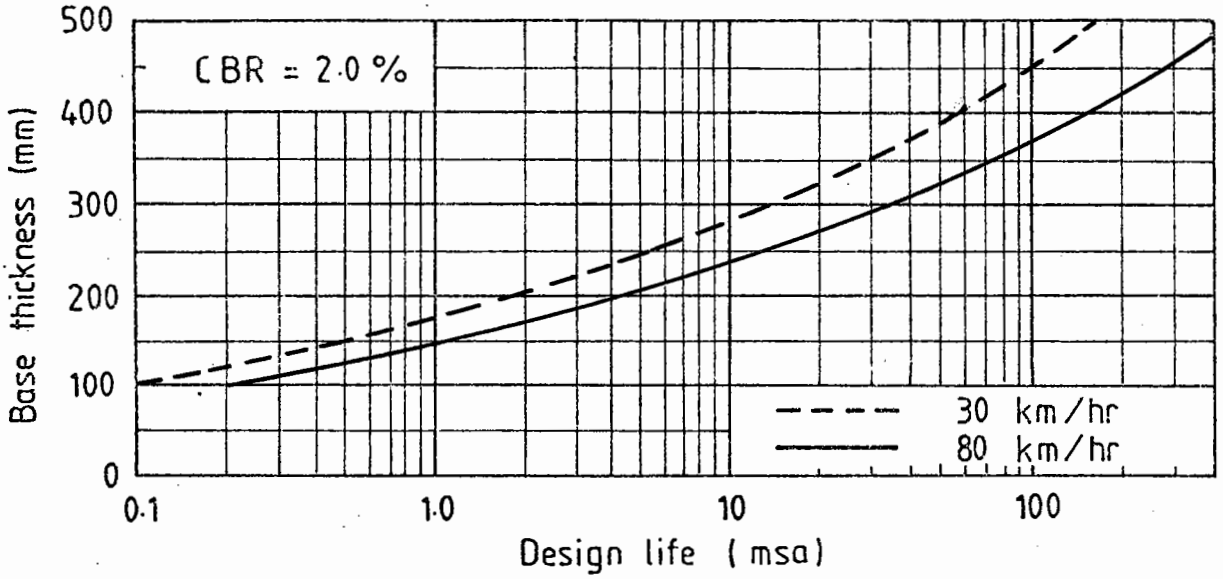

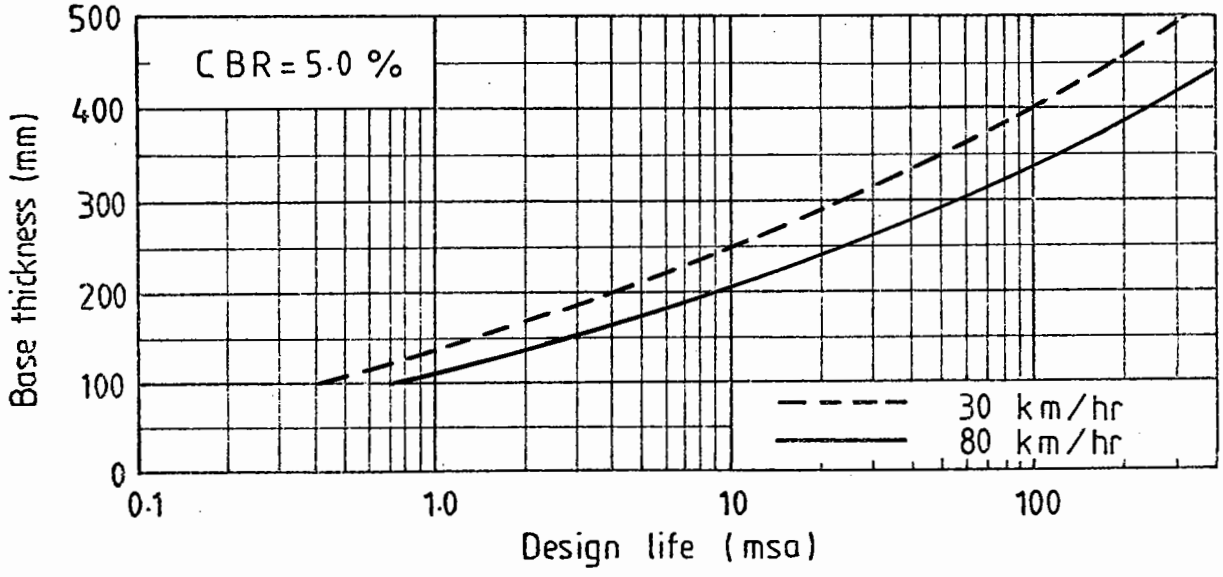

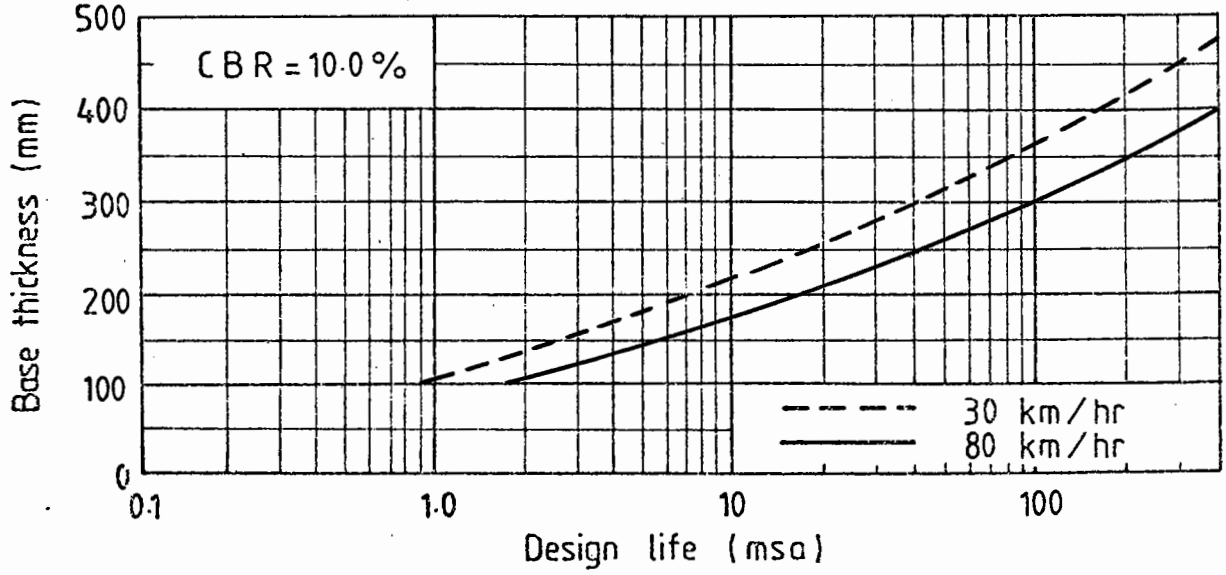

CHART 1N DBM BASE , FULL DEPTH ASPHALT TYPE A

SOUTHERN TEMPERATURE ZONE

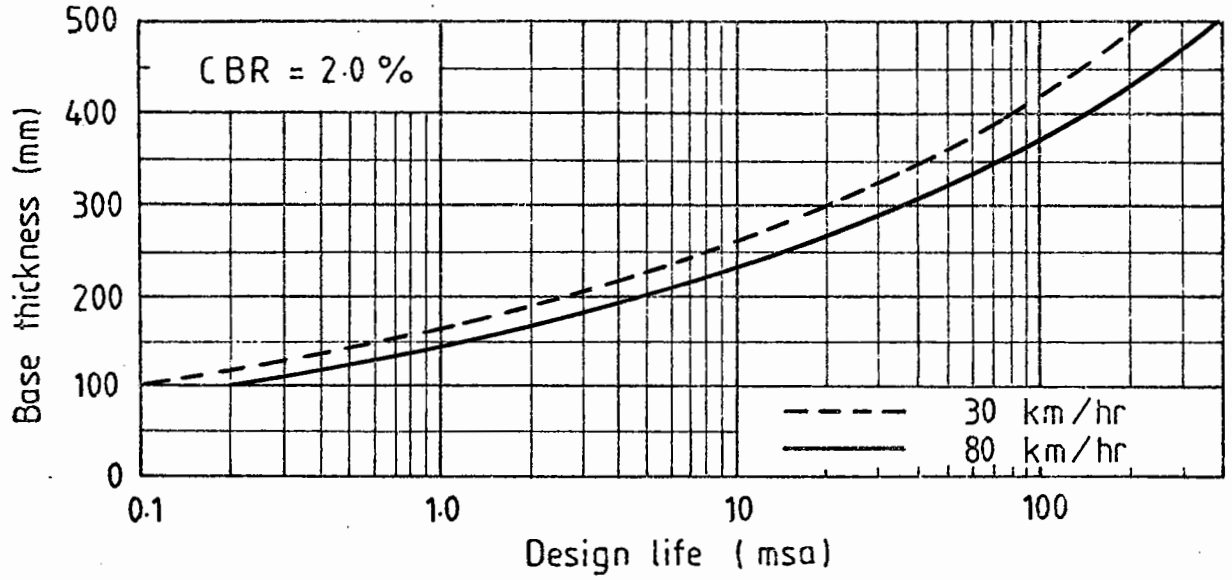

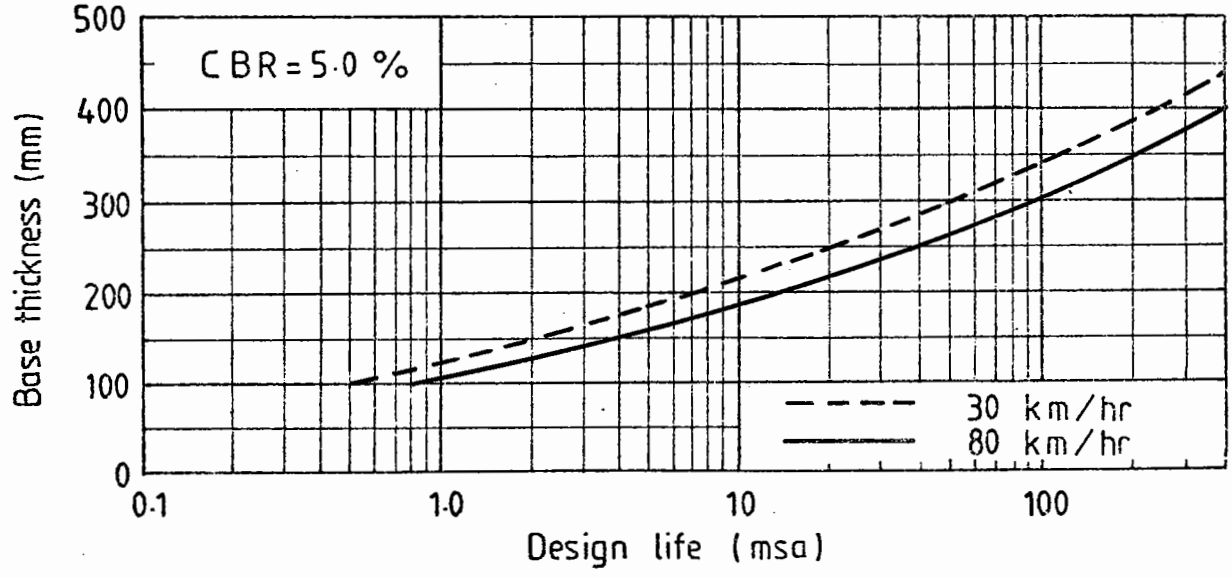

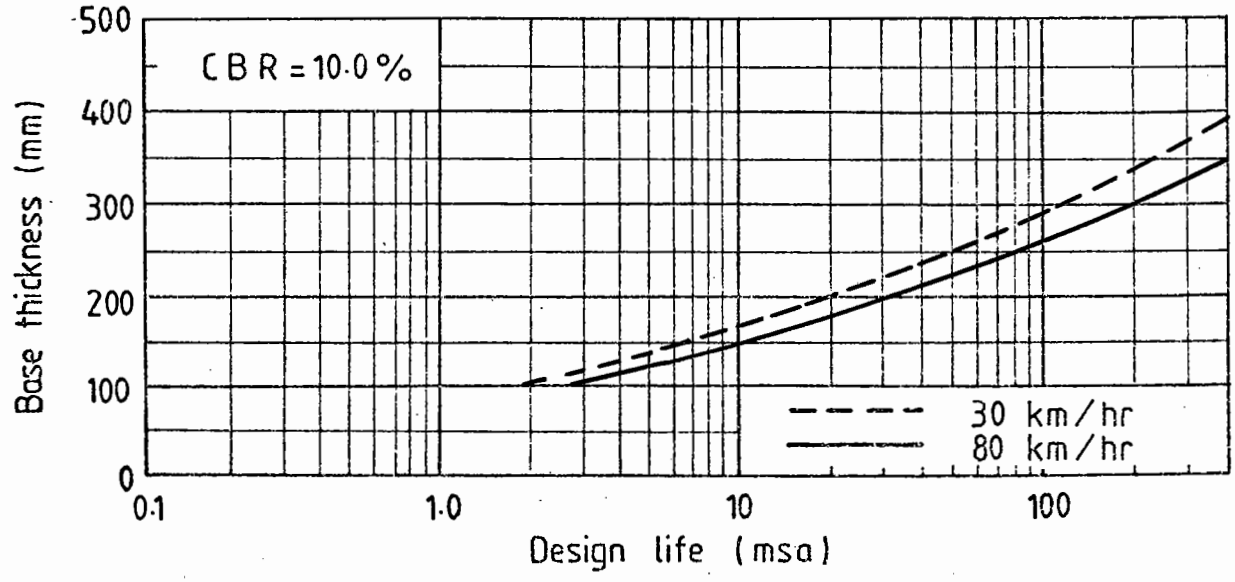

CHART 2S HRA BASE , FULL DEPTH ASPHALT TYPE A

NORTHERN TEMPERATURE ZONE

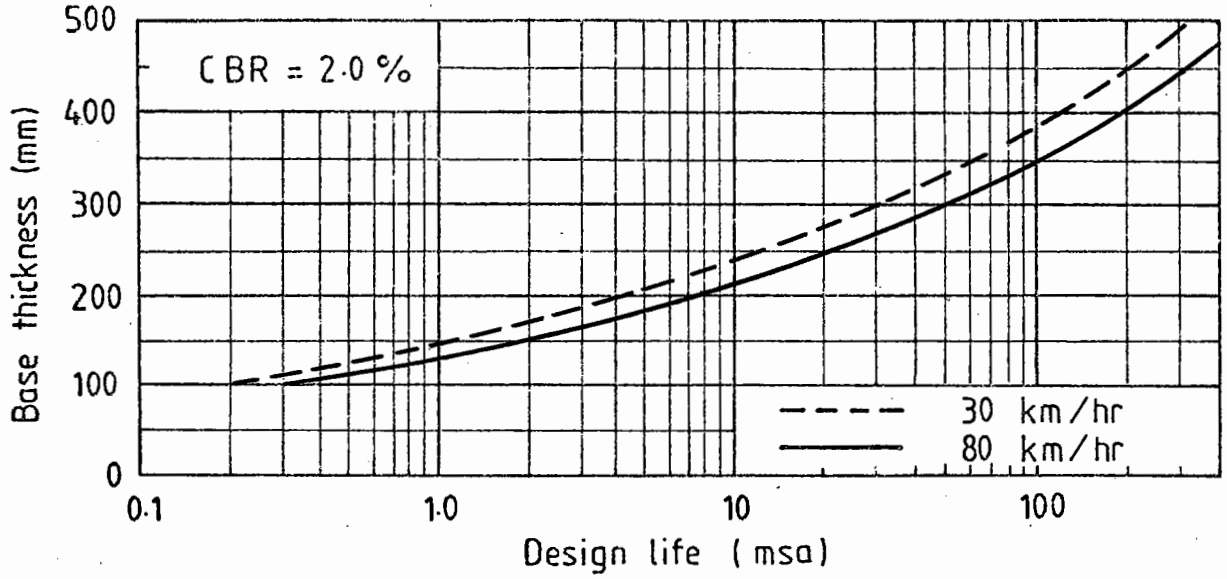

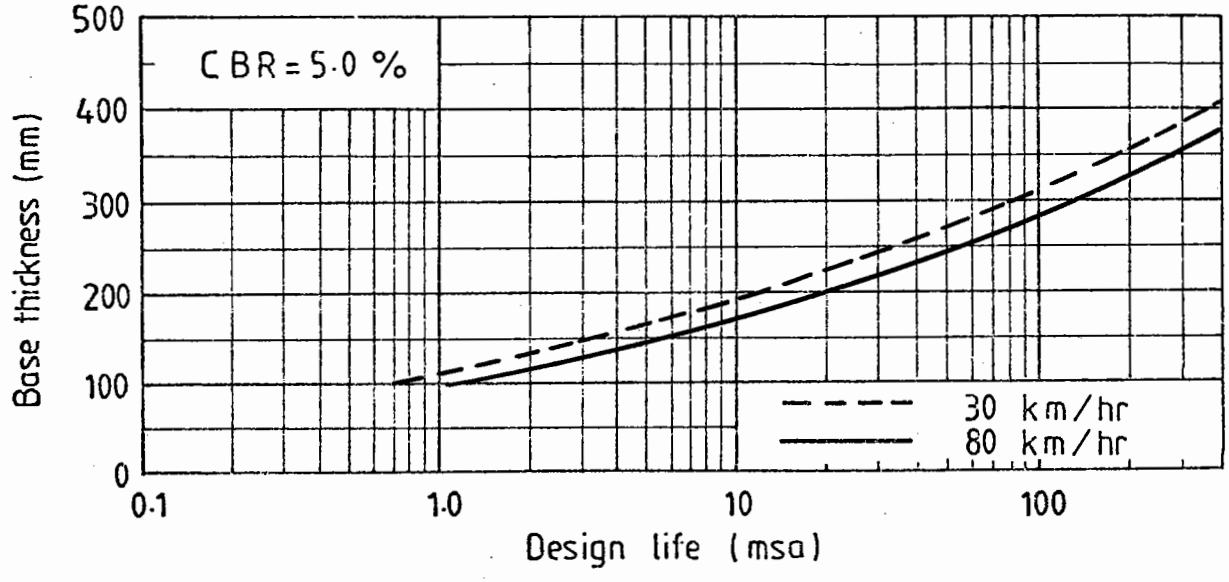

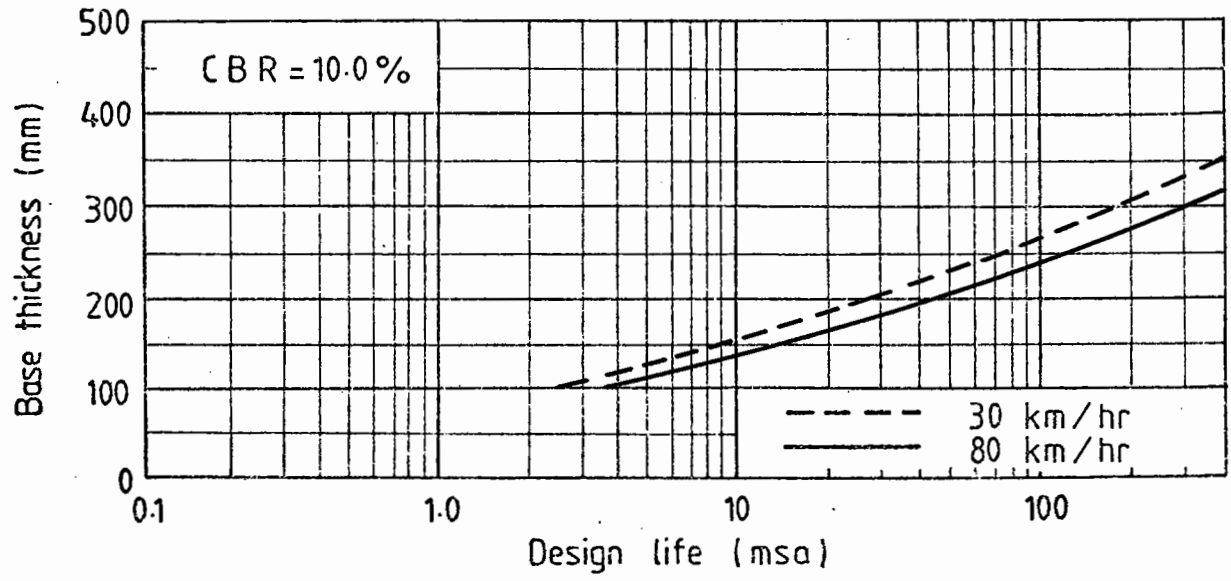

CHART 2N HRA BASE , FULL DEPTH ASPHALT TYPE A

SOUTHERN TEMPERATURE ZONE

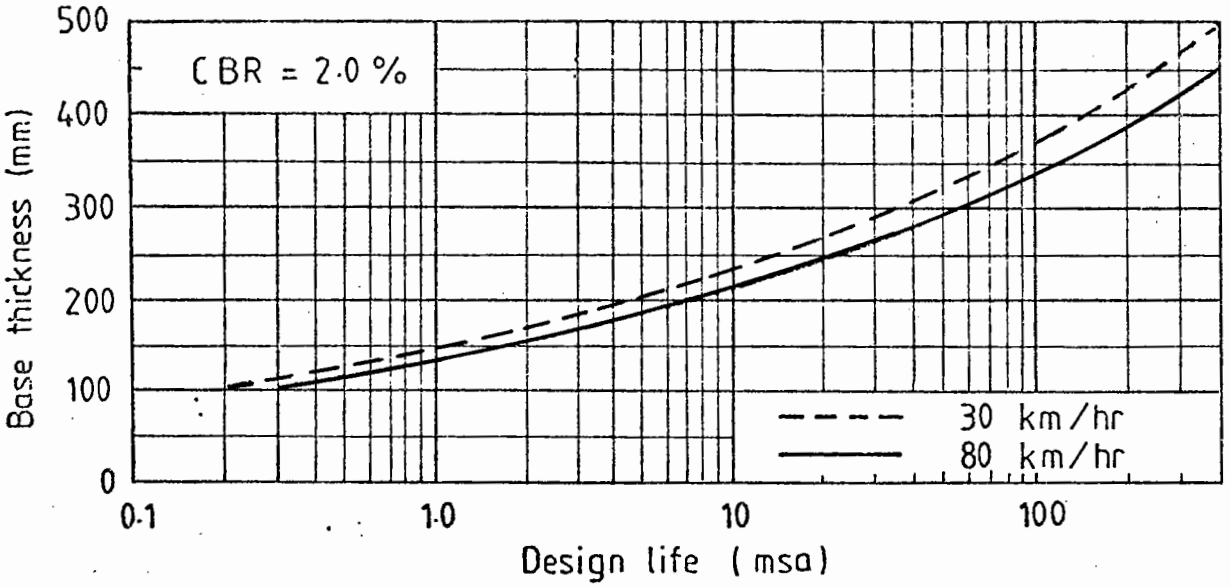

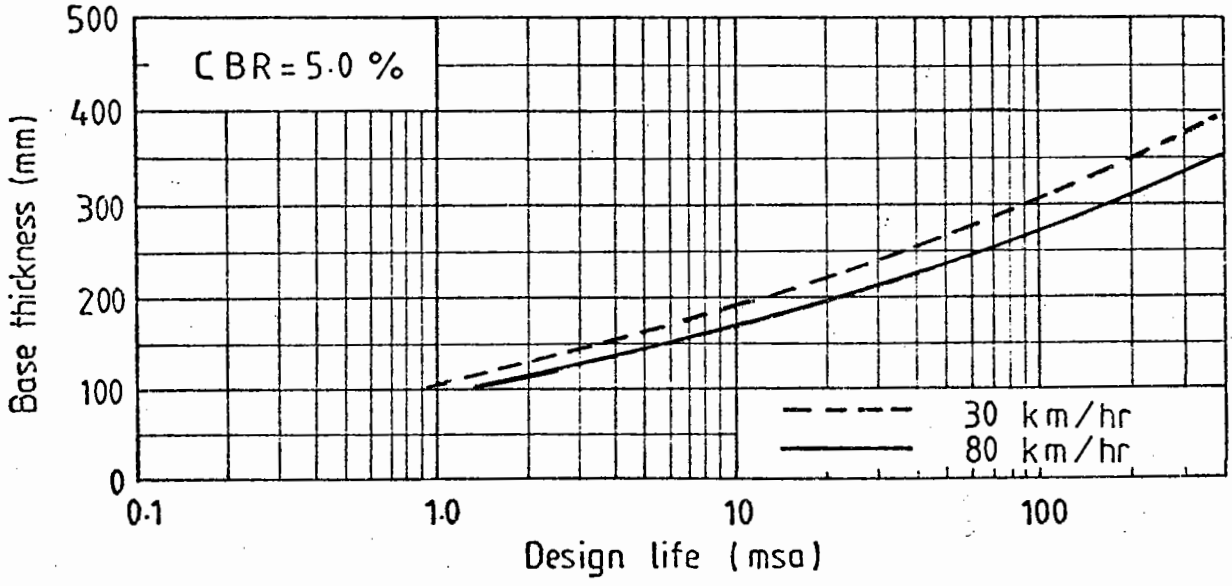

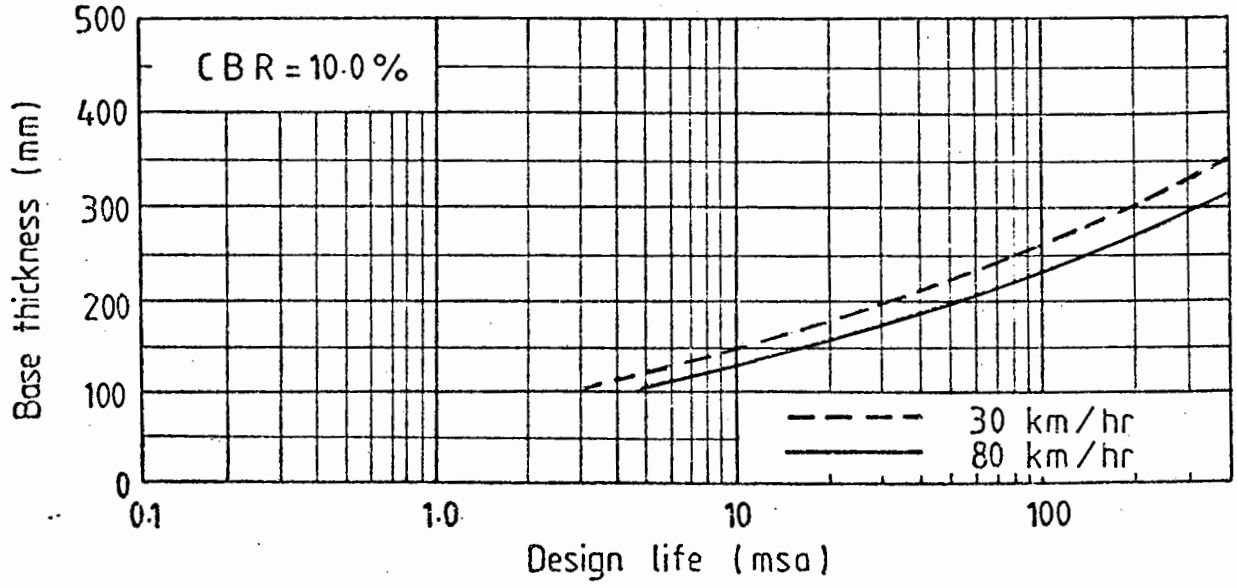

CHART 3S DESIGN MIX BASE, FULL DEPTH ASPHALT TYPE A

NORTHERN TEMPERATURE ZONE

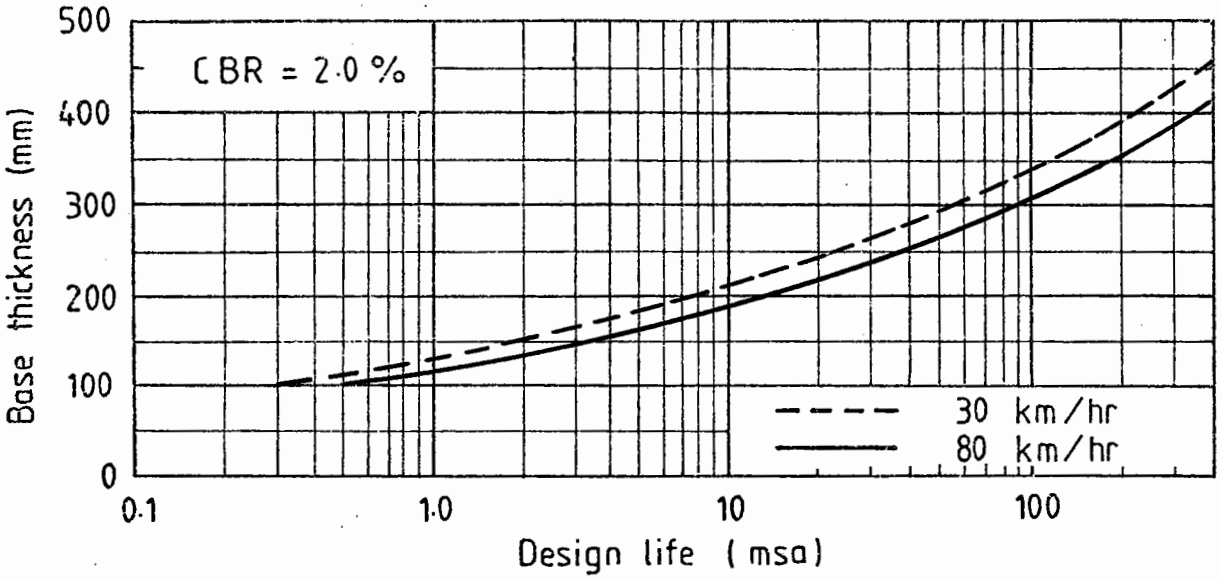

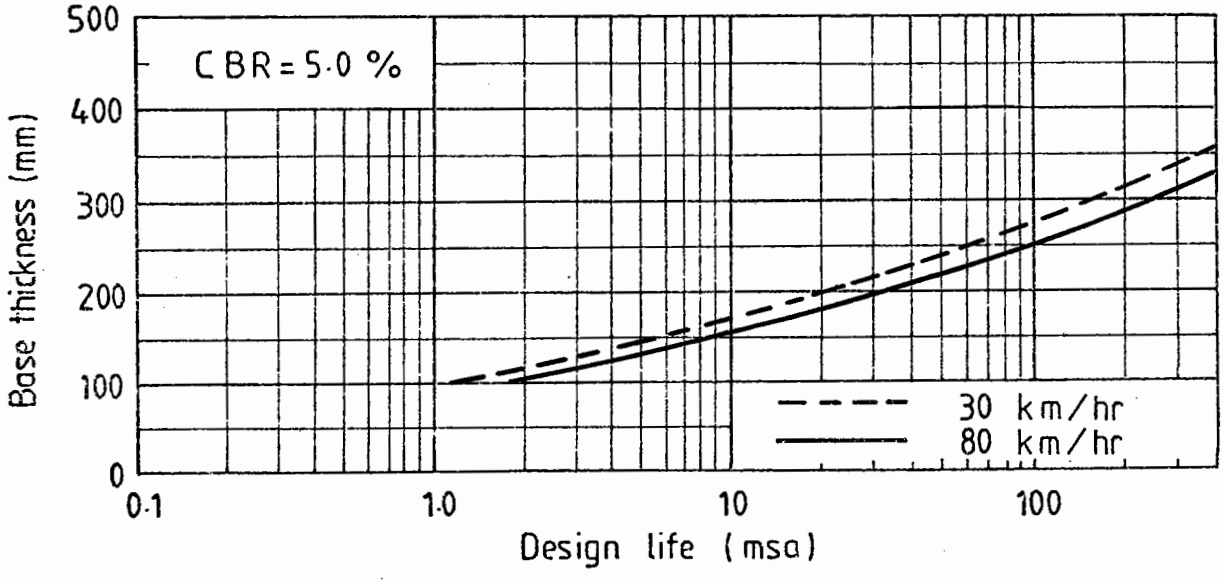

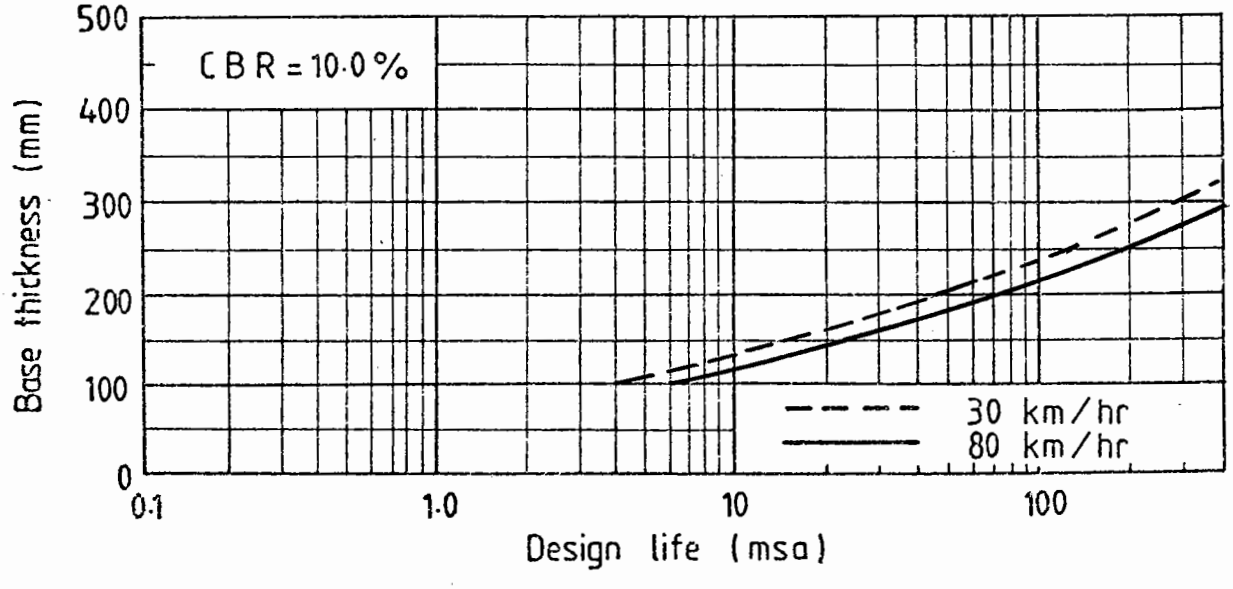

CHART 3N DESIGN MIX BASE , FULL DEPTH ASPHALT TYPE A

SOUTHERN TEMPERATURE ZONE

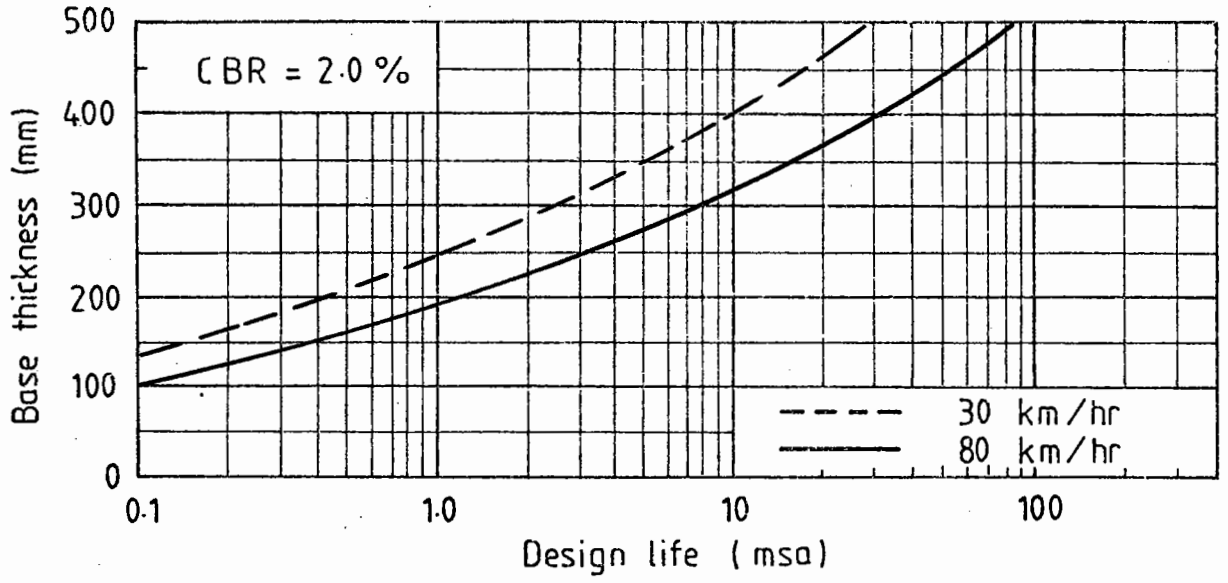

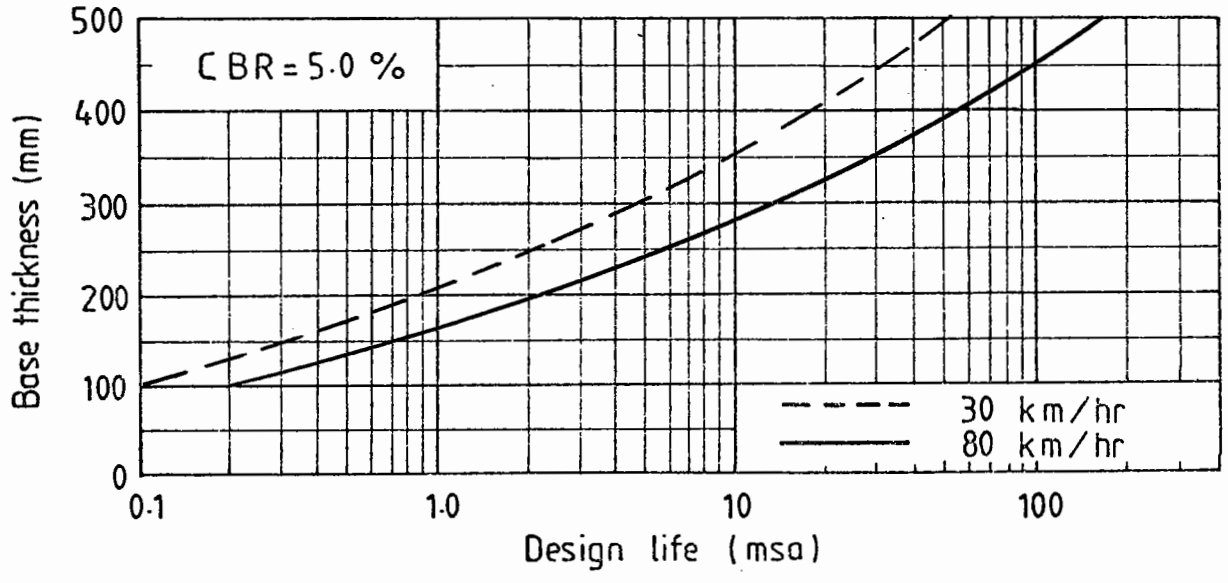

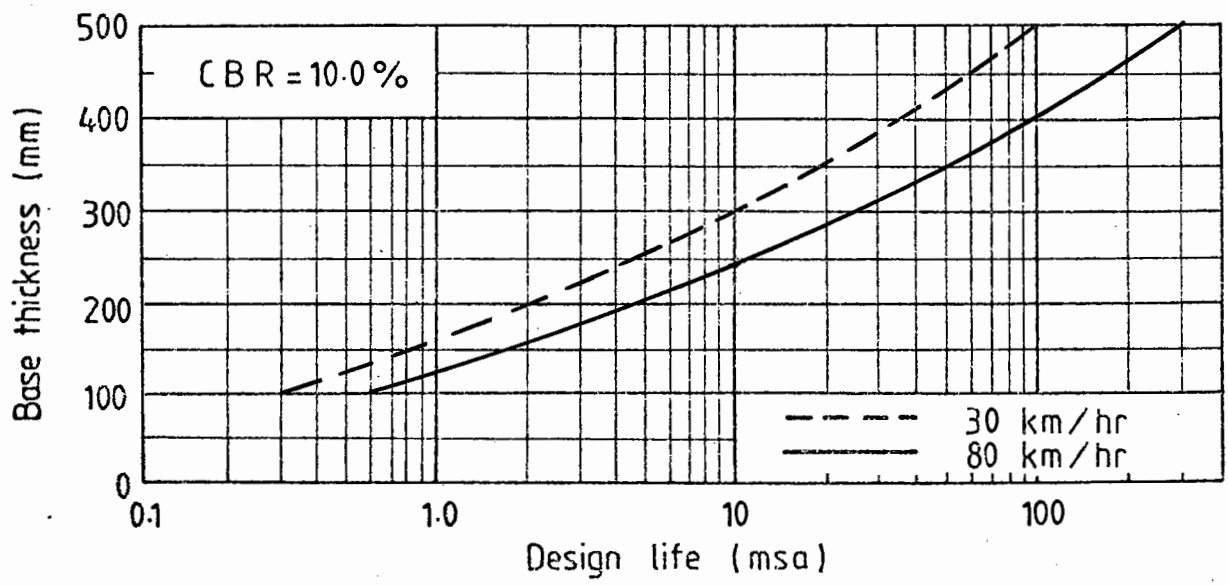

CHART 4S DBM BASE , FULL DEPTH ASPHALT TYPE B

NORTHERN TEMPERATURE ZONE

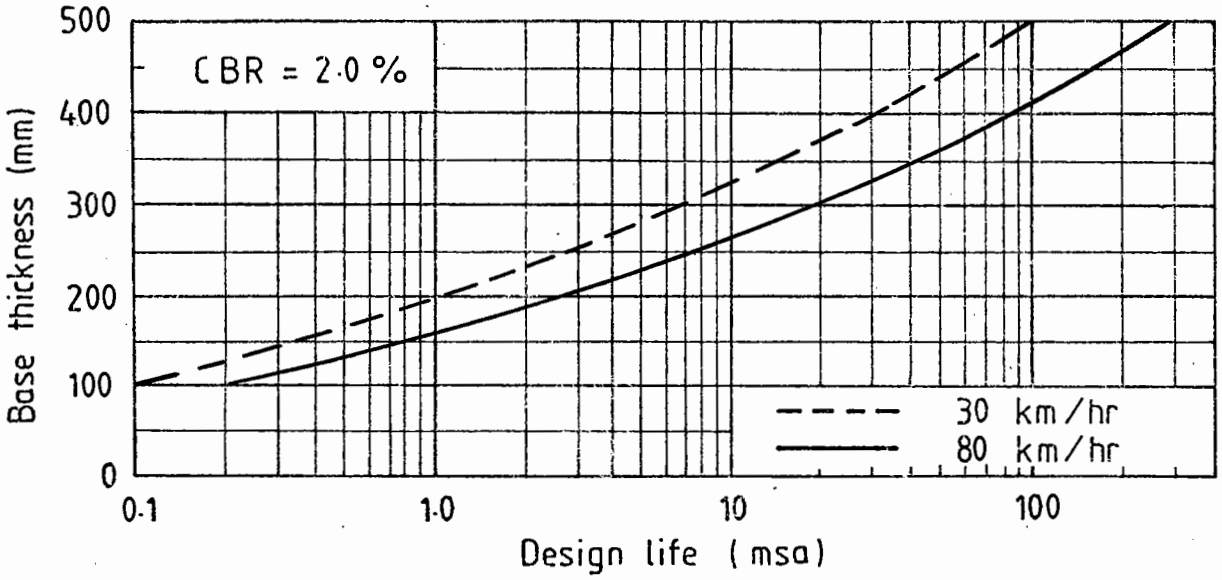

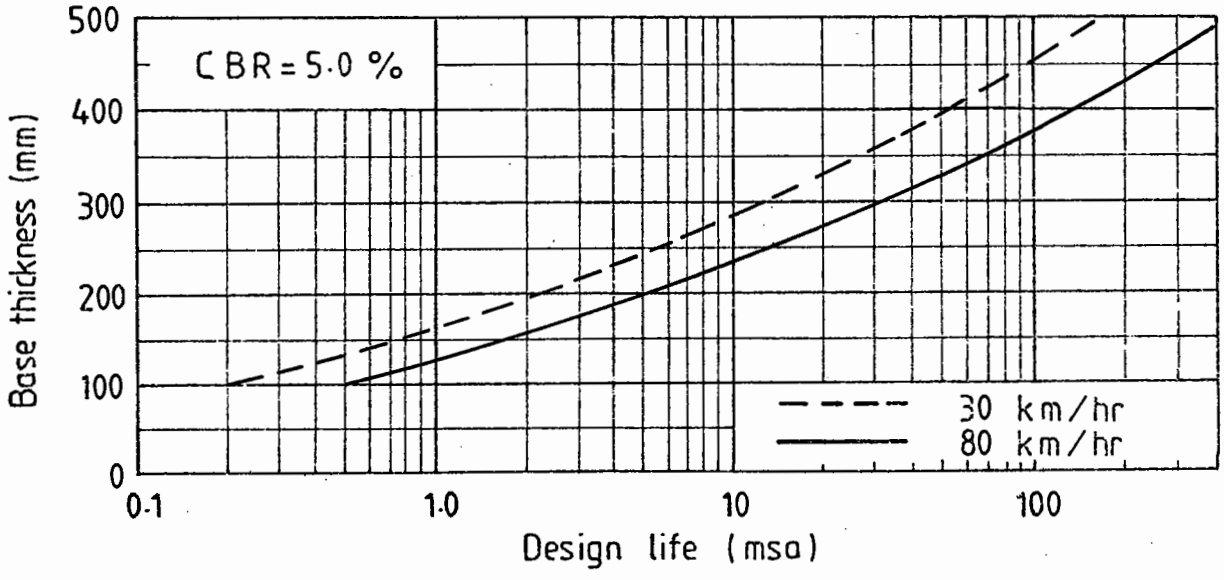

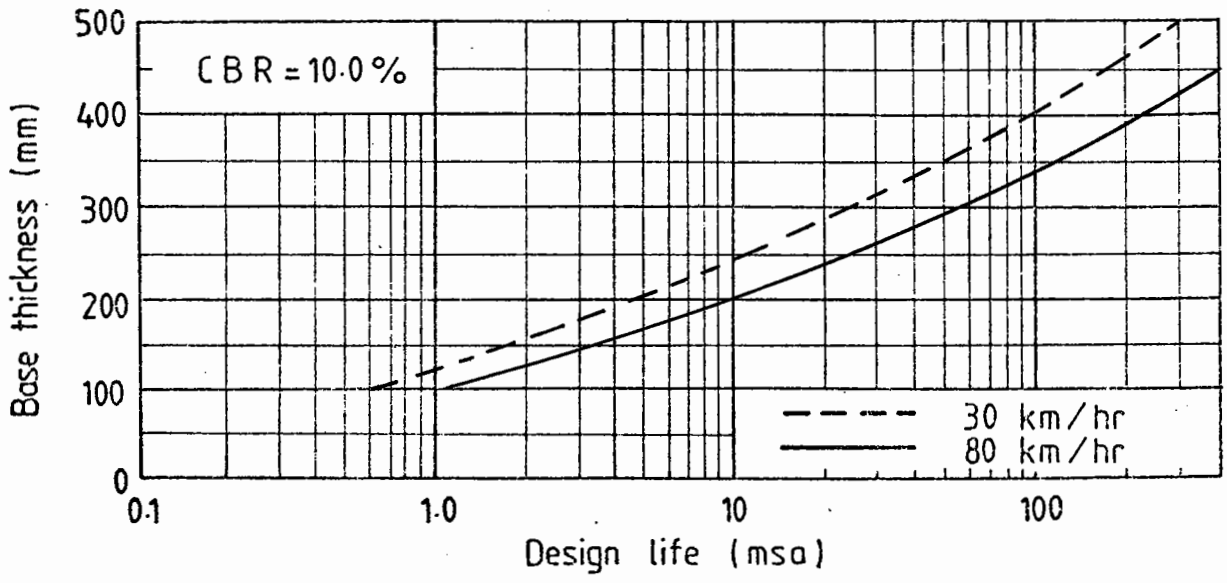

CHART 4N DBM BASE , FULL DEPTH ASPHALT TYPE B

SOUTHERN TEMPERATURE ZONE

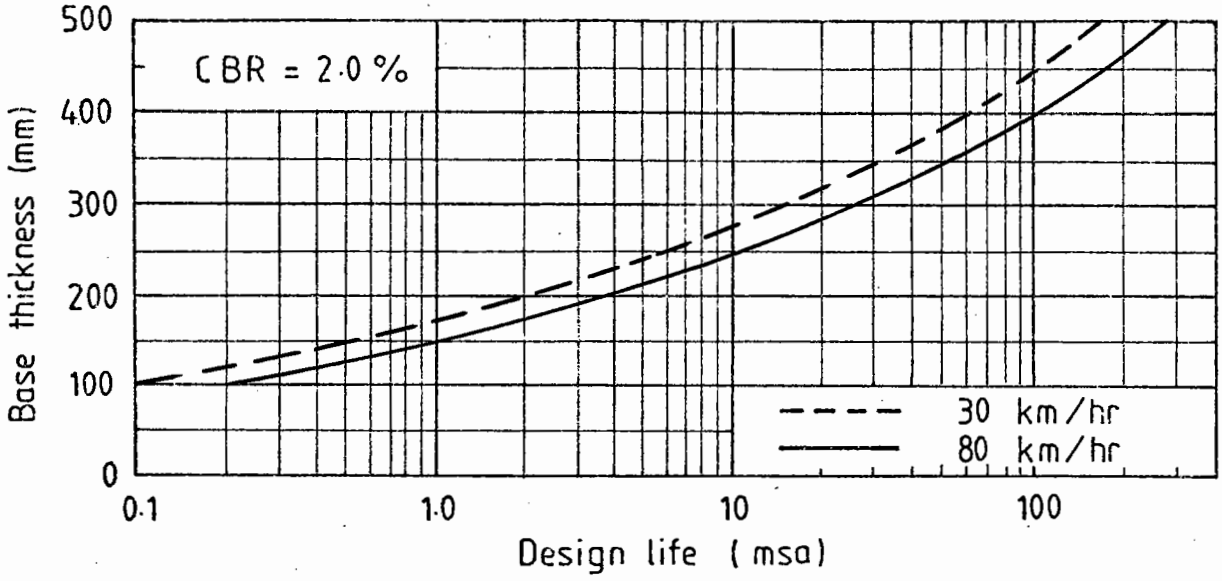

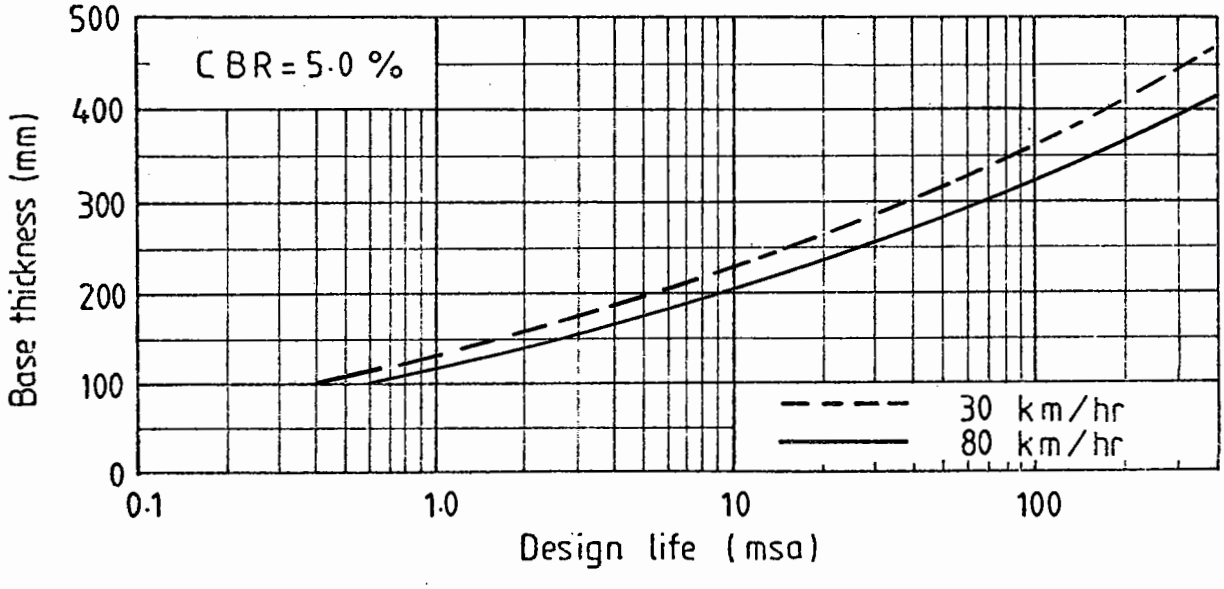

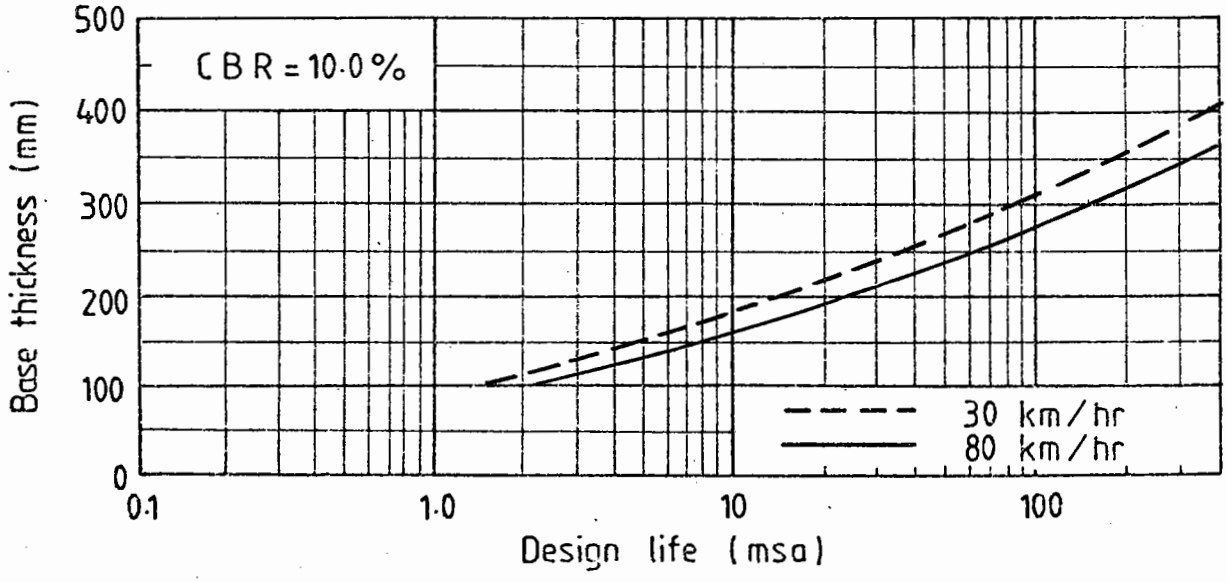

CHART 5S HRA BASE , FULL DEPTH ASPHALT TYPE B

NORTHERN TEMPERATURE ZONE

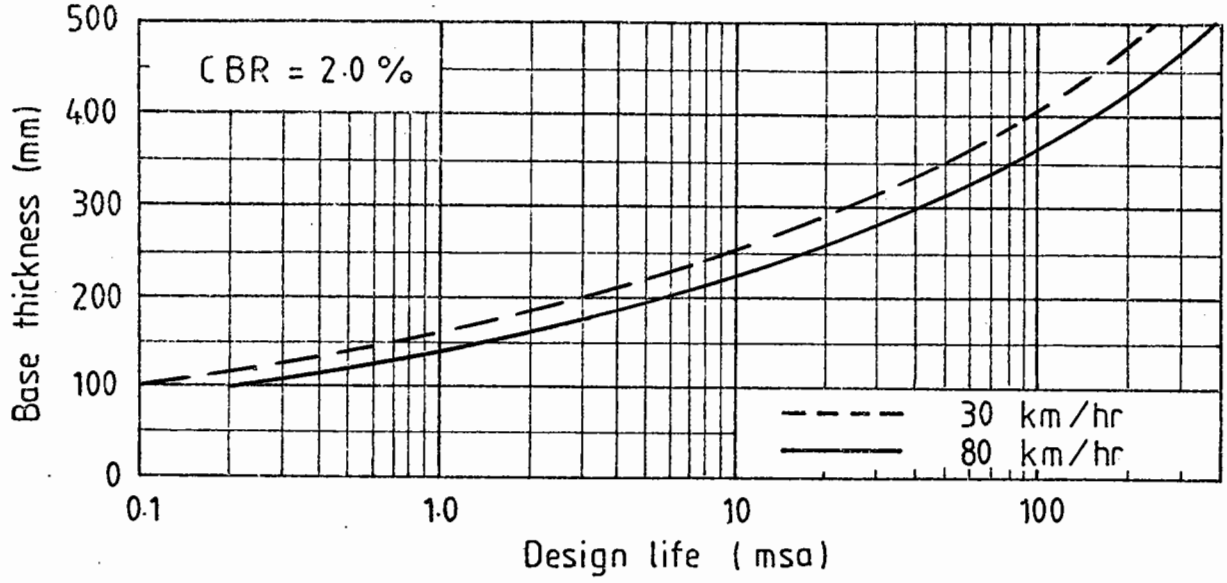

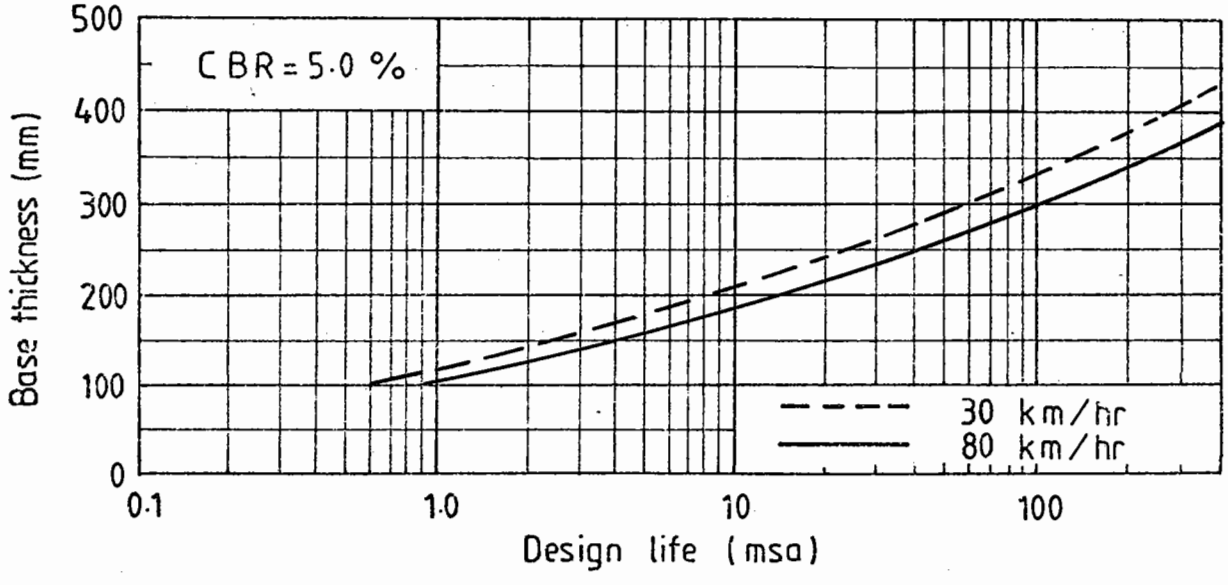

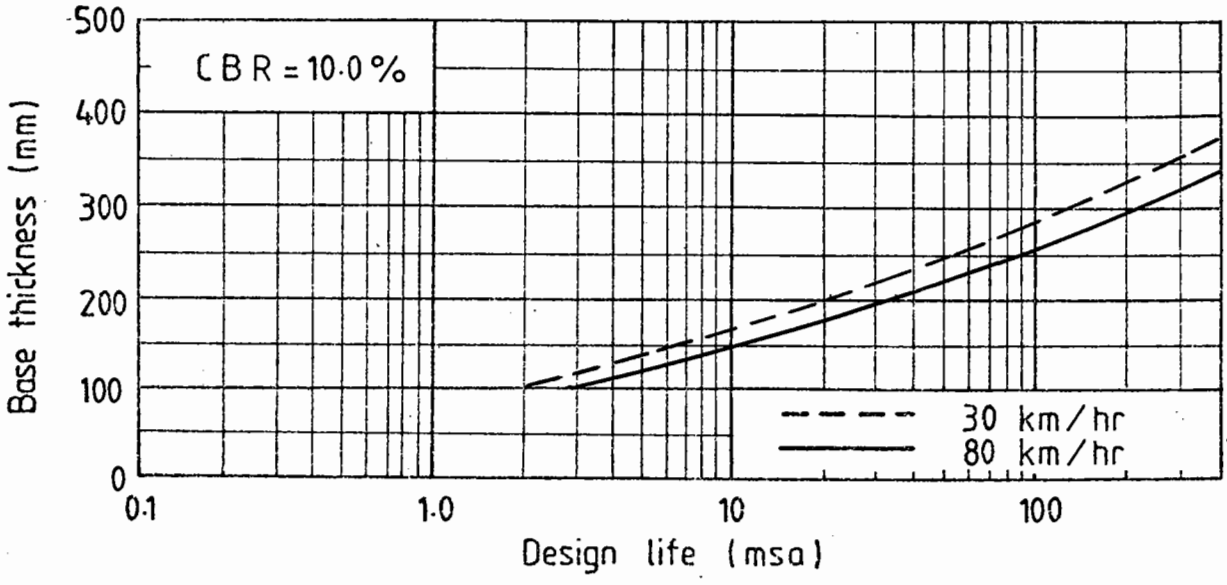

CHART 5N HRA BASE , FULL DEPTH ASPHALT TYPE B

SOUTHERN TEMPERATURE ZONE

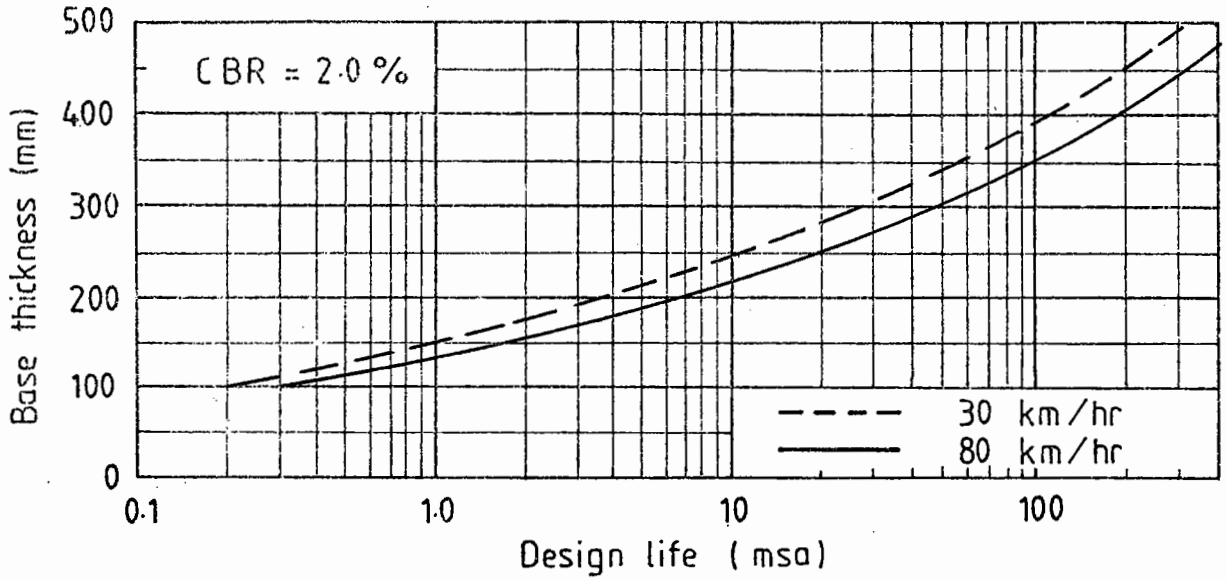

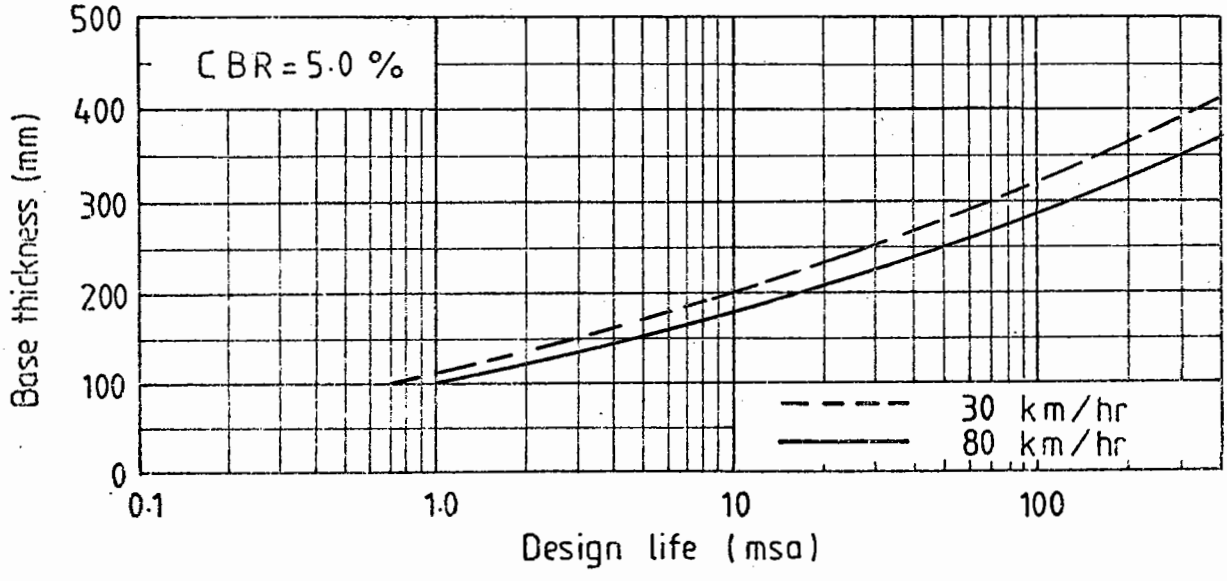

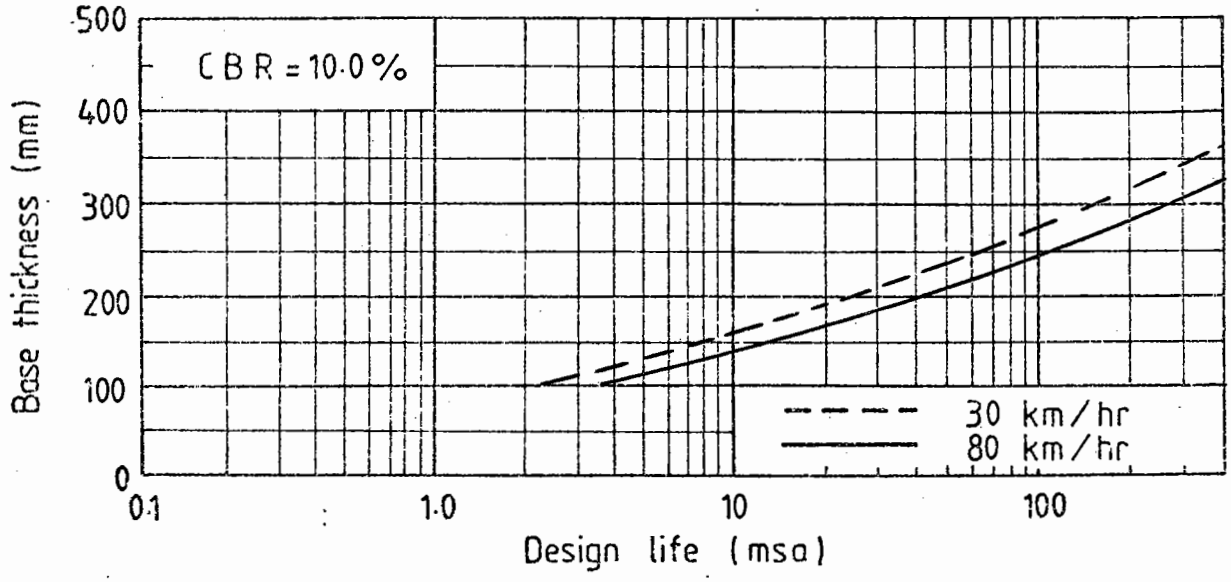

CHART 6S DESIGN MIX BASE , FULL DEPTH ASPHALT TYPE B

NORTHERN TEMPERATURE ZONE

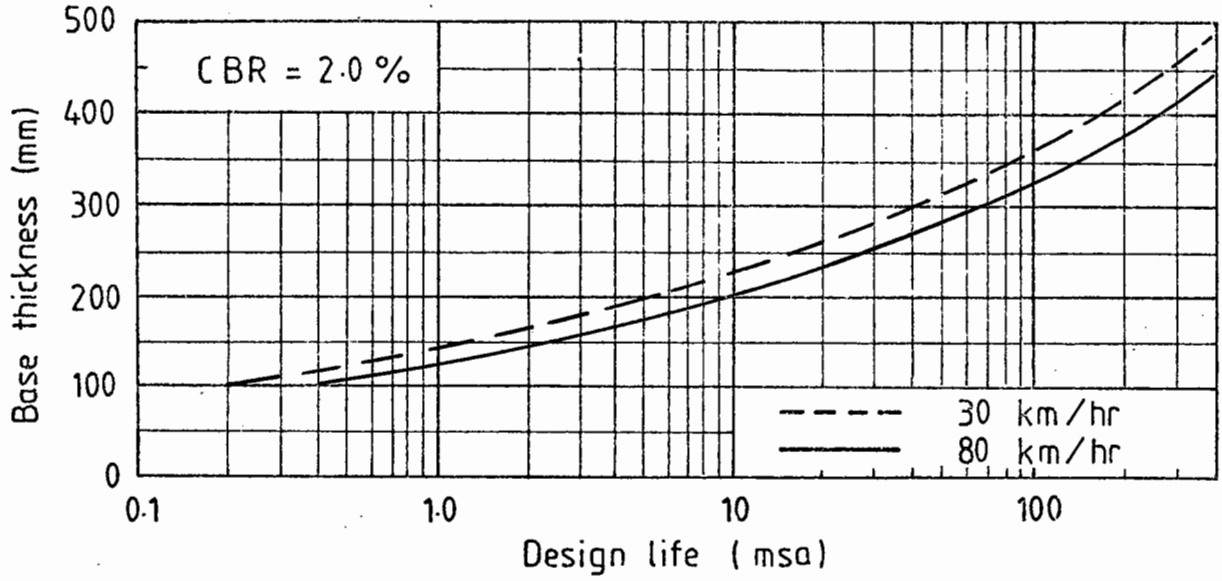

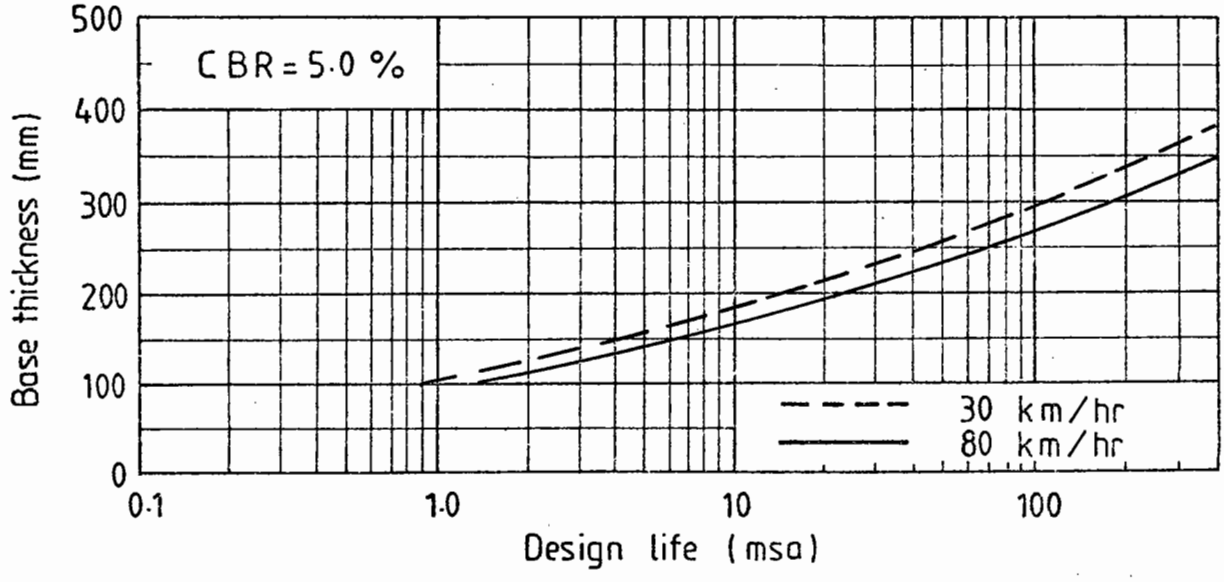

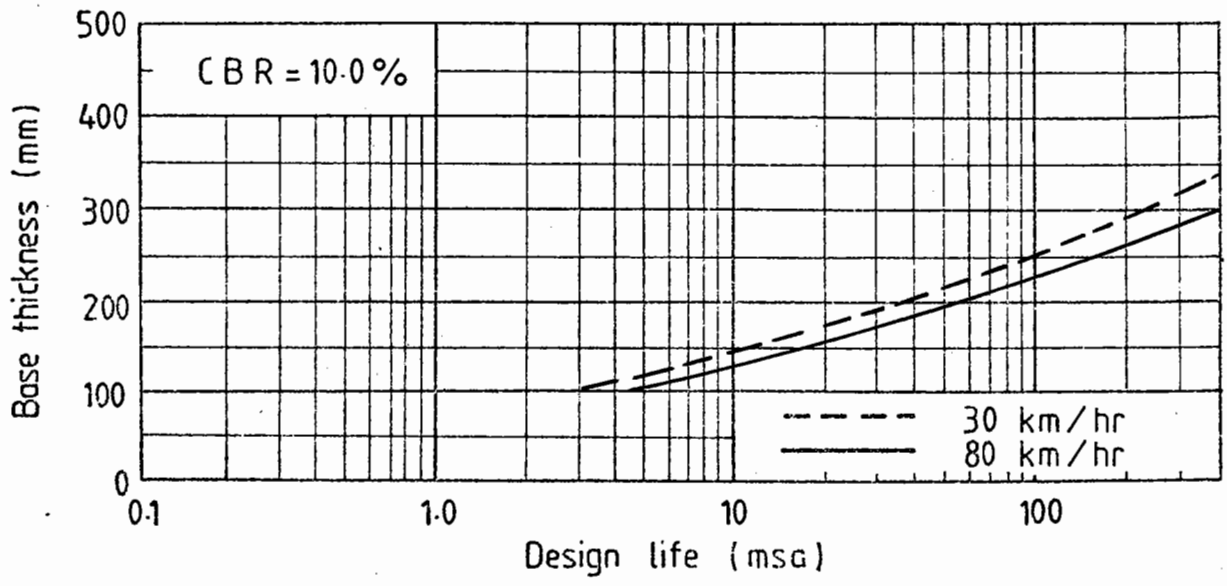

CHART 6N DESIGN MIX BASE FULL DEPTH ASPHALT TYPE B

SOUTHERN TEMPERATURE ZONE

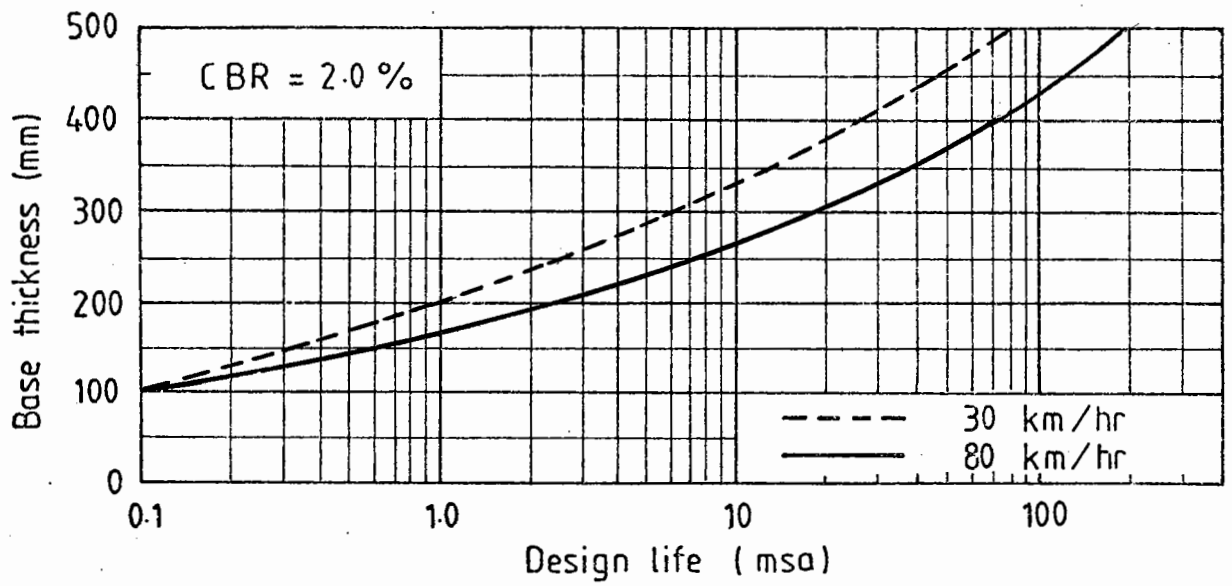

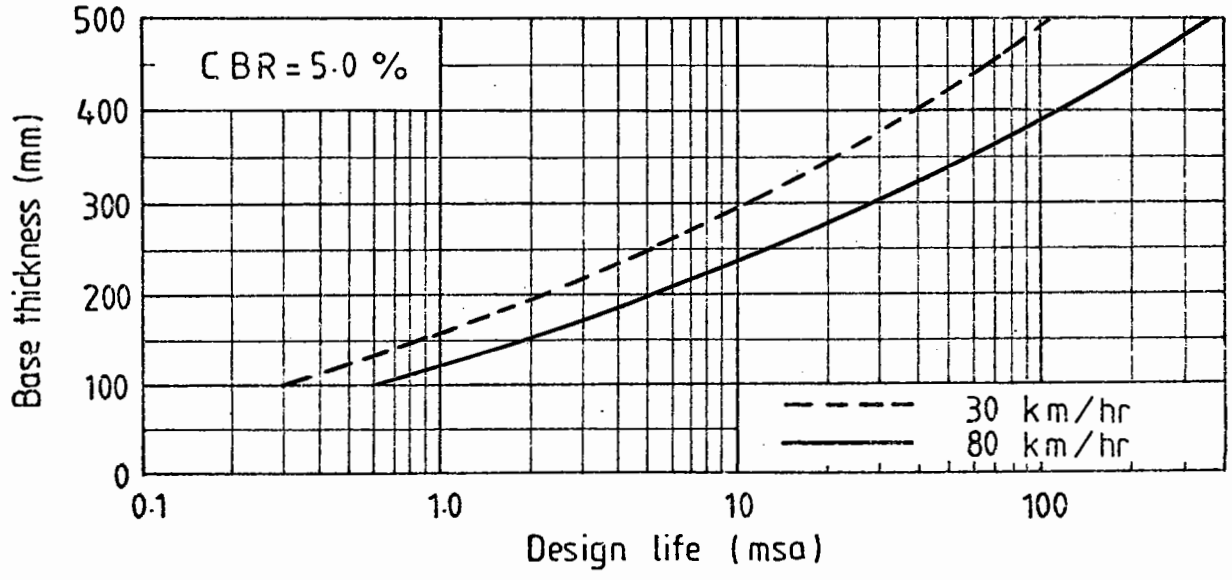

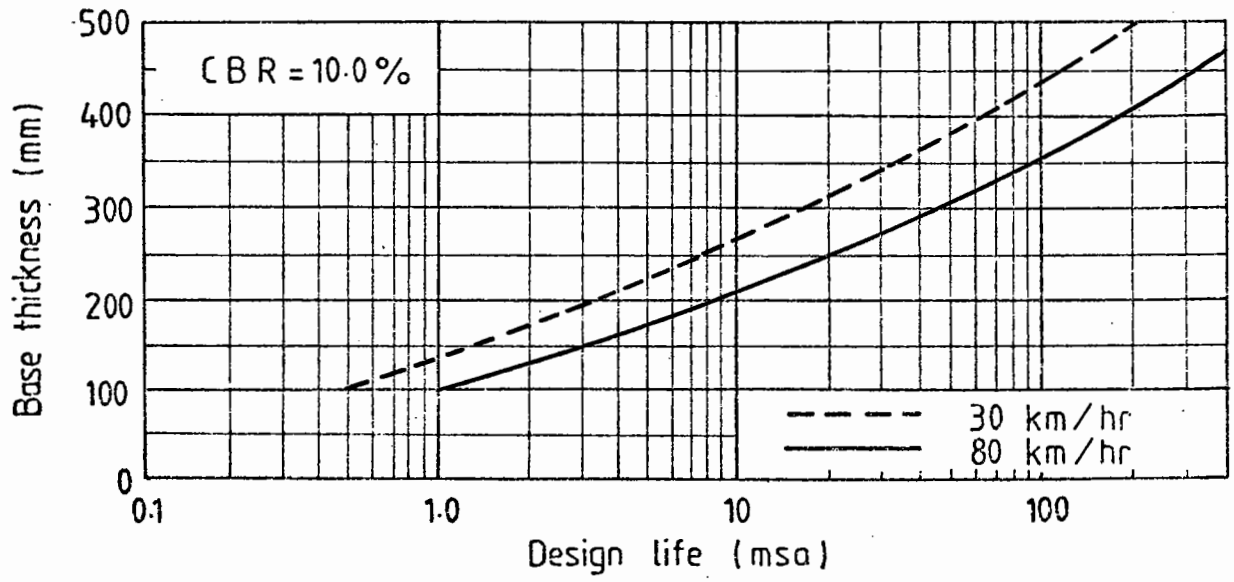

CHART 7S DBM BASE , GRANULAR SUB-BASE

NORTHERN TEMPERATURE ZONE

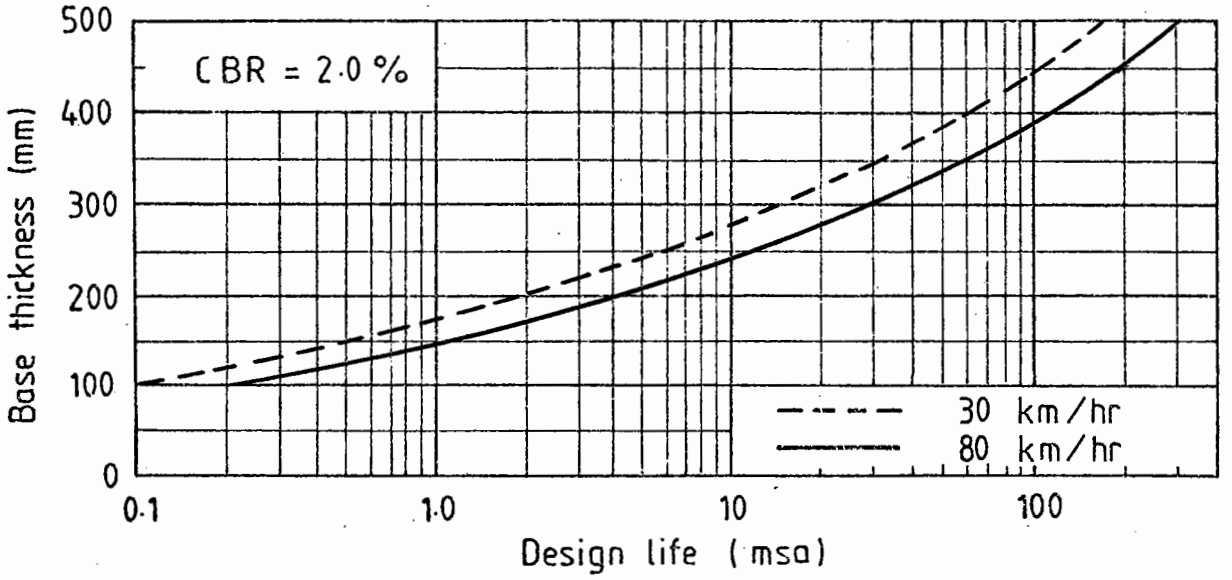

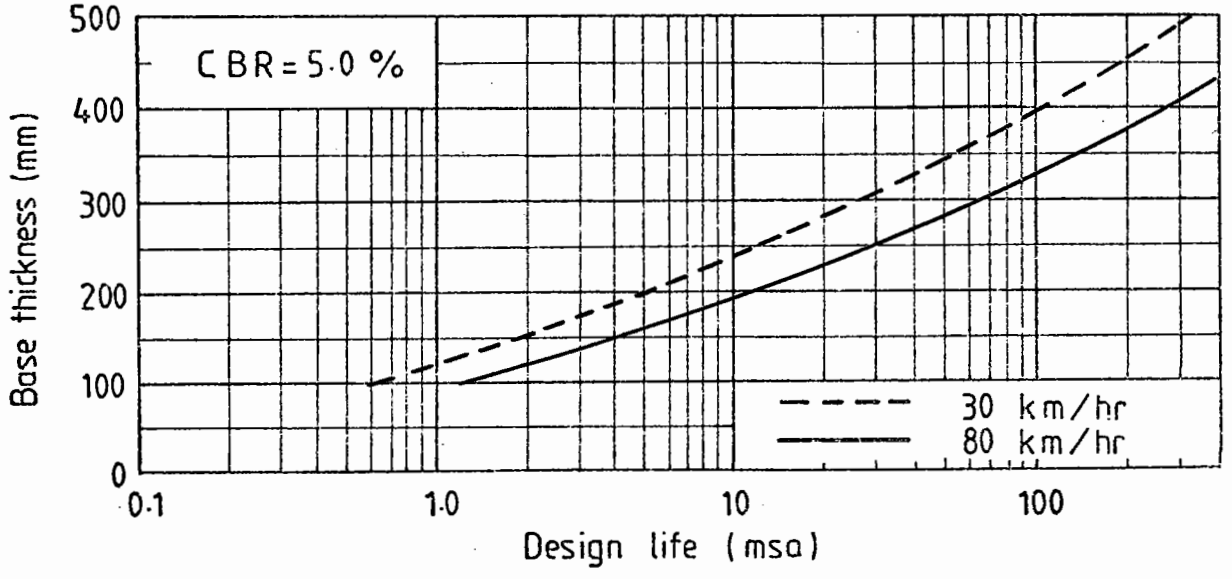

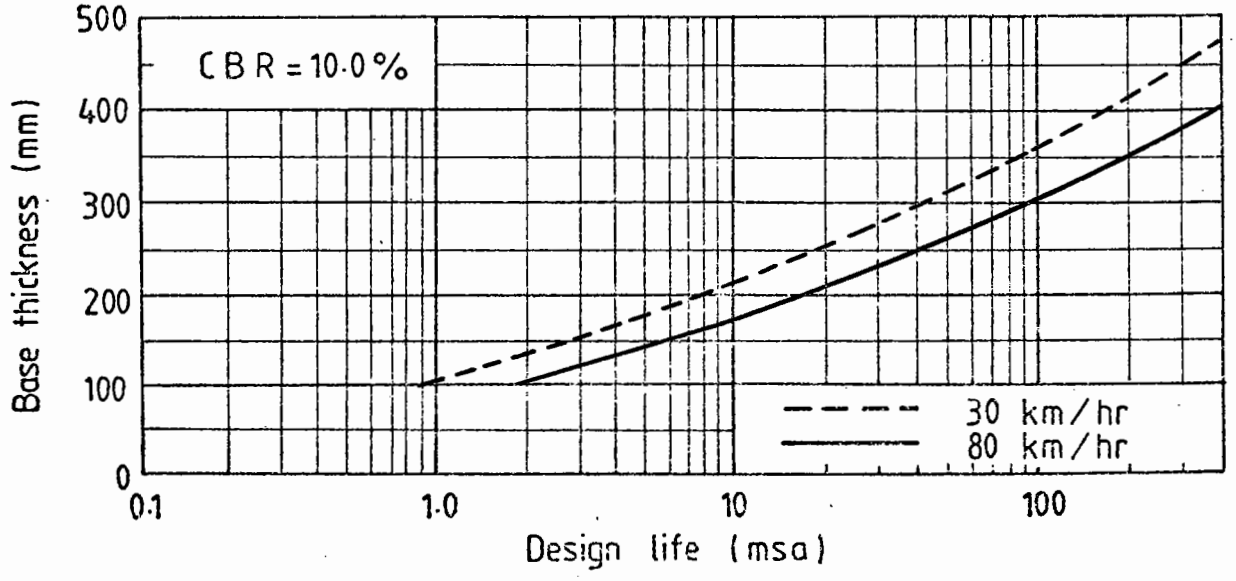

CHART 7N DBM BASE , GRANULAR SUB-BASE

SOUTHERN TEMPERATURE ZONE

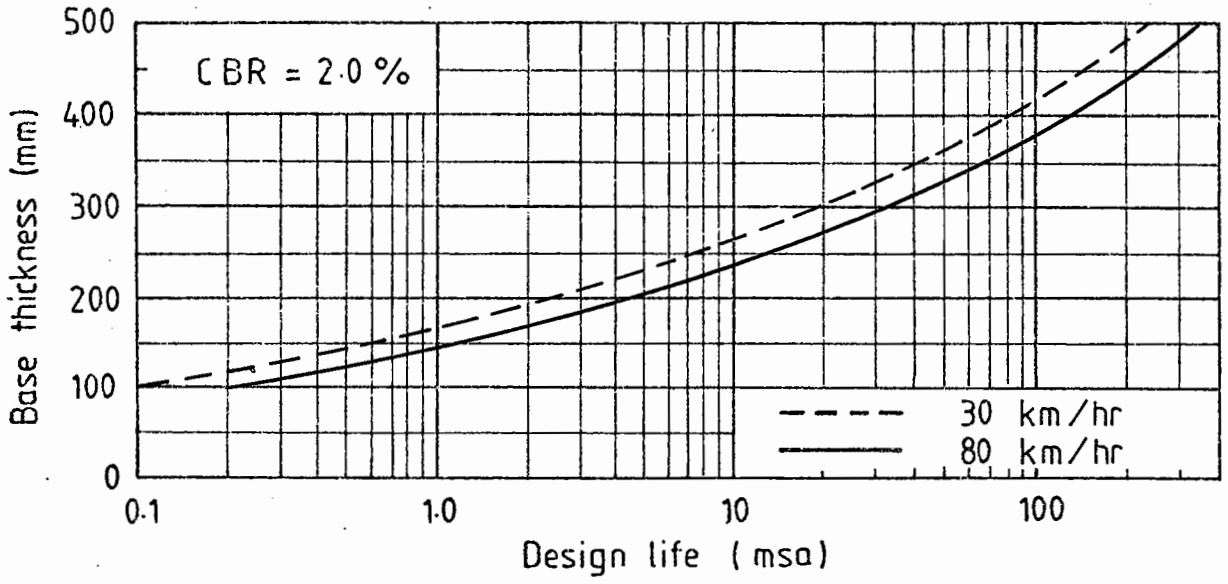

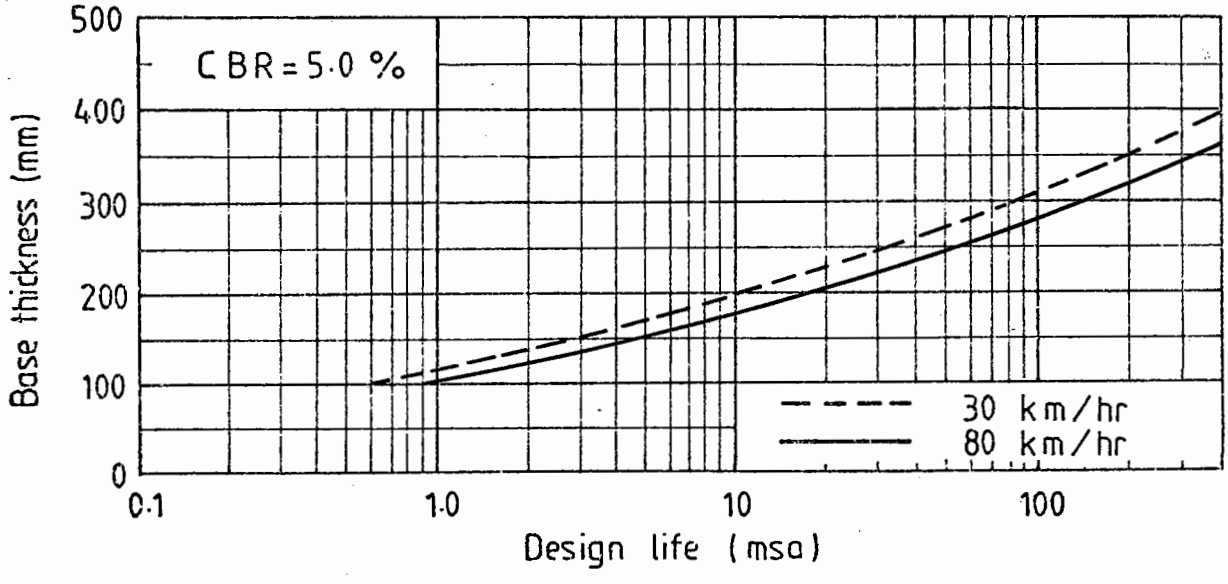

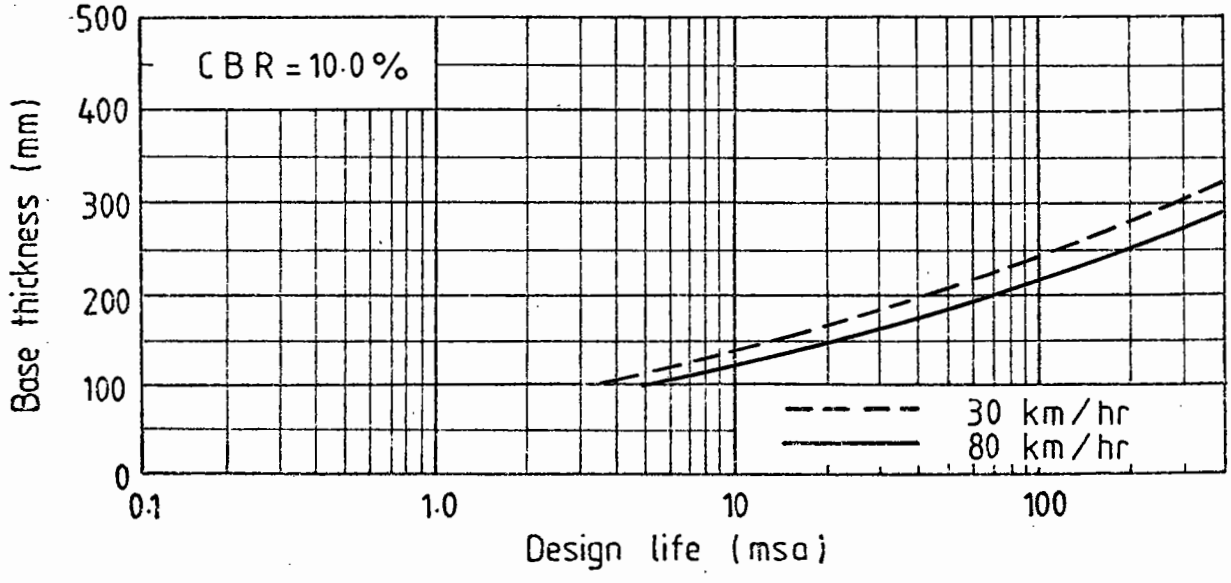

CHART 8S HRA BASE , GRANULAR SUB-BASE

NORTHERN TEMPERATURE ZONE

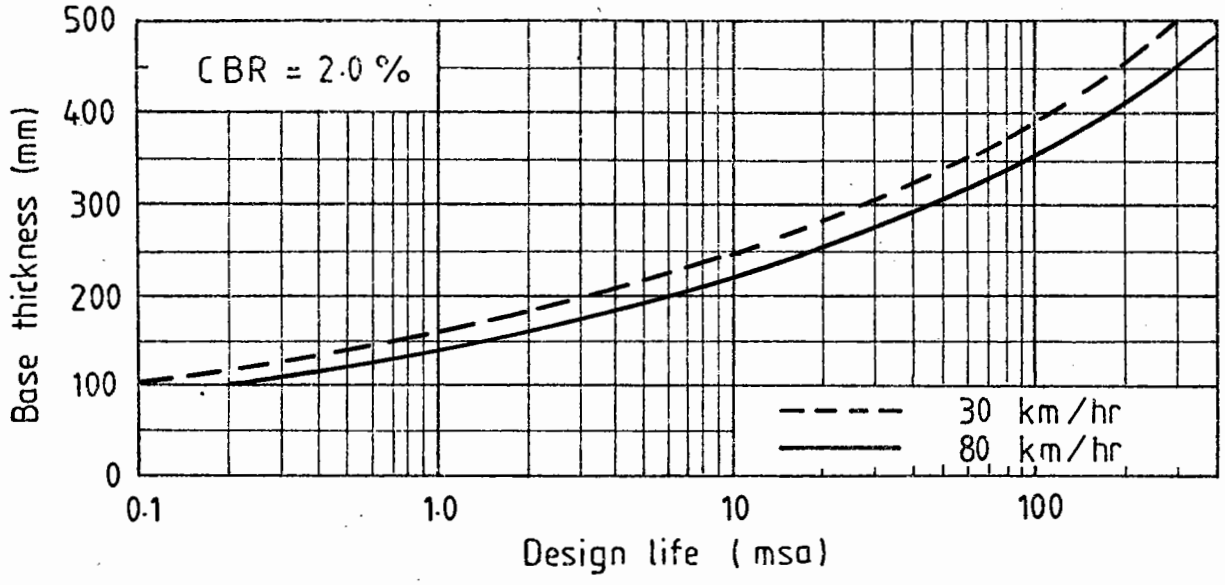

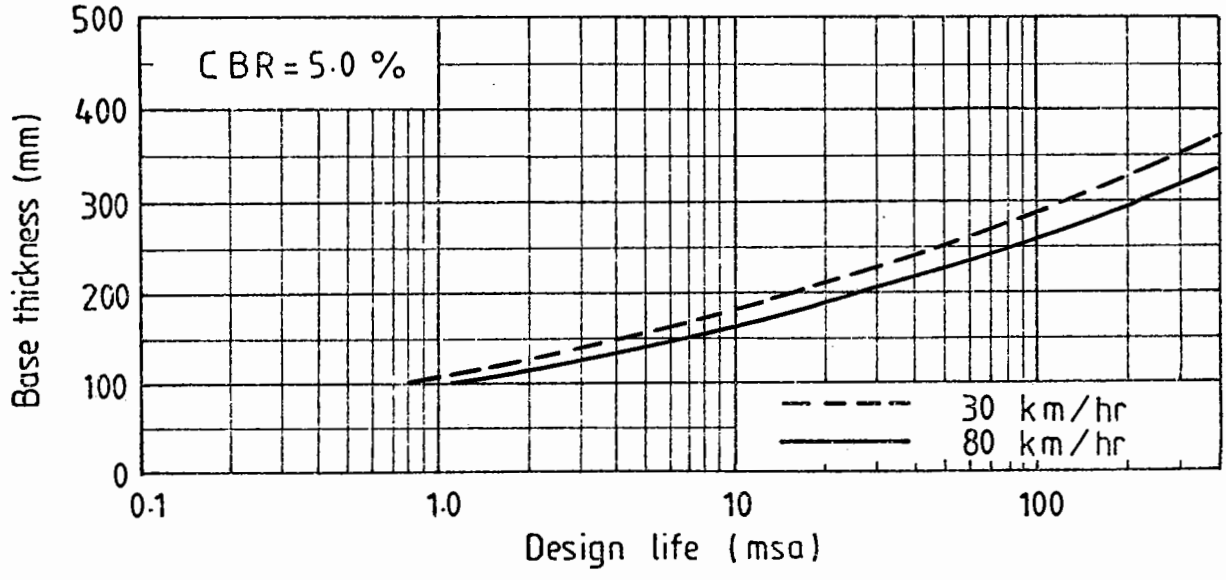

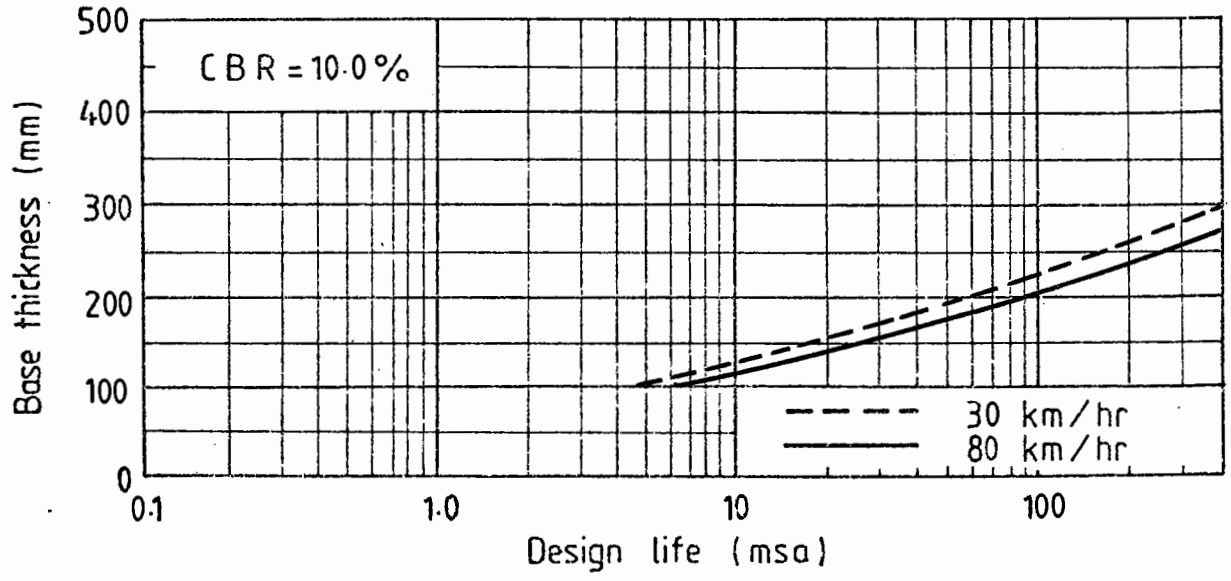

CHART 8N HRA BASE , GRANULAR SUB-BASE

NORTHERN TEMPERATURE ZONE

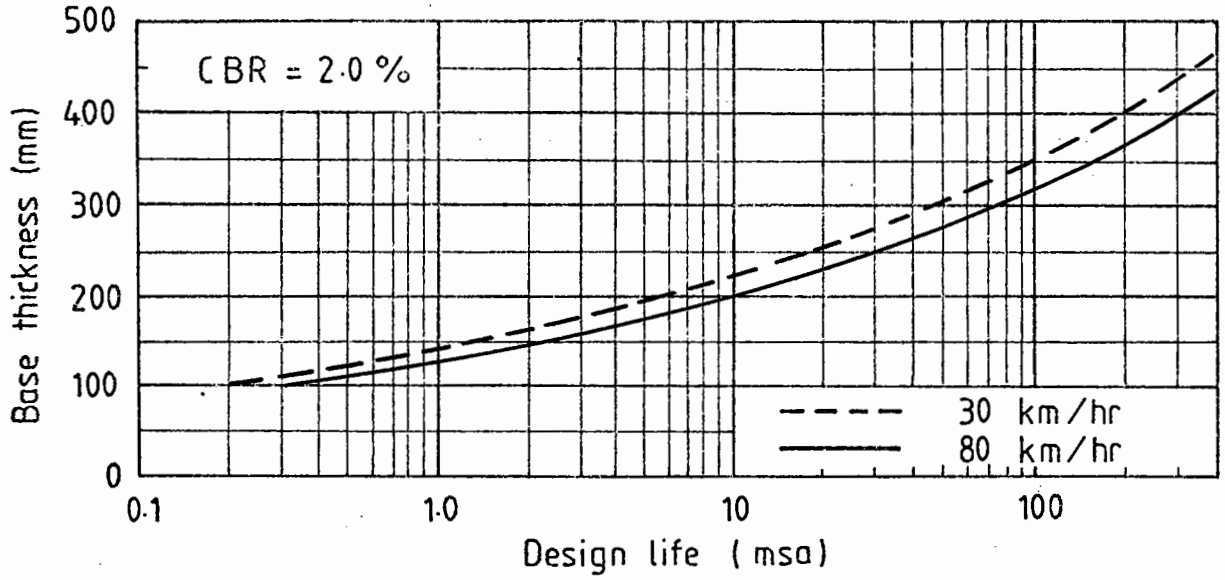

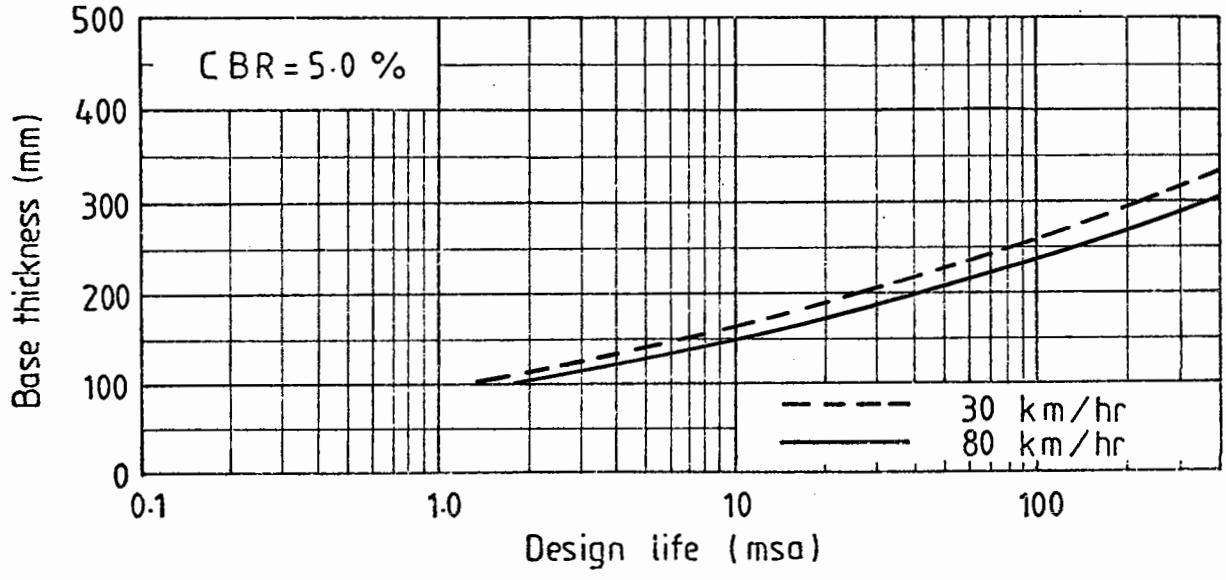

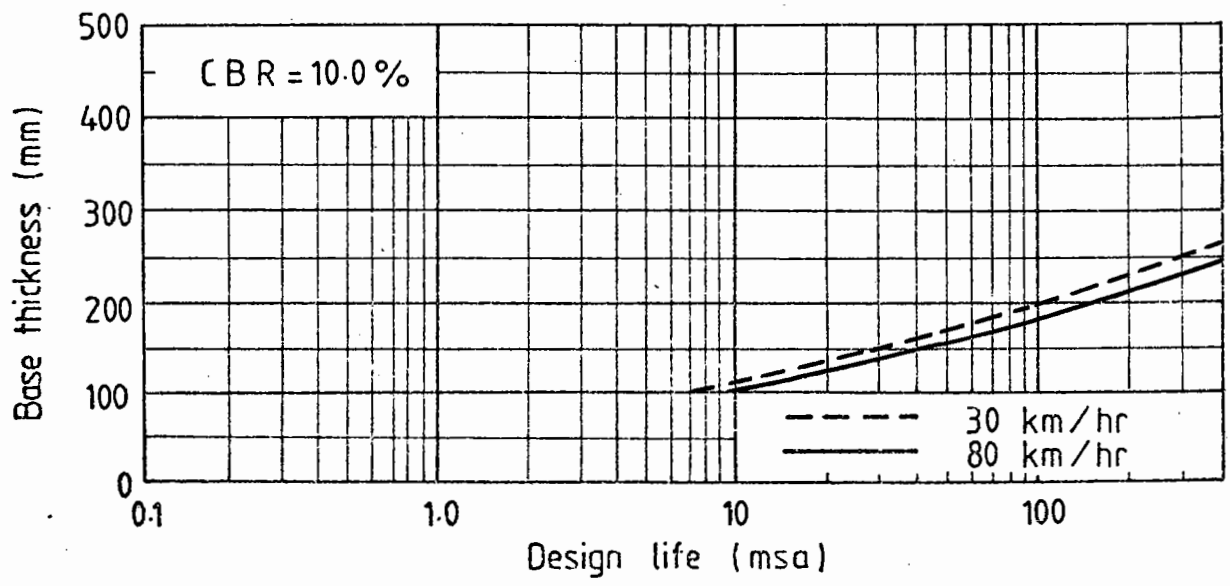

CHART 9N DESIGN MIX BASE , GRANULAR SUB-BASE

SOUTHERN TEMPERATURE ZONE

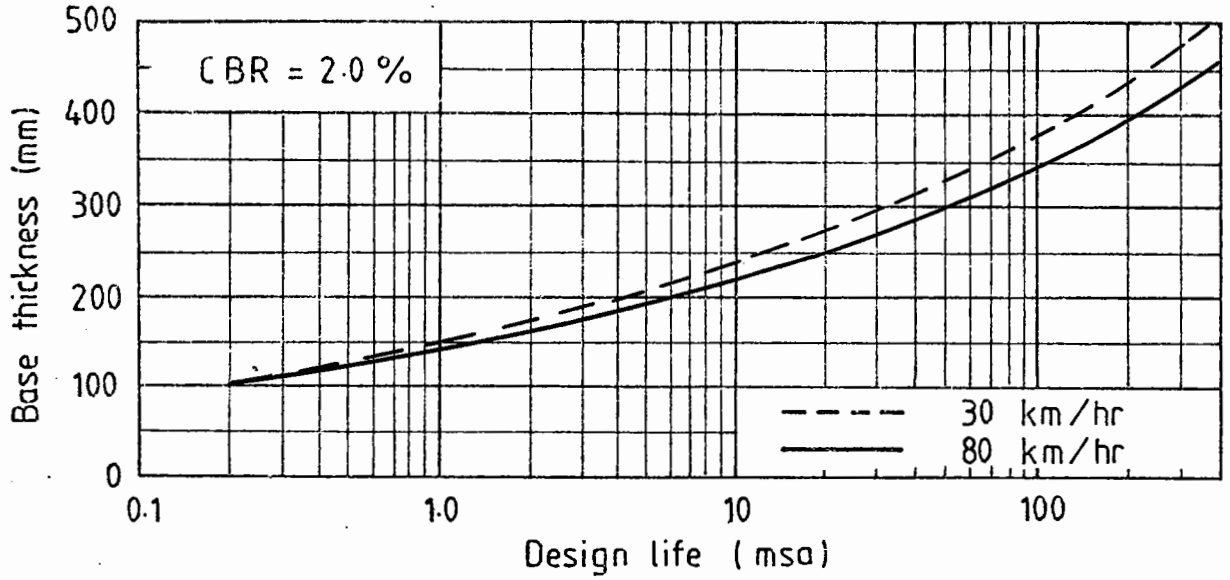

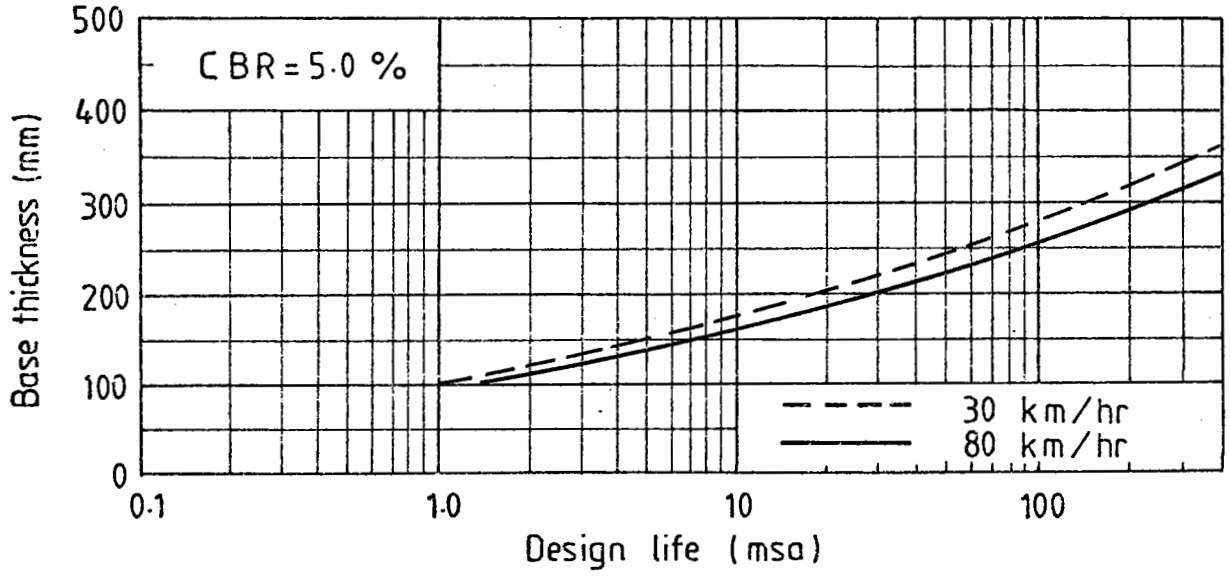

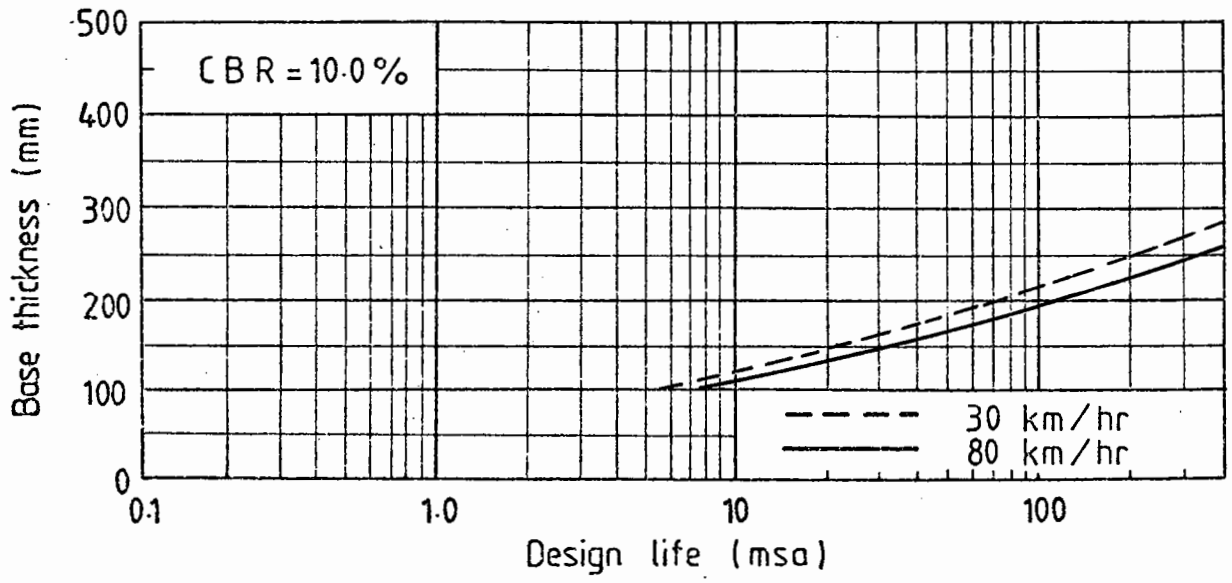

CHART 9S DESIGN MIX BASE , GRANULAR SUB-BASE

APPENDIX B

TABULATION OF DATA FOR PAVEMENT DESIGN MANUAL

CONTENTS

NOTATION

The following notation is used in the column headings for Tables B1 to B9.

Structure	The three types of structures used are represented by numbers 1 to 3, where: 1 is full depth asphalt type A 2 is full depth asphalt type B 3 is granular sub-base
Temp	The average annual air temperature in °Centigrade
Speed	Average speed of commercial vehicles in km/hr
h_2	Thickness of asphalt base in mm
h_3	Thickness of sub-base in mm
Modular ratio	The ratio of sub-base to subgrade stiffness modulus ratio
N_z	Calculated life of pavement against permanent deformation in millions of standard axles
N_t	Calculated life of pavement against fatigue cracking in millions of standard axles.

Table B1 INPUT DATA AND CALCULATED LIVES FOR DBM BASE, FULL DEPTH ASPHALT TYPE A

Structure	CBR (%)	Temp °C	Speed (km/hr)	Base h_2 (mm)	Subbase h_3 (mm)	Modular ratio	N_z (msa)	N_t (msa)
1	2	8.4	30	100	5	1.0	0.1	0.1
				250			6.3	5.2
				400			59.7	58.7
			80	100			0.2	0.3
				250			12.7	13.0
				400			116	154
		10.1	30	100			0.1	0.1
				250			3.7	1.7
				400			35.4	18.7
			80	100			0.1	0.1
				250			7.5	5.4
				400			70.9	60.8
	5	8.4	30	100			0.6	0.4
				250			16.6	9.8
				400			159	99.5
			80	100			0.9	0.7
				250			32.7	23.1
				400			327	255
		10.1	30	100			0.4	0.2
				250			9.9	3.6
				400			91.0	33.3
			80	100			0.6	0.4
				250			19.7	10.1
				400			191	103
	10	8.4	30	100			2.0	0.9
				250			38.7	18.7
				400			319	167
			80	100			3.1	1.7
				250			72.8	41.4
				400			656	404
		10.1	30	100			1.5	0.4
				250			24.1	61.1
				400			186	61.1
			80	100			2.3	0.9
				250			45.5	19.2
				400			383	173

Table B2 INPUT DATA AND CALCULATED LIVES FOR HRA BASE, FULL DEPTH ASPHALT TYPE A

Structure	CBR (%)	Temp °C	Speed (km/hr)	Base h_2 (mm)	Subbase h_3 (mm)	Modular ratio	N_z (msa)	N_t (msa)
1	2	8.4	30	100	5	1.0	0.2	1.5
				250			12.8	264
				400			124	>1000
			80	100			0.3	3.7
				250			21.3	718
				400			198	>1000
		10.1	30	100			0.1	0.6
				250			8.2	86.1
				400			82.8	>1000
			80	100			0.2	1.6
				250			14.1	270
				400			141	>1000
	5	8.4	30	100			0.7	4.9
				250			33.7	530
				400			374	>1000
			80	100			1.1	11.2
				200			18.8	345
				300			144	>1000
		10.1	30	100			0.5	2.0
				250			21.6	186
				400			239	>1000
			80	100			0.8	5.0
				250			38.9	542
				400			433	>1000
	10	8.4	30	100			2.5	14.0
				200			28.0	308
				300			175	>1000
			80	100			3.5	29.9
				200			44.1	725
				300			295	>1000
		10.1	30	100			1.8	6.2
				200			19.1	120
				300			113	>1000
			80	100			2.7	14.2
				200			31.8	314
				300			202	>1000

Table B3 INPUT DATA AND CALCULATED LIVES FOR DESIGN MIX BASE, FULL DEPTH ASPHALT TYPE A

Structure	CBR (%)	Temp °C	Speed (km/hr)	Base h_2 (mm)	Subbase h_3 (mm)	Modular ratio	N_z (msa)	N_t (msa)
1	2	8.4	30	100	5	1.0	0.3	1.4
				250			23.2	145
				400			223	> 1000
			80	100			0.5	3.0
				250			37.8	344
				400			350	> 1000
		10.1	30	100			0.2	0.6
				250			15.2	54.7
				400			152	> 1000
			80	100			0.3	1.4
				250			26.7	148
				400			252	> 1000
	5	8.4	30	100			1.2	3.7
				200			20.4	78.0
				300			157	780
			80	100			1.8	7.7
				200			33.1	173
				300			263	> 1000
		10.1	30	100			0.9	1.7
				200			13.5	32.5
				300			101	302
			80	100			1.3	3.8
				200			23.4	79.5
				300			181	796
	10	8.4	30	100			4.0	9.3
				200			49.0	155
				300			322	> 1000
			80	100			5.7	18.1
				200			76.5	327
				250			215	> 1000
		10.1	30	100			3.0	4.5
				200			33.5	68.2
				300			211	548
			80	100			4.4	9.4
				200			55.5	158
				300			372	> 1000

Table B4 INPUT DATA AND CALCULATED LIVES FOR DBM BASE, FULL DEPTH ASPHALT TYPE B

Structure	CBR (%)	Temp °C	Speed (km/hr)	Base h_2 (mm)	Subbase h_3 (mm)	Modular ratio	N_z (msa)	N_t (msa)
2	2	8.4	30	100	5	1.0	0.1	0.1
				250			4.5	2.9
				400			44.6	31.4
			80	100			0.2	0.2
				250			9.3	7.4
				400			88.0	84.9
		10.1	30	100			0.1	0.0
				250			2.6	1.0
				400			25.8	10.0
			80	100			0.1	0.1
				250			5.5	3.0
				400			53.2	32.5
	5	8.4	30	100			0.4	0.2
				250			12.2	5.7
				400			117	54.5
			80	100			0.7	0.5
				250			24.1	13.5
				400			244	142
		10.1	30	100			0.3	0.1
				250			7.3	2.1
				400			66.0	18.6
			80	100			0.5	0.2
				250			14.5	5.8
				400			141	56.4
	10	8.4	30	100			1.6	0.6
				250			29.3	11.2
				400			240	95.6
			80	100			2.5	1.1
				250			55.1	24.9
				400			492	232
		10.1	30	100			1.2	0.3
				250			18.3	4.5
				400			139	36.0
			80	100			1.8	0.6
				250			34.4	11.5
				400			288	98.6

Table B5 INPUT DATA AND CALCULATED LIVES FOR HRA BASE, FULL DEPTH ASPHALT TYPE B

Structure	CBR (%)	Temp °C	Speed (km/hr)	Base h_2 (mm)	Subbase h_3 (mm)	Modular ratio	N_z (msa)	N_t (msa)
2	2	8.4	30	100	5	1.0	0.1	0.8
				250			9.5	128
				400			95.8	> 1000
			80	100			0.2	2.0
				250			16.2	352
				400			157	> 1000
		10.1	30	100			0.1	0.3
				250			6.0	40.7
				400			63.0	> 1000
			80	100			0.2	0.8
				250			11.0	131
				400			109	> 1000
	5	8.4	30	100			0.6	2.6
				250			24.9	265
				400			283	> 1000
			80	100			0.9	6.0
				250			42.7	689
				400			490	> 1000
		10.1	30	100			0.4	1.1
				250			15.9	91.8
				400			178	> 1000
			80	100			0.6	2.7
				250			28.9	271
				400			328	> 1000
	10	8.4	30	100			2.0	7.6
				200			21.4	163
				300			130	> 1000
			80	100			2.8	16.5
				200			34.1	384
				300			221	> 1000
		10.1	30	100			1.5	3.4
				200			14.5	63.0
				300			83.4	595
			80	100			2.2	7.8
				200			24.3	166
				300			150	> 1000

Table B6 INPUT DATA AND CALCULATED LIVES FOR DESIGN MIX BASE, FULL DEPTH ASPHALT TYPE B

Structure	CBR (%)	Temp °C	Speed (km/hr)	Base h_2 (mm)	Subbase h_3 (mm)	Modular ratio	N_z (msa)	N_t (msa)
2	2	8.4	30	100	5	1.0	0.2	0.7
				250			170	725
				400			171	>1000
			80	100			0.4	1.6
				250			28.5	175
				400			275	>1000
		10.1	30	100			0.2	0.3
				250			10.9	26.8
				400			115	502
			80	100			0.3	0.7
				250			19.6	74.1
				400			195	>1000
	5	8.4	30	100			0.9	2.0
				200			15.0	41.0
				300			113	386
			80	100			1.4	4.2
				200			24.7	91.5
				300			194	908
		10.1	30	100			0.7	0.9
				200			9.9	16.9
				300			71.8	147
			80	100			1.0	2.1
				200			17.2	41.8
				300			131	394
	10	8.4	30	100			3.1	5.2
				200			36.8	83.8
				300			235	823
			80	100			4.5	10.2
				200			58.2	118
				300			397	>1000
		10.1	30	100			2.3	2.5
				200			25.1	36.6
				300			152	279
			80	100			3.5	5.3
				200			41.8	85.3
				300			271	696

Table B7 INPUT DATA AND CALCULATED LIVES FOR DBM BASE, GRANULAR SUB-BASE

Structure	CBR (%)	Temp °C	Speed (km/hr)	Base h_2 (mm)	Subbase h_3 (mm)	Modular ratio	N_z (msa)	N_t (msa)
3	2	8.4	30	100	200	5.0	0.1	0.4
				250		3.5	6.3	7.2
				400		3.5	62.9	72.7
			80	100		5.0	0.2	0.7
				250		3.5	11.7	16.8
				400		3.5	115	181
		10.1	30	100		5.0	0.1	0.2
				250		3.5	3.9	2.6
				400		3.5	39.2	25.1
			80	100		5.0	0.1	0.4
				250		3.5	7.4	7.4
				400		3.5	73.2	75.2
	5	8.4	30	100		2.0	0.8	0.6
				250		1.5	28.7	11.7
				400		1.5	288	113
			80	100		2.0	1.1	1.2
				250		1.5	52.3	26.6
				400		1.5	552	282
		10.1	30	100		2.0	0.6	0.3
				250		1.5	18.3	4.5
				400		1.5	175	39.6
			80	100		2.0	0.9	0.6
				250		1.5	33.4	12.0
				400		1.5	341	117
	10	8.4	30	100		1.0	4.3	0.9
				250		1.0	105	19.4
				400		1.0	916	172
			80	100		1.0	6.2	1.8
				250		1.0	182	42.5
				400		1.0	>1000	414
		10.1	30	100		1.0	3.3	0.5
				250		1.0	70.1	7.7
				400		1.0	566	63.6
			80	100		1.0	4.8	1.0
				250		1.0	121	19.9
				400		1.0	>1000	178

Table B.8 INPUT DATA AND CALCULATED LIVES FOR HRA BASE, GRANULAR SUB-BASE

Structure	CBR (%)	Temp °C	Speed (km/hr)	Base h_2 (mm)	Subbase h_3 (mm)	Modular ratio	N_z (msa)	N_t (msa)
3	2	8.4	30	100	200	5.0	0.1	4.0
				250		3.5	11.0	345
				400		3.5	116	>1000
			80	100		5.0	0.2	8.5
				250		3.5	17.7	894
				400		3.5	180	>1000
		10.1	30	100		5.0	0.1	1.8
				250		3.5	7.3	120
				400		3.5	79.8	>1000
			80	100		5.0	0.2	4.1
				250		3.5	12.6	353
				400		3.5	131	>1000
	5	8.4	30	100		2.0	0.8	8.6
				200		1.5	15.9	167
				300		1.5	129	>1000
			80	100		2.0	1.1	18.2
				200		1.5	24.8	403
				300		1.5	210	>1000
		10.1	30	100		2.0	0.6	3.9
				200		1.5	10.9	63.5
				300		1.5	85.4	697
			80	100		2.0	0.9	8.8
				200		1.5	18.0	170
				300		1.5	148	>1000
	10	8.4	30	100		1.0	4.5	14.6
				200		1.0	60.3	317
				300		1.0	416	>1000
			80	100		1.0	6.1	31.0
				150		1.0	26.5	172
				200		1.0	90.2	740
		10.1	30	100		1.0	3.5	6.6
				200		1.0	43.0	125
				300		1.0	281	>1000
			80	100		1.0	4.9	14.9
				150		1.0	20.4	78.1
				200		1.0	67.4	323

Table B9 INPUT DATA AND CALCULATED LIVES FOR DESIGN MIX BASE, GRANULAR SUB-BASE

Structure	CBR (%)	Temp °C	Speed (km/hr)	Base h_2 (mm)	Subbase h_3 (mm)	Modular ratio	N_z (msa)	N_t (msa)
3	2	8.4	30	100	200	5.0	0.2	3.0
				250		3.5	19.4	180
				400		3.5	204	>1000
			80	100		5.0	0.3	5.8
				250		3.5	30.7	411
				400		3.5	312	>1000
		10.1	30	100		5.0	0.2	1:5
				250		3.5	13.1	71.6
				400		3.5	143	>1000
			80	100		5.0	0.2	3.1
				250		3.5	22.1	183
				400		3.5	230	>1000
	5	8.4	30	100		2.0	1.3	6.0
				200		1.5	27.2	90.5
				300		1.5	231	865
			80	100		2.0	1.8	11.5
				200		1.5	42.2	196
				300		1.5	370	>1000
		10.1	30	100		2.0	1.0	3.8
				200		1.5	18.8	38.9
				300		1.5	154	343
			80	100		2.0	1.4	6.1
				200		1.5	30.8	92.2
				300		1.5	263	883
	10	8.4	30	100		1.0	7.0	9.6
				150		1.0	30.0	43.6
				200		1.0	101	158
			80	100		1.0	9.5	18.6
				150		1.0	42.7	88.6
				200		1.0	151	333
		10.1	30	100		1.0	5.4	4.7
				150		1.0	22.2	20.1
				200		1.0	72.4	70.2
			80	100		1.0	7.6	9.8
				150		1.0	33.1	44.4
				200		1.0	113	161